อิทธิพลจากการฉาบของตะกอนดินเหนียว และหินดินดานบริเวณรอยเลื่อน ต่อการมีศักย์ปิดกั้นไฮโดรคาร์บอนแปลงสัมประทาน B8/32 แอ่งปัตตานี อ่าวไทย

นาย ธรรมศักดิ์ เกิดนอก

วิทยานิพนธ์นี้เป็นส่วนหนึ่งของการศึกษาตามหลักสูตรปริญญาวิทยาศาสตรมหบัณฑิต
สาขาวิชาธรณีวิทยา ภาควิชาธรณีวิทยา
คณะวิทยาศาสตร์ จุฬาลงกรณ์มหาวิทยาลัย
ปีการศึกษา 2545

ISBN 974-17-3052-7

INFLUENCE OF CLAY AND SHALE SMEAR IN FAULT ZONE ON THE POTENTIAL SEALING OF HYDROCARBON IN BLOCK B8/32, PATTANI BASIN, GULF OF THAILAND

Mr. Thammasak Koednok

A Thesis Submitted in Partial Fulfillment of the Requirements
for the Degree of Master of Science in Geology
Department of Geology
Faculty of Science
Chulalongkorn University
Academic Year 2002

ISBN 974-17-3052-7

Thesis Title	Influence of Clay and Shale Smear in Fault Zone on the Potential Sealing of Hydrocarbon in Block B8/32, Pattani basin, Gulf of Thailand
By	Mr. Thammasak Koednok
Field of study	Geology
Thesis Advisor	Associate Professor Punya Charusiri, Ph.D.
Thesis Co-advisor	Luca Rigo De Righi, Ph.D.

Accepted by the Faculty of Science, Chulalongkorn University in Partial Fulfillment of the Requirements for the Master 's Degree

…….. Dean of Faculty of Science
(Associate Professor Wanchai Phothiphichitr, Ph.D.)

THESIS COMMITTEE

…….. Chairman
(Assistant Professor Veerote Daorerk, M.Sc.)

……. Thesis Advisor
(Associate Professor Punya Charusiri, Ph.D.)

…….. Thesis Co-advisor
(Luca Rigo de Righi, Ph.D.)

…….. Member
(Prapat Soponpongpipat, M.Sc.)

ธรรมศักดิ์ เกิดนอก : อิทธิพลจากการฉาบของตะกอนดินเหนียว และหินดินดานบริเวณรอยเลื่อนต่อการมีศักย์ปิดกั้นไฮโดรคาร์บอน แปลงสัมประทาน B8/32 แอ่งปัตตานี อ่าวไทย (INFLUENCE OF CLAY AND SHALE SMEAR IN FAULT ZONE ON THE POTENTIAL SEALING OF HYDROCARBON IN BLOCK B8/32, PATTANI BASIN, GULF OF THAILAND) อาจารย์ที่ปรึกษา รศ. ดร. ปัญญา จารุศิริ, อาจารย์ที่ปรึกษาร่วม ดร. ลูกา ลิโก, 257 หน้า. ISBN 974-17-3052-7

การศึกษารอยเลื่อนปิดกั้นเป็นจุดมุ่งหมายที่จะพิสูจน์และประเมินอิทธิพลการฉาบตัวของตะกอนดินเหนียวและหินดินดานบริเวณรอยเลื่อน ภายในชั้นหินอุ้มไฮโดรคาร์บอน พื้นที่เบญจมาศ-A ของ Block B8/32 แอ่งปัตตานีในอ่าวไทย โดยได้เลือกชั้นทรายและชั้นหินดินดานสลับกันหกชั้น ความหนา 1,230 ฟุต (378 เมตร) จากเก้าหลุมเจาะเพื่อการศึกษาครั้งนี้ ผลการแปลความหมายข้อมูลหยั่งธรณีหลุมเจาะชนิดแกรมม่าเรย์ชี้ว่าชั้นแทรกสลับเหล่านี้ทั้งหมดมีต้นกำเนิดจากการทำงานของแม่น้ำและลำธาร, ส่วนชั้นดินเหนียวเด่นสองชั้น (หนาเฉลี่ย 220 ฟุตหรือ 68 เมตร) ระบุถึงสะภาพแวดล้อมแบบทะเลสาบ ข้อมูลใต้ผิวดินจากชั้นทรายกักเก็บไฮโดรคาร์บอนที่ได้เลือกสรร เรียงลำดับจากบนลงล่างคือชั้น U-C6, U-B2, U-B3, U-B4, U-B5, และ U-B6 โดยมีความหนาในช่วง 14 ถึง 75 ฟุต (4 ถึง 18 เมตร) ได้ถูกนำมาใช้ในการสร้างแผนที่โครงสร้างธรณี (top depth structure map), แผนที่ชั้นความหนาสุทธิชั้นทราย [net sand (isopach) map], และแบบจำลองระนาบรอยเลื่อน (fault-plane-section) จากแผนที่โครงสร้างธรณีพบว่ารอยเลื่อนวางตัวแนวทิศเหนือภายในพื้นที่เบญจมาศ-A แสดงการเลื่อนแบบปกติด้วยมุมลาดเอียงที่สูงไปในทิศตะวันออกและมีระยะในการเลื่อนตัวในแนวดิ่งทั้งหมดเท่ากับ 325 ฟุต (100 เมตร) ส่วนแผนที่ชั้นความหนาสุทธิชั้นทรายระบุว่าชั้นทรายกักเก็บไฮโดรคาร์บอนที่มีปริมาณสูงสะสมตัวอยู่ทางทิศตะวันออกในฝั่งชั้นหินเลื่อนขึ้นของระนาบรอยเลื่อน ในการวิเคราะห์รอยเลื่อนปิดกั้น มีสามขั้นตอนหลักต่อเนื่องกันตามลำดับ คือ ขั้นแรก คือการสืบสวนความสามารถจะเป็นตัวกักเก็บ จากแบบจำลองระนาบรอยเลื่อนชั้นทรายทั้งหมดแปดชั้นจากฝั่งชั้นหินเลื่อนขึ้นและลงของระนาบรอยเลื่อนมีศักย์ต่อการปิดกั้น ชั้นเหล่านี้ประกอบไปด้วยชั้นทรายในฝั่งชั้นหินเลื่อนขึ้น U-C6, U-B2, U-B3, และ U-B5 และชั้นทรายในฝั่งชั้นหินเลื่อนลง U-C6, U-B3, U-B4, และ U-B6 อย่างไรก็ตาม 4 ชั้นทรายซึ่งได้แก่ ชั้นทราย U-B4 และ U-B6 ในฝั่งชั้นหินเลื่อนขึ้นและชั้นทราย U-B2 และ U-B5 ในฝั่งชั้นหินเลื่อนลงมีแนวโน้มจะเกิดการรั่วไหลของไฮโดรคาร์บอนได้ ณ บริเวณสัมผัสแต่ละชั้นทรายหนึ่งกับชั้นทรายอื่นข้ามรอยเลื่อน ขั้นที่สอง คือการประเมินรอยเลื่อนปิดกั้นโดยใช้ shale gouge ratio (SGR) โดยอาศัยการคำนวณปริมาตรหินดินดาน, ความหนาชั้นหิน, และระยะการเลื่อนตัวในแนวดิ่ง ได้ค่า SGR 40 ถึง 42 เปอร์เซ็นต์ สำหรับการคำนวณในชั้นทราย U-B4 สัมผัสกับ U-B2 และค่า 62 ถึง 86 เปอร์เซ็นต์ จากชั้น U-B6 สัมผัสกับ U-B5 ค่า SGR ในพื้นที่ศึกษานี้ มีค่ามากกว่าค่าเริ่มต้นสำหรับการกำเนิดการปิดกั้นไฮโดรคาร์บอนสถิตย์ (15 ถึง 20 เปอร์เซ็นต์) และขั้นที่สาม คือการยืนยันความสามารถในการปิดกั้นโดยวิเคราะห์จากความดันชั้นหินภาคตัดขวาง (pore-pressure profile) ผลลัพธ์แสดงถึงความแตกต่างของความดันข้ามรอยเลื่อน (across-fault pressure difference) อยู่ในช่วง 5 ถึง 23 ปอนด์ต่อตารางนิ้ว (0.3 ถึง 1.5 บาร์) ด้วยค่าความแตกต่างของความดันนี้แสดงความสามารถในการกำเนิดการปิดกั้นที่ดีในพื้นที่ชั้นทรายซ้อนทับ

โดยสรุปแล้ว รอยเลื่อนในพื้นที่เบญจมาศ-A สามารถกำเนิดการปิดกั้นได้โดยการฉาบของตะกอนดินเหนียวและหินดินดานบนระนาบรอยเลื่อน นอกจากนี้วิธีการและผลลัพธ์จากการศึกษาในครั้งนี้สามารถนำไปทำนายประสิทธิภาพและความสามารถในการเป็นตัวปิดกั้นของรอยเลื่อนต่อไฮโดรคาร์ในพื้นที่อื่นได้ที่ซึ่งมีลักษณะธรณีวิทยาและโครงสร้างคล้ายคลึงกัน

ภาควิชา……ธรณีวิทยา……ลายมือชื่อนิสิต……

สาขาวิชา……..ธรณีวิทยา……ลายมือชื่ออาจารย์ที่ปรึกษา……

ปีการศึกษา……2545……ลายมือชื่ออาจารย์ที่ปรึกษาร่วม……

4272295023: MAJOR GEOLOGY
KEY WORD: FAULT SEAL/ CLAY SMEAR/ BENCHAMAS-A FIELD/ PATTANI BASIN/ GULF OF THAILAND

THAMMASAK KOEDNOK: INFLUENCE OF CLAY AND SHALE SMEAR IN FAULT ZONE ON THE POTENTIAL SEALING OF HYDROCARBON IN BLOCK B8/32, PATTANI BASIN, GULF OF THAILAND. THESIS ADVISOR: ASSISTANT PROFESSOR PUNYA CHARUSIRI, Ph.D., THESIS CO-ADVISOR: LUCA RIGO DE RIGHI, Ph.D., 257 pp. ISBN 974-17-3052-7.

Fault seal study is aimed at identifying and evaluating influence of clay and shale smear in a fault zone in the hydrocarbon-bearing reservoirs, Benchamas-A field of Block B8/32, Pattani basin in the Gulf of Thailand. Six alternated sequences of 1,230 ft (378 m)-thick sands and shales from 9 drill holes, were selected for this study. Gamma-ray log interpretation indicates that these interbeds are mostly fluvial in origin, and two clay-dominated horizons (av. 220 ft or 68 m) suggest a lacustrine environment. Subsurface data from selected reservoir sand horizons, in a descending order, as U-C6, U-B2, U-B3, U-B4, U-B5, and U-B6 with thickness varying from 14 to 75 ft (4 to 18 m), were used for constructing top depth structure (reservoir sand horizon) maps, net-sand (isopach) maps, and a fault-plane section (or Allan fault diagram). Based on the top depth structure map, the N-trending fault in Benchamas-A field shows a normal sense of movement with high-dip angles to the east and a total vertical displacement of 325 ft (100 m). The net-sand maps indicate large volumes of reservoir sand located in the upthrown eastern side of the fault plane. To analyze the fault seal 3 majors consecutive stages are involved. The first stage is to investigate trapping potential using fault-plane-section analysis. Result from fault-plane-section, a total of 8 sand horizons for both upthrown and downthrown sides of a fault plane, have potentials for fault sealing. They are U-C6, U-B2, U-B3, and U-B5 sand horizons in the upthrown side and the U-B6, U-B3, U-B4, and U-B6 sand horizons in the downthrown side. However, 4 sand horizons including the U-B4 and U-B6 of the upthrown side and the U-B2 and U-B5 of the downthrown side, have leakage potentials where each horizon is juxtaposed against one another across the fault. The second stage is to evaluate fault seals using the shale gouge ratio (SGR) based on calculated shale volumes, bed thickness, and fault throws. The SGR values of 40 to 42% are calculated for the U-B4 sand horizon juxtaposed against the U-B2 sand horizon and 62 to 86% for the U-B6 and the U-B5 horizons. These SGR values are obviously greater than the threshold SGR values (15-20%) for static hydrocarbon sealing. The third step is to confirm seal capacity by using pore-pressure profile. The result shows that the across-fault pressure difference varies from 5 to 23 psi (0.3 to 1.5 bar). Such values of pressure difference suggest good sealing capacity in the sand offset areas.

In conclusion, the studied fault in Benchamas-A field can be sealed by clay and shale smears on the fault plane. Furthermore, the methodology and the result in this research can be applied to predict the fault seal capacity in the other areas of similar lithologies and structures.

Department……Geology……..Student's signature……

Field of study…….Geology……Advisor's signature……

Academic year……..2002……Co-advisor's signature……

ACKNOWLEDGEMENTS

The author is indebted to Associate Professor Dr. Punya Charusiri, his thesis advisor and Dr. Luca Rigo, his thesis co-advisor for their advice, reviewing manuscripts and general help throughout this research. Without their kind help, this achievement would not have been possible.

Grateful acknowledgements are extended to Chevron Offshore (Thailand) Limited, Government relationship and Benchamas asset team, for the permission to study the confidential data. Deep appreciation is given to Mrs. Rattikan Chaiwanit, Mr. Trem Smith, and Mr. George Mettingly for kindness in considering the research topic.

Special acknowledgements are due to Assistant Professor Pongsak Phongprayoon for his guidance and encouragement to study. Deep appreciation is given to Mr. Chaiyan Chaikiturajai and Mr. Atip Muangsuwan for their assistance, invaluable suggestions, and teaching the Allan diagram construction.

The author would like to express his appreciation to Graduate School, Department of Geology, and Chulalongkorn University for continuously providing numerous facilities and financial support.

Additionally, special thank is given to Miss Sukumarl Kedboonsai who has helped in the reading of the manuscript and comments for encouragement.

Finally, this thesis cannot be completed without the help and encouragement of his family and friend who patiently provided both moral and physical support.

CONTENTS

CONTENTS (continued)

CONTENTS (continued)

CONTENTS (continued)

LIST OF FIGURES

LIST OF FIGURES (continued)

LIST OF FIGURES (continued)

LIST OF FIGURES (continued)

LIST OF FIGURES (continued)

LIST OF FIGURES (continued)

LIST OF FIGURES (continued)

LIST OF FIGURES (continued)

LIST OF FIGURES (continued)

LIST OF FIGURES (continued)

LIST OF FIGURES (continued)

LIST OF FIGURES (continued)

LIST OF FIGURES (continued)

LIST OF FIGURES (continued)

LIST OF TABLES

LIST OF TABLES (continued)

CHAPTER I

INTRODUCTION

1.1 Background

Faults play an important role in creating hydrocarbon traps in Benchamas-A field. For a better appreciation of the risks associated with fault-controlled prospects and of the production from faulted fields, it is important to understand the processes that contribute to fault seals (Yielding et al., 1997). In fact, the problems that happen to prediction of reservoir distribution is difficult because of multiple faults, complex reservoir and seal geometry, and the opportunities of cross-fault leakage and migration (Williamson, 1992). The reason of many hydrocarbon fields in Thailand is related to structural trap especially fault trap therefore faults are possibly their sealed by clay smear (Pradidtan and Dook, 1992). Furthermore, clay smear plays an important part in upthrown fault trap at Pru Krathiam-B01, Phitsanulok, where a 312 ft (95 meters) oil column in deltaic “K” sand is sealed laterally by clay smear from overlying lacustrine deposits, and by juxtaposition against the same clays across the fault (Bal et al., 1992). Moreover, fault seal study in the North Pailin field, Pattani basin, the Gulf of Thailand shows fault is an effective seal to make the low-pay wells across a faults (Muangsuwan, 1998). Therefore fault seal study is one challenging topic to study and search for answer why the fault can be sealed.

Fault seal study has many methodologies to investigate the potential sealing on a fault surface. For example fault-plane section (Allan fault diagram) was used to predict trapped area in faulted closure (Allan, 1989); fault slicing, clay smearing and pore-pressure distribution were used to indicated strong seal potential along the fault plane (Jev et al., 1993); cores rock in fault zone and capillary pressure were used to correlate the properties of sheared zones with their trapping capacity (Berg et al., 1995); fluid types, pressure and organic

geochemistry were used to identify fluid composition in juxtaposed sands (Alexander, 1998); and shale gouge ratio (SGR) was used to predict clay smear on fault surface that can act as a seal (Yielding et al., 1997).

Fault seal study in this research was focused on influence of clay and shale to smear on the fault plane that caused to fault seals in Benchamas-A field, Pattani basin, the Gulf of Thailand. Clay smear study can be defined two types of lithology dependent attributes; they are gouge ratio and smear factor. Gouge ratio is an estimating of the proportion of fine-grained material entrained into the fault gouge from wall rocks. Smear factor methods (including clay smear potential and shale smear factor) estimate the profile thickness of shale drown along the fault zone during faulting (Yielding et al., 1997). As regard, a clay smear study by shale gouge ratio had performed many fields such as the Gullfaks field (North sea), Nun river field (Niger delta) and Oseberg Syd (North sea) as an aid to improve reservoir management of this complexly faulted structure. Therefore shale gouge ratio the same algorithm had been selected to predict clay smear in this research.

The cause of clay and shale in study area deposits in fluvial system some shale have more thickness in the duration of the flooding but some shale alternated or interbedded with sand beds in lithological sequence (U-B5 to U-C6). It is too difficult to apply algorithm directly in thick heterogeneous (sand-shale) sequences because it is often not feasible to map every shale bed and consider its effect at the fault surface. Therefore, shale gouge ratio algorithm had been applied because this algorithm considers only the bulk properties of the sequence at the scale of the throw windrow and it is easiest way to count the slipped beds in sand-shale sequence. Furthermore shale gouge ratio algorithm widely used to analyze fault seal study in petroleum exploration. For example The Gullfaks field (North sea), a shale gouge ratio of about 20% (volume of shale in the slipped interval) is a typical threshold between minimal across-fault pressure difference and significant seal (Yielding et al., 1999).

A number of mechanisms have been recognized whereby fault planes can act as a seal, show as stated below (Watts, 1987; Knipe, 1992);

1) Juxtaposition, in which reservoir sands are offset against a low-permeability unit (e.g., shale) with a high entry pressure;

2) Clay smear (i.e., entrainment of clay or shale) into the fault plane, thereby giving the fault itself a high entry pressure;

3) Cataclasis, which is the crushing of sand grains to produce a fault gouge of finer grained material, again giving the fault high entry pressure; and

4) Diagenesis, when preferential cementation along an originally permeable fault plane may partially or completely remove porosity, ultimately creating a hydraulic seal.

1.2 Objectives

Objectives in this study are:

1) To study and analyze properties of clay and shale due to the deformation on fault zone;

2) To find the best appropriate method to analyze the information of clay and shale smear on fault plane;

3) To identify potential sealing by using clay and shale smear on fault plane as a significant factor of evaluation; and

4) To evaluate influence of clay and shale smear on fault zone and discuss.

1.3 Study area

The Benchamas field is located in northwest of the Tantawan field in the concession area Block B8/32, Pattani Basin in the Gulf of Thailand

(**Figure 1.1**). The Benchamas field is one of major ChevronTexaco's production fields in the Gulf of Thailand. The Benchamas field currently produces approximately 160 million cubic feet of natural gas and 50,000 barrels of oil per day.

Benchamas-A field is a part of the Benchamas field that was selected to investigate the fault seal potential. The cause of hydrocarbons is trapped in fault closures and these fault look seem, it is controlled reservoir distribution on both side of upthrown and downthrown the Benchamas-A Fault. The Benchamas-A field was separated from the other Benchamas fields by the N-trending horst block (**Figure 1.2**). These field lies between latitude 10°29'30" N to 10°32'00" N and longitude 101°16'16" E to 101°17'28" E. Approximate area is 11.5 square kilometers.

There are 9 exploration and production wells, namely A, B, C, D, E, F, I, H and J (**Figure 1.2**). These 9 wells can be divided into two groups by using Benchamas-A Fault classified, they are upthrown side in the north (include: A, C, D, E, F and J) and down thrown side in the south (include: I, B).

1.4 Data sources

The data of study in Benchamas-A field have been kindly provided by ChevronTexaco (Chevron Offshore (Thailand) Limited) (Atip Muangsuwan, January 22, 2001). The data can be concluded as stated below:

1. Final well reports of the 9 wells (A, B, C, D, E, F, H, I and J);
2. Electrical wireline logs of the 9 wells (A, B, C, D, E, F, H, I and J) comprise caliper, gamma ray, resistivity, density - neutron and sonic log. Total depth to run logs was about 32,760 feet;
3. Results of repeat formation test (RFT) of 7 wells (A, B, D, E, F, I and J). Total test about 292 points;
4. Top depth structure map of 5 horizons (U-C, U-A, U-B6 and U-C6 scale 1: 10000);

5. Fault traces of 6 studies sand horizon onto the top depth structure map. They are U-C6, U-B2, U-B3, U-B4, U-B5, and U-B6; and

6. Well log key beds, of wells D and F.

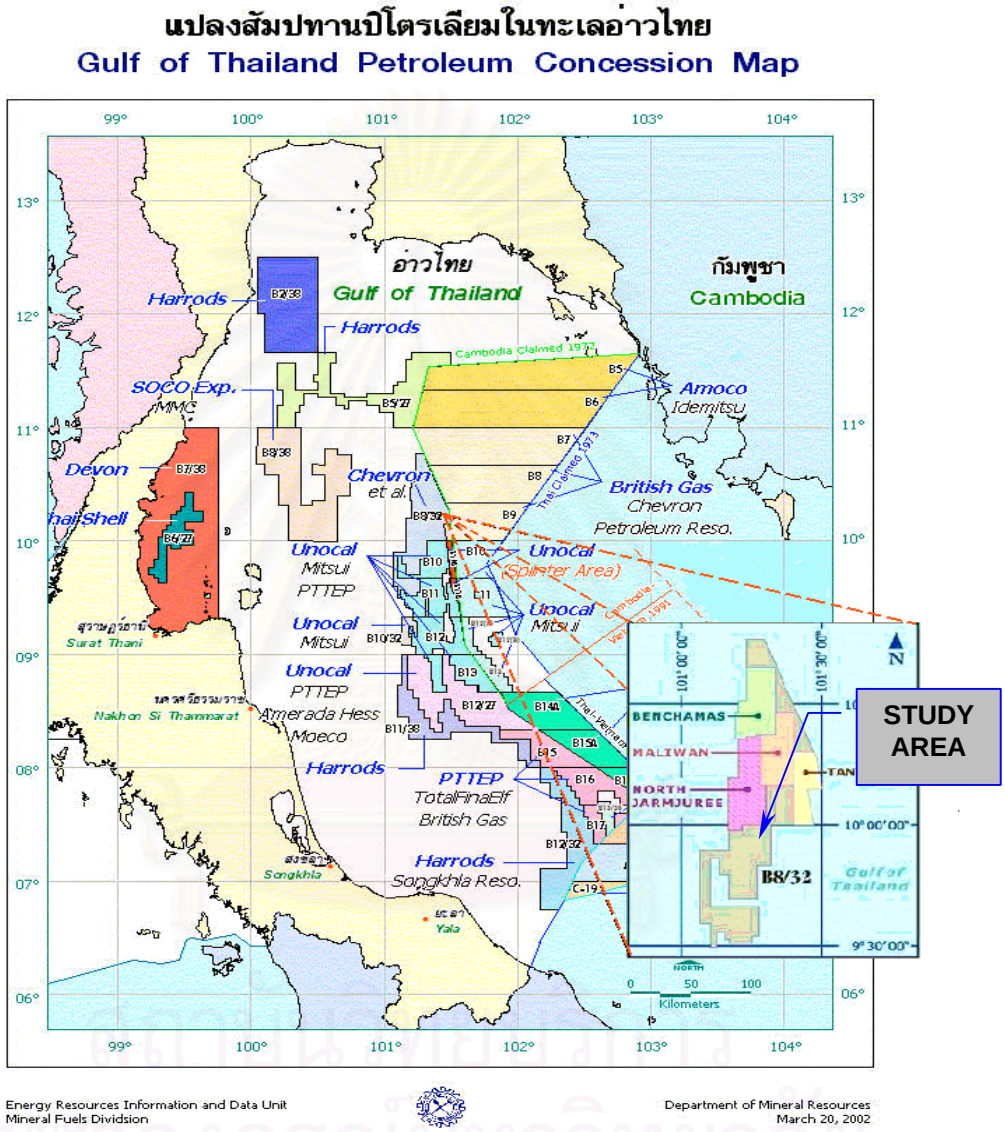

Figure 1.1 Location of the study area and concession areas block B8/32 in the Pattani Basin, the Gulf of Thailand (modified after Department of Mineral Resources, 2002).

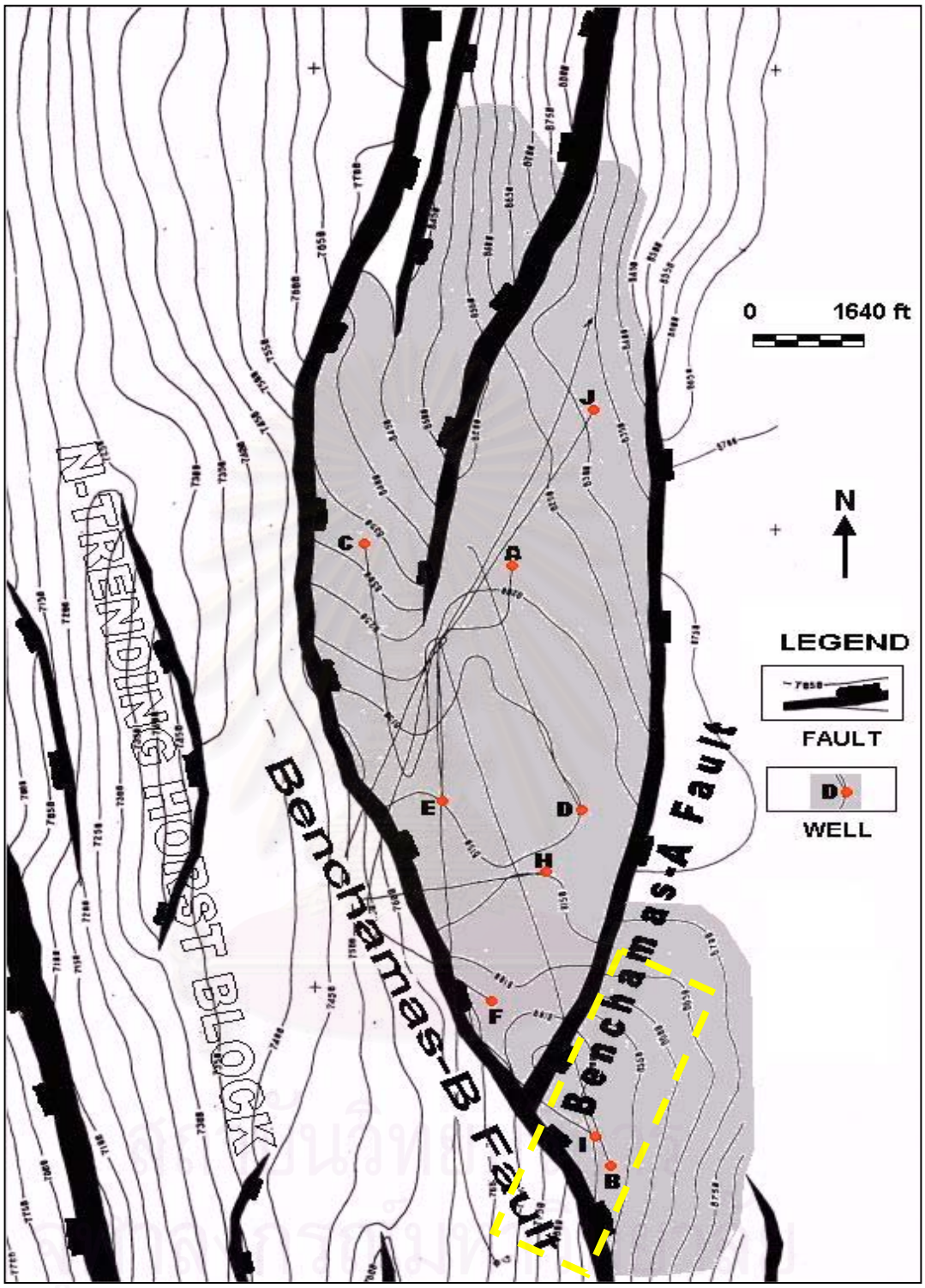

Figure 1.2 Top U-A horizon depth structure map shows the location of the studied wells and in side the yellow rectangle represents studied fault in the Benchamas-A field (modified after ChevronTexaco, 2001).

1.5 Previous works

There are many previous works and different algorithms that identify or predict fault sealing by clay smears. This section divided previous works into 2 sections. First it introduces the algorithms that have been proposed by other authors. Second it presents the previous studies that related to clay smear.

Algorithms for predicting clay smear

Bouvier et al. (1989) presented a study of the Nun River field in the Niger Delta. They described a clay smear potential (CSP) as a means of estimating the likelihood of clay smearing in area of sand-to-sand juxtaposition on fault. The clay smear potential is stated to represent the relative amount of clay that has been smeared from individual shale source beds at the certain point along the fault plane. CPS is stated to (1) increase with shale source bed thickness, (2) increase with the number of source beds displaced past a particular point along fault plane, and (3) decrease with increased fault throw. The equation represented in equation (Eq-1.1)

$$CSP = \sum [(\text{Shale bed thickness})^2 / \text{Distance from source bed}] \quad \text{(Eq-1. 1)}$$

In the CSP algorithm equation (Eq-1.1), The shale bed thickness is raised to the power of 2. This has been justified by fluid dynamics arguments by Lehner and Pilaar (1996), who stated that the out-flux from the shale or clay layer should be proportional to the square of its thickness if the material undergoes Newtonian flow. CSP as defined by equation (Eq-1.1) then has dimensions of distance. Therefore, The CSP was modified as below.

$$\text{Smear factor} = \sum [(\text{Shale bed thickness})^n / (\text{Distance from source bed})^m]$$

(Eq-1. 2)

The exponents m and n can be regarded as additional variables whose values may be justified by experimental or observational studies. When m = n, the result is dimensionless and is therefore independent of the units of measurement.

Lindsay et al. (1993) proposed a shale smear factor to constrain the likelihood of shale smear continuity. Based on their observations of abrasion smears in a lithified sequence, they define the shale smear factor (SSF).

SSF = Fault throw / Shale layer thickness (Eq-1. 3)

The shale smear factor remains constant between the offset terminations because it does not depend on smear distance. From case study of 80 faults, Lindsay et al. (1993) concluded that shale smears may become incomplete for an SSF greater than 7. The smaller values of SSF are more likely to correspond to continuous smears and therefore to sealing layer on fault surface. The values of SSF are not additive for compound smears because thin shale gives higher SSF and dominate the sum. In example, a simple application of SSF values would take the minimum value (most sealing) from the relevant shale beds at that point on the fault. Gibson (1994) presented observations from the Columbus Basin, offshore Trinidad. He showed that self-juxtaposed sands from poor fault seals and that significant fault seals are formed when clay smearing is able to occur down the fault plane. He applied the SSF method of Lindsay et al. (1993) and concluded that the more significant seals are developed where SSF is less than 4.

The CSP, smear factor, and SSF algorithms described depend upon a consideration of the thickness and offset of individual shale beds. Conversely, such an approach may be difficult to apply directly in thick heterogeneous sequences because it is often not feasible to map or count every shale bed and consider its effect at the fault surface.

Yielding et al. (1997) suggest the simpler approach of considering only the bulk properties of the sequence at the scale of reservoir mapping. They call the shale gouge ratio (SGR), which is simply the percentage of shale or clay in the slipped interval (to estimate the composition of subsurface fault zone). The shale thicknesses are measured in a “window” with a height equal to the throw; therefore, this window represents the column of rock that has slid past this point on the fault. When extended for cases where the stratigraphic breakdown is by reservoir zone rather than by individual beds. Then the net contribution of fine-grained material from each reservoir zone can be related to the clay content and thickness of the zone analyze. This parameter likely is good guide to the proportion of phyllosilicates in the fault zone material (Foxford et al., 1998). Furthermore, He was applied the pore pressure in reservoir zone between upthrow side and downthrow side to supported the potential fault sealing. SGR has been calibrated in this way for a number of data sets, including the adjacent Gullfaks Sør field. In general, static sealing behavior is observed when SGR is above 15-20 %; higher-pressure differences correlate with larger values of SGR. The other example, the Brent-Brent overlap data show a small static seal [up to 22 psi. (1.5 bar)] developing at gouge ratios of 15-20%. This is in excellent agreement with earlier calibrations from various areas (Yielding et al., 1997)

$$SGR = \sum [(\text{zone thickness}) \times (\text{zone clay fraction})] / \text{Fault throw} \times 100\% \quad \text{(Eq-1.4)}$$

The relationship of CSP, SSF and SGR can be summary in this way, clay/ shale smear indicate that their geometries are dependent on the thickness of source bed and on the fault throw or smear distance. These relationships have been used to define a number of fault-surface attributes that describe the likelihood of smears being developed at a particular point on the fault surface. These attributes are as follows.

1) Clay smear potential (CSP) Bouvier et al., (1989), which is the sum of (thickness^2/distance) for shale beds.

2) Generalized smear factor, which is the sum of (thickness^n/distance^m) for shale beds, with optional exponents for both thickness and distance.

3) Shale smear factor (SSF) (Lindsay et al., 1993), equal to throw/thickness.

4) Shale gouge ratio (SGR), which is net shale/clay percentage in the slipped interval.

Applying these algorithms to fault surface in a variety of data sets shows that they can be related together, the plot for SGR has similar distribution to that for CSP. No fault-sealed hydrocarbons are observed at values of less than 20% because the shale content of the slipped interval is too low. Above 20%, the maximum observed pressure difference progressively increases, reaching about 100 psi (about ~7 bar) at SGR of about 60%. This relationship agrees well with the statement by Weber (1987, p. 97) " it usually requires some 25 to 30% of shale to render a fault sealing". The distribution for SSF is almost a mirror image of that for SGR. Seal in not observed at SSF greater than 6, which agree very well with the outcrop observations of Lindsay et al. (1993) that shale smears may become incomplete for an SFF greater than 7.

Previous clay smear study

Vavra et al. (1984) presented the capacity of a seal to hold back hydrocarbons is thus controlled by the size of the largest interconnected continuous pore throats and the relative densities of the hydrocarbon (oil or gas) and formation water.

Weber (1987) presented his research. The relationship between amount of shale in slipped interval and pressure difference across fault that "it usually requires some 25 to 30% of shale to render a fault sealing.

Sneider (1987) presented any rock type can form a seal in the subsurface provided that minimum displacement pressure of the potential seal rock is greater than the established buoyancy pressure of the hydrocarbons within the accumulation.

Allan (1989) presented the Allan diagram or fault plan section that can used to predict: (1) which closures have a high probability of being traps and (2) the amounts of hydrocarbons these traps could contain. Further more this diagram can used to explain the migration pathway on fault plan.

Bouvier et al. (1989) calibrated their CPS calculation against known sealing and no sealing faults, and divided the observed range into high, medium, and low CPS. Low CPS represents little chance for the presence of continuous clay smear seal that can trap hydrocarbons. Jev et al. (1993) used the same technique on the Akaso field (in the Niger Delta) and quoted a CPS of less than 15 as no sealing and CSP of more than 30 as sealing for faults bounding undrilled prospects.

Bal et al. (1992) presented the trap geometries in the Phitsanulok basin are complex, and structures are generally faulted. Clay smear along fault planes are increased hydrocarbon columns and trap volumes. These traps often require 3D seismic data for proper resolution.

Jev et al. (1993) studied fault seal in Akaso field, Nigeria. They used fault slicing, clay smearing and RFT pressure data on fault trapping and dynamic leakage to investigate the back-split fault and main antithetic fault indicated strong seal potential with possible “leak windows” along the fault planes.

Gibson (1994) applied the shale smear factor (SSF) method of Lindsay et al. (1993) and concluded that the more significant seals are developed where SSF is less that 4 (i.e., the shale bed is more that 25% of the displaced section.).

Berg and Avery (1995) studied and described the characteristics of shear zones in core. The sheared zone display fabrics similar to Riedel shear and are termed wispy, crenulate, conjugate and miniscate, in order of increasing deformation. In addition Berg and Avery discussed the soft-sediment deformation, the term “fault” denotes the slip surface or displacement surface. The term “sheared zone” denotes the associated, highly deformed sediment adjacent to the fault. The sealing properties of growth faults gave the result, sheared zone are effective seals because ductile deformation has homogenized the original sediments and resulted in a uniform distribution of small pore and cause of increased capillary pressure (high displacement pressures) that hence increasing seal capacity in the sheared zone.

Fristad (1996) provided a fault-seal calibration for a group of structures in the Brent province of the North Sea. The faults cut the deltaic Brent Group reservoir sequence, which at the time of faulting was less than 500 meters deep. This shallow burial depth would suggest that the clays were unconsolidated during faulting, and evidence of clay smearing is seen in core.

Jardine (1997) presented the dominant petroleum system in Pattani basin is made up of Miocene gas-generating terrestrial coals/ shale and Oligocene oil-prone lacustrine shale. The structure evolution was favorable for entrapment of the expelled gas and oil. The main phase of lifting and basin subsidence that initially created the productive graben systems occurred in the early and middle Miocene.

Knipe (1997) presented the juxtaposition diagram that can used to analyze fault juxtaposition and sealing. The diagrams are based on the interaction of rock lithology and fault displacement (throw) magnitude to control juxtapositions and fault seal types.

Yielding et al. (1997) presented the factors control the likelihood of clay/ shale smearing: (1) thicker source beds can produce thicker clay smears; (2) shear-type smears decrease in thickness with distance from the source layer; (3) abrasion-type smears decrease in thickness with increasing throw; and (4) multiple source beds can give a combined continuous smear. These relationships imply that a quantitative approach to clay smear prediction might be possible.

Fisher and Knipe (1998) studies the relationship between shale gouge ratio and outcrop and classified fault rock is fundamentally based on their composition and hence shale gouge ratio (SGR) can be thought of as a predictor of fault-rock types for simple fault zone. Fault rocks with phyllosilicate content < ca. 15-20% are typically cataclasites or disaggergation zone, those with > ca. 40% phyllosilicate are clay shale smears, and intermediate compositions are sometimes referred to as clay-matrix gouges (Gibson, 1998) or Phyllosilicate-framework fault rock (Fisher and Knipe, 1998).

Gibson (1998) studied and measurement permeability of fault gouge samples in siliciclastic strata of the Columbus basin, offshore Trinidad. When increased phyllosilicate content results is lower permeability for the fault gouge.

Yielding et al. (1999) presented the Brent Group oil-water contact (OWC) on the upthrown side lies above the downthrown Brent Group, and hence the

footwall Brent Group oil and gas are trapped by juxtaposition against Upper Jurassic shales. On the downthrown side, however, the oil-bearing Brent Group is juxtaposed against the upthrown water-bearing Brent Group.

Bracken et al. (2000) presented the structural-stratigraphic model of Oligocene and Miocene reservoirs in Block B8/32, Gulf of Thailand. Benchamas reservoirs occur in braid belt and sandy, upper estuarine fluvio-deltaic sandstone. Reservoir intervals alternate with carbonaceous mudstones with relatively few reservoir quality sandstone beds. The fine-grained mudstones probably acted as regional seals during hydrocarbon migration and now act as top-seals in fault compartments.

Teerman et al. (2000) presented Benchamas field produces primarily light oil. The main source rock area is in the deeper graben areas to the east of the fields, in the Pattani Trough. A regional decrease in thermal gradient from concession areas to the south puts Block B8/32 in favorable location for bout gas and liquids generation. Faulting strongly controls migration pathways and seals.

Yielding et al. (2002) suggested that a shale gouge ratio value between 15 to 20% represented a threshold value between non-sealing and sealing fault in the Oseberg Syd.

CHAPTER II

GENERAL GEOLOGY OF PATTANI BASIN, GULF OF THAILAND

2.1 Geology of the northern part of the Gulf of Thailand overview

Numerous Tertiary basins are located in the northern part of the gulf of Thailand, namely Sakhon, Paknam, Hua Hin, North Western, Western, Kra, East Kra, North Kra, Prachuap, Chumphon and the northern part of Pattani basin. The Tertiary basins in the area are intracratonic rift basin (Pradidtan and Dook, 1992).

The northern part basin of the Gulf of Thailand appears to lie near the intersection of two major strike-slip fault systems (**Figure 2.1**). The NW-SE trending Three Pagodas Fault appears from the Myanmar border and appears to extend into the northern part of the Gulf. The NE-SW trending Ranong Fault cuts across peninsular Thailand and may extend into the north-western part of the Gulf (Achalabuti, 1974, and Polachan and Sattayarak, 1989). Polachan (1988) suggested that the dextral movement of the NW-SE strike-slip faults and the sinistral movement of the NE-SW strike-slip conjugate faults probably had occurred initially in the Oligocene.

In South East Asia, Tertiary tectonic has largely been caused by the interaction of the Indian and Eurasian plates (**Figure 2.2**). The Indian plate separated from Africa during Late Cretaceous time and through northward movement, eventually collided with the Eurasian plate in the Eocene. With continued penetration to the north, South East Asia was slowly pushed out to the southeast and progressively rotated clockwise, with the angle of subduction changing from perpendicular to oblique (Tapponnier et al., 1986). Progressively increasing oblique subduction accelerated dextral movement of the NW-SE strike-slip faults, including the Three Pagodas and Ping Faults.

The Gulf of Thailand can be divided by the N-S trending Ko Kra ridge into two areas, West and East. According to Bunopas (1981), the west Area, where

numerous narrow and small Tertiary basins are located, appears to be situated in the Shan-Thai block. The East Area, where the Pattani and Malay basins are located, appears to be part of the Indochina block.

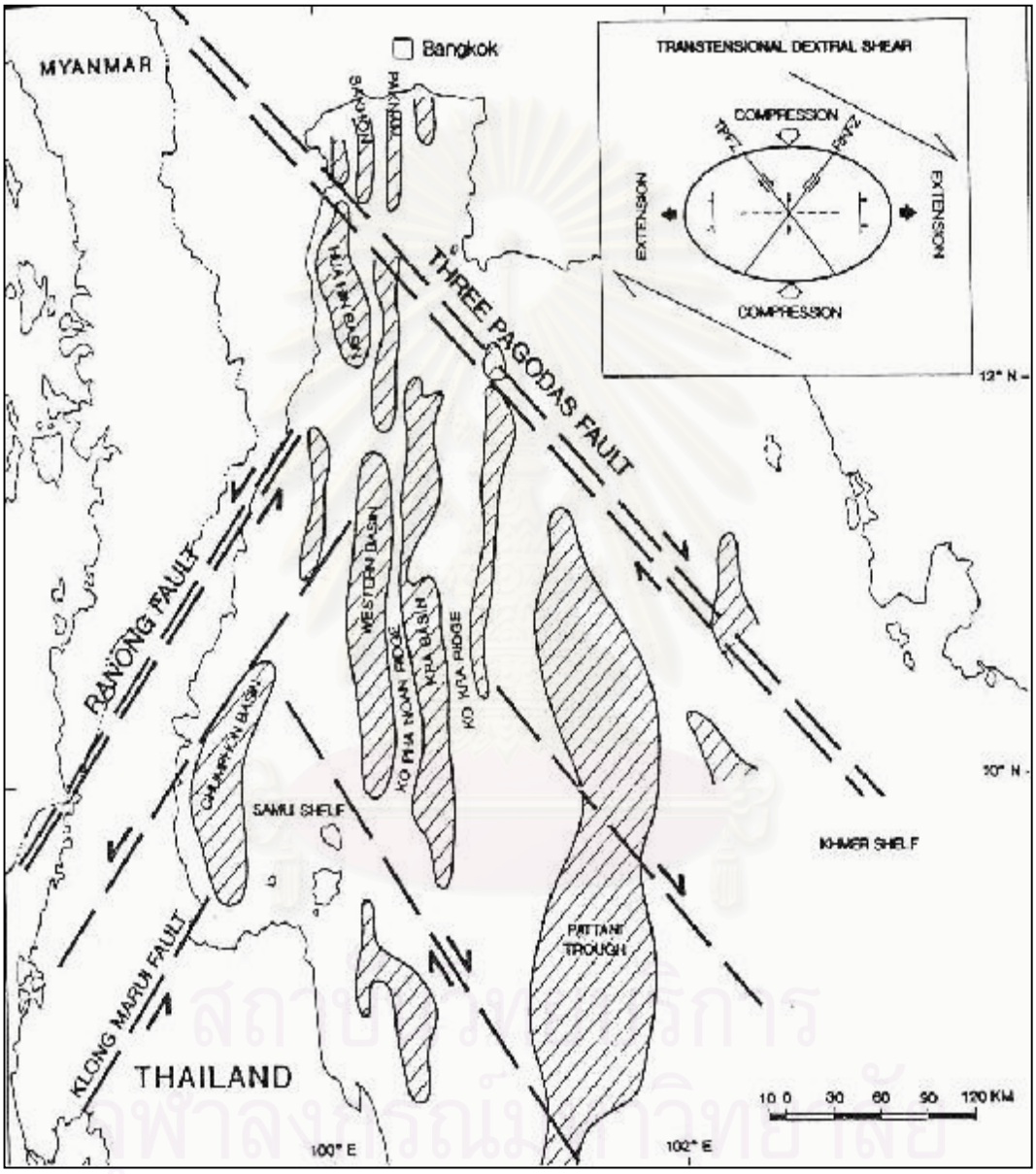

Figure 2.1 Structure elements indicate indicating dextral shear in the northern part of the Gulf of Thailand (Pradidtan and Dook, 1992).

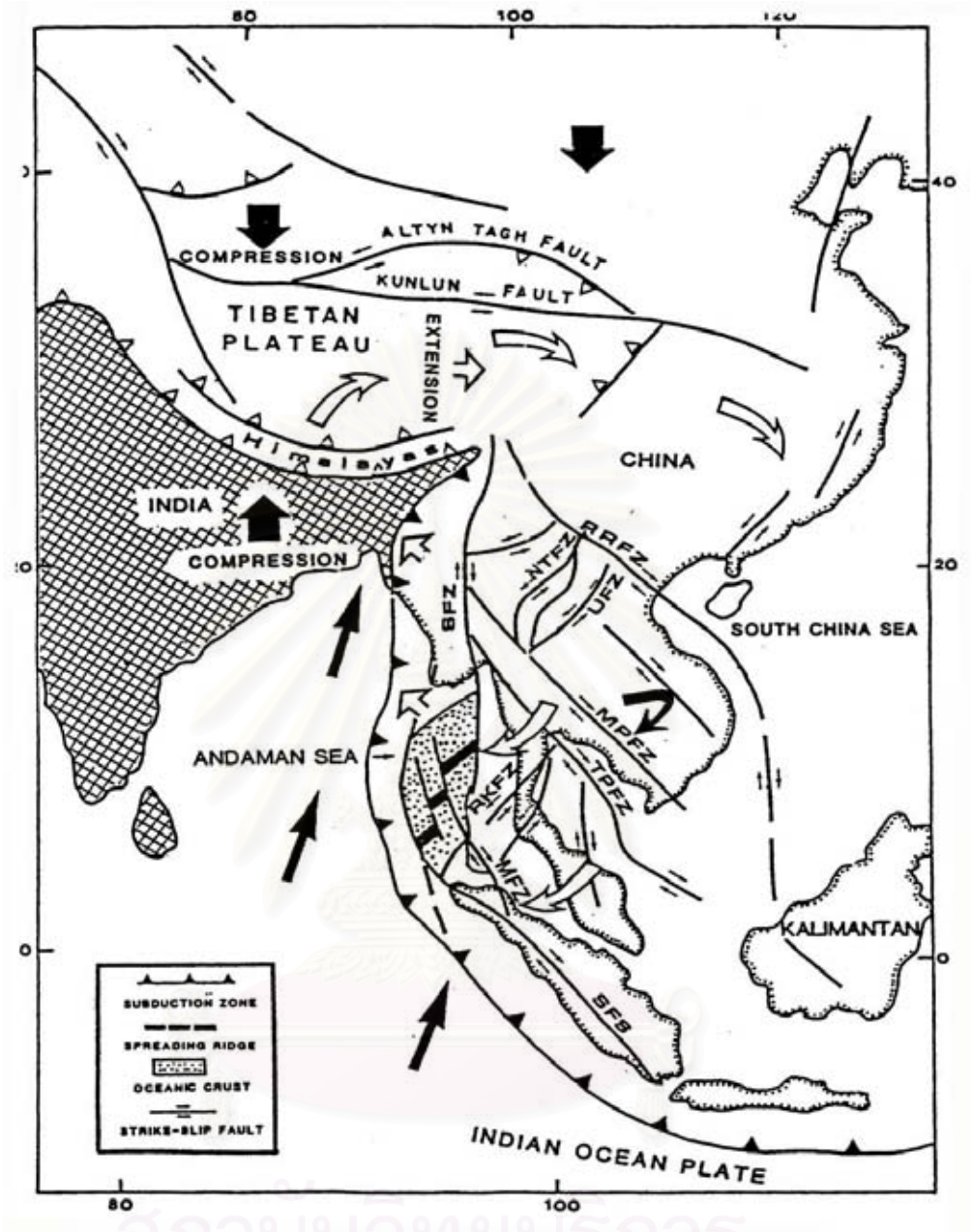

Figure 2.2 Tectonic map of Southeast Asia and the South China Sea showing the patterns of major faults and their relative movements. SFS (Sumatran fault system); MFZ (Mergui fault zone); TPFZ (Three Padodas fault zone); SFZ (Sagaing fault zone); RKFZ (Ranong and Klong Marui fault zone); MPFZ (Mae Ping fault zone); UFZ (Uttaradit fault zone); NTFZ (Northern Thailand fault zone) and RRFZ (Red River fault zone) (Packham, 1993).

The western and eastern parts of the Gulf of Thailand appear to be part of the Shan-Thai and Indochina blocks respectively. Pre-Tertiary basement in the northern part of the Gulf has been encountered by several wells. Lithologies penetrated include; Permian carbonates, Mesozoic carbonates, Paleozoic metaclastics and Cretaceous granite (Pradidtan and Dook, 1992). Tertiary sequences, unconformably overlying the Pre-Tertiary, are almost entirely nonmarine sediments. Paul and Lian (1975) described the presence of the Late Middle Miocene Unconformity in the Pattani basin. Woolland and Haws (1976) also recognized its presence elsewhere in the Gulf of Thailand. By comparison with radioactive dating of the unconformity in the Phitsanulok basin (Legendre et al., 1988), an absolute age between 10.4 to 13.6 Ma is suggested.

Pradidtan et al. (1990) use the unconformity to suggest two stratigraphic groups for the Tertiary sequences. Overlying the unconformity is Chao Phraya group. The second group, beneath the unconformity is named after the basin in which it occurs.

Post-rift sequence

Since the formation of the unconformity, generally quiescent thermal subsidence has been taking place. The lithology of the Chao Phraya group is rather homogeneous with relatively uniform thicknesses of approximately 3280 ft (1000 meters). A more marine influence is seen in the eastern basinal area. Flood plain and fluviatile sediments are predominant, with more littoral and paludal sediments occurring in the upper part of the group.

Syn-rift sequence

The stratigraphic groups below the unconformity are syn-rift related and were deposited in separate basins, particularly the lower and middle parts of the sequences. Therefore, they are potentially unique. In general, three distinct unit; Upper, Middle, and Lower can be recognized in these groups. In a few basins, four units have also been identified (**Figure 2.3**). Generally, these syn-rift sequences comprise alluvial and lacustrine sediments.

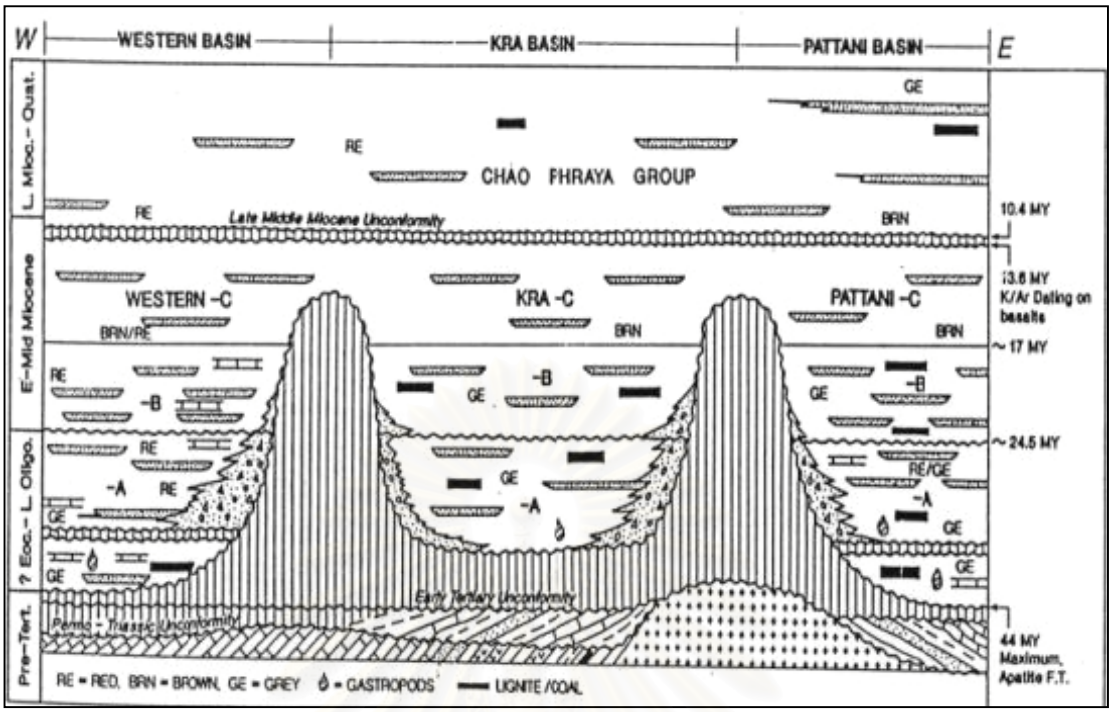

Figure 2.3 Generalized chronostratigraphics summary of the basins in the northern part of the Gulf of Thailand (Pradidtan and Dook, 1992).

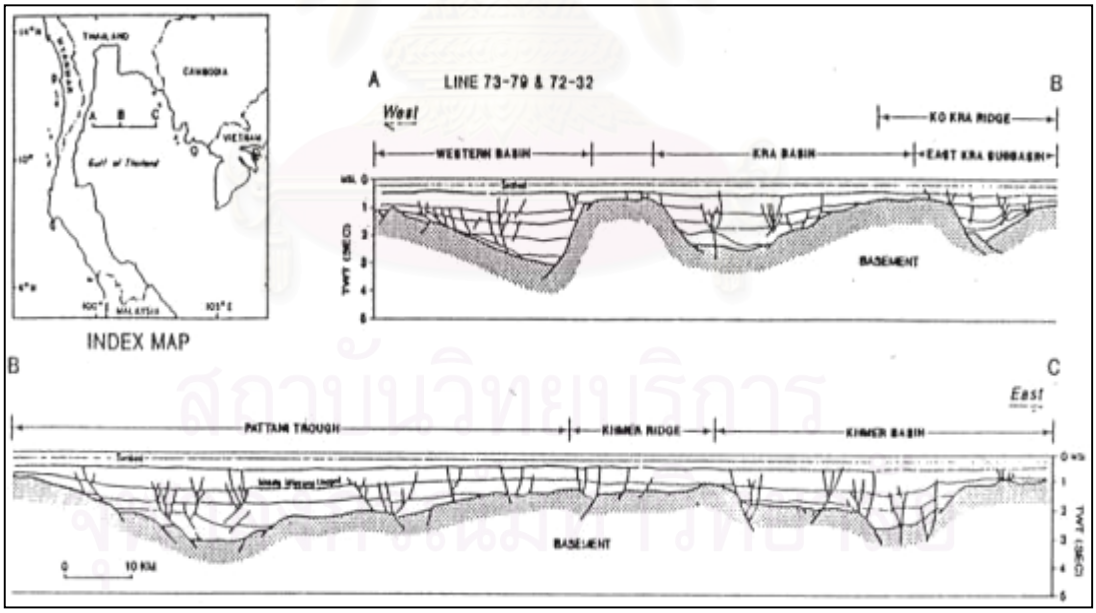

Figure 2.4 Cross-section across the northern part of the Gulf of Thailand (Pradidtan and Dook, 1992).

A map on top of the Pre-Tertiary basement and a regional cross section illustrated in **Figure 2.4** respectively, show the geometry and distribution of the basin in the northern part of the Gulf. Tertiary basins generally have half-graben geometry and are controlled by major boundary fault zone. The major boundary faults lie N-S trends and are products of extensional tectonics. The throw of these faults are extremely large. However, lateral variations in throw are frequently found. The major movement occurred in the early stage, during the Late Oligocene to Early Miocene, but analyses of the fault system suggest periods of rejuvenation (Pradidtan and Dook, 1992). Beside the boundary fault, numerous normal faults bout listric and basement involved can be identified. Generally, these lie in N-S trends. The throw of these faults are much less than the throw of the major boundary fault, and they are sufficient to isolate reservoirs.

2.2 Geology of Pattani basin

2.2.1 Structural evolution

The Pattani basin is the largest of a series of elongate N-S trending tertiary rifts formed in the Gulf of Thailand in response to the northward movement and collision of Indian plate into Eurasia. Initial rifting in the Oligocene (40-50 Ma.) created localized haft-grabens where oil-prone lacustrine shales were deposited in shallow lakes rimmed by alluvial fan complexes. The internally drained sub-basin coalesced in the lower Miocene during the main basin-forming rifting phase and river flow became the dominant drainage mechanism. As the Pattani basin subsided throughout the Miocene, gas-pone coals and carbonaceous shales formed in low-lying swamps dissected by fluvial flood-plain system. Sediments are non-marine in origin, mainly fluvio-lacustrine deposits. However, the eastern portion was influenced by marine incursion during the early Miocene age. A variety of trap types present in the basin such as anticlinal faults, tilted faults, rollover, and buried hills. A number of oil and gas fields have been found in Pattani. Most of the gas fields are distributed all over the central part of the Pattani basin while oil fields are gathered in the shallower part of the basin

margin. The characteristic of hydrocarbon bearing reservoirs in Pattani basin is found in Oligocene to middle Miocene fluvial and fluvial-deltaic sandstone. The data source rock chemists suggested two main sources of hydrocarbon in the area. The first source rock facie is the Miocene fluvial-deltaic coals and carbonaceous shale contains land plant debris is the primary source of gas and condensate in the region. The second source facie are the Oligocene, oil-prone lacustrine shale. The organic matter is dispersed, terrestrially derived, type III kerogen with minor type II kerogen and primarily consists of vitrinite. The average total organic carbon (TOC) contents are generally low to moderate (0.2-1.4 wt.%). The hydrogen index (HI) average is 100 mg HC/g TOC, the hydrocarbon potential range from 0.01 to 2.5 mg HC/g rock and the quality of the organic matter ranges from 0.31 to 1.9 mg HC/g TOC (Bustin and Chonchawalit, 1995).

The structural evolution of the Pattani region can be divided into seven main stages (Jardine, 1997):

1) Pre-rift folding and uplift of pre-Tertiary accreted basement terranes from the Cretaceous to the Eocene;

2) Initial rifting and creation of localized sub-basins (half-grabens) from late Eocene to late Oligocene time;

3) Structural inversion and erosion at the end of the Oligocene;

4) Rifting and basin formation in the lower Miocene;

5) Post-rift collapse and basin subsidence in the middle Miocene;

6) Widespread erosion in latest-middle to early upper Miocene time; and

7) Continued basin subsidence from the upper Miocene to the present.

During the main rifting and basin formation phase in the early and middle Miocene, Pattani trough subsided quite rapidly. “Accommodation” graben systems consisting of series of opposing normal faults developed in response to the rapid extension and deepening.

2.2.2 Depositional system

Since Oligocene time, more than 25000 ft of sediment thickness have been deposited in the central Pattani basin **Figure 2.5**. The basin fill is comprised of non-marine and marginal marine siliciclastic sediments shed from adjoining highlands to the north, east, and west. The various provenances provided sediment influx of differing characteristics, forming variability in reservoir size, reservoir quality, and source richness across the basin.

Five major sequences are identified (**Figure 2.6**), reflecting low-order relative sea-level changes during the Neogene. Two periods of non-deposition occur near 25 mya and 10 mya, represented by the Mid-Tertiary Unconformity (MTU) and the mid-Miocene Unconformity (MMU) respectively.

The evolution of the depositional environments active in the Pattani during Tertiary time began with initial localized lacustrine and alluvial deposition in the Oligocene (Sequence 1), changing to mostly fluvial and alluvial deposition in the lower Miocene (Sequence 2), to transgressive fluvial and marginal marine deposition in the lower middle Miocene (Sequence 3), then overall regressive fluvial and alluvial deposition in the upper middle Miocene (Sequence 4), and predominately transgressive marginal marine deposition in the upper Miocene (Sequence 5) (Jardine, 1997).

The main hydrocarbon-bearing reservoirs in the Pattani are fluvial and fluvial-deltaic sandstones within Sequences 4, 3, and upper Sequence 2. These sequences, overall sand percentages increase towards the basin margins where the main sediment source provinces are located. Major basin faults and graben systems guide fluvial meander-belt trends and create localized sand build-ups along downthrown fault blocks.

The timing of the structural evolution of the Pattani basin was favorable for entrapment of the expelled gas and oil. The main phase of rifting and basin subsidence, which initially created the productive graben systems, occurred in the early and middle Miocene. Therefore, the major fault system existed to trap hydrocarbons (mostly gas) expelled from Sequences 2 and 3 over a relatively

long period of time, from the middle Miocene to the present. Continued fault movements since the mid-Miocene is an important factor controlling variations of hydrocarbon pool size and abundances throughout the Pattani basin. Moreover oil generation and preservation occurs in cooler, shallower areas along the basin flanks, particularly in the northern Pattani where heat flows are lower.

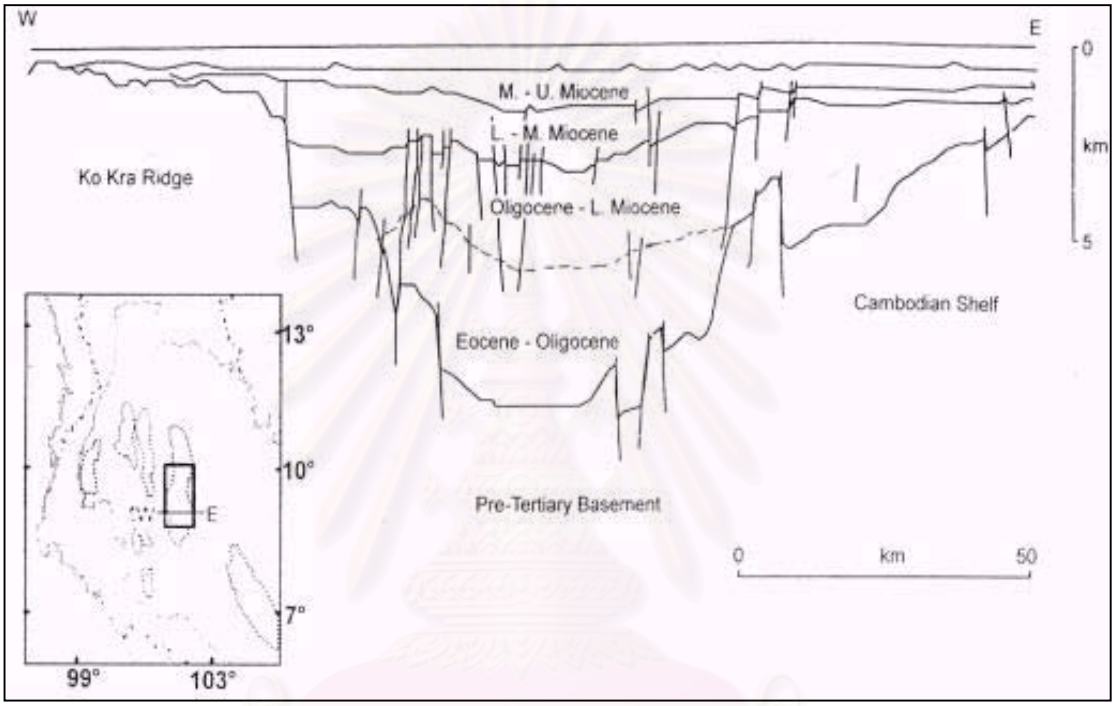

Figure 2.5 Idealized west-east cross section of the Pattani basin (Bustin and Chonchawalit, 1997).

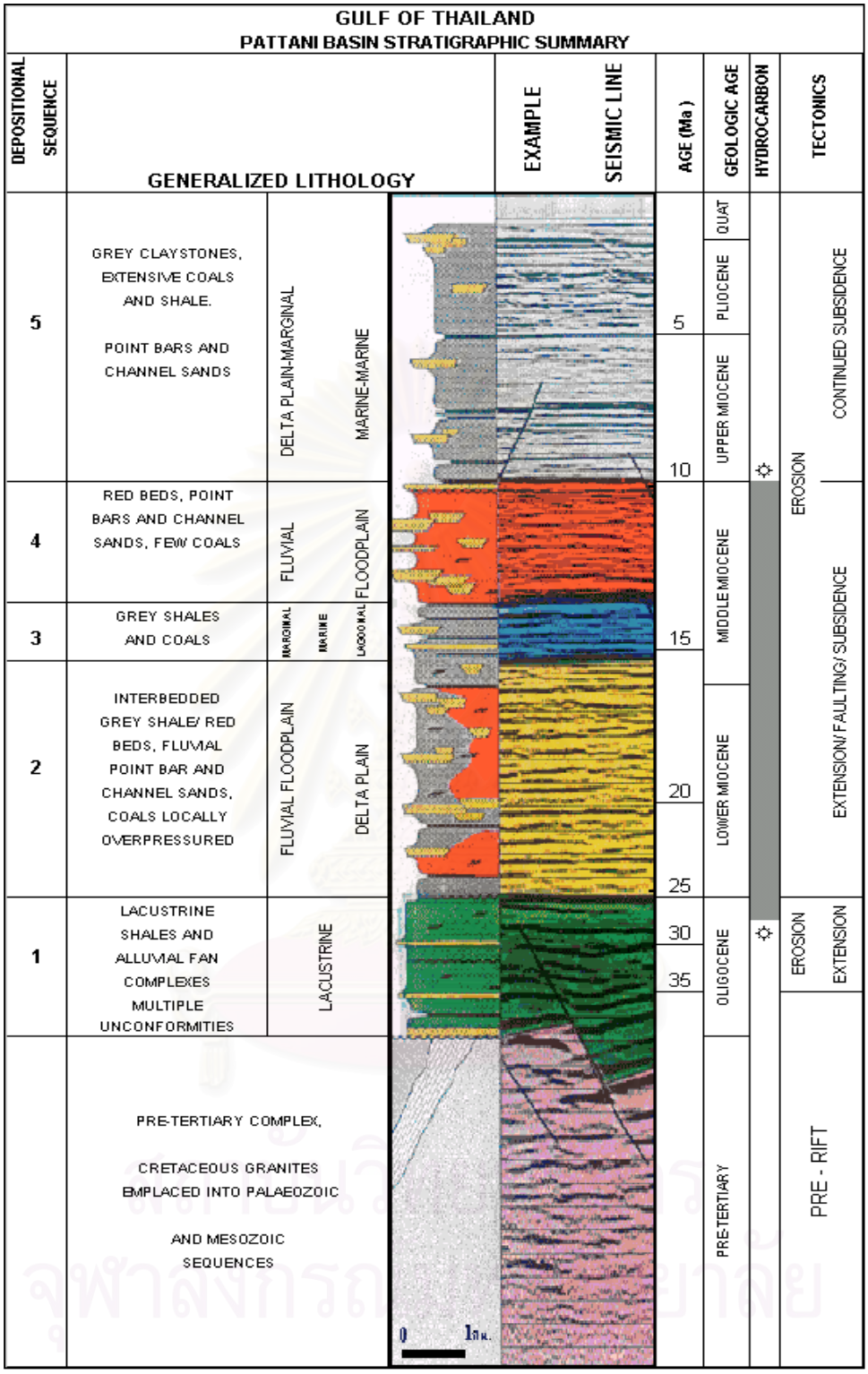

Figure 2.6 Stratigraphic summaries of the major depositional sequences within the Pattani basin (modified after Jardine, 1997).

CHAPTER III

GENERAL GEOLOGY BENCHAMAS-A

3.1 Geology of Benchamas field

Benchamas field is a one majority production field of Chevron Offshore (Thailand) limited (ChevronTexaco) in Block B8/32 in the northern Pattani basin, the Gulf of Thailand. Benchamas field is currently producing approximately 160 million cubic feet of natural gas and 50,000 barrels of oil per day.

Benchamas field can be divided into three sub-basinal structures there are Benchamas-A, Benchamas-B, and Benchamas-C. The hydrocarbon reservoirs in this area are distributed in fault compartments. Oligocene and Miocene sand are the primary reservoir targets. Hydrocarbon reservoir occur in braid-belt and sandy, upper estuarine fluvio-deltaic sandstone.

Reservoir-bearing intervals alternate with carbonaceous mudstones with relatively few reservoir quality sandstone beds (Bracken et al., 2000). The main source rock area is in the deeper graben areas to the east of the field, in the Pattani Trough. A regional decrease in thermal gradient from concession areas to the south puts Block B8/32 in a favorable location for both gas and liquids generation. Faulting strongly controls migration pathways and seals. Both oils and condensates display variations in isotopic composition and their capillary gas-chromatography character, suggesting differences in source input. Characterization of type II and II/III kerogens by pyrolysis and organic petrology indicate the occurrence of several different source facies and depositional environment. Restricted penetration of potential source rock intervals and lateral facies changes limits interpretation of source rock occurrence (Teerman et al., 2000).

3.2 Geology of Benchamas-A field

3.2.1 Field structure

The Benchamas-A field is located to the eastern flank of the main N-trending horst block in the Benchamas field (**Figure 3.1**). The main fault lies in N-S trends at the western of Benchamas-A field. The throw of this fault is extremely large (> 700 ft). However, lateral variations in throw are frequently found. The main fault is products of extensional tectonics, which created the sub-basinal haft-graben in adjacent area of this fault. Benchamas-A field is one another sub-basin that formed during extensional tectonic.

Benchamas-A field appears to lie near the intersection of two normal faults. They are Benchamas-A Fault and Benchamas-B Fault. Both faults have dip direction lie parallel together. Benchamas-B Fault appears in the western flank of Benchamas-A field. This fault makes the boundary Benchamas-A field separated form the main N-trending horst block. This fault have strike direction NW-SE, average dip angle 75°, dip direction to NE and throw vary from 625 to 750 ft. The Benchamas-B Fault cuts through the horizon in a descending order, as U-C, U-B, and U-A. The other planar fault namely Benchamas-A Fault. This fault appears in the eastern flank of Benchamas-A field. This fault have strike direction NE-SW, average dip angle 64°, dip direction to NE and throw vary from 210 to 325 ft.

The Benchamas-A Fault separated the Benchamas-A field into 2 areas they are upthrown areas at the north and downthrown areas at the south. The main production area is located in the upthrown side of the Benchamas-A Fault, whereas the downthrown side have a few well penetrated in this compartment. However, the result of drilling in well B and I show a good reservoir quality in downthrown side.

The horizon U-C, U-B, and U-A in upthrown side, they are gentle dipping to the NNE. The down-dip of these horizons appears at the north, whereas the up-dip appears at the south.

The horizon in downthrown side is steep dipping to the east. The down-dip appears at the east. The deepest area is located in the eastern area, whereas the highest area is located nearby the western of block.

Fault traps along both flanks (west and east) of Benchamas-A field are controller the hydrocarbon migration and accumulation in this area. **Figure 3.2** displays the different depth of hydrocarbon-water contact in overlap reservoir sand between upthrown and downthrown side of Benchamas-A Fault.

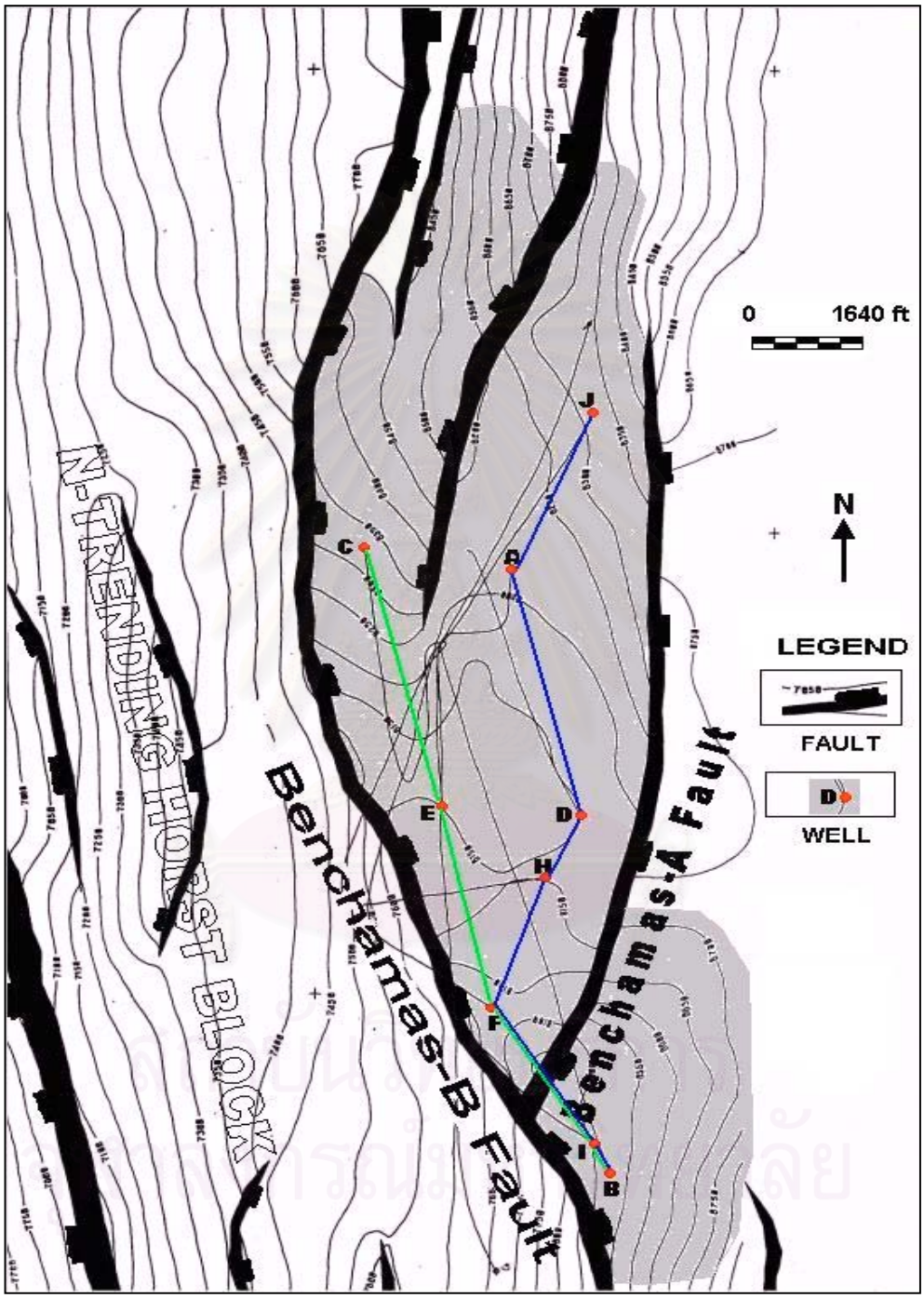

Figure 3.1 Top depth U-A structure map of Benchamas-A field (modified after ChevronTexaco, 2001).

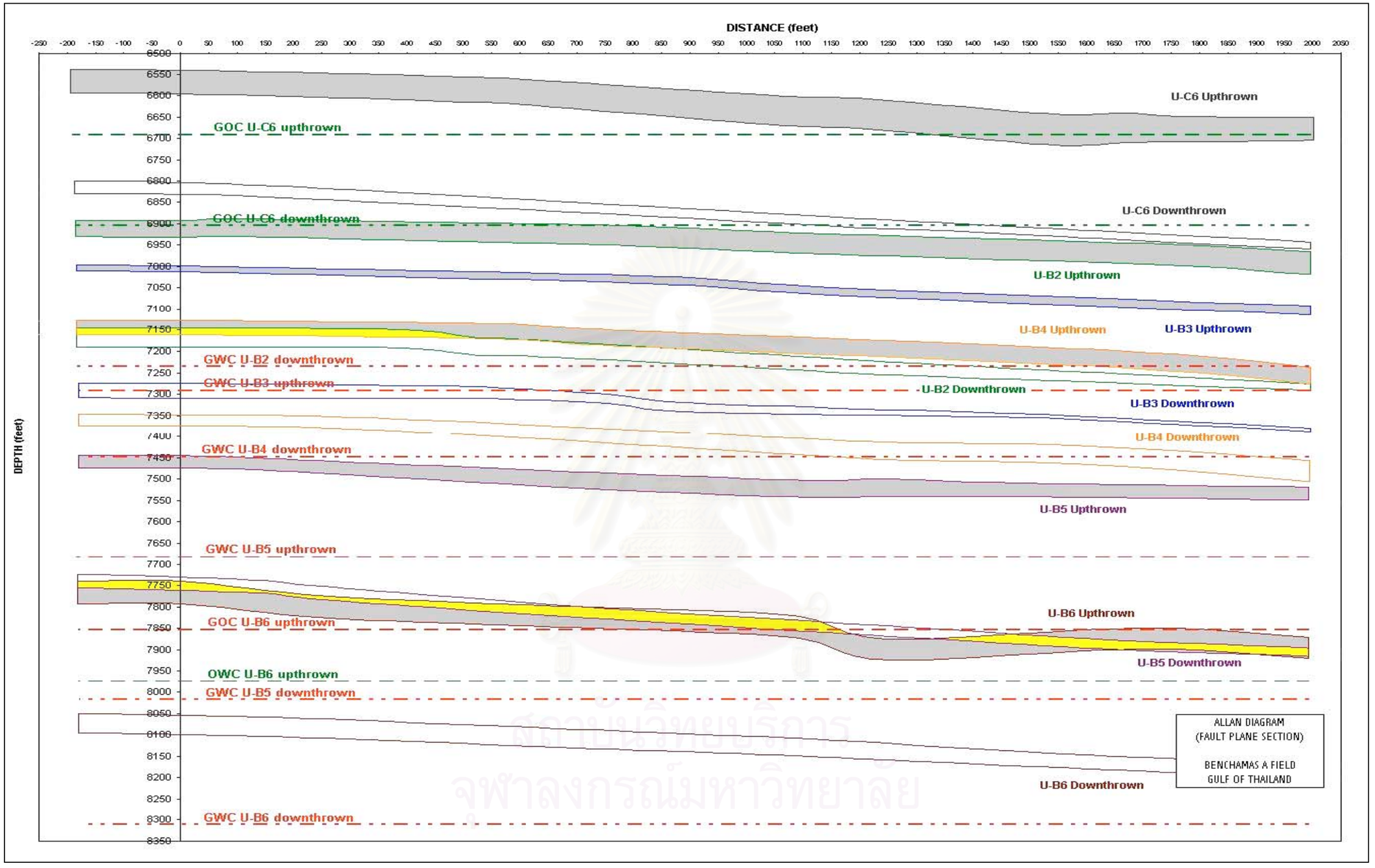

Figure 3.2 Fault-plane-section represents the hydrocarbon-water contact depth across the Benchamas-A Fault. Yellow color represents the overlap sand areas between sand horizon upthrown and downthrown side (GWC = gas-water contact, GOC = gas-oil contact, and OWC = Oil-water contact). The gray blocks represent the reservoir sand horizons in upthrown and the empty blocks represent the reservoir sand horizons in downthrown side.

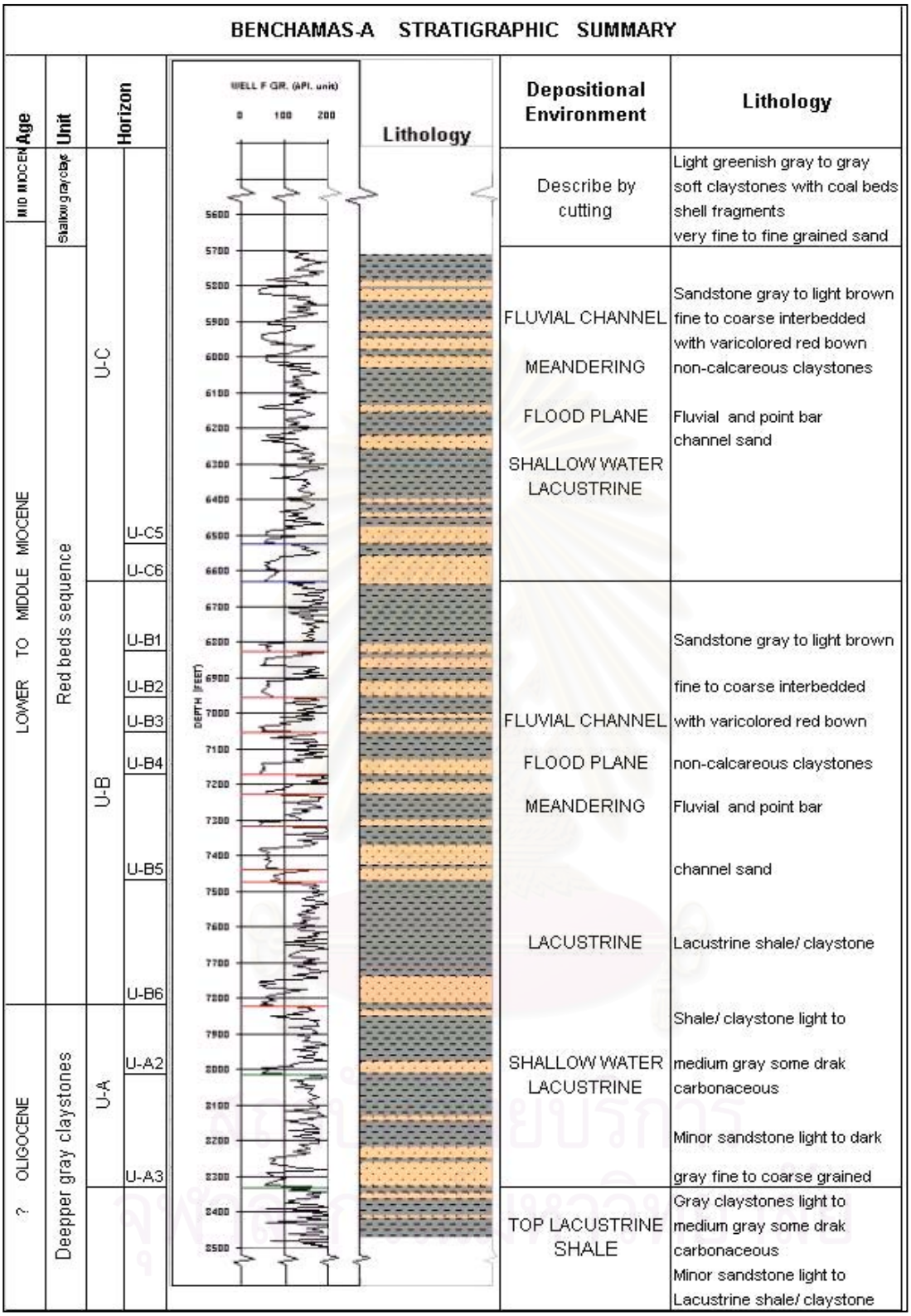

Figure 3.3 Stratigraphic summary of Benchamas-A field.

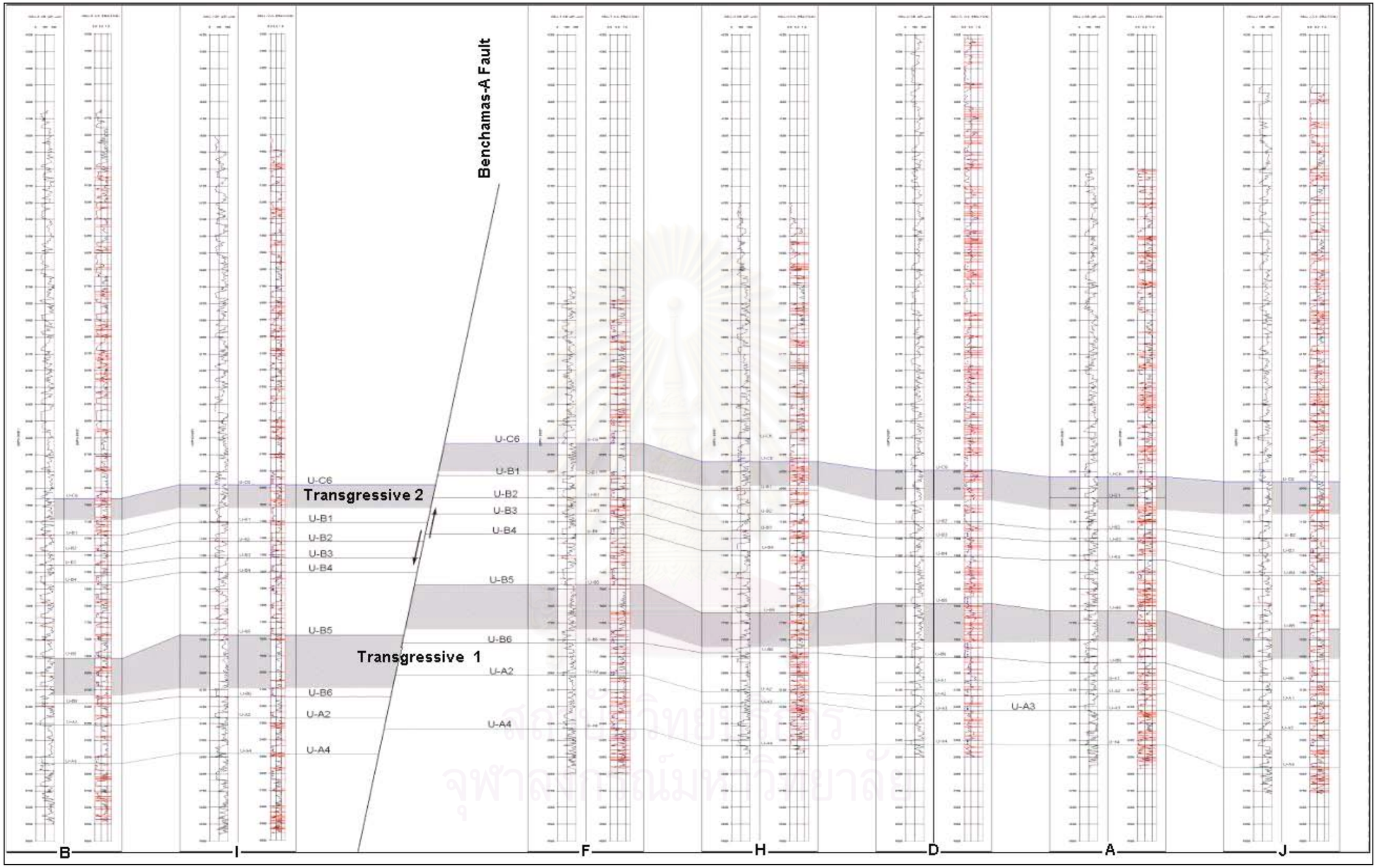

Figure 3.4 Two transgressive intervals (av. 220 ft) appear in well log correlation across the Benchamas-A Fault, suggest that the lacustrine environment (at the top lines indicate the maximum flooding surface). At the left represents the gamma ray log and at the right represents the shale volume (Vsh) log in each well.

3.2.2 Stratigraphic

3.2.2.1 Depositional system

Since Oligocene time, the sedimentary strata have been deposited in the Benchamas field. The basin fill is comprised of non-marine clastic sediment from adjoining highlands to the east. The depositional system in this area is controlled by water level (sea level?). The evolution of the depositional environment active in the Benchamas-A field happened at the same time of Pattani basin started extension. Duration Tertiary began with initial localized lacustrine and alluvial deposition in the Oligocene (Deep gray claystone), relative to tectonic event erosion and extension, changing to mostly fluvial deposition, in the lower Miocene (Red beds sequence), to transgressive fluvial and shallow water (marginal marine?) deposition in the middle to upper Miocene (Shallow gray clays), and predominately transgressive marginal marine deposition in the upper Miocene.

The cause of log pattern shown 2 cycles transgressive of the maximum flooding (hot shale) in this area (massive shale thickness > 130 ft below formation U-B5 and upper U-B1). When using these shale beds did a well correlation between well to well can be used to describe the depositional evolution into 3 phases for this area (**Figure 3.4**).

Oligocene time, the predominant of transgressive sequences appear in the area (U-A to U-B6). The location of deepest area in basin can be located at the southeast of the basin. Because the log patterns shown the dominated bell shaped curves (fining upward) in this interval and the high clay/ shale thickness appear several more than 120 ft in well D, E, F, and H, these suggests low energy deposits region in the lacustrine. Whereas, well C, A, and J appear the log patterns shown dense sand beds in the same interval this suggests the sediment transported into the area from the north and N-W of the area.

Lower to middle Miocene, the regressive sequences is dominate in the area and that to changed the depositional system in the area to fluvial system alternated with local flooding (U-B5 to U-B1). This sequences look seem the high transported energy supplied more sediments into the area and created

the sand layers distributed around the area. This sand layers are importance because they are the main target reservoirs in these sequences.

Middle to upper Miocene, the transgressive sequence dominant in the area again. This time look seem transgressive sequences appear in cover mostly area of Benchamas-A field. The log patterns can be indicated the maximum flooding surface lower sand horizon U-C6.

3.2.2.2 Lithological units

The penetrated from drilling exploration and production wells can basically be sub-divided into three gross lithological units, they are Shallow Gray Clays, Red beds sequence and Deeper Gray Claystone. The following divisions are based depend on a combination of cuttings samples and initial log correlations. The lithological units were deposited within a fluvio-lacustrine depositional system. The potential reservoir formation contains three majority horizons separated by intraformational seals. From youngest to oldest, these are the U-C, U-B and U-A horizon.

Lithological detail

Shallow Gray Clays: This section is dominated by light greenish gray-to-gray soft claystones with coal beds and rare shell fragments. These are commonly interbedded with very fine-to-fine grained loosely cemented sands or sandstone.

Red beds sequence: This section consisted of abundant thin to massive (up to 70 feet TVD.) sandstone interbedded with varicolored red brown, non-calcareous claystones. These claystones became firmer with depth as overburden increases. The sandstone are generally composed of clear, translucent gray to light brown, fine to coarse quartz grains held together in slightly to very argillaceous matrix. The sandstone was generally broken up into their individual grains and cementation was often difficult to discern. The top of this interval was picked lithologically at well site when red-brown claystones became predominate in the cuttings sample.

Deeper Gray claystones: The deeper gray claystones were picked by Maersk for their final report and termed by Maersk as “ Top Lacustrine

Shale" claystones in this section of the wells were light to medium gray with some dark carbonaceous material appearing. Minor sandstones were light to dark gray, fine to coarse grained, occasionally very coarse, subangular to subrounded, with an argillaceous matrix.

3.2.3 Benchamas-A reservoir

The majority reservoir, oil and gas accumulations within lower to middle Miocene sandstone, deposited within a fluvial system of low to moderate energy meandering channels. Sand thickness for these units range from 15 to 100 feet. Porosity ranges from 10% to 26%. The secondary reservoir target is deeper, late Oligocene to early Miocene, sand thickness for these units range from 5 to 25 feet and porosity is variable ranging from 5% to 18%.

Table 3.1 Summary of net pay sand and net sand in each horizon.

WELL	Net pay / horizon (feet)			Net sand to Gross ratio			Sand to shale ratio in horizon			Net pay / well (feet)
	U-C	U-B	U-A	U-C	U-B	U-A	U-C	U-B	U-A	
A	0	211	77	13	25	18	15	33	22	288
B	10	207	66	20	23	23	25	30	30	283
C	40	163	N/A	49	26	N/A	96	35	N/A	203
D	0	162	77	16	17	11	19	20	12	239
E	0	147	29	16	18	8	19	22	8	176
F	146	194	76	24	26	19	32	35	23	416
H	106	126	65	23	22	24	30	28	32	297
I	42	106	105	19	23	15	23	30	18	253
J	0	99	54	17	33	14	20	49	16	153
Average	38	157	68	22	24	17	31	31	20	-

Note: N/A = well did not penetrate.

The net-to-gross ratio when classified by based on horizon, every horizon presented low net-to-gross ratio. However if consider to the net pay per horizon, in the main sand horizon U-B have net pay highest. The cause of low net-to-gross ratio due to shale is a predominance of rock sequence in every well (**Table 3.1**). Shale bed appears in the formed of high thickness shale column (50 to 225 ft) and some interbedded in sand beds (12 to 25 ft).

3.2.4 Fault seal

Faulting strongly controls migration pathway and seals (**Figure 3.5)**. The cause of Benchamas-A Fault and Benchamas-B Fault are effectively control the reservoirs distribution between upthrown and downthrown that can observing the hydrocarbon distribution shows the hydrocarbons are trapped at sand/ sand overlaps, suggesting that clay smear contributes to the fault seal. The result of fault seal study on the Benchamas-A Fault can be classified 2 types of the fault seal in the Benchamas-A field. First, juxtaposition seals in which faulting juxtapose rock types or lithologies with different permeability (sand reservoir overlap with shale bed). For example reservoir formation U-C6 and U-B3, both upthrown and downthrown are juxtaposed against shale and created hydrocarbon trapped along the fault. Second, fault seal by clay smears that occurs by fine-grained materials such as shale and clay have slipped past this part of fault surface. The minimum shale gouge ratio (SGR) values (40% of SGR) that calculated from the Benchamas-A Fault when calibrated with differential pressure (ΔP = 9 psi) across a fault suggest the leaked area (U-B6 upthrown offset U-B5 downthrown) is sealed by clay smear.

When consider to the fine-grained source bed that provided amount of clay to slipped interval. Clay and shale sequences of fluvial system in this area are effective to generate clay smear along a fault plane. The characteristic of clastic sequences that appears in this area, shale and clay are predominant in the stratigraphic sequences. The massive shale beds 30 to 150 ft in thickness have been repeated appear in intervals of well log,

whereas sand beds 10 to 65 ft in thick appear discontinue in thickness and some sand interbedded by shale.

The migration of hydrocarbon in the Benchamas-A field have controlled by lateral lithology continuity and faulting. When the hydrocarbons have left the source rock they migrated through the up-dip bedding to the highest closure and fill-up this closure. When this closure have saturated with hydrocarbon, they start fill backward into the lower closure such as fault closure Benchamas-A Fault.

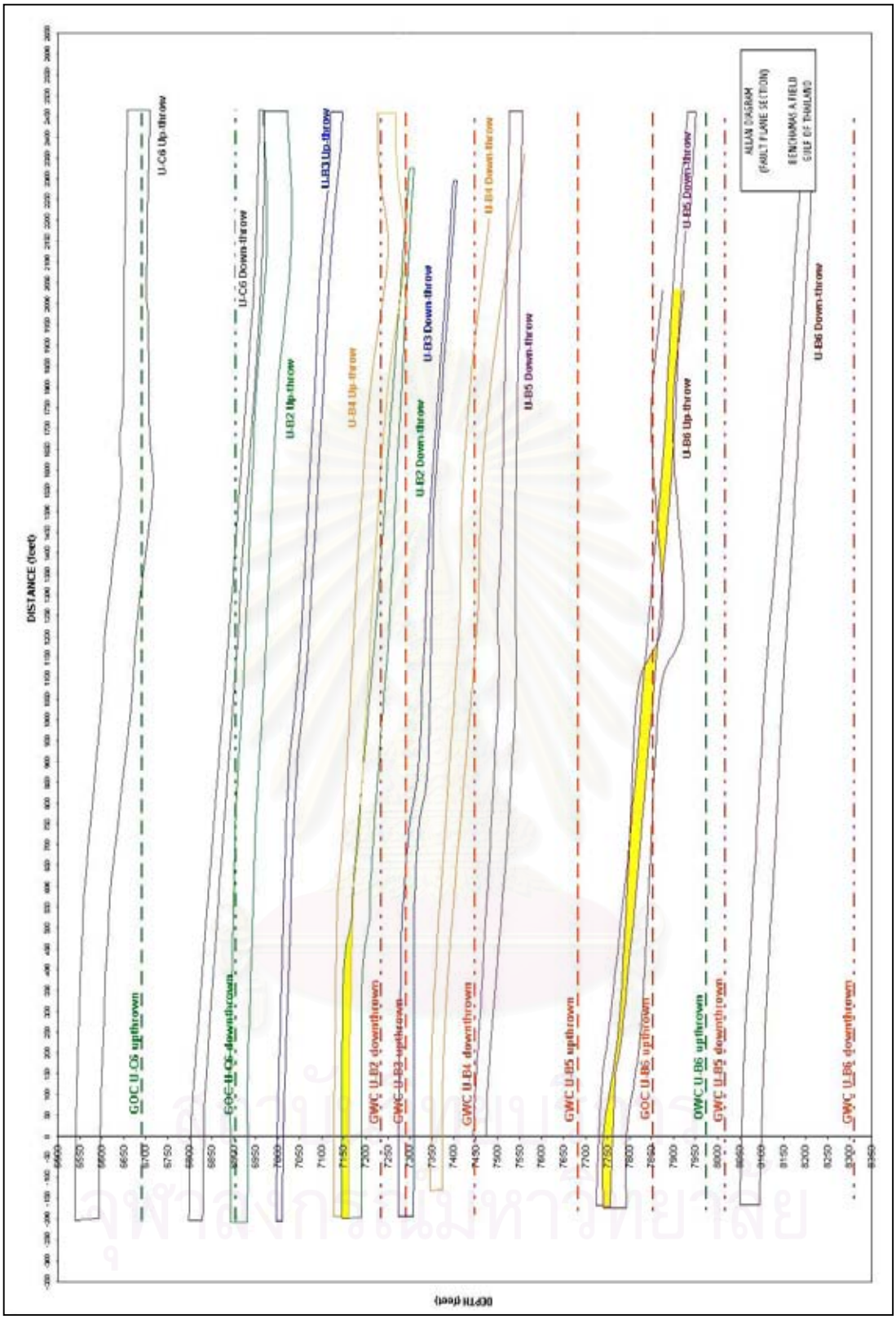

Figure 3.5 Allan fault diagram represents a potential fault sealing by observing the different hydrocarbons contact depth. Moreover, this diagram represents the overlap sand horizons between upthrown and downthrown (yellow color).

CHAPTER IV

METHODOLOGY

In this chapter, it is the methodology that using to analyze fault seal by influence of clay and shale smear on fault plane. All of the methodologies in this research referenced the methodology given by Needham et al. (1996), Yielding et al. (1997), Knipe (1997) and Freeman et al. (1998). However some systematic study in this research have to changed some step, which can be applied for these research. The work flow diagram that is used to explain the work step in this study has shown in **Figure 4.1**.

4.1 Literature review

In this chapter, it is the methodologies that using to analyze fault seal by influence of clay and shale smear on fault plane. All of the methodologies in this research referenced to the methodology given by Needham et al. (1996), Yielding et al. (1997), Knipe (1997) and Freeman et al. (1998). However for the available data in the study area, the systematic of study in this research have to changed some details, which can be apply for this study. The analytical of studying is based on the following assumptions:

1) The hanging wall stratigraphy is same as the footwall stratigraphy (Allan, 1989).
2) Each well has only one hydrostatic pressure gradient (assume a common aquifer in all reservoir zones).
3) All reservoir zones in the hanging wall are wet sand and have the same aquifer as the footwall (the same reason as the assumption no.1).
4) Where there are non-reservoirs (shale) juxtaposed against reservoirs (sands), those juxtaposed areas have sealing potential (Allan, 1989).

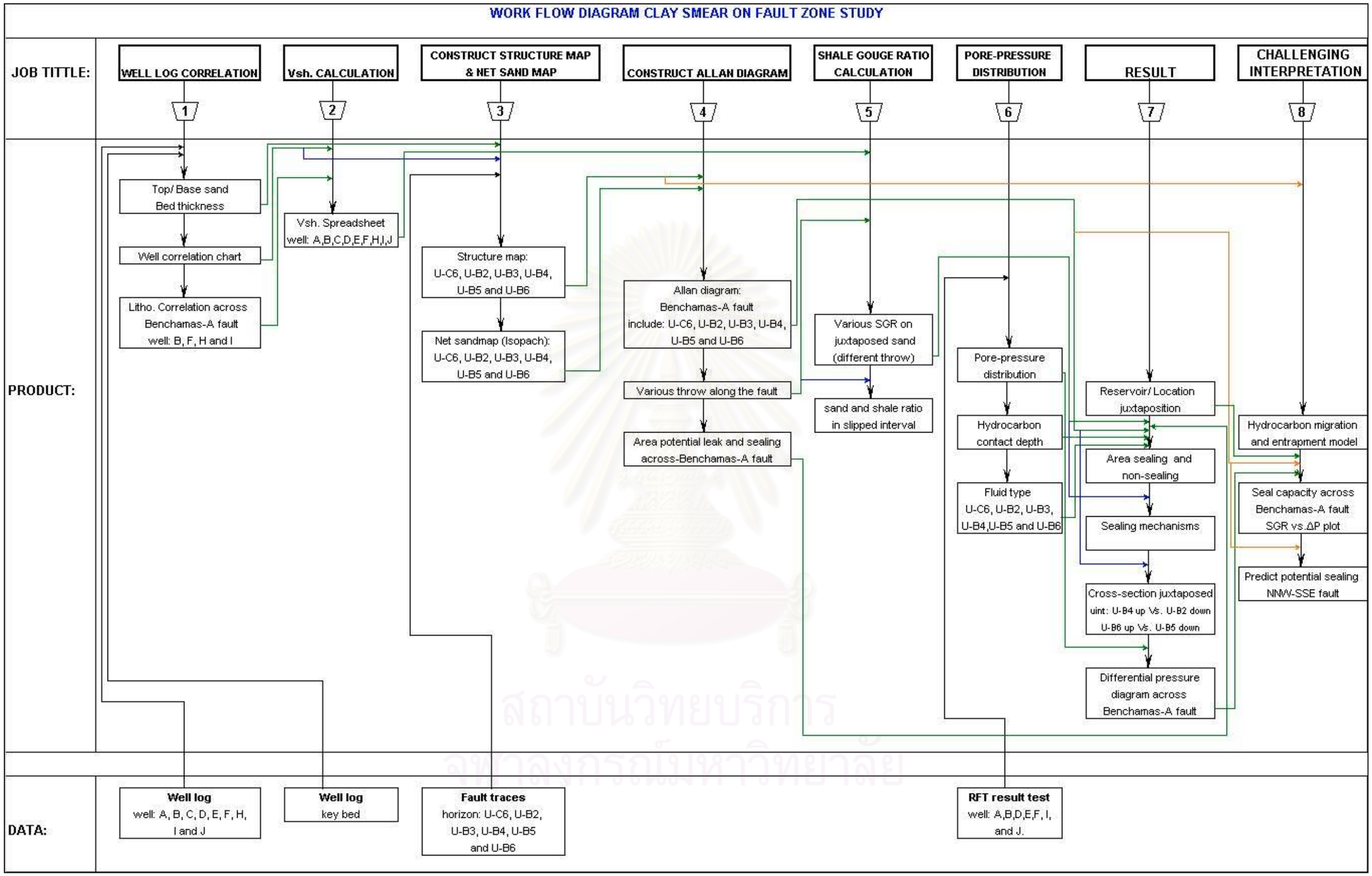

Figure 4.1 Diagram of the overview workflows for fault seal study.

The typical procedure is as follows.

1) Well log correlation. The characteristics of well log curves are used to correlate the horizon from well to well and create the stratigraphic layers model. These stratigraphic layers will give the ideal stratigraphic continuity on the fault plane that is used to analyze for calculation the shale gouge ratio in next step.

2) To calculate the shale volume (Vsh.) from well log. These shale volumes were assigned to each stratigraphic layer. Then the detail of stratigraphic layer includes; the zonal averages of Vsh. and bed thickness. The Benchamas-A fault is located was analyzed by using shale volume (Vsh.) data from well F, H, B and I. The reason to chose these wells to analyze because they are located adjacent to the Benchamas-A Fault.

3) Fault traces at 6 mapped horizons are used to construct the top depth structure map and net sand (isopach) map on each horizon.

4) The top sand depth on each structure map and the bed thickness of net sand map are used to create the Allan fault diagram (fault-plane section). In addition the grid line on the fault surface has been generate and use this grid node as a framework (grid node size 25 × 25 feet) for calculating a variety of attributes, such as fault throw along the fault, clay smear parameters and pore pressure distribution. For example, the depth difference between footwall and hanging wall for each horizon defines the fault throw at that point; these observations can be grid to give the throw distribution over the fault surface.

5) Juxtaposition analysis, the detailed mapping of the Allan fault diagram is used to define the location of potential leakage area on the fault.

6) Calculate clay smear by using the shale gouge ratio (SGR) method. Compositional data (e.g. Vsh., bed thickness, bed number) in slipped interval are used, in conjunction with the fault displacement, to calculate shale gouge ratio for estimate fault seal capacity.

7) To compare with pore pressure data. Repeat formation tester (RFT) measurements for each reservoir on both sides of the fault were input to display the pore pressure field in each fault block and across-fault pressure differences.

8) The results of fault seal study by clay smearing, have to answer the basic questions as below;

    1) Which reservoir units are juxtaposed, and where?

    2) Where on a fault surface is there seal and where is there leakage?

    3) What is the likelihood that sealed reservoir juxtaposition will support across-fault pressure difference?

    4) Which smear type is happen in fault zone?

4.2 Conceptual method

4.2.1 Log correlation

Data from 9 wells are available to correlate the horizon from well to well. The depth on each horizon is evaluated by using the gamma ray log that recorded in the well of study area. The characteristic relationship between gamma ray curves of each well in the same fault block, they showed the same continuous of pattern. Ligo, L. (personal communication, February 27, 2002) mentioned the typically characteristic of pattern that used for correlated gamma ray log, it is the strongheaded curve of gamma ray or “hot shale” which recorded in the zone of high thickness shale (massive shale). The cause of using shale beds for correlation the horizon is because the characteristic of depositional of fine grain (Shale and Clay) when, they were deposited in the low energy region the formed bed was appearances in lateral (horizon) continuity. The characteristics that had mention can be observed in the section between 6850 to 6910 feet and 8830 to 8895 feet (in well F, E, D, H, A, J, B, I, C) and all of them is helpful to correlate the lithology continuity on each horizon. But not of all the well

log data give the same characteristics; some well cannot be detected hot shale bed. Therefore the other techniques have to apply such as correlate by the thickness of bed, seismic cross section or sometime RFT were applied to check the same hydrostatic region.

4.2.2 Volume of shale calculation

For gathering clay-volume (Vsh) data, Petrophysical analysis of well data is used to define the clay or shale fraction in each stratigraphic unit.

Shale content, or volume of shale, is an important quantitative result of log analysis. Several methods can be used, depending on the logs available. Shale can be distributed in several different ways, as shown in **Figure 4.2**

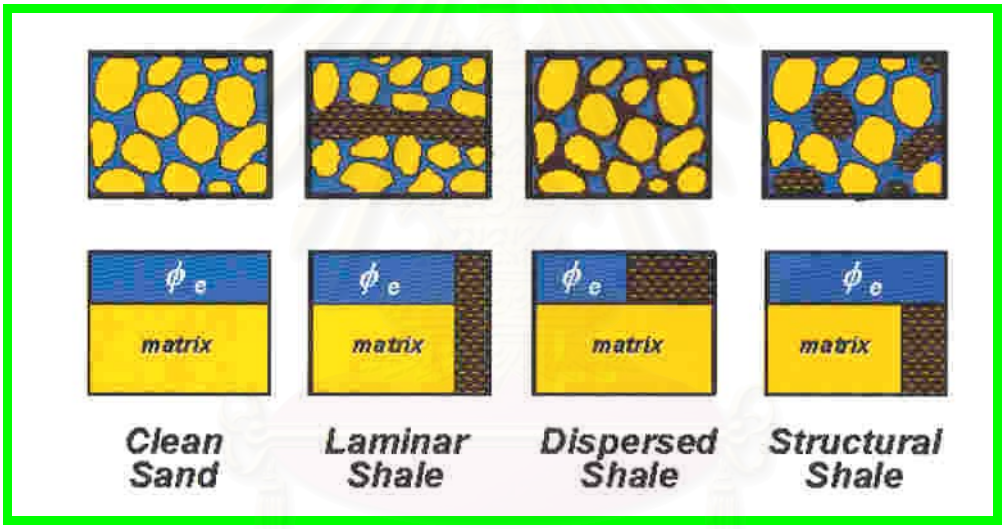

Figure 4.2 Shale matrix show, how shale is distributed in shaly sand (Crain, 2000).

The common shale indicating logs are the gamma ray (GR) that used in this research. The units of measurement for GR are API units or counts per second.

Estimation of shale content is done by observation of the gamma ray log with respect to the clean line (GR_{min}) and the shale base line (GR_{max}) (both values, they are the first order to calculate Vsh., when the minimum and maximum log readings is a linear interpolation). The base lines for the GR are shown in Figure 3.3 The shale base line for the gamma ray log may alter

with whole depth due to changes in logging instrumentation, hole size, mud properties, and varying shale character. Therefore, the shale base line should be chosen specifically in the shale immediately below the formation of interest. However, the clean line have been chosen quite some distance from the zone of interest if no clean sands may be nearby. If the well does not penetrate shale below the zone of interest, the shale base line must be chosen from the nearest shale above the zone. However shale properties may need to be adjusted by comparing shale volume calculated from logs with core description, thin section point count data, X-ray diffraction data, or scanning electron microscope data, the reason is too closely to get the result the best assumption of shale volume.

Shale volume from the gamma ray

The response equation for the gamma ray log follows the classical form:

$$
\begin{aligned}
GR = {} & PHIe * Sxo * GRw && \text{(water term)} \\
& + PHIe * (1 - Sxo) * GRh && \text{(hydrocarbon term)} \\
& + Vsh * GRsh && \text{(shale term)} \\
& + (1 - Vsh - PHIe) * Sum\,(Vi * GRi) && \text{(matrix term)}
\end{aligned}
\qquad \text{(Eq-4.1)}
$$

Where: GRh = log reading in 100% hydrocarbon

GRi = log reading in 100% of the component of matrix rock

GR = log reading

GRsh = log reading in 100% shale

GRw = log reading in 100% water

PHIe = effective porosity (fractional)

Sxo = water saturation in invaded zone (fractional)

Vi = volume of the component of matrix rock

Vsh = volume of shale (fractional

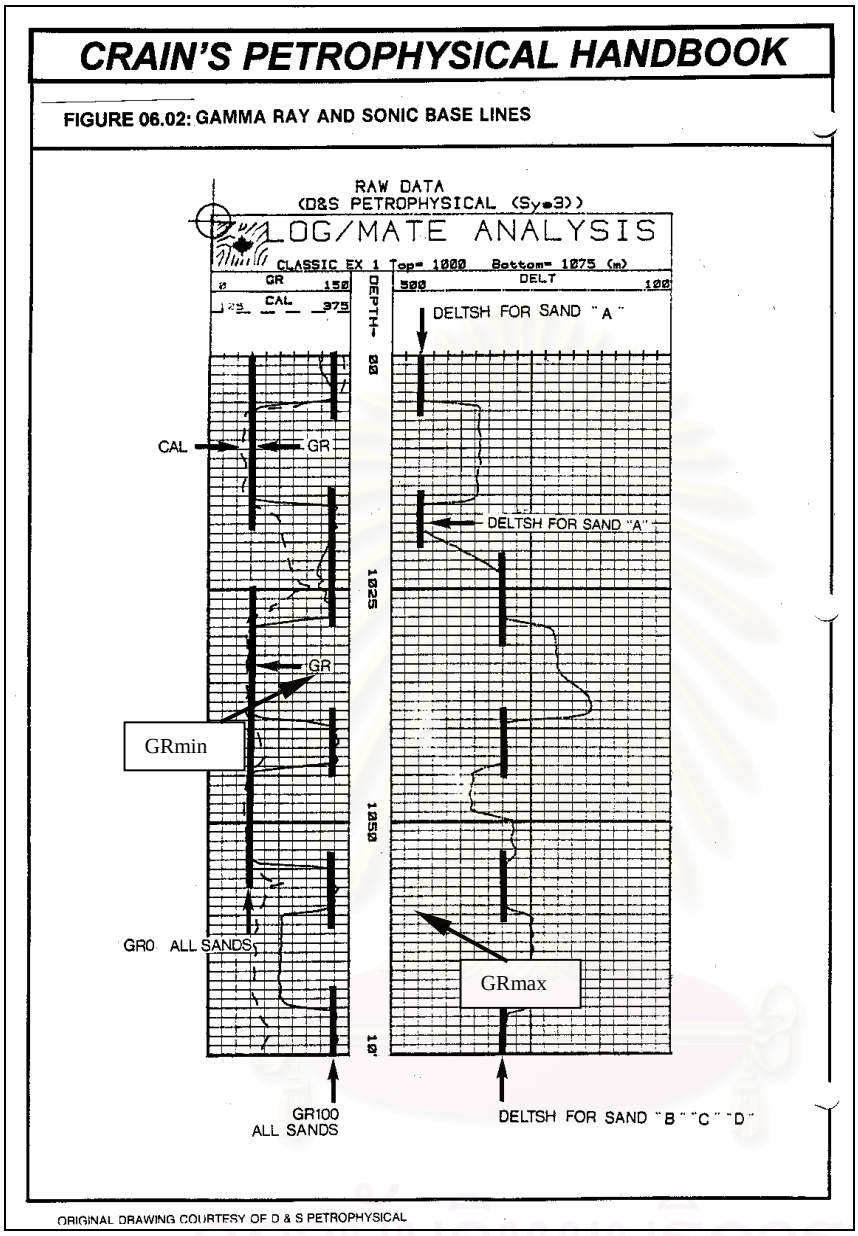

Figure 4.3 The gamma ray log with respect to the clean line (GR_{min}) and the shale base line (GR_{max}) (Crain, 2000).

Both GRw and GRh are zero. GRi is equal to the background radiation in non-shaly rock and is called GR_{min}. GRsh is the log reading in shale, called GR_{max}. The effect of porosity is very small, so that term also is assumed to be zero. The response equation thus reduces to:

$$GR = Vsh * GR_{max} + (1 - Vsh) * GR_{min} \qquad \text{(Eq-4.2)}$$

When solved for Vsh, equation 2 becomes:

$$Vshg = (GR - GR_{min}) / (GR_{max} - GR_{min}) \qquad \text{(Eq-4.3)}$$

In the study area, the gamma ray is not a linear prediction of shale volume. Then the shale volume calculation has to modify the linearly derived shale volume to obtain a more satisfying answer. The better method is **"Schlumberger Clavier equation for Tertiary sediments"** have been applied to calculate shale volume that can give more accuracy of shale volume in this area. When compared; the nonlinear values (shale volume) is more closely approximate the shale content described in the cutting samples, conventional cores and sidewall cores. Then the second order shale volume has been applied in equation (Eq-4.4)

$$Vshc = 0.083\,3\,(2^{(3.73Vshg)} - 1) \qquad \text{(Eq-4.4)}$$

Where:

Vshg = shale content from GR or SP (fractional)

Vshc = shale content corrected for non-linear effects (fractional)

4.2.3 Top depth structure map and net sand (isopach) map

To construct the structure map and net sand map in this section, have to understand the subsurface topography across the fault and use them to construct the Allan fault diagram. Furthermore the structure map can be applied to investigate the migration pathway and accumulation area of hydrocarbon in each horizon.

Top depth structure map: The fault trace lines (**Figure 4.4**) are the boundary that is used to control and limit the contour lines. The top sand depth (**Table 5.1**) in each horizon is the factors to generate the contour interval and distribution of contour on map.

Net sand (isopach) map: This process have the same methods to construct the structure map, which is using the same fault trace line and structure map in each horizon to control and limit the contour lines. In addition, the net sand thickness is used to generate the contour interval and contour distribution on map. The net sand map in this process is the isopach map that was measured only the thickness of sand reservoir (Vshale cut off < 35%).

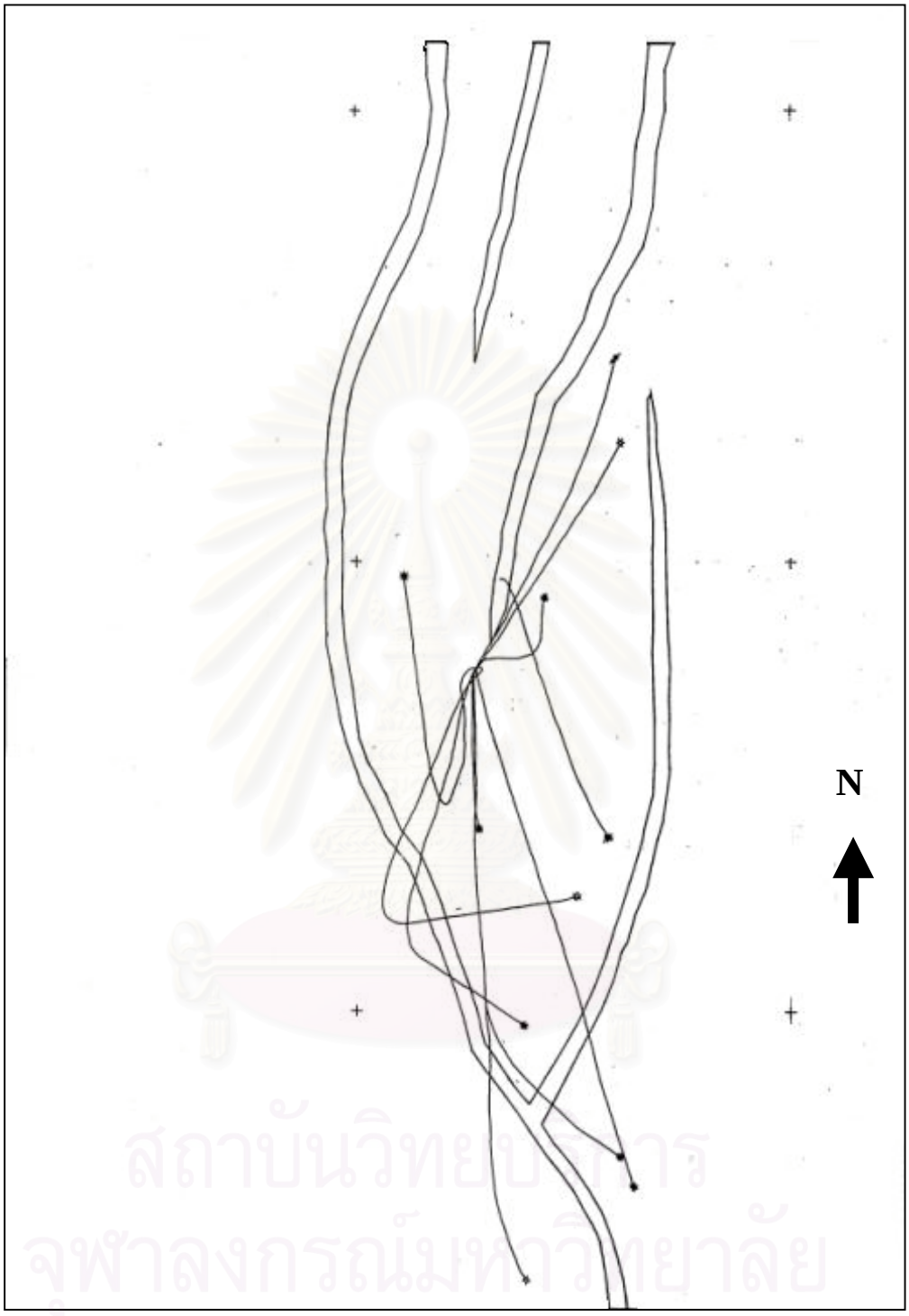

Figure 4.4 Example Fault trace line and the top sand in depth located on the well pathways on horizon. (modified from ChevronTexaco, 2002).

4.2.4 Fault-plane-section analysis (Allan fault diagram)

In this study, the analytical technique of fault-plane-section analysis have been used the Allan fault diagram analysis to approach and identify fault traps and probable permeability pathways along fault study. Fault-plane sections allow for quick identification of lithological and fluid juxtaposition across a fault (Allan, 1989). As defined by Allan (1989), a fault-plane section is " A display of the geometry of stratigraphy brought into contact by fault displacement, i.e., two side of a fault juxtaposed". (Also termed "fault section" or " fault surface section"). The plane of the section is not vertical, as in normal cross-section, but is the plane of the fault.

This fault plane was generated by assume "a fault would be a smooth surface passing through the foot-wall and hanging-wall cutoffs mapped on each horizon" (Yielding et al., 1999). The critical parameters to generate a fault-plane section in this part include structure, closure style, fault geometries and stratigraphic geometry. The need of the best structure map and stratigraphic correlation between wells in the area study are the importance factor. Better maps generate better fault-plane sections. Stratigraphic geometry is often the most difficult parameter to derive and often must be extrapolated over long distance and estimated from depositional models derived from seismic and subsurface data. Stratigraphic geometry is the thickness and distribution of permeable and impermeable units.

In this research was investigated the trapping potential of fault by virtue of stratigraphic juxtaposition. Six of the top depth reservoir structure and net sand maps including six horizons of, U-C6, U-B2, U-B3, U-B4, U-B5 and U-B6 were used to created the fault-plane section and stratigraphic units (reservoir zonations). The top depth structure contours on each horizon represented as the top sand wherever this contour line was cutoff by fault trace at any depth, it is the position of stratigraphic unit on the fault-plane section in depth as show in **Figure 4.4** and the sand thickness from net sand maps were projected from the top sand, it was represented the thickness of the sand horizon unit along a fault.

The ideal to analyses fault plane section is based on the following simple assumption (Allan, 1989):

1. Fault itself has no sealing properties.
2. Fault is not an open conduit.
3. Trapping and migration relationships a fault based on the fault juxtaposed stratigraphy.

The assumptions that cause of sealing fault or non-sealing fault in this research can be classified as follow the **Table 4.1**.

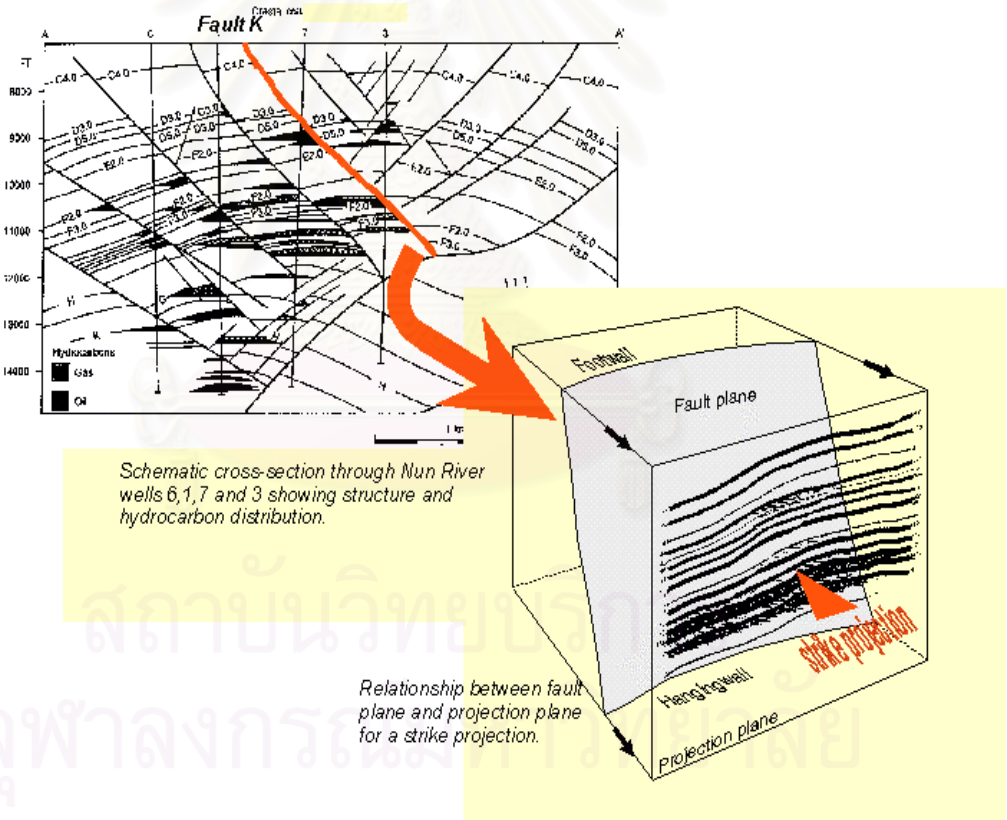

Figure 4.5 Example of fault-plane section; the ideal to generate fault plane by using horizon fault intersection line is projected onto the fault surface along trajectories to the plane (Yielding et al., 1997).

Table 4.1 Classification the potential sealing fault on fault-plane section.

Classification	Seal	Non-seal
1. Impermeable bed juxtaposed against permeable bed	Yes	No
2. Permeable bed against permeable bed	Yes	Yes
3. Difference fluid between sand on sand juxtaposition	Yes	Yes
4. Same fluid between sand on sand juxtaposition	Yes	Yes
5. Same fluid and same hydrocarbon level contact between sand on sand juxtaposition (GOC, GWC, OWC)	No	Yes
6. Same fluid but difference hydrocarbon level contact between sand on sand juxtaposition	Yes	No
7. Difference pore-pressure distribution sand on sand juxtaposition	Yes	No

Note: GOC = gas oil contact; GWC = gas water contact; OWC = oil water contact.

4.2.5 Shale gouge ratio (SGR) evaluation

The algorithm for predicting clay smear prediction in this research is the shale gouge ratio (SGR), it was defined in publications by Yielding et al. (1997) and Freeman et al. (1998). The shale gouge ratio is used to estimate the composition of subsurface fault zone, which is the proportion of shaly material in the fault zone.

The basic assumption in the Shale Gouge Ratio (SGR) algorithms is that the fault-gouge composition is governed by the buck composition of the wall rocks that have slipped past that point on the fault (Yielding et al. 1998). Faulting through clean sandstones generates cataclasites, whereas dragging clay beds along the fault generates clay smear. Fault seal in sand shale sequences is broadly predictable. The method is the juxtaposition pattern of the units at the fault plane. In general many traps, juxtaposition seal of shale against sand is a main component of the trap geometry, when the shale sequence thickness more

than sand sequence thickness. However, areas of sand against sand juxtaposition can also contribute to the trap because of the presence of fault rock, which impede fluid flow. Clay-rich fault rock tends to form the better seals because they contain finer-grained material and therefore have smaller pore-throats (Gibson, 1998). The first order controls on fault rock development are the lithologies (clay content) in the faulted sequence and amount of offset on the fault.

Classification of fault rocks is fundamentally based on their composition (Fisher and Knipe, 1998), and hence Shale Gouge Ratio (SGR) can be thought of as a predictor of fault-rock types for simple fault zone. Also Shale Gouge Ratio (SGR) likely is a good guide to the proportion of phyllosilicates in the fault zone material (Foxford et al., 1998). Fault rock with phyllosilicates content less than 15 to 20% are typically cataclasites or disaggergation zone, those with more than 40% phyllosilicates are clay smears, and intermediate compositions (15-40%) are sometime referred to as clay-matrix gouge (Gibson, 1998) or phyllosilicates framework fault rocks (Fisher and Knipe, 1998).

In 1992 Knipe suggested “ The mixture of phyllosilicates and framework (impure sandstone) silicates generates fault rocks where the porosity and permeability are controlled by the creations of anastomosing networks of micro-smears around framework fragments or clast. Then anastomosing zones of micro-smears may have properties similar to clay smears”. The relationship between hydraulic properties of a fault zone through a clastic sequence is strongly influenced by the proportion of phyllosilicates in the fault zone material (Gibson, 1998; Foxford et al. 1998). Then cause of hydraulic seal and non-communications of hydraulic properties between sand juxtaposed footwall and hanging wall because increased phyllosilicates contain reduces the pore-throat size and correspondingly increases the capillary pressure of the gouge.The cutoff shale gouge ratio value for this research was selected the SGR values between 15 to 20% to identify the fault sealing or leakage in the overlap

sand area between sand horizon upthrown and downthrown. SGR has been calibrated in comparisons of SGR and pressure difference for a number of data sets (Yielding et al., 1997). In general, static sealing behavior is observed when SGR is above 15-20%; higher pressure differences correlate with larger values of SGR.

The following factors control the likelihood of clay/shale smearing (Yielding at el., 1997);

1). Thicker source beds can produce thicker clay smears;

2) Shear-type smears decrease in thickness with distance from the source layer;

3) Abrasion-type smears decrease in thickness with increasing throw; and

4) Multiple source beds can give a combined continuous smear

Calculation of Shale Gouge Ratio (SGR) requires input of the shale content of the faulted section or can illustrate in **Figure 4.6**

The equation as show below:

SGR = Σ [(zone thickness) × (zone clay fraction)] / Fault throw × 100% (Eq-4.5)

Where:

Δz_n = individual thickness of rock in slipped interval.

Vsh. = volume of shale is in individual thickness.

t = throw window is the vertical slipped thickness that considered at any point on fault plane.

The various degree of shale gouge ratio in triangle diagram or Allan fault diagram grid cells, this research had been referenced the shale gouge ratio interval from manual Badleys's Triangle software and display in the same interval (e.g. 0-10%, 10-20%, 20-30%, etc.).

Color-coding for SGR (modified from Triangle software manual, 2001)

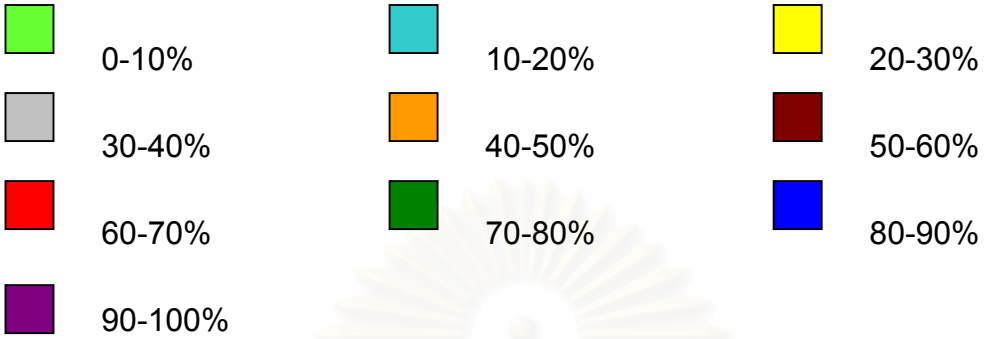

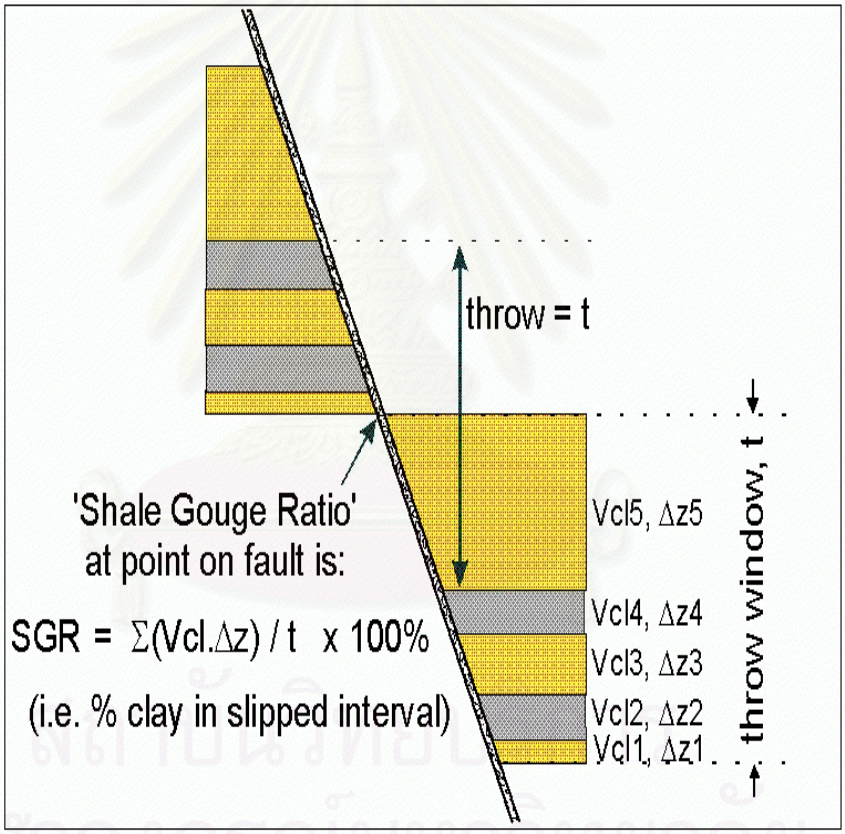

Figure 4.6 Diagram showing the definition of shale gouge ratio (SGR). For a sequence of reservoir zones with specified Vshale or Vclay (Vcl_n) and thickness (Δz_n), The SGR equals the net shale (or clay) content in the rock interval that has slipped past any point on the fault. t is the fault throw (vertical component of slip) (modified from Quantitative Fault Seal Prediction; Yielding et al., 1997).

4.2.6 Repeat formation test (RFT) evaluation

The result repeat formation test (RFT) in this section can be used the virtue of difference pore-pressure between upthrow and down throw defines the across-fault pressure difference along the fault plane (fault surface). It is assumed that within each layer in each compartment there are no pressure barriers, that is, all the changes in pressure field occur across the faults (Yielding, 1999).

The pore-pressure profile is defined by the repeat formation test data (RFT) in a well, in a fault-bound block can be used to construct the pressure field for the near side of each bounding fault to that block. This process involves tracking the pressure trend along each reservoir zone from the well to the fault using the appropriate fluid densities. The pore-pressure data can be classification fluid type and interpretation the physical properties of fluid in test zone such as fluid density, the depth of fluid contact (GOC, GWC and OWC) and how much fluid column high that can be derived from this pressure properties. By taking several pressures different depths in hydrocarbon zone. The measuring hydrocarbon pressures and the hydrocarbon is continues, the pressure is a function of depth and all pressure plotted against depth, should lie on a same straight line (difference kind of fluid, difference straight line). The pressure at any point can be derided from a law's of hydrostatic in equation (Eq-3.6) (static condition).

P = fluid density × gravitational const. × height of fluid column (Eq-4.6)

And when consider through continuous fluid column

$$P_Z = P_{in} + [\rho_{\text{of fluid}} \cdot g \cdot (Z - Z_{in})] \quad \text{(Eq-4.7) or}$$

$$P_Z = P_{in} + [\text{Grad.}_{\text{of fluid}} \cdot (Z - Z_{in})] \qquad \text{(Eq-4.8)}$$

Where Z_{in} = initial depth

Z = consider pressure at any depth

P_Z = pressure at depth Z

P_{in} = pressure at depth Z_{in}

$\rho_{\text{of fluid}}$ = density of fluid

g = gravitational const.

$\text{Grad.}_{\text{of fluid}}$ = gradient of fluid ($\rho_{\text{of fluid}} \cdot g$)

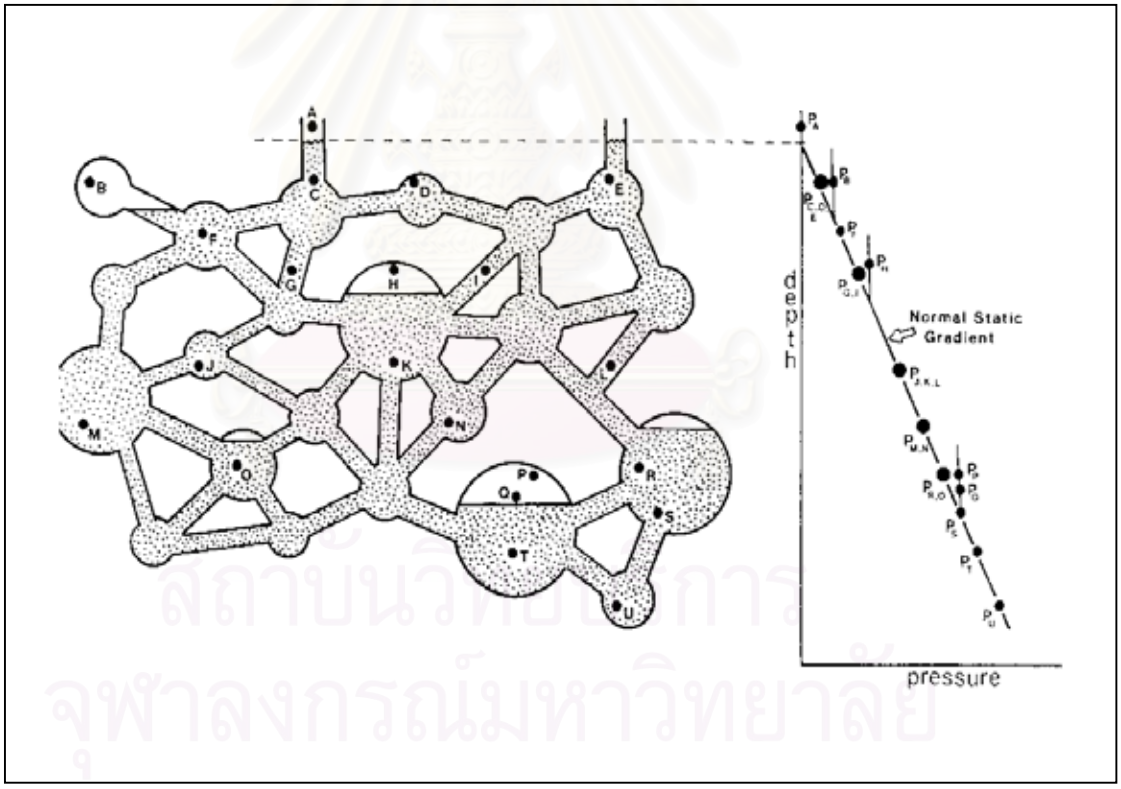

Figure 4.7 Pressure-depth relationships within a single fluid network. The top of the water column for system is in contact with the atmosphere (Dahlberg, 1994).

Pressures from locations at various depths in the system (**Figure 4.7**) are plotted on the graph at the right. All pressures in the fluid lie along the same line, which represents the normal static gradient for the system. Pressure in the confined gas portions of the system plot on the high side of the normal static gradient, since the gas is compressed by water pressure to an a mount proportional to the relative depth below the surface of gas-water interface. Such as, the pressure in gas body P, Q (which is the deepest in the system) is greater than point H, and B.

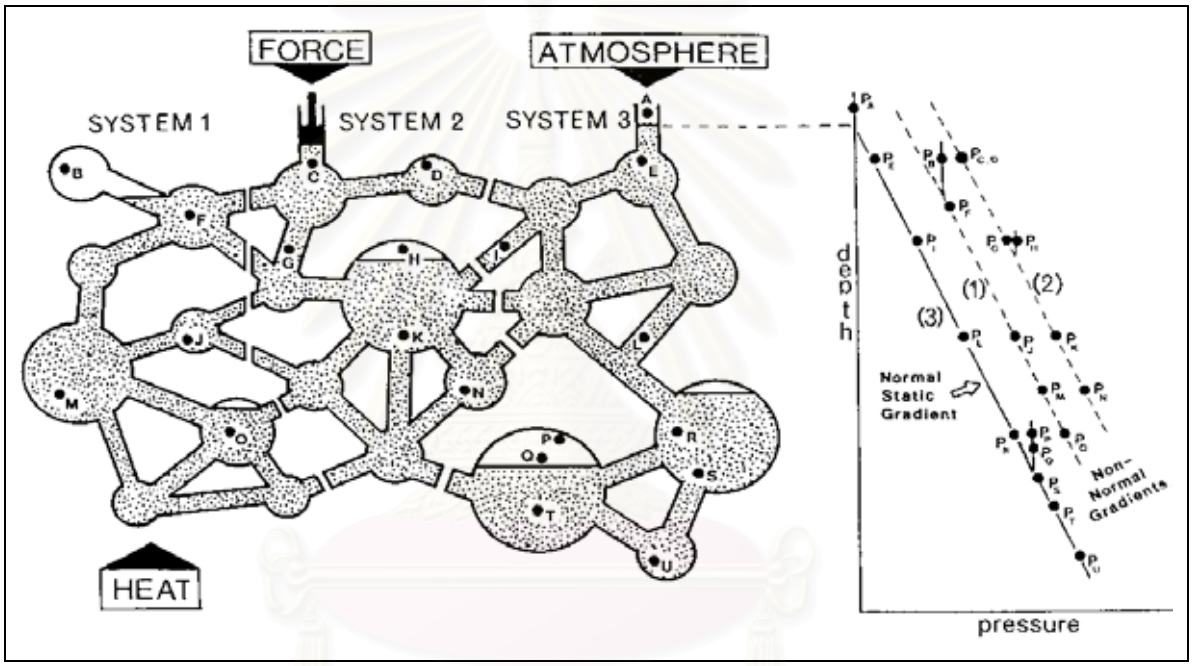

Figure 4.8 Pressure-depth relationships when original single network system is subdivided into three separate, isolated systems with the fluids acted on by different external influences (Dahlberg, 1994).

Figure 4.8 shows the system in **Figure 4.7** has been rearranged into three-separated system (in geology e.g. fault, barrier flow). System 1 is confined are exposed to heat, which raises the internal fluid pressure significantly. When the pressure reference points are plotted on the pressure-depth graph, the line

along which they lie reflects an elevated gradient for this system. The system 2, independent of the others, is under compression from the small piston located above point C, the proportional elevation in pressure at all locations within the system refer to Pascal's principal is reflected in the gradient, which is displaced significantly to the right of normal static gradient. And system 3, the system is the same original, as the normal static pressure. Then the fluid system and network can be applied to the pore fluids in rock.

Analysis and interpretation of RFT log data

A set of pressure-depth data from one RFT run has been record in Excel file for plotting in graph pressure-depth and analyze. The principal, pressure and depth both have the relationship in linear equation. Then when plotted data should lie on a same straight line. The pressure data from RFT log that using for analyzing is the shut-in pressure as showed in **Figure 4.9**.

The assumptions to analyze RFT data:

1. Each well has only one hydrostatic pressure gradient (hydrostatic normal pressure in all reservoirs).

2. All reservoir zones in hanging wall are water wet and have the same aquifer as the footwall.

3. The pressure is a function of depth and all pressure plotted against depth, should lie on a same straight line.

4. Each layer in each compartment there are no pressure barriers, that is, all the changes in pressure field occur across the faults (Yielding, 1999).

Data interpretation

1. In pressure-depth graph, each (1/slope) value is represented kind of fluid gradient.
2. The intersection point between two slope line is represented the transition zone or depth difference fluid contact in the system.

3. The continuous RFT data on a same straight line between well to well is represented reservoir continuity.

Table 4.2 Relationships among specific gravity, API gravity, hydrostatic pressure gradient (psi/ft), and total dissolved solids for brines (Dahlberg, 1994).

Specific gravity	API gravity	Hydrostatic pressure gradient	Total solids (ppm)
2.50	-7.5	1.083	210,000
2.00	-5.2	0.866	175,800
1.50	-2.7	0.650	143,500
1.25	3.0	0.541	69,500
1.20	10.0	0.520	0
1.14 (brines and heavy oils)	17.0	0.494	
1.12	25.0	0.485	
1.10	35.0	0.476	
1.05	45.0	0.455	
1 (fresh water)	60.0	0.433	
0.95		0.411	
0.90		0.390	
0.85 (light oil)		0.368	
0.80		0.346	
0.70		0.303	
0.55		0.238	
0.50		0.216	
0.40 (gas)		0.130	
0.20		0.086	
0.15		0.065	
0.10		0.043	

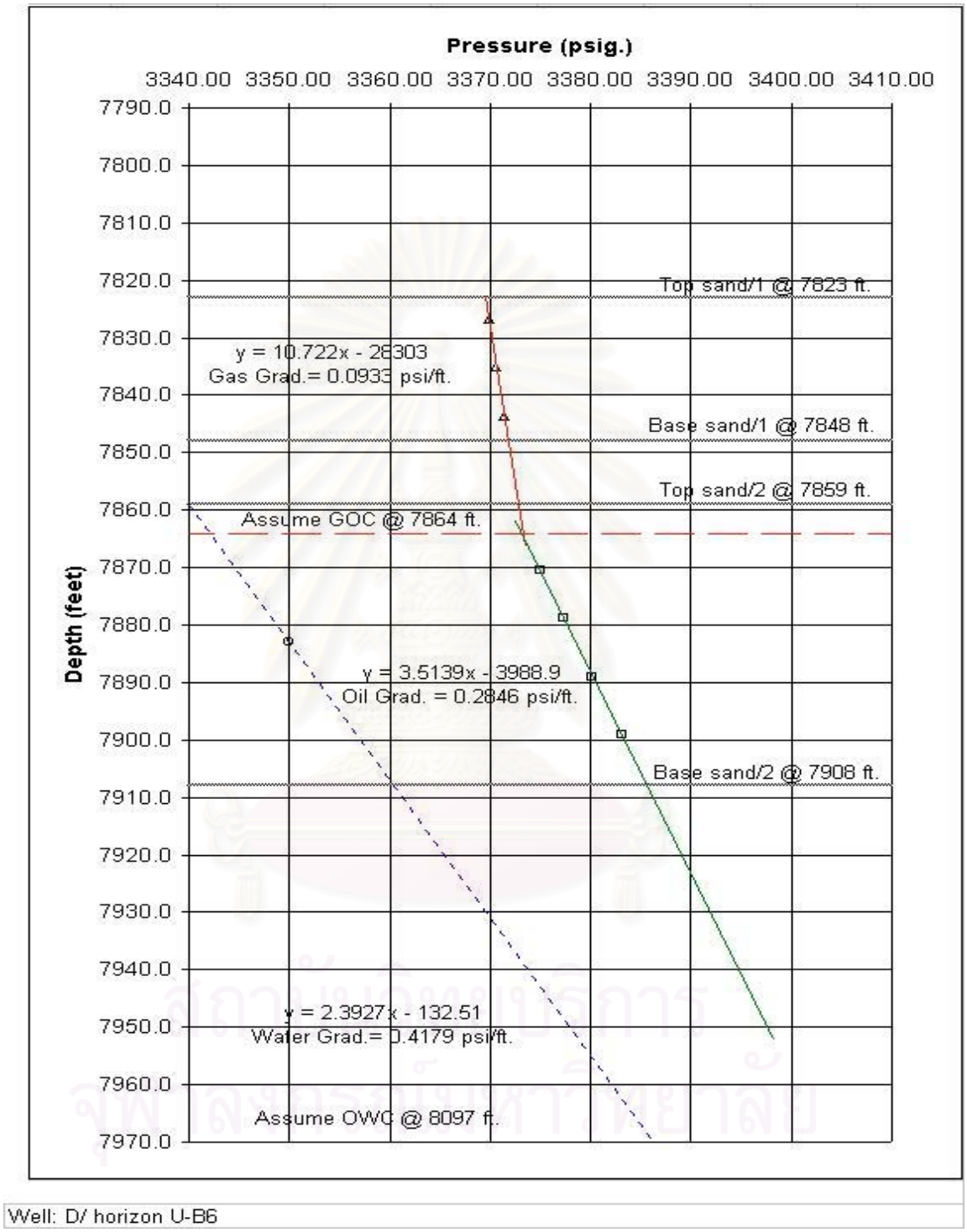

Figure 4.9 Example RFT data plotted in pressure-depth diagram. The gradient lines represent the different type of fluid in the same pay sand of well D in the Benchamas-A field.

4.3 Workflow

This section, the steps are used to analyze fault seal had been explain in logic diagram as show below:

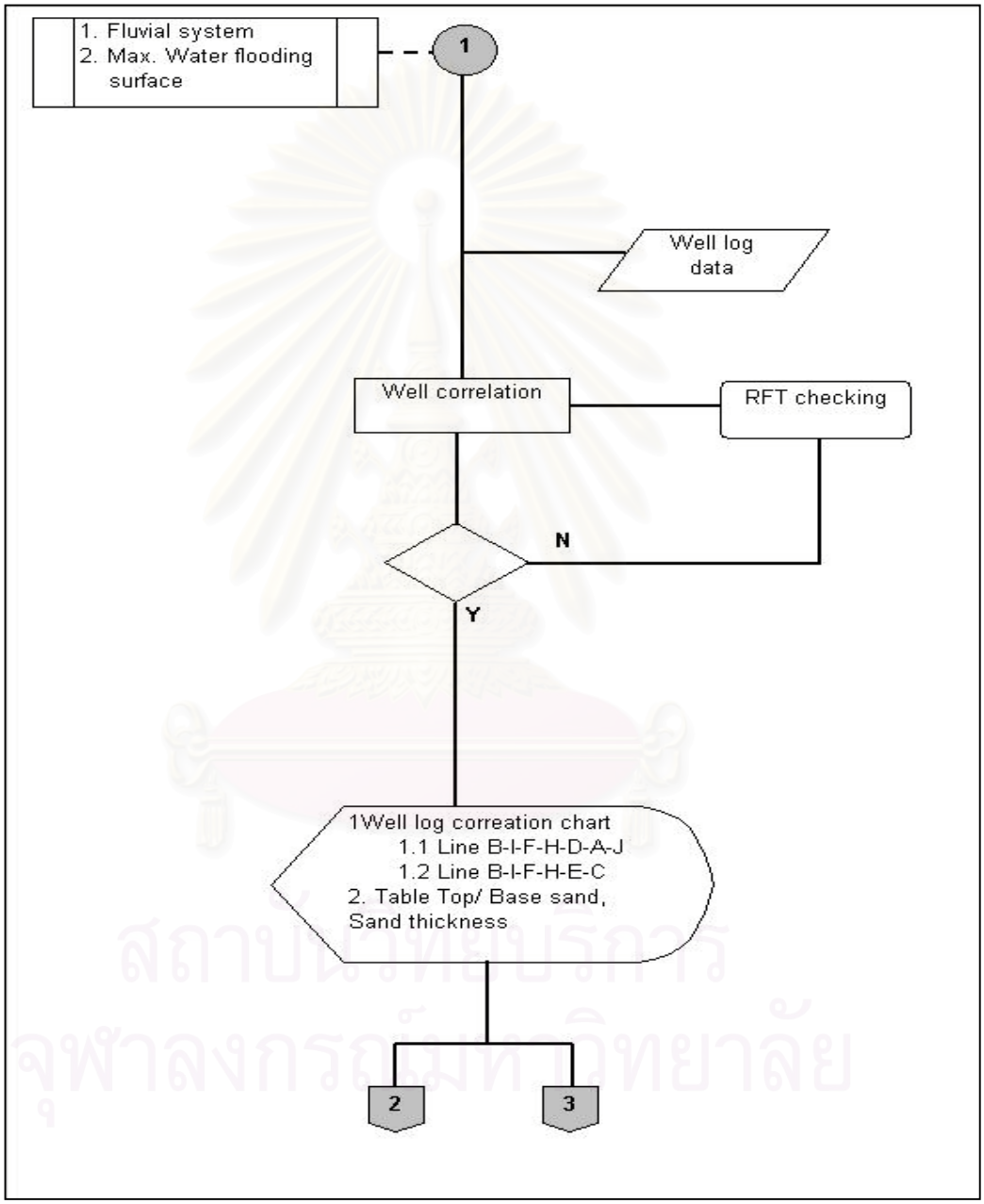

Figure 4.10 Chart illustrates workflow for the well correlation.

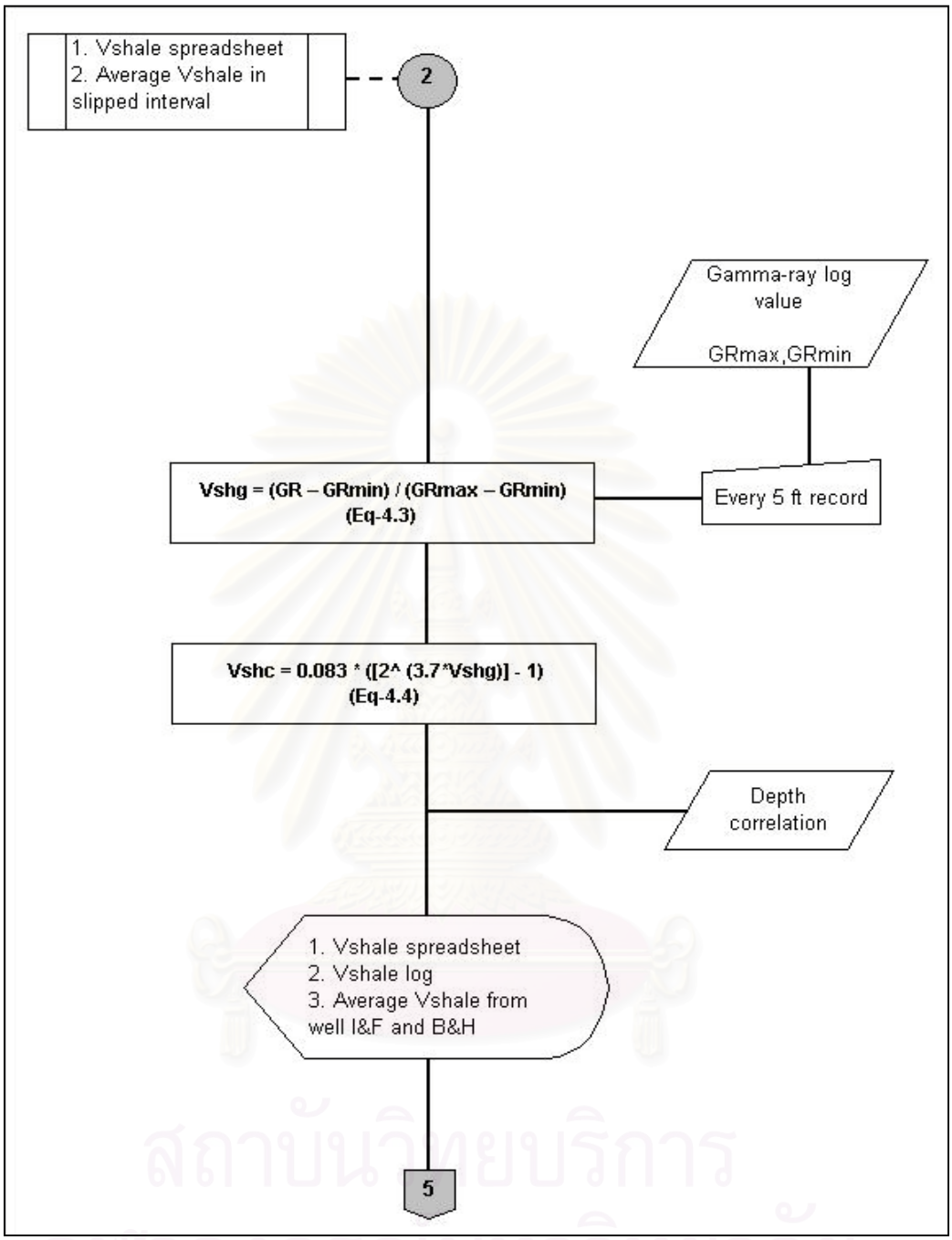

Figure 4.11 Chart illustrates workflow for the shale volume calculation.

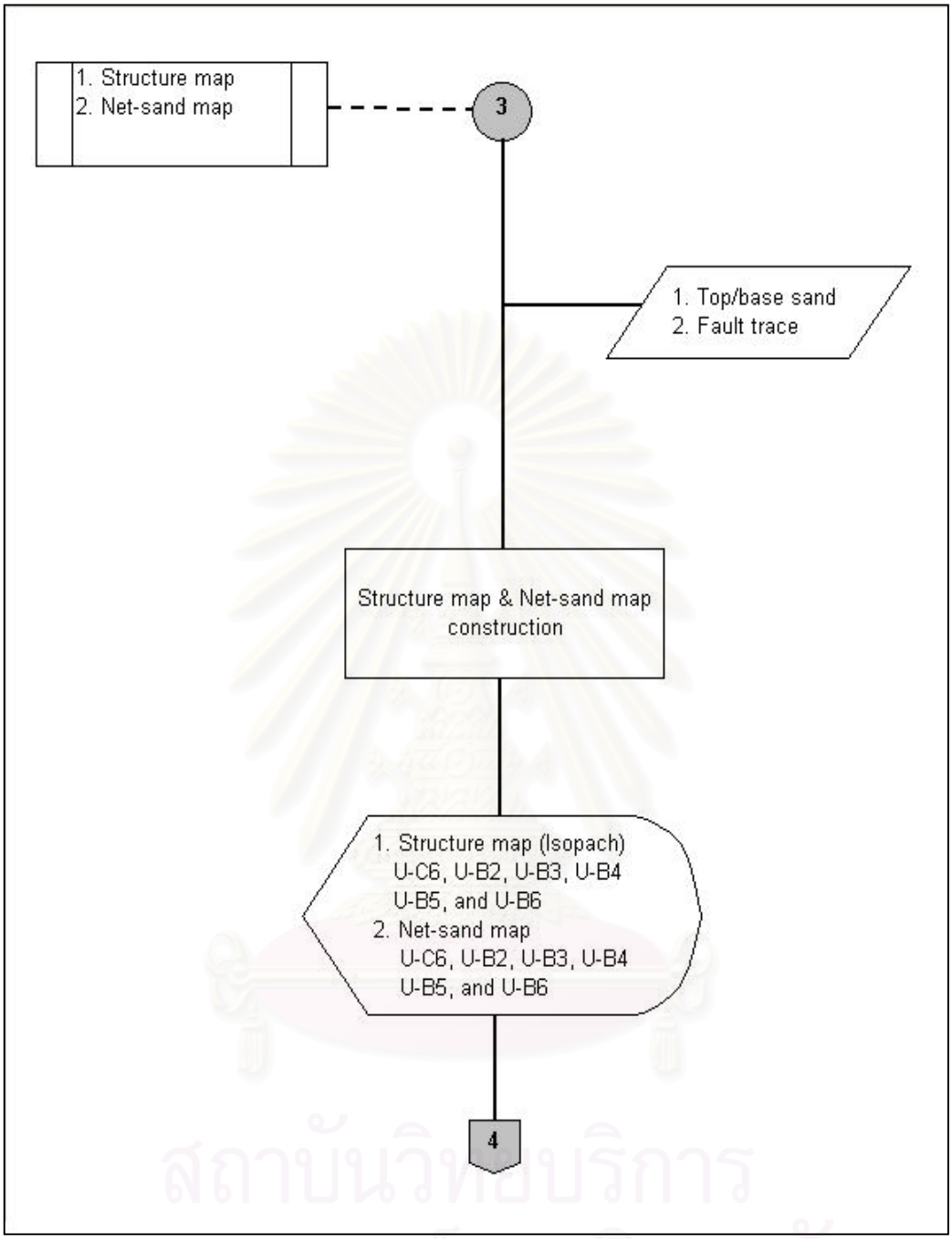

Figure 4.12 Chart illustrates workflow for top the depth structure map and net-sand map construction.

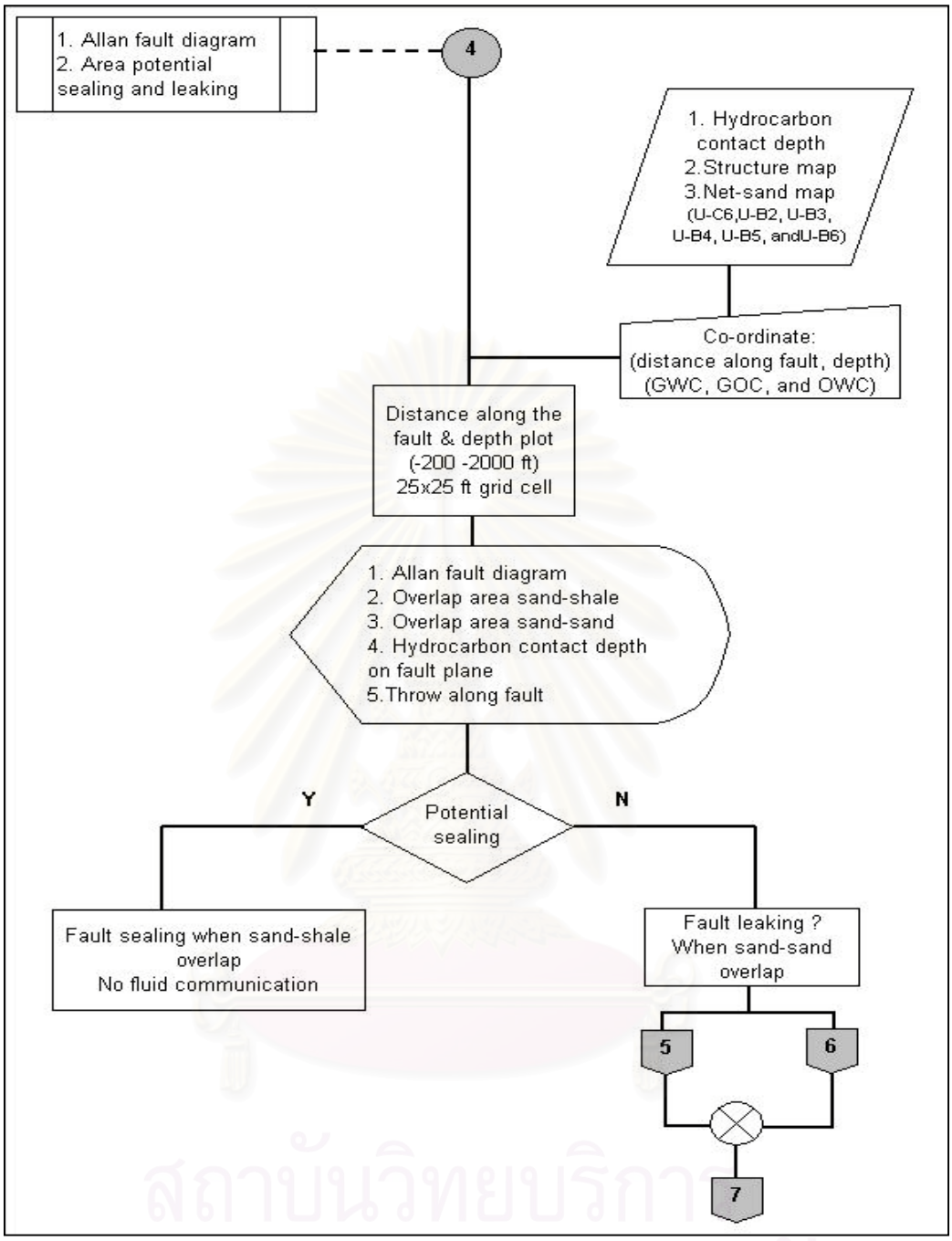

Figure 4.13 Chart illustrates workflow for the fault-plane-section (Allan fault diagram) construction.

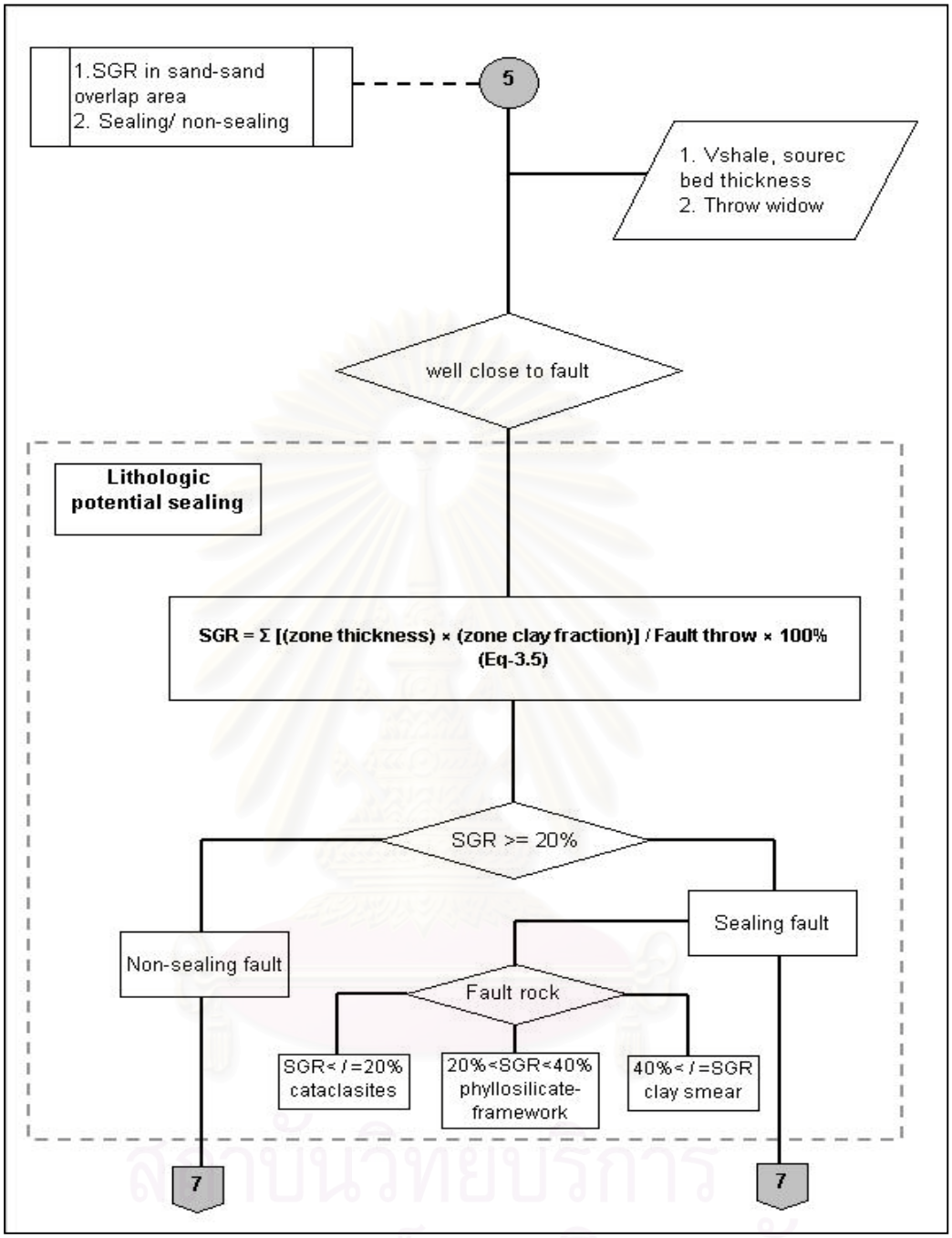

Figure 4.14 Chart illustrates workflow for the shale gouge ratio (SGR) calculation.

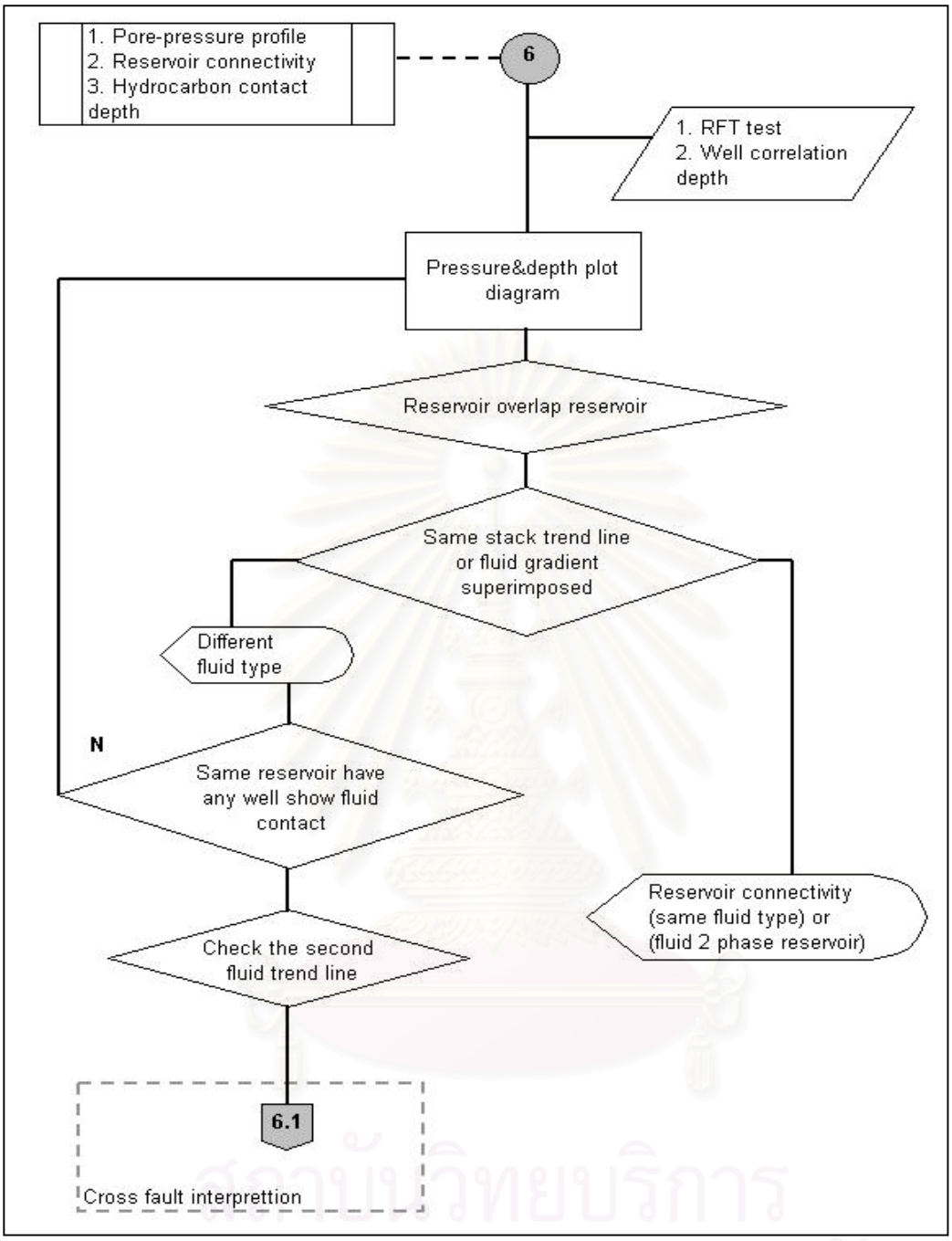

Figure 4.15 Chart illustrates workflow for the pore-pressure profile.

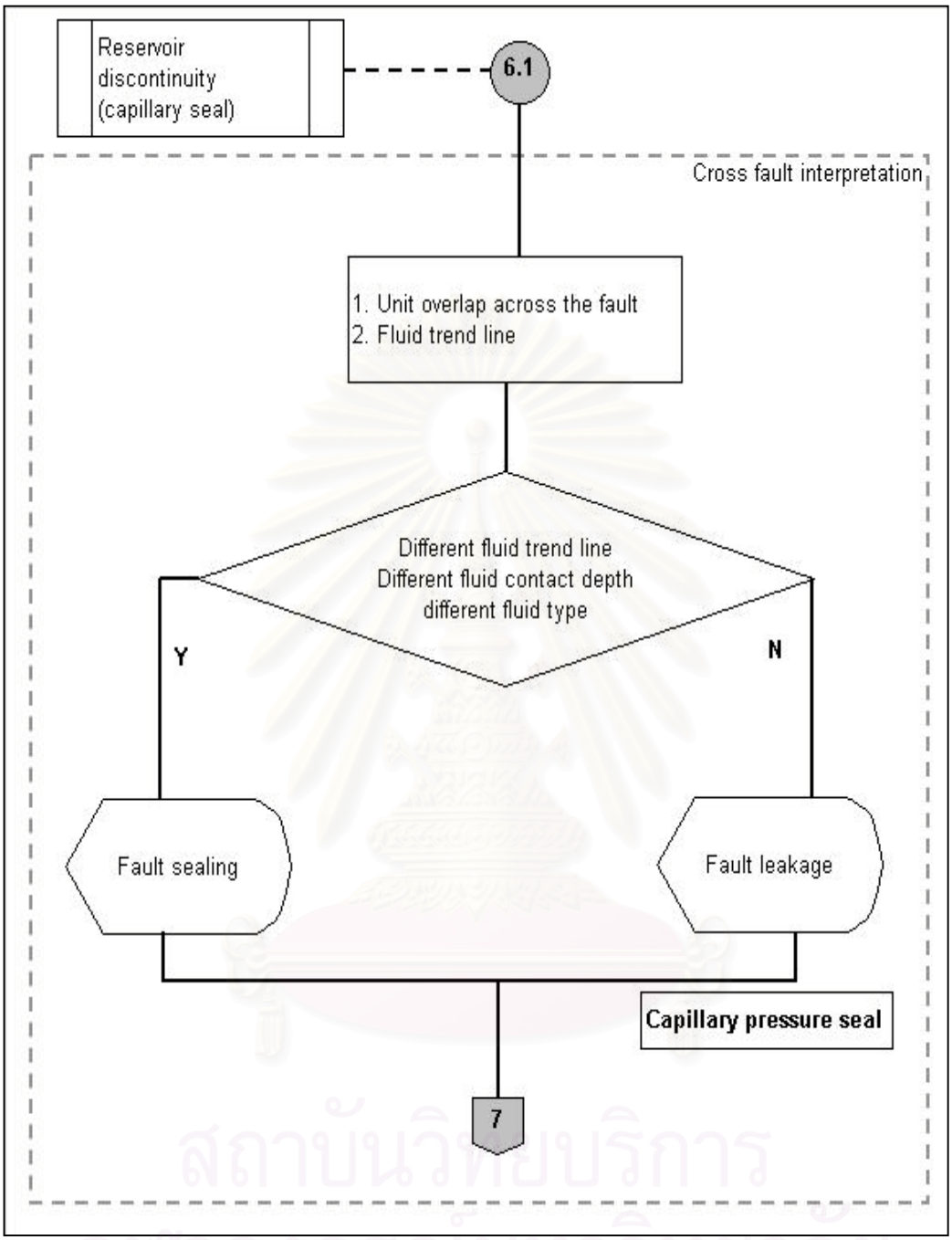

Figure 4.15 (continue).

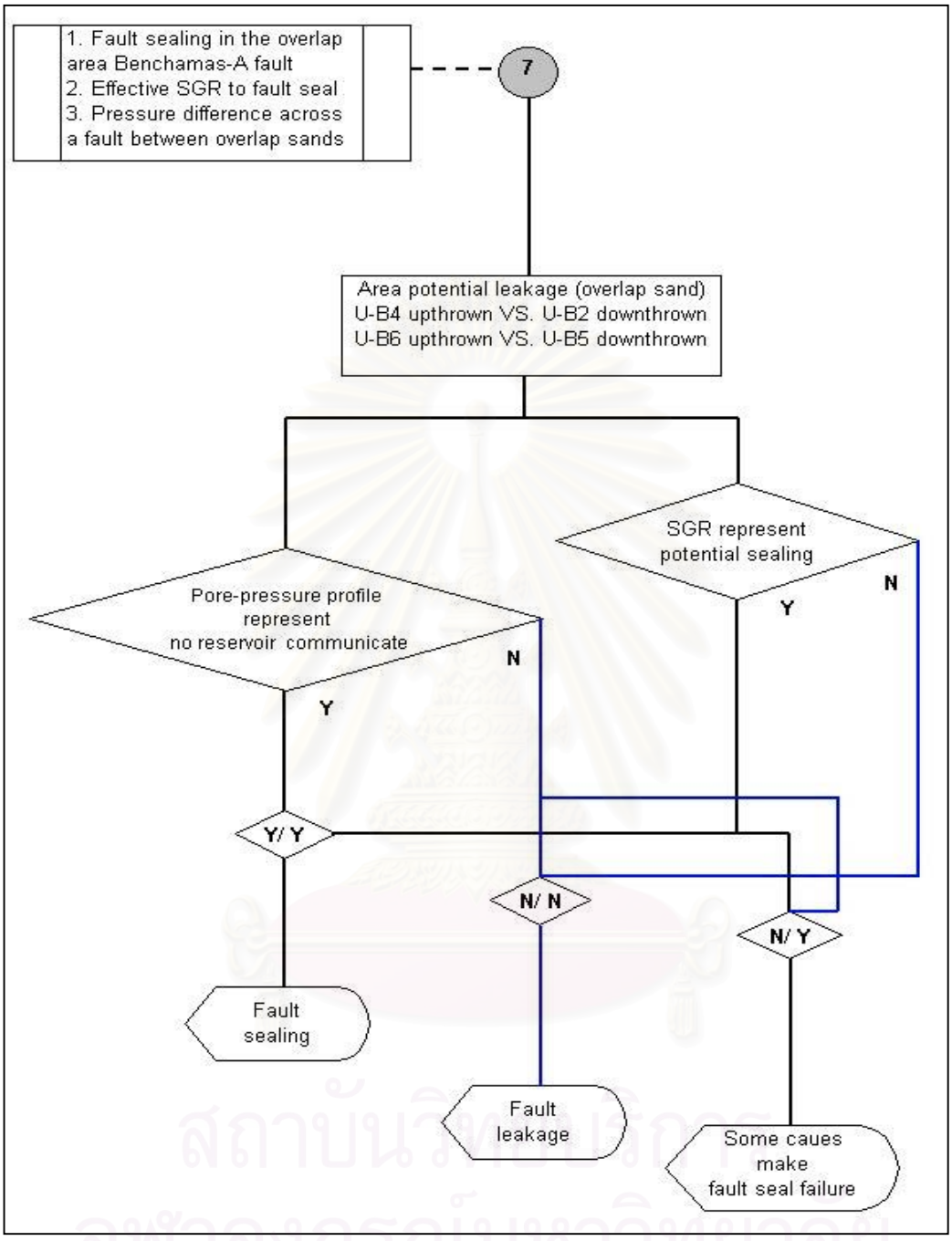

Figure 4.16 Chart illustrates workflow for the results interpretation.

CHAPTER V

RESULTS

This section concluded the results of data analysis, which divided into 10 parts. The analysis of each part had used the methodology and interpretation that had been mention in the chapter 4.

5.1 Well log correlation

The total 9 geophysical log data from 9 drill holes in the Benchamas-A field have employed to correlate lithology from well to well. The 3 main horizons in a descending order, as U-C, U-B and U-A are presented in well log. The individual characteristics in each horizon were used to correlate rock horizons through Benchamas-A field. The log patterns and characteristics of six sand horizons namely U-C6, U-B2, U-B3, U-B4, U-B5 and U-B6 presented the blocky log pattern and occasional fining-upward profile that represent the fluvial channel system. The top and base sand horizons are used to study presented in **Table 5.1** and well log correlation **Figures 5.1** and **5.2**.

5.2 Volume of shale

The results of shale volume calculation have presented in log column of shale volume with gamma-ray log (**Figure 5.1** and **5.2**) (see shale volume result in appendix A: shale volume spreadsheet). Shale volumes in reservoir vary from 0 to 35%. Every reservoirs are presented high shale volume contents because in some sand bed interbedded with shale. Shale beds are generally 40 to 80 ft thick and high thickness shale beds present in the transgressive sequences, it is located between horizon U-B5 and U-B6. This shale beds vary in thickness from 110 to 310 ft. They appear laterally cover the area of Benchamas-A field (**Figure 5.1**). The comparative sand to shale ratio in each main horizon were presented in **Table 5.2**, shale beds are the

predominance of the rock sequences in every main horizons. Shale beds appear about of 76 to 83% of gross thickness in each horizon.

Table 5.1 Top and base of the reservoir sand horizon in the Benchamas-A field.

(TVDSS) feet.	Well B		Well I		Well F		Well H		Well D		Well E		Well C		Well A		Well J	
Horizon name	Top	Base	Top	Base	Top	Base	Top	Base	Top	Base	Top	Base	Top	Base	Top	Base	Top	Base
U-C6	6919	6960	6808	6877	6557	6632	6642	6739	6704	6790	6701	6800	6642	6742	6754	6831	5753	6860
U-B1	7168	7176	7080	7103	6801	6825	6885	6914	-	-	6925	6936	6870	6891	6925	6956	-	-
U-B2	7246	7275	7168	7213	6905	6954	6976	7055	7047	7110	7020	7085	6977	7020	7068	7145	7158	7197
U-B3	7346	7358	7282	7313	7023	7053	7127	7151	7165	7192	7139	7165	7140	7177	7197	7217	7259	7285
U-B4	7421	7459	7369	7400	7135	7173	7227	7271	7276	7308	7239	7268	7205	7234	7293	7329	7382	7420
U-B5	7877	7898	7739	7769	7450	7474	7530	7536	7546	7583	7505	7548	7490	7530	7583	7610	7706	7736
U-B6	8140	8179	8092	8131	7745	7821	7850	7880	7822	7907	7770	7890	7819	7918	7819	7937	7925	8048
U-A1	-	-	-	-	-	-	-	-	8048	8058	8030	8050	-	-	8025	8042	8140	8163
U-A2	8284	8311	8237	8265	7994	8013	8100	8112	8107	8136	-	-	-	-	8108	8120	-	-
U-A3	-	-	-	-	-	-	8175	8180	8201	8224	8177	8185	-	-	8190	8220	8331	8341
U-A4	8500	8539	8445	8478	8290	8330	8395	8431	8396	8427	8350	8378	-	-	8397	8427	8537	8560

Note: [-] = the top or base disappeared from well log.

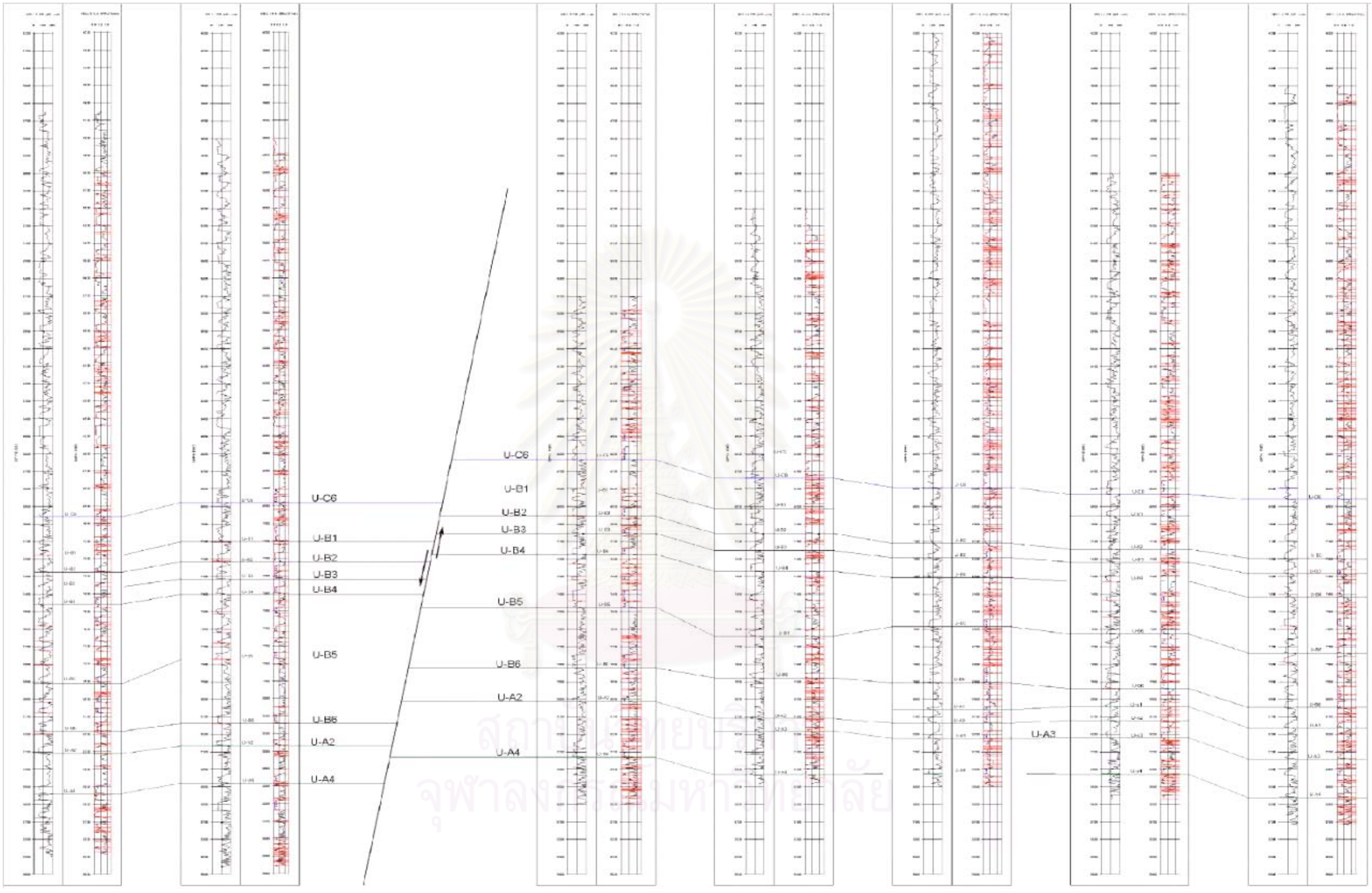

Figure 5.1 North to south well log correlation in Benchamas-A field. Well B-I-F-H-D-A-J. Gamma-ray log presents at left, whereas Vshale logs presents at the left side of the well log in each well. At the left represent the gamma-ray log and at the right represent the shale volume log.

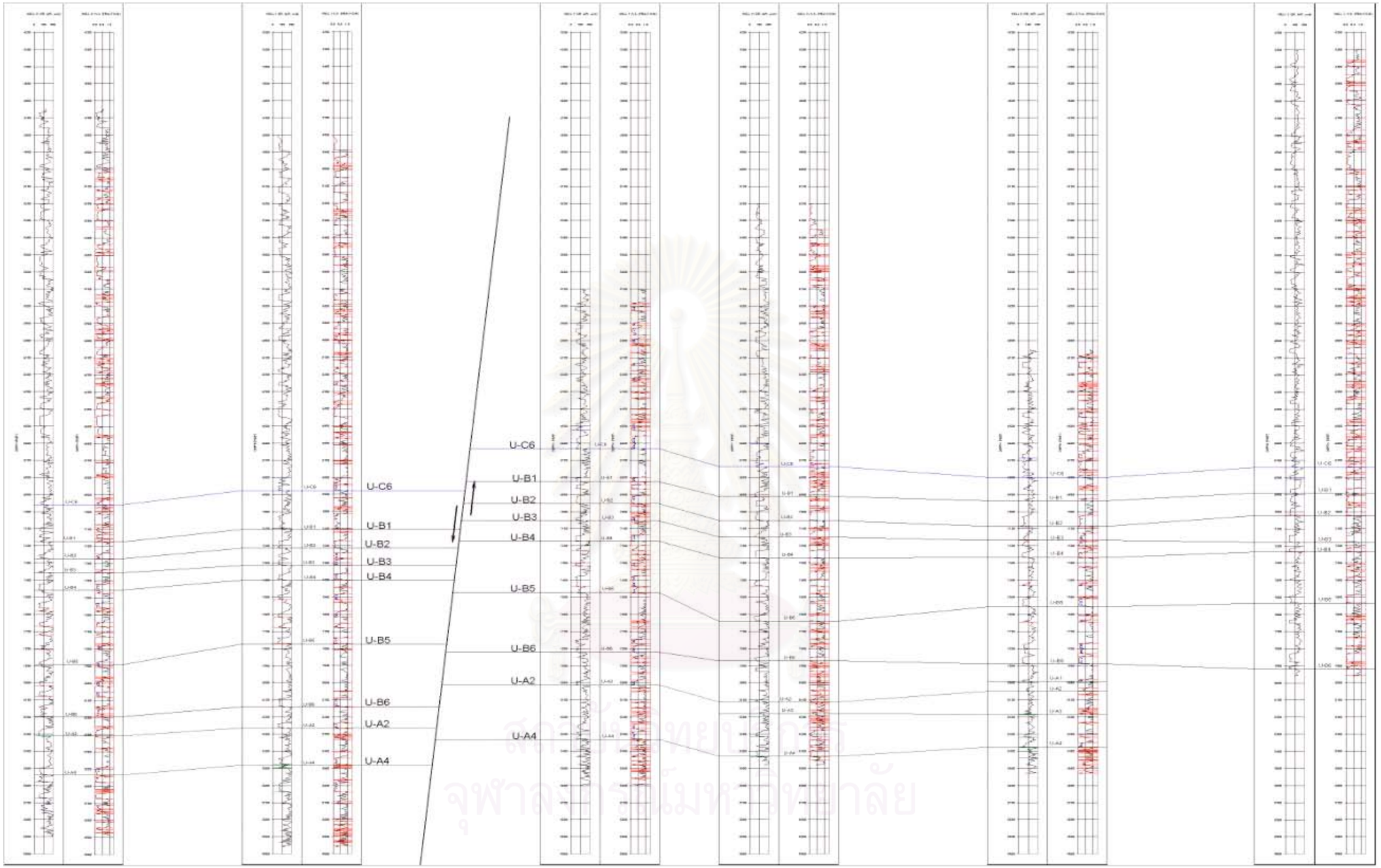

Figure 5.2 North to south well log correlation in Benchamas-A field. Well B-I-F-H-E-C. Gamma-ray log presents at left, whereas Vshale logs presents at right in each well.

Table 5.2 Summary of the sand to shale ratio in each horizon interval the Benchamas-A field.

WELL	Net pay / horizon (feet)			Net sand to Gross ratio			Sand to shale ratio in horizon			Net pay / well (feet)
	U-C	U-B	U-A	U-C	U-B	U-A	U-C	U-B	U-A	
A	0	211	77	13	25	18	15	33	22	288
B	10	207	66	20	23	23	25	30	30	283
C	40	163	N/A	49	26	N/A	96	35	N/A	203
D	0	162	77	16	17	11	19	20	12	239
E	0	147	29	16	18	8	19	22	8	176
F	146	194	76	24	26	19	32	35	23	416
H	106	126	65	23	22	24	30	28	32	297
I	42	106	105	19	23	15	23	30	18	253
J	0	99	54	17	33	14	20	49	16	153
Average	38	157	68	22	24	17	31	31	20	-

5.3 Top depth structure map and Net sand map

Top depth structure map of reservoir sand horizon U-C6, U-B2, U-B3, U-B4, U-B5 and U-B6 had been constructed and they are used to describe the structure in the study area. The Benchamas-B Fault separated Benchamas-A field from the main N-trending horst block, Benchamas-A block moved downward to the east. The Benchamas-B Fault is the boundary at the western flank of Benchamas-A field that setup fault traps at the western side. At the eastern flank, the Benchamas-A Fault appears in direction NE-SW and separated Benchamas-A field into two areas, they are upthrown areas and downthrown areas. The Benchamas-A Fault is a fault boundary at the eastern flank of Benchamas-A field. The hydrocarbon traps along this fault on both side of upthrown and downthrown. Almost horizons in upthrown present down dip direction to the north, whereas the horizons in downthrown present the down dip direction to the east.

Top depth structure map and net sand map description

Horizon U-C6 sand reservoirs are distributed from sub sea depths of 6530 to 6800 ft in the upthrown side and 6800 to 6950 ft in the downthrown (**Figure 5.3**). The high sand thickness (> 50 ft) appears at the location of well F and H (**Figure 5.4**). Sand beds gradually decreases in thickness to the north. Well F and H encountered oil reservoir 58 ft and 73 ft in thickness whereas, the other wells in the same fault compartment encountered wet sand at the north The oil-water contact presents at depth 6691 ft. Downthrown, well B and I encountered wet sand 17 ft and 27 ft.

Horizon U-B2 sand reservoirs are distributed from sub sea depths of 6900 to 7250 ft in upthrown and 7160 to 7300 ft in downthrown (**Figure 5.5**). The high sand thickness (> 40ft) appears at the location of well C, F and H (**Figure 5.6**). The up-dip appears at the south of area. The upthrown appears wet sand, whereas the downthrown presents gas reservoir. Well I encountered gas reservoir 41 ft. Gas-water contact presents at depth 7212 ft.

Horizon U-B3 this horizon, sheet sand covers in the area. Sand reservoirs are distributed from sub sea depths of 6900 to 7250 ft in upthrown and 7160 to 7300 ft in downthrown (**Figure 5.7**). The average sand thickness is 22 ft. The up-dip bedding appears at the south of area where well A, C, D, E, F, H, and J encountered gas reservoir 16, 37, 23, 25, 17, 21, and 22 ft in sequent (**Figure 5.8**). Gas-water contact in upthrown presents at depth 7292 ft, whereas downthrown appears wet sand.

Horizon U-B4 sand reservoirs are distributed from sub sea depths of 7130 to 7390 ft in upthrown and 7360 to 7500 ft in downthrown (**Figure 5.9**). The high sand thickness (> 40ft) appears at the location of well F (**Figure 5.10**). The up-dip appears at the south of area. The upthrown

appears wet sand, whereas the downthrown presents the gas reservoir. Well I encountered into gas reservoir 30 ft in thickness. Gas-water contact presents at depth 7421 ft.

Horizon U-B5 sand reservoirs are distributed from sub sea depths of 7450 to 7750 ft in upthrown and 7730 to 8050 ft in downthrown (**Figure 5.11**). Wells C and E encountered gas reservoir 40 ft and 43 ft in thickness (**Figure 5.12**). The up-dip appears at the south of area. The upthrown appears gas reservoir, gas-water-contact presents at depth 7683 ft, whereas the downthrown appears gas reservoir, gas-water contact presents at depth 8018 ft. Well B and I encountered gas reservoir 30 ft and 21 ft in thickness.

Horizon U-B6 only this horizon, the deposition look seem sediment in the location well F and H have deposited in low energy region due to sand bed gradual decreases thickness to the south. Sand reservoirs are distributed from sub sea depths of 7750 to 8000 ft in upthrown and 8090 to 8200 ft in downthrown (**Figure 5.13**). Well A, C, D, E, F and H encountered gas zone 48, 64, 74, 49, 52 and 49 ft in sequent, well J encountered gas and oil zone 100 ft (**Figure 5.14**). The up-dip appears at the south of area. The upthrown presents gas-water contact at depth 7854 ft and oil-water contact at depth 7974 ft whereas, the downthrown appears gas reservoir, gas-water-contact presents at depth 8311 ft. Well B and I encountered gas reservoir 17 ft and 27 ft in thickness. Well B the pore-pressure represents sub-normal pressure, these indicated horizon U-B6 downthrown have reservoir discontinuity.

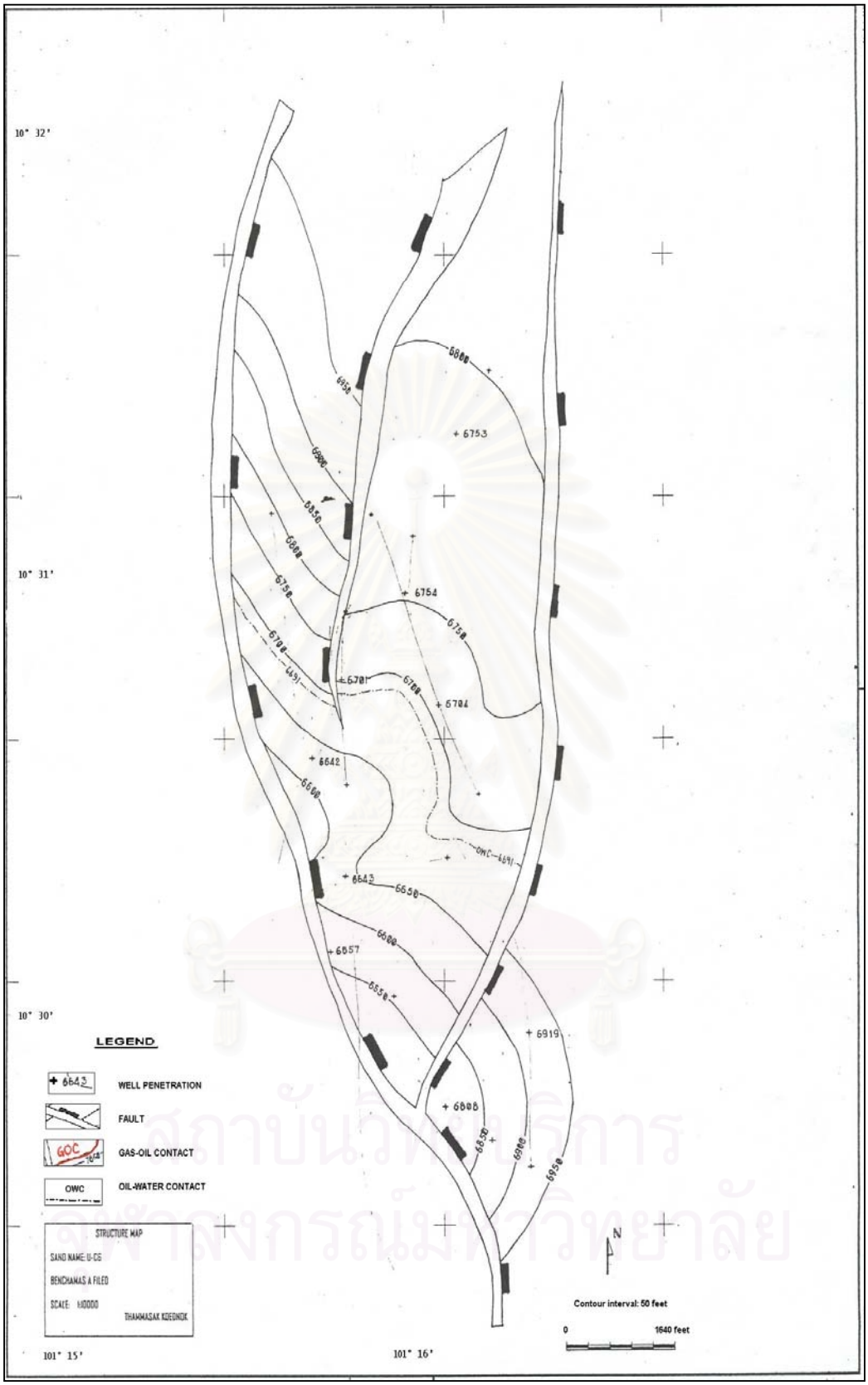

Figure 5.3 Top U-C6 reservoir depth structure map of Benchamas-A field.

Figure 5.4 U-C6 net sand (isopach) map of Benchamas-A field.

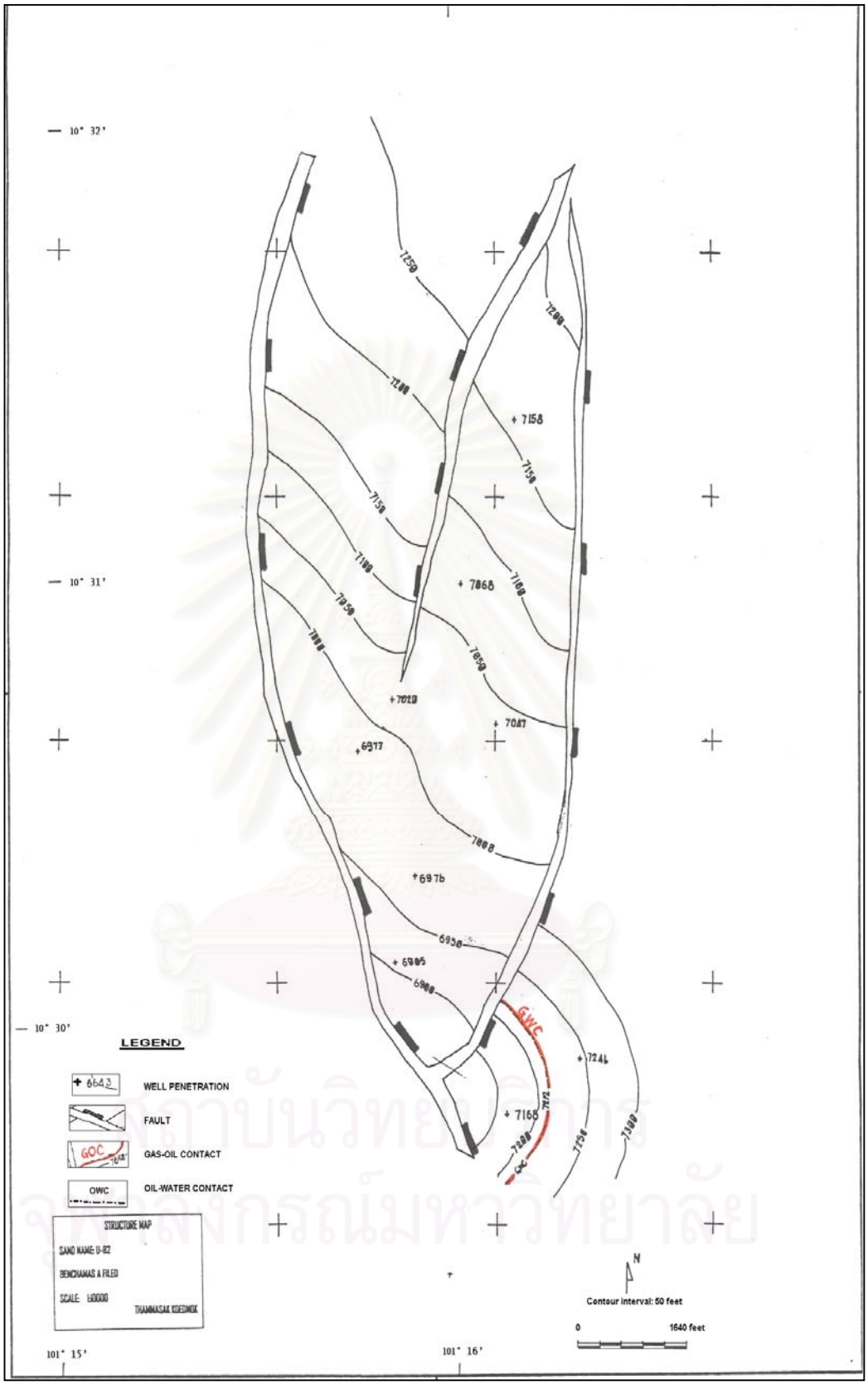

Figure 5.5 Top U-B2 reservoir depth structure map of Benchamas-A field.

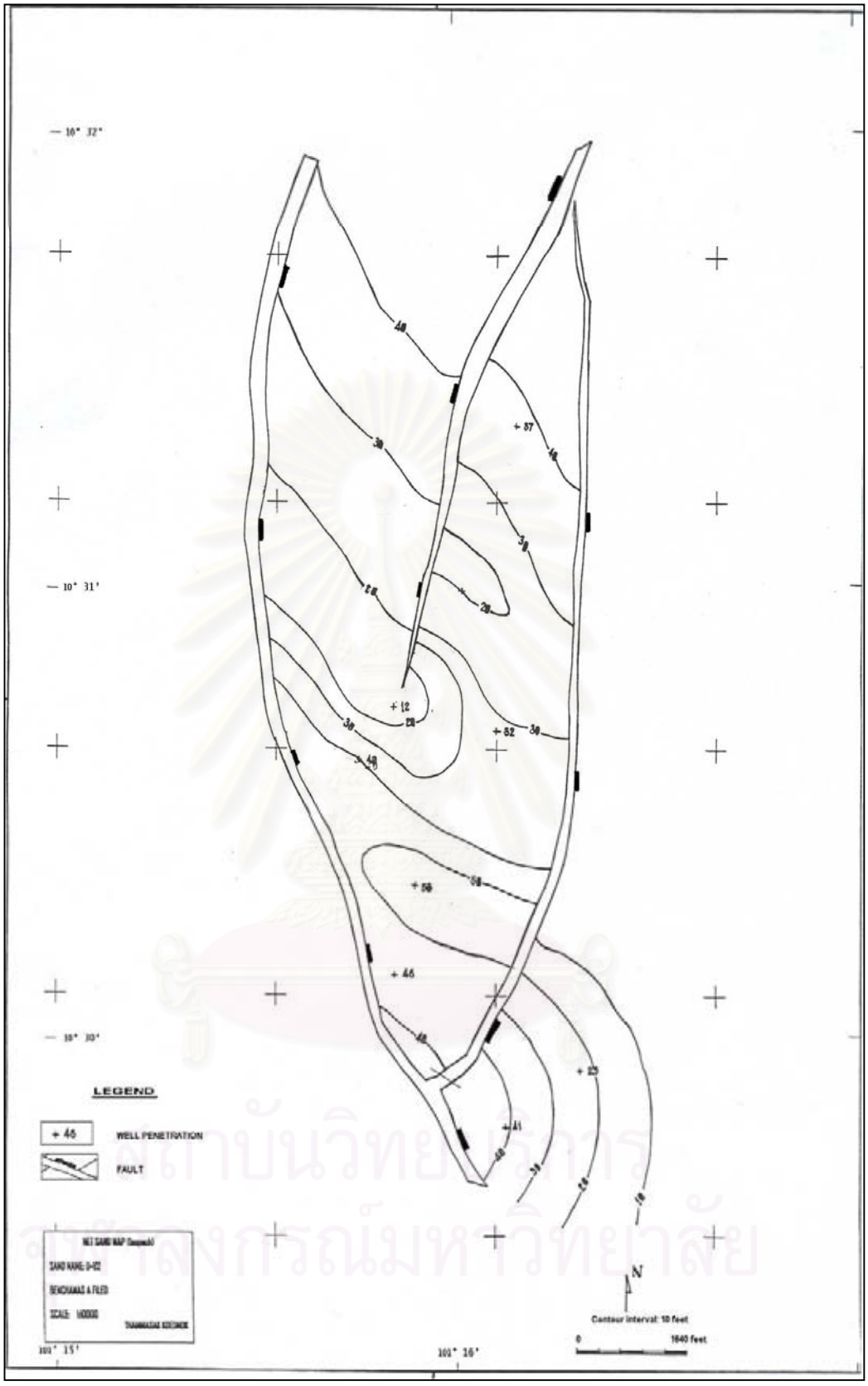

Figure 5.6 U-B2 net sand (isopach) map of Benchamas-A field.

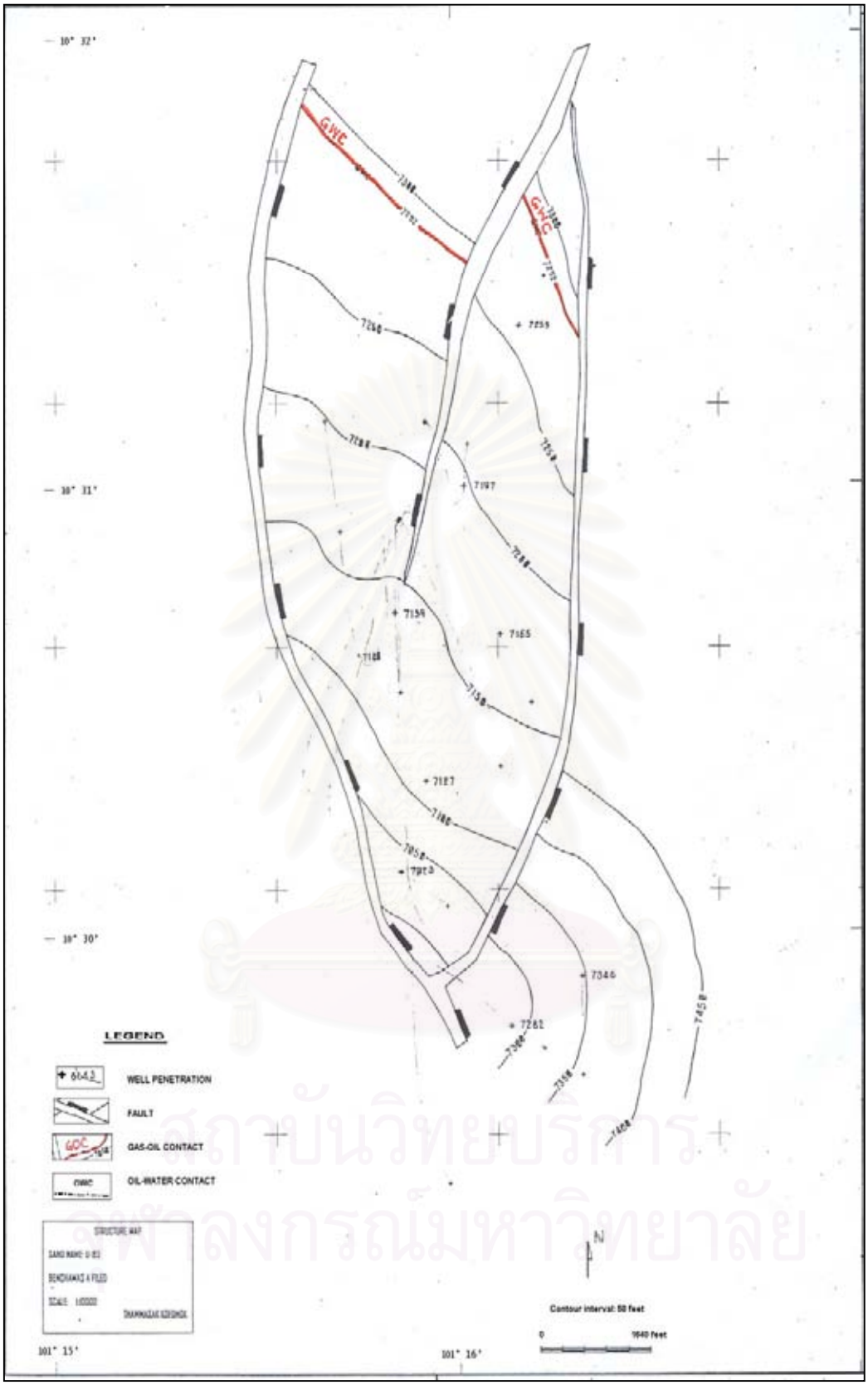

Figure 5.7 Top U-B3 reservoir depth structure map of Benchamas-A field.

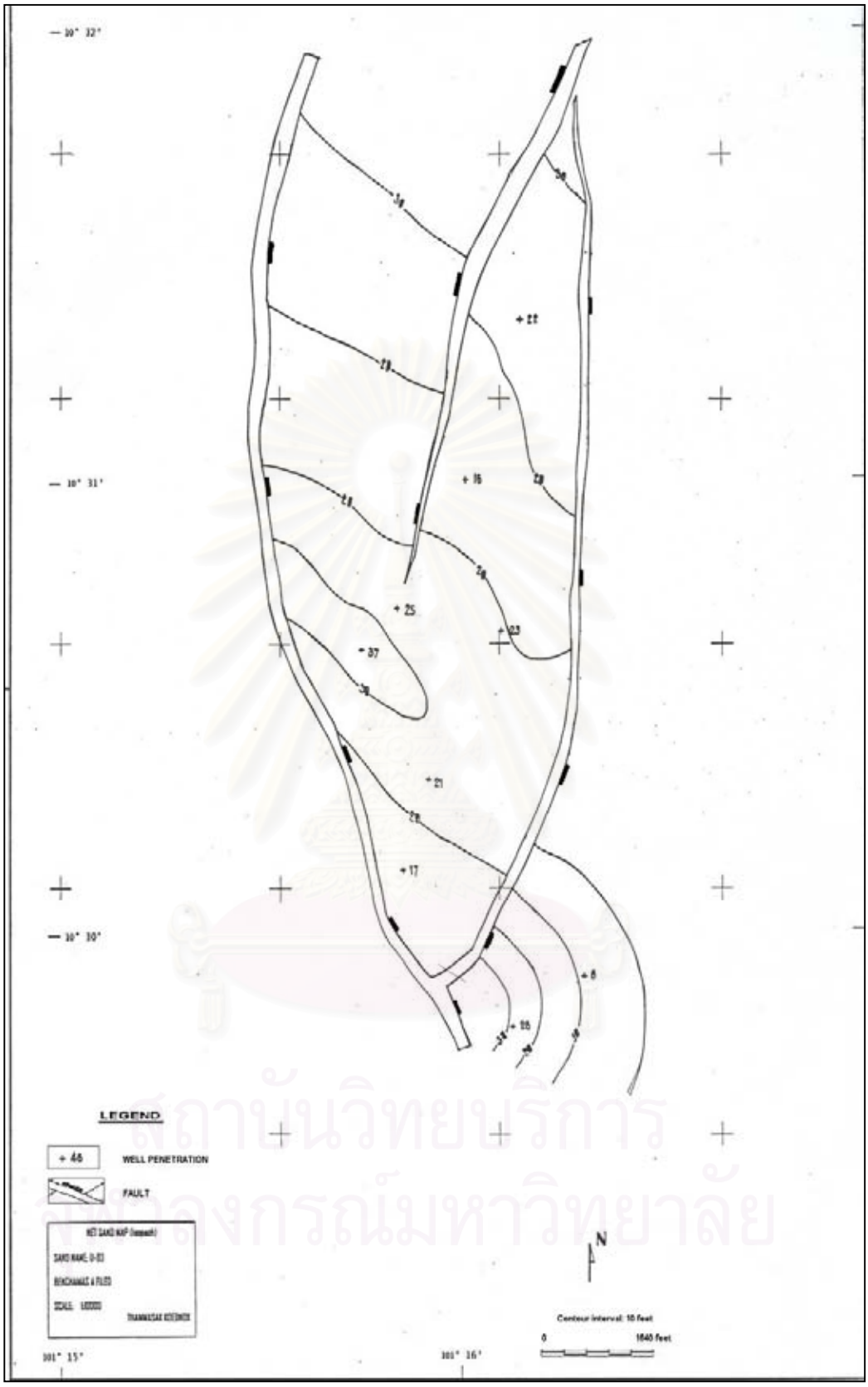

Figure 5.8 U-B3 net sand (isopach) map of Benchamas-A field.

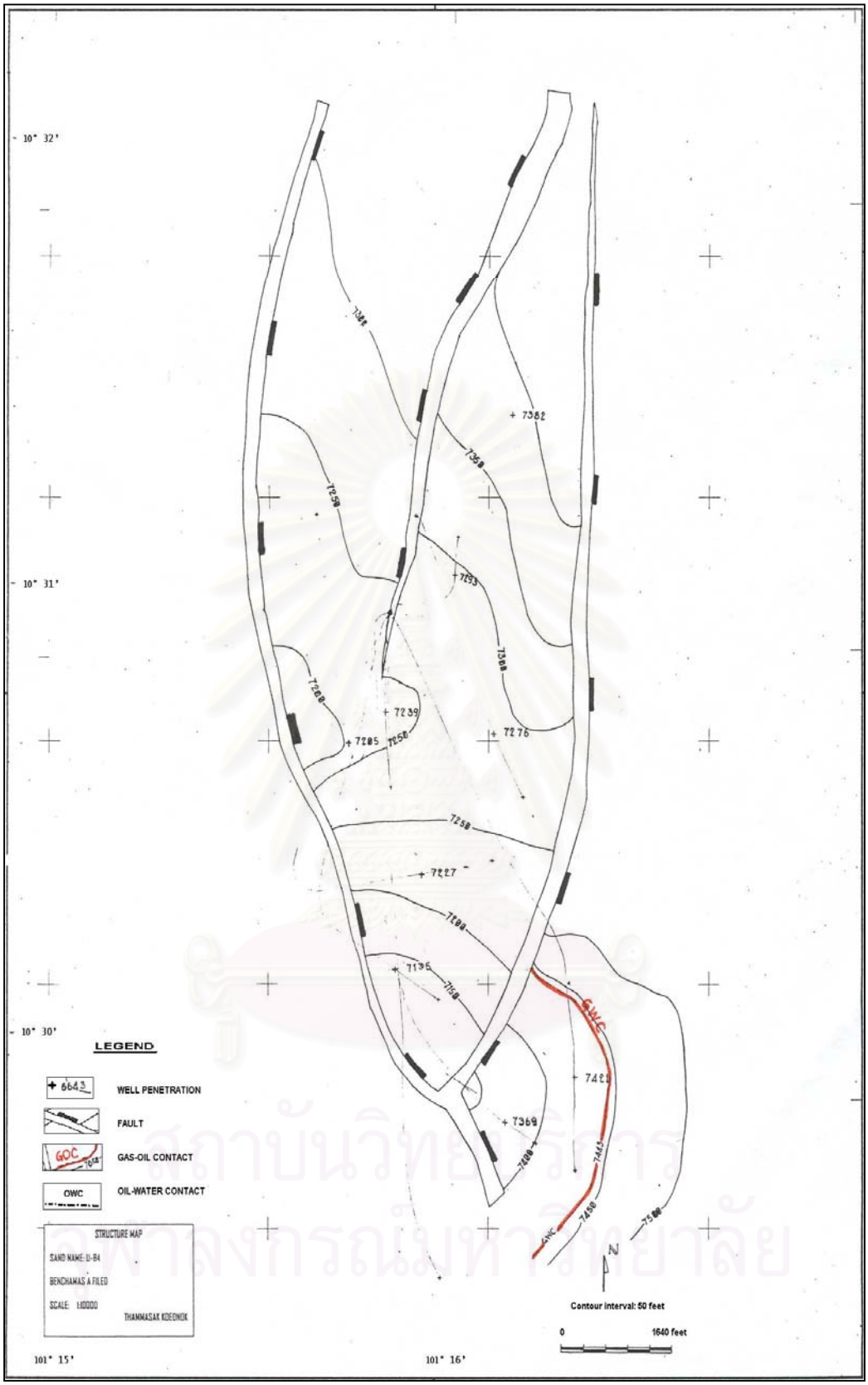

Figure 5.9 Top U-B4 reservoir depth structure map of Benchamas-A field.

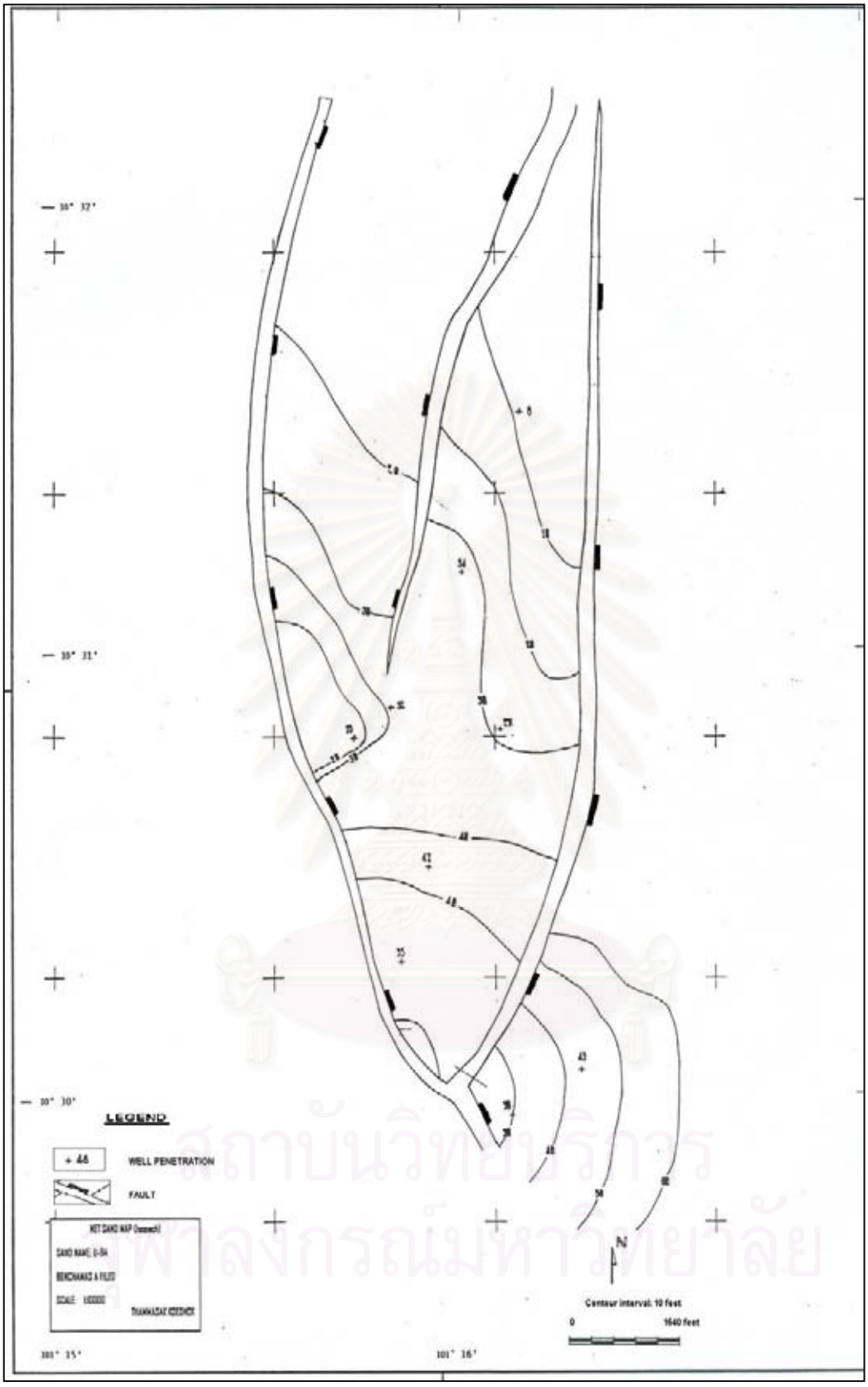

Figure 5.10 U-B4 net sand (isopach) map of Benchamas-A field.

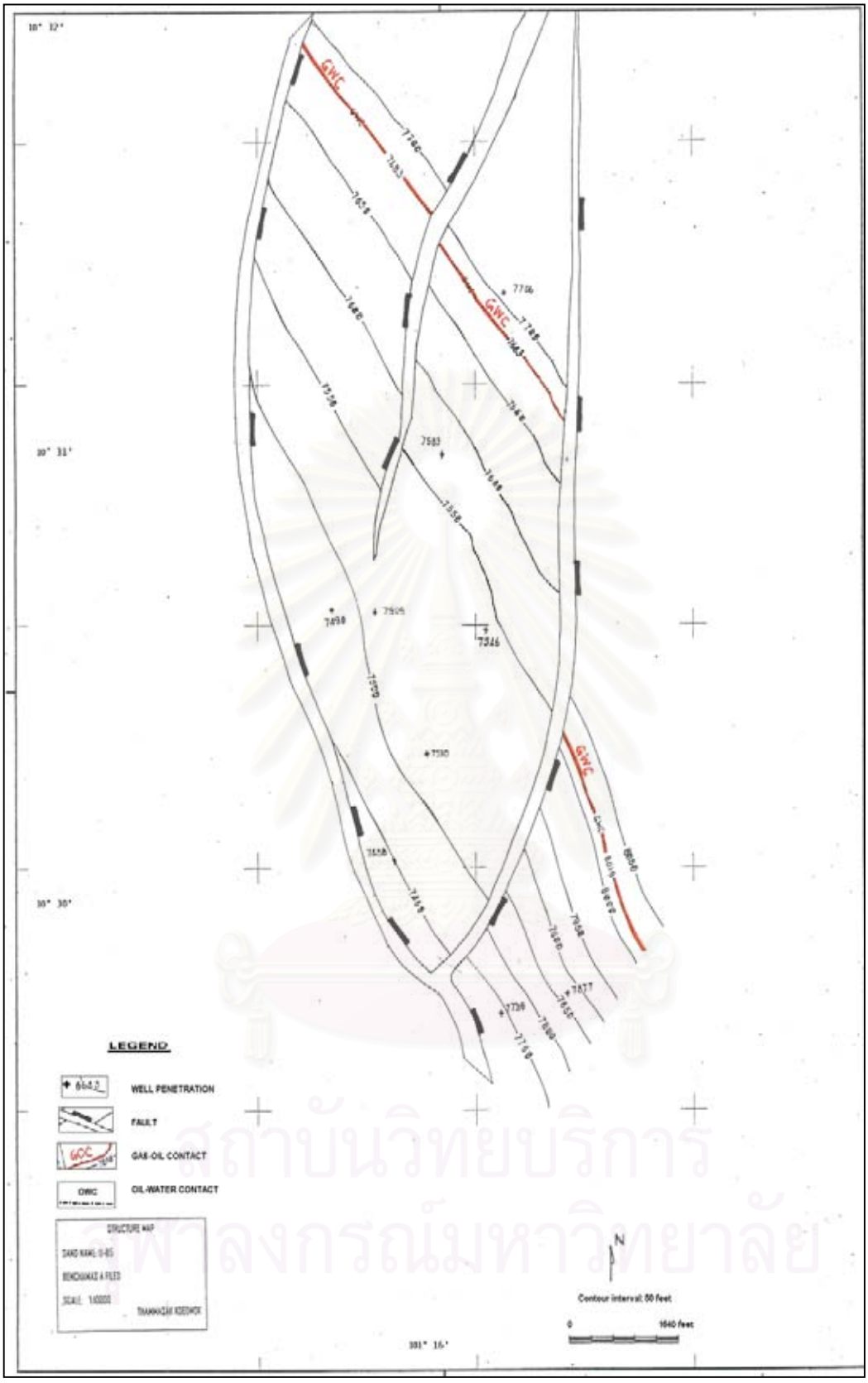

Figure 5.11 Top U-C5 reservoir depth structure map of Benchamas-A field.

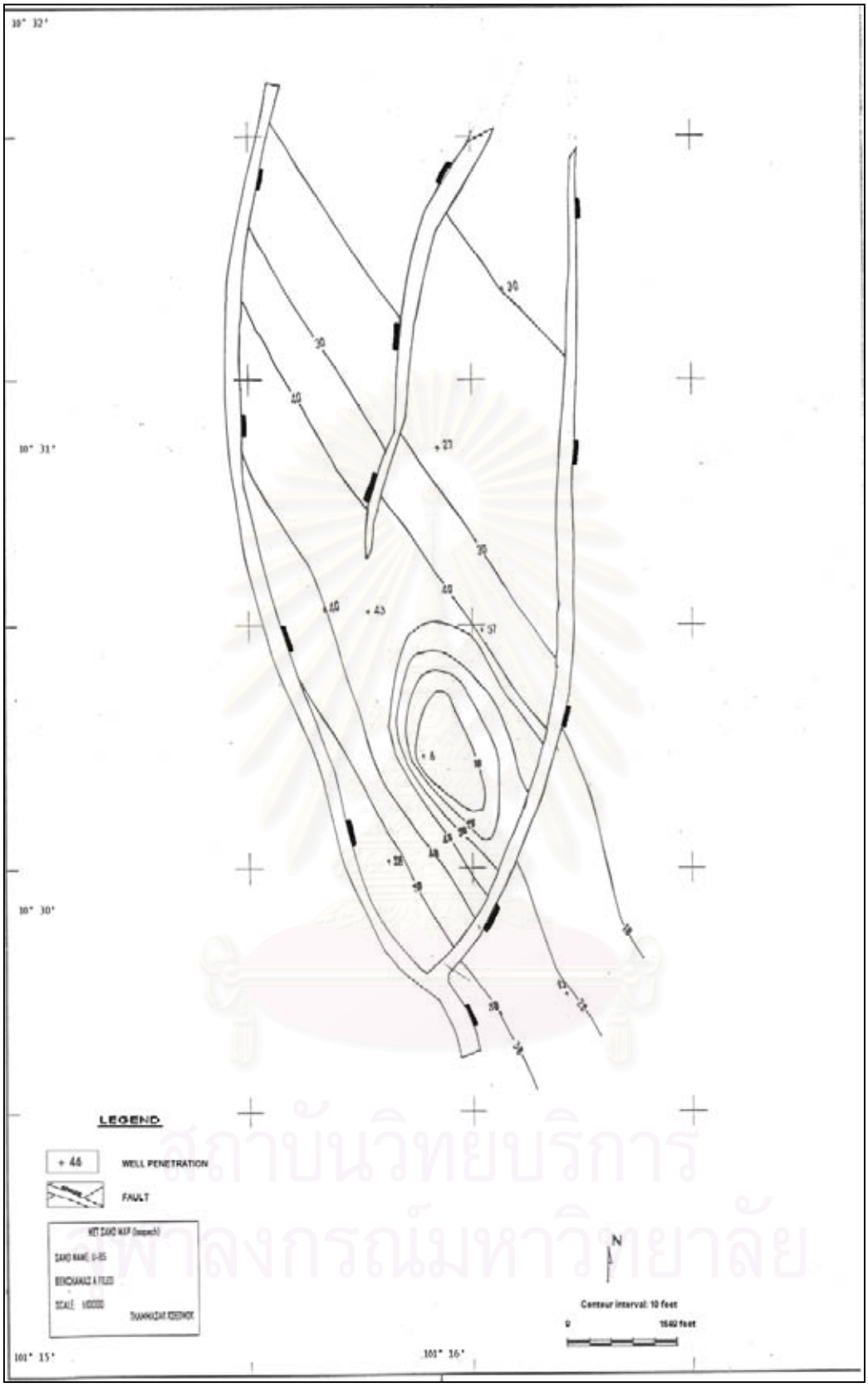

Figure 5.12 U-B5 net sand (isopach) map of Benchamas-A field.

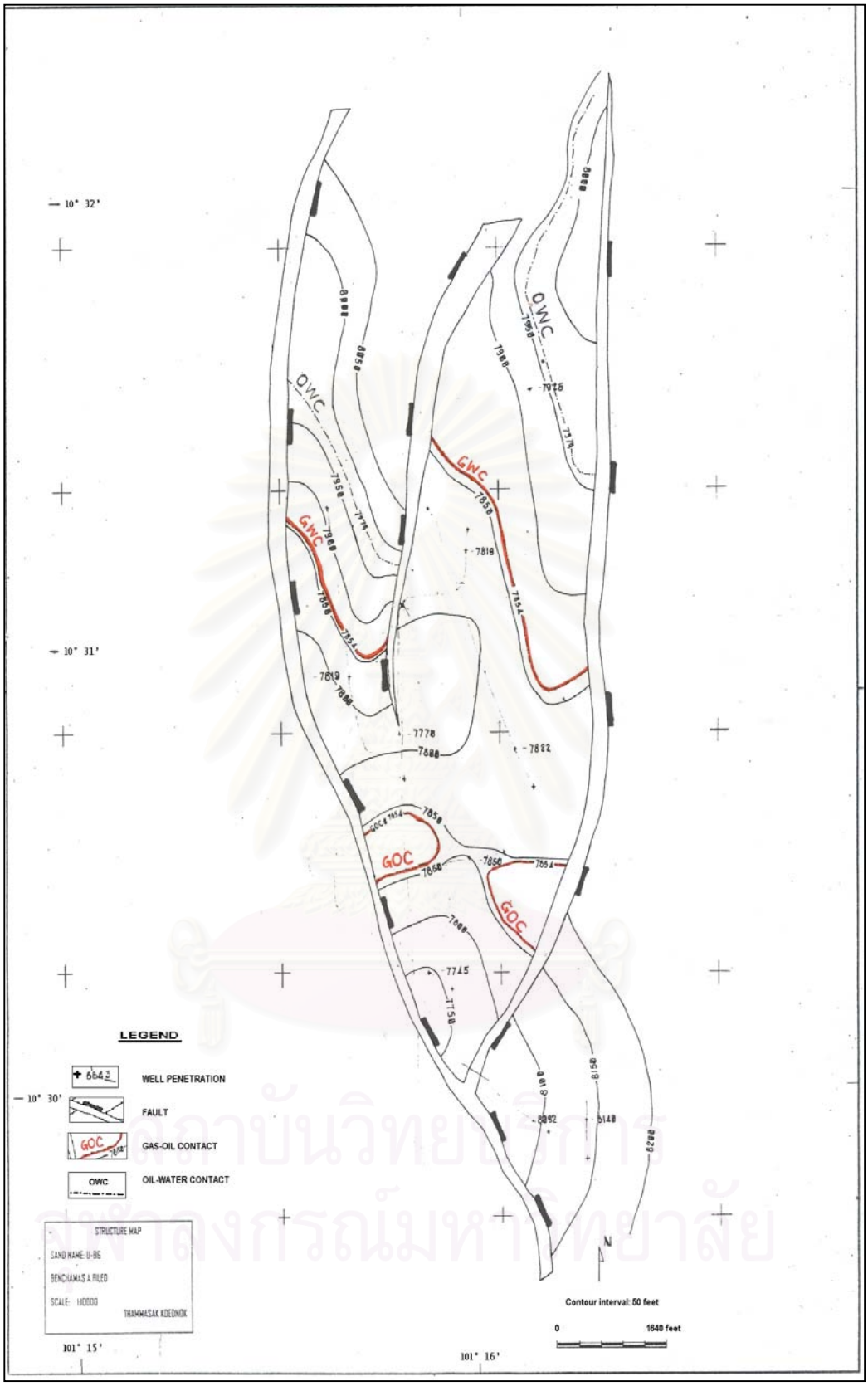

Figure 5.13 Top U-B6 reservoir depth structure map of Benchamas-A field.

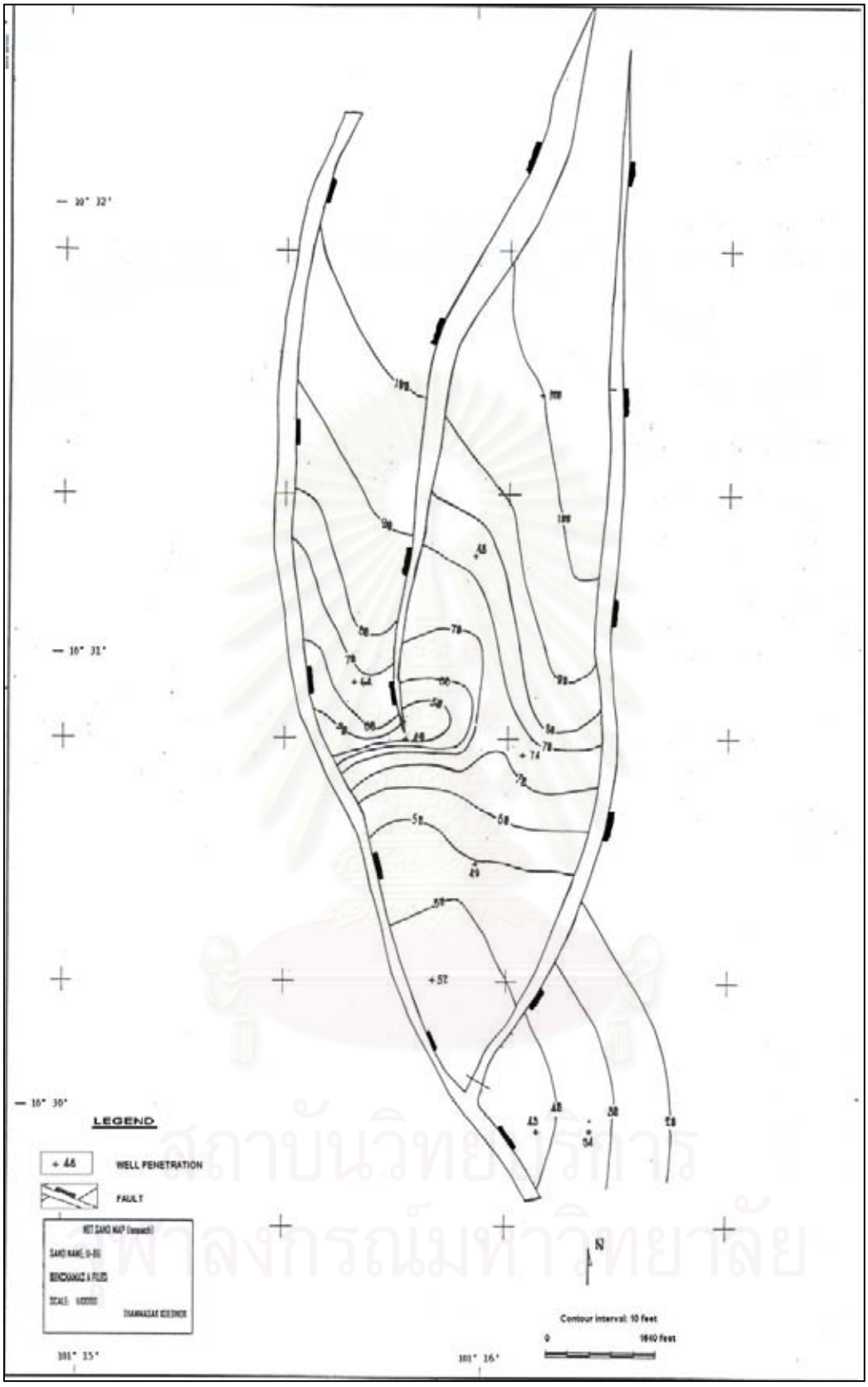

Figure 5.14 U-B6 net sand (isopach) map of Benchamas-A field.

5.4 Fault-plane-section analysis

Allan fault diagram was constructed from top depth structure and net sand maps as shown in **Figure 5.15**. The distance along the fault from (-200) to 2000 ft is used to consider the potential sealing on the Benchamas-A Fault. Area potential sealing and leakage across the Benchamas-A Fault can be identified into 2 groups they are;

First, sand-to-shale (reservoir to nonreservoir) juxtaposition, this juxtaposition consists of horizon U-C6 upthrown and downthrown, U-B2 upthrown, U-B3 upthrown and downthrown, U-B4 downthrown, U-B5 upthrown, U-B6 downthrown.

Second, sand-to-sand (reservoir to reservoir) juxtaposition, this sand-to-sand offset consists of horizon U-B4 upthrown juxtaposed against U-B2 downthrown and U-6 upthrown juxtaposed against U-B5 downthrown. The sand-to-shale juxtaposition is considered as a sealing fault in structure closure whereas sand-to-sand juxtaposition is considered as a leakage fault.

Sand-to-shale juxtaposition can be recognized as the lithological sealing because fault cannot be act as an open conduit when hydrocarbon-bearing sand-on-shale closures are present (Alexander et al., 1998). Therefore the horizon U-C6 upthrown and downthrown, U-B2 upthrown, U-B3 upthrown and downthrown, U-B4 downthrown, U-B5 upthrown, and U-B6 downthrown, all of them have sealed by lithological sealing. Moreover, when consider to the level of hydrocarbon contacts, all of them have different depth contact across Benchamas-A Fault (**Figure 5.16**).

Sand-to-sand juxtaposition can be recognized as the fault is an open conduit or hydrocarbon can be spill across Benchamas-A Fault. Horizon U-B4 upthrown against U-B2 downthrown and U-6 upthrown against U-B5 downthrown these overlap sands appear on the fault-plane section but the hydrocarbon contact depth in both side of fault appear different contact depth and fluid are the different type (**Figures 5.17 (a)** and **(b)**). However, to investigate the potential sealing, have to confirm with pore-pressure (RFT test) and check fluids have communicated between sand-to-sand juxtaposition or not.

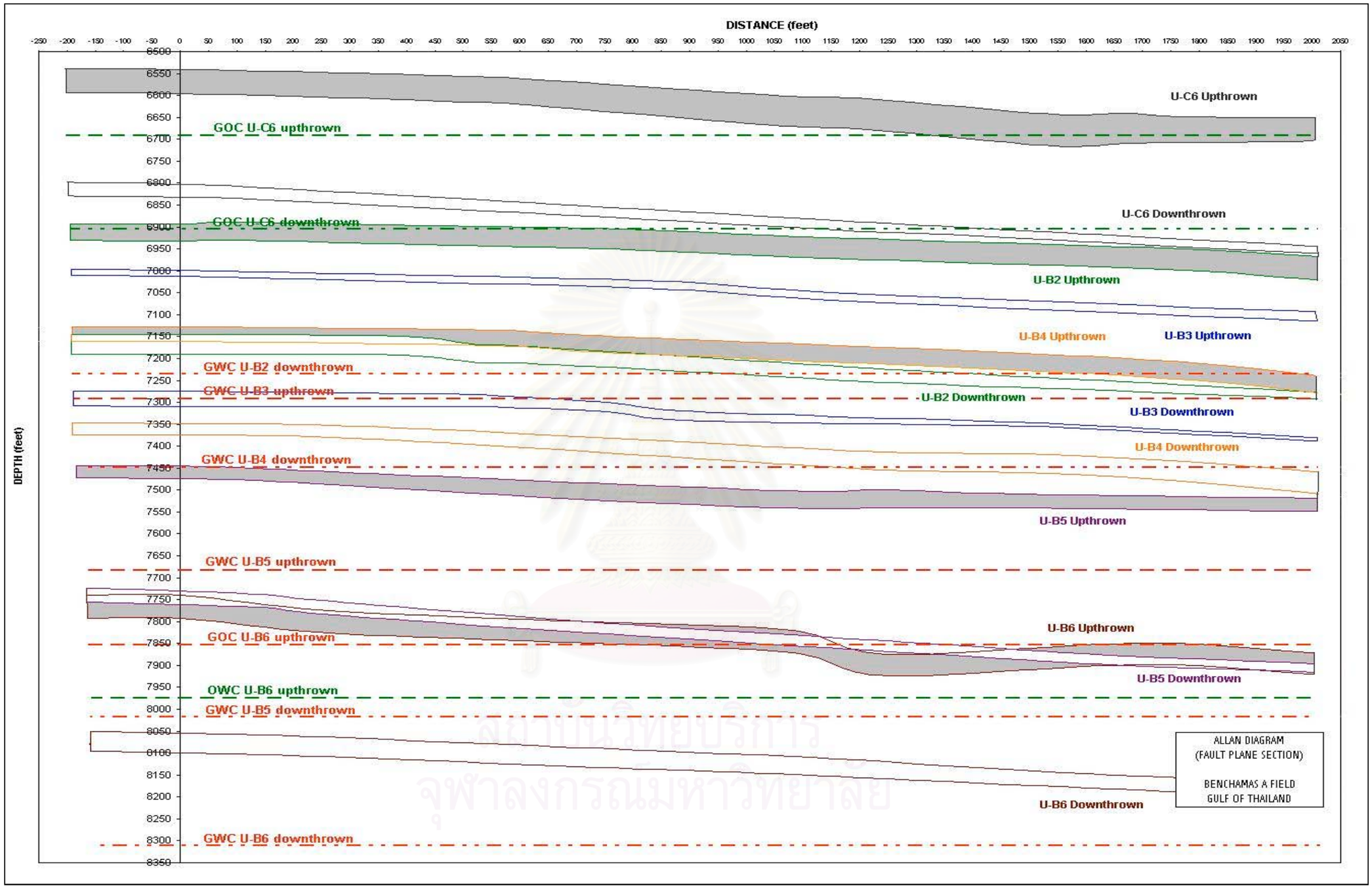

Figure 5.15 The diagram illustrating structure and stratigraphic geometry of Benchamas-A Fault on Allan fault diagram (fault-plane section), by consideration the actual thickness. This diagram was investigated distance along a fault from –200 to 2000 ft. The yellow color represents the area of sand-to-sand juxtaposition. GWG = Gas-water contact, OWC = Oil-water contact, GOC = Gas-oil contact. The gray blocks represent the reservoir horizons in the upthrown side and the empty blocks represent the reservoir horizons in the downthrown side.

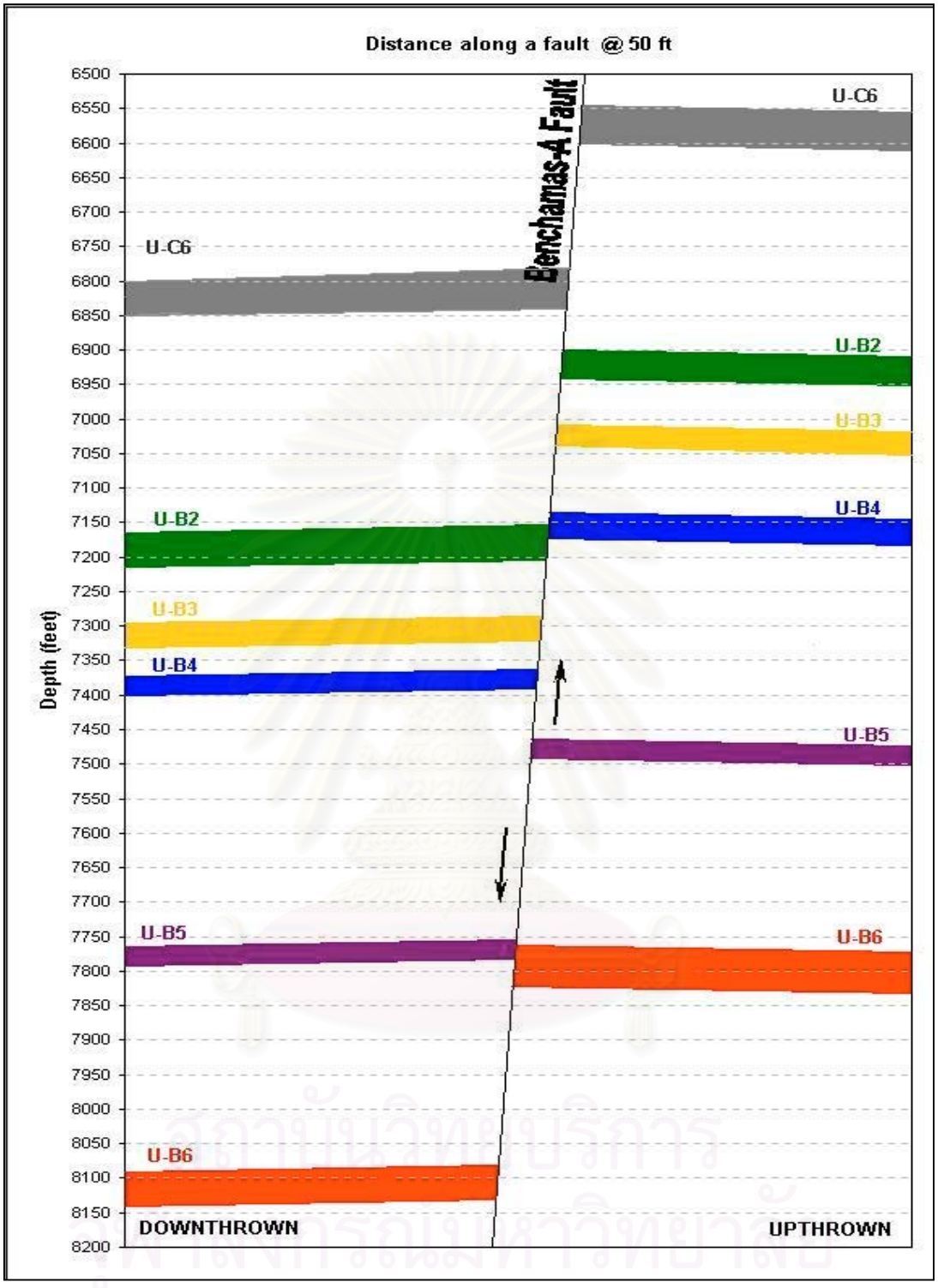

Figure 5.16 Cross-section diagram illustrates the reservoir sand horizons juxtaposed against the other sand horizons across the Benchamas-A Fault. The sand horizons juxtaposed against clay/ shale bed across a fault considered as a fault sealing, whereas the sand horizons juxtaposed against the other sand across a fault consider as a fault leakage unit.

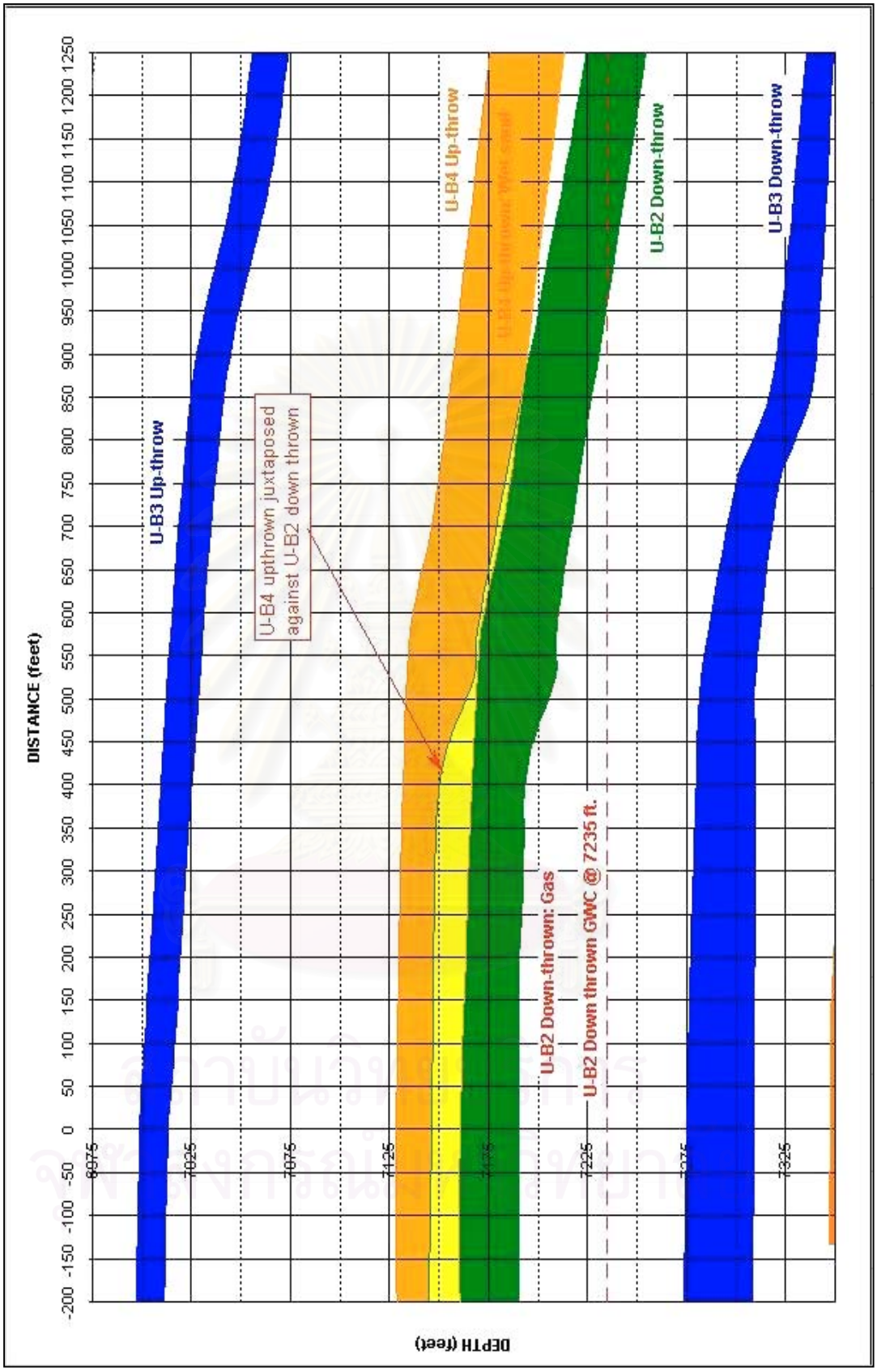

Figure 5.17 (a) Close-up section where the wet sand horizon U-B4 upthrown juxtaposed against gas reservoir horizon U-B2 downthrown.

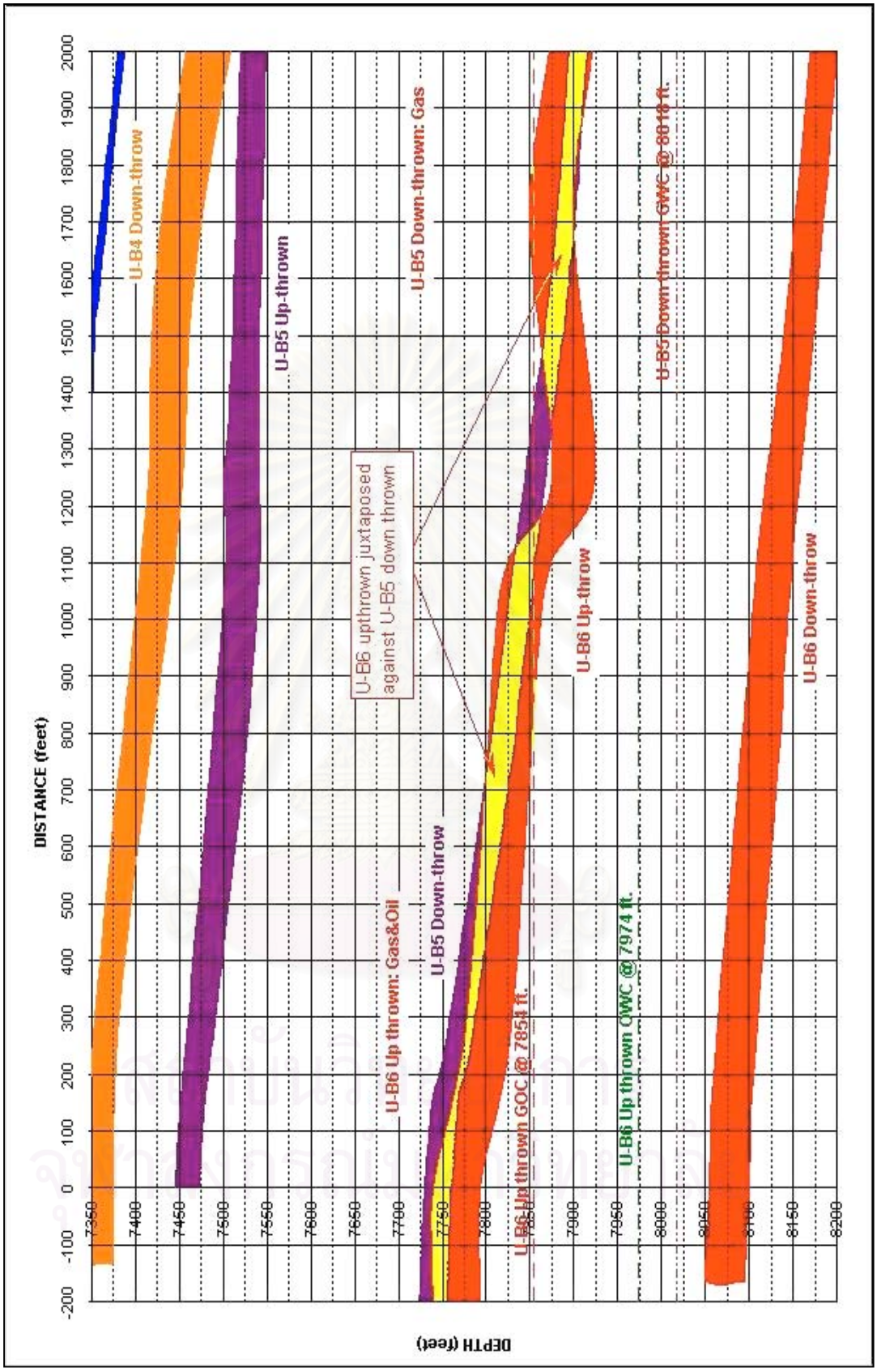

Figure 5.17 (b) Close-up section where the gas and oil reservoir horizon U-B6 upthrown juxtaposed against gas reservoir horizon U-B5 downthrown.

5.5 Migration and entrapment of hydrocarbon in study area

The migration of hydrocarbon in Benchamas-A field have controlled by lateral lithology continuity and fault closure. When the hydrocarbons have left the source rock they migrated through the up-dip bedding to the highest closure and fill-up this closure unit this closure have saturated with hydrocarbon, they will start fill backward to the lower closure such as along a fault closure. The probability of hydrocarbon can be migrated across Benchamas-A Fault, it would be happened before or early movement of Benchamas-A Fault. Because the values of shale gouge ratio got high 30 to 40% when this Benchamas-A Fault, has started to move in a few feet (25-50 ft). Moreover, on the Benchamas-A Fault have sealed by clay smear that is more effective to trap the hydrocarbon accumulated in both side of faulted compartments. Therefore the location that appropriated to hydrocarbon accumulation would be happened at the up-dip closure adjacent Benchamas-A Fault (**Figure 5.18**).

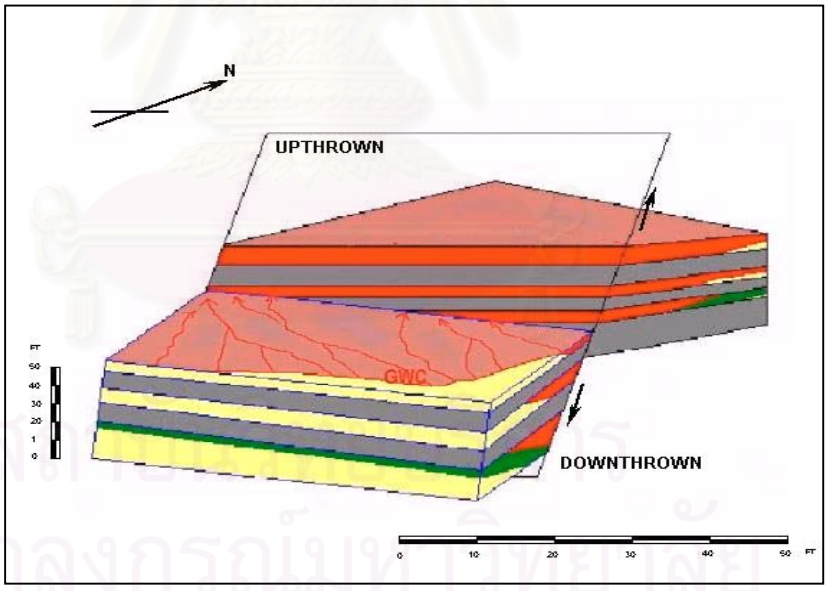

Figure 5.18 Hydrocarbon migration and entrapment model of Benchamas-A field. The hydrocarbon reservoirs occur in sand layers with entrapping shale sequences and normal faulting. Yellow and gray color represent sand and shale beds respectively. Red and green color represent gas and oil respectively. The red arrows represent the hydrocarbon migration pathways.

5.6 Result of shale gouge ratio (SGR)

The results of shale gouge ratio in overlap areas on the fault plane have been displayed into two algorithms and both represent similar results.

First, using the Vshale, source bed thickness, and throw from Allan fault diagram to calculate SGR. These results were assigned into the grid cells for presenting the degree of SGR on the fault plane (**Figure 5.19**). The results have changed with throw along the fault. Wet sand horizons U-B4 upthrown overlap with gas reservoir U-B2 downthrown shown 40 to 43% of SGR, whereas the overlap area gas and oil reservoir U-B6 upthrown overlap with U-B5 downthrown shown 62 to 86% of SGR.

Second, using the Vshale, source bed thickness, and throw from juxtaposition diagram to calculated SGR values by using the juxtaposition diagram. The result on juxtaposition diagram displays the shale gouge ratio only the overlap sand-sand, therefore the SGR values have changed with throw until the end of interested interval. Wet sand U-B4 upthrown overlap with gas reservoir U-B2 downthrown shown 40 to 60% of SGR (**Figure 5.20 (a)**), whereas the overlap area gas and oil reservoir U-B6 upthrown overlap with U-B5 downthrown presents 50 to 70% of SGR (**Figure 5.20 (b)**). The comparison of SGR results in the leakage area from the Allan fault diagram with the cutoff SGR value at 20% (Yielding et al., 1999) that indicate all the overlap sand-sand area on the Benchamas-A Fault have sealed potentials.

As a result both algorithms were presented, showing the Benchamas-A Fault was sealed. Moreover, high SGR values appear in this fault zone represented high phyllosilicates content in the fault zone material (Foxford et al., 1998). For this reason the pore-throat size could be decreased and correspondingly increases the capillary entry pressure of the gouge, this association is an answer “ How does the clay smear can make a fault seal?” More ever, the minimum SGR in Benchamas-A Fault is higher than 40%, this represents fault seal by clay smears mechanism. Therefore Benchamas-A Fault is high probability to generate clay smear along the fault plane and traps hydrocarbon along the fault.

Table 5.3 Average shale volume (Vshale) data are used in analyzing Benchamas-A Fault.

Vshale average from F and I			Vshale average from H and B		
Depth feet	Formation name	Vsh. avg.	Depth feet	Formation name	Vsh. avg.
0-25	U-C6	0.20	0-25	U-C6	0.21
25-50		0.32	25-50		0.11
50-75		0.10	50-75		0.03
75-100		0.87	75-100		0.72
100-125		0.90	100-125		0.80
125-150		0.81	125-150		0.80
150-175		0.71	150-175		0.43
175-200		0.88	175-200		0.60
200-225		0.97	200-225		0.52
225-250		0.11	225-250		0.17
250-275		0.46	250-275		0.68
275-300		0.13	275-300		0.48
300-325		0.87	300-325		0.88
325-350		0.92	325-350	U-B2	0.18
350-375	U-B2	0.12	350-375		0.02
375-400		0.11	375-400		0.94
400-425		0.86	400-425		0.75
425-450		0.44	425-450	U-B3	0.29
450-475	U-B3	0.16	450-475		0.79
475-500		0.86	475-500		0.76
500-525		0.86	500-525	U-B4	0.09
525-550		0.87	525-550		0.14
550-575	U-B4	0.10	550-575		0.92
575-600		0.94	575-600		0.79
600-625		0.55	600-625		0.33
625-650		0.19	625-650		0.67
650-675		0.72	650-675		0.42
675-700		0.96	675-700		0.55
700-725		0.75	700-725		0.58
725-750		0.13	725-750		0.78
750-775		0.92	750-775		0.59
775-800		0.94	775-800		1.00
800-825		0.23	800-825	U-B5	0.23
825-850		0.47	825-850		0.72
850-875		0.87	850-875		0.87
875-900	U-B5	0.19	875-900		0.66
900-925		0.92	900-925		0.09
925-950		0.85	925-950		0.80
950-975		0.74	950-975		0.93
975-1000		0.92	975-1000		0.31
1000-1025		0.83	1000-1025		0.95
1025-1050		0.86	1025-1050		0.66
1050-1075		0.83	1050-1075		0.14
1075-1100		0.83	1075-1100		0.86
1100-1125		0.86	1100-1125		0.88
1125-1150		0.89	1125-1150	U-B6	0.19
1150-1175		0.83	1150-1175		0.42
1175-1200	U-B6	0.190	1175-1200		0.23
1200-1225		0.190			

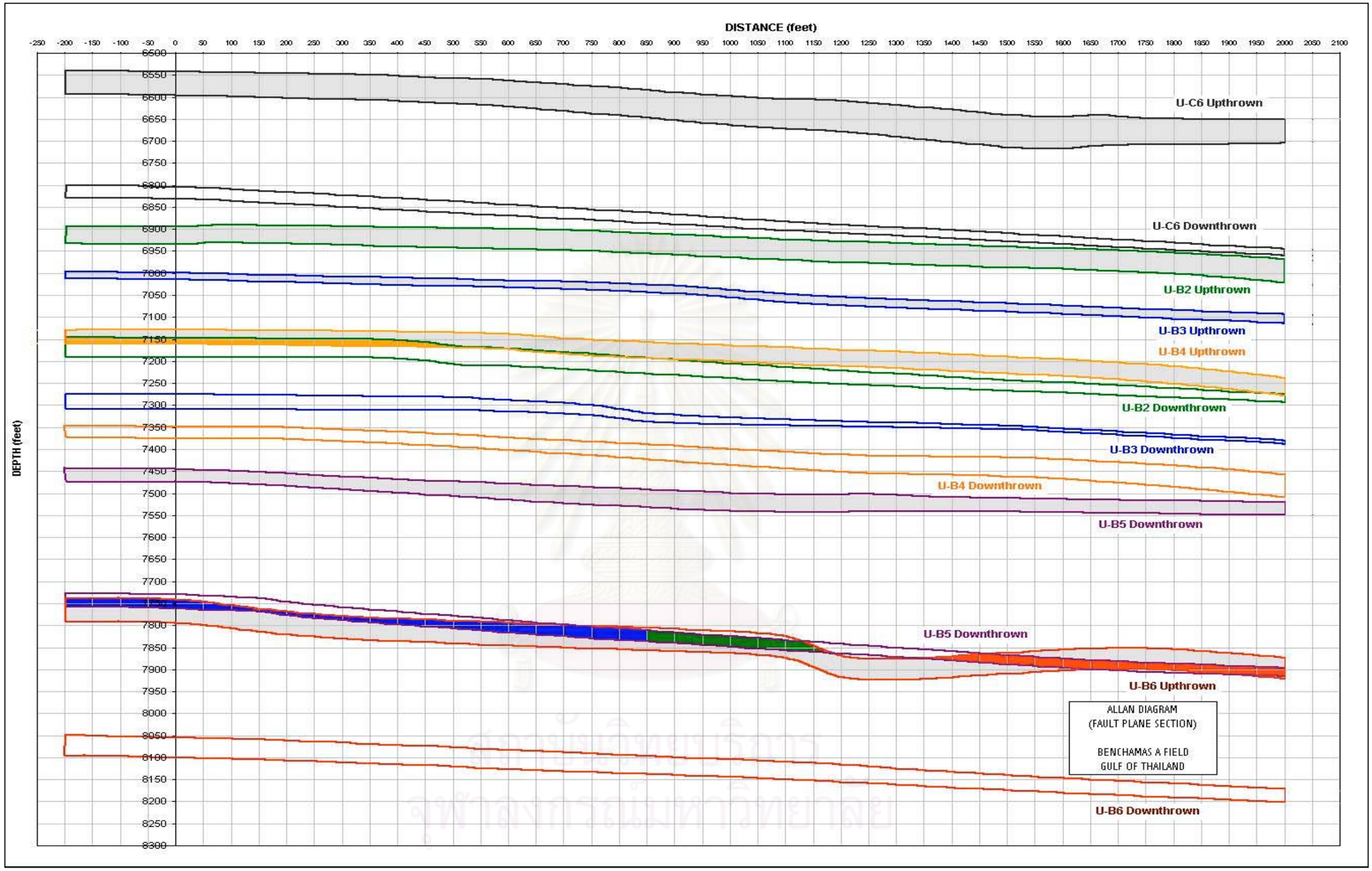

Figure 5.19 Allan fault diagram represents the shale gouge ratio vale in offset sand upthrown and downthrown. The color-coding represents the shale gouge ratio value. The SGR calculation uses the Vshale values listed in **Table 5.3**. The gray blocks represent the reservoir horizons in the upthrown side and the empty blocks represent the reservoir horizons in the downthrown side. = 40 - 50% SGR, = 60 - 70% SGR, = 70 - 80% SGR, = 80 - 90% SGR.

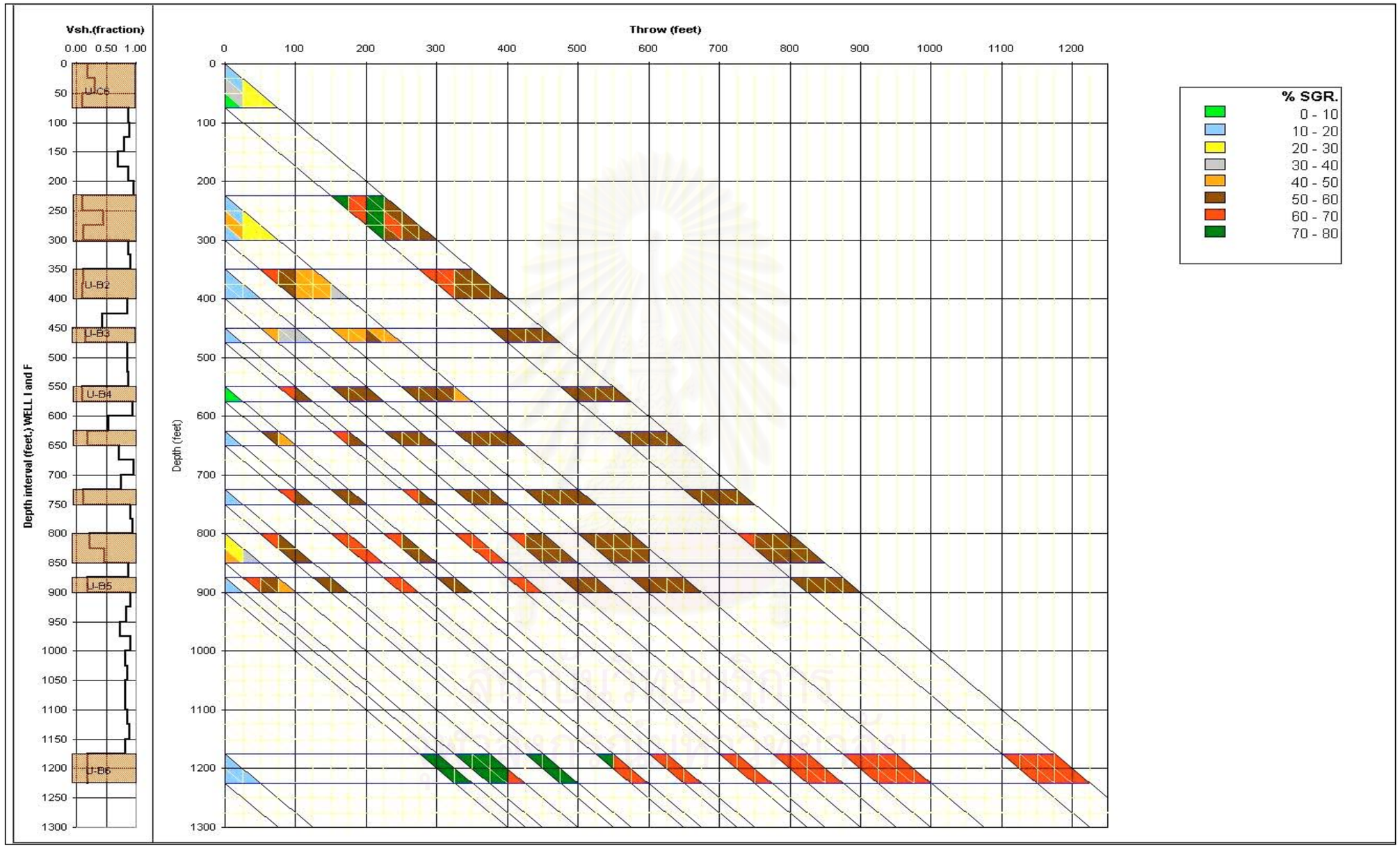

Figure 5.20 Juxtaposition diagram illustrating the variation of shale gouge ratio (SGR) with throw for typical horizons U-C6, U-B2, U-B3, U-B4, U-B5, and U-B6. Horizontal lines represent upthrown reservoir zone, and diagonal lines represent downthrown zone. The SGR calculation uses the Vshale values listed in **Table 5.3**. In **(a)**, SGR was calculated by using average Vshale from well F and I. (modified from Triangle diagram manual, 2001).

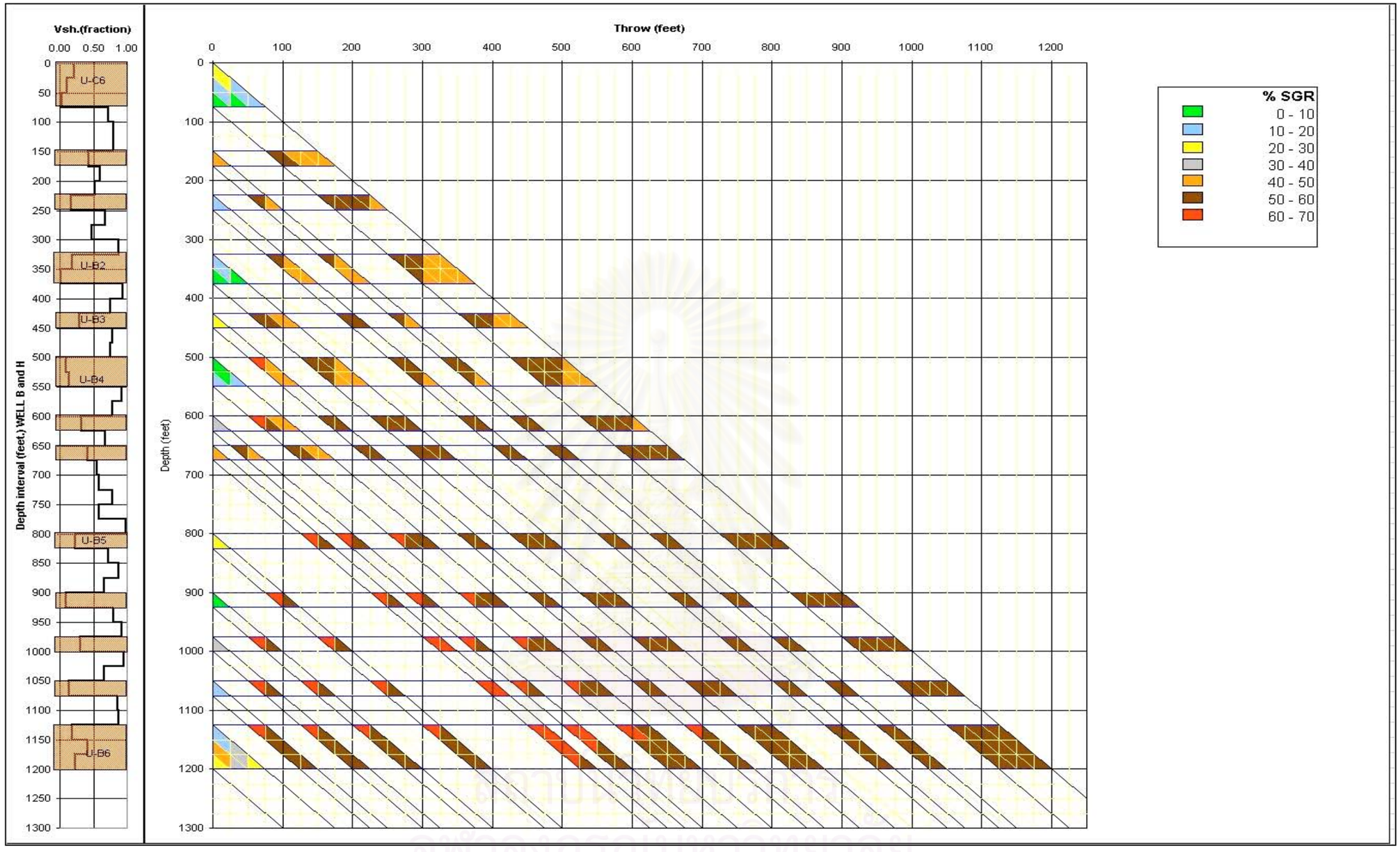

Figure 5.20 (continued). In **(b)** SGR was calculated by using average Vshale from well H and B.

5.7 Pore pressure distribution

The pore-pressure profile defined by the RFT data in a well in a fault-bound block can be used to construct the pressure field for the near side of each bounding fault to that block. This process involves tracking the pressure trend along each reservoir zone from the well to the fault using the appropriate fluid densities. It is assumed that within each layer in each compartment there are no pressure barriers, that is, all the changes in pressure-field occur across the fault. **Figure 5.21** represent the pore-pressure distribution in Benchamas-A field and gave ideal reservoir continuity across Benchamas-A Fault.

5.7.1 Pore-pressure distribution in each horizon

The result of RFT analyze in this part have been classified by 6 horizons. The RFT data in each well as the same horizon are used to construct the pore pressure field. Therefore these pore pressure will give the detail of fluid properties such as fluid gradient, type, column high, continuity and contact depth. The details of analysis have been explained as below.

Horizon U-C6

RFT data from well F and I were used to analyze in this horizon.

Horizon overview: This horizon has the RFT data test 1 well in upthrown side and 1 well in downthrown side. Then the data overview can be used the individual data in well F and I to explain the result in this horizon (**Figures 5.22 and 5.23**).

Fluid type: Oil.

Fluid gradient:

Upthrown side: Oil gradient = 0.3059 psi/ft

Water gradient = 0.4101 psi/ft

Downthrown side: Oil gradient = 0.2910 psi/ft

Water gradient = 0.4147 psi/ft

Fluid contact depth:

Upthrown side: OWC = 6691 ft

Downthrown side: OWC = 6905 ft

Horizon U-B2

RFT data from well F and I were used to analyze in this horizon.

Horizon overview: This horizon has the RFT data test, 1 well in upthrown side and 1 well in downthrown side. Then the data overview can be used the individual data in well F and I to explain the result in this horizon (**Figures 5.24 and 5.25**).

Fluid type: Gas and water.

Fluid gradient:

Upthrown side: N/A (wet sand) psi/ft

Water gradient = 0.4205 psi/ft

Downthrown side: Gas gradient = 0.0883 psi/ft

Water gradient = 0.4147 psi/ft

Fluid contact depth:

Upthrown side: GWC = N/A ft

Downthrown side: GWC = 7235 ft

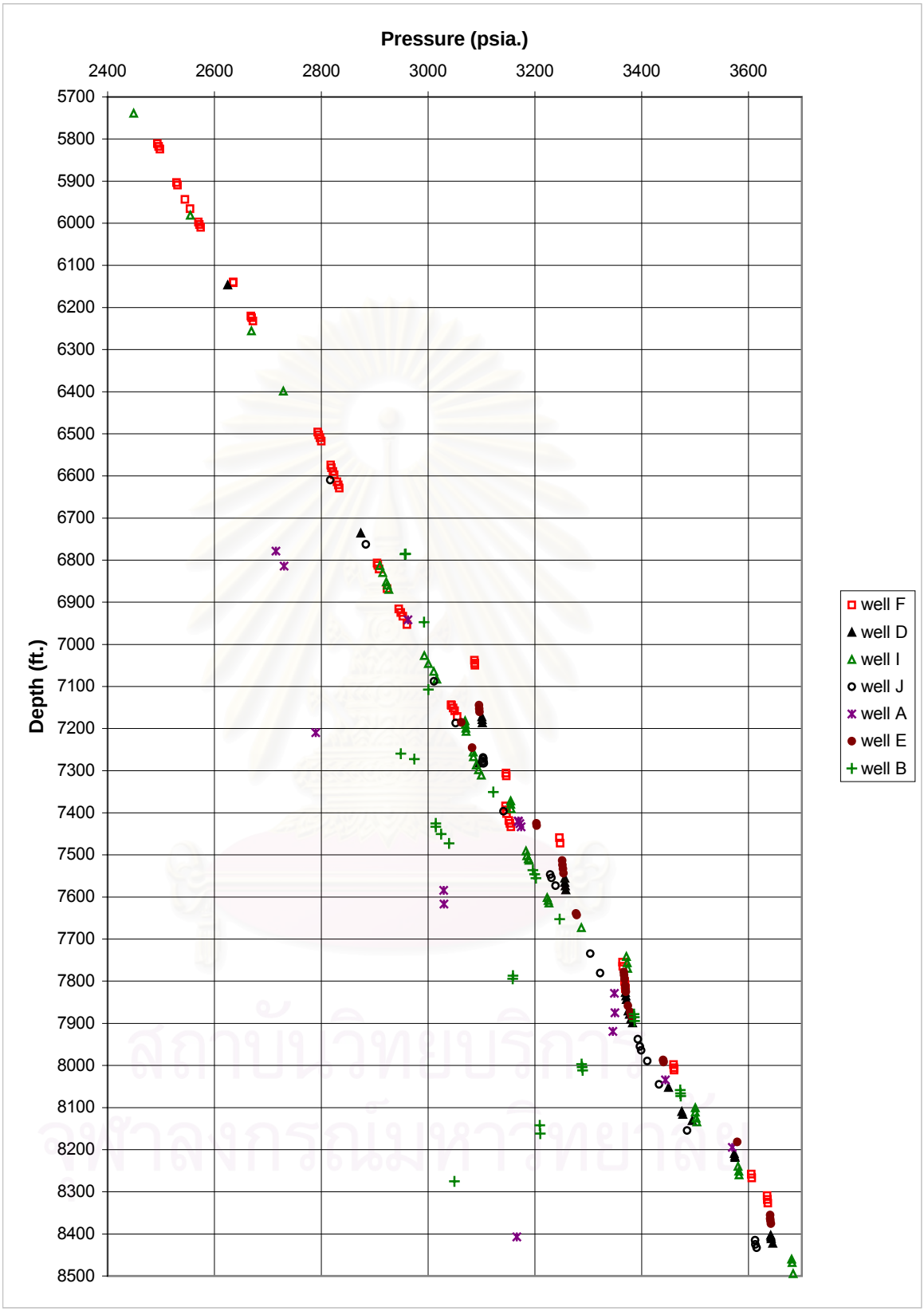

Figure 5.21 Repeat formation test (RFT) data plotted in pressure-depth diagram shown pore-pressure distribution in Benchamas-A field.

Horizon U-B3

RFT data from well F, E, D, J and I were used to analyze in this horizon.

Horizon overview: This horizon has the RFT data test, 4 wells in upthrown side and 1 well in downthrown side. Then the data overview can be used the individual data in well I to explain the result in downthrown horizon, whereas the conclusion RFT analyze from wells F, E, D and J are used to explain the result in upthrown side (**Figures 5.26 and 2.27**).

Fluid type: Gas and water.

Fluid gradient:

Upthrown side: Gas gradient = 0.0776psi/ft

Water gradient = 0.4207 psi/ft

Downthrown side: N/A (wet sand) psi/ft

Water gradient = 0.4079 psi/ft

Fluid contact depth:

Upthrown side: GWC = 7292 ft

Downthrown side: GWC = N/A ft

Horizon U-B4

RFT data from well F, E, D, J, B and I were used to analyze in this horizon.

Horizon overview: This horizon has the RFT data test, 4 wells in upthrown side and 2 wells in downthrown side. Then the data overview can be used the conclusion RFT analyze from well I, and B are used to explain the result in downthrown side. Whereas only data in well F can be used to explain the result in up thrown horizon because the other test points in well E, D and J there are not fit on curve when analyze the gradient (**Figures 5.28 and 5.29**).

Fluid type: Gas and water.

Fluid gradient:

Upthrown side: Gas gradient = N/A (wet sand) psi/ft

Water gradient = 0.4207 psi/ft

Downthrown side: Gas gradient = 0.0772 psi/ft

Water gradient = 0.4138 psi/ft

Fluid contact depth:

Upthrown side: GWC = N/A ft

Downthrown side: GWC = 7449 ft

Horizon U-B5

RFT data from well F, E, D, B, and I were used to analyze in this horizon.

Horizon overview: This horizon has the RFT data test, 3 wells in upthrown side and 2 well in downthrown side. Then the data overview can be used the conclusion RFT analyze. The wells I, and B are used to explain the result in downthrown side. And the wells F, E, D are used to explain the result in upthrown side. Water summary from well F, E and D is used to calculate GWC (**Figures 5.30 and 5.31**).

Fluid type: Gas.

Fluid gradient:

Upthrown side: Gas gradient =0.0980 psi/ft

Water gradient = 0.4176 psi/ft

Downthrown side: Gas gradient = 0.1047 psi/ft

Water gradient = 0.4138 psi/ft

Fluid contact depth:

Upthrown side: GWC = 7683 ft

Downthrown side: GWC = 8018 ft

Horizon U-B6

RFT data from well F, E, D, J, B, and I were used to analyze in this horizon.

Horizon overview: This horizon has the RFT data test, 4 wells in upthrow side and 2 well in downthrown side. Then the data overview can be used the conclusion RFT analyze. The wells I, and B are used to explain the result in downthrown side. And the wells F, E, D and J are used to explain the result in upthrown side (**Figures 5.32 and 5.33**).

Fluid type: Gas, Oil and Water.

Fluid gradient:

Upthrown side: Gas gradient = 0.0852 psi/ft

Oil gradient = 0.2439 psi/ft

Water gradient = 0.4571 psi/ft

Downthrown side: Gas gradient = 0.0953 psi/ft

Water gradient = 0.4147 psi/ft

Fluid contact depth:

Upthrown side: GOC = 7854 ft

OWC = 7974 ft

Downthrown side: GWC = 8311 ft

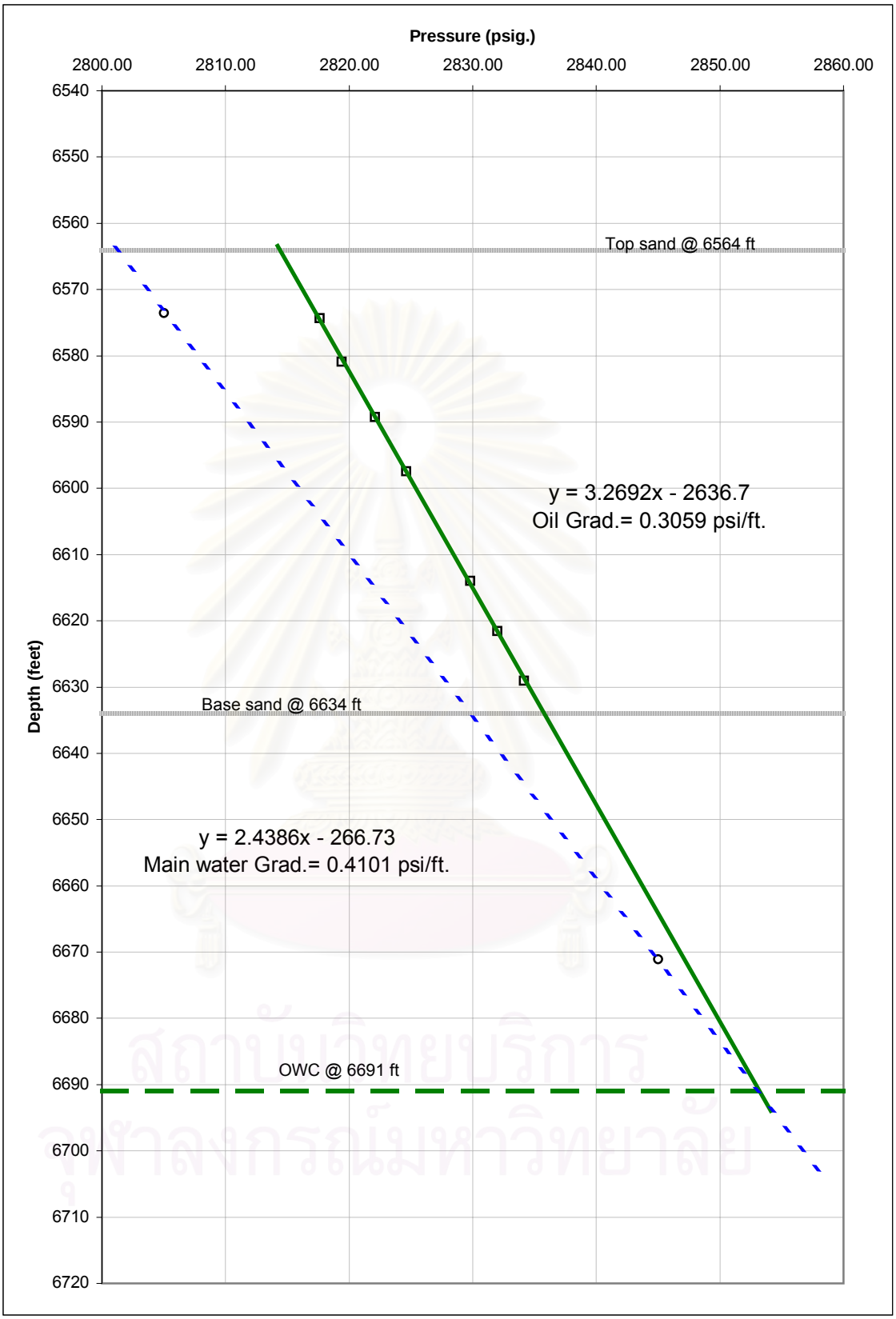

Figure 5.22 Pressure-depth diagram shown pore-pressure distribution in the oil reservoir horizon U-C6 upthrown side.

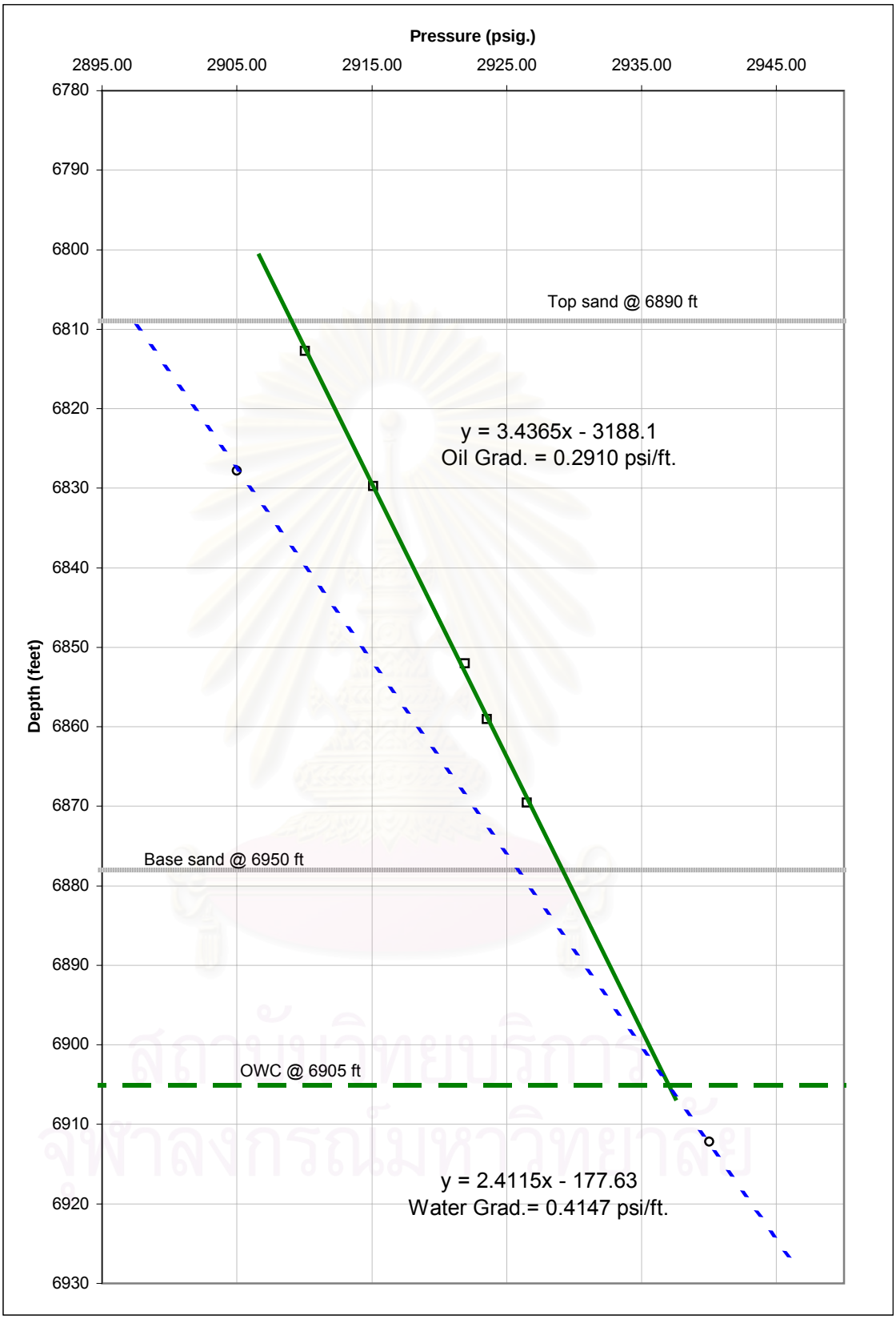

Figure 5.23 Pressure-depth diagram shown pore-pressure distribution in the oil reservoir horizon U-C6 downthrown side.

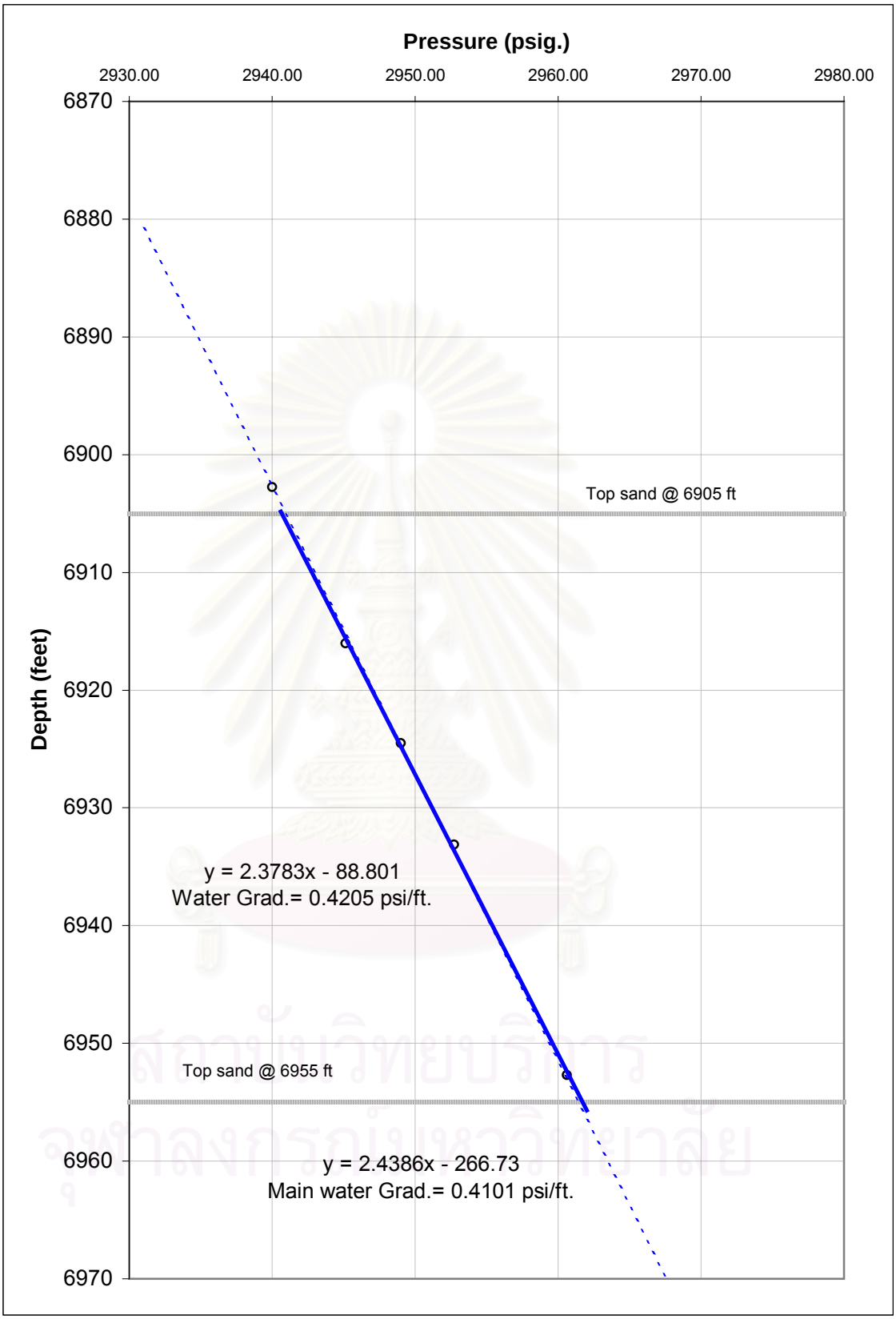

Figure 5.24 Pressure-depth diagram shown pore-pressure distribution in the wet sand horizon U-B2 upthrown side.

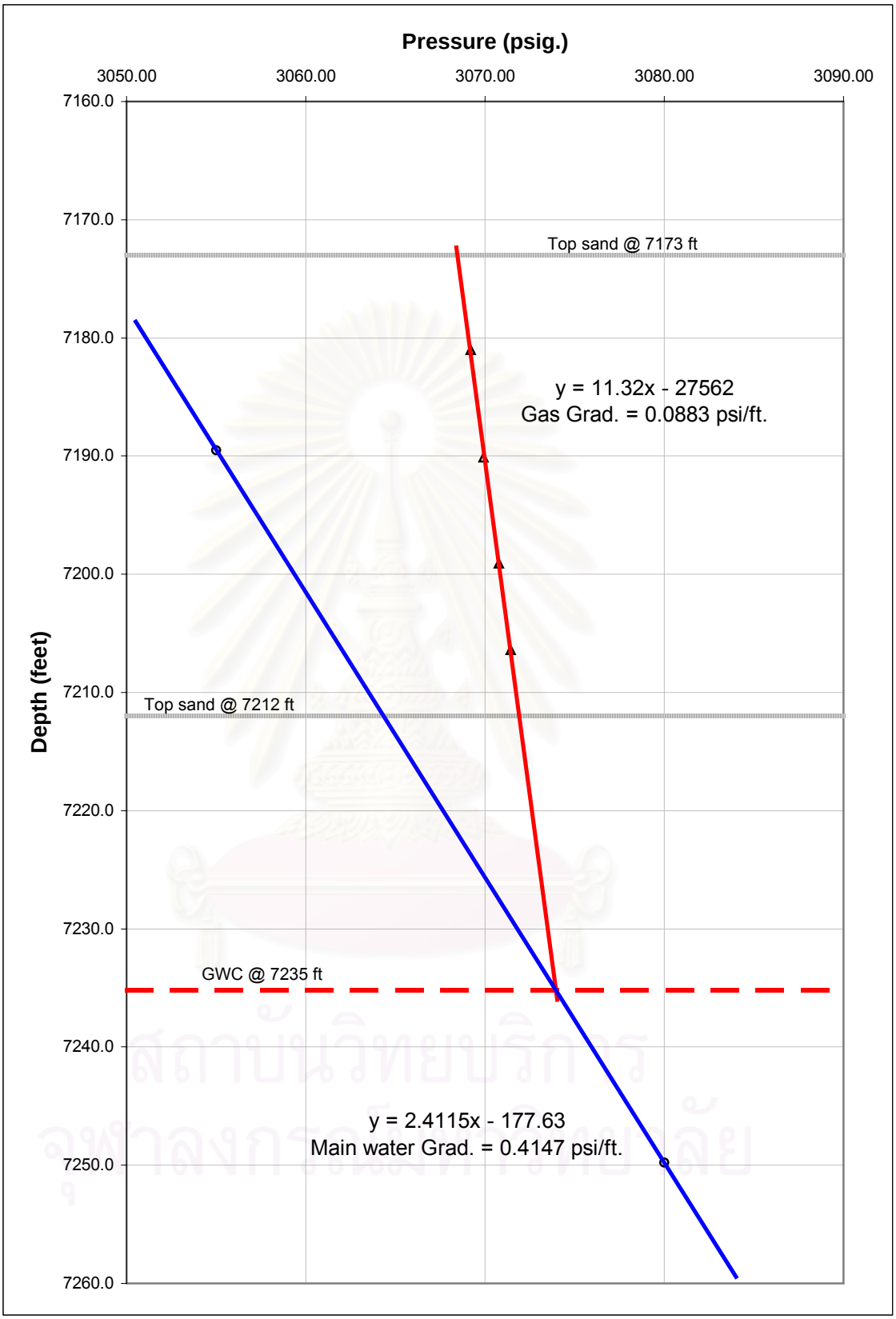

Figure 5.25 Pressure-depth diagram shown pore-pressure distribution in the gas reservoir sand horizon U-B2 downthrown side.

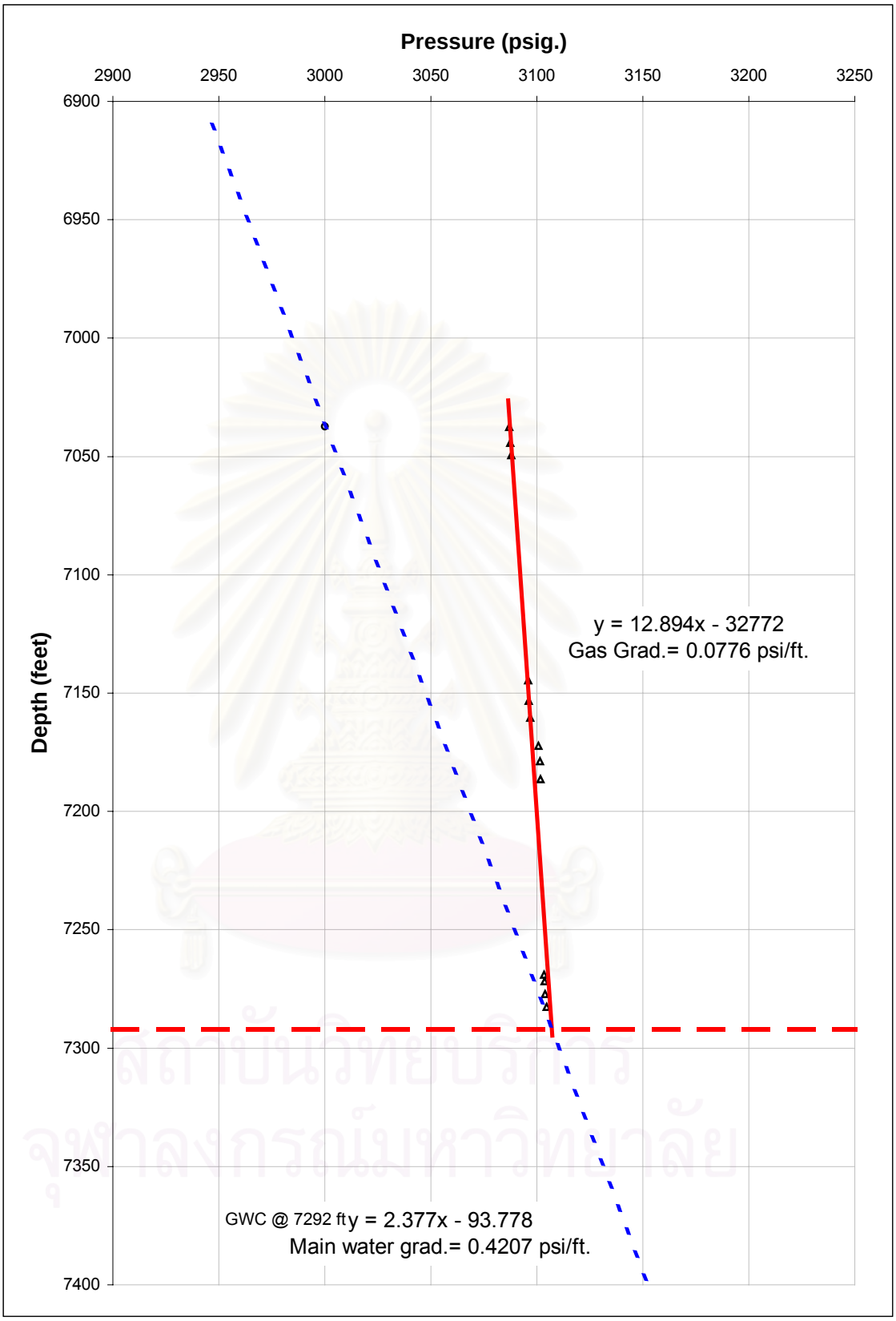

Figure 5.26 Pressure-depth diagram shown pore-pressure distribution in the gas reservoir sand horizon U-B3 upthrown side.

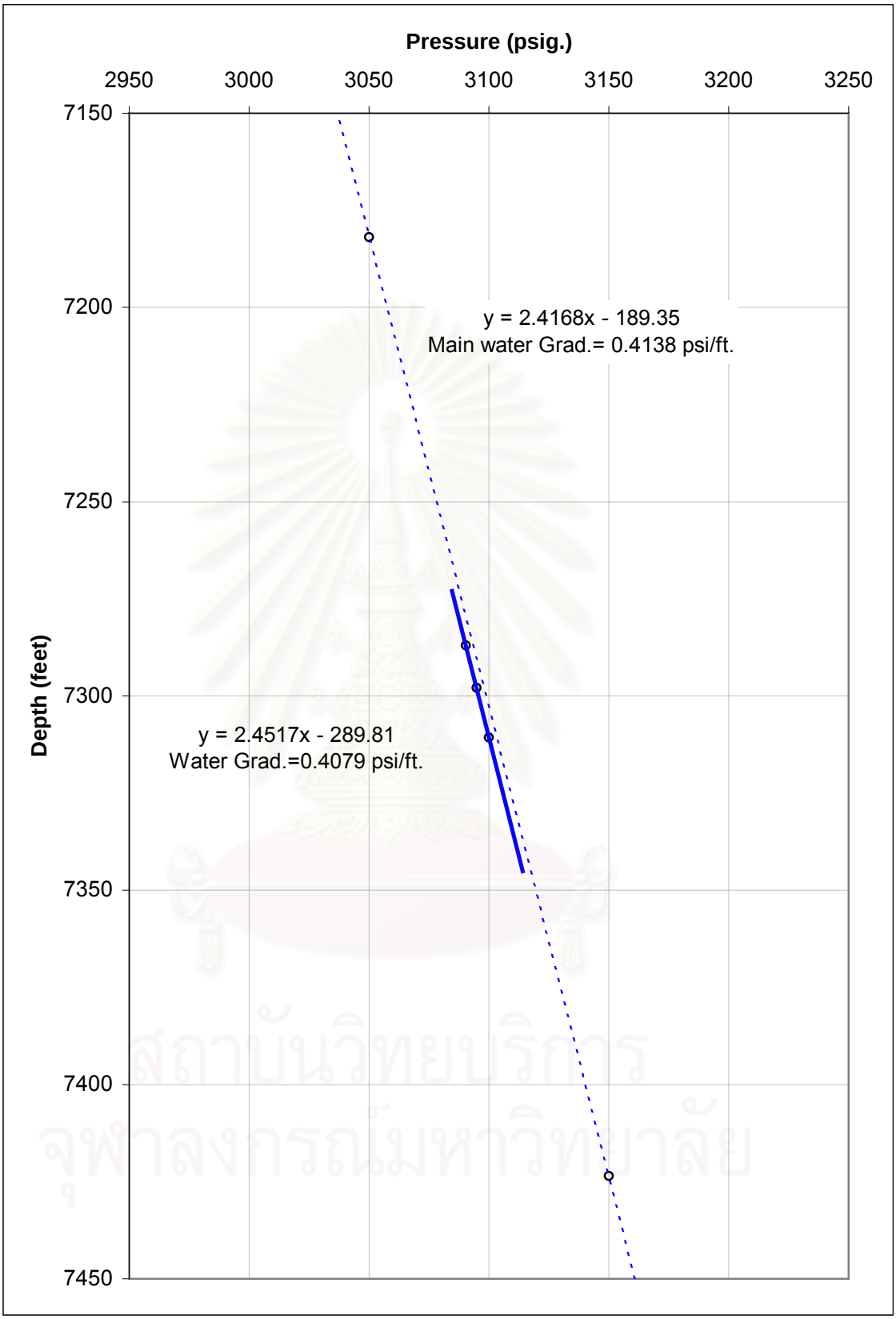

Figure 5.27 Pressure-depth diagram shown pore-pressure distribution in the wet sand horizon U-B3 downthrown side.

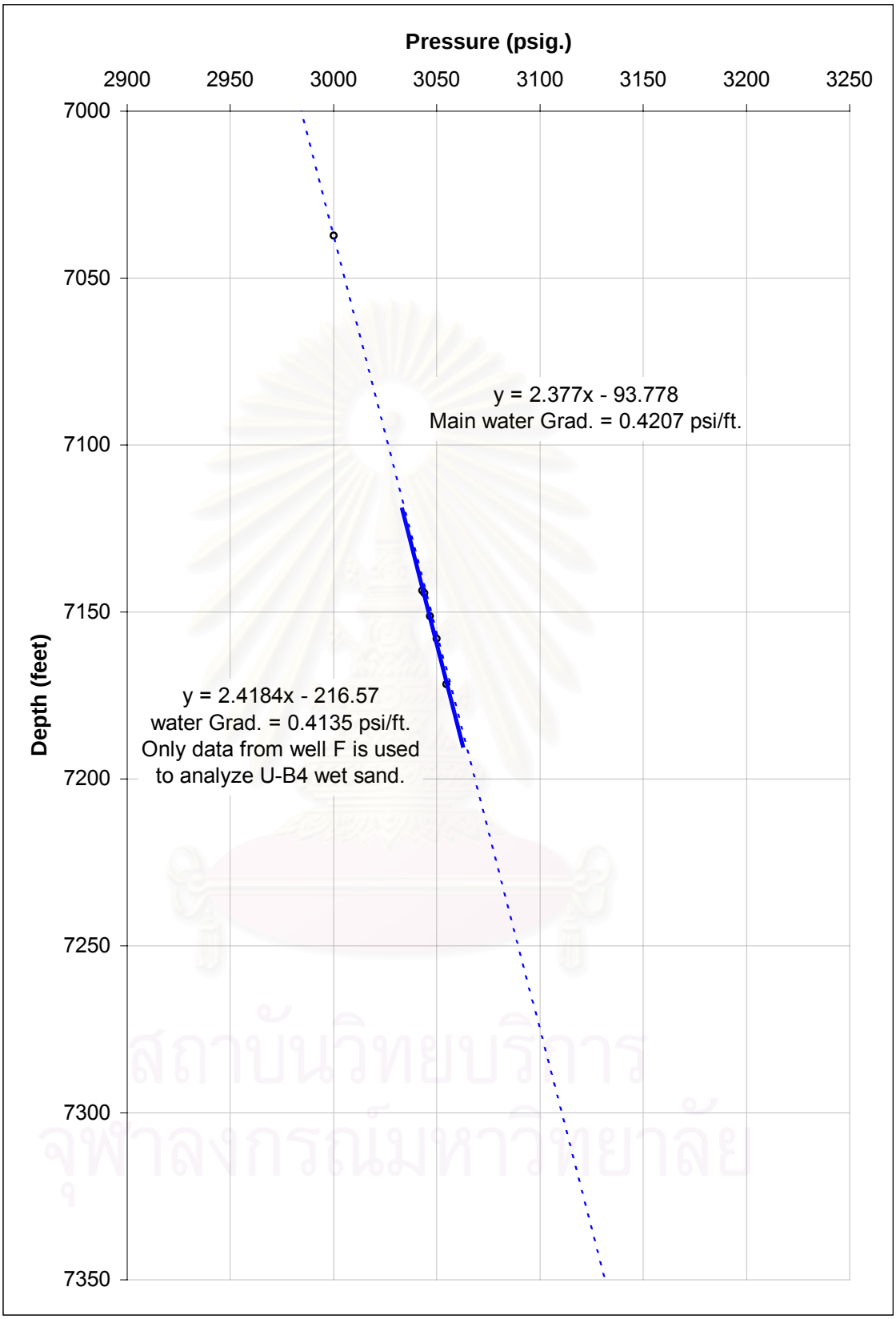

Figure 5.28 Pressure-depth diagram shown pore-pressure distribution in the wet sand horizon U-B4 upthrown side.

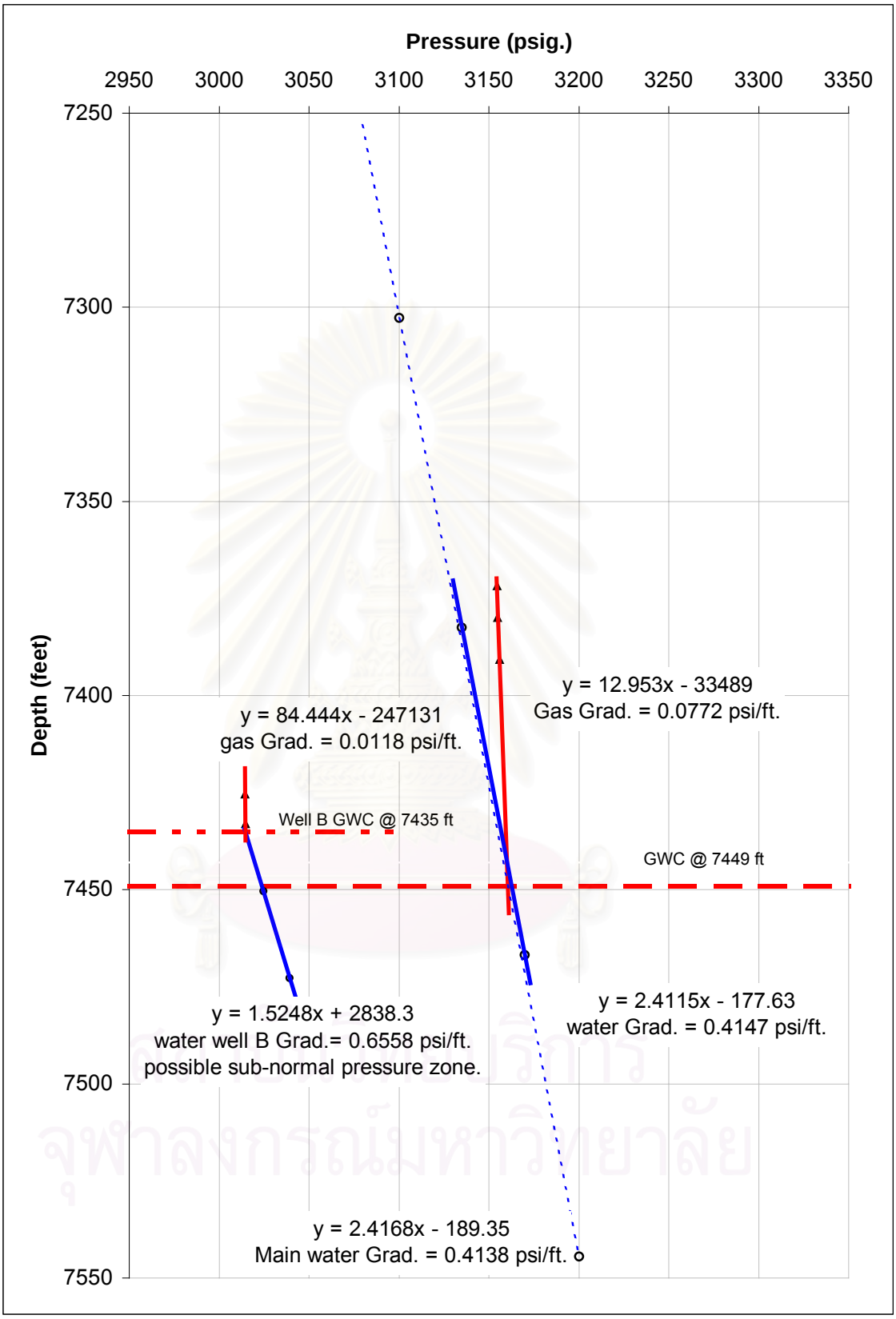

Figure 5.29 Pressure-depth diagram shown pore-pressure distribution in the gas reservoir horizon U-B4 downthrown side.

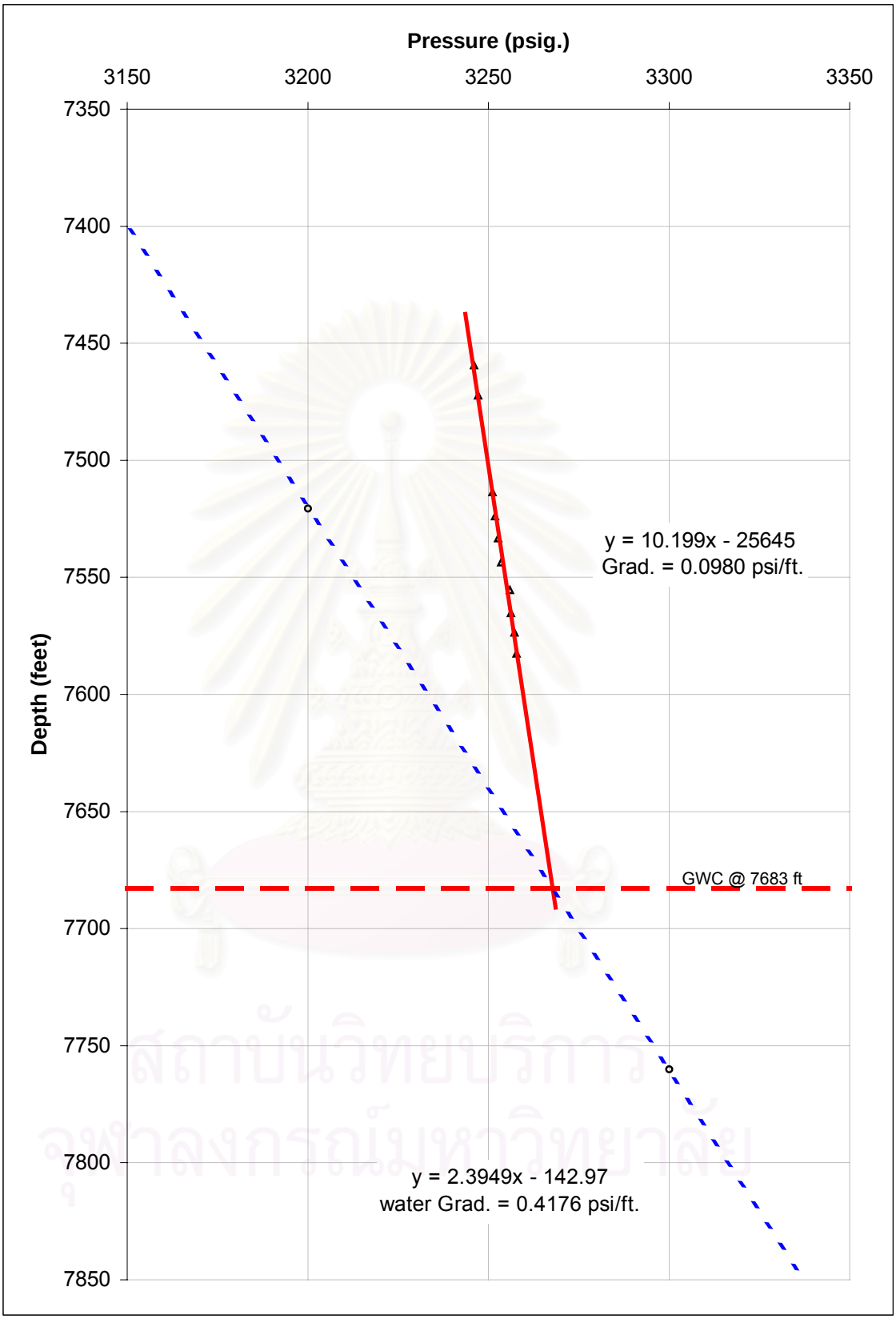

Figure 5.30 Pressure-depth diagram shown pore-pressure distribution in the gas reservoir horizon U-B5 upthrown side.

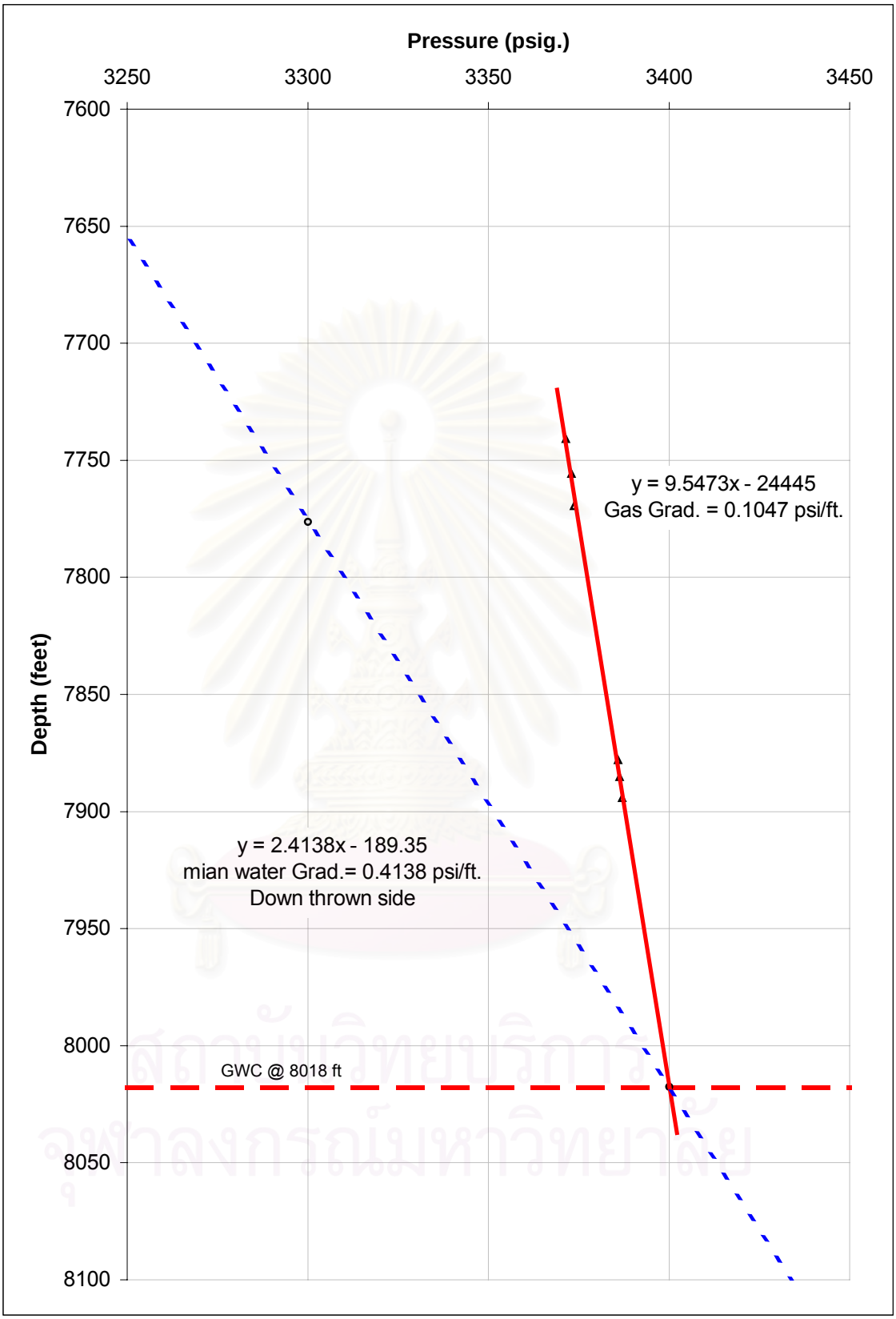

Figure 5.31 Pressure-depth diagram shown pore-pressure distribution in the gas reservoir horizon U-B5 downthrown side.

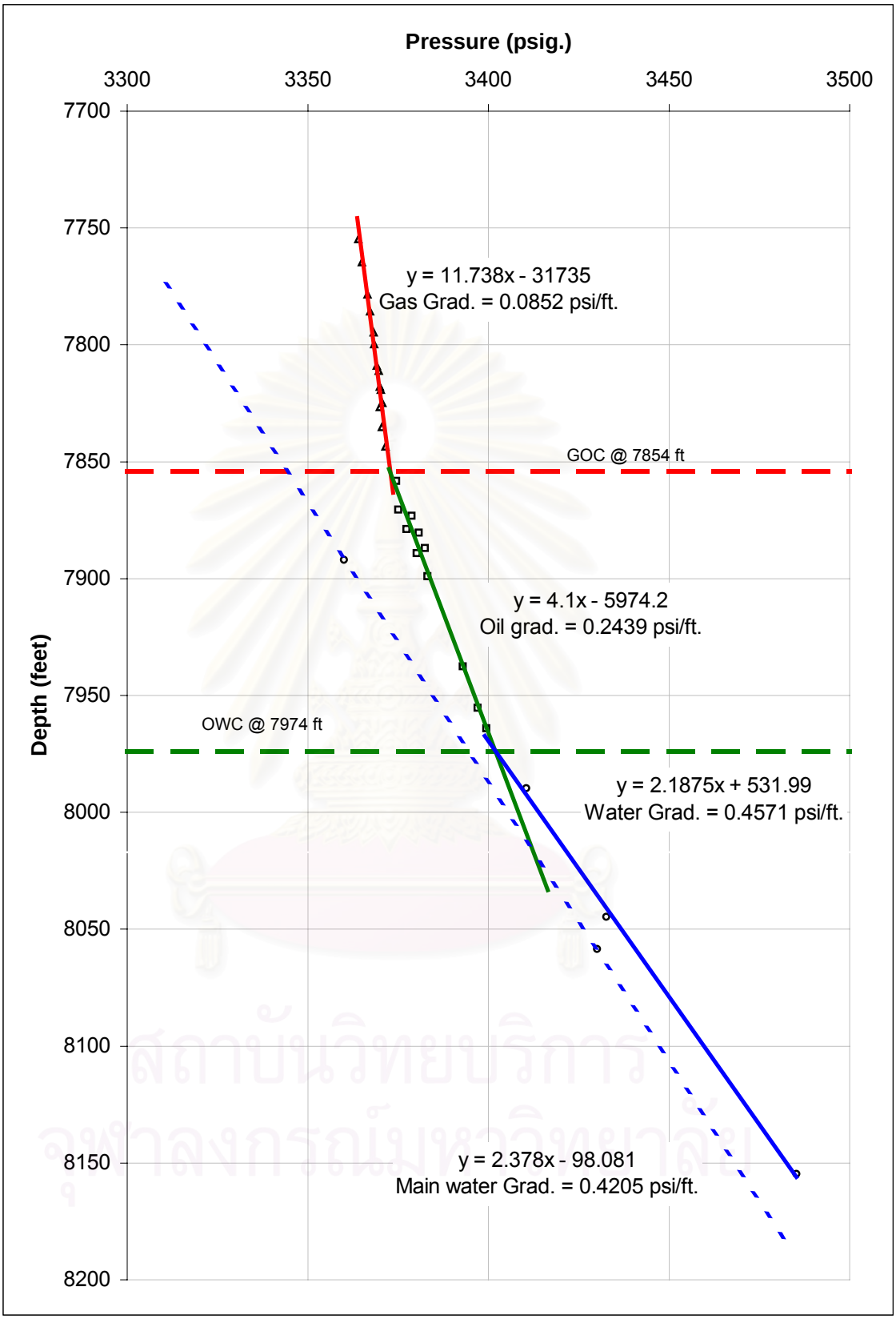

Figure 5.32 Pressure-depth diagram shown pore-pressure distribution in the gas and oil reservoir horizon U-B6 upthrown side.

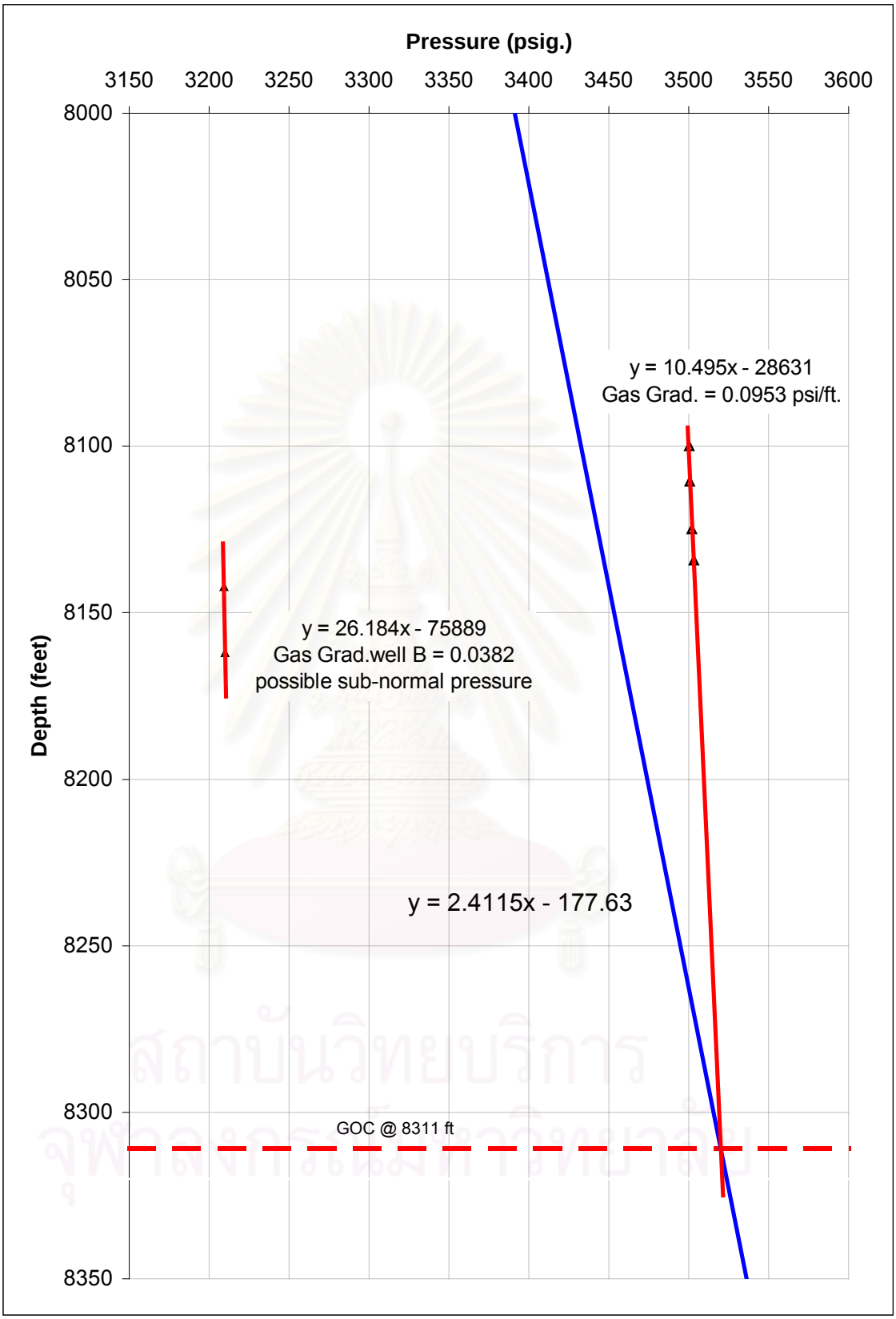

Figure 5.33 Pressure-depth diagram shown pore-pressure distribution in the gas reservoir horizon U-B6 downthrown side.

5.7.2 Horizon sand-to-sand juxtaposition

The wet sand horizon U-B4 in the upthrown side juxtaposed against gas reservoir horizon U-B2 in downthrown side, both sand have different fluid type (**Figure 5.34**). The wet sand horizon U-B4 has water gradient about 0.4135 psi/ft, whereas the gas reservoir horizon U-B2 in downthrown has a gas gradient about 0.0883 psi/ft, water gradient about 0.4147 psi/ft, and GWC at 7235 ft. **Figure 5.34** is a schematic cross section across the Benchamas-A Fault showing the considerable amount of sand horizon U-B4 upthrown offset with gas reservoir horizon U-B2 downthrown. The gas-water contact (GWC) in gas reservoir U-B2 in the downthrown side lies below the wet sand horizon U-B4 downthrown.

The pressure data (**Figure 5.35**) shows that reservoir horizon U-B2 downthrown is overpressured by about 15 psi with respect to the upthrown U-B4 sand horizon at the offset sand (7147 to 7175 ft), hence these two sands are different fluid compartment. Moreover, in the case of Benchamas-A Fault not seal and sand horizon U-B4 upthrown has pore-pressure lowers than U-B2 gas reservoir, fluid like a gas phase must be cross-flow across the Benchamas-A Fault by buoyancy drive and accumulated into U-B4 sand horizon. For this reason the overlap sand between U-B4 upthrown and U-B2 downthrown can be recognized as the fluid networks did not occur across the fault and that fluid accumulation took place in the isolating compartments, hence gas reservoir U-B2 downthrown is sealed by capillary seal at these overlap area (28 ft).

The gas and oil reservoir horizon U-B6 in the upthrown juxtaposed against downthrown gas reservoir horizon U-B5 (7739 to 7904 ft), both side have some fluid different type (**Figure 5.36**). U-B6 upthrown consists of gas and oil, gas gradient 0.0852 psi/ft, and oil gradient about 0.2439 psi/ft, GOC at 7854 ft, and OWC at 7974 ft. The gas reservoir U-B5 downthrown has a gas gradient about 0.1047 psi/ft and GWC at 8018 ft.

Hydrocarbon contacted depth in both sands are different level contact (**Figure 5.37**). When compared the pore-pressure between reservoir horizon U-B6 upthrown against U-B5 downthrown, the different pressure across a

fault vary from 5 to 10 psi, both reservoirs are completely different fluid gradient lines and separated form the other one (cannot superimpose). As the same case before, if Benchamas-A Fault is not seal the pressure must be make equalize pressure between the upper-part where gas is bearing sands juxtaposition. For this reason, the overlap sand horizons between U-B6 upthrown and U-B5 downthrown can be recognized both sands are not fluid in communication across the Benchamas-A Fault, hence hydrocarbon reservoir U-B6 upthrown and U-B5 downthrown is sealed by capillary seal at these overlap area (265 ft).

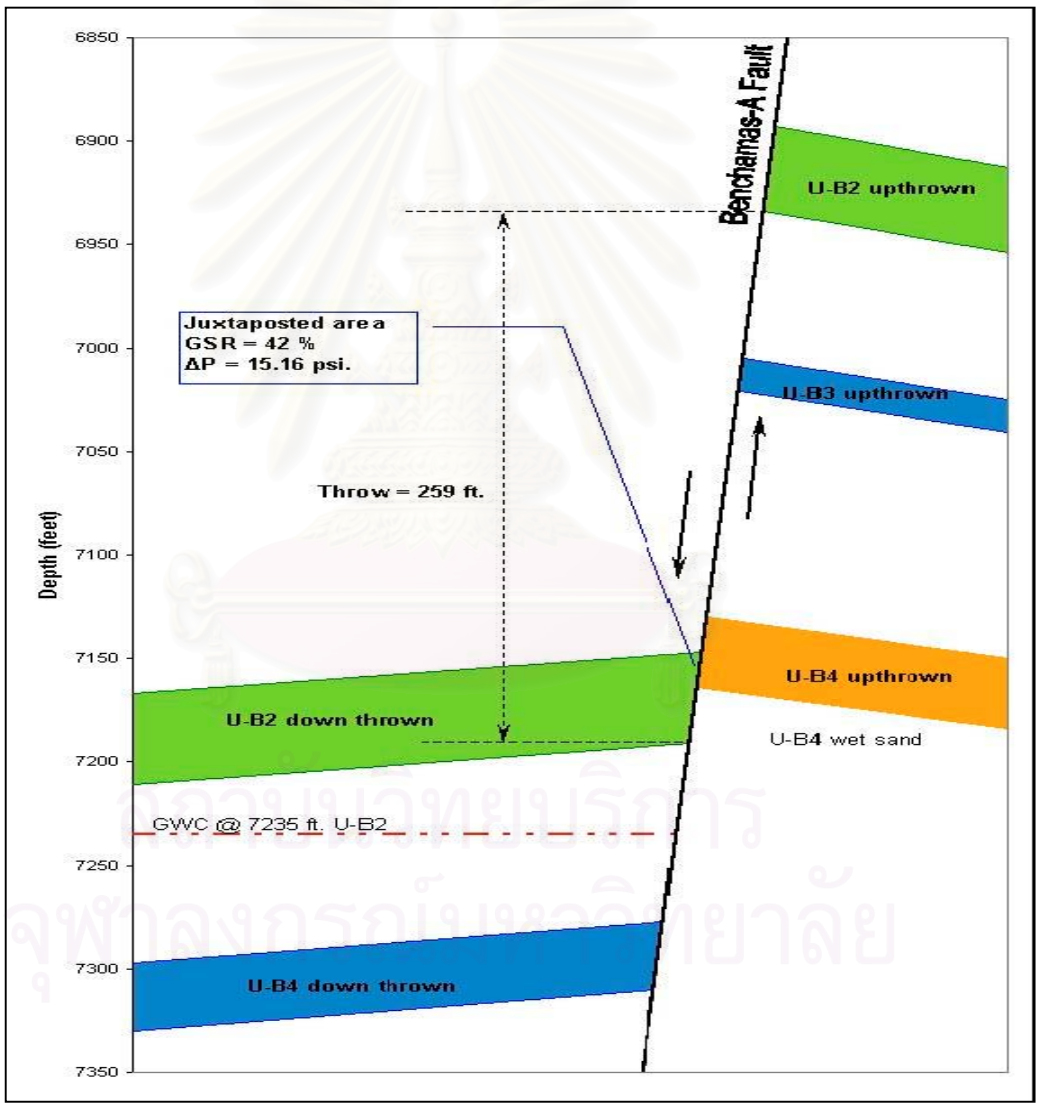

Figure 5.34 Cross-section across a fault where the overlap sands horizons U-B4 upthrown and U-B2 downthrown (distance a long the fault = 250 ft). U-B4 upthrown is wet sand, whereas U-B2 downthrown is gas reservoir and GWC at 7235 ft. The overlap = 17 ft in vertical.

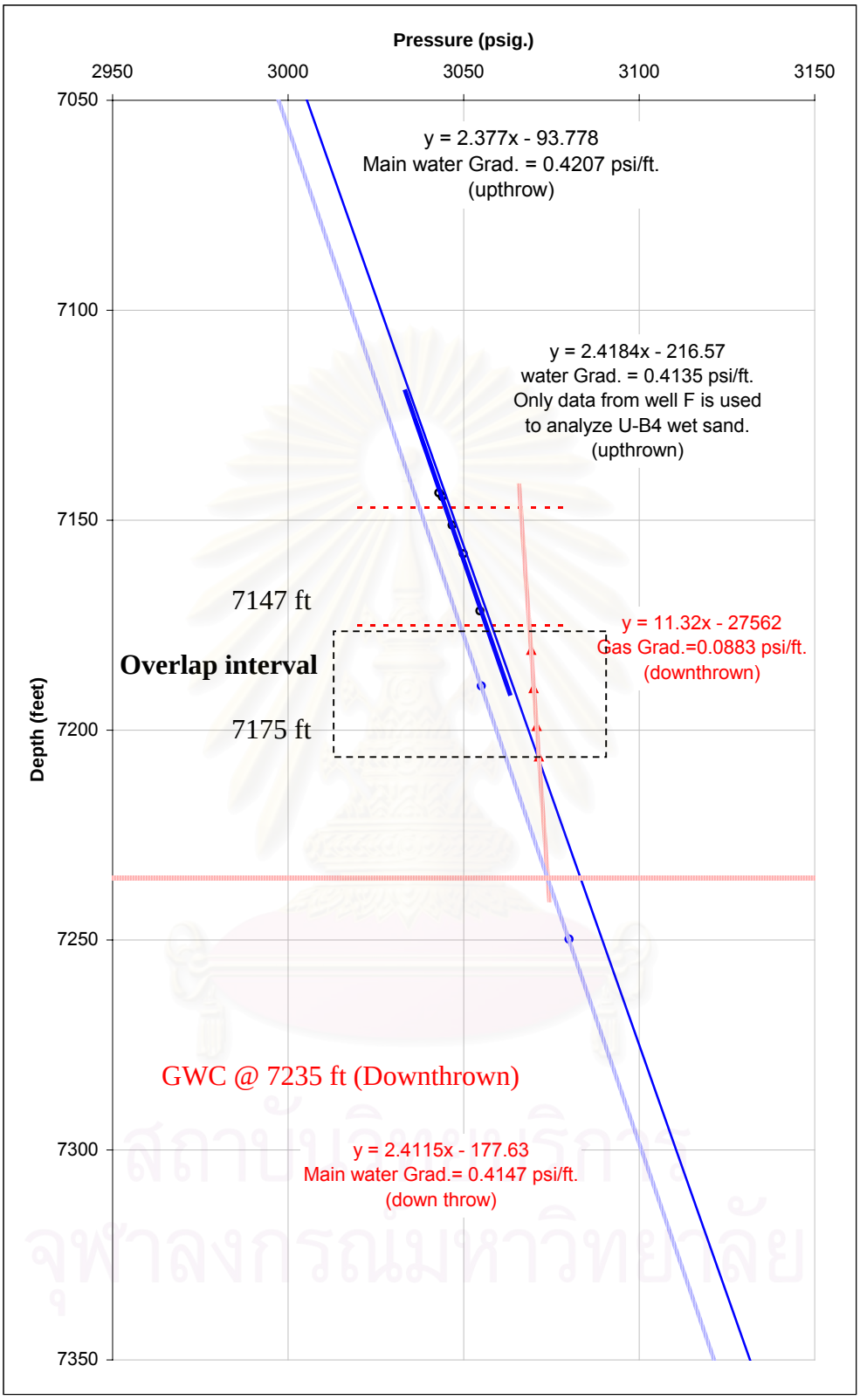

Figure 5.35 Pressure-depth diagram shown pore-pressure distribution in horizon U-B4 upthrown and U-B2 downthrown. The maximum across-fault pressure difference = 21 psi at the top of reservoir horizon U-B2 downthrown.

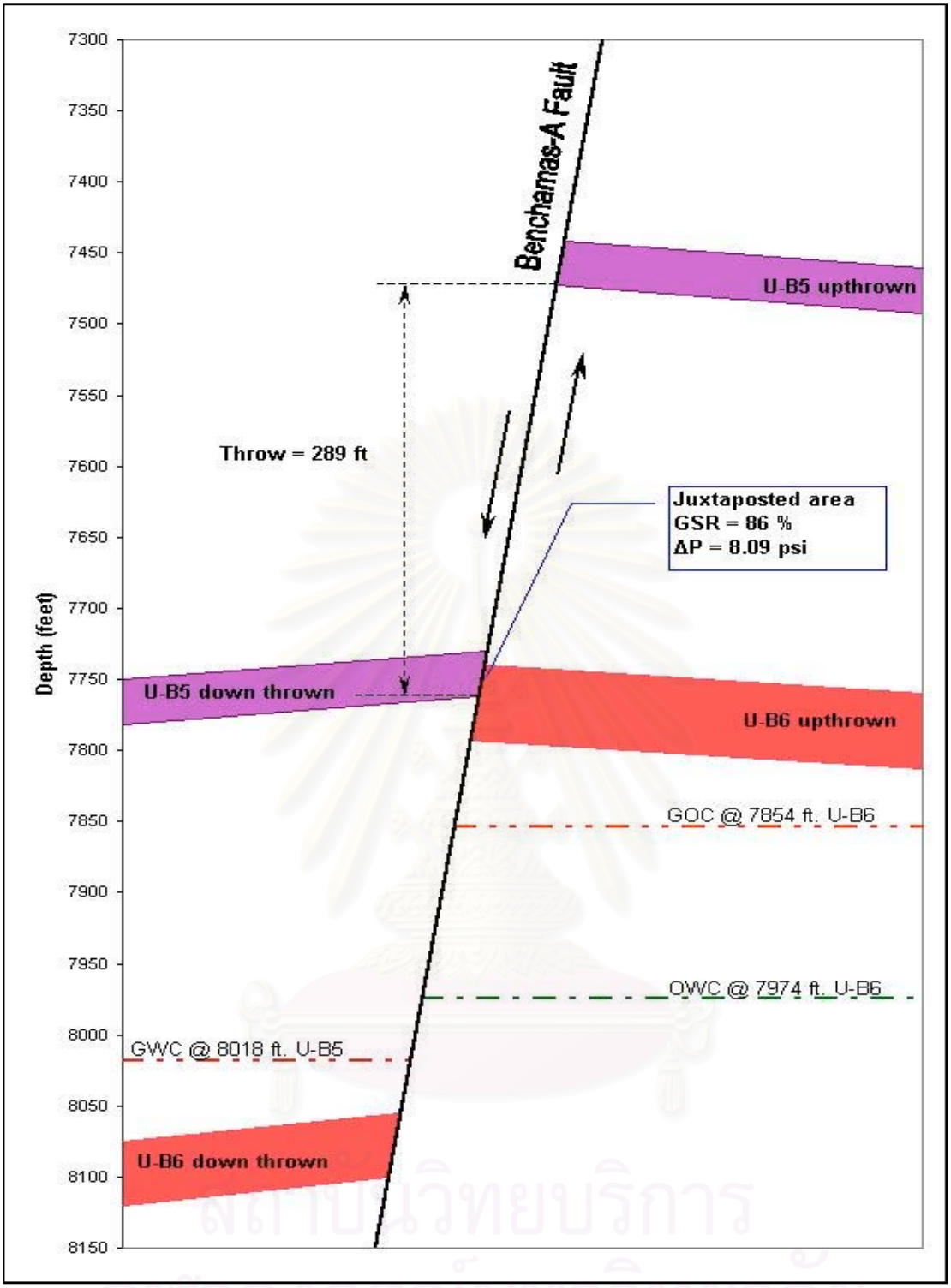

Figure 5.36 (a) Cross-section of overlap sand horizon U-B6 upthrown and U-B5 downthrown (distance a long the fault = 0 ft). U-B6 upthrown is the gas and oil reservoir, GOC at 7854 ft, and OWC at 7974 ft, whereas U-B5 downthrown is gas reservoir and GWC at 8018 ft. The overlap = 22 ft.

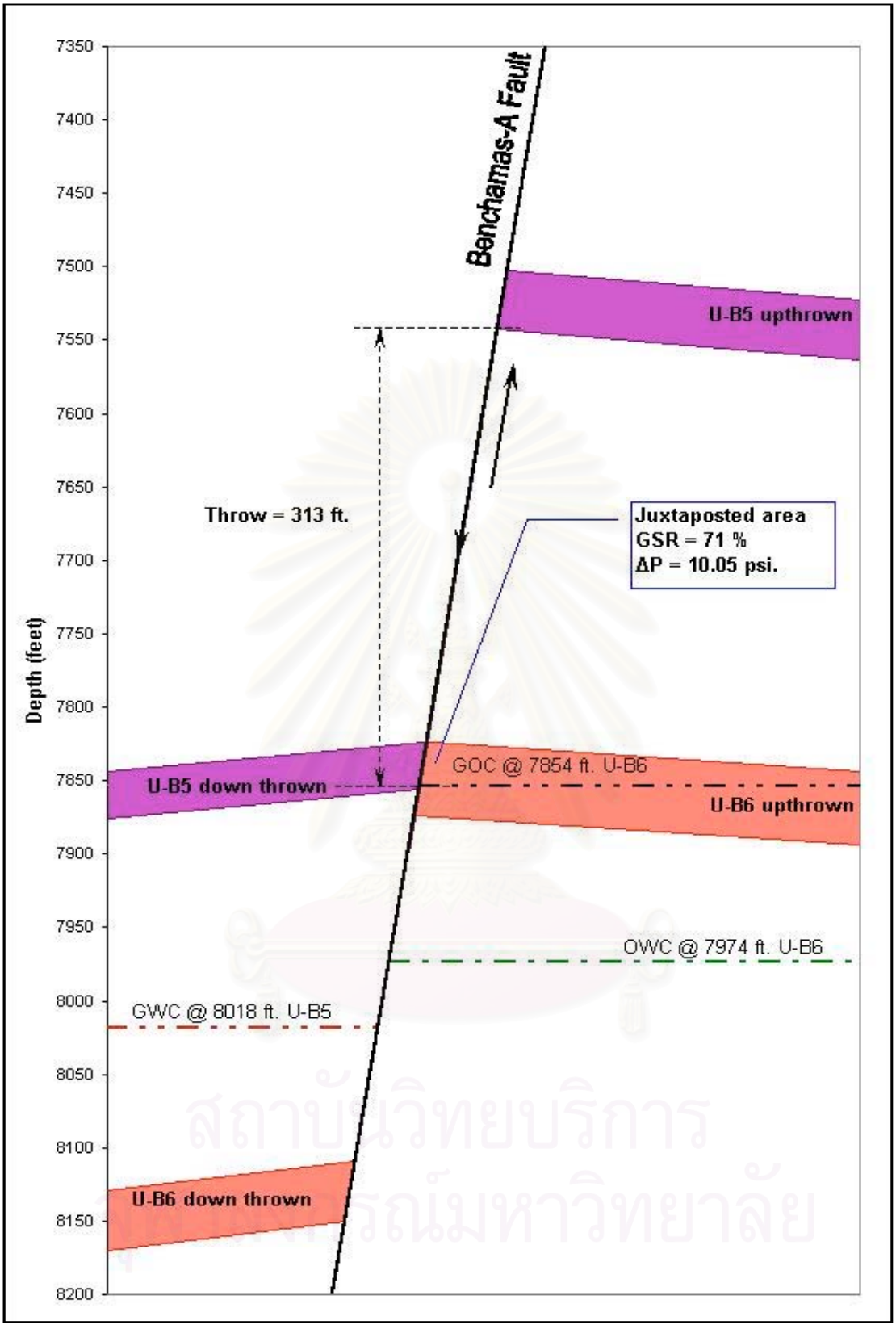

Figure 5.36 (b) Cross-section of overlap sand U-B6 upthrown and U-B5 downthrown (distance a long the fault = 1100 ft). The overlap = 21 ft in vertical.

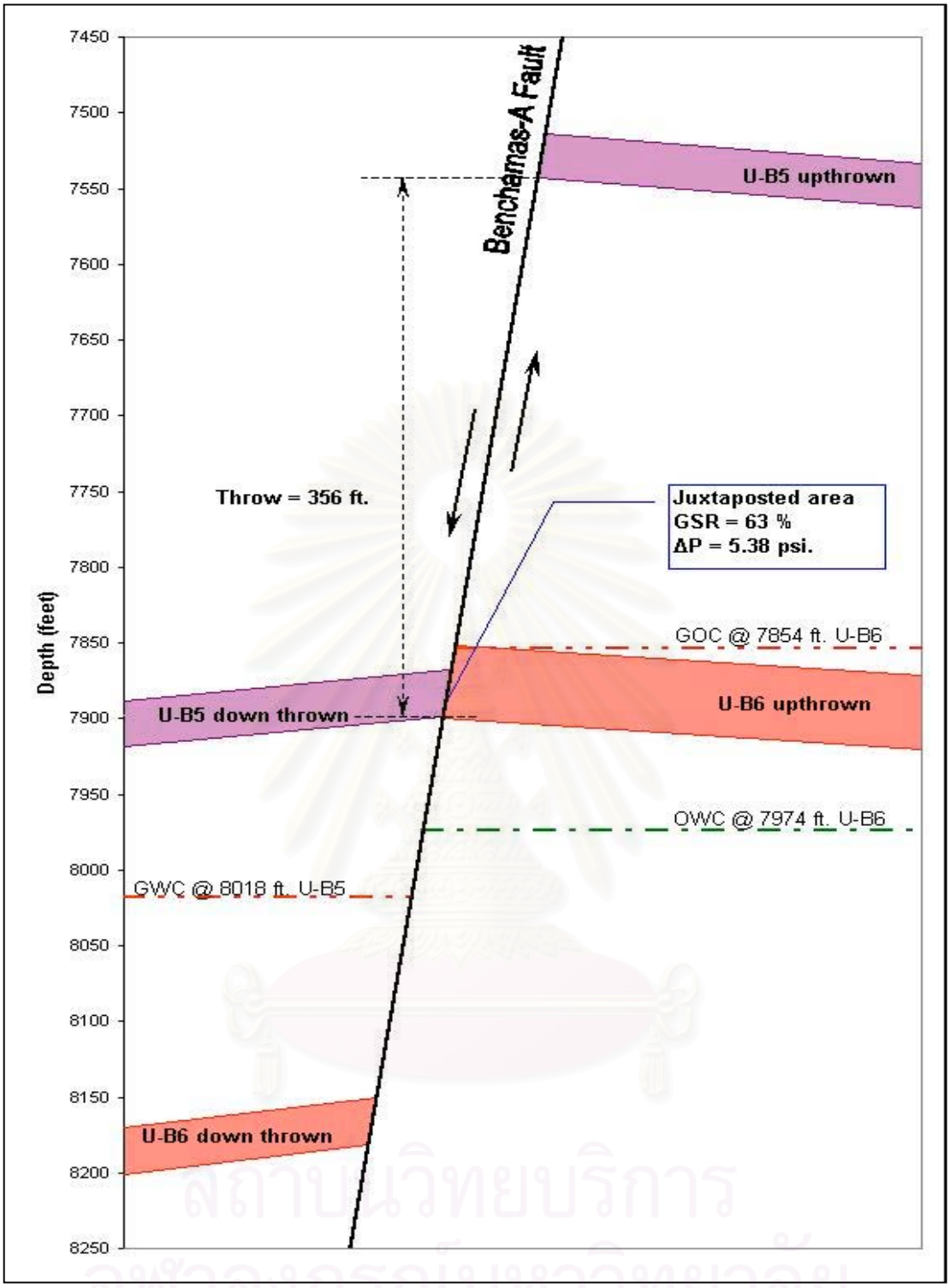

Figure 5.36 (c) Cross-section of overlap sand U-B6 upthrown and U-B5 downthrown (distance a long the fault = 1650 ft). The overlap = 21 ft in vertical.

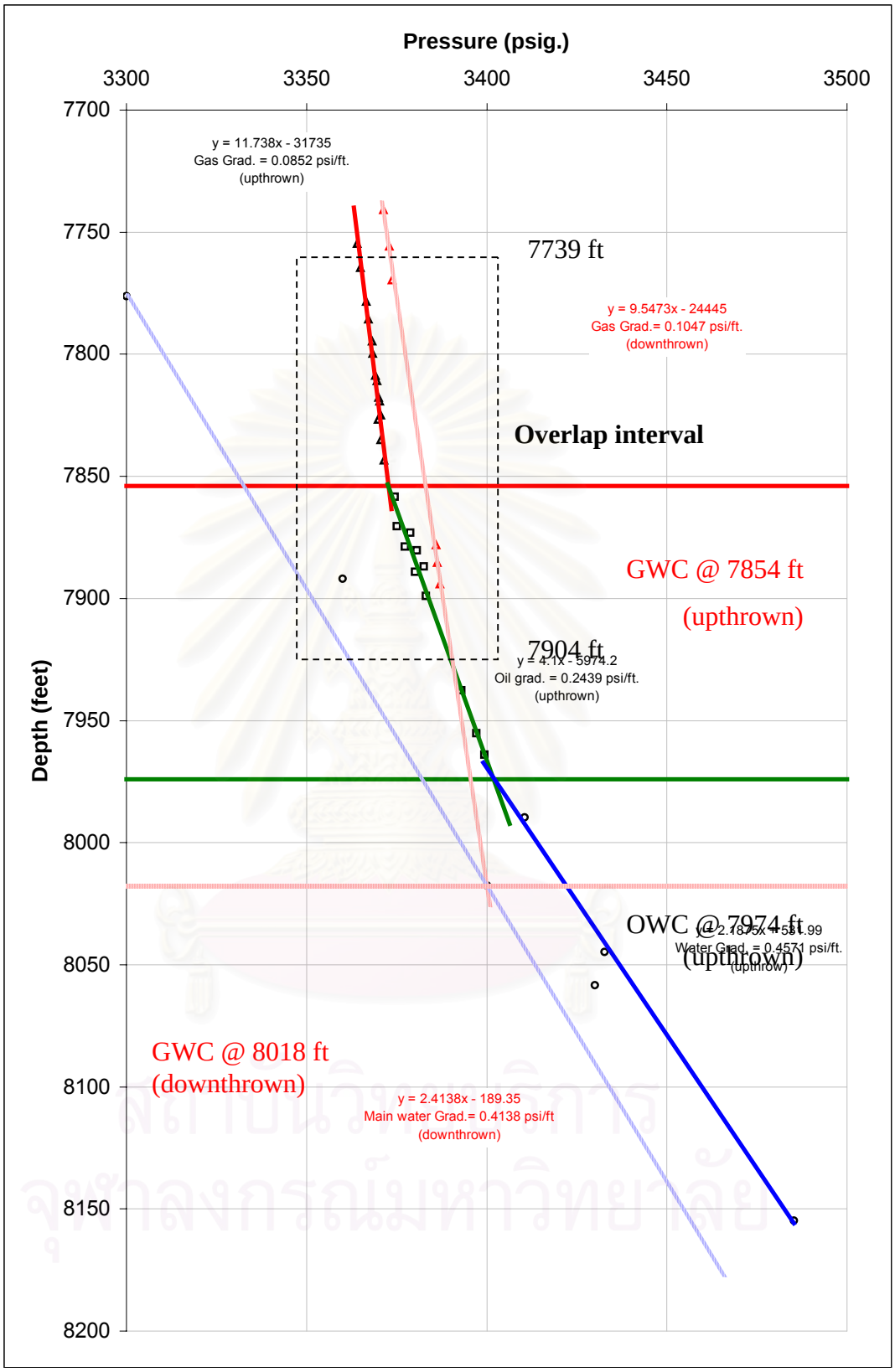

Figure 5.37 Pressure-depth diagram shown pore-pressure distribution in horizon U-B6 upthrown and U-B5 downthrown. The differential pressure across-fault = 8 to 10 psi.

5.8 Cross-fault pressure difference and static seal

Shale gouge ratio is, in itself, not a measure of sealing capacity of the fault surface. Instead, they are estimates of the relative likelihood of clay smear being developed at the fault surface. In order to use these attributes as estimates of seal capacity, it must be calibrated in datasets where sealing behavior is documented from well data (Yielding, 1999). The difference between these distributions is the pressure difference across the fault zone. In the case of static seal (preproduction) this pressure difference is a minimum estimate of the seal capacity (capillary entry pressure) of the fault zone.

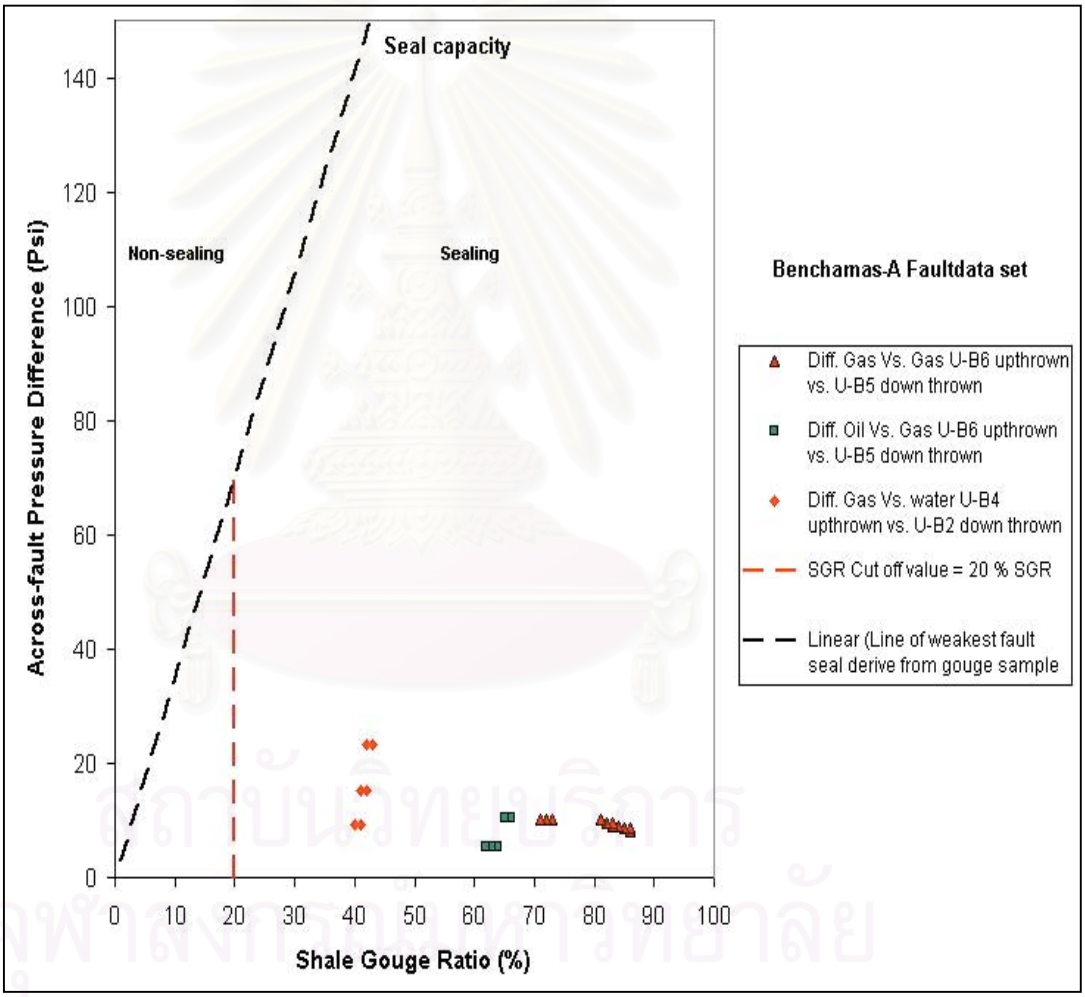

Figure 5.38 Fault seal capacity plots for Benchamas-A Fault, illustrating the relationship between across-pressure difference and shale gouge ratio (SGR). Each point corresponds to one grid node on the offset area (attributes gridded at 25325 ft). Line of the weakest fault seal was derived from Yielding et al., (2002).

The seal capacity on Benchamas-A Fault have investigated by comparison of the shale gouge ratio and across-fault pressure difference, at sand horizon U-B4 upthrown overlap with the gas reservoir horizon U-B2 downthrown and the gas-oil reservoir U-B6 upthrown offset with the gas reservoir U-B5 downthrown. The dashed line represents an estimate of seal capacity of the fault. Points close to this line are expected to be near the capillary entry pressure for that part of the fault, i.e. may be critical in controlling the seal potential. The interpretation of this plot is that the area below the envelope represents the static fault seals, whereas the area above the envelope represents seal failure of fault rocks (**Figure 5.38**). The minimum of shale gouge ratio at 40% that can be supported across-fault pressure difference at 9 psi and rapidly increasing seal capacity when the shale gouge ratio 40 to 42%. Moreover, all of the datasets that plotted in **Figure 5.38** lie in the area of static seal and no any overlap sands have pressure flow across the Benchamas-A Fault (at $\Delta P = 0$). This indicates the Benchamas-A Fault seals, at any overlap sands on a fault surface. The minimum SGR represent at 40% that means the number of fine-grained source beds, shale volumes, and fault throw are the factors to generate the high number of SGR on the Benchamas-A Fault.

5.9 Result of clay smear in fault zone

Benchamas-A Fault is considered as a fault sealing by clay smear. For every overlap interval are presented shale gouge ratio higher than 40%. The overlap sands U-B4 upthrown against U-B2 downthrown and U-B6 upthrown against U-B5 downthrown both areas have shale gouge ratio higher than 20% that is used to indicate the general minimum seal capacity in knew fault sealing and non-sealing (Yielding et al., 1999). Moreover, pore-pressure and fluid properties between upthrown and downthrown in overlap sand represented no fluid in communication across Benchamas-A Fault because on the overlap sands have capillary seal by fine-grain material, i.e., phyllosilicate.

5.10 Potential fault sealing prediction model on Benchamas-B Fault

The Benchamas-B Fault is located at the western of Benchamas-A field. This fault is one important fault trap because this fault controls the structure closure at the western of basin. This fault has the throw higher than Benchamas-A Fault and the lithological detail would be the same therefore the clay smear is possible to created seal on this fault as same as Benchamas-A Fault. Additionally, the comparison of shale gouge ratio results that calculated from the juxtaposition diagram and Allan fault plane (grid cells) (**Figures 5.19, 5.20, and b**) both algorithms gave the similar results. Therefore the juxtaposition diagram could be applied to estimate the potential sealing on Benchamas-B Fault.

To estimate the potential sealing on this Benchamas-B Fault, the juxtaposition diagram had been applied to investigate the shale gouge ratio history and compare these shale gouge ratio value with the shale gouge ratio in Benchamas-A Fault that effective to seals and traps hydrocarbon on the faulted reservoirs.

The juxtaposition diagram (Bentley and Barry, 1991, and Knipe 1997) was constructed to present the overlap sands and shale gouge ratio history that presented at each throw in the overlap sand areas onto the fault plane. The horizontal lines represent an upthrown side to a fault, the diagonal lines represent the downthrown side. Throw increases linearly to the right (shown along the top margin). The triangular and parallelogram area represent the different zone juxtapositions at various parts of a fault plane. Shale volume value from the adjacent wells has been assigned to the reservoir zones. At every location on the juxtaposition diagram (**Figure 5.39**), the shale volumes in slipped interval have been used to calculate shale gouge ratio, which is then displayed using the color-coding. Blue represents low shale gouge ratio, i.e., low phyllosilicate content in the fault gouge. Such areas will be expected to have low capillary entry pressure and relatively good permeability. Conversely, the red areas have high shale gouge ratio, indicating shaly fault gouge with high capillary entry pressure and low fault zone permeability.

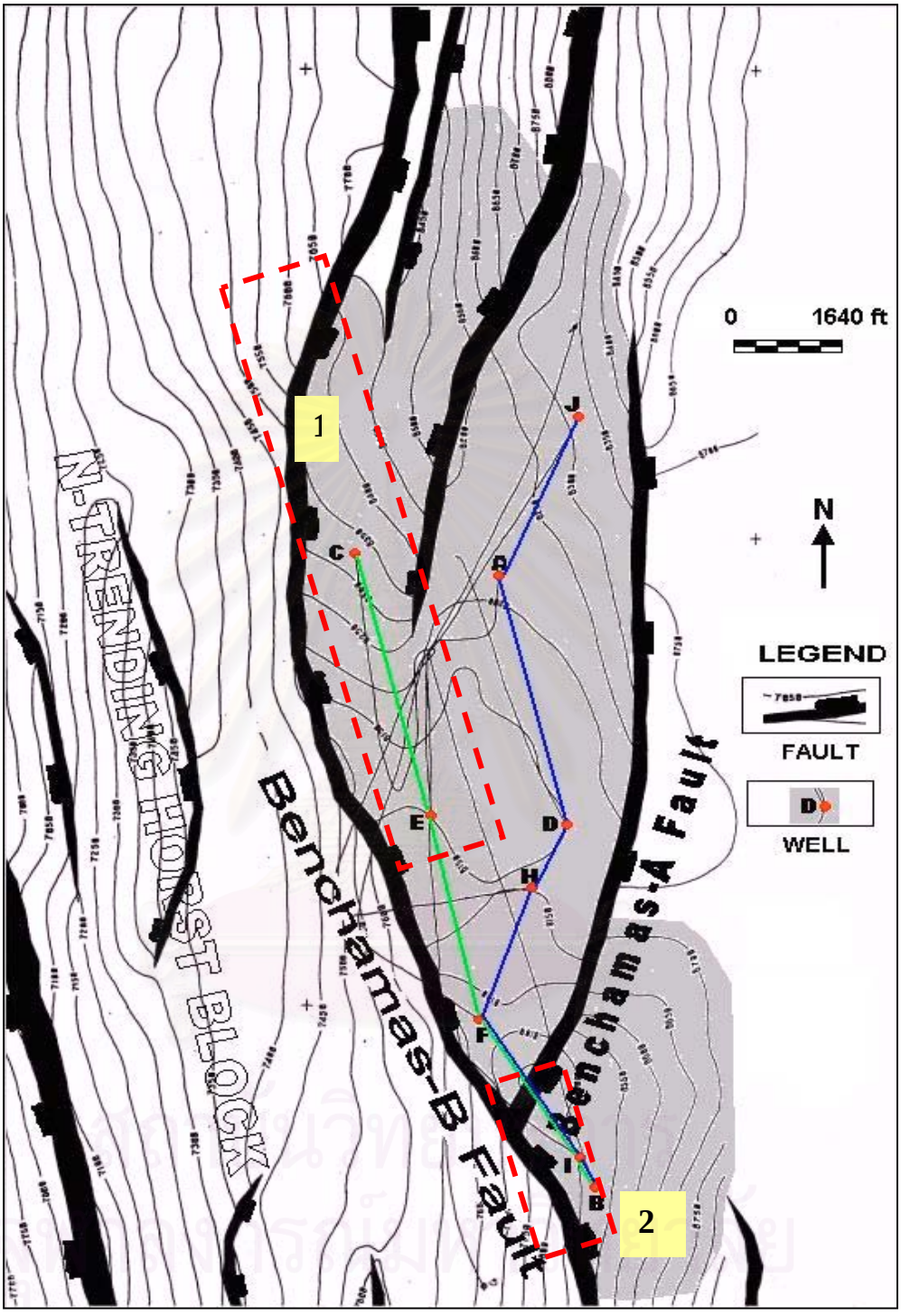

Figure 5.39 Benchamas-B Fault locates in the western area of the Benchamas-A field. The red rectangular represents the area of fault study.

Assumptions are used to interpret the potential sealing of Benchamas-B Fault as follows;

1) The upthrown stratigraphy is the same as downthrown stratigraphy. By using well data from well B, C, E, F, H, and I;

2) Where there is non-reservoir (shales) juxtaposed against reservoir (sands), those juxtaposed area have sealing potential (Allan, 1989);

3) Potential fault sealing have presented by triangle diagram that can represent only the history degree of shale gouge ratio in the overlap area (since there are no throw data); and

4) Fault has potential sealing at 20% SGR and 40% indicate seal by clay smearing.

The juxtaposition diagrams in **Figure 5.40** represent the potential sealing model on the Benchamas-B Fault at the western of basin. The color-coding represents the degree of shale gouge ratio at any overlap sand between upthrown and downthrown on the Benchamas-B Fault plane. The reservoir sand that present in the **Figure 5.40** include sand horizon U-C6, U-B2, U-B3, U-B4, U-B5, and U-B6. **Figure 5.40** can be used to describe sealing potential on the Benchamas-B Fault as follow below;

1) To estimate the potential sealing, this process has divided the datasets for interpretation into 2 groups. At the northern part of the Benchamas-B Fault (area 1) using the dataset form well C, E, H, and F to calculated the SGR values that represent in **Figure 5.40 (a)**. The other dataset (area2) using the data from well B and I to calculated the SGR values that represent in **Figure 5.40 (b)**.

2) At any overlap sands, the value of shale gouge ratio represents higher than 40% when throw more than 100 ft.

3) When the upper sand horizon moved downward to overlap the other lower sand horizon, shale gouge ratio presents higher than 40% at any overlap sand, these represents more probability clay smear occurs on fault plane.

4) The cause of throw on the Benchamas-B Fault > 450 ft, this throw is higher than Benchamas-A Fault throws. Therefore the shale gouge ratio would be presented at a high throw that due to move pass many fine-grained source beds.

5) The comparative degree of shale gouge ratio looks similar between Benchamas-B Fault and Benchamas-A Fault.

In conclusion, the Benchamas-B Fault is more probability to seal by clay smears like the Benchamas-A Fault the cause of high degree of shale gouge ratio and higher than 20%. Moreover, the hydrocarbon traps along the Benchamas-B Fault can observe in the upthrown and downthrown sides of the Benchamas-A field. Therefore, the hydrocarbon distribution in the western area have controlled by the Benchamas-B Fault.

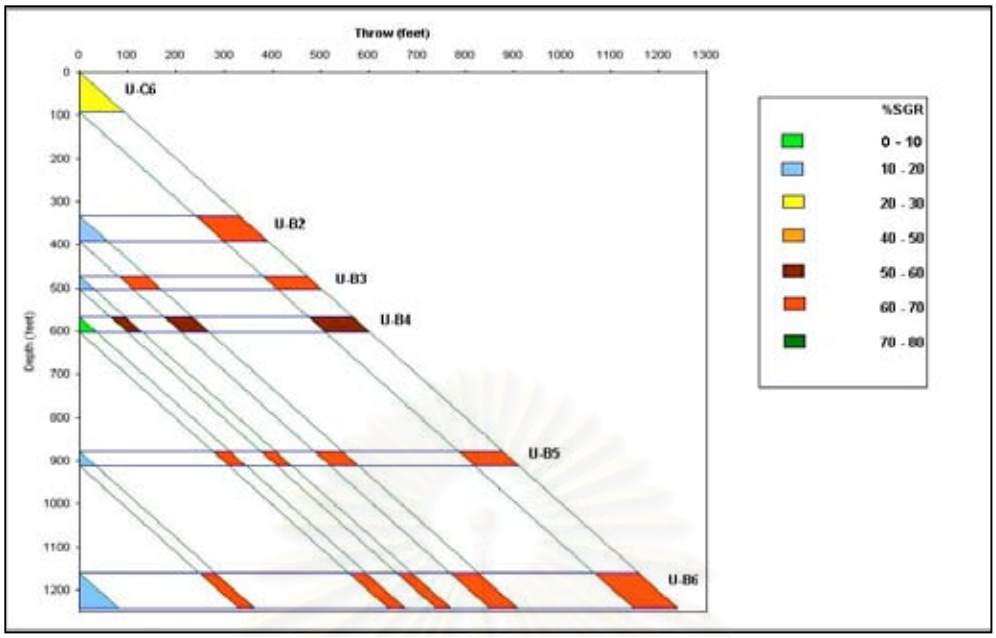

(a) SGR calculated by using lithological data from well C, E, F, and H.

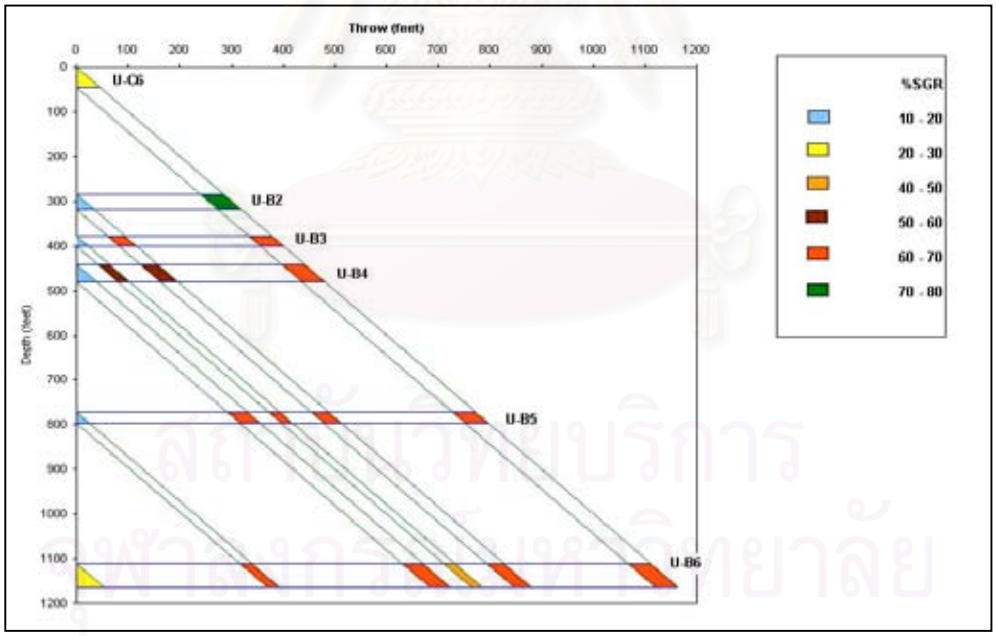

(b) SGR calculated by using lithological data from well B, and I.

Figure 5.40 Juxtaposition diagram present the offset sand and shale gouge ratio history that happen at each throw on the overlap sand horizons between upthrown and downthrown side of Benchamas-B Fault (modified from Juxtaposition diagram manual, 2001).

CHAPTER VI

DISCUSSION

Based on the results in previous chapter, there are enough data to make a discussion, which can be divided into 4 topics as shown below.

6.1 Well correlation across the fault

Regarding to the early stage of procedures, well correlations have to be applied to correlate the rock layer across a fault. The result, at the first time, is that horizons U-B5 and U-B6 at downthrown side displayed a movement pattern (throw) less than the upper rock layers on the fault-plane section. In reality, fault structure is unlikely to display like this. Therefore, the well correlations have to be rechecked by using interval thickness and pore-pressure profile to correlate rock layers U-B5 and U-B6 in downthrown side. The second result displayed a movement pattern similar to the upper layers. Therefore, cause of uncorrected horizon correlation across-fault could lead to errors of Allan fault diagram and affect fault seal interpretation.

6.2 Evaluation of the average horizon thickness across the fault

SGR calculation needs input data from the average shale volume and bed thickness of well pairs adjacent to the fault to calculate and display the sealing potentials on the fault plane. To evaluate the average values of both parameters across a fault require careful investigation. Because the horizon thickness that appears in well pairs across a fault is not be the same. Some are similar in and some very different in thickness. Therefore this value is very sensitive to error and may cause seal predicting variation. For example, **Table 5.3** presents the average Vshale interval of 25 ft, before this table was created, the well pairs data (GR log, Vshale log) adjacent to the fault were used to correlate the best matching of rock layer thickness across a fault. One problem that happened and caused confusion in calculation of the average

thickness of sand horizon across a fault, it is the large difference in thickness appears in each the well pairs. For example, horizon U-C6 in well pairs B and H all are the same lithological unit but are different in thickness. To solve this problem and to obtain the reasonable outcome, the average bed thickness was used to control the interval thickness in horizon U-C6, a thickness of 25 ft appears in well B, whereas 95 ft in thickness appears in well H. Therefore, the calculated average bed thickness of 60 ft across fault is applied to control amount of interval thickness for horizon U-C6. The displayed interval thickness would be little higher than or close to 60 ft, then 75 ft was assigned into the average bed thickness for horizon U-C6 and divided the thickness of horizon into 3 intervals (25+25+25 = 75 ft).

6.3 Influence of clay and shale smears on fault zones

Clay and shale smear is an effectiveness to create fault seals in the clastic (sand-shale) sequences. The Benchamas-A field consists of thick sand-shale sequences as it appears in the lithological column. When fault cuts through these sequences, the amount of fine-grained materials will supply into the fault zone and cause the high capillary entry pressure due to fine grain materials have small pore-throat size that can be increased seal capacity in fault zone (Yielding et al., 2002). This high capillary entry pressure can balance the buoyancy pressure generated by the height of hydrocarbon column. For the Benchamas-A field the capillary pressure is not high when compared to the seal capacity on the Benchamas-A Fault (see **Figure 5.38**). Because the SGR at 40% can supports the across-fault pressure difference to 147 psi (Benchamas-A Fault = 9 psi). Therefore, the seal capacity for Benchamas-A Fault could support more hydrocarbon column height.

6.4 Comparison with the other SGR researches

Fault seal analysis in this research, was done using only manual process to generate the results. Based on this current result, the horizon and stratigraphic correlation across a fault is recommended in the routine work for generating a fault-plane section, such as uncorrected sand horizon

correlation. Application of FAPS software (Fault Analysis Projection System) (Yielding et al., 1999) is considered as the alternative way to study fault seal capacity. Because this software can generates the high resolution of fault–plane section. So this correlation problems can be solve by this software.

Muangsuwan (1998) studied the fault seal affect to low-pay wells in the North Pailin field, Pattani basin, Gulf of Thailand. The FAPS software (Fault Analysis Projection System) was applied to generate reservoir juxtapositions and to calculate and calibrate fault seal estimates. Testing result reveals reasonable achievement, and the result can answer all basic questions such as which reservoir units are juxtaposed, and where on a fault surface is sealed and where the leakage is etc.

However, as shown in **Figure 6.1** the result of fault seal capacity of this research is compared with those of the other SGR researchers, as Northern North Sea, Niger Delta, and Gulf of Thailand. The data set for Benchamas-A field as shown by dots of yellow, green, and red color. The data set for Benchamas-A field are plotted at the boundary between the data sets of the Gulf of Thailand or the North Pailin field (red area) and some those of Northern North Sea.

The comparison of result data with the other researches can be discussed as stated below.

Data set of fault seal for the Benchamas-A Fault laid on the left side of the data set of the fault seal analysis of the North Pailin field in the Gulf of Thailand (red area), **Figure 6.1** represents the result of the fault seal capacity for The Benchamas-A field consistent to the North Pailin field due to the high SGR values but small across-fault pressure difference. The cause of the small size of hydrocarbon reservoirs in the Pattani basin, it is a reason of small across-fault pressure difference in the overlap reservoir-reservoir. Additionally, the similar of SGR values of both fields would be they are located in the same basin that similar the lithology and structure styles (sand shale sequences in fluvial system and high fault throw).

The cause of high SGR value in the Benchamas-A field may be due to many factors, such as depositional system, alternated clay/ shale sequences, advantage of multiple fine-grained source bed sequences, high thickness of fine-grained source beds, large throws and different clay mineral deposits. Therefore, in this section one would compare the Benchamas-A field with the other areas in the scope of similar sequences/ lithologies (sand/ shale sequences) and structure style. The minimum of SGR value at the Benchamas-A Fault (40%) is higher than some part of the Gullfaks field in Northern North Sea (**Figure 6.1**), this is probably the cause of different characteristic of fine-grained source beds. The fine-grained source beds in the Benchamas-A field are much thick and appear alternated with sand beds. Upon faulting, these fine-grained source beds can be continuously supply more fine-grained materials into the slipped interval by integrating of fine-grained materials. This can lead to high fault seal capacity in the Benchamas-A field.

In general the static seal on the fault plane needs the shale gouge ratio just only 15 to 20 percents to creates fault sealing. For example, in the Gullfaks field represented a small static seal developing at gouge ratios of 15 to 20 percents in the sand self-juxtaposition (Yielding et al., 1999). Therefore, in the Benchamas-A field represents the minimum shale gouge ratio up to 40 percent that mean the Benchamas-A Fault is more possible all the overlapped sands on the fault plane have seal and traps hydrocarbon along the fault plane.

Niger Delta is another example of fault seal study, the stratigraphic sequences comprise a delta-plain, delta-front sand and shale and a varyingly thick sequence of continental sands of predominantly fluvio-deltaic origin (Jev et al., 1993). The fault sealing appeared when SGR value is higher than 20% and probably reaching about 100 psi at SGR of about 60% (Yielding et al., 1999). The low SGR happened in the overlapped area of the upper part of the fault plane where small throws or in the self-juxtaposition occurred in the massive sand bed. Conversely, the likelihood of clay smear then increases downward again as the clays become thicker and more closely spaced. This increases SGR in the Niger Delta field looks similar to the Benchamas-A field

due to multiple of fine-grained source beds that induced the high fine-grained material into the fault zone and increased fault seal capacity.

Therefore in areas where sediments bear similar lithology and structure styles, shale gouge ratio distribution on the fault-plane section can be employed to evaluate fault seal capacity. This theses study gives an insight into the importance of sealing and leaking faults in term of basic evaluating and developing faulted field. Moreover, the manual process in this research is the basic to teach and train the software users to understand the basic of fault seal analysis and can solve the problem that would be happened during the process interpretation.

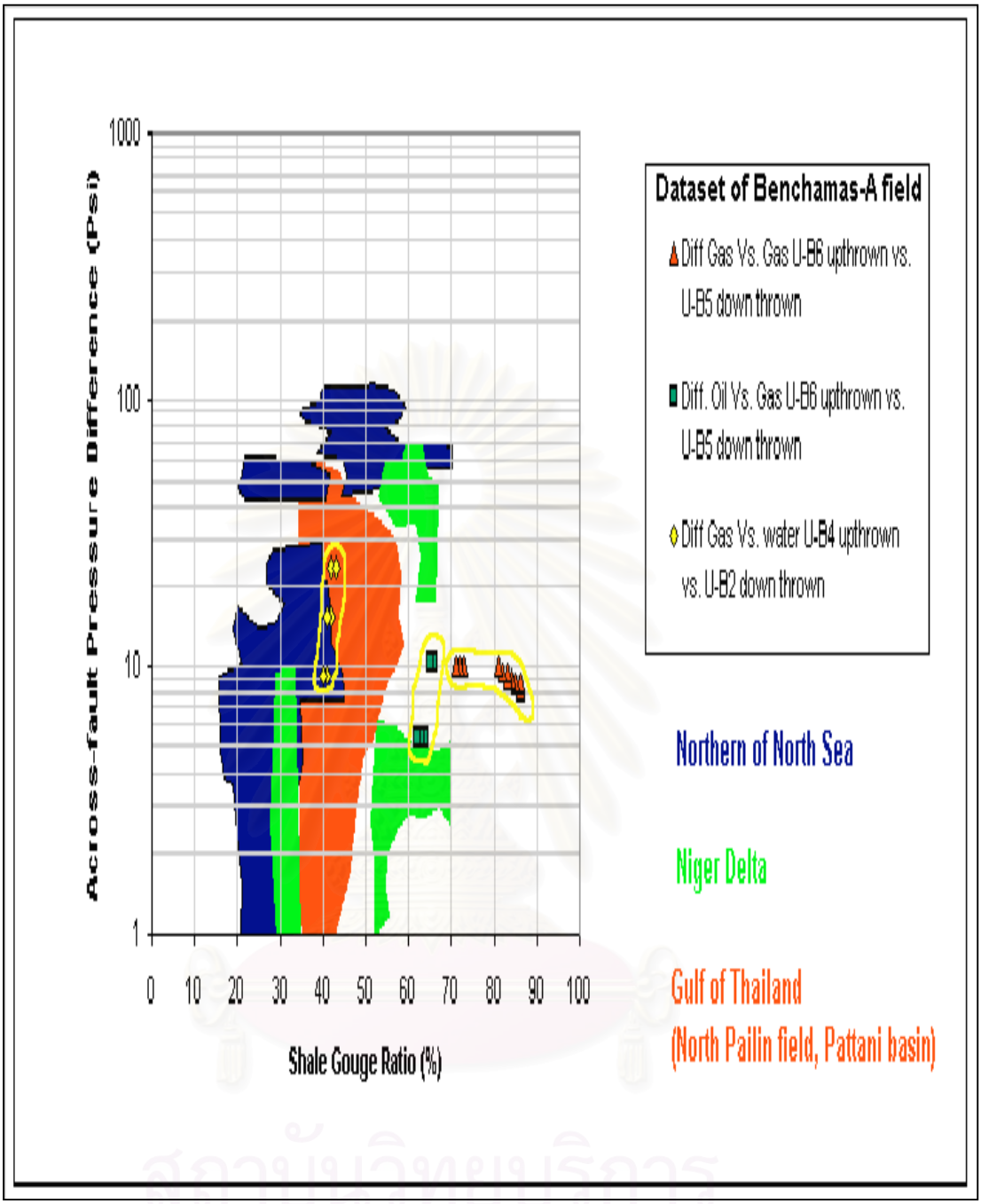

Figure 6.1 Comparison of across-fault pressure difference to shale gouge ratio in the Benchamas-A field with the other areas (modified after Yielding, 2002).

CHAPTER VII

CONCLUSION

Analysis on clay and shale smear in the fault zone can indicate and identify smearing that has effectively created a fault seal in the Benchamas-A field in Block B8/32, Pattani basin in the Gulf of Thailand. The results from this research can be concluded below.

Log interpretation indicates that six sequences of 1,230 ft (378 m)-thick alternated sandstone and shale sequences are mostly fluvial in origin. Moreover, well log correlations combined with top depth structure maps indicate that clay/ shale beds distributed in the laterally covered area of the Benchamas-A field can prevent the vertical migration of hydrocarbon in the fault compartments. The reservoir, oil and gas accumulations within late Oligocene to middle Miocene sandstone, deposited within a fluvial system of low to moderate energy meandering channels. Sand thicknesses for these units vary from 15 to 100 ft, based on net-sand (isopach) maps, large volumes of reservoir sand locate nearby Benchamas-A Fault in the southern part of the study area. Faults in the Benchamas-A field show normal sense of movement with high-dip angles (64°) to the east and approximately vertical displacement of about 325 ft. The faults are regarded half-graben. The initial hydrocarbon-water contacts onto the top depth structure maps indicate the hydrocarbon accumulation area is located in the south where the NNW-trending fault (the Benchamas-B Fault) intersects the N-trending fault (the Benchamas-A Fault). The fault-plane section (or Allan fault diagram) can be used to analyze the qualitative fault seal properties. Eight sand horizons for both upthrown and downthrown sides of a fault plane have potentials for fault sealing when these sand horizons are juxtaposed against the shale bed across the fault plane. These sand horizons include the U-C6, U-B2, U-B3, and U-B5 sand horizons in the upthrown and U-B6, U-B3, U-B4, and U-B6 sand horizons in the downthrown. However, four sand horizons have potential of leakages where the sand horizons juxtaposed against the other sand horizons across the fault plane. These leakage areas include, the

upthrown U-B4 sand horizon juxtaposed with the downthrown U-B2 sand horizon, the overlap varies from 8 to 17 ft and the upthrown U-B6 sand horizon juxtaposed with the downthrown U-B5 sand horizon, at the overlap vary from 8 to 25 ft.

To calculate the SGR values in the sand overlap areas represented quantitative potential seal within the range of 40 to 42% in the overlap sand upthrown U-B4 and the downthrown U-B2 and 62 to 86% in the overlap sand upthrown U-B6 and the downthrown U-B5. The SGR (> 20%) in overlap reservoir sand areas indicate that the Benchamas-A Fault have been sealed and the cause of SGR value higher than 40% that indicated this fault sealed by clay smear mechanism. Causes of high SGR values are due to 2 factors including, A) Tertiary fine-grained source beds of lacustrine and fluvial clay/ shale sequences and B) high vertical slip of fault movement. The clay and shale beds in this study area can be regarded as the excellent fine-grained source because they can provide high volumes of fine-grained materials in to the fault zone and lead to high capillary entry pressure in the fault zone. Pore-pressure profile confirms that the Benchamas-A Fault has sealed. There are 3 supporting evidences. The first evidence is that across-fault pressure difference presented varies from 5 to 23 psi. The second one is that no fluid gradient lines are superimposed between the overlap reservoir sands. This indicates that fluid networks did not occur across the fault and that fluid accumulation took place in the isolating compartments. The third one is that different fluid contact depth at 263 ft for gas and at 43 ft for oil appear in the overlap reservoir sand horizon U-B6 upthrown against the reservoir sand horizon U-B5 downthrown. Therefore, fluids cannot flow across the fault to equalize the across-fault pressure difference.

In conclusion, through the methodology and results, this research can be applied to predict and evaluate the risk of the critical fault seal capacity in the other areas of similar lithologies and structural trap. Furthermore geological history, geopressure, field production history, core samples, etc. can be used for effective fault seal prediction in the future. They are still required to be used for improvement and calibration for the best fault seal attribute.

REFERENCES

Allan, U.S. 1989. Model for Hydrocarbon Migration and Entrapment Within Fault Structures. The American Association of Petroleum Geologists Bulletin 73(7): 803-811.

Alexander, L.L., and Handschy, J.W. 1998. Fluid Flow in a Faulted Reservoir System: Fault Trap Analysis for the Block 330 Field in Eugene Island, South Addition, Offshore Louisiana. The American Association of Petroleum Geologists Bulletin 82(3): 387-411.

Bal, A.A., Burgisser, H.M., Harris, D.K., Herber, S.M.R., Thumprasertwong, S., and Winkler, F.J. 1992. The Tertiary Phitsanulok Lacustrine Basin, Thailand. National Conference on “Geologic Resources of Thailand: Potential for Future Development”, 247-258. Department of Mineral Resources, Bangkok, Thailand.

Berg R.R., and Avery A.H. 1995. Sealing Properties of Tertiary Growth Fault, Texas Gulf Coast. The American Association of Petroleum Geologists Bulletin 79(3): 375-393.

Bj¬rlykke, K. 1989. Radioactive Logs. Sedimentology and Petroleum Geology p.315

Bustin, R. M., and Chonchawalit, A. 1997. Petroleum Source Rock Potential and Evolution of Tertiary Strata, Pattani Basin, Gulf of Thailand. The American Association of Petroleum Geologists Bulletin 81 (12): 2000-2023.

Dahlberg, E. C. 1995. Fluids, Pressure, and Gradients. Applied Hydrodynamics in Petroleum Exploration 2: 1-14.

Dahlberg, E. C. 1995. Formation Pressure Measurements and Data. Applied Hydrodynamics in Petroleum Exploration 2: 15-33.

Dahlberg, E. C. 1995. Pressure Variation with Depth: Geologic Interpretation of P - D Plots. Applied Hydrodynamics in Petroleum Exploration 2: 99-104.

Dahlberg, E. C. 1995. Pressure Variation with Depth: Subsurface Correlations Based on pressure data. Applied Hydrodynamics in Petroleum Exploration 2: 99-104.

Jardine, E. 1997. Dual Petroleum Systems Governing the Prolific Pattani Basin, Offshore Thailand. International Conference on Stratigraphy and Tectonic Evolution of Southeast Asia and the South Pacific, 525-534. Department of Mineral Resources, Bangkok, Thailand.

Jev, B.I., Sijpesteijn, C.H.K., Peters, M.P.A.M., Watts, N.L., and Wilkie, J.T. 1993. Akaso Field, Nigeria: Using of Integrated 3-D Seismic, Fault Slicing, Clay Smearing, and RFT Pressure Data Fault Trapping and Dynamic Leakage. The American Association of Petroleum Geologists Bulletin 77(8): 1389-1404.

Knipe, R. J. 1997. Juxtaposition and Seal Diagrams to Help Analyze Fault Seals in Hydrocarbon Reservoirs. The American Association of Petroleum Geologists Bulletin 81(2): 187-195.

Muangsuwan, A., 1998. Applications of Geological, Geophysical and Geochemical Data to Investigate 3 Low-pay wells in North Pailin, Pattani Basin, Gulf of Thailand. Msc Thesis, Universiti Brunei Darussalam.

Packham, G. H. 1993. Plate Tectonics and the Development of Sedimentary Basin of the Dextral Regime in Western Southeast Asia. Journal of Southeast Asia Earth sciences (8): 497-551.

Pradidtan, S., and Dook, R. 1992.Petroleum Geology of the Northern Part of the Gulf of Thailand. National Conference on “Geologic Resources of Thailand: Potential for Future Development”, 235-246. Department of Mineral Resources, Bangkok, Thailand.

Polachn, S., and Sattayarak, N. 1989, Strike-slip tectonics and the development of Tertiary in Thailand, in Thanasuthipitak, T. and Ounchanum, P. (eds), International Symposium on Intermontane Basins: Geology and Resources, pp. 243-253. Chiang Mai University, Thailand.

Sneider, R.M. 1987. Practical Petrophysics for Exploration and Development. AAPG Education Department Short Course Notes, variously paginated.

Vavra, C.L., Kaldi J.G., and Sneider, R.M. 1992. Geological Applications of Capillary Pressure: A Review. The American Association of Petroleum Geologists Bulletin 76(6): 840-850.

Williamson, C. R. 1992. Funan Field – First Gas Production From The Eastern Pattani Basin. National Conference on "Geologic Resources of Thailand: Potential for Future Development", 225-234. Department of Mineral Resources, Bangkok, Thailand.

Yielding, G., Freeman B., and Needham, D.T. 1997. Quantitative Fault Seal Prediction. The American Association of Petroleum Geologists Bulletin 81(6): 897-917.

Yielding, G. 2002. Shale Gouge Ratio – Calibration by Geohistory. Hydrocarbon Seal Quantification NPF Special Publication 11: 1-15.

Yielding, G., ¬verland, J. A., and Byberg, G. 1999. Characterization of Fault Zones for Reservoir Modeling: An Example from the Gullfaks Field, Northern North Sea. The American Association of Petroleum Geologists Bulletin 83(6): 925-951.

Badleys.co.uk. 2001. Triangle diagram manual [Online]. Available from: www.badleys.co.uk/Shale_Gouge.html [2001, May 15]

Bracken, B.R., Denison, C.N., and Livingston, J. 2000. Stratigraphic Architecture and Intra-reservoir seals in Miocene Fluvial to marginal Marine Reservoirs, Pattani Basin, Gulf of Thailand.

Petroleum System of Southeast Asia [online]. Available from: http://aapg.confex.com/aapg/ba2000/techprogram/section_1096.htm [2003, January 24]

Crain, E. R. (Ross). 2000. Calculating Shale Volume: Non Linear GR and SP relationships. eText Home Study Course in Petrophysics and Well Log Analysis [online]. Available from: http://www.spec2000.net [2002, March 21]

Teerman, S.C., Denison, C.N., and Livingston, J. 2000. An Integrated Petroleum System Study, Northern Gulf of Thailand: Applications to the Block B8/32 Area. Petroleum System of Southeast Asia [online]. Available from:

http://aapg.confex.com/aapg/ba2000/techprogram/section_1096.htm [2003, January 24]

APPENDIES

APPENDIX A

SHALE VOLUME SPREDSHEET

Table A.1 Shale volume (Vsh) calculation from **well: A**

Vsh.calculation (Clavier Eq.)					Depth
GR.	Max	Min	GR.fraction	Vsh.	(feet)
98	160	60	0.3800	0.21	5000
123	160	60	0.6300	0.43	5005
135	160	60	0.7500	0.57	5010
106	160	60	0.4600	0.27	5015
130	160	60	0.7000	0.51	5020
140	160	60	0.8000	0.64	5025
65	160	60	0.0500	0.02	5030
65	160	60	0.0500	0.02	5035
68	160	60	0.0800	0.04	5040
75	160	60	0.1500	0.07	5045
155	160	60	0.9500	0.89	5050
150	160	60	0.9000	0.79	5055
150	160	60	0.9000	0.79	5060
99	160	60	0.3900	0.22	5065
77	160	60	0.1700	0.08	5070
60	160	60	0.0000	0.00	5075
60	160	60	0.0000	0.00	5080
75	160	60	0.1500	0.07	5085
70	160	60	0.1000	0.04	5090
60	160	60	0.0000	0.00	5095
55	160	60	-0.0500	0.00	5100
121	160	60	0.6100	0.41	5105
160	160	60	1.0000	1.00	5110
166	160	60	1.0600	1.00	5115
165	160	60	1.0500	1.00	5120
125	160	60	0.6500	0.45	5125
98	160	60	0.3800	0.21	5130
72	160	60	0.1200	0.05	5135
148	160	60	0.8800	0.76	5140
161	160	60	1.0100	1.00	5145
148	160	60	0.8800	0.76	5150
150	160	60	0.9000	0.79	5155
183	160	60	1.2300	1.00	5160
163	160	60	1.0300	1.00	5165
175	160	60	1.1500	1.00	5170
129	160	60	0.6900	0.50	5175
185	160	60	1.2500	1.00	5180
160	160	60	1.0000	1.00	5185
173	160	60	1.1300	1.00	5190
190	160	60	1.3000	1.00	5195
155	160	60	0.9500	0.89	5200
170	160	60	1.1000	1.00	5205
108	160	60	0.4800	0.29	5210
150	160	60	0.9000	0.79	5215
135	160	60	0.7500	0.57	5220
125	160	60	0.6500	0.45	5225
200	160	60	1.4000	1.00	5230

Vsh.calculation (Clavier Eq.)					Depth
GR.	Max	Min	GR.fraction	Vsh.	(feet)
150	160	60	0.9000	0.79	5235
153	160	60	0.9300	0.85	5240
165	160	60	1.0500	1.00	5245
170	160	60	1.1000	1.00	5250
163	160	60	1.0300	1.00	5255
150	160	60	0.9000	0.79	5260
142	160	60	0.8200	0.67	5265
140	160	60	0.8000	0.64	5270
133	160	60	0.7300	0.54	5275
140	160	60	0.8000	0.64	5280
130	160	60	0.7000	0.51	5285
133	160	60	0.7300	0.54	5290
120	160	60	0.6000	0.40	5295
173	160	60	1.1300	1.00	5300
187	160	60	1.2700	1.00	5305
142	160	60	0.8200	0.67	5310
157	160	60	0.9700	0.93	5315
197	160	60	1.3700	1.00	5320
200	160	60	1.4000	1.00	5325
146	160	60	0.8600	0.73	5330
157	160	60	0.9700	0.93	5335
140	160	60	0.8000	0.64	5340
153	160	60	0.9300	0.85	5345
140	160	60	0.8000	0.64	5350
115	160	60	0.5500	0.35	5355
100	160	60	0.4000	0.23	5360
85	160	60	0.2500	0.13	5365
110	160	60	0.5000	0.31	5370
67	160	60	0.0700	0.03	5375
60	160	60	0.0000	0.00	5380
60	160	60	0.0000	0.00	5385
54	160	60	-0.0600	0.00	5390
62	160	60	0.0200	0.01	5395
80	160	60	0.2000	0.10	5400
168	160	60	1.0800	1.00	5405
127	160	60	0.6700	0.47	5410
158	160	60	0.9800	0.95	5415
112	160	60	0.5200	0.32	5420
177	160	60	1.1700	1.00	5425
155	160	60	0.9500	0.89	5430
140	160	60	0.8000	0.64	5435
134	160	60	0.7400	0.56	5440
150	160	60	0.9000	0.79	5445
117	160	60	0.5700	0.37	5450
187	160	60	1.2700	1.00	5455
195	160	60	1.3500	1.00	5460
183	160	60	1.2300	1.00	5465

Table A.1 Shale volume (Vsh) calculation from **well: A** (continued)

Vsh.calculation (Clavier Eq.)					Depth
GR.	Max	Min	GR.fraction	Vsh.	(feet)
141	160	60	0.8100	0.65	5470
200	160	60	1.4000	1.00	5475
161	160	60	1.0100	1.00	5480
150	160	60	0.9000	0.79	5485
124	160	60	0.6400	0.44	5490
127	160	60	0.6700	0.47	5495
170	160	60	1.1000	1.00	5500
130	160	60	0.7000	0.51	5505
160	160	60	1.0000	1.00	5510
126	160	60	0.6600	0.46	5515
175	160	60	1.1500	1.00	5520
120	160	60	0.6000	0.40	5525
132	160	60	0.7200	0.53	5530
130	160	60	0.7000	0.51	5535
150	160	60	0.9000	0.79	5540
157	160	60	0.9700	0.93	5545
100	160	60	0.4000	0.23	5550
107	160	60	0.4700	0.28	5555
85	160	60	0.2500	0.13	5560
200	160	60	1.4000	1.00	5565
155	160	60	0.9500	0.89	5570
187	160	60	1.2700	1.00	5575
130	160	60	0.7000	0.51	5580
164	160	60	1.0400	1.00	5585
161	160	60	1.0100	1.00	5590
112	160	60	0.5200	0.32	5595
127	160	60	0.6700	0.47	5600
165	160	60	1.0500	1.00	5605
160	160	60	1.0000	1.00	5610
109	160	60	0.4900	0.30	5615
80	160	60	0.2000	0.10	5620
68	160	60	0.0800	0.04	5625
62	160	60	0.0200	0.01	5630
65	160	60	0.0500	0.02	5635
65	160	60	0.0500	0.02	5640
58	160	60	-0.0200	0.00	5645
63	160	60	0.0300	0.01	5650
65	160	60	0.0500	0.02	5655
120	160	60	0.6000	0.40	5660
115	160	60	0.5500	0.35	5665
143	160	60	0.8300	0.68	5670
178	160	60	1.1800	1.00	5675
82	160	60	0.2200	0.11	5680
150	160	60	0.9000	0.79	5685
124	160	60	0.6400	0.44	5690
200	160	60	1.4000	1.00	5695
140	160	60	0.8000	0.64	5700

Vsh.calculation (Clavier Eq.)					Depth
GR.	Max	Min	GR.fraction	Vsh.	(feet)
150	160	60	0.9000	0.79	5705
98	160	60	0.3800	0.21	5710
107	160	60	0.4700	0.28	5715
93	160	60	0.3300	0.18	5720
62	160	60	0.0200	0.01	5725
65	160	60	0.0500	0.02	5730
53	160	60	-0.0700	0.00	5735
195	160	60	1.3500	1.00	5740
140	160	60	0.8000	0.64	5745
165	160	60	1.0500	1.00	5750
155	160	60	0.9500	0.89	5755
157	160	60	0.9700	0.93	5760
102	160	60	0.4200	0.24	5765
88	160	60	0.2800	0.14	5770
120	160	60	0.6000	0.40	5775
72	160	60	0.1200	0.05	5780
72	160	60	0.1200	0.05	5785
104	160	60	0.4400	0.26	5790
62	160	60	0.0200	0.01	5795
78	160	60	0.1800	0.09	5800
80	160	60	0.2000	0.10	5805
81	160	60	0.2100	0.10	5810
60	160	60	0.0000	0.00	5815
55	160	60	-0.0500	0.00	5820
127	160	60	0.6700	0.47	5825
47	160	60	-0.1300	0.00	5830
85	160	60	0.2500	0.13	5835
150	160	60	0.9000	0.79	5840
136	160	60	0.7600	0.58	5845
140	160	60	0.8000	0.64	5850
105	160	60	0.4500	0.27	5855
150	160	60	0.9000	0.79	5860
153	160	60	0.9300	0.85	5865
168	160	60	1.0800	1.00	5870
190	155	43	1.3125	1.00	5875
161	155	43	1.0536	1.00	5880
200	155	43	1.4018	1.00	5885
185	155	43	1.2679	1.00	5890
158	155	43	1.0268	1.00	5895
168	155	43	1.1161	1.00	5900
150	155	43	0.9554	0.90	5905
153	155	43	0.9821	0.96	5910
130	155	43	0.7768	0.60	5915
143	155	43	0.8929	0.78	5920
165	155	43	1.0893	1.00	5925
200	155	43	1.4018	1.00	5930
123	155	43	0.7143	0.53	5935

Table A.1 Shale volume (Vsh) calculation from **well: A** (continued)

Vsh.calculation (Clavier Eq.)					Depth
GR.	Max	Min	GR.fraction	Vsh.	(feet)
139	155	43	0.8571	0.72	5940
130	155	43	0.7768	0.60	5945
150	155	43	0.9554	0.90	5950
137	155	43	0.8393	0.69	5955
167	155	43	1.1071	1.00	5960
145	155	43	0.9107	0.81	5965
112	155	43	0.6161	0.42	5970
150	155	43	0.9554	0.90	5975
138	155	43	0.8482	0.71	5980
152	155	43	0.9732	0.94	5985
153	155	43	0.9821	0.96	5990
162	155	43	1.0625	1.00	5995
153	155	43	0.9821	0.96	6000
173	155	43	1.1607	1.00	6005
180	155	43	1.2232	1.00	6010
199	155	43	1.3929	1.00	6015
150	155	43	0.9554	0.90	6020
168	155	43	1.1161	1.00	6025
183	155	43	1.2500	1.00	6030
153	155	43	0.9821	0.96	6035
100	155	43	0.5089	0.31	6040
175	155	43	1.1786	1.00	6045
135	155	43	0.8214	0.67	6050
128	155	43	0.7589	0.58	6055
140	155	43	0.8661	0.74	6060
200	155	43	1.4018	1.00	6065
140	155	43	0.8661	0.74	6070
157	155	43	1.0179	1.00	6075
130	155	43	0.7768	0.60	6080
105	155	43	0.5536	0.36	6085
110	155	43	0.5982	0.40	6090
195	155	43	1.3571	1.00	6095
160	155	43	1.0446	1.00	6100
150	155	43	0.9554	0.90	6105
153	155	43	0.9821	0.96	6110
92	155	43	0.4375	0.26	6115
59	155	43	0.1429	0.07	6120
150	155	43	0.9554	0.90	6125
178	155	43	1.2054	1.00	6130
130	155	43	0.7768	0.60	6135
133	155	43	0.8036	0.64	6140
150	155	43	0.9554	0.90	6145
125	155	43	0.7321	0.55	6150
153	155	43	0.9821	0.96	6155
110	155	43	0.5982	0.40	6160
110	155	43	0.5982	0.40	6165
163	155	43	1.0714	1.00	6170

Vsh.calculation (Clavier Eq.)					Depth
GR.	Max	Min	GR.fraction	Vsh.	(feet)
61	155	43	0.1607	0.08	6175
81	155	43	0.3393	0.18	6180
134	155	43	0.8125	0.65	6185
120	155	43	0.6875	0.49	6190
52	155	43	0.0804	0.04	6195
50	155	43	0.0625	0.03	6200
78	155	43	0.3125	0.17	6205
68	155	43	0.2232	0.11	6210
60	155	43	0.1518	0.07	6215
75	155	43	0.2857	0.15	6220
145	155	43	0.9107	0.81	6225
152	155	43	0.9732	0.94	6230
139	155	43	0.8571	0.72	6235
145	155	43	0.9107	0.81	6240
149	155	43	0.9464	0.88	6245
130	155	43	0.7768	0.60	6250
195	177	60	1.1538	1.00	6255
187	177	60	1.0855	1.00	6260
190	177	60	1.1111	1.00	6265
140	177	60	0.6838	0.49	6270
103	177	60	0.3675	0.20	6275
147	177	60	0.7436	0.56	6280
145	177	60	0.7265	0.54	6285
175	177	60	0.9829	0.96	6290
173	177	60	0.9658	0.92	6295
112	177	60	0.4444	0.26	6300
158	177	60	0.8376	0.69	6305
132	177	60	0.6154	0.42	6310
120	177	60	0.5128	0.32	6315
110	177	60	0.4274	0.25	6320
137	177	60	0.6581	0.46	6325
190	177	60	1.1111	1.00	6330
164	177	60	0.8889	0.78	6335
150	177	60	0.7692	0.59	6340
100	177	60	0.3419	0.19	6345
180	177	60	1.0256	1.00	6350
157	177	60	0.8291	0.68	6355
123	177	60	0.5385	0.34	6360
149	177	60	0.7607	0.58	6365
112	177	60	0.4444	0.26	6370
87	177	60	0.2308	0.11	6375
145	177	60	0.7265	0.54	6380
148	177	60	0.7521	0.57	6385
158	177	60	0.8376	0.69	6390
120	177	60	0.5128	0.32	6395
143	177	60	0.7094	0.52	6400
105	177	60	0.3846	0.22	6405

Table A.1 Shale volume (Vsh) calculation from **well: A** (continued)

Vsh.calculation (Clavier Eq.)					Depth
GR.	Max	Min	GR.fraction	Vsh.	(feet)
168	177	60	0.9231	0.84	6410
180	177	60	1.0256	1.00	6415
133	177	60	0.6239	0.42	6420
173	177	60	0.9658	0.92	6425
170	177	60	0.9402	0.87	6430
150	177	60	0.7692	0.59	6435
178	177	60	1.0085	1.00	6440
128	177	60	0.5812	0.38	6445
180	177	60	1.0256	1.00	6450
160	177	60	0.8547	0.72	6455
157	177	60	0.8291	0.68	6460
160	177	60	0.8547	0.72	6465
158	177	60	0.8376	0.69	6470
168	177	60	0.9231	0.84	6475
160	177	60	0.8547	0.72	6480
181	177	60	1.0342	1.00	6485
200	177	60	1.1966	1.00	6490
176	177	60	0.9915	0.98	6495
192	177	60	1.1282	1.00	6500
170	177	60	0.9402	0.87	6505
173	177	60	0.9658	0.92	6510
185	177	60	1.0684	1.00	6515
147	177	60	0.7436	0.56	6520
137	177	60	0.6581	0.46	6525
110	177	60	0.4274	0.25	6530
168	177	60	0.9231	0.84	6535
96	177	60	0.3077	0.16	6540
79	177	60	0.1624	0.08	6545
61	177	60	0.0085	0.00	6550
55	177	60	-0.0427	0.00	6555
44	177	60	-0.1368	0.00	6560
50	177	60	-0.0855	0.00	6565
179	177	60	1.0171	1.00	6570
159	177	60	0.8462	0.71	6575
178	177	60	1.0085	1.00	6580
177	177	60	1.0000	1.00	6585
159	177	60	0.8462	0.71	6590
165	177	60	0.8974	0.79	6595
181	177	60	1.0342	1.00	6600
110	177	60	0.4274	0.25	6605
138	177	60	0.6667	0.47	6610
165	177	60	0.8974	0.79	6615
170	177	60	0.9402	0.87	6620
142	177	60	0.7009	0.51	6625
162	177	60	0.8718	0.75	6630
200	177	60	1.1966	1.00	6635
177	177	60	1.0000	1.00	6640

Vsh.calculation (Clavier Eq.)					Depth
GR.	Max	Min	GR.fraction	Vsh.	(feet)
190	177	60	1.1111	1.00	6645
113	177	60	0.4530	0.27	6650
175	177	60	0.9829	0.96	6655
165	177	60	0.8974	0.79	6660
147	177	60	0.7436	0.56	6665
130	177	60	0.5983	0.40	6670
150	177	60	0.7692	0.59	6675
100	177	60	0.3419	0.19	6680
171	177	60	0.9487	0.89	6685
193	177	60	1.1368	1.00	6690
180	177	60	1.0256	1.00	6695
110	177	60	0.4274	0.25	6700
157	177	60	0.8291	0.68	6705
150	177	60	0.7692	0.59	6710
153	177	60	0.7949	0.63	6715
170	177	60	0.9402	0.87	6720
162	177	60	0.8718	0.75	6725
120	177	60	0.5128	0.32	6730
196	177	60	1.1624	1.00	6735
186	177	60	1.0769	1.00	6740
170	177	60	0.9402	0.87	6745
135	177	60	0.6410	0.44	6750
63	177	60	0.0256	0.01	6755
67	177	60	0.0598	0.03	6760
62	177	60	0.0171	0.01	6765
80	177	60	0.1709	0.08	6770
60	177	60	0.0000	0.00	6775
75	177	60	0.1282	0.06	6780
53	177	60	-0.0598	0.00	6785
54	177	60	-0.0513	0.00	6790
118	177	60	0.4957	0.30	6795
85	177	60	0.2137	0.10	6800
118	177	60	0.4957	0.30	6805
99	177	60	0.3333	0.18	6810
51	177	60	-0.0769	0.00	6815
66	177	60	0.0513	0.02	6820
54	177	60	-0.0513	0.00	6825
59	177	60	-0.0085	0.00	6830
200	177	60	1.1966	1.00	6835
180	177	60	1.0256	1.00	6840
140	177	60	0.6838	0.49	6845
160	177	60	0.8547	0.72	6850
154	177	60	0.8034	0.64	6855
173	177	60	0.9658	0.92	6860
160	177	60	0.8547	0.72	6865
200	177	60	1.1966	1.00	6870
172	177	60	0.9573	0.90	6875

Table A.1 Shale volume (Vsh) calculation from **well: A** (continued)

Vsh.calculation (Clavier Eq.)					Depth
GR.	Max	Min	GR.fraction	Vsh.	(feet)
200	177	60	1.1966	1.00	6880
163	177	60	0.8803	0.76	6885
103	177	60	0.3675	0.20	6890
185	177	60	1.0684	1.00	6895
187	177	60	1.0855	1.00	6900
165	177	60	0.8974	0.79	6905
180	177	60	1.0256	1.00	6910
145	177	60	0.7265	0.54	6915
155	177	60	0.8120	0.65	6920
108	177	60	0.4103	0.23	6925
55	177	60	-0.0427	0.00	6930
60	177	60	0.0000	0.00	6935
60	177	60	0.0000	0.00	6940
65	177	60	0.0427	0.02	6945
54	177	60	-0.0513	0.00	6950
120	177	60	0.5128	0.32	6955
160	177	60	0.8547	0.72	6960
143	177	60	0.7094	0.52	6965
197	177	60	1.1709	1.00	6970
180	177	60	1.0256	1.00	6975
200	177	60	1.1966	1.00	6980
130	177	60	0.5983	0.40	6985
178	177	60	1.0085	1.00	6990
150	177	60	0.7692	0.59	6995
133	177	60	0.6239	0.42	7000
168	177	60	0.9231	0.84	7005
172	177	60	0.9573	0.90	7010
140	177	60	0.6838	0.49	7015
145	177	60	0.7265	0.54	7020
147	177	60	0.7436	0.56	7025
121	177	60	0.5214	0.33	7030
153	177	60	0.7949	0.63	7035
60	177	60	0.0000	0.00	7040
50	177	60	-0.0855	0.00	7045
186	177	60	1.0769	1.00	7050
150	177	60	0.7692	0.59	7055
180	177	60	1.0256	1.00	7060
127	177	60	0.5726	0.37	7065
79	177	60	0.1624	0.08	7070
82	177	60	0.1880	0.09	7075
65	177	60	0.0427	0.02	7080
175	177	60	0.9829	0.96	7085
115	177	60	0.4701	0.28	7090
150	177	60	0.7692	0.59	7095
60	177	60	0.0000	0.00	7100
152	177	60	0.7863	0.62	7105
134	177	60	0.6325	0.43	7110

Vsh.calculation (Clavier Eq.)					Depth
GR.	Max	Min	GR.fraction	Vsh.	(feet)
103	177	60	0.3675	0.20	7115
128	177	60	0.5812	0.38	7120
90	177	60	0.2564	0.13	7125
75	177	60	0.1282	0.06	7130
75	177	60	0.1282	0.06	7135
73	177	60	0.1111	0.05	7140
140	177	60	0.6838	0.49	7145
195	177	60	1.1538	1.00	7150
198	177	60	1.1795	1.00	7155
158	177	60	0.8376	0.69	7160
175	177	60	0.9829	0.96	7165
130	177	60	0.5983	0.40	7170
190	177	60	1.1111	1.00	7175
132	177	60	0.6154	0.42	7180
133	177	60	0.6239	0.42	7185
130	177	60	0.5983	0.40	7190
200	177	60	1.1966	1.00	7195
79	177	60	0.1624	0.08	7200
60	177	60	0.0000	0.00	7205
60	177	60	0.0000	0.00	7210
143	177	60	0.7094	0.52	7215
118	177	60	0.4957	0.30	7220
120	177	60	0.5128	0.32	7225
200	177	60	1.1966	1.00	7230
200	177	60	1.1966	1.00	7235
143	177	60	0.7094	0.52	7240
175	177	60	0.9829	0.96	7245
190	177	60	1.1111	1.00	7250
195	177	60	1.1538	1.00	7255
152	177	60	0.7863	0.62	7260
84	177	60	0.2051	0.10	7265
159	177	60	0.8462	0.71	7270
180	177	60	1.0256	1.00	7275
110	177	60	0.4274	0.25	7280
123	177	60	0.5385	0.34	7285
143	177	60	0.7094	0.52	7290
45	177	60	-0.1282	0.00	7295
50	177	60	-0.0855	0.00	7300
50	177	60	-0.0855	0.00	7305
53	177	60	-0.0598	0.00	7310
63	177	60	0.0256	0.01	7315
50	177	60	-0.0855	0.00	7320
75	177	60	0.1282	0.06	7325
200	177	60	1.1966	1.00	7330
163	177	60	0.8803	0.76	7335
177	200	50	0.8467	0.71	7340
177	200	50	0.8467	0.71	7345

Table A.1 Shale volume (Vsh) calculation from **well: A** (continued)

Vsh.calculation (Clavier Eq.)					Depth
GR.	Max	Min	GR.fraction	Vsh.	(feet)
176	200	50	0.8400	0.70	7350
182	200	50	0.8800	0.76	7355
195	200	50	0.9667	0.92	7360
175	200	50	0.8333	0.69	7365
161	200	50	0.7400	0.56	7370
157	200	50	0.7133	0.52	7375
190	200	50	0.9333	0.86	7380
173	200	50	0.8200	0.67	7385
108	200	50	0.3867	0.22	7390
127	200	50	0.5133	0.32	7395
200	200	50	1.0000	1.00	7400
200	200	50	1.0000	1.00	7405
169	200	50	0.7933	0.63	7410
73	200	50	0.1533	0.07	7415
52	200	50	0.0133	0.01	7420
60	200	50	0.0667	0.03	7425
60	200	50	0.0667	0.03	7430
62	200	50	0.0800	0.04	7435
103	200	50	0.3533	0.19	7440
159	200	50	0.7267	0.54	7445
140	200	50	0.6000	0.40	7450
162	200	50	0.7467	0.57	7455
190	200	50	0.9333	0.86	7460
135	200	50	0.5667	0.37	7465
200	200	50	1.0000	1.00	7470
187	200	50	0.9133	0.82	7475
193	200	50	0.9533	0.90	7480
200	200	50	1.0000	1.00	7485
200	200	50	1.0000	1.00	7490
160	200	50	0.7333	0.55	7495
200	200	50	1.0000	1.00	7500
139	200	50	0.5933	0.39	7505
181	200	50	0.8733	0.75	7510
118	200	50	0.4533	0.27	7515
65	200	50	0.1000	0.04	7520
87	200	50	0.2467	0.12	7525
199	200	50	0.9933	0.98	7530
155	200	50	0.7000	0.51	7535
128	200	50	0.5200	0.32	7540
168	200	50	0.7867	0.62	7545
162	200	50	0.7467	0.57	7550
200	200	50	1.0000	1.00	7555
118	200	50	0.4533	0.27	7560
193	200	50	0.9533	0.90	7565
181	200	50	0.8733	0.75	7570
135	200	50	0.5667	0.37	7575
200	200	50	1.0000	1.00	7580

Vsh.calculation (Clavier Eq.)					Depth
GR.	Max	Min	GR.fraction	Vsh.	(feet)
47	200	50	-0.0200	0.00	7585
79	200	50	0.1933	0.09	7590
155	200	50	0.7000	0.51	7595
200	200	50	1.0000	1.00	7600
78	200	50	0.1867	0.09	7605
63	200	50	0.0867	0.04	7610
60	200	50	0.0667	0.03	7615
53	200	50	0.0200	0.01	7620
52	200	50	0.0133	0.01	7625
180	200	50	0.8667	0.74	7630
193	200	50	0.9533	0.90	7635
178	200	50	0.8533	0.72	7640
165	200	50	0.7667	0.59	7645
180	200	50	0.8667	0.74	7650
91	200	50	0.2733	0.14	7655
105	200	50	0.3667	0.20	7660
130	200	50	0.5333	0.34	7665
73	200	50	0.1533	0.07	7670
42	200	50	-0.0533	0.00	7675
70	200	50	0.1333	0.06	7680
162	200	50	0.7467	0.57	7685
188	200	50	0.9200	0.83	7690
190	200	50	0.9333	0.86	7695
174	200	50	0.8267	0.68	7700
152	200	50	0.6800	0.49	7705
180	200	50	0.8667	0.74	7710
198	200	50	0.9867	0.97	7715
130	200	50	0.5333	0.34	7720
190	200	50	0.9333	0.86	7725
195	200	50	0.9667	0.92	7730
200	200	50	1.0000	1.00	7735
160	200	50	0.7333	0.55	7740
200	200	50	1.0000	1.00	7745
200	200	50	1.0000	1.00	7750
155	200	50	0.7000	0.51	7755
155	200	50	0.7000	0.51	7760
170	200	50	0.8000	0.64	7765
130	200	50	0.5333	0.34	7770
170	200	50	0.8000	0.64	7775
198	200	50	0.9867	0.97	7780
170	200	50	0.8000	0.64	7785
182	200	50	0.8800	0.76	7790
190	200	50	0.9333	0.86	7795
108	200	50	0.3867	0.22	7800
167	200	50	0.7800	0.61	7805
180	200	50	0.8667	0.74	7810
130	200	50	0.5333	0.34	7815

Table A.1 Shale volume (Vsh) calculation from **well: A** (continued)

Vsh.calculation (Clavier Eq.)					Depth
GR.	Max	Min	GR.fraction	Vsh.	(feet)
82	200	50	0.2133	0.10	7820
47	200	50	-0.0200	0.00	7825
58	200	50	0.0533	0.02	7830
75	200	50	0.1667	0.08	7835
74	200	50	0.1600	0.08	7840
70	200	50	0.1333	0.06	7845
67	200	50	0.1133	0.05	7850
199	200	50	0.9933	0.98	7855
120	200	50	0.4667	0.28	7860
65	200	50	0.1000	0.04	7865
67	200	50	0.1133	0.05	7870
62	200	50	0.0800	0.04	7875
74	200	50	0.1600	0.08	7880
95	200	50	0.3000	0.16	7885
66	200	50	0.1067	0.05	7890
92	200	50	0.2800	0.14	7895
198	200	50	0.9867	0.97	7900
104	200	50	0.3600	0.20	7905
53	200	50	0.0200	0.01	7910
51	200	50	0.0067	0.00	7915
60	200	50	0.0667	0.03	7920
47	200	50	-0.0200	0.00	7925
48	200	50	-0.0133	0.00	7930
75	200	50	0.1667	0.08	7935
178	200	50	0.8533	0.72	7940
194	200	50	0.9600	0.91	7945
187	200	50	0.9133	0.82	7950
185	200	50	0.9000	0.79	7955
155	200	50	0.7000	0.51	7960
170	200	50	0.8000	0.64	7965
172	200	50	0.8133	0.66	7970
143	200	50	0.6200	0.42	7975
184	200	50	0.8933	0.78	7980
186	200	50	0.9067	0.81	7985
187	200	50	0.9133	0.82	7990
170	200	50	0.8000	0.64	7995
200	200	50	1.0000	1.00	8000
115	200	50	0.4333	0.25	8005
140	200	50	0.6000	0.40	8010
182	200	50	0.8800	0.76	8015
98	200	50	0.3200	0.17	8020
84	200	50	0.2267	0.11	8025
73	200	50	0.1533	0.07	8030
43	200	50	-0.0467	0.00	8035
60	200	50	0.0667	0.03	8040
161	200	50	0.7400	0.56	8045
178	200	50	0.8533	0.72	8050

Vsh.calculation (Clavier Eq.)					Depth
GR.	Max	Min	GR.fraction	Vsh.	(feet)
154	200	50	0.6933	0.50	8055
120	200	50	0.4667	0.28	8060
121	200	50	0.4733	0.28	8065
175	200	50	0.8333	0.69	8070
172	200	50	0.8133	0.66	8075
154	200	50	0.6933	0.50	8080
181	200	50	0.8733	0.75	8085
141	200	50	0.6067	0.41	8090
181	200	50	0.8733	0.75	8095
158	200	50	0.7200	0.53	8100
140	200	50	0.6000	0.40	8105
79	200	50	0.1933	0.09	8110
65	200	50	0.1000	0.04	8115
72	200	50	0.1467	0.07	8120
160	200	50	0.7333	0.55	8125
139	200	50	0.5933	0.39	8130
197	200	50	0.9800	0.95	8135
190	200	50	0.9333	0.86	8140
185	200	50	0.9000	0.79	8145
160	200	50	0.7333	0.55	8150
175	200	50	0.8333	0.69	8155
136	200	50	0.5733	0.37	8160
161	200	50	0.7400	0.56	8165
157	200	50	0.7133	0.52	8170
162	200	50	0.7467	0.57	8175
170	200	50	0.8000	0.64	8180
163	200	50	0.7533	0.57	8185
57	200	50	0.0467	0.02	8190
50	200	50	0.0000	0.00	8195
62	200	50	0.0800	0.04	8200
62	200	50	0.0800	0.04	8205
67	200	50	0.1133	0.05	8210
62	200	50	0.0800	0.04	8215
65	200	50	0.1000	0.04	8220
130	200	50	0.5333	0.34	8225
110	200	70	0.3077	0.16	8230
163	200	70	0.7154	0.53	8235
150	200	70	0.6154	0.42	8240
200	200	70	1.0000	1.00	8245
100	200	70	0.2308	0.11	8250
197	200	70	0.9769	0.95	8255
128	200	70	0.4462	0.26	8260
185	200	70	0.8846	0.77	8265
195	200	70	0.9615	0.91	8270
194	200	70	0.9538	0.90	8275
160	200	70	0.6923	0.50	8280
157	200	70	0.6692	0.47	8285

Table A.1 Shale volume (Vsh) calculation from **well: A** (continued)

Vsh.calculation (Clavier Eq.)					Depth
GR.	Max	Min	GR.fraction	Vsh.	(feet)
120	200	70	0.3846	0.22	8290
102	200	70	0.2462	0.12	8295
195	200	70	0.9615	0.91	8300
200	200	70	1.0000	1.00	8305
172	200	70	0.7846	0.62	8310
200	200	70	1.0000	1.00	8315
174	200	70	0.8000	0.64	8320
190	200	70	0.9231	0.84	8325
170	200	70	0.7692	0.59	8330
200	200	70	1.0000	1.00	8335
165	200	70	0.7308	0.55	8340
200	200	70	1.0000	1.00	8345
60	200	70	-0.0769	0.00	8350
170	200	70	0.7692	0.59	8355
74	200	70	0.0308	0.01	8360
72	200	70	0.0154	0.01	8365
80	200	70	0.0769	0.03	8370
200	200	70	1.0000	1.00	8375
200	200	70	1.0000	1.00	8380
126	200	70	0.4308	0.25	8385
180	200	70	0.8462	0.71	8390
153	200	70	0.6385	0.44	8395
90	200	70	0.1538	0.07	8400
77	200	70	0.0538	0.02	8405
100	200	70	0.2308	0.11	8410
85	200	70	0.1154	0.05	8415
84	200	70	0.1077	0.05	8420
62	200	70	-0.0615	0.00	8425
200	200	70	1.0000	1.00	8430
148	200	70	0.6000	0.40	8435
120	200	70	0.3846	0.22	8440
200	200	70	1.0000	1.00	8445
192	200	70	0.9385	0.87	8450
130	200	70	0.4615	0.27	8455
77	200	70	0.0538	0.02	8460
200	200	70	1.0000	1.00	8465
200	200	70	1.0000	1.00	8470
80	200	70	0.0769	0.03	8475
100	200	70	0.2308	0.11	8480
200	200	70	1.0000	1.00	8485
177	200	70	0.8231	0.67	8490
170	200	70	0.7692	0.59	8495
200	200	70	1.0000	1.00	8500
195	200	70	0.9615	0.91	8505
100	200	70	0.2308	0.11	8510
200	200	70	1.0000	1.00	8515
138	200	70	0.5231	0.33	8520

Vsh.calculation (Clavier Eq.)					Depth
GR.	Max	Min	GR.fraction	Vsh.	(feet)
90	200	70	0.1538	0.07	8525
190	200	70	0.9231	0.84	8530
200	200	70	1.0000	1.00	8535
200	200	70	1.0000	1.00	8540
200	200	70	1.0000	1.00	8545
105	200	70	0.2692	0.14	8550
110	200	70	0.3077	0.16	8555
119	200	70	0.3769	0.21	8560
110	200	70	0.3077	0.16	8565
110	200	70	0.3077	0.16	8570

Table A.2 Shale volume (Vsh) calculation from **well: B**

Vsh.calculation (Clavier Eq.)					Depth
GR.	Max	Min	GR.fraction	Vsh.	(feet)
115	160	30	0.654	0.46	4650
130	160	30	0.769	0.59	4655
105	160	30	0.577	0.38	4660
125	160	30	0.731	0.55	4665
48	160	30	0.138	0.06	4670
50	160	30	0.154	0.07	4675
63	160	30	0.254	0.13	4680
60	160	30	0.231	0.11	4685
50	160	30	0.154	0.07	4690
100	160	30	0.538	0.34	4695
65	160	30	0.269	0.14	4700
100	160	30	0.538	0.34	4705
63	160	30	0.254	0.13	4710
82	160	30	0.400	0.23	4715
150	160	30	0.923	0.84	4720
120	160	30	0.692	0.50	4725
113	160	30	0.638	0.44	4730
75	160	30	0.346	0.19	4735
67	160	30	0.285	0.15	4740
60	160	30	0.231	0.11	4745
58	160	30	0.215	0.11	4750
60	160	30	0.231	0.11	4755
160	160	30	1.000	1.00	4760
165	160	30	1.038	1.00	4765
140	160	30	0.846	0.71	4770
143	160	30	0.869	0.74	4775
140	160	30	0.846	0.71	4780
160	160	30	1.000	1.00	4785
140	160	30	0.846	0.71	4790
147	160	30	0.900	0.79	4795
138	160	30	0.831	0.68	4800
170	160	30	1.077	1.00	4805
147	160	30	0.900	0.79	4810
145	160	30	0.885	0.77	4815
120	160	30	0.692	0.50	4820
155	160	30	0.962	0.91	4825
133	160	30	0.792	0.63	4830
108	160	30	0.600	0.40	4835
167	160	30	1.054	1.00	4840
58	160	30	0.215	0.11	4845
155	160	30	0.962	0.91	4850
140	160	30	0.846	0.71	4855
140	160	30	0.846	0.71	4860
153	160	30	0.946	0.88	4865
148	160	30	0.908	0.81	4870
140	160	30	0.846	0.71	4875
178	160	30	1.138	1.00	4880

Vsh.calculation (Clavier Eq.)					Depth
GR.	Max	Min	GR.fraction	Vsh.	(feet)
142	160	30	0.862	0.73	4885
157	160	30	0.977	0.95	4890
174	160	30	1.108	1.00	4895
150	160	30	0.923	0.84	4900
130	160	30	0.769	0.59	4905
142	160	30	0.862	0.73	4910
157	160	30	0.977	0.95	4915
118	160	30	0.677	0.48	4920
145	160	30	0.885	0.77	4925
190	160	30	1.231	1.00	4930
120	160	30	0.692	0.50	4935
140	160	30	0.846	0.71	4940
147	160	30	0.900	0.79	4945
160	160	30	1.000	1.00	4950
168	160	30	1.062	1.00	4955
158	160	30	0.985	0.96	4960
138	160	30	0.831	0.68	4965
132	160	30	0.785	0.62	4970
65	160	30	0.269	0.14	4975
58	160	30	0.215	0.11	4980
55	160	30	0.192	0.09	4985
120	160	30	0.692	0.50	4990
150	160	30	0.923	0.84	4995
165	160	30	1.038	1.00	5000
122	160	30	0.708	0.52	5005
150	160	30	0.923	0.84	5010
175	160	30	1.115	1.00	5015
120	160	30	0.692	0.50	5020
80	160	30	0.385	0.22	5025
93	160	30	0.485	0.29	5030
85	160	30	0.423	0.24	5035
80	160	30	0.385	0.22	5040
73	160	30	0.331	0.18	5045
150	160	30	0.923	0.84	5050
190	160	30	1.231	1.00	5055
87	160	30	0.438	0.26	5060
103	160	30	0.562	0.36	5065
140	160	30	0.846	0.71	5070
200	160	30	1.308	1.00	5075
150	160	30	0.923	0.84	5080
158	160	30	0.985	0.96	5085
160	160	30	1.000	1.00	5090
170	160	30	1.077	1.00	5095
160	160	30	1.000	1.00	5100
142	160	30	0.862	0.73	5105
150	160	30	0.923	0.84	5110
150	160	30	0.923	0.84	5115

Table A.2 Shale volume (Vsh) calculation from **well: B** (continued)

Vsh.calculation (Clavier Eq.)					Depth
GR.	Max	Min	GR.fraction	Vsh.	(feet)
63	160	30	0.254	0.13	5120
75	160	30	0.346	0.19	5125
133	160	30	0.792	0.63	5130
162	160	30	1.015	1.00	5135
180	160	30	1.154	1.00	5140
142	160	30	0.862	0.73	5145
130	160	30	0.769	0.59	5150
153	160	30	0.946	0.88	5155
155	160	30	0.962	0.91	5160
128	160	30	0.754	0.57	5165
80	160	30	0.385	0.22	5170
65	160	30	0.269	0.14	5175
160	160	30	1.000	1.00	5180
150	160	30	0.923	0.84	5185
140	160	30	0.846	0.71	5190
155	160	30	0.962	0.91	5195
138	160	30	0.831	0.68	5200
80	160	30	0.385	0.22	5205
58	160	30	0.215	0.11	5210
67	160	30	0.285	0.15	5215
70	160	30	0.308	0.16	5220
70	160	30	0.308	0.16	5225
80	160	30	0.385	0.22	5230
162	160	30	1.015	1.00	5235
110	160	30	0.615	0.42	5240
112	160	30	0.631	0.43	5245
67	160	30	0.285	0.15	5250
70	160	30	0.308	0.16	5255
70	160	30	0.308	0.16	5260
65	160	30	0.269	0.14	5265
67	160	30	0.285	0.15	5270
60	160	30	0.231	0.11	5275
70	160	30	0.308	0.16	5280
82	160	30	0.400	0.23	5285
55	160	30	0.192	0.09	5290
98	160	30	0.523	0.33	5295
127	160	30	0.746	0.56	5300
153	160	30	0.946	0.88	5305
150	160	30	0.923	0.84	5310
170	160	30	1.077	1.00	5315
150	160	30	0.923	0.84	5320
173	160	30	1.100	1.00	5325
168	160	30	1.062	1.00	5330
138	160	30	0.831	0.68	5335
122	160	30	0.708	0.52	5340
115	160	30	0.654	0.46	5345
140	160	30	0.846	0.71	5350

Vsh.calculation (Clavier Eq.)					Depth
GR.	Max	Min	GR.fraction	Vsh.	(feet)
145	160	30	0.885	0.77	5355
145	160	30	0.885	0.77	5360
130	160	30	0.769	0.59	5365
140	160	30	0.846	0.71	5370
140	160	30	0.846	0.71	5375
150	160	30	0.923	0.84	5380
168	160	30	1.062	1.00	5385
160	160	30	1.000	1.00	5390
160	160	30	1.000	1.00	5395
181	160	30	1.162	1.00	5400
189	160	30	1.223	1.00	5405
155	160	30	0.962	0.91	5410
145	160	30	0.885	0.77	5415
158	160	30	0.985	0.96	5420
155	160	30	0.962	0.91	5425
127	160	30	0.746	0.56	5430
135	160	30	0.808	0.65	5435
120	160	30	0.692	0.50	5440
70	160	30	0.308	0.16	5445
62	160	30	0.246	0.12	5450
82	160	30	0.400	0.23	5455
85	160	30	0.423	0.24	5460
118	160	30	0.677	0.48	5465
142	160	30	0.862	0.73	5470
175	160	30	1.115	1.00	5475
180	160	30	1.154	1.00	5480
65	160	30	0.269	0.14	5485
142	160	30	0.862	0.73	5490
130	160	30	0.769	0.59	5495
132	160	30	0.785	0.62	5500
77	160	30	0.362	0.20	5505
60	160	30	0.231	0.11	5510
60	160	30	0.231	0.11	5515
55	160	30	0.192	0.09	5520
53	160	30	0.177	0.08	5525
57	160	30	0.208	0.10	5530
50	160	30	0.154	0.07	5535
70	160	30	0.308	0.16	5540
78	160	30	0.369	0.20	5545
78	160	30	0.369	0.20	5550
80	160	30	0.385	0.22	5555
60	160	30	0.231	0.11	5560
59	160	30	0.223	0.11	5565
90	160	30	0.462	0.27	5570
140	160	30	0.846	0.71	5575
140	160	30	0.846	0.71	5580
121	160	30	0.700	0.51	5585

Table A.2 Shale volume (Vsh) calculation from **well: B** (continued)

Vsh.calculation (Clavier Eq.)					Depth
GR.	Max	Min	GR.fraction	Vsh.	(feet)
80	160	30	0.385	0.22	5590
68	160	30	0.292	0.15	5595
62	160	30	0.246	0.12	5600
60	160	30	0.231	0.11	5605
70	160	30	0.308	0.16	5610
53	160	30	0.177	0.08	5615
52	160	30	0.169	0.08	5620
120	160	30	0.692	0.50	5625
80	160	30	0.385	0.22	5630
100	160	30	0.538	0.34	5635
80	160	30	0.385	0.22	5640
200	160	30	1.308	1.00	5645
142	160	30	0.862	0.73	5650
170	160	30	1.077	1.00	5655
160	160	30	1.000	1.00	5660
145	160	30	0.885	0.77	5665
170	160	30	1.077	1.00	5670
130	160	30	0.769	0.59	5675
140	160	30	0.846	0.71	5680
130	160	30	0.769	0.59	5685
187	160	30	1.208	1.00	5690
200	160	30	1.308	1.00	5695
167	160	30	1.054	1.00	5700
200	160	30	1.308	1.00	5705
197	160	30	1.285	1.00	5710
128	160	30	0.754	0.57	5715
168	160	30	1.062	1.00	5720
125	160	30	0.731	0.55	5725
115	160	30	0.654	0.46	5730
158	160	30	0.985	0.96	5735
147	160	30	0.900	0.79	5740
123	160	30	0.715	0.53	5745
150	160	30	0.923	0.84	5750
117	160	30	0.669	0.47	5755
125	160	30	0.731	0.55	5760
175	160	30	1.115	1.00	5765
185	160	30	1.192	1.00	5770
190	160	30	1.231	1.00	5775
42	160	30	0.092	0.04	5780
60	160	30	0.231	0.11	5785
55	160	30	0.192	0.09	5790
110	160	30	0.615	0.42	5795
110	160	30	0.615	0.42	5800
153	160	30	0.946	0.88	5805
148	160	30	0.908	0.81	5810
198	160	30	1.292	1.00	5815
121	160	30	0.700	0.51	5820

Vsh.calculation (Clavier Eq.)					Depth
GR.	Max	Min	GR.fraction	Vsh.	(feet)
178	160	30	1.138	1.00	5825
143	160	30	0.869	0.74	5830
174	160	30	1.108	1.00	5835
190	160	30	1.231	1.00	5840
150	160	30	0.923	0.84	5845
148	160	30	0.908	0.81	5850
190	160	30	1.231	1.00	5855
143	160	30	0.869	0.74	5860
120	160	30	0.692	0.50	5865
53	160	30	0.177	0.08	5870
70	160	30	0.308	0.16	5875
62	160	30	0.246	0.12	5880
78	160	30	0.369	0.20	5885
62	160	30	0.246	0.12	5890
70	160	30	0.308	0.16	5895
120	160	30	0.692	0.50	5900
100	160	30	0.538	0.34	5905
142	160	30	0.862	0.73	5910
145	160	30	0.885	0.77	5915
178	160	30	1.138	1.00	5920
160	160	30	1.000	1.00	5925
100	160	30	0.538	0.34	5930
90	160	30	0.462	0.27	5935
200	160	30	1.308	1.00	5940
140	160	30	0.846	0.71	5945
120	160	30	0.692	0.50	5950
118	160	30	0.677	0.48	5955
160	160	30	1.000	1.00	5960
60	160	30	0.231	0.11	5965
52	160	30	0.169	0.08	5970
68	160	30	0.292	0.15	5975
80	160	30	0.385	0.22	5980
67	160	30	0.285	0.15	5985
200	160	30	1.308	1.00	5990
120	160	30	0.692	0.50	5995
150	160	30	0.923	0.84	6000
163	160	30	1.023	1.00	6005
143	160	30	0.869	0.74	6010
150	160	30	0.923	0.84	6015
142	160	30	0.862	0.73	6020
150	160	30	0.923	0.84	6025
147	160	30	0.900	0.79	6030
128	160	30	0.754	0.57	6035
108	160	30	0.600	0.40	6040
110	160	30	0.615	0.42	6045
108	160	30	0.600	0.40	6050
78	160	30	0.369	0.20	6055

Table A.2 Shale volume (Vsh) calculation from **well: B** (continued)

Vsh.calculation (Clavier Eq.)					Depth
GR.	Max	Min	GR.fraction	Vsh.	(feet)
80	160	30	0.385	0.22	6060
62	160	30	0.246	0.12	6065
58	160	30	0.215	0.11	6070
55	160	30	0.192	0.09	6075
62	160	30	0.246	0.12	6080
165	160	30	1.038	1.00	6085
121	160	30	0.700	0.51	6090
150	160	30	0.923	0.84	6095
113	160	30	0.638	0.44	6100
98	160	30	0.523	0.33	6105
142	160	30	0.862	0.73	6110
158	160	30	0.985	0.96	6115
160	160	30	1.000	1.00	6120
85	160	30	0.423	0.24	6125
98	160	30	0.523	0.33	6130
147	160	30	0.900	0.79	6135
90	160	30	0.462	0.27	6140
70	160	30	0.308	0.16	6145
120	160	30	0.692	0.50	6150
110	160	30	0.615	0.42	6155
180	160	30	1.154	1.00	6160
150	160	30	0.923	0.84	6165
160	160	30	1.000	1.00	6170
138	160	30	0.831	0.68	6175
128	160	30	0.754	0.57	6180
83	160	30	0.408	0.23	6185
168	160	30	1.062	1.00	6190
165	160	30	1.038	1.00	6195
140	160	30	0.846	0.71	6200
180	160	30	1.154	1.00	6205
140	160	30	0.846	0.71	6210
155	160	30	0.962	0.91	6215
112	160	30	0.631	0.43	6220
142	160	30	0.862	0.73	6225
167	160	30	1.054	1.00	6230
182	160	30	1.169	1.00	6235
122	160	30	0.708	0.52	6240
140	160	30	0.846	0.71	6245
102	160	30	0.554	0.36	6250
158	160	30	0.985	0.96	6255
103	160	30	0.562	0.36	6260
138	160	30	0.831	0.68	6265
140	160	30	0.846	0.71	6270
170	160	30	1.077	1.00	6275
190	160	30	1.231	1.00	6280
140	160	30	0.846	0.71	6285
135	160	30	0.808	0.65	6290

Vsh.calculation (Clavier Eq.)					Depth
GR.	Max	Min	GR.fraction	Vsh.	(feet)
140	160	30	0.846	0.71	6295
140	160	30	0.846	0.71	6300
197	160	30	1.285	1.00	6305
140	160	30	0.846	0.71	6310
165	160	30	1.038	1.00	6315
138	160	30	0.831	0.68	6320
132	160	30	0.785	0.62	6325
58	160	30	0.215	0.11	6330
58	160	30	0.215	0.11	6335
182	160	30	1.169	1.00	6340
168	160	30	1.062	1.00	6345
137	160	30	0.823	0.67	6350
163	160	30	1.023	1.00	6355
135	160	30	0.808	0.65	6360
78	160	30	0.369	0.20	6365
68	160	30	0.292	0.15	6370
70	160	30	0.308	0.16	6375
60	160	30	0.231	0.11	6380
63	160	30	0.254	0.13	6385
60	160	30	0.231	0.11	6390
58	160	30	0.215	0.11	6395
120	160	30	0.692	0.50	6400
150	160	30	0.923	0.84	6405
197	160	30	1.285	1.00	6410
160	160	30	1.000	1.00	6415
160	160	30	1.000	1.00	6420
170	160	30	1.077	1.00	6425
163	160	30	1.023	1.00	6430
138	160	30	0.831	0.68	6435
100	160	30	0.538	0.34	6440
50	160	30	0.154	0.07	6445
55	160	30	0.192	0.09	6450
53	160	30	0.177	0.08	6455
58	160	30	0.215	0.11	6460
57	160	30	0.208	0.10	6465
62	160	30	0.246	0.12	6470
58	160	30	0.215	0.11	6475
58	160	30	0.215	0.11	6480
60	160	30	0.231	0.11	6485
58	160	30	0.215	0.11	6490
60	160	30	0.231	0.11	6495
80	160	30	0.385	0.22	6500
120	160	30	0.692	0.50	6505
100	160	30	0.538	0.34	6510
78	160	30	0.369	0.20	6515
70	160	30	0.308	0.16	6520
70	160	30	0.308	0.16	6525

Table A.2 Shale volume (Vsh) calculation from **well: B** (continued)

Vsh.calculation (Clavier Eq.)					Depth
GR.	Max	Min	GR.fraction	Vsh.	(feet)
70	160	30	0.308	0.16	6530
72	160	30	0.323	0.17	6535
65	160	30	0.269	0.14	6540
75	160	30	0.346	0.19	6545
110	160	30	0.615	0.42	6550
160	160	30	1.000	1.00	6555
108	160	30	0.600	0.40	6560
60	160	30	0.231	0.11	6565
160	160	30	1.000	1.00	6570
150	160	30	0.923	0.84	6575
150	160	30	0.923	0.84	6580
165	160	30	1.038	1.00	6585
170	160	30	1.077	1.00	6590
183	160	30	1.177	1.00	6595
138	160	30	0.831	0.68	6600
137	160	30	0.823	0.67	6605
132	160	30	0.785	0.62	6610
130	160	30	0.769	0.59	6615
130	160	30	0.769	0.59	6620
155	160	30	0.962	0.91	6625
123	160	30	0.715	0.53	6630
130	160	30	0.769	0.59	6635
125	160	30	0.731	0.55	6640
145	160	30	0.885	0.77	6645
140	160	30	0.846	0.71	6650
137	160	30	0.823	0.67	6655
138	160	30	0.831	0.68	6660
140	160	30	0.846	0.71	6665
121	160	30	0.700	0.51	6670
175	160	30	1.115	1.00	6675
165	160	30	1.038	1.00	6680
190	160	30	1.231	1.00	6685
160	160	30	1.000	1.00	6690
142	160	30	0.862	0.73	6695
160	160	30	1.000	1.00	6700
162	160	30	1.015	1.00	6705
100	160	30	0.538	0.34	6710
200	160	30	1.308	1.00	6715
150	160	30	0.923	0.84	6720
142	160	30	0.862	0.73	6725
162	160	30	1.015	1.00	6730
170	160	30	1.077	1.00	6735
168	160	30	1.062	1.00	6740
125	160	30	0.731	0.55	6745
125	160	30	0.731	0.55	6750
143	160	30	0.869	0.74	6755
145	160	30	0.885	0.77	6760

Vsh.calculation (Clavier Eq.)					Depth
GR.	Max	Min	GR.fraction	Vsh.	(feet)
138	160	30	0.831	0.68	6765
140	160	30	0.846	0.71	6770
158	160	30	0.985	0.96	6775
75	160	30	0.346	0.19	6780
57	160	30	0.208	0.10	6785
162	160	30	1.015	1.00	6790
120	160	30	0.692	0.50	6795
165	160	30	1.038	1.00	6800
140	160	30	0.846	0.71	6805
130	160	30	0.769	0.59	6810
142	160	30	0.862	0.73	6815
195	160	30	1.269	1.00	6820
180	160	30	1.154	1.00	6825
160	160	30	1.000	1.00	6830
130	160	30	0.769	0.59	6835
165	160	30	1.038	1.00	6840
178	160	30	1.138	1.00	6845
179	160	30	1.146	1.00	6850
160	160	30	1.000	1.00	6855
145	160	30	0.885	0.77	6860
176	160	30	1.123	1.00	6865
170	160	30	1.077	1.00	6870
178	160	30	1.138	1.00	6875
150	160	30	0.923	0.84	6880
170	160	30	1.077	1.00	6885
180	160	30	1.154	1.00	6890
158	160	30	0.985	0.96	6895
200	160	30	1.308	1.00	6900
162	160	30	1.015	1.00	6905
160	160	30	1.000	1.00	6910
158	160	30	0.985	0.96	6915
78	160	30	0.369	0.20	6920
180	160	30	1.154	1.00	6925
140	160	30	0.846	0.71	6930
103	160	24	0.581	0.38	6935
118	160	24	0.691	0.50	6940
58	160	24	0.250	0.13	6945
60	160	24	0.265	0.13	6950
70	160	24	0.338	0.18	6955
100	160	24	0.559	0.36	6960
150	160	24	0.926	0.84	6965
130	160	24	0.779	0.61	6970
103	160	24	0.581	0.38	6975
200	160	24	1.294	1.00	6980
120	160	24	0.706	0.52	6985
170	160	24	1.074	1.00	6990
160	160	24	1.000	1.00	6995

Table A.2 Shale volume (Vsh) calculation from **well: B** (continued)

Vsh.calculation (Clavier Eq.)					Depth
GR.	Max	Min	GR.fraction	Vsh.	(feet)
110	160	24	0.632	0.43	7000
103	160	24	0.581	0.38	7005
75	160	24	0.375	0.21	7010
177	160	24	1.125	1.00	7015
160	160	24	1.000	1.00	7020
170	160	24	1.074	1.00	7025
138	160	24	0.838	0.69	7030
130	160	24	0.779	0.61	7035
183	160	24	1.169	1.00	7040
160	160	24	1.000	1.00	7045
174	160	24	1.103	1.00	7050
177	160	24	1.125	1.00	7055
152	160	24	0.941	0.87	7060
132	160	24	0.794	0.63	7065
190	160	24	1.221	1.00	7070
95	160	24	0.522	0.33	7075
200	160	24	1.294	1.00	7080
150	160	24	0.926	0.84	7085
133	160	24	0.801	0.64	7090
65	160	24	0.301	0.16	7095
60	160	24	0.265	0.13	7100
57	160	24	0.243	0.12	7105
60	160	24	0.265	0.13	7110
73	160	24	0.360	0.20	7115
200	160	24	1.294	1.00	7120
150	160	24	0.926	0.84	7125
120	160	24	0.706	0.52	7130
62	160	24	0.279	0.14	7135
50	160	24	0.191	0.09	7140
68	160	24	0.324	0.17	7145
50	160	24	0.191	0.09	7150
165	160	24	1.037	1.00	7155
113	160	24	0.654	0.46	7160
115	160	24	0.669	0.47	7165
70	160	24	0.338	0.18	7170
70	160	24	0.338	0.18	7175
180	160	24	1.147	1.00	7180
140	160	24	0.853	0.72	7185
160	160	24	1.000	1.00	7190
167	160	24	1.051	1.00	7195
180	160	24	1.147	1.00	7200
172	160	24	1.088	1.00	7205
182	160	24	1.162	1.00	7210
180	160	24	1.147	1.00	7215
200	160	24	1.294	1.00	7220
140	160	24	0.853	0.72	7225
170	160	24	1.074	1.00	7230

Vsh.calculation (Clavier Eq.)					Depth
GR.	Max	Min	GR.fraction	Vsh.	(feet)
167	160	24	1.051	1.00	7235
102	160	24	0.574	0.37	7240
116	160	24	0.676	0.48	7245
110	160	24	0.632	0.43	7250
50	160	24	0.191	0.09	7255
40	160	24	0.118	0.05	7260
87	160	24	0.463	0.28	7265
60	160	24	0.265	0.13	7270
160	160	24	1.000	1.00	7275
164	160	24	1.029	1.00	7280
145	160	24	0.890	0.78	7285
130	160	24	0.779	0.61	7290
178	160	24	1.132	1.00	7295
163	160	24	1.022	1.00	7300
150	160	24	0.926	0.84	7305
158	160	24	0.985	0.97	7310
130	160	24	0.779	0.61	7315
200	160	24	1.294	1.00	7320
163	160	24	1.022	1.00	7325
160	160	24	1.000	1.00	7330
158	160	24	0.985	0.97	7335
105	160	24	0.596	0.40	7340
115	160	24	0.669	0.47	7345
45	160	24	0.154	0.07	7350
50	160	24	0.191	0.09	7355
173	160	24	1.096	1.00	7360
168	160	24	1.059	1.00	7365
168	160	24	1.059	1.00	7370
190	160	24	1.221	1.00	7375
120	160	24	0.706	0.52	7380
180	160	24	1.147	1.00	7385
150	160	24	0.926	0.84	7390
130	160	24	0.779	0.61	7395
158	160	24	0.985	0.97	7400
200	160	24	1.294	1.00	7405
123	160	24	0.728	0.54	7410
172	160	24	1.088	1.00	7415
160	160	24	1.000	1.00	7420
45	160	24	0.154	0.07	7425
60	160	24	0.265	0.13	7430
53	160	24	0.213	0.10	7435
58	160	24	0.250	0.13	7440
55	160	24	0.228	0.11	7445
45	160	24	0.154	0.07	7450
50	160	24	0.191	0.09	7455
60	160	24	0.265	0.13	7460
105	160	24	0.596	0.40	7465

Table A.2 Shale volume (Vsh) calculation from **well: B** (continued)

Vsh.calculation (Clavier Eq.)					Depth
GR.	Max	Min	GR.fraction	Vsh.	(feet)
73	160	24	0.360	0.20	7470
102	160	24	0.574	0.37	7475
190	160	24	1.221	1.00	7480
193	160	24	1.243	1.00	7485
125	160	24	0.743	0.56	7490
165	160	24	1.037	1.00	7495
160	160	24	1.000	1.00	7500
157	160	24	0.978	0.95	7505
185	160	24	1.184	1.00	7510
173	160	24	1.096	1.00	7515
180	160	24	1.147	1.00	7520
120	160	24	0.706	0.52	7525
123	160	24	0.728	0.54	7530
45	160	24	0.154	0.07	7535
40	160	24	0.118	0.05	7540
60	160	24	0.265	0.13	7545
53	160	24	0.213	0.10	7550
50	160	24	0.191	0.09	7555
52	160	24	0.206	0.10	7560
160	160	24	1.000	1.00	7565
133	160	24	0.801	0.64	7570
100	160	24	0.559	0.36	7575
50	160	24	0.191	0.09	7580
188	160	24	1.206	1.00	7585
150	160	24	0.926	0.84	7590
121	160	24	0.713	0.52	7595
190	160	24	1.221	1.00	7600
187	160	24	1.199	1.00	7605
180	160	24	1.147	1.00	7610
120	160	24	0.706	0.52	7615
177	160	24	1.125	1.00	7620
172	160	24	1.088	1.00	7625
130	160	24	0.779	0.61	7630
130	160	24	0.779	0.61	7635
138	160	24	0.838	0.69	7640
98	160	24	0.544	0.35	7645
50	160	24	0.191	0.09	7650
55	160	24	0.228	0.11	7655
53	160	24	0.213	0.10	7660
60	160	24	0.265	0.13	7665
67	160	24	0.316	0.17	7670
157	160	24	0.978	0.95	7675
200	160	24	1.294	1.00	7680
200	160	24	1.294	1.00	7685
190	160	24	1.221	1.00	7690
170	160	24	1.074	1.00	7695
138	160	24	0.838	0.69	7700

Vsh.calculation (Clavier Eq.)					Depth
GR.	Max	Min	GR.fraction	Vsh.	(feet)
130	160	24	0.779	0.61	7705
95	160	24	0.522	0.33	7710
50	160	24	0.191	0.09	7715
62	160	24	0.279	0.14	7720
110	160	24	0.632	0.43	7725
180	160	24	1.147	1.00	7730
178	160	24	1.132	1.00	7735
175	160	24	1.110	1.00	7740
160	160	24	1.000	1.00	7745
190	160	24	1.221	1.00	7750
178	160	24	1.132	1.00	7755
185	160	24	1.184	1.00	7760
150	160	24	0.926	0.84	7765
110	160	24	0.632	0.43	7770
160	160	24	1.000	1.00	7775
150	160	24	0.926	0.84	7780
60	160	24	0.265	0.13	7785
117	160	24	0.684	0.49	7790
95	160	24	0.522	0.33	7795
60	160	24	0.265	0.13	7800
110	160	24	0.632	0.43	7805
137	160	24	0.831	0.68	7810
165	160	24	1.037	1.00	7815
170	160	24	1.074	1.00	7820
120	160	24	0.706	0.52	7825
157	160	24	0.978	0.95	7830
140	160	24	0.853	0.72	7835
165	160	24	1.037	1.00	7840
155	160	24	0.963	0.92	7845
172	160	24	1.088	1.00	7850
182	160	24	1.162	1.00	7855
140	160	24	0.853	0.72	7860
150	160	24	0.926	0.84	7865
122	160	24	0.721	0.53	7870
70	160	24	0.338	0.18	7875
63	160	24	0.287	0.15	7880
45	160	24	0.154	0.07	7885
60	160	24	0.265	0.13	7890
80	160	24	0.412	0.24	7895
80	160	24	0.412	0.24	7900
80	160	24	0.412	0.24	7905
180	160	24	1.147	1.00	7910
145	160	24	0.890	0.78	7915
162	160	24	1.015	1.00	7920
150	160	24	0.926	0.84	7925
125	160	24	0.743	0.56	7930
187	160	24	1.199	1.00	7935

Table A.2 Shale volume (Vsh) calculation from **well: B** (continued)

Vsh.calculation (Clavier Eq.)					Depth
GR.	Max	Min	GR.fraction	Vsh.	(feet)
200	160	24	1.294	1.00	7940
150	160	24	0.926	0.84	7945
180	160	24	1.147	1.00	7950
177	160	24	1.125	1.00	7955
167	160	24	1.051	1.00	7960
113	160	24	0.654	0.46	7965
170	160	24	1.074	1.00	7970
110	160	24	0.632	0.43	7975
102	160	24	0.574	0.37	7980
138	160	24	0.838	0.69	7985
118	160	24	0.691	0.50	7990
50	160	24	0.191	0.09	7995
60	160	24	0.265	0.13	8000
62	160	24	0.279	0.14	8005
60	160	24	0.265	0.13	8010
70	160	24	0.338	0.18	8015
187	160	24	1.199	1.00	8020
150	160	24	0.926	0.84	8025
197	160	24	1.272	1.00	8030
182	160	24	1.162	1.00	8035
180	160	24	1.147	1.00	8040
155	160	24	0.963	0.92	8045
140	160	24	0.853	0.72	8050
55	160	24	0.228	0.11	8055
60	160	24	0.265	0.13	8060
50	160	24	0.191	0.09	8065
42	160	24	0.132	0.06	8070
60	160	24	0.265	0.13	8075
155	160	24	0.963	0.92	8080
170	160	24	1.074	1.00	8085
155	160	24	0.963	0.92	8090
150	160	24	0.926	0.84	8095
198	160	24	1.279	1.00	8100
180	160	24	1.147	1.00	8105
200	160	24	1.294	1.00	8110
195	160	24	1.257	1.00	8115
150	160	24	0.926	0.84	8120
198	160	24	1.279	1.00	8125
150	160	24	0.926	0.84	8130
90	160	24	0.485	0.29	8135
45	160	24	0.154	0.07	8140
113	160	24	0.654	0.46	8145
140	160	24	0.853	0.72	8150
70	160	24	0.338	0.18	8155
65	160	24	0.301	0.16	8160
78	160	24	0.397	0.22	8165
70	160	24	0.338	0.18	8170

Vsh.calculation (Clavier Eq.)					Depth
GR.	Max	Min	GR.fraction	Vsh.	(feet)
70	160	24	0.338	0.18	8175
130	160	24	0.779	0.61	8180
83	160	24	0.434	0.25	8185
62	160	24	0.279	0.14	8190
75	160	24	0.375	0.21	8195
200	160	24	1.294	1.00	8200
188	160	24	1.206	1.00	8205
119	160	24	0.699	0.51	8210
188	160	24	1.206	1.00	8215
150	160	24	0.926	0.84	8220
200	160	24	1.294	1.00	8225
162	160	24	1.015	1.00	8230
157	160	24	0.978	0.95	8235
200	160	24	1.294	1.00	8240
190	160	24	1.221	1.00	8245
190	160	24	1.221	1.00	8250
112	160	24	0.647	0.45	8255
200	160	24	1.294	1.00	8260
138	160	24	0.838	0.69	8265
103	160	24	0.581	0.38	8270
68	164	40	0.226	0.11	8275
62	164	40	0.177	0.08	8280
45	164	40	0.040	0.02	8285
42	164	40	0.016	0.01	8290
50	164	40	0.081	0.04	8295
48	164	40	0.065	0.03	8300
47	164	40	0.056	0.02	8305
40	164	40	0.000	0.00	8310
177	164	40	1.105	1.00	8315
157	164	40	0.944	0.88	8320
132	164	40	0.742	0.56	8325
126	164	40	0.694	0.50	8330
131	164	40	0.734	0.55	8335
150	164	40	0.887	0.77	8340
135	164	40	0.766	0.59	8345
175	164	40	1.089	1.00	8350
170	164	40	1.048	1.00	8355
175	164	40	1.089	1.00	8360
175	164	40	1.089	1.00	8365
170	164	40	1.048	1.00	8370
178	164	40	1.113	1.00	8375
110	164	40	0.565	0.37	8380
155	164	40	0.927	0.84	8385
140	164	40	0.806	0.65	8390
190	164	40	1.210	1.00	8395
175	164	40	1.089	1.00	8400
179	164	40	1.121	1.00	8405

Table A.2 Shale volume (Vsh) calculation from **well: B** (continued)

Vsh.calculation (Clavier Eq.)					Depth
GR.	Max	Min	GR.fraction	Vsh.	(feet)
170	164	40	1.048	1.00	8410
175	164	40	1.089	1.00	8415
150	164	40	0.887	0.77	8420
137	164	40	0.782	0.61	8425
160	164	40	0.968	0.93	8430
178	164	40	1.113	1.00	8435
165	164	40	1.008	1.00	8440
170	164	40	1.048	1.00	8445
172	164	40	1.065	1.00	8450
153	164	40	0.911	0.81	8455
152	164	40	0.903	0.80	8460
168	164	40	1.032	1.00	8465
172	164	40	1.065	1.00	8470
170	164	40	1.048	1.00	8475
183	164	40	1.153	1.00	8480
145	164	40	0.847	0.71	8485
162	164	40	0.984	0.96	8490
90	164	40	0.403	0.23	8495
50	164	40	0.081	0.04	8500
48	164	40	0.065	0.03	8505
55	164	40	0.121	0.06	8510
60	164	40	0.161	0.08	8515
67	164	40	0.218	0.11	8520
65	164	40	0.202	0.10	8525
65	164	40	0.202	0.10	8530
60	164	40	0.161	0.08	8535
200	164	40	1.290	1.00	8540
155	164	40	0.927	0.84	8545
45	164	40	0.040	0.02	8550
80	164	40	0.323	0.17	8555
78	164	40	0.306	0.16	8560
58	164	40	0.145	0.07	8565
55	164	40	0.121	0.06	8570
42	164	40	0.016	0.01	8575
187	164	40	1.185	1.00	8580
190	164	40	1.210	1.00	8585
185	164	40	1.169	1.00	8590
157	164	40	0.944	0.88	8595
188	164	40	1.194	1.00	8600
177	164	40	1.105	1.00	8605
128	164	40	0.710	0.52	8610
180	164	40	1.129	1.00	8615
90	164	40	0.403	0.23	8620
165	164	40	1.008	1.00	8625
121	164	40	0.653	0.46	8630
160	164	40	0.968	0.93	8635
170	164	40	1.048	1.00	8640

Vsh.calculation (Clavier Eq.)					Depth
GR.	Max	Min	GR.fraction	Vsh.	(feet)
80	164	40	0.323	0.17	8645
60	164	40	0.161	0.08	8650
50	164	40	0.081	0.04	8655
50	164	40	0.081	0.04	8660
52	164	40	0.097	0.04	8665
57	164	40	0.137	0.06	8670
155	164	40	0.927	0.84	8675
160	164	40	0.968	0.93	8680
179	164	40	1.121	1.00	8685
163	164	40	0.992	0.98	8690
130	164	40	0.726	0.54	8695
170	164	40	1.048	1.00	8700
122	164	40	0.661	0.46	8705
180	164	40	1.129	1.00	8710
70	164	40	0.242	0.12	8715
80	164	40	0.323	0.17	8720
80	164	40	0.323	0.17	8725
100	164	40	0.484	0.29	8730
138	164	40	0.790	0.62	8735
100	164	40	0.484	0.29	8740
67	164	40	0.218	0.11	8745
195	164	40	1.250	1.00	8750
150	164	40	0.887	0.77	8755
75	164	40	0.282	0.15	8760
160	164	40	0.968	0.93	8765
188	164	40	1.194	1.00	8770
200	164	40	1.290	1.00	8775
130	164	40	0.726	0.54	8780
190	164	40	1.210	1.00	8785
147	164	40	0.863	0.73	8790
168	164	40	1.032	1.00	8795
154	164	40	0.919	0.83	8800
170	164	40	1.048	1.00	8805
125	164	40	0.685	0.49	8810
170	164	40	1.048	1.00	8815
170	164	40	1.048	1.00	8820
150	164	40	0.887	0.77	8825
190	164	40	1.210	1.00	8830
150	164	40	0.887	0.77	8835
150	164	40	0.887	0.77	8840
90	164	40	0.403	0.23	8845
60	164	40	0.161	0.08	8850
142	164	40	0.823	0.67	8855
180	164	40	1.129	1.00	8860
200	164	40	1.290	1.00	8865
100	164	40	0.484	0.29	8870
180	164	40	1.129	1.00	8875

Table A.2 Shale volume (Vsh) calculation from **well: B** (continued)

Vsh.calculation (Clavier Eq.)					Depth
GR.	Max	Min	GR.fraction	Vsh.	(feet)
130	164	40	0.726	0.54	8880
200	164	40	1.290	1.00	8885
185	164	40	1.169	1.00	8890
190	164	40	1.210	1.00	8895
190	164	40	1.210	1.00	8900

Table A.3 Shale volume (Vsh) calculation from **well: C**

Vsh.calculation (Clavier Eq.)					Depth
GR.	Max	Min	GR.fraction	Vsh.	(feet)
140	138	43	1.0211	1.00	4300
118	138	43	0.7895	0.62	4305
120	138	43	0.8105	0.65	4310
125	138	43	0.8632	0.73	4315
122	138	43	0.8316	0.68	4320
122	138	43	0.8316	0.68	4325
128	138	43	0.8947	0.79	4330
132	138	43	0.9368	0.86	4335
120	138	43	0.8105	0.65	4340
130	138	43	0.9158	0.82	4345
120	138	43	0.8105	0.65	4350
132	138	43	0.9368	0.86	4355
125	138	43	0.8632	0.73	4360
103	138	43	0.6316	0.43	4365
120	138	43	0.8105	0.65	4370
108	138	43	0.6842	0.49	4375
63	138	43	0.2105	0.10	4380
55	138	43	0.1263	0.06	4385
55	138	43	0.1263	0.06	4390
70	138	43	0.2842	0.15	4395
122	138	43	0.8316	0.68	4400
130	138	43	0.9158	0.82	4405
130	138	43	0.9158	0.82	4410
120	138	43	0.8105	0.65	4415
122	138	43	0.8316	0.68	4420
118	138	43	0.7895	0.62	4425
125	138	43	0.8632	0.73	4430
130	138	43	0.9158	0.82	4435
135	138	43	0.9684	0.93	4440
120	138	43	0.8105	0.65	4445
95	138	43	0.5474	0.35	4450
102	138	43	0.6211	0.42	4455
87	138	43	0.4632	0.28	4460
75	138	43	0.3368	0.18	4465
45	138	43	0.0211	0.01	4470
42	138	43	-0.0105	0.00	4475
60	138	43	0.1789	0.09	4480
52	138	43	0.0947	0.04	4485
127	138	43	0.8842	0.77	4490
70	138	43	0.2842	0.15	4495
60	138	43	0.1789	0.09	4500
53	138	43	0.1053	0.05	4505
112	138	43	0.7263	0.54	4510
78	138	43	0.3684	0.20	4515
60	138	43	0.1789	0.09	4520
65	138	43	0.2316	0.12	4525
52	138	43	0.0947	0.04	4530

Vsh.calculation (Clavier Eq.)					Depth
GR.	Max	Min	GR.fraction	Vsh.	(feet)
47	138	43	0.0421	0.02	4535
55	138	43	0.1263	0.06	4540
125	138	43	0.8632	0.73	4545
120	138	43	0.8105	0.65	4550
127	138	43	0.8842	0.77	4555
130	138	43	0.9158	0.82	4560
118	138	43	0.7895	0.62	4565
120	138	43	0.8105	0.65	4570
115	138	43	0.7579	0.58	4575
160	138	43	1.2316	1.00	4580
135	138	43	0.9684	0.93	4585
120	138	43	0.8105	0.65	4590
68	138	43	0.2632	0.13	4595
50	138	43	0.0737	0.03	4600
62	138	43	0.2000	0.10	4605
53	138	43	0.1053	0.05	4610
77	138	43	0.3579	0.20	4615
78	138	43	0.3684	0.20	4620
125	138	43	0.8632	0.73	4625
140	138	43	1.0211	1.00	4630
122	138	43	0.8316	0.68	4635
110	138	43	0.7053	0.51	4640
127	138	43	0.8842	0.77	4645
115	138	43	0.7579	0.58	4650
130	138	43	0.9158	0.82	4655
138	138	43	1.0000	1.00	4660
145	138	43	1.0737	1.00	4665
135	138	43	0.9684	0.93	4670
133	138	43	0.9474	0.88	4675
115	138	43	0.7579	0.58	4680
130	138	43	0.9158	0.82	4685
120	138	43	0.8105	0.65	4690
134	138	43	0.9579	0.91	4695
125	138	43	0.8632	0.73	4700
128	138	43	0.8947	0.79	4705
133	138	43	0.9474	0.88	4710
135	138	43	0.9684	0.93	4715
122	138	43	0.8316	0.68	4720
140	138	43	1.0211	1.00	4725
145	138	43	1.0737	1.00	4730
115	138	43	0.7579	0.58	4735
138	138	43	1.0000	1.00	4740
120	138	43	0.8105	0.65	4745
113	138	43	0.7368	0.55	4750
150	138	43	1.1263	1.00	4755
127	138	43	0.8842	0.77	4760
110	138	43	0.7053	0.51	4765

Table A.3 Shale volume (Vsh) calculation from **well: C** (continued)

Vsh.calculation (Clavier Eq.)					Depth
GR.	Max	Min	GR.fraction	Vsh.	(feet)
110	138	43	0.7053	0.51	4770
93	138	43	0.5263	0.33	4775
95	138	43	0.5474	0.35	4780
100	138	43	0.6000	0.40	4785
60	138	43	0.1789	0.09	4790
60	138	43	0.1789	0.09	4795
60	138	43	0.1789	0.09	4800
57	138	43	0.1474	0.07	4805
163	138	43	1.2632	1.00	4810
140	138	43	1.0211	1.00	4815
130	138	43	0.9158	0.82	4820
142	138	43	1.0421	1.00	4825
110	138	43	0.7053	0.51	4830
125	138	43	0.8632	0.73	4835
80	138	43	0.3895	0.22	4840
200	138	43	1.6526	1.00	4845
65	138	43	0.2316	0.12	4850
55	138	43	0.1263	0.06	4855
75	138	43	0.3368	0.18	4860
60	138	43	0.1789	0.09	4865
67	138	43	0.2526	0.13	4870
140	138	43	1.0211	1.00	4875
152	138	43	1.1474	1.00	4880
122	138	43	0.8316	0.68	4885
106	138	43	0.6632	0.47	4890
105	138	43	0.6526	0.45	4895
118	138	43	0.7895	0.62	4900
75	138	43	0.3368	0.18	4905
65	138	43	0.2316	0.12	4910
63	138	43	0.2105	0.10	4915
60	138	43	0.1789	0.09	4920
90	138	43	0.4947	0.30	4925
60	138	43	0.1789	0.09	4930
60	138	43	0.1789	0.09	4935
68	138	43	0.2632	0.13	4940
63	138	43	0.2105	0.10	4945
67	138	43	0.2526	0.13	4950
55	138	43	0.1263	0.06	4955
53	138	43	0.1053	0.05	4960
53	138	43	0.1053	0.05	4965
60	138	43	0.1789	0.09	4970
77	138	43	0.3579	0.20	4975
95	138	43	0.5474	0.35	4980
80	138	43	0.3895	0.22	4985
90	138	43	0.4947	0.30	4990
62	138	43	0.2000	0.10	4995
57	138	43	0.1474	0.07	5000

Vsh.calculation (Clavier Eq.)					Depth
GR.	Max	Min	GR.fraction	Vsh.	(feet)
125	138	43	0.8632	0.73	5005
110	138	43	0.7053	0.51	5010
132	138	43	0.9368	0.86	5015
122	138	43	0.8316	0.68	5020
80	138	43	0.3895	0.22	5025
128	138	43	0.8947	0.79	5030
118	138	43	0.7895	0.62	5035
122	138	43	0.8316	0.68	5040
125	138	43	0.8632	0.73	5045
115	138	43	0.7579	0.58	5050
140	138	43	1.0211	1.00	5055
122	138	43	0.8316	0.68	5060
122	138	43	0.8316	0.68	5065
137	138	43	0.9895	0.97	5070
143	138	43	1.0526	1.00	5075
142	138	43	1.0421	1.00	5080
123	138	43	0.8421	0.70	5085
145	138	43	1.0737	1.00	5090
133	138	43	0.9474	0.88	5095
97	138	43	0.5684	0.37	5100
135	138	43	0.9684	0.93	5105
140	138	43	1.0211	1.00	5110
135	138	43	0.9684	0.93	5115
180	138	43	1.4421	1.00	5120
60	138	43	0.1789	0.09	5125
73	138	43	0.3158	0.17	5130
65	138	43	0.2316	0.12	5135
65	138	43	0.2316	0.12	5140
80	138	43	0.3895	0.22	5145
142	138	43	1.0421	1.00	5150
130	138	43	0.9158	0.82	5155
120	138	43	0.8105	0.65	5160
137	138	43	0.9895	0.97	5165
128	138	43	0.8947	0.79	5170
130	138	43	0.9158	0.82	5175
82	138	43	0.4105	0.23	5180
62	138	43	0.2000	0.10	5185
67	138	43	0.2526	0.13	5190
70	138	43	0.2842	0.15	5195
72	138	43	0.3053	0.16	5200
60	138	43	0.1789	0.09	5205
48	138	43	0.0526	0.02	5210
48	138	43	0.0526	0.02	5215
47	138	43	0.0421	0.02	5220
85	138	43	0.4421	0.26	5225
135	138	43	0.9684	0.93	5230
143	138	43	1.0526	1.00	5235

Table A.3 Shale volume (Vsh) calculation from **well: C** (continued)

Vsh.calculation (Clavier Eq.)					Depth
GR.	Max	Min	GR.fraction	Vsh.	(feet)
103	138	43	0.6316	0.43	5240
115	138	43	0.7579	0.58	5245
120	138	43	0.8105	0.65	5250
103	138	43	0.6316	0.43	5255
83	138	43	0.4211	0.24	5260
90	138	43	0.4947	0.30	5265
80	138	43	0.3895	0.22	5270
78	138	43	0.3684	0.20	5275
60	138	43	0.1789	0.09	5280
125	138	43	0.8632	0.73	5285
120	138	43	0.8105	0.65	5290
145	138	43	1.0737	1.00	5295
90	138	43	0.4947	0.30	5300
177	138	43	1.4105	1.00	5305
128	138	43	0.8947	0.79	5310
107	138	43	0.6737	0.48	5315
125	138	43	0.8632	0.73	5320
110	138	43	0.7053	0.51	5325
120	138	43	0.8105	0.65	5330
160	138	43	1.2316	1.00	5335
140	138	43	1.0211	1.00	5340
130	138	43	0.9158	0.82	5345
133	138	43	0.9474	0.88	5350
138	138	43	1.0000	1.00	5355
158	138	43	1.2105	1.00	5360
105	138	43	0.6526	0.45	5365
150	138	43	1.1263	1.00	5370
155	138	43	1.1789	1.00	5375
118	138	43	0.7895	0.62	5380
125	138	43	0.8632	0.73	5385
120	138	43	0.8105	0.65	5390
102	138	43	0.6211	0.42	5395
132	138	43	0.9368	0.86	5400
113	138	43	0.7368	0.55	5405
122	138	43	0.8316	0.68	5410
120	138	43	0.8105	0.65	5415
130	138	43	0.9158	0.82	5420
118	138	43	0.7895	0.62	5425
140	138	43	1.0211	1.00	5430
110	138	43	0.7053	0.51	5435
113	138	43	0.7368	0.55	5440
140	138	43	1.0211	1.00	5445
138	138	43	1.0000	1.00	5450
145	138	43	1.0737	1.00	5455
147	138	43	1.0947	1.00	5460
127	138	43	0.8842	0.77	5465
118	138	43	0.7895	0.62	5470

Vsh.calculation (Clavier Eq.)					Depth
GR.	Max	Min	GR.fraction	Vsh.	(feet)
140	138	43	1.0211	1.00	5475
145	138	43	1.0737	1.00	5480
97	138	43	0.5684	0.37	5485
100	138	43	0.6000	0.40	5490
120	138	43	0.8105	0.65	5495
110	138	43	0.7053	0.51	5500
47	138	43	0.0421	0.02	5505
47	138	43	0.0421	0.02	5510
70	138	43	0.2842	0.15	5515
130	138	43	0.9158	0.82	5520
160	138	43	1.2316	1.00	5525
122	138	43	0.8316	0.68	5530
118	138	43	0.7895	0.62	5535
110	138	43	0.7053	0.51	5540
135	138	43	0.9684	0.93	5545
105	138	43	0.6526	0.45	5550
200	138	43	1.6526	1.00	5555
143	138	43	1.0526	1.00	5560
103	138	43	0.6316	0.43	5565
108	138	43	0.6842	0.49	5570
100	138	43	0.6000	0.40	5575
58	138	43	0.1579	0.07	5580
48	138	43	0.0526	0.02	5585
45	138	43	0.0211	0.01	5590
90	138	43	0.4947	0.30	5595
95	138	43	0.5474	0.35	5600
150	138	43	1.1263	1.00	5605
130	138	43	0.9158	0.82	5610
110	138	43	0.7053	0.51	5615
135	138	43	0.9684	0.93	5620
110	138	43	0.7053	0.51	5625
102	138	43	0.6211	0.42	5630
88	138	43	0.4737	0.28	5635
75	138	43	0.3368	0.18	5640
53	138	43	0.1053	0.05	5645
57	138	43	0.1474	0.07	5650
60	138	43	0.1789	0.09	5655
62	138	43	0.2000	0.10	5660
62	138	43	0.2000	0.10	5665
63	138	43	0.2105	0.10	5670
102	138	43	0.6211	0.42	5675
120	138	43	0.8105	0.65	5680
78	138	43	0.3684	0.20	5685
62	138	43	0.2000	0.10	5690
110	138	43	0.7053	0.51	5695
138	138	43	1.0000	1.00	5700
97	138	43	0.5684	0.37	5705

Table A.3 Shale volume (Vsh) calculation from **well: C** (continued)

Vsh.calculation (Clavier Eq.)					Depth
GR.	Max	Min	GR.fraction	Vsh.	(feet)
133	138	43	0.9474	0.88	5710
127	138	43	0.8842	0.77	5715
160	138	43	1.2316	1.00	5720
147	138	43	1.0947	1.00	5725
122	138	43	0.8316	0.68	5730
122	138	43	0.8316	0.68	5735
122	138	43	0.8316	0.68	5740
85	138	43	0.4421	0.26	5745
125	138	43	0.8632	0.73	5750
100	138	43	0.6000	0.40	5755
178	138	43	1.4211	1.00	5760
138	138	43	1.0000	1.00	5765
120	138	43	0.8105	0.65	5770
80	138	43	0.3895	0.22	5775
180	138	43	1.4421	1.00	5780
122	138	43	0.8316	0.68	5785
140	138	43	1.0211	1.00	5790
98	138	43	0.5789	0.38	5795
110	138	43	0.7053	0.51	5800
128	138	43	0.8947	0.79	5805
133	138	43	0.9474	0.88	5810
120	138	43	0.8105	0.65	5815
120	138	43	0.8105	0.65	5820
130	138	43	0.9158	0.82	5825
118	138	43	0.7895	0.62	5830
110	138	43	0.7053	0.51	5835
153	138	43	1.1579	1.00	5840
110	138	43	0.7053	0.51	5845
127	138	43	0.8842	0.77	5850
140	138	43	1.0211	1.00	5855
143	138	43	1.0526	1.00	5860
163	138	43	1.2632	1.00	5865
138	138	43	1.0000	1.00	5870
122	138	43	0.8316	0.68	5875
130	138	43	0.9158	0.82	5880
110	138	43	0.7053	0.51	5885
138	138	43	1.0000	1.00	5890
130	138	43	0.9158	0.82	5895
135	138	43	0.9684	0.93	5900
110	138	43	0.7053	0.51	5905
98	138	43	0.5789	0.38	5910
165	138	43	1.2842	1.00	5915
120	138	43	0.8105	0.65	5920
125	138	43	0.8632	0.73	5925
120	138	43	0.8105	0.65	5930
118	138	43	0.7895	0.62	5935
83	138	43	0.4211	0.24	5940

Vsh.calculation (Clavier Eq.)					Depth
GR.	Max	Min	GR.fraction	Vsh.	(feet)
140	138	43	1.0211	1.00	5945
118	138	43	0.7895	0.62	5950
160	138	43	1.2316	1.00	5955
125	138	43	0.8632	0.73	5960
125	138	43	0.8632	0.73	5965
65	138	43	0.2316	0.12	5970
138	138	43	1.0000	1.00	5975
115	138	43	0.7579	0.58	5980
122	138	43	0.8316	0.68	5985
125	138	43	0.8632	0.73	5990
118	138	43	0.7895	0.62	5995
95	138	43	0.5474	0.35	6000
53	138	43	0.1053	0.05	6005
60	138	43	0.1789	0.09	6010
128	138	43	0.8947	0.79	6015
103	138	43	0.6316	0.43	6020
135	138	43	0.9684	0.93	6025
158	138	43	1.2105	1.00	6030
138	138	43	1.0000	1.00	6035
140	138	43	1.0211	1.00	6040
70	138	43	0.2842	0.15	6045
47	138	43	0.0421	0.02	6050
45	138	43	0.0211	0.01	6055
42	138	43	-0.0105	0.00	6060
45	138	43	0.0211	0.01	6065
59	138	43	0.1684	0.08	6070
98	138	43	0.5789	0.38	6075
115	138	43	0.7579	0.58	6080
117	138	43	0.7789	0.61	6085
122	138	43	0.8316	0.68	6090
127	138	43	0.8842	0.77	6095
117	138	43	0.7789	0.61	6100
132	138	43	0.9368	0.86	6105
128	138	43	0.8947	0.79	6110
150	138	43	1.1263	1.00	6115
135	138	43	0.9684	0.93	6120
120	138	43	0.8105	0.65	6125
126	138	43	0.8737	0.75	6130
65	138	43	0.2316	0.12	6135
200	138	43	1.6526	1.00	6140
130	138	43	0.9158	0.82	6145
123	138	43	0.8421	0.70	6150
158	138	43	1.2105	1.00	6155
117	138	43	0.7789	0.61	6160
83	138	43	0.4211	0.24	6165
118	138	43	0.7895	0.62	6170
103	138	43	0.6316	0.43	6175

Table A.3 Shale volume (Vsh) calculation from **well: C** (continued)

Vsh.calculation (Clavier Eq.)					Depth
GR.	Max	Min	GR.fraction	Vsh.	(feet)
115	138	43	0.7579	0.58	6180
70	138	43	0.2842	0.15	6185
125	138	43	0.8632	0.73	6190
102	138	43	0.6211	0.42	6195
120	138	43	0.8105	0.65	6200
143	138	43	1.0526	1.00	6205
126	138	43	0.8737	0.75	6210
120	138	43	0.8105	0.65	6215
120	138	43	0.8105	0.65	6220
110	138	43	0.7053	0.51	6225
142	138	43	1.0421	1.00	6230
140	138	43	1.0211	1.00	6235
100	138	43	0.6000	0.40	6240
123	138	43	0.8421	0.70	6245
140	138	43	1.0211	1.00	6250
110	138	43	0.7053	0.51	6255
100	138	43	0.6000	0.40	6260
117	138	43	0.7789	0.61	6265
95	138	43	0.5474	0.35	6270
98	138	43	0.5789	0.38	6275
145	138	43	1.0737	1.00	6280
118	138	43	0.7895	0.62	6285
120	138	43	0.8105	0.65	6290
108	138	43	0.6842	0.49	6295
145	138	43	1.0737	1.00	6300
108	138	43	0.6842	0.49	6305
133	138	43	0.9474	0.88	6310
110	138	43	0.7053	0.51	6315
108	138	43	0.6842	0.49	6320
125	138	43	0.8632	0.73	6325
62	138	43	0.2000	0.10	6330
102	138	43	0.6211	0.42	6335
122	138	43	0.8316	0.68	6340
105	138	43	0.6526	0.45	6345
45	138	43	0.0211	0.01	6350
50	138	43	0.0737	0.03	6355
50	138	43	0.0737	0.03	6360
50	138	43	0.0737	0.03	6365
138	138	43	1.0000	1.00	6370
135	138	43	0.9684	0.93	6375
128	138	43	0.8947	0.79	6380
142	138	43	1.0421	1.00	6385
140	138	43	1.0211	1.00	6390
128	138	43	0.8947	0.79	6395
115	138	43	0.7579	0.58	6400
140	138	43	1.0211	1.00	6405
140	138	43	1.0211	1.00	6410

Vsh.calculation (Clavier Eq.)					Depth
GR.	Max	Min	GR.fraction	Vsh.	(feet)
135	138	43	0.9684	0.93	6415
130	138	43	0.9158	0.82	6420
130	138	43	0.9158	0.82	6425
100	138	43	0.6000	0.40	6430
130	138	43	0.9158	0.82	6435
150	138	43	1.1263	1.00	6440
130	138	43	0.9158	0.82	6445
107	138	43	0.6737	0.48	6450
135	138	43	0.9684	0.93	6455
138	138	43	1.0000	1.00	6460
78	138	43	0.3684	0.20	6465
82	138	43	0.4105	0.23	6470
160	138	43	1.2316	1.00	6475
60	138	43	0.1789	0.09	6480
63	138	43	0.2105	0.10	6485
68	138	43	0.2632	0.13	6490
80	138	43	0.3895	0.22	6495
140	138	43	1.0211	1.00	6500
140	138	43	1.0211	1.00	6505
152	138	43	1.1474	1.00	6510
140	138	43	1.0211	1.00	6515
132	138	43	0.9368	0.86	6520
90	138	43	0.4947	0.30	6525
118	138	43	0.7895	0.62	6530
100	138	43	0.6000	0.40	6535
90	138	43	0.4947	0.30	6540
120	138	43	0.8105	0.65	6545
120	138	43	0.8105	0.65	6550
140	138	43	1.0211	1.00	6555
125	138	43	0.8632	0.73	6560
80	138	43	0.3895	0.22	6565
155	138	43	1.1789	1.00	6570
135	138	43	0.9684	0.93	6575
68	138	43	0.2632	0.13	6580
78	138	43	0.3684	0.20	6585
58	138	43	0.1579	0.07	6590
50	138	43	0.0737	0.03	6595
55	138	43	0.1263	0.06	6600
68	138	43	0.2632	0.13	6605
55	138	43	0.1263	0.06	6610
50	138	43	0.0737	0.03	6615
120	138	43	0.8105	0.65	6620
162	138	43	1.2526	1.00	6625
130	138	43	0.9158	0.82	6630
100	138	43	0.6000	0.40	6635
190	138	43	1.5474	1.00	6640
180	138	43	1.4421	1.00	6645

Table A.3 Shale volume (Vsh) calculation from **well: C** (continued)

Vsh.calculation (Clavier Eq.)					Depth
GR.	Max	Min	GR.fraction	Vsh.	(feet)
100	138	43	0.6000	0.40	6650
58	138	43	0.1579	0.07	6655
52	138	43	0.0947	0.04	6660
58	138	43	0.1579	0.07	6665
50	138	43	0.0737	0.03	6670
47	138	43	0.0421	0.02	6675
60	138	43	0.1789	0.09	6680
120	138	43	0.8105	0.65	6685
80	138	43	0.3895	0.22	6690
82	138	43	0.4105	0.23	6695
70	138	43	0.2842	0.15	6700
63	138	43	0.2105	0.10	6705
147	138	43	1.0947	1.00	6710
147	138	43	1.0947	1.00	6715
130	138	43	0.9158	0.82	6720
83	138	43	0.4211	0.24	6725
80	138	43	0.3895	0.22	6730
62	138	43	0.2000	0.10	6735
113	138	43	0.7368	0.55	6740
177	138	43	1.4105	1.00	6745
175	138	43	1.3895	1.00	6750
130	138	43	0.9158	0.82	6755
110	138	43	0.7053	0.51	6760
115	138	43	0.7579	0.58	6765
80	138	43	0.3895	0.22	6770
135	138	43	0.9684	0.93	6775
120	138	43	0.8105	0.65	6780
90	138	43	0.4947	0.30	6785
45	138	43	0.0211	0.01	6790
45	138	43	0.0211	0.01	6795
52	138	43	0.0947	0.04	6800
52	138	43	0.0947	0.04	6805
58	138	43	0.1579	0.07	6810
157	138	43	1.2000	1.00	6815
160	138	43	1.2316	1.00	6820
153	138	43	1.1579	1.00	6825
162	138	43	1.2526	1.00	6830
160	138	43	1.2316	1.00	6835
155	138	43	1.1789	1.00	6840
140	138	43	1.0211	1.00	6845
155	138	43	1.1789	1.00	6850
145	138	43	1.0737	1.00	6855
140	138	43	1.0211	1.00	6860
120	138	43	0.8105	0.65	6865
70	138	43	0.2842	0.15	6870
50	138	43	0.0737	0.03	6875
47	138	43	0.0421	0.02	6880

Vsh.calculation (Clavier Eq.)					Depth
GR.	Max	Min	GR.fraction	Vsh.	(feet)
50	138	43	0.0737	0.03	6885
50	138	43	0.0737	0.03	6890
130	138	43	0.9158	0.82	6895
95	138	43	0.5474	0.35	6900
118	138	43	0.7895	0.62	6905
58	138	43	0.1579	0.07	6910
70	138	43	0.2842	0.15	6915
60	138	43	0.1789	0.09	6920
55	138	43	0.1263	0.06	6925
50	138	43	0.0737	0.03	6930
50	138	43	0.0737	0.03	6935
55	138	43	0.1263	0.06	6940
87	138	43	0.4632	0.28	6945
121	138	43	0.8211	0.67	6950
70	138	43	0.2842	0.15	6955
65	138	43	0.2316	0.12	6960
157	138	43	1.2000	1.00	6965
120	138	43	0.8105	0.65	6970
110	138	43	0.7053	0.51	6975
58	138	43	0.1579	0.07	6980
55	138	43	0.1263	0.06	6985
55	138	43	0.1263	0.06	6990
52	138	43	0.0947	0.04	6995
57	138	43	0.1474	0.07	7000
50	138	43	0.0737	0.03	7005
45	138	43	0.0211	0.01	7010
47	138	43	0.0421	0.02	7015
60	138	43	0.1789	0.09	7020
105	138	43	0.6526	0.45	7025
142	138	43	1.0421	1.00	7030
155	138	43	1.1789	1.00	7035
110	138	43	0.7053	0.51	7040
110	138	43	0.7053	0.51	7045
132	138	43	0.9368	0.86	7050
130	138	43	0.9158	0.82	7055
190	138	43	1.5474	1.00	7060
130	138	43	0.9158	0.82	7065
100	138	43	0.6000	0.40	7070
130	138	43	0.9158	0.82	7075
122	138	43	0.8316	0.68	7080
142	138	43	1.0421	1.00	7085
87	138	43	0.4632	0.28	7090
118	138	43	0.7895	0.62	7095
167	138	43	1.3053	1.00	7100
130	138	43	0.9158	0.82	7105
140	138	43	1.0211	1.00	7110
90	138	43	0.4947	0.30	7115

Table A.3 Shale volume (Vsh) calculation from **well: C** (continued)

Vsh.calculation (Clavier Eq.)					Depth
GR.	Max	Min	GR.fraction	Vsh.	(feet)
145	138	43	1.0737	1.00	7120
110	145	40	0.6667	0.47	7125
100	145	40	0.5714	0.37	7130
113	145	40	0.6952	0.50	7135
40	145	40	0.0000	0.00	7140
40	145	40	0.0000	0.00	7145
43	145	40	0.0286	0.01	7150
47	145	40	0.0667	0.03	7155
42	145	40	0.0190	0.01	7160
43	145	40	0.0286	0.01	7165
41	145	40	0.0095	0.00	7170
42	145	40	0.0190	0.01	7175
141	145	40	0.9619	0.91	7180
137	145	40	0.9238	0.84	7185
120	145	40	0.7619	0.59	7190
123	145	40	0.7905	0.62	7195
130	145	40	0.8571	0.72	7200
150	145	40	1.0476	1.00	7205
110	145	40	0.6667	0.47	7210
62	145	40	0.2095	0.10	7215
40	145	40	0.0000	0.00	7220
40	145	40	0.0000	0.00	7225
42	145	40	0.0190	0.01	7230
110	145	40	0.6667	0.47	7235
170	145	40	1.2381	1.00	7240
153	145	40	1.0762	1.00	7245
140	145	40	0.9524	0.89	7250
150	145	40	1.0476	1.00	7255
140	145	40	0.9524	0.89	7260
130	145	40	0.8571	0.72	7265
120	145	40	0.7619	0.59	7270
150	145	40	1.0476	1.00	7275
100	145	40	0.5714	0.37	7280
120	145	40	0.7619	0.59	7285
133	145	40	0.8857	0.77	7290
118	145	40	0.7429	0.56	7295
140	145	40	0.9524	0.89	7300
153	145	40	1.0762	1.00	7305
137	145	40	0.9238	0.84	7310
90	145	40	0.4762	0.29	7315
63	145	40	0.2190	0.11	7320
143	145	40	0.9810	0.96	7325
120	145	40	0.7619	0.59	7330
140	145	40	0.9524	0.89	7335
127	145	40	0.8286	0.68	7340
90	145	40	0.4762	0.29	7345
160	145	40	1.1429	1.00	7350

Vsh.calculation (Clavier Eq.)					Depth
GR.	Max	Min	GR.fraction	Vsh.	(feet)
147	145	40	1.0190	1.00	7355
142	145	40	0.9714	0.93	7360
137	145	40	0.9238	0.84	7365
140	145	40	0.9524	0.89	7370
113	145	40	0.6952	0.50	7375
143	145	40	0.9810	0.96	7380
108	145	40	0.6476	0.45	7385
81	145	40	0.3905	0.22	7390
42	145	40	0.0190	0.01	7395
68	145	40	0.2667	0.14	7400
157	145	40	1.1143	1.00	7405
140	145	40	0.9524	0.89	7410
105	145	40	0.6190	0.42	7415
140	145	40	0.9524	0.89	7420
170	145	40	1.2381	1.00	7425
140	145	40	0.9524	0.89	7430
127	145	40	0.8286	0.68	7435
120	145	40	0.7619	0.59	7440
173	145	40	1.2667	1.00	7445
163	145	40	1.1714	1.00	7450
145	145	40	1.0000	1.00	7455
140	145	40	0.9524	0.89	7460
125	145	40	0.8095	0.65	7465
160	145	40	1.1429	1.00	7470
145	145	40	1.0000	1.00	7475
138	145	40	0.9333	0.86	7480
108	145	40	0.6476	0.45	7485
102	145	40	0.5905	0.39	7490
35	145	40	-0.0476	0.00	7495
50	145	40	0.0952	0.04	7500
53	145	40	0.1238	0.06	7505
60	145	40	0.1905	0.09	7510
57	145	40	0.1619	0.08	7515
60	145	40	0.1905	0.09	7520
57	145	40	0.1619	0.08	7525
50	145	40	0.0952	0.04	7530
162	145	40	1.1619	1.00	7535
155	145	40	1.0952	1.00	7540
125	145	40	0.8095	0.65	7545
135	145	40	0.9048	0.80	7550
140	145	40	0.9524	0.89	7555
120	145	40	0.7619	0.59	7560
110	145	40	0.6667	0.47	7565
170	145	40	1.2381	1.00	7570
137	145	40	0.9238	0.84	7575
107	145	40	0.6381	0.44	7580
148	145	40	1.0286	1.00	7585

Table A.3 Shale volume (Vsh) calculation from **well: C** (continued)

Vsh.calculation (Clavier Eq.)					Depth
GR.	Max	Min	GR.fraction	Vsh.	(feet)
123	145	40	0.7905	0.62	7590
100	145	40	0.5714	0.37	7595
158	145	40	1.1238	1.00	7600
143	145	40	0.9810	0.96	7605
101	145	40	0.5810	0.38	7610
159	145	40	1.1333	1.00	7615
120	145	40	0.7619	0.59	7620
90	145	40	0.4762	0.29	7625
120	145	40	0.7619	0.59	7630
38	145	40	-0.0190	0.00	7635
40	145	40	0.0000	0.00	7640
43	145	40	0.0286	0.01	7645
40	145	40	0.0000	0.00	7650
160	145	40	1.1429	1.00	7655
110	145	40	0.6667	0.47	7660
150	145	40	1.0476	1.00	7665
140	145	40	0.9524	0.89	7670
163	145	40	1.1714	1.00	7675
120	145	40	0.7619	0.59	7680
159	145	40	1.1333	1.00	7685
163	145	40	1.1714	1.00	7690
142	145	40	0.9714	0.93	7695
135	145	40	0.9048	0.80	7700
115	145	40	0.7143	0.53	7705
140	145	40	0.9524	0.89	7710
105	145	40	0.6190	0.42	7715
138	145	40	0.9333	0.86	7720
140	145	40	0.9524	0.89	7725
140	145	40	0.9524	0.89	7730
110	145	40	0.6667	0.47	7735
140	145	40	0.9524	0.89	7740
158	145	40	1.1238	1.00	7745
145	145	40	1.0000	1.00	7750
165	145	40	1.1905	1.00	7755
162	145	40	1.1619	1.00	7760
140	145	40	0.9524	0.89	7765
150	145	40	1.0476	1.00	7770
150	145	40	1.0476	1.00	7775
140	145	40	0.9524	0.89	7780
100	145	40	0.5714	0.37	7785
140	145	40	0.9524	0.89	7790
150	145	40	1.0476	1.00	7795
123	145	40	0.7905	0.62	7800
143	145	40	0.9810	0.96	7805
157	145	40	1.1143	1.00	7810
118	145	40	0.7429	0.56	7815
140	145	40	0.9524	0.89	7820

Vsh.calculation (Clavier Eq.)					Depth
GR.	Max	Min	GR.fraction	Vsh.	(feet)
130	145	40	0.8571	0.72	7825
70	145	40	0.2857	0.15	7830
42	145	40	0.0190	0.01	7835
40	145	40	0.0000	0.00	7840
39	145	40	-0.0095	0.00	7845
50	145	40	0.0952	0.04	7850
40	145	40	0.0000	0.00	7855
63	145	40	0.2190	0.11	7860
58	145	40	0.1714	0.08	7865
45	145	40	0.0476	0.02	7870
45	145	40	0.0476	0.02	7875
150	145	40	1.0476	1.00	7880
100	145	40	0.5714	0.37	7885
110	145	40	0.6667	0.47	7890
115	124	27	0.9072	0.81	7895
132	124	27	1.0825	1.00	7900
40	124	27	0.1340	0.06	7905
50	124	27	0.2371	0.12	7910
35	124	27	0.0825	0.04	7915
104	124	27	0.7938	0.63	7920
120	124	27	0.9588	0.91	7925
150	124	27	1.2680	1.00	7930
145	124	27	1.2165	1.00	7935
120	124	27	0.9588	0.91	7940
110	124	27	0.8557	0.72	7945
120	124	27	0.9588	0.91	7950
130	124	27	1.0619	1.00	7955
87	124	27	0.6186	0.42	7960

Table A.4 Shale volume (Vsh) calculation from **well: D**

Vsh.calculation (Clavier Eq.)					Depth
GR.	Max	Min	GR.fraction	Vsh.	(feet)
93	183	60	0.2683	0.14	4200
100	183	60	0.3252	0.17	4205
125	183	60	0.5285	0.33	4210
110	183	60	0.4065	0.23	4215
103	183	60	0.3496	0.19	4220
130	183	60	0.5691	0.37	4225
150	183	60	0.7317	0.55	4230
158	183	60	0.7967	0.63	4235
150	183	60	0.7317	0.55	4240
180	183	60	0.9756	0.94	4245
123	183	60	0.5122	0.32	4250
140	183	60	0.6504	0.45	4255
136	183	60	0.6179	0.42	4260
155	183	60	0.7724	0.60	4265
140	183	60	0.6504	0.45	4270
130	183	60	0.5691	0.37	4275
145	183	60	0.6911	0.50	4280
140	183	60	0.6504	0.45	4285
120	183	60	0.4878	0.30	4290
100	183	60	0.3252	0.17	4295
103	183	60	0.3496	0.19	4300
105	183	60	0.3659	0.20	4305
56	183	60	-0.0325	0.00	4310
60	183	60	0.0000	0.00	4315
95	183	60	0.2846	0.15	4320
150	183	60	0.7317	0.55	4325
143	183	60	0.6748	0.48	4330
150	183	60	0.7317	0.55	4335
140	183	60	0.6504	0.45	4340
130	183	60	0.5691	0.37	4345
132	183	60	0.5854	0.39	4350
127	183	60	0.5447	0.35	4355
125	183	60	0.5285	0.33	4360
150	183	60	0.7317	0.55	4365
150	183	60	0.7317	0.55	4370
113	183	60	0.4309	0.25	4375
108	183	60	0.3902	0.22	4380
90	183	60	0.2439	0.12	4385
68	183	60	0.0650	0.03	4390
68	183	60	0.0650	0.03	4395
70	183	60	0.0813	0.04	4400
66	183	60	0.0488	0.02	4405
60	183	60	0.0000	0.00	4410
100	183	60	0.3252	0.17	4415
70	183	60	0.0813	0.04	4420
68	183	60	0.0650	0.03	4425
65	183	60	0.0407	0.02	4430

Vsh.calculation (Clavier Eq.)					Depth
GR.	Max	Min	GR.fraction	Vsh.	(feet)
73	183	60	0.1057	0.05	4435
68	183	60	0.0650	0.03	4440
90	183	60	0.2439	0.12	4445
75	183	60	0.1220	0.06	4450
72	183	60	0.0976	0.04	4455
70	183	60	0.0813	0.04	4460
72	183	60	0.0976	0.04	4465
78	183	60	0.1463	0.07	4470
66	183	60	0.0488	0.02	4475
62	183	60	0.0163	0.01	4480
90	183	60	0.2439	0.12	4485
145	183	60	0.6911	0.50	4490
168	183	60	0.8780	0.76	4495
137	183	60	0.6260	0.43	4500
133	183	60	0.5935	0.39	4505
140	183	60	0.6504	0.45	4510
152	183	60	0.7480	0.57	4515
135	183	60	0.6098	0.41	4520
140	183	60	0.6504	0.45	4525
110	183	60	0.4065	0.23	4530
106	183	60	0.3740	0.21	4535
55	183	60	-0.0407	0.00	4540
60	183	60	0.0000	0.00	4545
50	183	60	-0.0813	0.00	4550
53	183	60	-0.0569	0.00	4555
55	183	60	-0.0407	0.00	4560
110	183	60	0.4065	0.23	4565
100	183	60	0.3252	0.17	4570
90	183	60	0.2439	0.12	4575
80	183	60	0.1626	0.08	4580
65	183	60	0.0407	0.02	4585
62	183	60	0.0163	0.01	4590
60	183	60	0.0000	0.00	4595
58	183	60	-0.0163	0.00	4600
90	183	60	0.2439	0.12	4605
120	183	60	0.4878	0.30	4610
78	183	60	0.1463	0.07	4615
72	183	60	0.0976	0.04	4620
68	183	60	0.0650	0.03	4625
140	183	60	0.6504	0.45	4630
145	183	60	0.6911	0.50	4635
160	183	60	0.8130	0.66	4640
143	183	60	0.6748	0.48	4645
123	183	60	0.5122	0.32	4650
143	183	60	0.6748	0.48	4655
140	183	60	0.6504	0.45	4660
150	183	60	0.7317	0.55	4665

Table A.4 Shale volume (Vsh) calculation from **well: D** (continued)

Vsh.calculation (Clavier Eq.)					Depth
GR.	Max	Min	GR.fraction	Vsh.	(feet)
140	183	60	0.6504	0.45	4670
145	183	60	0.6911	0.50	4675
148	183	60	0.7154	0.53	4680
135	183	60	0.6098	0.41	4685
150	183	60	0.7317	0.55	4690
186	183	60	1.0244	1.00	4695
146	183	60	0.6992	0.51	4700
158	183	60	0.7967	0.63	4705
150	183	60	0.7317	0.55	4710
125	183	60	0.5285	0.33	4715
120	183	60	0.4878	0.30	4720
145	183	60	0.6911	0.50	4725
158	183	60	0.7967	0.63	4730
150	183	60	0.7317	0.55	4735
147	183	60	0.7073	0.52	4740
150	183	60	0.7317	0.55	4745
153	183	60	0.7561	0.58	4750
150	183	60	0.7317	0.55	4755
148	183	60	0.7154	0.53	4760
130	183	60	0.5691	0.37	4765
103	183	60	0.3496	0.19	4770
95	183	60	0.2846	0.15	4775
160	183	60	0.8130	0.66	4780
200	183	60	1.1382	1.00	4785
152	183	60	0.7480	0.57	4790
170	183	60	0.8943	0.78	4795
148	183	60	0.7154	0.53	4800
135	183	60	0.6098	0.41	4805
147	183	60	0.7073	0.52	4810
140	183	60	0.6504	0.45	4815
137	183	60	0.6260	0.43	4820
142	183	60	0.6667	0.47	4825
140	183	60	0.6504	0.45	4830
150	183	60	0.7317	0.55	4835
140	183	60	0.6504	0.45	4840
150	183	60	0.7317	0.55	4845
140	183	60	0.6504	0.45	4850
128	183	60	0.5528	0.35	4855
110	183	60	0.4065	0.23	4860
112	183	60	0.4228	0.24	4865
118	183	60	0.4715	0.28	4870
78	183	60	0.1463	0.07	4875
65	183	60	0.0407	0.02	4880
70	183	60	0.0813	0.04	4885
68	183	60	0.0650	0.03	4890
70	183	60	0.0813	0.04	4895
140	183	60	0.6504	0.45	4900

Vsh.calculation (Clavier Eq.)					Depth
GR.	Max	Min	GR.fraction	Vsh.	(feet)
145	183	60	0.6911	0.50	4905
160	183	60	0.8130	0.66	4910
148	183	60	0.7154	0.53	4915
133	183	60	0.5935	0.39	4920
88	183	60	0.2276	0.11	4925
70	183	60	0.0813	0.04	4930
72	183	60	0.0976	0.04	4935
70	183	60	0.0813	0.04	4940
154	183	60	0.7642	0.59	4945
180	183	60	0.9756	0.94	4950
158	183	60	0.7967	0.63	4955
158	183	60	0.7967	0.63	4960
150	183	60	0.7317	0.55	4965
107	183	60	0.3821	0.21	4970
170	183	60	0.8943	0.78	4975
150	183	60	0.7317	0.55	4980
138	183	60	0.6341	0.44	4985
163	183	60	0.8374	0.69	4990
68	183	60	0.0650	0.03	4995
68	183	60	0.0650	0.03	5000
126	183	60	0.5366	0.34	5005
125	183	60	0.5285	0.33	5010
75	183	60	0.1220	0.06	5015
62	183	60	0.0163	0.01	5020
68	183	60	0.0650	0.03	5025
78	183	60	0.1463	0.07	5030
88	183	60	0.2276	0.11	5035
88	183	60	0.2276	0.11	5040
125	183	60	0.5285	0.33	5045
128	183	60	0.5528	0.35	5050
115	183	60	0.4472	0.26	5055
121	183	60	0.4959	0.30	5060
61	183	60	0.0081	0.00	5065
68	183	60	0.0650	0.03	5070
58	183	60	-0.0163	0.00	5075
130	183	60	0.5691	0.37	5080
120	183	60	0.4878	0.30	5085
137	183	60	0.6260	0.43	5090
130	183	60	0.5691	0.37	5095
140	183	60	0.6504	0.45	5100
152	183	60	0.7480	0.57	5105
65	183	60	0.0407	0.02	5110
80	183	60	0.1626	0.08	5115
125	183	60	0.5285	0.33	5120
150	183	60	0.7317	0.55	5125
160	183	60	0.8130	0.66	5130
148	183	60	0.7154	0.53	5135

Table A.4 Shale volume (Vsh) calculation from **well: D** (continued)

Vsh.calculation (Clavier Eq.)					Depth
GR.	Max	Min	GR.fraction	Vsh.	(feet)
135	183	60	0.6098	0.41	5140
150	183	60	0.7317	0.55	5145
146	183	60	0.6992	0.51	5150
178	183	60	0.9593	0.91	5155
155	183	60	0.7724	0.60	5160
150	183	60	0.7317	0.55	5165
148	183	60	0.7154	0.53	5170
90	183	60	0.2439	0.12	5175
80	183	60	0.1626	0.08	5180
75	183	60	0.1220	0.06	5185
85	183	60	0.2033	0.10	5190
80	183	60	0.1626	0.08	5195
72	183	60	0.0976	0.04	5200
103	183	60	0.3496	0.19	5205
170	183	60	0.8943	0.78	5210
178	183	60	0.9593	0.91	5215
140	183	60	0.6504	0.45	5220
141	183	60	0.6585	0.46	5225
152	183	60	0.7480	0.57	5230
138	183	60	0.6341	0.44	5235
138	183	60	0.6341	0.44	5240
128	183	60	0.5528	0.35	5245
128	183	60	0.5528	0.35	5250
160	183	60	0.8130	0.66	5255
145	183	60	0.6911	0.50	5260
138	183	60	0.6341	0.44	5265
155	183	60	0.7724	0.60	5270
150	183	60	0.7317	0.55	5275
145	183	60	0.6911	0.50	5280
150	183	60	0.7317	0.55	5285
190	183	60	1.0569	1.00	5290
197	183	60	1.1138	1.00	5295
148	183	60	0.7154	0.53	5300
155	183	60	0.7724	0.60	5305
158	183	60	0.7967	0.63	5310
152	183	60	0.7480	0.57	5315
142	183	60	0.6667	0.47	5320
138	183	60	0.6341	0.44	5325
142	183	60	0.6667	0.47	5330
128	183	60	0.5528	0.35	5335
100	183	60	0.3252	0.17	5340
102	183	60	0.3415	0.18	5345
95	183	60	0.2846	0.15	5350
70	183	60	0.0813	0.04	5355
82	183	60	0.1789	0.09	5360
140	183	60	0.6504	0.45	5365
178	183	60	0.9593	0.91	5370

Vsh.calculation (Clavier Eq.)					Depth
GR.	Max	Min	GR.fraction	Vsh.	(feet)
125	183	60	0.5285	0.33	5375
178	183	60	0.9593	0.91	5380
130	183	60	0.5691	0.37	5385
135	183	60	0.6098	0.41	5390
82	183	60	0.1789	0.09	5395
128	183	60	0.5528	0.35	5400
120	183	60	0.4878	0.30	5405
138	183	60	0.6341	0.44	5410
190	183	60	1.0569	1.00	5415
120	183	60	0.4878	0.30	5420
180	183	60	0.9756	0.94	5425
138	183	60	0.6341	0.44	5430
148	183	60	0.7154	0.53	5435
140	183	60	0.6504	0.45	5440
160	183	60	0.8130	0.66	5445
135	183	60	0.6098	0.41	5450
130	183	60	0.5691	0.37	5455
150	183	60	0.7317	0.55	5460
152	183	60	0.7480	0.57	5465
145	183	60	0.6911	0.50	5470
135	183	60	0.6098	0.41	5475
115	183	60	0.4472	0.26	5480
150	183	60	0.7317	0.55	5485
150	183	60	0.7317	0.55	5490
140	183	60	0.6504	0.45	5495
102	183	60	0.3415	0.18	5500
115	183	60	0.4472	0.26	5505
158	183	60	0.7967	0.63	5510
130	183	60	0.5691	0.37	5515
160	183	60	0.8130	0.66	5520
150	183	60	0.7317	0.55	5525
152	183	60	0.7480	0.57	5530
147	183	60	0.7073	0.52	5535
140	183	60	0.6504	0.45	5540
138	183	60	0.6341	0.44	5545
150	183	60	0.7317	0.55	5550
145	183	60	0.6911	0.50	5555
105	183	60	0.3659	0.20	5560
87	183	60	0.2195	0.11	5565
87	183	60	0.2195	0.11	5570
72	183	60	0.0976	0.04	5575
70	183	60	0.0813	0.04	5580
65	183	60	0.0407	0.02	5585
72	183	60	0.0976	0.04	5590
55	183	60	-0.0407	0.00	5595
200	183	60	1.1382	1.00	5600
138	185	66	0.6050	0.41	5605

Table A.4 Shale volume (Vsh) calculation from **well: D** (continued)

Vsh.calculation (Clavier Eq.)					Depth
GR.	Max	Min	GR.fraction	Vsh.	(feet)
115	185	66	0.4118	0.24	5610
165	185	66	0.8319	0.68	5615
152	185	66	0.7227	0.54	5620
143	185	66	0.6471	0.45	5625
183	185	66	0.9832	0.96	5630
150	185	66	0.7059	0.52	5635
148	185	66	0.6891	0.50	5640
150	185	66	0.7059	0.52	5645
100	185	66	0.2857	0.15	5650
130	185	66	0.5378	0.34	5655
135	185	66	0.5798	0.38	5660
150	185	66	0.7059	0.52	5665
154	185	66	0.7395	0.56	5670
158	185	66	0.7731	0.60	5675
170	185	66	0.8739	0.75	5680
140	185	66	0.6218	0.42	5685
140	185	66	0.6218	0.42	5690
135	185	66	0.5798	0.38	5695
150	185	66	0.7059	0.52	5700
123	185	66	0.4790	0.29	5705
115	185	66	0.4118	0.24	5710
102	185	66	0.3025	0.16	5715
127	185	66	0.5126	0.32	5720
145	185	66	0.6639	0.47	5725
68	185	66	0.0168	0.01	5730
60	185	66	-0.0504	0.00	5735
78	185	66	0.1008	0.05	5740
68	185	66	0.0168	0.01	5745
73	185	66	0.0588	0.03	5750
83	185	66	0.1429	0.07	5755
70	185	66	0.0336	0.01	5760
72	185	66	0.0504	0.02	5765
100	185	66	0.2857	0.15	5770
113	185	66	0.3950	0.22	5775
97	185	66	0.2605	0.13	5780
108	185	66	0.3529	0.19	5785
112	185	66	0.3866	0.22	5790
80	185	66	0.1176	0.05	5795
60	185	66	-0.0504	0.00	5800
67	185	66	0.0084	0.00	5805
70	185	66	0.0336	0.01	5810
60	185	66	-0.0504	0.00	5815
65	185	66	-0.0084	0.00	5820
68	185	66	0.0168	0.01	5825
60	185	66	-0.0504	0.00	5830
62	185	66	-0.0336	0.00	5835
73	185	66	0.0588	0.03	5840

Vsh.calculation (Clavier Eq.)					Depth
GR.	Max	Min	GR.fraction	Vsh.	(feet)
140	185	66	0.6218	0.42	5845
138	185	66	0.6050	0.41	5850
155	185	66	0.7479	0.57	5855
102	185	66	0.3025	0.16	5860
60	185	66	-0.0504	0.00	5865
178	185	66	0.9412	0.87	5870
145	185	66	0.6639	0.47	5875
138	185	66	0.6050	0.41	5880
128	185	66	0.5210	0.33	5885
130	185	66	0.5378	0.34	5890
150	185	66	0.7059	0.52	5895
122	185	66	0.4706	0.28	5900
147	185	66	0.6807	0.49	5905
147	185	66	0.6807	0.49	5910
148	185	66	0.6891	0.50	5915
140	185	66	0.6218	0.42	5920
140	185	66	0.6218	0.42	5925
142	185	66	0.6387	0.44	5930
150	185	66	0.7059	0.52	5935
155	185	66	0.7479	0.57	5940
118	185	66	0.4370	0.26	5945
133	185	66	0.5630	0.36	5950
133	185	66	0.5630	0.36	5955
102	185	66	0.3025	0.16	5960
110	185	66	0.3697	0.20	5965
138	185	66	0.6050	0.41	5970
113	185	66	0.3950	0.22	5975
80	185	66	0.1176	0.05	5980
117	185	66	0.4286	0.25	5985
135	185	66	0.5798	0.38	5990
198	185	66	1.1092	1.00	5995
132	185	66	0.5546	0.36	6000
160	185	66	0.7899	0.62	6005
112	185	66	0.3866	0.22	6010
148	185	66	0.6891	0.50	6015
140	185	66	0.6218	0.42	6020
145	185	66	0.6639	0.47	6025
148	185	66	0.6891	0.50	6030
125	185	66	0.4958	0.30	6035
138	185	66	0.6050	0.41	6040
100	185	66	0.2857	0.15	6045
115	185	66	0.4118	0.24	6050
132	185	66	0.5546	0.36	6055
200	185	66	1.1261	1.00	6060
145	185	66	0.6639	0.47	6065
140	185	66	0.6218	0.42	6070
138	185	66	0.6050	0.41	6075

Table A.4 Shale volume (Vsh) calculation from **well: D** (continued)

Vsh.calculation (Clavier Eq.)					Depth
GR.	Max	Min	GR.fraction	Vsh.	(feet)
132	185	66	0.5546	0.36	6080
116	185	66	0.4202	0.24	6085
155	185	66	0.7479	0.57	6090
140	185	66	0.6218	0.42	6095
142	185	66	0.6387	0.44	6100
160	185	66	0.7899	0.62	6105
153	185	66	0.7311	0.55	6110
150	185	66	0.7059	0.52	6115
138	185	66	0.6050	0.41	6120
110	185	66	0.3697	0.20	6125
65	185	66	-0.0084	0.00	6130
53	185	66	-0.1092	0.00	6135
55	185	66	-0.0924	0.00	6140
57	185	66	-0.0756	0.00	6145
68	185	66	0.0168	0.01	6150
70	185	66	0.0336	0.01	6155
63	185	66	-0.0252	0.00	6160
145	190	60	0.6538	0.46	6165
138	190	60	0.6000	0.40	6170
170	190	60	0.8462	0.71	6175
130	190	60	0.5385	0.34	6180
120	190	60	0.4615	0.27	6185
140	190	60	0.6154	0.42	6190
158	190	60	0.7538	0.57	6195
142	190	60	0.6308	0.43	6200
110	190	60	0.3846	0.22	6205
198	190	60	1.0615	1.00	6210
190	190	60	1.0000	1.00	6215
130	190	60	0.5385	0.34	6220
140	190	60	0.6154	0.42	6225
152	190	60	0.7077	0.52	6230
155	190	60	0.7308	0.55	6235
122	190	60	0.4769	0.29	6240
183	190	60	0.9462	0.88	6245
120	190	60	0.4615	0.27	6250
125	190	60	0.5000	0.31	6255
100	190	60	0.3077	0.16	6260
140	190	60	0.6154	0.42	6265
120	190	60	0.4615	0.27	6270
177	190	60	0.9000	0.79	6275
140	190	60	0.6154	0.42	6280
138	190	60	0.6000	0.40	6285
110	190	60	0.3846	0.22	6290
142	190	60	0.6308	0.43	6295
148	190	60	0.6769	0.48	6300
150	190	60	0.6923	0.50	6305
87	190	60	0.2077	0.10	6310

Vsh.calculation (Clavier Eq.)					Depth
GR.	Max	Min	GR.fraction	Vsh.	(feet)
118	190	60	0.4462	0.26	6315
153	190	60	0.7154	0.53	6320
158	190	60	0.7538	0.57	6325
128	190	60	0.5231	0.33	6330
108	190	60	0.3692	0.20	6335
128	190	60	0.5231	0.33	6340
90	190	60	0.2308	0.11	6345
160	190	60	0.7692	0.59	6350
162	190	60	0.7846	0.62	6355
128	190	60	0.5231	0.33	6360
130	190	60	0.5385	0.34	6365
165	190	60	0.8077	0.65	6370
173	190	60	0.8692	0.74	6375
148	190	60	0.6769	0.48	6380
125	190	60	0.5000	0.31	6385
103	190	60	0.3308	0.18	6390
53	190	60	-0.0538	0.00	6395
55	190	60	-0.0385	0.00	6400
59	190	60	-0.0077	0.00	6405
55	190	60	-0.0385	0.00	6410
105	190	60	0.3462	0.19	6415
140	190	60	0.6154	0.42	6420
70	190	60	0.0769	0.03	6425
70	190	60	0.0769	0.03	6430
75	190	60	0.1154	0.05	6435
70	190	60	0.0769	0.03	6440
130	190	60	0.5385	0.34	6445
170	190	60	0.8462	0.71	6450
152	190	60	0.7077	0.52	6455
180	190	60	0.9231	0.84	6460
132	190	60	0.5538	0.36	6465
138	190	60	0.6000	0.40	6470
187	190	60	0.9769	0.95	6475
135	190	60	0.5769	0.38	6480
132	190	60	0.5538	0.36	6485
67	190	60	0.0538	0.02	6490
65	190	60	0.0385	0.02	6495
63	190	60	0.0231	0.01	6500
52	190	60	-0.0615	0.00	6505
50	190	60	-0.0769	0.00	6510
110	190	60	0.3846	0.22	6515
148	190	60	0.6769	0.48	6520
165	190	60	0.8077	0.65	6525
120	190	60	0.4615	0.27	6530
150	190	60	0.6923	0.50	6535
200	190	60	1.0769	1.00	6540
128	190	60	0.5231	0.33	6545

Table A.4 Shale volume (Vsh) calculation from **well: D** (continued)

Vsh.calculation (Clavier Eq.)					Depth
GR.	Max	Min	GR.fraction	Vsh.	(feet)
130	190	60	0.5385	0.34	6550
170	190	60	0.8462	0.71	6555
140	190	60	0.6154	0.42	6560
150	190	60	0.6923	0.50	6565
175	190	60	0.8846	0.77	6570
158	190	60	0.7538	0.57	6575
120	190	60	0.4615	0.27	6580
90	190	60	0.2308	0.11	6585
63	190	60	0.0231	0.01	6590
63	190	60	0.0231	0.01	6595
70	190	60	0.0769	0.03	6600
160	190	60	0.7692	0.59	6605
162	190	60	0.7846	0.62	6610
157	190	60	0.7462	0.56	6615
120	190	60	0.4615	0.27	6620
180	190	60	0.9231	0.84	6625
160	190	60	0.7692	0.59	6630
120	190	60	0.4615	0.27	6635
140	190	60	0.6154	0.42	6640
142	190	60	0.6308	0.43	6645
142	190	60	0.6308	0.43	6650
118	190	60	0.4462	0.26	6655
150	190	60	0.6923	0.50	6660
152	190	60	0.7077	0.52	6665
130	190	60	0.5385	0.34	6670
162	190	60	0.7846	0.62	6675
160	190	60	0.7692	0.59	6680
110	190	60	0.3846	0.22	6685
200	190	60	1.0769	1.00	6690
165	190	60	0.8077	0.65	6695
158	190	60	0.7538	0.57	6700
110	190	60	0.3846	0.22	6705
105	190	60	0.3462	0.19	6710
72	190	60	0.0923	0.04	6715
128	190	60	0.5231	0.33	6720
55	190	60	-0.0385	0.00	6725
60	190	60	0.0000	0.00	6730
60	190	60	0.0000	0.00	6735
62	190	60	0.0154	0.01	6740
68	190	60	0.0615	0.03	6745
68	190	60	0.0615	0.03	6750
70	190	60	0.0769	0.03	6755
50	190	60	-0.0769	0.00	6760
118	190	60	0.4462	0.26	6765
93	190	60	0.2538	0.13	6770
72	190	60	0.0923	0.04	6775
70	190	60	0.0769	0.03	6780

Vsh.calculation (Clavier Eq.)					Depth
GR.	Max	Min	GR.fraction	Vsh.	(feet)
63	190	60	0.0231	0.01	6785
72	190	60	0.0923	0.04	6790
167	190	60	0.8231	0.67	6795
140	190	60	0.6154	0.42	6800
182	190	60	0.9385	0.87	6805
158	190	60	0.7538	0.57	6810
143	190	60	0.6385	0.44	6815
180	190	60	0.9231	0.84	6820
190	190	60	1.0000	1.00	6825
130	190	60	0.5385	0.34	6830
187	190	60	0.9769	0.95	6835
172	190	60	0.8615	0.73	6840
175	190	60	0.8846	0.77	6845
123	190	60	0.4846	0.29	6850
170	190	60	0.8462	0.71	6855
170	190	60	0.8462	0.71	6860
90	190	60	0.2308	0.11	6865
100	190	60	0.3077	0.16	6870
92	190	60	0.2462	0.12	6875
63	190	60	0.0231	0.01	6880
112	190	60	0.4000	0.23	6885
75	190	60	0.1154	0.05	6890
130	190	60	0.5385	0.34	6895
150	190	60	0.6923	0.50	6900
108	190	60	0.3692	0.20	6905
162	190	60	0.7846	0.62	6910
145	190	60	0.6538	0.46	6915
122	190	60	0.4769	0.29	6920
160	190	60	0.7692	0.59	6925
162	190	60	0.7846	0.62	6930
172	190	60	0.8615	0.73	6935
170	190	60	0.8462	0.71	6940
138	190	60	0.6000	0.40	6945
162	190	60	0.7846	0.62	6950
175	190	60	0.8846	0.77	6955
162	190	60	0.7846	0.62	6960
170	190	60	0.8462	0.71	6965
138	190	60	0.6000	0.40	6970
110	190	60	0.3846	0.22	6975
55	190	60	-0.0385	0.00	6980
60	190	60	0.0000	0.00	6985
60	190	60	0.0000	0.00	6990
58	190	60	-0.0154	0.00	6995
62	190	60	0.0154	0.01	7000
112	190	60	0.4000	0.23	7005
110	190	60	0.3846	0.22	7010
145	190	60	0.6538	0.46	7015

Table A.4 Shale volume (Vsh) calculation from **well: D** (continued)

Vsh.calculation (Clavier Eq.)					Depth
GR.	Max	Min	GR.fraction	Vsh.	(feet)
160	190	60	0.7692	0.59	7020
172	190	60	0.8615	0.73	7025
73	190	60	0.1000	0.04	7030
70	190	60	0.0769	0.03	7035
175	190	60	0.8846	0.77	7040
150	190	60	0.6923	0.50	7045
80	190	60	0.1538	0.07	7050
70	190	60	0.0769	0.03	7055
73	190	60	0.1000	0.04	7060
68	190	60	0.0615	0.03	7065
63	190	60	0.0231	0.01	7070
60	190	60	0.0000	0.00	7075
70	190	60	0.0769	0.03	7080
70	190	60	0.0769	0.03	7085
87	190	60	0.2077	0.10	7090
90	190	60	0.2308	0.11	7095
83	190	60	0.1769	0.08	7100
92	190	60	0.2462	0.12	7105
120	190	60	0.4615	0.27	7110
110	190	60	0.3846	0.22	7115
150	190	60	0.6923	0.50	7120
132	190	60	0.5538	0.36	7125
160	190	60	0.7692	0.59	7130
187	190	60	0.9769	0.95	7135
132	190	60	0.5538	0.36	7140
128	190	60	0.5231	0.33	7145
167	190	60	0.8231	0.67	7150
140	190	60	0.6154	0.42	7155
112	190	60	0.4000	0.23	7160
123	208	52	0.4551	0.27	7165
50	208	52	-0.0128	0.00	7170
52	208	52	0.0000	0.00	7175
52	208	52	0.0000	0.00	7180
52	208	52	0.0000	0.00	7185
53	208	52	0.0064	0.00	7190
172	208	52	0.7692	0.59	7195
162	208	52	0.7051	0.51	7200
108	208	52	0.3590	0.20	7205
190	208	52	0.8846	0.77	7210
170	208	52	0.7564	0.58	7215
165	208	52	0.7244	0.54	7220
150	208	52	0.6282	0.43	7225
140	208	52	0.5641	0.37	7230
160	208	52	0.6923	0.50	7235
110	208	52	0.3718	0.21	7240
168	208	52	0.7436	0.56	7245
100	208	52	0.3077	0.16	7250

Vsh.calculation (Clavier Eq.)					Depth
GR.	Max	Min	GR.fraction	Vsh.	(feet)
170	208	52	0.7564	0.58	7255
165	208	52	0.7244	0.54	7260
130	208	52	0.5000	0.31	7265
127	208	52	0.4808	0.29	7270
135	208	52	0.5321	0.34	7275
47	208	52	-0.0321	0.00	7280
45	208	52	-0.0449	0.00	7285
57	208	52	0.0321	0.01	7290
60	208	52	0.0513	0.02	7295
52	208	52	0.0000	0.00	7300
50	208	52	-0.0128	0.00	7305
178	208	52	0.8077	0.65	7310
180	208	52	0.8205	0.67	7315
165	208	52	0.7244	0.54	7320
170	208	52	0.7564	0.58	7325
200	208	52	0.9487	0.89	7330
180	208	52	0.8205	0.67	7335
143	208	52	0.5833	0.38	7340
158	208	52	0.6795	0.48	7345
140	208	52	0.5641	0.37	7350
142	208	52	0.5769	0.38	7355
140	208	52	0.5641	0.37	7360
100	208	52	0.3077	0.16	7365
162	208	52	0.7051	0.51	7370
150	208	52	0.6282	0.43	7375
140	208	52	0.5641	0.37	7380
130	208	52	0.5000	0.31	7385
180	208	52	0.8205	0.67	7390
130	208	52	0.5000	0.31	7395
140	208	52	0.5641	0.37	7400
145	208	52	0.5962	0.40	7405
170	208	52	0.7564	0.58	7410
120	208	52	0.4359	0.25	7415
188	208	52	0.8718	0.75	7420
175	208	52	0.7885	0.62	7425
161	208	52	0.6987	0.51	7430
197	208	52	0.9295	0.85	7435
132	208	52	0.5128	0.32	7440
150	208	52	0.6282	0.43	7445
140	208	52	0.5641	0.37	7450
142	208	52	0.5769	0.38	7455
155	208	52	0.6603	0.46	7460
170	208	52	0.7564	0.58	7465
102	208	52	0.3205	0.17	7470
190	208	52	0.8846	0.77	7475
187	208	52	0.8654	0.74	7480
132	208	52	0.5128	0.32	7485

Table A.4 Shale volume (Vsh) calculation from **well: D** (continued)

Vsh.calculation (Clavier Eq.)					Depth
GR.	Max	Min	GR.fraction	Vsh.	(feet)
182	208	52	0.8333	0.69	7490
150	208	52	0.6282	0.43	7495
140	208	52	0.5641	0.37	7500
130	208	52	0.5000	0.31	7505
175	208	52	0.7885	0.62	7510
150	208	52	0.6282	0.43	7515
135	208	52	0.5321	0.34	7520
185	208	52	0.8526	0.72	7525
180	208	52	0.8205	0.67	7530
180	208	52	0.8205	0.67	7535
178	208	52	0.8077	0.65	7540
160	208	52	0.6923	0.50	7545
65	208	52	0.0833	0.04	7550
63	208	52	0.0705	0.03	7555
63	208	52	0.0705	0.03	7560
52	208	52	0.0000	0.00	7565
60	208	52	0.0513	0.02	7570
63	208	52	0.0705	0.03	7575
58	208	52	0.0385	0.02	7580
43	208	52	-0.0577	0.00	7585
130	208	52	0.5000	0.31	7590
128	208	52	0.4872	0.30	7595
170	208	52	0.7564	0.58	7600
140	208	52	0.5641	0.37	7605
82	208	52	0.1923	0.09	7610
160	208	52	0.6923	0.50	7615
165	208	52	0.7244	0.54	7620
170	208	52	0.7564	0.58	7625
123	208	52	0.4551	0.27	7630
160	208	52	0.6923	0.50	7635
160	208	52	0.6923	0.50	7640
193	208	52	0.9038	0.80	7645
161	208	52	0.6987	0.51	7650
185	208	52	0.8526	0.72	7655
80	208	52	0.1795	0.09	7660
185	208	52	0.8526	0.72	7665
120	208	52	0.4359	0.25	7670
200	208	52	0.9487	0.89	7675
185	208	52	0.8526	0.72	7680
190	208	52	0.8846	0.77	7685
183	208	52	0.8397	0.70	7690
170	208	52	0.7564	0.58	7695
150	208	52	0.6282	0.43	7700
145	208	52	0.5962	0.40	7705
168	208	52	0.7436	0.56	7710
135	208	52	0.5321	0.34	7715
170	208	52	0.7564	0.58	7720

Vsh.calculation (Clavier Eq.)					Depth
GR.	Max	Min	GR.fraction	Vsh.	(feet)
170	208	52	0.7564	0.58	7725
183	208	52	0.8397	0.70	7730
142	208	52	0.5769	0.38	7735
175	208	52	0.7885	0.62	7740
167	208	52	0.7372	0.55	7745
167	208	52	0.7372	0.55	7750
138	208	52	0.5513	0.35	7755
152	208	52	0.6410	0.44	7760
110	208	52	0.3718	0.21	7765
168	208	52	0.7436	0.56	7770
158	208	52	0.6795	0.48	7775
140	208	52	0.5641	0.37	7780
135	208	52	0.5321	0.34	7785
142	208	52	0.5769	0.38	7790
180	208	52	0.8205	0.67	7795
160	208	52	0.6923	0.50	7800
195	208	52	0.9167	0.82	7805
185	208	52	0.8526	0.72	7810
138	208	52	0.5513	0.35	7815
115	208	52	0.4038	0.23	7820
58	208	52	0.0385	0.02	7825
75	208	52	0.1474	0.07	7830
68	208	52	0.1026	0.05	7835
68	208	52	0.1026	0.05	7840
60	208	52	0.0513	0.02	7845
175	208	52	0.7885	0.62	7850
135	208	52	0.5321	0.34	7855
70	208	52	0.1154	0.05	7860
68	208	52	0.1026	0.05	7865
70	208	52	0.1154	0.05	7870
70	208	52	0.1154	0.05	7875
67	208	52	0.0962	0.04	7880
67	208	52	0.0962	0.04	7885
65	208	52	0.0833	0.04	7890
68	208	52	0.1026	0.05	7895
67	208	52	0.0962	0.04	7900
55	208	52	0.0192	0.01	7905
167	208	52	0.7372	0.55	7910
160	208	52	0.6923	0.50	7915
160	208	52	0.6923	0.50	7920
145	208	52	0.5962	0.40	7925
172	208	52	0.7692	0.59	7930
178	208	52	0.8077	0.65	7935
158	208	52	0.6795	0.48	7940
133	208	52	0.5192	0.32	7945
152	208	52	0.6410	0.44	7950
123	208	52	0.4551	0.27	7955

Table A.4 Shale volume (Vsh) calculation from **well: D** (continued)

Vsh.calculation (Clavier Eq.)					Depth
GR.	Max	Min	GR.fraction	Vsh.	(feet)
117	208	52	0.4167	0.24	7960
160	208	52	0.6923	0.50	7965
100	208	52	0.3077	0.16	7970
150	208	52	0.6282	0.43	7975
173	208	52	0.7756	0.60	7980
140	208	52	0.5641	0.37	7985
155	208	52	0.6603	0.46	7990
148	208	52	0.6154	0.42	7995
105	208	52	0.3397	0.18	8000
130	208	52	0.5000	0.31	8005
160	208	52	0.6923	0.50	8010
162	208	52	0.7051	0.51	8015
161	208	52	0.6987	0.51	8020
200	208	52	0.9487	0.89	8025
186	208	52	0.8590	0.73	8030
200	208	52	0.9487	0.89	8035
185	208	52	0.8526	0.72	8040
160	208	52	0.6923	0.50	8045
42	208	52	-0.0641	0.00	8050
45	208	52	-0.0449	0.00	8055
120	208	52	0.4359	0.25	8060
145	208	52	0.5962	0.40	8065
160	208	52	0.6923	0.50	8070
147	208	52	0.6090	0.41	8075
155	208	52	0.6603	0.46	8080
182	208	52	0.8333	0.69	8085
120	208	52	0.4359	0.25	8090
115	208	52	0.4038	0.23	8095
118	208	52	0.4231	0.24	8100
85	208	52	0.2115	0.10	8105
50	208	52	-0.0128	0.00	8110
55	208	52	0.0192	0.01	8115
50	208	52	-0.0128	0.00	8120
73	208	52	0.1346	0.06	8125
63	208	52	0.0705	0.03	8130
140	208	52	0.5641	0.37	8135
172	208	52	0.7692	0.59	8140
164	208	52	0.7179	0.53	8145
178	208	52	0.8077	0.65	8150
175	208	52	0.7885	0.62	8155
170	208	52	0.7564	0.58	8160
163	208	52	0.7115	0.52	8165
173	208	52	0.7756	0.60	8170
170	208	52	0.7564	0.58	8175
150	208	52	0.6282	0.43	8180
170	208	52	0.7564	0.58	8185
141	208	52	0.5705	0.37	8190

Vsh.calculation (Clavier Eq.)					Depth
GR.	Max	Min	GR.fraction	Vsh.	(feet)
112	208	52	0.3846	0.22	8195
98	208	52	0.2949	0.15	8200
83	208	52	0.1987	0.10	8205
55	208	52	0.0192	0.01	8210
58	208	52	0.0385	0.02	8215
55	208	52	0.0192	0.01	8220
135	208	52	0.5321	0.34	8225
178	208	52	0.8077	0.65	8230
175	208	52	0.7885	0.62	8235
138	208	52	0.5513	0.35	8240
115	208	52	0.4038	0.23	8245
160	208	52	0.6923	0.50	8250
110	208	52	0.3718	0.21	8255
160	208	52	0.6923	0.50	8260
160	208	52	0.6923	0.50	8265
150	208	52	0.6282	0.43	8270
175	208	52	0.7885	0.62	8275
140	208	52	0.5641	0.37	8280
172	208	52	0.7692	0.59	8285
130	208	52	0.5000	0.31	8290
120	208	52	0.4359	0.25	8295
142	208	52	0.5769	0.38	8300
127	208	52	0.4808	0.29	8305
103	208	52	0.3269	0.18	8310
142	208	52	0.5769	0.38	8315
168	208	52	0.7436	0.56	8320
123	208	52	0.4551	0.27	8325
140	208	52	0.5641	0.37	8330
160	223	56	0.6228	0.42	8335
130	223	56	0.4431	0.26	8340
138	223	56	0.4910	0.30	8345
187	223	56	0.7844	0.62	8350
200	223	56	0.8623	0.73	8355
192	223	56	0.8144	0.66	8360
197	223	56	0.8443	0.70	8365
153	223	56	0.5808	0.38	8370
135	223	56	0.4731	0.28	8375
178	223	56	0.7305	0.55	8380
182	223	56	0.7545	0.58	8385
198	223	56	0.8503	0.71	8390
143	223	56	0.5210	0.33	8395
55	223	56	-0.0060	0.00	8400
58	223	56	0.0120	0.00	8405
60	223	56	0.0240	0.01	8410
57	223	56	0.0060	0.00	8415
55	223	56	-0.0060	0.00	8420
50	223	56	-0.0359	0.00	8425

Table A.4 Shale volume (Vsh) calculation from **well: D** (continued)

Vsh.calculation (Clavier Eq.)					Depth
GR.	Max	Min	GR.fraction	Vsh.	(feet)
147	223	56	0.5449	0.35	8430
165	223	56	0.6527	0.45	8435
200	223	56	0.8623	0.73	8440
160	223	56	0.6228	0.42	8445
97	223	56	0.2455	0.12	8450
120	223	56	0.3832	0.21	8455
168	223	56	0.6707	0.47	8460
140	223	56	0.5030	0.31	8465
187	223	56	0.7844	0.62	8470
182	223	56	0.7545	0.58	8475
87	223	56	0.1856	0.09	8480
163	223	56	0.6407	0.44	8485
160	223	56	0.6228	0.42	8490
200	223	56	0.8623	0.73	8495
177	223	56	0.7246	0.54	8500

Table A.5 Shale volume (Vsh) calculation from **well: E**

Vsh.calculation (Clavier Eq.)					Depth
GR.	Max	Min	GR.fraction	Vsh.	(feet)
120	133	35	0.8673	0.74	6050
125	133	35	0.9184	0.83	6055
122	133	35	0.8878	0.77	6060
197	133	35	1.6531	1.00	6065
122	133	35	0.8878	0.77	6070
150	133	35	1.1735	1.00	6075
105	133	35	0.7143	0.53	6080
120	133	35	0.8673	0.74	6085
93	133	35	0.5918	0.39	6090
40	133	35	0.0510	0.02	6095
140	133	35	1.0714	1.00	6100
105	133	35	0.7143	0.53	6105
133	133	35	1.0000	1.00	6110
127	133	35	0.9388	0.87	6115
125	133	35	0.9184	0.83	6120
120	133	35	0.8673	0.74	6125
45	133	35	0.1020	0.05	6130
43	133	35	0.0816	0.04	6135
41	133	35	0.0612	0.03	6140
42	133	35	0.0714	0.03	6145
50	133	35	0.1531	0.07	6150
44	133	35	0.0918	0.04	6155
125	133	35	0.9184	0.83	6160
113	133	35	0.7959	0.63	6165
120	133	35	0.8673	0.74	6170
130	133	35	0.9694	0.93	6175
125	133	35	0.9184	0.83	6180
100	133	35	0.6633	0.47	6185
90	133	35	0.5612	0.36	6190
110	133	35	0.7653	0.59	6195
120	133	35	0.8673	0.74	6200
138	133	35	1.0510	1.00	6205
120	133	35	0.8673	0.74	6210
130	133	35	0.9694	0.93	6215
140	133	35	1.0714	1.00	6220
140	133	35	1.0714	1.00	6225
140	133	35	1.0714	1.00	6230
162	133	35	1.2959	1.00	6235
115	133	35	0.8163	0.66	6240
98	133	35	0.6429	0.44	6245
73	133	35	0.3878	0.22	6250
110	133	35	0.7653	0.59	6255
83	133	35	0.4898	0.30	6260
108	133	35	0.7449	0.56	6265
57	133	35	0.2245	0.11	6270
130	133	35	0.9694	0.93	6275
128	133	35	0.9490	0.89	6280

Vsh.calculation (Clavier Eq.)					Depth
GR.	Max	Min	GR.fraction	Vsh.	(feet)
98	133	35	0.6429	0.44	6285
100	133	35	0.6633	0.47	6290
47	133	35	0.1224	0.06	6295
122	133	35	0.8878	0.77	6300
117	133	35	0.8367	0.69	6305
140	133	35	1.0714	1.00	6310
125	133	35	0.9184	0.83	6315
100	133	35	0.6633	0.47	6320
140	133	35	1.0714	1.00	6325
138	133	35	1.0510	1.00	6330
110	133	35	0.7653	0.59	6335
140	133	35	1.0714	1.00	6340
125	133	35	0.9184	0.83	6345
83	133	35	0.4898	0.30	6350
125	133	35	0.9184	0.83	6355
155	133	35	1.2245	1.00	6360
110	133	35	0.7653	0.59	6365
108	133	35	0.7449	0.56	6370
150	133	35	1.1735	1.00	6375
142	133	35	1.0918	1.00	6380
138	133	35	1.0510	1.00	6385
110	133	35	0.7653	0.59	6390
175	133	35	1.4286	1.00	6395
125	133	35	0.9184	0.83	6400
140	133	35	1.0714	1.00	6405
123	133	35	0.8980	0.79	6410
95	133	35	0.6122	0.41	6415
150	133	35	1.1735	1.00	6420
50	133	35	0.1531	0.07	6425
41	133	35	0.0612	0.03	6430
42	133	35	0.0714	0.03	6435
54	133	35	0.1939	0.09	6440
43	133	35	0.0816	0.04	6445
120	133	35	0.8673	0.74	6450
128	133	35	0.9490	0.89	6455
138	133	35	1.0510	1.00	6460
157	133	35	1.2449	1.00	6465
130	133	35	0.9694	0.93	6470
125	133	35	0.9184	0.83	6475
162	133	35	1.2959	1.00	6480
100	133	35	0.6633	0.47	6485
60	133	35	0.2551	0.13	6490
143	133	35	1.1020	1.00	6495
120	133	35	0.8673	0.74	6500
80	133	35	0.4592	0.27	6505
45	133	35	0.1020	0.05	6510
62	133	35	0.2755	0.14	6515

Table A.5 Shale volume (Vsh) calculation from **well: E** (continued)

Vsh.calculation (Clavier Eq.)					Depth
GR.	Max	Min	GR.fraction	Vsh.	(feet)
125	133	35	0.9184	0.83	6520
123	133	35	0.8980	0.79	6525
100	133	35	0.6633	0.47	6530
40	133	35	0.0510	0.02	6535
45	133	35	0.1020	0.05	6540
63	133	35	0.2857	0.15	6545
100	133	35	0.6633	0.47	6550
163	133	35	1.3061	1.00	6555
155	133	35	1.2245	1.00	6560
110	133	35	0.7653	0.59	6565
140	133	35	1.0714	1.00	6570
100	133	35	0.6633	0.47	6575
135	133	35	1.0204	1.00	6580
140	133	35	1.0714	1.00	6585
143	133	35	1.1020	1.00	6590
150	133	35	1.1735	1.00	6595
138	133	35	1.0510	1.00	6600
50	133	35	0.1531	0.07	6605
60	133	35	0.2551	0.13	6610
135	133	35	1.0204	1.00	6615
110	133	35	0.7653	0.59	6620
150	133	35	1.1735	1.00	6625
140	133	35	1.0714	1.00	6630
120	133	35	0.8673	0.74	6635
105	133	35	0.7143	0.53	6640
120	133	35	0.8673	0.74	6645
82	133	35	0.4796	0.29	6650
95	133	35	0.6122	0.41	6655
93	133	35	0.5918	0.39	6660
40	133	35	0.0510	0.02	6665
42	133	35	0.0714	0.03	6670
43	133	35	0.0816	0.04	6675
42	133	35	0.0714	0.03	6680
50	133	35	0.1531	0.07	6685
138	133	35	1.0510	1.00	6690
103	133	35	0.6939	0.50	6695
140	133	35	1.0714	1.00	6700
110	133	35	0.7653	0.59	6705
45	133	35	0.1020	0.05	6710
50	133	35	0.1531	0.07	6715
62	133	35	0.2755	0.14	6720
67	133	35	0.3265	0.17	6725
61	133	35	0.2653	0.14	6730
51	133	35	0.1633	0.08	6735
48	133	35	0.1327	0.06	6740
54	133	35	0.1939	0.09	6745
52	133	35	0.1735	0.08	6750

Vsh.calculation (Clavier Eq.)					Depth
GR.	Max	Min	GR.fraction	Vsh.	(feet)
122	133	35	0.8878	0.77	6755
72	133	35	0.3776	0.21	6760
63	133	35	0.2857	0.15	6765
46	133	35	0.1122	0.05	6770
155	133	35	1.2245	1.00	6775
143	133	35	1.1020	1.00	6780
157	133	35	1.2449	1.00	6785
62	133	35	0.2755	0.14	6790
40	133	35	0.0510	0.02	6795
48	133	35	0.1327	0.06	6800
173	133	35	1.4082	1.00	6805
110	133	35	0.7653	0.59	6810
140	133	35	1.0714	1.00	6815
195	133	35	1.6327	1.00	6820
142	133	35	1.0918	1.00	6825
147	133	35	1.1429	1.00	6830
137	133	35	1.0408	1.00	6835
120	133	35	0.8673	0.74	6840
105	133	35	0.7143	0.53	6845
135	133	35	1.0204	1.00	6850
90	133	35	0.5612	0.36	6855
115	133	35	0.8163	0.66	6860
55	133	35	0.2041	0.10	6865
57	133	35	0.2245	0.11	6870
158	133	35	1.2551	1.00	6875
150	133	35	1.1735	1.00	6880
130	133	35	0.9694	0.93	6885
142	133	35	1.0918	1.00	6890
170	133	35	1.3776	1.00	6895
160	133	35	1.2755	1.00	6900
145	133	35	1.1224	1.00	6905
140	133	35	1.0714	1.00	6910
150	133	35	1.1735	1.00	6915
167	133	35	1.3469	1.00	6920
97	133	35	0.6327	0.43	6925
62	133	35	0.2755	0.14	6930
100	133	35	0.6633	0.47	6935
150	140	32	1.0926	1.00	6940
130	140	32	0.9074	0.81	6945
125	140	32	0.8611	0.73	6950
120	140	32	0.8148	0.66	6955
107	140	32	0.6944	0.50	6960
145	140	32	1.0463	1.00	6965
137	140	32	0.9722	0.94	6970
115	140	32	0.7685	0.59	6975
117	140	32	0.7870	0.62	6980
178	140	32	1.3519	1.00	6985

Table A.5 Shale volume (Vsh) calculation from **well: E** (continued)

Vsh.calculation (Clavier Eq.)					Depth
GR.	Max	Min	GR.fraction	Vsh.	(feet)
130	140	32	0.9074	0.81	6990
140	140	32	1.0000	1.00	6995
150	140	32	1.0926	1.00	7000
150	140	32	1.0926	1.00	7005
120	140	32	0.8148	0.66	7010
143	140	32	1.0278	1.00	7015
120	140	32	0.8148	0.66	7020
75	140	32	0.3981	0.23	7025
40	140	32	0.0741	0.03	7030
55	140	32	0.2130	0.10	7035
57	140	32	0.2315	0.11	7040
60	140	32	0.2593	0.13	7045
53	140	32	0.1944	0.09	7050
53	140	32	0.1944	0.09	7055
55	140	32	0.2130	0.10	7060
55	140	32	0.2130	0.10	7065
80	140	32	0.4444	0.26	7070
53	140	32	0.1944	0.09	7075
50	140	32	0.1667	0.08	7080
5	140	32	-0.2500	0.00	7085
138	140	32	0.9815	0.96	7090
140	140	32	1.0000	1.00	7095
135	140	32	0.9537	0.90	7100
153	140	32	1.1204	1.00	7105
120	140	32	0.8148	0.66	7110
107	140	32	0.6944	0.50	7115
142	140	32	1.0185	1.00	7120
140	140	32	1.0000	1.00	7125
85	140	32	0.4907	0.30	7130
105	140	32	0.6759	0.48	7135
90	140	32	0.5370	0.34	7140
60	140	32	0.2593	0.13	7145
70	140	32	0.3519	0.19	7150
50	140	32	0.1667	0.08	7155
60	140	32	0.2593	0.13	7160
95	140	32	0.5833	0.38	7165
85	140	32	0.4907	0.30	7170
108	140	32	0.7037	0.51	7175
60	140	32	0.2593	0.13	7180
55	140	32	0.2130	0.10	7185
45	140	32	0.1204	0.05	7190
45	140	32	0.1204	0.05	7195
47	140	32	0.1389	0.06	7200
112	140	32	0.7407	0.56	7205
135	140	32	0.9537	0.90	7210
90	140	32	0.5370	0.34	7215
157	140	32	1.1574	1.00	7220

Vsh.calculation (Clavier Eq.)					Depth
GR.	Max	Min	GR.fraction	Vsh.	(feet)
142	140	32	1.0185	1.00	7225
118	140	32	0.7963	0.63	7230
117	140	32	0.7870	0.62	7235
50	140	32	0.1667	0.08	7240
38	140	32	0.0556	0.02	7245
42	140	32	0.0926	0.04	7250
38	140	32	0.0556	0.02	7255
35	140	32	0.0278	0.01	7260
60	140	32	0.2593	0.13	7265
120	140	32	0.8148	0.66	7270
165	140	32	1.2315	1.00	7275
137	140	32	0.9722	0.94	7280
160	140	32	1.1852	1.00	7285
160	140	32	1.1852	1.00	7290
147	140	32	1.0648	1.00	7295
138	140	32	0.9815	0.96	7300
140	140	32	1.0000	1.00	7305
140	140	32	1.0000	1.00	7310
142	140	32	1.0185	1.00	7315
153	140	32	1.1204	1.00	7320
87	140	32	0.5093	0.32	7325
168	140	32	1.2593	1.00	7330
132	140	32	0.9259	0.84	7335
110	140	32	0.7222	0.53	7340
110	140	32	0.7222	0.53	7345
155	140	32	1.1389	1.00	7350
158	140	32	1.1667	1.00	7355
135	140	32	0.9537	0.90	7360
140	140	32	1.0000	1.00	7365
135	140	32	0.9537	0.90	7370
108	140	32	0.7037	0.51	7375
138	140	32	0.9815	0.96	7380
150	140	32	1.0926	1.00	7385
142	140	32	1.0185	1.00	7390
128	140	32	0.8889	0.78	7395
142	140	32	1.0185	1.00	7400
134	140	32	0.9444	0.88	7405
120	140	32	0.8148	0.66	7410
105	140	32	0.6759	0.48	7415
120	140	32	0.8148	0.66	7420
50	140	32	0.1667	0.08	7425
42	140	32	0.0926	0.04	7430
145	140	32	1.0463	1.00	7435
110	140	32	0.7222	0.53	7440
137	140	32	0.9722	0.94	7445
107	140	32	0.6944	0.50	7450
135	140	32	0.9537	0.90	7455

Table A.5 Shale volume (Vsh) calculation from **well: E** (continued)

Vsh.calculation (Clavier Eq.)					Depth
GR.	Max	Min	GR.fraction	Vsh.	(feet)
132	140	32	0.9259	0.84	7460
145	140	32	1.0463	1.00	7465
180	140	32	1.3704	1.00	7470
160	140	32	1.1852	1.00	7475
157	140	32	1.1574	1.00	7480
145	140	32	1.0463	1.00	7485
160	140	32	1.1852	1.00	7490
140	140	32	1.0000	1.00	7495
80	140	32	0.4444	0.26	7500
123	140	32	0.8426	0.70	7505
54	140	32	0.2037	0.10	7510
40	140	32	0.0741	0.03	7515
47	140	32	0.1389	0.06	7520
55	140	32	0.2130	0.10	7525
60	140	32	0.2593	0.13	7530
50	140	32	0.1667	0.08	7535
42	140	32	0.0926	0.04	7540
38	140	32	0.0556	0.02	7545
58	140	32	0.2407	0.12	7550
136	140	32	0.9630	0.92	7555
142	140	32	1.0185	1.00	7560
133	140	32	0.9352	0.86	7565
180	140	32	1.3704	1.00	7570
150	140	32	1.0926	1.00	7575
175	140	32	1.3241	1.00	7580
170	140	32	1.2778	1.00	7585
133	140	32	0.9352	0.86	7590
180	140	32	1.3704	1.00	7595
150	140	32	1.0926	1.00	7600
92	140	32	0.5556	0.36	7605
155	140	32	1.1389	1.00	7610
163	140	32	1.2130	1.00	7615
132	140	32	0.9259	0.84	7620
133	140	32	0.9352	0.86	7625
130	140	32	0.9074	0.81	7630
120	140	32	0.8148	0.66	7635
48	140	32	0.1481	0.07	7640
120	140	32	0.8148	0.66	7645
142	140	32	1.0185	1.00	7650
150	140	32	1.0926	1.00	7655
130	140	32	0.9074	0.81	7660
128	140	32	0.8889	0.78	7665
130	140	32	0.9074	0.81	7670
150	140	32	1.0926	1.00	7675
180	140	32	1.3704	1.00	7680
135	140	32	0.9537	0.90	7685
157	140	32	1.1574	1.00	7690

Vsh.calculation (Clavier Eq.)					Depth
GR.	Max	Min	GR.fraction	Vsh.	(feet)
175	140	32	1.3241	1.00	7695
160	140	32	1.1852	1.00	7700
161	140	32	1.1944	1.00	7705
150	140	32	1.0926	1.00	7710
148	140	32	1.0741	1.00	7715
140	140	32	1.0000	1.00	7720
121	140	32	0.8241	0.67	7725
110	140	32	0.7222	0.53	7730
160	140	32	1.1852	1.00	7735
140	140	32	1.0000	1.00	7740
162	140	32	1.2037	1.00	7745
170	140	32	1.2778	1.00	7750
140	140	32	1.0000	1.00	7755
140	140	32	1.0000	1.00	7760
138	140	32	0.9815	0.96	7765
100	140	32	0.6296	0.43	7770
50	140	32	0.1667	0.08	7775
50	140	32	0.1667	0.08	7780
65	140	32	0.3056	0.16	7785
55	140	32	0.2130	0.10	7790
54	140	32	0.2037	0.10	7795
100	140	32	0.6296	0.43	7800
72	140	32	0.3704	0.21	7805
58	140	32	0.2407	0.12	7810
62	140	32	0.2778	0.14	7815
62	140	32	0.2778	0.14	7820
60	140	32	0.2593	0.13	7825
100	140	32	0.6296	0.43	7830
130	140	32	0.9074	0.81	7835
165	140	32	1.2315	1.00	7840
130	140	32	0.9074	0.81	7845
55	140	32	0.2130	0.10	7850
42	140	32	0.0926	0.04	7855
40	140	32	0.0741	0.03	7860
40	140	32	0.0741	0.03	7865
45	140	32	0.1204	0.05	7870
43	140	32	0.1019	0.05	7875
50	140	32	0.1667	0.08	7880
38	140	32	0.0556	0.02	7885
140	140	32	1.0000	1.00	7890
142	140	32	1.0185	1.00	7895
130	140	32	0.9074	0.81	7900
160	140	32	1.1852	1.00	7905
150	140	32	1.0926	1.00	7910
152	140	32	1.1111	1.00	7915
152	140	32	1.1111	1.00	7920
135	140	32	0.9537	0.90	7925

Table A.5 Shale volume (Vsh) calculation from **well: E** (continued)

Vsh.calculation (Clavier Eq.)					Depth
GR.	Max	Min	GR.fraction	Vsh.	(feet)
155	140	32	1.1389	1.00	7930
145	140	32	1.0463	1.00	7935
198	140	32	1.5370	1.00	7940
142	140	32	1.0185	1.00	7945
168	140	32	1.2593	1.00	7950
140	140	32	1.0000	1.00	7955
125	140	32	0.8611	0.73	7960
160	140	32	1.1852	1.00	7965
133	140	32	0.9352	0.86	7970
140	140	32	1.0000	1.00	7975
100	140	32	0.6296	0.43	7980
48	140	32	0.1481	0.07	7985
40	140	32	0.0741	0.03	7990
140	140	32	1.0000	1.00	7995
127	140	32	0.8796	0.76	8000
138	140	32	0.9815	0.96	8005
120	140	32	0.8148	0.66	8010
138	140	32	0.9815	0.96	8015
163	140	32	1.2130	1.00	8020
150	140	32	1.0926	1.00	8025
110	140	32	0.7222	0.53	8030
85	140	32	0.4907	0.30	8035
102	140	32	0.6481	0.45	8040
85	140	32	0.4907	0.30	8045
115	140	32	0.7685	0.59	8050
157	140	32	1.1574	1.00	8055
140	140	32	1.0000	1.00	8060
110	140	32	0.7222	0.53	8065
100	140	32	0.6296	0.43	8070
137	140	32	0.9722	0.94	8075
160	140	32	1.1852	1.00	8080
150	140	32	1.0926	1.00	8085
120	140	32	0.8148	0.66	8090
130	140	32	0.9074	0.81	8095
150	140	32	1.0926	1.00	8100
110	140	32	0.7222	0.53	8105
122	140	32	0.8333	0.69	8110
147	140	32	1.0648	1.00	8115
107	140	32	0.6944	0.50	8120
132	140	32	0.9259	0.84	8125
160	140	32	1.1852	1.00	8130
130	140	32	0.9074	0.81	8135
120	140	32	0.8148	0.66	8140
128	140	32	0.8889	0.78	8145
100	140	32	0.6296	0.43	8150
120	140	32	0.8148	0.66	8155
130	140	32	0.9074	0.81	8160

Vsh.calculation (Clavier Eq.)					Depth
GR.	Max	Min	GR.fraction	Vsh.	(feet)
65	140	32	0.3056	0.16	8165
123	140	32	0.8426	0.70	8170
138	140	32	0.9815	0.96	8175
60	140	32	0.2593	0.13	8180
160	140	32	1.1852	1.00	8185
160	140	32	1.1852	1.00	8190
140	140	32	1.0000	1.00	8195
110	140	32	0.7222	0.53	8200
160	140	32	1.1852	1.00	8205
140	140	32	1.0000	1.00	8210
130	140	32	0.9074	0.81	8215
153	140	32	1.1204	1.00	8220
140	140	32	1.0000	1.00	8225
120	140	32	0.8148	0.66	8230
80	140	32	0.4444	0.26	8235
115	140	32	0.7685	0.59	8240
135	140	32	0.9537	0.90	8245
142	140	32	1.0185	1.00	8250
145	140	32	1.0463	1.00	8255
165	140	32	1.2315	1.00	8260
153	140	32	1.1204	1.00	8265
141	140	32	1.0093	1.00	8270
115	140	32	0.7685	0.59	8275
108	140	32	0.7037	0.51	8280
158	140	32	1.1667	1.00	8285
170	140	32	1.2778	1.00	8290
150	140	32	1.0926	1.00	8295
62	140	32	0.2778	0.14	8300
72	140	32	0.3704	0.21	8305
60	140	32	0.2593	0.13	8310
63	140	32	0.2870	0.15	8315
162	140	32	1.2037	1.00	8320
150	140	32	1.0926	1.00	8325
145	140	32	1.0463	1.00	8330
180	140	32	1.3704	1.00	8335
120	140	32	0.8148	0.66	8340
140	140	32	1.0000	1.00	8345
97	140	32	0.6019	0.40	8350
73	140	32	0.3796	0.21	8355
75	140	32	0.3981	0.23	8360
67	140	32	0.3241	0.17	8365
55	140	32	0.2130	0.10	8370
40	140	32	0.0741	0.03	8375
190	155	46	1.3211	1.00	8380
141	155	46	0.8716	0.75	8385
90	155	46	0.4037	0.23	8390
130	155	46	0.7706	0.60	8395

Table A.5 Shale volume (Vsh) calculation from **well: E** (continued)

Vsh.calculation (Clavier Eq.)					Depth
GR.	Max	Min	GR.fraction	Vsh.	(feet)
100	155	46	0.4954	0.30	8400
142	155	46	0.8807	0.76	8405
107	155	46	0.5596	0.36	8410
200	155	46	1.4128	1.00	8415
140	155	46	0.8624	0.73	8420
170	155	46	1.1376	1.00	8425
110	155	46	0.5872	0.39	8430
110	155	46	0.5872	0.39	8435
197	155	46	1.3853	1.00	8440
160	155	46	1.0459	1.00	8445
100	155	46	0.4954	0.30	8450
170	155	46	1.1376	1.00	8455
120	155	46	0.6789	0.48	8460
110	155	46	0.5872	0.39	8465
100	155	46	0.4954	0.30	8470
120	155	46	0.6789	0.48	8475
85	155	46	0.3578	0.20	8480
180	155	46	1.2294	1.00	8485
185	155	46	1.2752	1.00	8490
150	155	46	0.9541	0.90	8495
140	155	46	0.8624	0.73	8500
120	155	46	0.6789	0.48	8505
108	155	46	0.5688	0.37	8510
117	155	46	0.6514	0.45	8515
130	155	46	0.7706	0.60	8520
190	155	46	1.3211	1.00	8525
62	155	46	0.1468	0.07	8530

Table A.6 Shale volume (Vsh) calculation from **well: F**

Vsh.calculation (Clavier Eq.)					Depth
GR.	Max	Min	GR.fraction	Vsh.	(feet)
155	138	38	1.1700	1.00	5700
110	138	38	0.7200	0.53	5705
155	138	38	1.1700	1.00	5710
135	138	38	0.9700	0.93	5715
125	138	38	0.8700	0.74	5720
155	138	38	1.1700	1.00	5725
145	138	38	1.0700	1.00	5730
195	138	38	1.5700	1.00	5735
155	138	38	1.1700	1.00	5740
155	138	38	1.1700	1.00	5745
140	138	38	1.0200	1.00	5750
125	138	38	0.8700	0.74	5755
190	138	38	1.5200	1.00	5760
160	138	38	1.2200	1.00	5765
180	138	38	1.4200	1.00	5770
127	138	38	0.8900	0.78	5775
100	138	38	0.6200	0.42	5780
60	138	38	0.2200	0.11	5785
150	138	38	1.1200	1.00	5790
155	138	38	1.1700	1.00	5795
140	138	38	1.0200	1.00	5800
70	138	38	0.3200	0.17	5805
40	138	38	0.0200	0.01	5810
40	138	38	0.0200	0.01	5815
45	138	38	0.0700	0.03	5820
40	138	38	0.0200	0.01	5825
158	138	38	1.2000	1.00	5830
110	138	38	0.7200	0.53	5835
145	138	38	1.0700	1.00	5840
165	138	38	1.2700	1.00	5845
145	138	38	1.0700	1.00	5850
200	138	38	1.6200	1.00	5855
120	138	38	0.8200	0.67	5860
160	138	38	1.2200	1.00	5865
150	138	38	1.1200	1.00	5870
110	138	38	0.7200	0.53	5875
175	138	38	1.3700	1.00	5880
148	138	38	1.1000	1.00	5885
110	138	38	0.7200	0.53	5890
100	138	38	0.6200	0.42	5895
72	138	38	0.3400	0.18	5900
62	138	38	0.2400	0.12	5905
61	138	38	0.2300	0.11	5910
125	138	38	0.8700	0.74	5915
125	138	38	0.8700	0.74	5920
110	138	38	0.7200	0.53	5925
105	138	38	0.6700	0.47	5930

Vsh.calculation (Clavier Eq.)					Depth
GR.	Max	Min	GR.fraction	Vsh.	(feet)
50	138	38	0.1200	0.05	5935
50	138	38	0.1200	0.05	5940
50	138	38	0.1200	0.05	5945
50	138	38	0.1200	0.05	5950
70	138	38	0.3200	0.17	5955
97	138	38	0.5900	0.39	5960
70	138	38	0.3200	0.17	5965
170	138	38	1.3200	1.00	5970
145	138	38	1.0700	1.00	5975
150	138	38	1.1200	1.00	5980
120	138	38	0.8200	0.67	5985
110	138	38	0.7200	0.53	5990
60	138	38	0.2200	0.11	5995
60	138	38	0.2200	0.11	6000
60	138	38	0.2200	0.11	6005
60	138	38	0.2200	0.11	6010
67	138	38	0.2900	0.15	6015
157	138	38	1.1900	1.00	6020
85	138	38	0.4700	0.28	6025
158	138	38	1.2000	1.00	6030
115	138	38	0.7700	0.60	6035
150	138	38	1.1200	1.00	6040
178	138	38	1.4000	1.00	6045
150	138	38	1.1200	1.00	6050
120	138	38	0.8200	0.67	6055
122	138	38	0.8400	0.70	6060
137	138	38	0.9900	0.98	6065
100	138	38	0.6200	0.42	6070
140	138	38	1.0200	1.00	6075
115	138	38	0.7700	0.60	6080
145	138	38	1.0700	1.00	6085
140	138	38	1.0200	1.00	6090
160	138	38	1.2200	1.00	6095
180	138	38	1.4200	1.00	6100
118	138	38	0.8000	0.64	6105
110	138	38	0.7200	0.53	6110
160	138	38	1.2200	1.00	6115
130	138	38	0.9200	0.83	6120
120	138	38	0.8200	0.67	6125
140	138	38	1.0200	1.00	6130
70	138	38	0.3200	0.17	6135
40	138	38	0.0200	0.01	6140
60	138	38	0.2200	0.11	6145
140	138	38	1.0200	1.00	6150
150	138	38	1.1200	1.00	6155
170	138	38	1.3200	1.00	6160
160	138	38	1.2200	1.00	6165

Table A.6 Shale volume (Vsh) calculation from **well: F** (continued)

Vsh.calculation (Clavier Eq.)					Depth
GR.	Max	Min	GR.fraction	Vsh.	(feet)
140	138	38	1.0200	1.00	6170
100	138	38	0.6200	0.42	6175
110	138	38	0.7200	0.53	6180
135	140	42	0.9490	0.89	6185
110	140	42	0.6939	0.50	6190
155	140	42	1.1531	1.00	6195
145	140	42	1.0510	1.00	6200
150	140	42	1.1020	1.00	6205
110	140	42	0.6939	0.50	6210
125	140	42	0.8469	0.71	6215
60	140	42	0.1837	0.09	6220
65	140	42	0.2347	0.12	6225
130	140	42	0.8980	0.79	6230
50	140	42	0.0816	0.04	6235
90	140	42	0.4898	0.30	6240
130	140	42	0.8980	0.79	6245
130	140	42	0.8980	0.79	6250
140	140	42	1.0000	1.00	6255
155	140	42	1.1531	1.00	6260
105	140	42	0.6429	0.44	6265
165	140	42	1.2551	1.00	6270
170	140	42	1.3061	1.00	6275
150	140	42	1.1020	1.00	6280
130	140	42	0.8980	0.79	6285
170	140	42	1.3061	1.00	6290
160	140	42	1.2041	1.00	6295
160	140	42	1.2041	1.00	6300
90	140	42	0.4898	0.30	6305
170	140	42	1.3061	1.00	6310
190	140	42	1.5102	1.00	6315
145	140	42	1.0510	1.00	6320
145	140	42	1.0510	1.00	6325
140	140	42	1.0000	1.00	6330
120	140	42	0.7959	0.63	6335
70	140	42	0.2857	0.15	6340
150	140	42	1.1020	1.00	6345
145	140	42	1.0510	1.00	6350
160	140	42	1.2041	1.00	6355
140	140	42	1.0000	1.00	6360
150	140	42	1.1020	1.00	6365
130	140	42	0.8980	0.79	6370
135	140	42	0.9490	0.89	6375
150	140	42	1.1020	1.00	6380
170	140	42	1.3061	1.00	6385
150	140	42	1.1020	1.00	6390
130	140	42	0.8980	0.79	6395
80	140	42	0.3878	0.22	6400

Vsh.calculation (Clavier Eq.)					Depth
GR.	Max	Min	GR.fraction	Vsh.	(feet)
140	140	42	1.0000	1.00	6405
150	140	42	1.1020	1.00	6410
170	140	42	1.3061	1.00	6415
165	140	42	1.2551	1.00	6420
153	140	42	1.1327	1.00	6425
115	140	42	0.7449	0.56	6430
90	140	42	0.4898	0.30	6435
140	140	42	1.0000	1.00	6440
110	140	42	0.6939	0.50	6445
150	140	42	1.1020	1.00	6450
150	140	42	1.1020	1.00	6455
100	140	42	0.5918	0.39	6460
180	140	42	1.4082	1.00	6465
190	140	42	1.5102	1.00	6470
100	140	42	0.5918	0.39	6475
125	140	42	0.8469	0.71	6480
75	140	42	0.3367	0.18	6485
60	140	42	0.1837	0.09	6490
60	140	42	0.1837	0.09	6495
60	140	42	0.1837	0.09	6500
125	140	42	0.8469	0.71	6505
70	140	42	0.2857	0.15	6510
55	140	42	0.1327	0.06	6515
55	140	42	0.1327	0.06	6520
100	140	42	0.5918	0.39	6525
130	140	42	0.8980	0.79	6530
155	140	42	1.1531	1.00	6535
140	140	42	1.0000	1.00	6540
155	140	42	1.1531	1.00	6545
180	140	42	1.4082	1.00	6550
155	140	42	1.1531	1.00	6555
90	140	42	0.4898	0.30	6560
90	140	42	0.4898	0.30	6565
80	140	42	0.3878	0.22	6570
55	140	42	0.1327	0.06	6575
65	140	42	0.2347	0.12	6580
55	140	42	0.1327	0.06	6585
65	140	42	0.2347	0.12	6590
60	140	42	0.1837	0.09	6595
100	140	42	0.5918	0.39	6600
80	140	42	0.3878	0.22	6605
80	140	42	0.3878	0.22	6610
70	140	42	0.2857	0.15	6615
65	140	42	0.2347	0.12	6620
60	140	42	0.1837	0.09	6625
50	140	42	0.0816	0.04	6630
170	140	42	1.3061	1.00	6635

Table A.6 Shale volume (Vsh) calculation from **well: F** (continued)

Vsh.calculation (Clavier Eq.)					Depth
GR.	Max	Min	GR.fraction	Vsh.	(feet)
120	140	42	0.7959	0.63	6640
150	140	42	1.1020	1.00	6645
140	140	42	1.0000	1.00	6650
200	140	42	1.6122	1.00	6655
185	140	42	1.4592	1.00	6660
120	140	42	0.7959	0.63	6665
170	140	42	1.3061	1.00	6670
190	140	42	1.5102	1.00	6675
185	140	42	1.4592	1.00	6680
140	140	42	1.0000	1.00	6685
200	140	42	1.6122	1.00	6690
170	140	42	1.3061	1.00	6695
150	140	42	1.1020	1.00	6700
110	140	42	0.6939	0.50	6705
200	140	42	1.6122	1.00	6710
110	140	42	0.6939	0.50	6715
120	140	42	0.7959	0.63	6720
200	140	42	1.6122	1.00	6725
135	140	42	0.9490	0.89	6730
150	140	42	1.1020	1.00	6735
180	140	42	1.4082	1.00	6740
200	140	42	1.6122	1.00	6745
140	140	42	1.0000	1.00	6750
170	140	42	1.3061	1.00	6755
180	140	42	1.4082	1.00	6760
160	140	42	1.2041	1.00	6765
170	143	39	1.2596	1.00	6770
140	143	39	0.9712	0.93	6775
165	143	39	1.2115	1.00	6780
150	143	39	1.0673	1.00	6785
170	143	39	1.2596	1.00	6790
165	143	39	1.2115	1.00	6795
120	143	39	0.7788	0.61	6800
40	143	39	0.0096	0.00	6805
70	143	39	0.2981	0.16	6810
60	143	39	0.2019	0.10	6815
60	143	39	0.2019	0.10	6820
70	143	39	0.2981	0.16	6825
190	143	39	1.4519	1.00	6830
140	143	39	0.9712	0.93	6835
140	143	39	0.9712	0.93	6840
55	143	39	0.1538	0.07	6845
60	143	39	0.2019	0.10	6850
55	143	39	0.1538	0.07	6855
55	143	39	0.1538	0.07	6860
45	143	39	0.0577	0.02	6865
165	143	39	1.2115	1.00	6870

Vsh.calculation (Clavier Eq.)					Depth
GR.	Max	Min	GR.fraction	Vsh.	(feet)
180	143	39	1.3558	1.00	6875
145	143	39	1.0192	1.00	6880
180	143	39	1.3558	1.00	6885
120	143	39	0.7788	0.61	6890
190	143	39	1.4519	1.00	6895
130	143	39	0.8750	0.75	6900
140	143	39	0.9712	0.93	6905
60	143	39	0.2019	0.10	6910
65	143	39	0.2500	0.13	6915
60	143	39	0.2019	0.10	6920
65	143	39	0.2500	0.13	6925
60	143	39	0.2019	0.10	6930
50	143	39	0.1058	0.05	6935
50	143	39	0.1058	0.05	6940
55	143	39	0.1538	0.07	6945
70	143	39	0.2981	0.16	6950
80	143	39	0.3942	0.22	6955
165	143	39	1.2115	1.00	6960
180	143	39	1.3558	1.00	6965
100	143	39	0.5865	0.39	6970
150	143	39	1.0673	1.00	6975
195	143	39	1.5000	1.00	6980
180	143	39	1.3558	1.00	6985
130	143	39	0.8750	0.75	6990
170	143	39	1.2596	1.00	6995
130	143	39	0.8750	0.75	7000
165	143	39	1.2115	1.00	7005
90	143	39	0.4904	0.30	7010
170	143	39	1.2596	1.00	7015
160	143	39	1.1635	1.00	7020
90	143	39	0.4904	0.30	7025
115	143	39	0.7308	0.55	7030
70	143	39	0.2981	0.16	7035
43	143	39	0.0385	0.02	7040
55	143	39	0.1538	0.07	7045
50	143	39	0.1058	0.05	7050
180	143	39	1.3558	1.00	7055
160	143	39	1.1635	1.00	7060
100	143	39	0.5865	0.39	7065
70	143	39	0.2981	0.16	7070
170	143	39	1.2596	1.00	7075
175	143	39	1.3077	1.00	7080
115	143	39	0.7308	0.55	7085
200	143	39	1.5481	1.00	7090
150	143	39	1.0673	1.00	7095
160	143	39	1.1635	1.00	7100
123	143	39	0.8077	0.65	7105

Table A.6 Shale volume (Vsh) calculation from **well: F** (continued)

Vsh.calculation (Clavier Eq.)					Depth
GR.	Max	Min	GR.fraction	Vsh.	(feet)
190	143	39	1.4519	1.00	7110
130	143	39	0.8750	0.75	7115
200	143	39	1.5481	1.00	7120
175	143	39	1.3077	1.00	7125
120	143	39	0.7788	0.61	7130
140	143	39	0.9712	0.93	7135
50	143	39	0.1058	0.05	7140
50	143	39	0.1058	0.05	7145
55	143	39	0.1538	0.07	7150
50	143	39	0.1058	0.05	7155
55	143	39	0.1538	0.07	7160
45	143	39	0.0577	0.02	7165
50	143	39	0.1058	0.05	7170
200	143	39	1.5481	1.00	7175
185	143	39	1.4038	1.00	7180
195	143	39	1.5000	1.00	7185
150	143	39	1.0673	1.00	7190
200	143	39	1.5481	1.00	7195
120	143	39	0.7788	0.61	7200
110	143	39	0.6827	0.49	7205
95	143	39	0.5385	0.34	7210
100	143	39	0.5865	0.39	7215
60	143	39	0.2019	0.10	7220
60	143	39	0.2019	0.10	7225
125	143	39	0.8269	0.68	7230
190	143	39	1.4519	1.00	7235
180	143	39	1.3558	1.00	7240
180	143	39	1.3558	1.00	7245
95	143	39	0.5385	0.34	7250
160	143	39	1.1635	1.00	7255
180	143	39	1.3558	1.00	7260
185	143	39	1.4038	1.00	7265
120	143	39	0.7788	0.61	7270
160	143	39	1.1635	1.00	7275
135	143	39	0.9231	0.84	7280
100	143	39	0.5865	0.39	7285
120	143	39	0.7788	0.61	7290
135	143	39	0.9231	0.84	7295
140	143	39	0.9712	0.93	7300
40	143	39	0.0096	0.00	7305
50	143	39	0.1058	0.05	7310
40	143	39	0.0096	0.00	7315
195	143	39	1.5000	1.00	7320
195	143	39	1.5000	1.00	7325
200	143	39	1.5481	1.00	7330
190	143	39	1.4519	1.00	7335
100	143	39	0.5865	0.39	7340

Vsh.calculation (Clavier Eq.)					Depth
GR.	Max	Min	GR.fraction	Vsh.	(feet)
200	150	32	1.4237	1.00	7345
200	150	32	1.4237	1.00	7350
130	150	32	0.8305	0.68	7355
150	150	32	1.0000	1.00	7360
175	150	32	1.2119	1.00	7365
155	150	32	1.0424	1.00	7370
130	150	32	0.8305	0.68	7375
50	150	32	0.1525	0.07	7380
40	150	32	0.0678	0.03	7385
65	150	32	0.2797	0.14	7390
60	150	32	0.2373	0.12	7395
60	150	32	0.2373	0.12	7400
65	150	32	0.2797	0.14	7405
55	150	32	0.1949	0.09	7410
70	150	32	0.3220	0.17	7415
65	150	32	0.2797	0.14	7420
60	150	32	0.2373	0.12	7425
60	150	32	0.2373	0.12	7430
60	150	32	0.2373	0.12	7435
155	150	32	1.0424	1.00	7440
105	150	32	0.6186	0.42	7445
100	150	32	0.5763	0.38	7450
75	150	32	0.3644	0.20	7455
80	150	32	0.4068	0.23	7460
90	150	32	0.4915	0.30	7465
80	150	32	0.4068	0.23	7470
55	150	32	0.1949	0.09	7475
170	150	32	1.1695	1.00	7480
180	150	32	1.2542	1.00	7485
160	150	32	1.0847	1.00	7490
180	150	32	1.2542	1.00	7495
170	150	32	1.1695	1.00	7500
165	150	32	1.1271	1.00	7505
190	150	32	1.3390	1.00	7510
160	150	32	1.0847	1.00	7515
140	150	32	0.9153	0.82	7520
150	150	32	1.0000	1.00	7525
190	150	32	1.3390	1.00	7530
200	150	32	1.4237	1.00	7535
140	150	32	0.9153	0.82	7540
180	150	32	1.2542	1.00	7545
160	150	32	1.0847	1.00	7550
140	150	32	0.9153	0.82	7555
170	150	32	1.1695	1.00	7560
130	150	32	0.8305	0.68	7565
140	150	32	0.9153	0.82	7570
180	150	32	1.2542	1.00	7575

Table A.6 Shale volume (Vsh) calculation from **well: F** (continued)

Vsh.calculation (Clavier Eq.)					Depth
GR.	Max	Min	GR.fraction	Vsh.	(feet)
140	150	32	0.9153	0.82	7580
150	150	32	1.0000	1.00	7585
120	150	32	0.7458	0.56	7590
170	150	32	1.1695	1.00	7595
160	150	32	1.0847	1.00	7600
130	150	32	0.8305	0.68	7605
140	150	32	0.9153	0.82	7610
200	150	32	1.4237	1.00	7615
165	150	32	1.1271	1.00	7620
175	150	32	1.2119	1.00	7625
130	150	32	0.8305	0.68	7630
195	150	32	1.3814	1.00	7635
100	150	32	0.5763	0.38	7640
195	150	32	1.3814	1.00	7645
100	150	32	0.5763	0.38	7650
170	150	32	1.1695	1.00	7655
200	150	32	1.4237	1.00	7660
140	150	32	0.9153	0.82	7665
130	150	32	0.8305	0.68	7670
125	150	32	0.7881	0.62	7675
110	150	32	0.6610	0.46	7680
120	150	32	0.7458	0.56	7685
180	150	32	1.2542	1.00	7690
145	150	32	0.9576	0.90	7695
180	150	32	1.2542	1.00	7700
170	150	32	1.1695	1.00	7705
120	150	32	0.7458	0.56	7710
160	150	32	1.0847	1.00	7715
160	150	32	1.0847	1.00	7720
200	150	32	1.4237	1.00	7725
140	150	32	0.9153	0.82	7730
120	150	32	0.7458	0.56	7735
175	150	32	1.2119	1.00	7740
175	150	32	1.2119	1.00	7745
45	150	32	0.1102	0.05	7750
40	150	32	0.0678	0.03	7755
80	150	32	0.4068	0.23	7760
45	150	32	0.1102	0.05	7765
60	150	32	0.2373	0.12	7770
150	150	32	1.0000	1.00	7775
125	150	32	0.7881	0.62	7780
95	150	32	0.5339	0.34	7785
70	150	32	0.3220	0.17	7790
60	150	32	0.2373	0.12	7795
60	150	32	0.2373	0.12	7800
80	150	32	0.4068	0.23	7805
50	150	32	0.1525	0.07	7810

Vsh.calculation (Clavier Eq.)					Depth
GR.	Max	Min	GR.fraction	Vsh.	(feet)
60	150	32	0.2373	0.12	7815
45	150	32	0.1102	0.05	7820
160	150	32	1.0847	1.00	7825
155	150	32	1.0424	1.00	7830
170	150	32	1.1695	1.00	7835
120	150	32	0.7458	0.56	7840
140	150	32	0.9153	0.82	7845
70	150	32	0.3220	0.17	7850
90	150	32	0.4915	0.30	7855
180	150	32	1.2542	1.00	7860
170	164	40	1.0484	1.00	7865
177	164	40	1.1048	1.00	7870
180	164	40	1.1290	1.00	7875
110	164	40	0.5645	0.37	7880
160	164	40	0.9677	0.93	7885
170	164	40	1.0484	1.00	7890
177	164	40	1.1048	1.00	7895
150	164	40	0.8871	0.77	7900
130	164	40	0.7258	0.54	7905
160	164	40	0.9677	0.93	7910
150	164	40	0.8871	0.77	7915
140	164	40	0.8065	0.65	7920
180	164	40	1.1290	1.00	7925
200	164	40	1.2903	1.00	7930
145	164	40	0.8468	0.71	7935
180	164	40	1.1290	1.00	7940
120	164	40	0.6452	0.45	7945
177	164	40	1.1048	1.00	7950
170	164	40	1.0484	1.00	7955
170	164	40	1.0484	1.00	7960
130	164	40	0.7258	0.54	7965
180	164	40	1.1290	1.00	7970
195	164	40	1.2500	1.00	7975
140	164	40	0.8065	0.65	7980
115	164	40	0.6048	0.40	7985
120	164	40	0.6452	0.45	7990
50	164	40	0.0806	0.04	7995
70	164	40	0.2419	0.12	8000
55	164	40	0.1210	0.06	8005
50	164	40	0.0806	0.04	8010
140	164	40	0.8065	0.65	8015
195	164	40	1.2500	1.00	8020
180	164	40	1.1290	1.00	8025
115	164	40	0.6048	0.40	8030
140	164	40	0.8065	0.65	8035
137	164	40	0.7823	0.61	8040
170	164	40	1.0484	1.00	8045

Table A.6 Shale volume (Vsh) calculation from **well: F** (continued)

Vsh.calculation (Clavier Eq.)					Depth
GR.	Max	Min	GR.fraction	Vsh.	(feet)
125	164	40	0.6855	0.49	8050
165	164	40	1.0081	1.00	8055
160	164	40	0.9677	0.93	8060
155	164	40	0.9274	0.84	8065
160	164	40	0.9677	0.93	8070
180	164	40	1.1290	1.00	8075
170	164	40	1.0484	1.00	8080
160	164	40	0.9677	0.93	8085
155	164	40	0.9274	0.84	8090
165	164	40	1.0081	1.00	8095
170	164	40	1.0484	1.00	8100
180	164	40	1.1290	1.00	8105
175	164	40	1.0887	1.00	8110
105	164	40	0.5242	0.33	8115
180	164	40	1.1290	1.00	8120
180	164	40	1.1290	1.00	8125
195	164	40	1.2500	1.00	8130
155	164	40	0.9274	0.84	8135
167	164	40	1.0242	1.00	8140
105	164	40	0.5242	0.33	8145
140	164	40	0.8065	0.65	8150
165	164	40	1.0081	1.00	8155
165	164	40	1.0081	1.00	8160
180	164	40	1.1290	1.00	8165
110	164	40	0.5645	0.37	8170
180	164	40	1.1290	1.00	8175
180	164	40	1.1290	1.00	8180
120	164	40	0.6452	0.45	8185
160	164	40	0.9677	0.93	8190
180	164	40	1.1290	1.00	8195
180	164	40	1.1290	1.00	8200
180	164	40	1.1290	1.00	8205
135	164	40	0.7661	0.59	8210
140	164	40	0.8065	0.65	8215
160	164	40	0.9677	0.93	8220
140	164	40	0.8065	0.65	8225
120	164	40	0.6452	0.45	8230
160	164	40	0.9677	0.93	8235
120	164	40	0.6452	0.45	8240
90	164	40	0.4032	0.23	8245
65	164	40	0.2016	0.10	8250
80	164	40	0.3226	0.17	8255
70	164	40	0.2419	0.12	8260
70	164	40	0.2419	0.12	8265
100	164	40	0.4839	0.29	8270
135	164	40	0.7661	0.59	8275
197	164	40	1.2661	1.00	8280

Vsh.calculation (Clavier Eq.)					Depth
GR.	Max	Min	GR.fraction	Vsh.	(feet)
140	164	40	0.8065	0.65	8285
60	164	40	0.1613	0.08	8290
70	164	40	0.2419	0.12	8295
75	164	40	0.2823	0.15	8300
105	164	40	0.5242	0.33	8305
80	164	40	0.3226	0.17	8310
70	164	40	0.2419	0.12	8315
60	164	40	0.1613	0.08	8320
55	164	40	0.1210	0.06	8325
200	164	40	1.2903	1.00	8330
120	164	40	0.6452	0.45	8335
110	164	40	0.5645	0.37	8340
197	164	40	1.2661	1.00	8345
150	164	40	0.8871	0.77	8350
180	164	40	1.1290	1.00	8355
180	164	40	1.1290	1.00	8360
110	164	40	0.5645	0.37	8365
120	164	40	0.6452	0.45	8370
100	164	40	0.4839	0.29	8375
170	164	40	1.0484	1.00	8380
200	164	40	1.2903	1.00	8385
60	164	40	0.1613	0.08	8390
180	164	40	1.1290	1.00	8395
150	164	40	0.8871	0.77	8400
200	164	40	1.2903	1.00	8405
200	164	40	1.2903	1.00	8410
130	164	40	0.7258	0.54	8415
200	164	40	1.2903	1.00	8420
110	164	40	0.5645	0.37	8425
60	164	40	0.1613	0.08	8430
200	164	40	1.2903	1.00	8435
200	164	40	1.2903	1.00	8440
150	164	40	0.8871	0.77	8445
175	164	40	1.0887	1.00	8450
190	164	40	1.2097	1.00	8455
110	164	40	0.5645	0.37	8460
160	164	40	0.9677	0.93	8465
200	164	40	1.2903	1.00	8470
200	164	40	1.2903	1.00	8475
70	164	40	0.2419	0.12	8480
200	164	40	1.2903	1.00	8485
145	164	40	0.8468	0.71	8490
200	164	40	1.2903	1.00	8495
160	164	40	0.9677	0.93	8500
190	164	40	1.2097	1.00	8505
110	164	40	0.5645	0.37	8510
160	164	40	0.9677	0.93	8515

Table A.6 Shale volume (Vsh) calculation from **well: F** (continued)

Vsh.calculation (Clavier Eq.)					Depth
GR.	Max	Min	GR.fraction	Vsh.	(feet)
110	164	40	0.5645	0.37	8520
200	164	40	1.2903	1.00	8525
130	164	40	0.7258	0.54	8530
175	164	40	1.0887	1.00	8535
190	164	40	1.2097	1.00	8540
150	164	40	0.8871	0.77	8545
200	164	40	1.2903	1.00	8550
120	164	40	0.6452	0.45	8555
100	164	40	0.4839	0.29	8560
140	164	40	0.8065	0.65	8565
180	164	40	1.1290	1.00	8570
200	164	40	1.2903	1.00	8575
200	164	40	1.2903	1.00	8580
200	164	40	1.2903	1.00	8585
190	164	40	1.2097	1.00	8590
110	164	40	0.5645	0.37	8595
90	164	40	0.4032	0.23	8600

Table A.7 Shale volume (Vsh) calculation from **well: H**

Vsh.calculation (Clavier Eq.)					Depth
GR.	Max	Min	GR.fraction	Vsh.	(feet)
100	158	68	0.3556	0.19	5200
82	158	68	0.1556	0.07	5205
80	158	68	0.1333	0.06	5210
90	158	68	0.2444	0.12	5215
97	158	68	0.3222	0.17	5220
73	158	68	0.0556	0.02	5225
75	158	68	0.0778	0.03	5230
80	158	68	0.1333	0.06	5235
80	158	68	0.1333	0.06	5240
75	158	68	0.0778	0.03	5245
65	158	68	-0.0333	0.00	5250
95	158	68	0.3000	0.16	5255
48	158	68	-0.2222	0.00	5260
78	158	68	0.1111	0.05	5265
68	158	68	0.0000	0.00	5270
68	158	68	0.0000	0.00	5275
63	158	68	-0.0556	0.00	5280
75	158	68	0.0778	0.03	5285
82	158	68	0.1556	0.07	5290
117	158	68	0.5444	0.35	5295
110	158	68	0.4667	0.28	5300
121	158	68	0.5889	0.39	5305
105	158	68	0.4111	0.24	5310
120	158	68	0.5778	0.38	5315
125	158	68	0.6333	0.43	5320
90	158	68	0.2444	0.12	5325
88	158	68	0.2222	0.11	5330
75	158	68	0.0778	0.03	5335
62	158	68	-0.0667	0.00	5340
52	158	68	-0.1778	0.00	5345
60	158	68	-0.0889	0.00	5350
150	158	68	0.9111	0.81	5355
150	158	68	0.9111	0.81	5360
153	158	68	0.9444	0.88	5365
142	158	68	0.8222	0.67	5370
153	158	68	0.9444	0.88	5375
152	158	68	0.9333	0.86	5380
117	158	68	0.5444	0.35	5385
118	158	68	0.5556	0.36	5390
115	158	68	0.5222	0.33	5395
70	158	68	0.0222	0.01	5400
62	158	68	-0.0667	0.00	5405
63	158	68	-0.0556	0.00	5410
70	158	68	0.0222	0.01	5415
78	158	68	0.1111	0.05	5420
70	158	68	0.0222	0.01	5425
62	158	68	-0.0667	0.00	5430

Vsh.calculation (Clavier Eq.)					Depth
GR.	Max	Min	GR.fraction	Vsh.	(feet)
153	158	68	0.9444	0.88	5435
87	158	68	0.2111	0.10	5440
138	158	68	0.7778	0.61	5445
98	158	68	0.3333	0.18	5450
82	158	68	0.1556	0.07	5455
80	158	68	0.1333	0.06	5460
90	158	68	0.2444	0.12	5465
85	158	68	0.1889	0.09	5470
62	158	68	-0.0667	0.00	5475
115	158	68	0.5222	0.33	5480
110	158	68	0.4667	0.28	5485
97	158	68	0.3222	0.17	5490
130	158	68	0.6889	0.50	5495
122	158	68	0.6000	0.40	5500
143	158	68	0.8333	0.69	5505
137	158	68	0.7667	0.59	5510
117	158	68	0.5444	0.35	5515
121	158	68	0.5889	0.39	5520
117	158	68	0.5444	0.35	5525
100	158	68	0.3556	0.19	5530
73	158	68	0.0556	0.02	5535
60	158	68	-0.0889	0.00	5540
75	158	68	0.0778	0.03	5545
62	158	68	-0.0667	0.00	5550
62	158	68	-0.0667	0.00	5555
67	158	68	-0.0111	0.00	5560
138	158	68	0.7778	0.61	5565
95	158	68	0.3000	0.16	5570
110	158	68	0.4667	0.28	5575
133	158	68	0.7222	0.53	5580
82	158	68	0.1556	0.07	5585
150	158	68	0.9111	0.81	5590
73	158	68	0.0556	0.02	5595
160	158	68	1.0222	1.00	5600
80	158	68	0.1333	0.06	5605
70	158	68	0.0222	0.01	5610
83	158	68	0.1667	0.08	5615
80	158	68	0.1333	0.06	5620
55	158	68	-0.1444	0.00	5625
63	158	68	-0.0556	0.00	5630
82	158	68	0.1556	0.07	5635
168	158	68	1.1111	1.00	5640
163	158	68	1.0556	1.00	5645
117	158	68	0.5444	0.35	5650
175	158	68	1.1889	1.00	5655
170	158	68	1.1333	1.00	5660
180	158	68	1.2444	1.00	5665

Table A.7 Shale volume (Vsh) calculation from **well: H** (continued)

Vsh.calculation (Clavier Eq.)					Depth
GR.	Max	Min	GR.fraction	Vsh.	(feet)
170	158	68	1.1333	1.00	5670
165	158	68	1.0778	1.00	5675
102	158	68	0.3778	0.21	5680
110	158	68	0.4667	0.28	5685
130	158	68	0.6889	0.50	5690
170	158	68	1.1333	1.00	5695
200	158	68	1.4667	1.00	5700
150	158	68	0.9111	0.81	5705
140	158	68	0.8000	0.64	5710
143	158	68	0.8333	0.69	5715
178	158	68	1.2222	1.00	5720
150	158	68	0.9111	0.81	5725
147	158	68	0.8778	0.76	5730
170	158	68	1.1333	1.00	5735
153	158	68	0.9444	0.88	5740
168	158	68	1.1111	1.00	5745
170	158	68	1.1333	1.00	5750
172	158	68	1.1556	1.00	5755
150	158	68	0.9111	0.81	5760
142	158	68	0.8222	0.67	5765
160	158	68	1.0222	1.00	5770
175	158	68	1.1889	1.00	5775
197	158	68	1.4333	1.00	5780
200	158	68	1.4667	1.00	5785
168	158	68	1.1111	1.00	5790
160	158	68	1.0222	1.00	5795
128	158	68	0.6667	0.47	5800
105	158	68	0.4111	0.24	5805
177	158	68	1.2111	1.00	5810
190	158	68	1.3556	1.00	5815
153	158	68	0.9444	0.88	5820
173	158	68	1.1667	1.00	5825
98	158	68	0.3333	0.18	5830
157	158	68	0.9889	0.97	5835
180	158	68	1.2444	1.00	5840
123	158	68	0.6111	0.41	5845
175	158	68	1.1889	1.00	5850
197	158	68	1.4333	1.00	5855
155	158	68	0.9667	0.92	5860
87	158	68	0.2111	0.10	5865
155	158	68	0.9667	0.92	5870
140	158	68	0.8000	0.64	5875
182	158	68	1.2667	1.00	5880
170	158	68	1.1333	1.00	5885
143	158	68	0.8333	0.69	5890
168	158	68	1.1111	1.00	5895
143	158	68	0.8333	0.69	5900

Vsh.calculation (Clavier Eq.)					Depth
GR.	Max	Min	GR.fraction	Vsh.	(feet)
190	158	68	1.3556	1.00	5905
177	158	68	1.2111	1.00	5910
200	158	68	1.4667	1.00	5915
140	158	68	0.8000	0.64	5920
168	158	68	1.1111	1.00	5925
110	158	68	0.4667	0.28	5930
118	158	68	0.5556	0.36	5935
127	158	68	0.6556	0.46	5940
63	158	68	-0.0556	0.00	5945
50	158	68	-0.2000	0.00	5950
170	158	68	1.1333	1.00	5955
168	158	68	1.1111	1.00	5960
160	158	68	1.0222	1.00	5965
158	158	68	1.0000	1.00	5970
130	158	68	0.6889	0.50	5975
120	158	68	0.5778	0.38	5980
55	158	68	-0.1444	0.00	5985
55	158	68	-0.1444	0.00	5990
65	158	68	-0.0333	0.00	5995
68	158	68	0.0000	0.00	6000
62	158	68	-0.0667	0.00	6005
62	158	68	-0.0667	0.00	6010
90	158	68	0.2444	0.12	6015
143	158	68	0.8333	0.69	6020
118	158	68	0.5556	0.36	6025
145	158	68	0.8556	0.72	6030
180	158	68	1.2444	1.00	6035
122	158	68	0.6000	0.40	6040
125	158	68	0.6333	0.43	6045
155	158	68	0.9667	0.92	6050
200	158	68	1.4667	1.00	6055
80	158	68	0.1333	0.06	6060
70	158	68	0.0222	0.01	6065
62	158	68	-0.0667	0.00	6070
67	158	68	-0.0111	0.00	6075
70	158	68	0.0222	0.01	6080
65	158	68	-0.0333	0.00	6085
90	158	68	0.2444	0.12	6090
75	158	68	0.0778	0.03	6095
90	158	68	0.2444	0.12	6100
138	158	68	0.7778	0.61	6105
140	158	68	0.8000	0.64	6110
132	158	68	0.7111	0.52	6115
132	158	68	0.7111	0.52	6120
131	158	68	0.7000	0.51	6125
145	158	68	0.8556	0.72	6130
142	158	68	0.8222	0.67	6135

Table A.7 Shale volume (Vsh) calculation from **well: H** (continued)

Vsh.calculation (Clavier Eq.)					Depth
GR.	Max	Min	GR.fraction	Vsh.	(feet)
138	158	68	0.7778	0.61	6140
125	158	68	0.6333	0.43	6145
120	158	68	0.5778	0.38	6150
153	158	68	0.9444	0.88	6155
160	158	68	1.0222	1.00	6160
175	158	68	1.1889	1.00	6165
120	158	68	0.5778	0.38	6170
170	162	65	1.0825	1.00	6175
175	162	65	1.1340	1.00	6180
125	162	65	0.6186	0.42	6185
150	162	65	0.8763	0.75	6190
187	162	65	1.2577	1.00	6195
160	162	65	0.9794	0.95	6200
160	162	65	0.9794	0.95	6205
165	162	65	1.0309	1.00	6210
168	162	65	1.0619	1.00	6215
133	162	65	0.7010	0.51	6220
158	162	65	0.9588	0.91	6225
190	162	65	1.2887	1.00	6230
160	162	65	0.9794	0.95	6235
190	162	65	1.2887	1.00	6240
170	162	65	1.0825	1.00	6245
167	162	65	1.0515	1.00	6250
190	162	65	1.2887	1.00	6255
140	162	65	0.7732	0.60	6260
200	162	65	1.3918	1.00	6265
158	162	65	0.9588	0.91	6270
155	162	65	0.9278	0.85	6275
142	162	65	0.7938	0.63	6280
123	162	65	0.5979	0.40	6285
120	162	65	0.5670	0.37	6290
100	162	65	0.3608	0.20	6295
197	162	65	1.3608	1.00	6300
160	162	65	0.9794	0.95	6305
158	162	65	0.9588	0.91	6310
158	162	65	0.9588	0.91	6315
195	162	65	1.3402	1.00	6320
170	162	65	1.0825	1.00	6325
153	162	65	0.9072	0.81	6330
107	162	65	0.4330	0.25	6335
173	162	65	1.1134	1.00	6340
190	162	65	1.2887	1.00	6345
165	162	65	1.0309	1.00	6350
100	162	65	0.3608	0.20	6355
160	162	65	0.9794	0.95	6360
168	162	65	1.0619	1.00	6365
150	162	65	0.8763	0.75	6370

Vsh.calculation (Clavier Eq.)					Depth
GR.	Max	Min	GR.fraction	Vsh.	(feet)
190	162	65	1.2887	1.00	6375
190	162	65	1.2887	1.00	6380
160	162	65	0.9794	0.95	6385
168	162	65	1.0619	1.00	6390
155	162	65	0.9278	0.85	6395
150	162	65	0.8763	0.75	6400
50	162	65	-0.1546	0.00	6405
100	162	65	0.3608	0.20	6410
45	162	65	-0.2062	0.00	6415
47	162	65	-0.1856	0.00	6420
167	162	65	1.0515	1.00	6425
140	162	65	0.7732	0.60	6430
190	162	65	1.2887	1.00	6435
147	162	65	0.8454	0.70	6440
142	162	65	0.7938	0.63	6445
140	162	65	0.7732	0.60	6450
150	162	65	0.8763	0.75	6455
200	162	65	1.3918	1.00	6460
115	162	65	0.5155	0.32	6465
160	162	65	0.9794	0.95	6470
175	162	65	1.1340	1.00	6475
190	162	65	1.2887	1.00	6480
192	162	65	1.3093	1.00	6485
120	162	65	0.5670	0.37	6490
57	162	65	-0.0825	0.00	6495
75	162	65	0.1031	0.05	6500
140	162	65	0.7732	0.60	6505
160	162	65	0.9794	0.95	6510
160	162	65	0.9794	0.95	6515
138	162	65	0.7526	0.57	6520
140	162	65	0.7732	0.60	6525
190	162	65	1.2887	1.00	6530
150	162	65	0.8763	0.75	6535
140	162	65	0.7732	0.60	6540
200	162	65	1.3918	1.00	6545
115	162	65	0.5155	0.32	6550
190	162	65	1.2887	1.00	6555
165	162	65	1.0309	1.00	6560
140	162	65	0.7732	0.60	6565
75	162	65	0.1031	0.05	6570
78	162	65	0.1340	0.06	6575
90	162	65	0.2577	0.13	6580
70	162	65	0.0515	0.02	6585
60	162	65	-0.0515	0.00	6590
85	162	65	0.2062	0.10	6595
58	162	65	-0.0722	0.00	6600
200	162	65	1.3918	1.00	6605

Table A.7 Shale volume (Vsh) calculation from **well: H** (continued)

Vsh.calculation (Clavier Eq.)					Depth
GR.	Max	Min	GR.fraction	Vsh.	(feet)
180	162	65	1.1856	1.00	6610
140	162	65	0.7732	0.60	6615
195	162	65	1.3402	1.00	6620
170	162	65	1.0825	1.00	6625
190	162	65	1.2887	1.00	6630
190	162	65	1.2887	1.00	6635
120	162	65	0.5670	0.37	6640
92	162	65	0.2784	0.14	6645
113	162	65	0.4948	0.30	6650
63	162	65	-0.0206	0.00	6655
73	162	65	0.0825	0.04	6660
68	162	65	0.0309	0.01	6665
70	162	65	0.0515	0.02	6670
67	162	65	0.0206	0.01	6675
110	162	65	0.4639	0.28	6680
108	162	65	0.4433	0.26	6685
65	162	65	0.0000	0.00	6690
78	162	65	0.1340	0.06	6695
72	162	65	0.0722	0.03	6700
72	162	65	0.0722	0.03	6705
68	162	65	0.0309	0.01	6710
62	162	65	-0.0309	0.00	6715
150	162	65	0.8763	0.75	6720
123	162	65	0.5979	0.40	6725
63	162	65	-0.0206	0.00	6730
65	162	65	0.0000	0.00	6735
178	162	65	1.1649	1.00	6740
175	162	65	1.1340	1.00	6745
130	162	65	0.6701	0.47	6750
122	162	65	0.5876	0.39	6755
78	162	65	0.1340	0.06	6760
83	162	65	0.1856	0.09	6765
188	162	65	1.2680	1.00	6770
170	182	63	0.8992	0.79	6775
130	182	63	0.5630	0.36	6780
178	182	63	0.9664	0.92	6785
180	182	63	0.9832	0.96	6790
105	182	63	0.3529	0.19	6795
187	182	63	1.0420	1.00	6800
200	182	63	1.1513	1.00	6805
190	182	63	1.0672	1.00	6810
150	182	63	0.7311	0.55	6815
117	182	63	0.4538	0.27	6820
200	182	63	1.1513	1.00	6825
200	182	63	1.1513	1.00	6830
127	182	63	0.5378	0.34	6835
200	182	63	1.1513	1.00	6840

Vsh.calculation (Clavier Eq.)					Depth
GR.	Max	Min	GR.fraction	Vsh.	(feet)
150	182	63	0.7311	0.55	6845
185	182	63	1.0252	1.00	6850
98	182	63	0.2941	0.15	6855
155	182	63	0.7731	0.60	6860
195	182	63	1.1092	1.00	6865
146	182	63	0.6975	0.51	6870
163	182	63	0.8403	0.70	6875
155	182	63	0.7731	0.60	6880
105	182	63	0.3529	0.19	6885
65	182	63	0.0168	0.01	6890
45	182	63	-0.1513	0.00	6895
62	182	63	-0.0084	0.00	6900
62	182	63	-0.0084	0.00	6905
50	182	63	-0.1092	0.00	6910
138	182	63	0.6303	0.43	6915
140	182	63	0.6471	0.45	6920
157	182	63	0.7899	0.62	6925
130	182	63	0.5630	0.36	6930
150	182	63	0.7311	0.55	6935
60	182	63	-0.0252	0.00	6940
65	182	63	0.0168	0.01	6945
65	182	63	0.0168	0.01	6950
68	182	63	0.0420	0.02	6955
60	182	63	-0.0252	0.00	6960
60	182	63	-0.0252	0.00	6965
178	182	63	0.9664	0.92	6970
180	182	63	0.9832	0.96	6975
143	182	63	0.6723	0.48	6980
200	182	63	1.1513	1.00	6985
178	182	63	0.9664	0.92	6990
100	182	63	0.3109	0.16	6995
87	182	63	0.2017	0.10	7000
72	182	63	0.0756	0.03	7005
70	182	63	0.0588	0.03	7010
85	182	63	0.1849	0.09	7015
72	182	63	0.0756	0.03	7020
60	182	63	-0.0252	0.00	7025
58	182	63	-0.0420	0.00	7030
60	182	63	-0.0252	0.00	7035
62	182	63	-0.0084	0.00	7040
60	182	63	-0.0252	0.00	7045
87	182	63	0.2017	0.10	7050
195	182	63	1.1092	1.00	7055
175	182	63	0.9412	0.87	7060
192	182	63	1.0840	1.00	7065
190	182	63	1.0672	1.00	7070
180	182	63	0.9832	0.96	7075

Table A.7 Shale volume (Vsh) calculation from **well: H** (continued)

Vsh.calculation (Clavier Eq.)					Depth
GR.	Max	Min	GR.fraction	Vsh.	(feet)
200	182	63	1.1513	1.00	7080
160	182	63	0.8151	0.66	7085
190	182	63	1.0672	1.00	7090
120	182	63	0.4790	0.29	7095
121	182	63	0.4874	0.30	7100
173	182	63	0.9244	0.84	7105
165	182	63	0.8571	0.72	7110
117	182	63	0.4538	0.27	7115
121	182	63	0.4874	0.30	7120
117	182	63	0.4538	0.27	7125
82	182	63	0.1597	0.07	7130
65	182	63	0.0168	0.01	7135
55	182	63	-0.0672	0.00	7140
50	182	63	-0.1092	0.00	7145
60	182	63	-0.0252	0.00	7150
167	182	63	0.8739	0.75	7155
112	182	63	0.4118	0.24	7160
180	182	63	0.9832	0.96	7165
185	182	63	1.0252	1.00	7170
170	182	63	0.8992	0.79	7175
117	182	63	0.4538	0.27	7180
200	182	63	1.1513	1.00	7185
130	182	63	0.5630	0.36	7190
135	182	63	0.6050	0.41	7195
175	182	63	0.9412	0.87	7200
200	182	63	1.1513	1.00	7205
175	182	63	0.9412	0.87	7210
190	182	63	1.0672	1.00	7215
198	182	63	1.1345	1.00	7220
135	182	63	0.6050	0.41	7225
58	182	63	-0.0420	0.00	7230
50	182	63	-0.1092	0.00	7235
58	182	63	-0.0420	0.00	7240
60	182	63	-0.0252	0.00	7245
60	182	63	-0.0252	0.00	7250
55	182	63	-0.0672	0.00	7255
55	182	63	-0.0672	0.00	7260
70	182	63	0.0588	0.03	7265
63	182	63	0.0000	0.00	7270
200	182	63	1.1513	1.00	7275
200	182	63	1.1513	1.00	7280
165	182	63	0.8571	0.72	7285
190	182	63	1.0672	1.00	7290
173	182	63	0.9244	0.84	7295
182	182	63	1.0000	1.00	7300
200	182	63	1.1513	1.00	7305
130	182	63	0.5630	0.36	7310

Vsh.calculation (Clavier Eq.)					Depth
GR.	Max	Min	GR.fraction	Vsh.	(feet)
172	182	63	0.9160	0.82	7315
160	182	63	0.8151	0.66	7320
198	182	63	1.1345	1.00	7325
135	182	63	0.6050	0.41	7330
200	182	63	1.1513	1.00	7335
160	182	63	0.8151	0.66	7340
142	182	63	0.6639	0.47	7345
130	182	63	0.5630	0.36	7350
200	182	63	1.1513	1.00	7355
192	182	63	1.0840	1.00	7360
170	182	63	0.8992	0.79	7365
170	182	63	0.8992	0.79	7370
180	182	63	0.9832	0.96	7375
168	182	63	0.8824	0.76	7380
170	182	63	0.8992	0.79	7385
165	182	63	0.8571	0.72	7390
150	182	63	0.7311	0.55	7395
110	182	63	0.3950	0.22	7400
57	182	63	-0.0504	0.00	7405
70	182	63	0.0588	0.03	7410
52	182	63	-0.0924	0.00	7415
50	182	63	-0.1092	0.00	7420
42	182	63	-0.1765	0.00	7425
50	182	63	-0.1092	0.00	7430
160	182	63	0.8151	0.66	7435
187	182	63	1.0420	1.00	7440
200	182	63	1.1513	1.00	7445
200	200	60	1.0000	1.00	7450
195	200	60	0.9643	0.92	7455
160	200	60	0.7143	0.53	7460
178	200	60	0.8429	0.70	7465
180	200	60	0.8571	0.72	7470
170	200	60	0.7857	0.62	7475
122	200	60	0.4429	0.26	7480
182	200	60	0.8714	0.75	7485
190	200	60	0.9286	0.85	7490
170	200	60	0.7857	0.62	7495
200	200	60	1.0000	1.00	7500
183	200	60	0.8786	0.76	7505
187	200	60	0.9071	0.81	7510
200	200	60	1.0000	1.00	7515
180	200	60	0.8571	0.72	7520
90	200	60	0.2143	0.10	7525
60	200	60	0.0000	0.00	7530
163	200	60	0.7357	0.55	7535
160	200	60	0.7143	0.53	7540
170	200	60	0.7857	0.62	7545

Table A.7 Shale volume (Vsh) calculation from **well: H** (continued)

Vsh.calculation (Clavier Eq.)					Depth
GR.	Max	Min	GR.fraction	Vsh.	(feet)
190	200	60	0.9286	0.85	7550
160	200	60	0.7143	0.53	7555
192	200	60	0.9429	0.87	7560
200	200	60	1.0000	1.00	7565
158	200	60	0.7000	0.51	7570
180	200	60	0.8571	0.72	7575
200	200	60	1.0000	1.00	7580
190	200	60	0.9286	0.85	7585
187	200	60	0.9071	0.81	7590
130	200	60	0.5000	0.31	7595
177	200	60	0.8357	0.69	7600
162	200	60	0.7286	0.54	7605
48	200	60	-0.0857	0.00	7610
40	200	60	-0.1429	0.00	7615
42	200	60	-0.1286	0.00	7620
50	200	60	-0.0714	0.00	7625
53	200	60	-0.0500	0.00	7630
62	200	60	0.0143	0.01	7635
130	200	60	0.5000	0.31	7640
190	200	60	0.9286	0.85	7645
200	200	60	1.0000	1.00	7650
143	200	60	0.5929	0.39	7655
190	200	60	0.9286	0.85	7660
170	200	60	0.7857	0.62	7665
180	200	60	0.8571	0.72	7670
195	200	60	0.9643	0.92	7675
200	200	60	1.0000	1.00	7680
178	200	60	0.8429	0.70	7685
90	200	60	0.2143	0.10	7690
147	200	60	0.6214	0.42	7695
200	200	60	1.0000	1.00	7700
140	200	60	0.5714	0.37	7705
200	200	60	1.0000	1.00	7710
200	200	60	1.0000	1.00	7715
200	200	60	1.0000	1.00	7720
190	200	60	0.9286	0.85	7725
200	200	60	1.0000	1.00	7730
187	200	60	0.9071	0.81	7735
200	200	60	1.0000	1.00	7740
130	200	60	0.5000	0.31	7745
168	200	60	0.7714	0.60	7750
170	200	60	0.7857	0.62	7755
180	200	60	0.8571	0.72	7760
200	200	60	1.0000	1.00	7765
110	200	60	0.3571	0.20	7770
163	200	60	0.7357	0.55	7775
150	200	60	0.6429	0.44	7780

Vsh.calculation (Clavier Eq.)					Depth
GR.	Max	Min	GR.fraction	Vsh.	(feet)
90	200	60	0.2143	0.10	7785
83	200	60	0.1643	0.08	7790
197	200	60	0.9786	0.95	7795
170	200	60	0.7857	0.62	7800
183	200	60	0.8786	0.76	7805
173	200	60	0.8071	0.65	7810
190	200	60	0.9286	0.85	7815
190	200	60	0.9286	0.85	7820
185	200	60	0.8929	0.78	7825
162	200	60	0.7286	0.54	7830
200	200	60	1.0000	1.00	7835
185	200	60	0.8929	0.78	7840
198	200	60	0.9857	0.97	7845
120	200	60	0.4286	0.25	7850
43	200	60	-0.1214	0.00	7855
52	200	60	-0.0571	0.00	7860
60	200	60	0.0000	0.00	7865
70	200	60	0.0714	0.03	7870
78	200	60	0.1286	0.06	7875
175	200	60	0.8214	0.67	7880
193	200	60	0.9500	0.89	7885
160	200	60	0.7143	0.53	7890
85	200	60	0.1786	0.09	7895
165	200	60	0.7500	0.57	7900
140	200	60	0.5714	0.37	7905
190	200	60	0.9286	0.85	7910
50	200	60	-0.0714	0.00	7915
68	200	60	0.0571	0.02	7920
60	200	60	0.0000	0.00	7925
53	200	60	-0.0500	0.00	7930
197	200	60	0.9786	0.95	7935
192	200	60	0.9429	0.87	7940
180	200	60	0.8571	0.72	7945
150	200	60	0.6429	0.44	7950
180	200	60	0.8571	0.72	7955
180	200	60	0.8571	0.72	7960
140	200	60	0.5714	0.37	7965
180	200	60	0.8571	0.72	7970
170	200	60	0.7857	0.62	7975
180	200	60	0.8571	0.72	7980
163	200	60	0.7357	0.55	7985
190	200	60	0.9286	0.85	7990
153	200	60	0.6643	0.47	7995
200	200	60	1.0000	1.00	8000
190	200	60	0.9286	0.85	8005
150	200	60	0.6429	0.44	8010
194	200	60	0.9571	0.90	8015

Table A.7 Shale volume (Vsh) calculation from **well: H** (continued)

Vsh.calculation (Clavier Eq.)					Depth
GR.	Max	Min	GR.fraction	Vsh.	(feet)
158	200	60	0.7000	0.51	8020
180	200	60	0.8571	0.72	8025
200	200	60	1.0000	1.00	8030
200	200	60	1.0000	1.00	8035
190	200	60	0.9286	0.85	8040
90	200	60	0.2143	0.10	8045
160	200	60	0.7143	0.53	8050
165	200	60	0.7500	0.57	8055
180	200	60	0.8571	0.72	8060
187	200	60	0.9071	0.81	8065
170	200	60	0.7857	0.62	8070
130	200	60	0.5000	0.31	8075
190	200	60	0.9286	0.85	8080
198	200	60	0.9857	0.97	8085
140	200	60	0.5714	0.37	8090
140	200	60	0.5714	0.37	8095
95	200	60	0.2500	0.13	8100
58	200	60	-0.0143	0.00	8105
60	200	60	0.0000	0.00	8110
193	200	60	0.9500	0.89	8115
140	200	60	0.5714	0.37	8120
155	200	60	0.6786	0.48	8125
200	200	60	1.0000	1.00	8130
190	200	60	0.9286	0.85	8135
160	200	60	0.7143	0.53	8140
178	200	60	0.8429	0.70	8145
198	200	60	0.9857	0.97	8150
195	200	60	0.9643	0.92	8155
130	200	60	0.5000	0.31	8160
197	200	60	0.9786	0.95	8165
160	200	60	0.7143	0.53	8170
100	200	60	0.2857	0.15	8175
132	200	60	0.5143	0.32	8180
150	200	60	0.6429	0.44	8185
137	200	60	0.5500	0.35	8190
197	200	60	0.9786	0.95	8195
180	200	60	0.8571	0.72	8200
170	200	60	0.7857	0.62	8205
135	200	60	0.5357	0.34	8210
200	200	60	1.0000	1.00	8215
135	200	60	0.5357	0.34	8220
200	200	60	1.0000	1.00	8225
180	200	60	0.8571	0.72	8230
115	200	60	0.3929	0.22	8235
200	200	60	1.0000	1.00	8240
158	200	60	0.7000	0.51	8245
185	200	60	0.8929	0.78	8250

Vsh.calculation (Clavier Eq.)					Depth
GR.	Max	Min	GR.fraction	Vsh.	(feet)
180	200	60	0.8571	0.72	8255
155	200	60	0.6786	0.48	8260
200	200	60	1.0000	1.00	8265
180	200	60	0.8571	0.72	8270
198	200	60	0.9857	0.97	8275
120	200	60	0.4286	0.25	8280
132	200	60	0.5143	0.32	8285
110	200	60	0.3571	0.20	8290
70	200	60	0.0714	0.03	8295
70	200	60	0.0714	0.03	8300
68	200	60	0.0571	0.02	8305
58	200	60	-0.0143	0.00	8310
183	200	60	0.8786	0.76	8315
187	200	60	0.9071	0.81	8320
178	200	60	0.8429	0.70	8325
150	200	60	0.6429	0.44	8330
150	200	60	0.6429	0.44	8335
160	200	60	0.7143	0.53	8340
193	200	60	0.9500	0.89	8345
200	200	60	1.0000	1.00	8350
170	200	60	0.7857	0.62	8355
195	200	60	0.9643	0.92	8360
100	200	60	0.2857	0.15	8365
67	200	60	0.0500	0.02	8370
70	200	60	0.0714	0.03	8375
200	200	60	1.0000	1.00	8380
158	200	60	0.7000	0.51	8385
197	200	60	0.9786	0.95	8390
145	200	60	0.6071	0.41	8395
62	200	60	0.0143	0.01	8400
70	200	60	0.0714	0.03	8405
75	200	60	0.1071	0.05	8410
90	200	60	0.2143	0.10	8415
80	200	60	0.1429	0.07	8420
70	200	60	0.0714	0.03	8425
45	200	60	-0.1071	0.00	8430
182	200	60	0.8714	0.75	8435
158	200	60	0.7000	0.51	8440
160	200	60	0.7143	0.53	8445
182	200	60	0.8714	0.75	8450
123	200	60	0.4500	0.27	8455
200	200	60	1.0000	1.00	8460
195	200	60	0.9643	0.92	8465
200	200	60	1.0000	1.00	8470
200	200	60	1.0000	1.00	8475
155	200	60	0.6786	0.48	8480
155	200	60	0.6786	0.48	8485

Table A.8 Shale volume (Vsh) calculation from **well: I**

Vsh.calculation (Clavier Eq.)					Depth
GR.	Max	Min	GR.fraction	Vsh.	(feet)
45	158	48	-0.0273	0.00	4800
50	158	48	0.018	0.01	4805
58	158	48	0.091	0.04	4810
58	158	48	0.091	0.04	4815
75	158	48	0.245	0.12	4820
79	158	48	0.282	0.15	4825
85	158	48	0.336	0.18	4830
90	158	48	0.382	0.21	4835
100	158	48	0.473	0.28	4840
90	158	48	0.382	0.21	4845
60	158	48	0.109	0.05	4850
53	158	48	0.045	0.02	4855
70	158	48	0.200	0.10	4860
60	158	48	0.109	0.05	4865
79	158	48	0.282	0.15	4870
62	158	48	0.127	0.06	4875
70	158	48	0.200	0.10	4880
62	158	48	0.127	0.06	4885
70	158	48	0.200	0.10	4890
158	158	48	1.000	1.00	4895
175	158	48	1.155	1.00	4900
170	158	48	1.109	1.00	4905
185	158	48	1.245	1.00	4910
150	158	48	0.927	0.84	4915
162	158	48	1.036	1.00	4920
152	158	48	0.945	0.88	4925
120	158	48	0.655	0.46	4930
90	158	48	0.382	0.21	4935
65	158	48	0.155	0.07	4940
60	158	48	0.109	0.05	4945
77	158	48	0.264	0.13	4950
112	158	48	0.582	0.38	4955
108	158	48	0.545	0.35	4960
90	158	48	0.382	0.21	4965
150	158	48	0.927	0.84	4970
143	158	48	0.864	0.73	4975
113	158	48	0.591	0.39	4980
130	158	48	0.745	0.56	4985
120	158	48	0.655	0.46	4990
170	158	48	1.109	1.00	4995
150	158	48	0.927	0.84	5000
152	158	48	0.945	0.88	5005
110	158	48	0.564	0.36	5010
62	158	48	0.127	0.06	5015
85	158	48	0.336	0.18	5020
87	158	48	0.355	0.19	5025
75	158	48	0.245	0.12	5030

Vsh.calculation (Clavier Eq.)					Depth
GR.	Max	Min	GR.fraction	Vsh.	(feet)
83	158	48	0.318	0.17	5035
80	158	48	0.291	0.15	5040
70	158	48	0.200	0.10	5045
120	158	48	0.655	0.46	5050
200	158	48	1.382	1.00	5055
160	158	48	1.018	1.00	5060
170	158	48	1.109	1.00	5065
158	158	48	1.000	1.00	5070
140	158	48	0.836	0.69	5075
127	158	48	0.718	0.53	5080
150	158	48	0.927	0.84	5085
98	158	48	0.455	0.27	5090
90	158	48	0.382	0.21	5095
87	158	48	0.355	0.19	5100
60	158	48	0.109	0.05	5105
70	158	48	0.200	0.10	5110
60	158	48	0.109	0.05	5115
62	158	48	0.127	0.06	5120
53	158	48	0.045	0.02	5125
68	158	48	0.182	0.09	5130
65	158	48	0.155	0.07	5135
132	158	48	0.764	0.59	5140
145	158	48	0.882	0.76	5145
167	158	48	1.082	1.00	5150
160	158	48	1.018	1.00	5155
152	158	48	0.945	0.88	5160
180	158	48	1.200	1.00	5165
182	158	48	1.218	1.00	5170
185	158	48	1.245	1.00	5175
137	158	48	0.809	0.65	5180
175	158	48	1.155	1.00	5185
143	158	48	0.864	0.73	5190
140	158	48	0.836	0.69	5195
115	158	48	0.609	0.41	5200
65	158	48	0.155	0.07	5205
58	158	48	0.091	0.04	5210
70	158	48	0.200	0.10	5215
100	158	48	0.473	0.28	5220
102	158	48	0.491	0.30	5225
95	158	48	0.427	0.25	5230
90	158	48	0.382	0.21	5235
143	158	48	0.864	0.73	5240
110	158	48	0.564	0.36	5245
173	158	48	1.136	1.00	5250
130	158	48	0.745	0.56	5255
120	158	48	0.655	0.46	5260
70	158	48	0.200	0.10	5265

Table A.8 Shale volume (Vsh) calculation from **well: I** (continued)

Vsh.calculation (Clavier Eq.)					Depth
GR.	Max	Min	GR.fraction	Vsh.	(feet)
98	158	48	0.455	0.27	5270
170	158	48	1.109	1.00	5275
133	158	48	0.773	0.60	5280
170	158	48	1.109	1.00	5285
97	158	48	0.445	0.26	5290
80	158	48	0.291	0.15	5295
73	158	48	0.227	0.11	5300
85	158	48	0.336	0.18	5305
77	158	48	0.264	0.13	5310
70	158	48	0.200	0.10	5315
78	158	48	0.273	0.14	5320
60	158	48	0.109	0.05	5325
173	158	48	1.136	1.00	5330
197	158	48	1.355	1.00	5335
155	158	48	0.973	0.94	5340
183	158	48	1.227	1.00	5345
170	158	48	1.109	1.00	5350
153	158	48	0.955	0.90	5355
145	158	48	0.882	0.76	5360
143	158	48	0.864	0.73	5365
200	158	48	1.382	1.00	5370
148	158	48	0.909	0.81	5375
158	158	48	1.000	1.00	5380
115	158	48	0.609	0.41	5385
123	158	48	0.682	0.49	5390
57	158	48	0.082	0.04	5395
70	158	48	0.200	0.10	5400
55	158	48	0.064	0.03	5405
70	158	48	0.200	0.10	5410
65	158	48	0.155	0.07	5415
78	158	48	0.273	0.14	5420
60	158	48	0.109	0.05	5425
80	158	48	0.291	0.15	5430
160	158	48	1.018	1.00	5435
142	158	48	0.855	0.72	5440
110	158	48	0.564	0.36	5445
120	158	48	0.655	0.46	5450
140	158	48	0.836	0.69	5455
65	158	48	0.155	0.07	5460
58	158	48	0.091	0.04	5465
62	158	48	0.127	0.06	5470
70	158	48	0.200	0.10	5475
80	158	48	0.291	0.15	5480
63	158	48	0.136	0.06	5485
80	158	48	0.291	0.15	5490
72	158	48	0.218	0.11	5495
80	158	48	0.291	0.15	5500

Vsh.calculation (Clavier Eq.)					Depth
GR.	Max	Min	GR.fraction	Vsh.	(feet)
75	158	48	0.245	0.12	5505
73	158	48	0.227	0.11	5510
147	158	48	0.900	0.79	5515
137	158	48	0.809	0.65	5520
197	165	44	1.264	1.00	5525
130	165	44	0.711	0.52	5530
173	165	44	1.066	1.00	5535
160	165	44	0.959	0.91	5540
160	165	44	0.959	0.91	5545
158	165	44	0.942	0.87	5550
170	165	44	1.041	1.00	5555
105	165	44	0.504	0.31	5560
200	165	44	1.289	1.00	5565
150	165	44	0.876	0.75	5570
170	165	44	1.041	1.00	5575
197	165	44	1.264	1.00	5580
187	165	44	1.182	1.00	5585
127	165	44	0.686	0.49	5590
140	165	44	0.793	0.63	5595
160	165	44	0.959	0.91	5600
200	165	44	1.289	1.00	5605
198	165	44	1.273	1.00	5610
130	165	44	0.711	0.52	5615
143	165	44	0.818	0.66	5620
158	165	44	0.942	0.87	5625
143	165	44	0.818	0.66	5630
194	165	44	1.240	1.00	5635
162	165	44	0.975	0.94	5640
147	165	44	0.851	0.71	5645
163	165	44	0.983	0.96	5650
170	165	44	1.041	1.00	5655
123	165	44	0.653	0.46	5660
147	165	44	0.851	0.71	5665
180	165	44	1.124	1.00	5670
170	165	44	1.041	1.00	5675
165	165	44	1.000	1.00	5680
163	165	44	0.983	0.96	5685
200	165	44	1.289	1.00	5690
173	165	44	1.066	1.00	5695
170	165	44	1.041	1.00	5700
118	165	44	0.612	0.41	5705
150	165	44	0.876	0.75	5710
120	165	44	0.628	0.43	5715
185	165	44	1.165	1.00	5720
162	165	44	0.975	0.94	5725
90	165	44	0.380	0.21	5730
70	165	44	0.215	0.11	5735

Table A.8 Shale volume (Vsh) calculation from **well: I** (continued)

Vsh.calculation (Clavier Eq.)					Depth
GR.	Max	Min	GR.fraction	Vsh.	(feet)
53	165	44	0.074	0.03	5740
57	165	44	0.107	0.05	5745
63	165	44	0.157	0.07	5750
65	165	44	0.174	0.08	5755
60	165	44	0.132	0.06	5760
63	165	44	0.157	0.07	5765
160	165	44	0.959	0.91	5770
198	165	44	1.273	1.00	5775
178	165	44	1.107	1.00	5780
138	165	44	0.777	0.61	5785
110	165	44	0.545	0.35	5790
178	165	44	1.107	1.00	5795
135	165	44	0.752	0.57	5800
172	165	44	1.058	1.00	5805
180	165	44	1.124	1.00	5810
137	165	44	0.769	0.59	5815
112	165	44	0.562	0.36	5820
155	165	44	0.917	0.83	5825
150	165	44	0.876	0.75	5830
98	165	44	0.446	0.26	5835
80	165	44	0.298	0.16	5840
70	165	44	0.215	0.11	5845
187	165	44	1.182	1.00	5850
150	165	44	0.876	0.75	5855
118	165	44	0.612	0.41	5860
177	165	44	1.099	1.00	5865
142	165	44	0.810	0.65	5870
175	165	44	1.083	1.00	5875
143	165	44	0.818	0.66	5880
142	165	44	0.810	0.65	5885
155	165	44	0.917	0.83	5890
110	165	44	0.545	0.35	5895
108	165	44	0.529	0.33	5900
112	165	44	0.562	0.36	5905
120	165	44	0.628	0.43	5910
105	165	44	0.504	0.31	5915
90	165	44	0.380	0.21	5920
70	165	44	0.215	0.11	5925
60	165	44	0.132	0.06	5930
190	165	44	1.207	1.00	5935
180	165	44	1.124	1.00	5940
148	165	44	0.860	0.73	5945
160	165	44	0.959	0.91	5950
170	165	44	1.041	1.00	5955
105	165	44	0.504	0.31	5960
127	165	44	0.686	0.49	5965
197	165	44	1.264	1.00	5970

Vsh.calculation (Clavier Eq.)					Depth
GR.	Max	Min	GR.fraction	Vsh.	(feet)
78	165	44	0.281	0.15	5975
60	165	44	0.132	0.06	5980
67	165	44	0.190	0.09	5985
60	165	44	0.132	0.06	5990
59	165	44	0.124	0.06	5995
165	165	44	1.000	1.00	6000
102	165	44	0.479	0.29	6005
122	165	44	0.645	0.45	6010
110	165	44	0.545	0.35	6015
140	165	44	0.793	0.63	6020
173	165	44	1.066	1.00	6025
162	165	44	0.975	0.94	6030
160	165	44	0.959	0.91	6035
140	165	44	0.793	0.63	6040
165	165	44	1.000	1.00	6045
160	165	44	0.959	0.91	6050
200	165	44	1.289	1.00	6055
158	165	44	0.942	0.87	6060
200	165	44	1.289	1.00	6065
175	165	44	1.083	1.00	6070
110	165	44	0.545	0.35	6075
170	165	44	1.041	1.00	6080
107	165	44	0.521	0.33	6085
155	165	44	0.917	0.83	6090
198	165	44	1.273	1.00	6095
160	165	44	0.959	0.91	6100
150	165	44	0.876	0.75	6105
192	165	44	1.223	1.00	6110
97	165	44	0.438	0.26	6115
157	165	44	0.934	0.86	6120
130	165	44	0.711	0.52	6125
127	165	44	0.686	0.49	6130
130	165	44	0.711	0.52	6135
195	165	44	1.248	1.00	6140
165	165	44	1.000	1.00	6145
168	165	44	1.025	1.00	6150
170	165	44	1.041	1.00	6155
80	165	44	0.298	0.16	6160
118	165	44	0.612	0.41	6165
65	165	44	0.174	0.08	6170
50	165	44	0.050	0.02	6175
60	165	44	0.132	0.06	6180
78	165	44	0.281	0.15	6185
100	165	44	0.463	0.28	6190
147	165	44	0.851	0.71	6195
145	165	44	0.835	0.69	6200
200	165	44	1.289	1.00	6205

Table A.8 Shale volume (Vsh) calculation from **well: I** (continued)

Vsh.calculation (Clavier Eq.)					Depth
GR.	Max	Min	GR.fraction	Vsh.	(feet)
140	165	44	0.793	0.63	6210
170	165	44	1.041	1.00	6215
150	165	44	0.876	0.75	6220
165	165	44	1.000	1.00	6225
170	165	44	1.041	1.00	6230
122	165	44	0.645	0.45	6235
145	165	44	0.835	0.69	6240
67	165	44	0.190	0.09	6245
60	165	44	0.132	0.06	6250
55	165	44	0.091	0.04	6255
60	165	44	0.132	0.06	6260
165	165	44	1.000	1.00	6265
128	165	44	0.694	0.50	6270
165	165	44	1.000	1.00	6275
200	165	44	1.289	1.00	6280
133	165	44	0.736	0.55	6285
150	165	44	0.876	0.75	6290
185	165	44	1.165	1.00	6295
162	165	44	0.975	0.94	6300
153	165	44	0.901	0.80	6305
108	165	44	0.529	0.33	6310
120	165	44	0.628	0.43	6315
160	165	44	0.959	0.91	6320
142	165	44	0.810	0.65	6325
160	165	44	0.959	0.91	6330
145	165	44	0.835	0.69	6335
140	165	44	0.793	0.63	6340
138	165	44	0.777	0.61	6345
140	165	44	0.793	0.63	6350
108	165	44	0.529	0.33	6355
50	165	44	0.050	0.02	6360
63	165	44	0.157	0.07	6365
132	165	44	0.727	0.54	6370
140	165	44	0.793	0.63	6375
100	165	44	0.463	0.28	6380
123	165	44	0.653	0.46	6385
60	165	44	0.132	0.06	6390
58	165	44	0.116	0.05	6395
68	165	44	0.198	0.10	6400
60	165	44	0.132	0.06	6405
62	165	44	0.149	0.07	6410
62	165	44	0.149	0.07	6415
63	165	44	0.157	0.07	6420
62	165	44	0.149	0.07	6425
50	165	44	0.050	0.02	6430
55	165	44	0.091	0.04	6435
60	165	44	0.132	0.06	6440

Vsh.calculation (Clavier Eq.)					Depth
GR.	Max	Min	GR.fraction	Vsh.	(feet)
65	165	44	0.174	0.08	6445
140	165	44	0.793	0.63	6450
170	165	44	1.041	1.00	6455
195	165	44	1.248	1.00	6460
200	165	44	1.289	1.00	6465
197	165	44	1.264	1.00	6470
170	165	44	1.041	1.00	6475
190	165	44	1.207	1.00	6480
145	165	44	0.835	0.69	6485
162	165	44	0.975	0.94	6490
120	165	44	0.628	0.43	6495
153	165	44	0.901	0.80	6500
108	165	44	0.529	0.33	6505
143	165	44	0.818	0.66	6510
130	165	44	0.711	0.52	6515
180	165	44	1.124	1.00	6520
178	165	44	1.107	1.00	6525
172	165	44	1.058	1.00	6530
110	165	44	0.545	0.35	6535
90	165	44	0.380	0.21	6540
180	165	44	1.124	1.00	6545
120	165	44	0.628	0.43	6550
153	165	44	0.901	0.80	6555
142	165	44	0.810	0.65	6560
115	165	44	0.587	0.39	6565
80	165	44	0.298	0.16	6570
178	165	44	1.107	1.00	6575
183	165	44	1.149	1.00	6580
162	165	44	0.975	0.94	6585
130	165	44	0.711	0.52	6590
150	165	44	0.876	0.75	6595
130	165	44	0.711	0.52	6600
170	165	44	1.041	1.00	6605
80	165	44	0.298	0.16	6610
170	165	44	1.041	1.00	6615
175	165	44	1.083	1.00	6620
145	165	44	0.835	0.69	6625
140	165	44	0.793	0.63	6630
180	165	44	1.124	1.00	6635
160	165	44	0.959	0.91	6640
140	165	44	0.793	0.63	6645
178	165	44	1.107	1.00	6650
158	165	44	0.942	0.87	6655
180	165	44	1.124	1.00	6660
197	165	44	1.264	1.00	6665
177	165	44	1.099	1.00	6670
160	165	44	0.959	0.91	6675

Table A.8 Shale volume (Vsh) calculation from **well: I** (continued)

Vsh.calculation (Clavier Eq.)					Depth
GR.	Max	Min	GR.fraction	Vsh.	(feet)
200	165	44	1.289	1.00	6680
160	165	44	0.959	0.91	6685
152	165	44	0.893	0.78	6690
200	165	44	1.289	1.00	6695
140	165	44	0.793	0.63	6700
117	165	44	0.603	0.40	6705
158	165	44	0.942	0.87	6710
170	165	44	1.041	1.00	6715
98	165	44	0.446	0.26	6720
177	165	44	1.099	1.00	6725
197	165	44	1.264	1.00	6730
200	165	44	1.289	1.00	6735
180	165	44	1.124	1.00	6740
155	165	44	0.917	0.83	6745
178	165	44	1.107	1.00	6750
178	165	44	1.107	1.00	6755
170	165	44	1.041	1.00	6760
190	165	44	1.207	1.00	6765
160	165	44	0.959	0.91	6770
170	165	44	1.041	1.00	6775
174	165	44	1.074	1.00	6780
178	172	37	1.044	1.00	6785
182	172	37	1.074	1.00	6790
145	172	37	0.800	0.64	6795
140	172	37	0.763	0.59	6800
135	172	37	0.726	0.54	6805
78	172	37	0.304	0.16	6810
78	172	37	0.304	0.16	6815
130	172	37	0.689	0.50	6820
117	172	37	0.593	0.39	6825
60	172	37	0.170	0.08	6830
59	172	37	0.163	0.08	6835
180	172	37	1.059	1.00	6840
170	172	37	0.985	0.97	6845
60	172	37	0.170	0.08	6850
50	172	37	0.096	0.04	6855
53	172	37	0.119	0.05	6860
78	172	37	0.304	0.16	6865
54	172	37	0.126	0.06	6870
60	172	37	0.170	0.08	6875
173	172	37	1.007	1.00	6880
157	172	37	0.889	0.78	6885
130	172	37	0.689	0.50	6890
155	172	37	0.874	0.75	6895
170	172	37	0.985	0.97	6900
160	172	37	0.911	0.81	6905
198	172	37	1.193	1.00	6910

Vsh.calculation (Clavier Eq.)					Depth
GR.	Max	Min	GR.fraction	Vsh.	(feet)
165	172	37	0.948	0.89	6915
130	172	37	0.689	0.50	6920
170	172	37	0.985	0.97	6925
200	172	37	1.207	1.00	6930
108	172	37	0.526	0.33	6935
145	172	37	0.800	0.64	6940
190	172	37	1.133	1.00	6945
143	172	37	0.785	0.62	6950
180	172	37	1.059	1.00	6955
137	172	37	0.741	0.56	6960
170	172	37	0.985	0.97	6965
120	172	37	0.615	0.41	6970
130	172	37	0.689	0.50	6975
140	172	37	0.763	0.59	6980
98	172	37	0.452	0.27	6985
178	172	37	1.044	1.00	6990
150	172	37	0.837	0.69	6995
163	172	37	0.933	0.86	7000
187	172	37	1.111	1.00	7005
165	172	37	0.948	0.89	7010
98	172	37	0.452	0.27	7015
108	172	37	0.526	0.33	7020
62	172	37	0.185	0.09	7025
57	172	37	0.148	0.07	7030
78	172	37	0.304	0.16	7035
80	172	37	0.319	0.17	7040
60	172	37	0.170	0.08	7045
75	172	37	0.281	0.15	7050
83	172	37	0.341	0.18	7055
95	172	37	0.430	0.25	7060
100	172	37	0.467	0.28	7065
130	172	37	0.689	0.50	7070
90	172	37	0.393	0.22	7075
77	172	37	0.296	0.15	7080
80	172	37	0.319	0.17	7085
70	172	37	0.244	0.12	7090
115	172	37	0.578	0.38	7095
70	172	37	0.244	0.12	7100
200	172	37	1.207	1.00	7105
187	172	37	1.111	1.00	7110
197	172	37	1.185	1.00	7115
120	172	37	0.615	0.41	7120
150	172	37	0.837	0.69	7125
185	172	37	1.096	1.00	7130
180	172	37	1.059	1.00	7135
150	172	37	0.837	0.69	7140
181	172	37	1.067	1.00	7145

Table A.8 Shale volume (Vsh) calculation from **well: I** (continued)

Vsh.calculation (Clavier Eq.)					Depth
GR.	Max	Min	GR.fraction	Vsh.	(feet)
195	172	37	1.170	1.00	7150
162	172	37	0.926	0.84	7155
163	172	37	0.933	0.86	7160
163	172	37	0.933	0.86	7165
95	172	37	0.430	0.25	7170
60	172	37	0.170	0.08	7175
60	172	37	0.170	0.08	7180
63	172	37	0.193	0.09	7185
70	172	37	0.244	0.12	7190
78	172	37	0.304	0.16	7195
80	172	37	0.319	0.17	7200
55	172	37	0.133	0.06	7205
60	172	37	0.170	0.08	7210
150	172	37	0.837	0.69	7215
130	172	37	0.689	0.50	7220
170	172	37	0.985	0.97	7225
168	172	37	0.970	0.93	7230
190	172	37	1.133	1.00	7235
158	172	37	0.896	0.79	7240
83	172	37	0.341	0.18	7245
68	172	37	0.230	0.11	7250
57	172	37	0.148	0.07	7255
60	172	37	0.170	0.08	7260
70	172	37	0.244	0.12	7265
87	172	37	0.370	0.21	7270
160	172	37	0.911	0.81	7275
113	172	37	0.563	0.36	7280
62	172	37	0.185	0.09	7285
60	172	37	0.170	0.08	7290
65	172	37	0.207	0.10	7295
68	172	37	0.230	0.11	7300
52	172	37	0.111	0.05	7305
57	172	37	0.148	0.07	7310
178	172	37	1.044	1.00	7315
200	172	37	1.207	1.00	7320
187	172	37	1.111	1.00	7325
185	172	37	1.096	1.00	7330
160	172	37	0.911	0.81	7335
170	172	37	0.985	0.97	7340
180	172	37	1.059	1.00	7345
165	172	37	0.948	0.89	7350
183	172	37	1.081	1.00	7355
142	172	37	0.778	0.61	7360
125	172	37	0.652	0.45	7365
60	172	37	0.170	0.08	7370
62	172	37	0.185	0.09	7375
73	172	37	0.267	0.14	7380

Vsh.calculation (Clavier Eq.)					Depth
GR.	Max	Min	GR.fraction	Vsh.	(feet)
65	172	37	0.207	0.10	7385
60	172	37	0.170	0.08	7390
45	172	37	0.059	0.03	7395
160	172	37	0.911	0.81	7400
170	172	37	0.985	0.97	7405
200	172	37	1.207	1.00	7410
195	172	37	1.170	1.00	7415
163	172	37	0.933	0.86	7420
195	172	37	1.170	1.00	7425
137	172	37	0.741	0.56	7430
198	172	37	1.193	1.00	7435
85	172	37	0.356	0.19	7440
100	172	37	0.467	0.28	7445
153	172	37	0.859	0.73	7450
138	172	37	0.748	0.57	7455
120	172	37	0.615	0.41	7460
175	172	37	1.022	1.00	7465
180	172	37	1.059	1.00	7470
150	172	37	0.837	0.69	7475
155	172	37	0.874	0.75	7480
98	172	37	0.452	0.27	7485
52	172	37	0.111	0.05	7490
50	172	37	0.096	0.04	7495
67	172	37	0.222	0.11	7500
78	172	37	0.304	0.16	7505
62	172	37	0.185	0.09	7510
130	172	37	0.689	0.50	7515
142	172	37	0.778	0.61	7520
140	172	37	0.763	0.59	7525
110	172	37	0.541	0.34	7530
145	172	37	0.800	0.64	7535
181	172	37	1.067	1.00	7540
190	172	37	1.133	1.00	7545
170	172	37	0.985	0.97	7550
185	172	37	1.096	1.00	7555
200	172	37	1.207	1.00	7560
185	172	37	1.096	1.00	7565
163	172	37	0.933	0.86	7570
180	172	37	1.059	1.00	7575
135	172	37	0.726	0.54	7580
125	172	37	0.652	0.45	7585
100	172	37	0.467	0.28	7590
87	172	37	0.370	0.21	7595
50	172	37	0.096	0.04	7600
55	172	37	0.133	0.06	7605
55	172	37	0.133	0.06	7610
58	172	37	0.156	0.07	7615

Table A.8 Shale volume (Vsh) calculation from **well: I** (continued)

Vsh.calculation (Clavier Eq.)					Depth
GR.	Max	Min	GR.fraction	Vsh.	(feet)
200	172	37	1.207	1.00	7620
200	172	37	1.207	1.00	7625
150	172	37	0.837	0.69	7630
200	172	37	1.207	1.00	7635
180	172	37	1.059	1.00	7640
200	172	37	1.207	1.00	7645
170	172	37	0.985	0.97	7650
110	172	37	0.541	0.34	7655
120	172	37	0.615	0.41	7660
97	172	37	0.444	0.26	7665
65	172	37	0.207	0.10	7670
60	172	37	0.170	0.08	7675
170	172	37	0.985	0.97	7680
182	172	37	1.074	1.00	7685
180	172	37	1.059	1.00	7690
140	172	37	0.763	0.59	7695
142	172	37	0.778	0.61	7700
165	172	37	0.948	0.89	7705
180	172	37	1.059	1.00	7710
192	172	37	1.148	1.00	7715
190	172	37	1.133	1.00	7720
180	172	37	1.059	1.00	7725
170	172	37	0.985	0.97	7730
170	172	37	0.985	0.97	7735
45	172	37	0.059	0.03	7740
70	172	37	0.244	0.12	7745
80	172	37	0.319	0.17	7750
63	172	37	0.193	0.09	7755
65	172	37	0.207	0.10	7760
47	172	37	0.074	0.03	7765
45	172	37	0.059	0.03	7770
192	172	37	1.148	1.00	7775
178	172	37	1.044	1.00	7780
150	172	37	0.837	0.69	7785
180	175	40	1.037	1.00	8020
160	175	40	0.889	0.78	8025
182	175	40	1.052	1.00	8030
195	175	40	1.148	1.00	8035
160	175	40	0.889	0.78	8040
200	175	40	1.185	1.00	8045
100	175	40	0.444	0.26	8050
200	175	40	1.185	1.00	8055
200	175	40	1.185	1.00	8060
195	175	40	1.148	1.00	8065
190	175	40	1.111	1.00	8070
140	175	40	0.741	0.56	8075
200	175	40	1.185	1.00	8080

Vsh.calculation (Clavier Eq.)					Depth
GR.	Max	Min	GR.fraction	Vsh.	(feet)
140	172	37	0.763	0.59	7790
200	172	37	1.207	1.00	7795
160	172	37	0.911	0.81	7800
110	172	37	0.541	0.34	7805
143	172	37	0.785	0.62	7810
170	175	40	0.963	0.92	7815
160	175	40	0.889	0.78	7820
175	175	40	1.000	1.00	7825
150	175	40	0.815	0.66	7830
142	175	40	0.756	0.58	7835
140	175	40	0.741	0.56	7840
138	175	40	0.726	0.54	7845
128	175	40	0.652	0.45	7850
175	175	40	1.000	1.00	7855
187	175	40	1.089	1.00	7860
190	175	40	1.111	1.00	7865
180	175	40	1.037	1.00	7870
170	175	40	0.963	0.92	7875
140	175	40	0.741	0.56	7880
200	175	40	1.185	1.00	7885
140	175	40	0.741	0.56	7890
170	175	40	0.963	0.92	7895
190	175	40	1.111	1.00	7900
200	175	40	1.185	1.00	7905
200	175	40	1.185	1.00	7910
175	175	40	1.000	1.00	7915
140	175	40	0.741	0.56	7920
138	175	40	0.726	0.54	7925
160	175	40	0.889	0.78	7930
162	175	40	0.904	0.80	7935
180	175	40	1.037	1.00	7940
180	175	40	1.037	1.00	7945
170	175	40	0.963	0.92	7950
193	175	40	1.133	1.00	7955
170	175	40	0.963	0.92	7960
200	175	40	1.185	1.00	7965
165	175	40	0.926	0.84	7970
178	175	40	1.022	1.00	7975
200	175	40	1.185	1.00	7980
145	175	40	0.778	0.61	7985
140	175	40	0.741	0.56	7990
188	175	40	1.096	1.00	7995
195	175	40	1.148	1.00	8000
175	175	40	1.000	1.00	8005
160	175	40	0.889	0.78	8010
200	175	40	1.185	1.00	8015

Table A.8 Shale volume (Vsh) calculation from **well: I** (continued)

Vsh.calculation (Clavier Eq.)					Depth
GR.	Max	Min	GR.fraction	Vsh.	(feet)
180	175	40	1.037	1.00	8085
120	175	40	0.593	0.39	8090
57	175	40	0.126	0.06	8095
50	175	40	0.074	0.03	8100
80	175	40	0.296	0.15	8105
65	175	40	0.185	0.09	8110
63	175	40	0.170	0.08	8115
65	175	40	0.185	0.09	8120
67	175	40	0.200	0.10	8125
67	175	40	0.200	0.10	8130
65	175	40	0.185	0.09	8135
138	175	40	0.726	0.54	8140
200	175	40	1.185	1.00	8145
187	175	40	1.089	1.00	8150
180	175	40	1.037	1.00	8155
190	175	40	1.111	1.00	8160
150	175	40	0.815	0.66	8165
125	175	40	0.630	0.43	8170
200	175	40	1.185	1.00	8175
200	175	40	1.185	1.00	8180
200	175	40	1.185	1.00	8185
150	175	40	0.815	0.66	8190
200	175	40	1.185	1.00	8195
183	175	40	1.059	1.00	8200
190	175	40	1.111	1.00	8205
160	175	40	0.889	0.78	8210
180	175	40	1.037	1.00	8215
142	175	40	0.756	0.58	8220
137	175	40	0.719	0.53	8225
198	175	40	1.170	1.00	8230
185	175	40	1.074	1.00	8235
50	175	40	0.074	0.03	8240
53	175	40	0.096	0.04	8245
63	175	40	0.170	0.08	8250
52	175	40	0.089	0.04	8255
59	175	40	0.141	0.07	8260
130	175	40	0.667	0.47	8265
185	175	40	1.074	1.00	8270
190	175	40	1.111	1.00	8275
180	175	40	1.037	1.00	8280
183	175	40	1.059	1.00	8285
158	175	40	0.874	0.75	8290
180	175	40	1.037	1.00	8295
175	175	40	1.000	1.00	8300
108	175	40	0.504	0.31	8305
200	175	40	1.185	1.00	8310
130	175	40	0.667	0.47	8315

Vsh.calculation (Clavier Eq.)					Depth
GR.	Max	Min	GR.fraction	Vsh.	(feet)
60	175	40	0.148	0.07	8320
180	175	40	1.037	1.00	8325
123	175	40	0.615	0.41	8330
182	175	40	1.052	1.00	8335
183	175	40	1.059	1.00	8340
163	175	40	0.911	0.81	8345
175	175	40	1.000	1.00	8350
162	175	40	0.904	0.80	8355
190	175	40	1.111	1.00	8360
127	175	40	0.644	0.45	8365
167	175	40	0.941	0.87	8370
170	175	40	0.963	0.92	8375
160	175	40	0.889	0.78	8380
142	175	40	0.756	0.58	8385
170	175	40	0.963	0.92	8390
186	175	40	1.081	1.00	8395
108	175	40	0.504	0.31	8400
185	175	40	1.074	1.00	8405
200	175	40	1.185	1.00	8410
180	175	40	1.037	1.00	8415
195	175	40	1.148	1.00	8420
200	175	40	1.185	1.00	8425
150	175	40	0.815	0.66	8430
130	175	40	0.667	0.47	8435
120	175	40	0.593	0.39	8440
57	175	40	0.126	0.06	8445
80	175	40	0.296	0.15	8450
107	175	40	0.496	0.30	8455
78	175	40	0.281	0.15	8460
77	175	40	0.274	0.14	8465
70	175	40	0.222	0.11	8470
108	175	40	0.504	0.31	8475
200	175	40	1.185	1.00	8480
95	175	40	0.407	0.23	8485
140	175	40	0.741	0.56	8490
60	175	40	0.148	0.07	8495
170	175	40	0.963	0.92	8500
160	175	40	0.889	0.78	8505
178	175	40	1.022	1.00	8510
173	175	40	0.985	0.97	8515
200	175	40	1.185	1.00	8520
183	175	40	1.059	1.00	8525
133	175	40	0.689	0.50	8530
193	175	40	1.133	1.00	8535
170	175	40	0.963	0.92	8540
187	175	40	1.089	1.00	8545
180	175	40	1.037	1.00	8550

Table A.8 Shale volume (Vsh) calculation from **well: I** (continued)

Vsh.calculation (Clavier Eq.)					Depth
GR.	Max	Min	GR.fraction	Vsh.	(feet)
160	175	40	0.889	0.78	8555
132	175	40	0.681	0.49	8560
190	175	40	1.111	1.00	8565
93	175	40	0.393	0.22	8570
140	175	40	0.741	0.56	8575
190	175	40	1.111	1.00	8580
103	175	40	0.467	0.28	8585
67	175	40	0.200	0.10	8590
70	175	40	0.222	0.11	8595
60	175	40	0.148	0.07	8600
77	175	40	0.274	0.14	8605
72	175	40	0.237	0.12	8610
73	175	40	0.244	0.12	8615
60	175	40	0.148	0.07	8620
82	175	40	0.311	0.16	8625
63	175	40	0.170	0.08	8630
100	175	40	0.444	0.26	8635
195	175	40	1.148	1.00	8640
170	185	56	0.884	0.77	8645
155	185	56	0.767	0.59	8650
197	185	56	1.093	1.00	8655
120	185	56	0.496	0.30	8660
178	185	56	0.946	0.88	8665
170	185	56	0.884	0.77	8670
140	185	56	0.651	0.45	8675
200	185	56	1.116	1.00	8680
155	185	56	0.767	0.59	8685
145	185	56	0.690	0.50	8690
120	185	56	0.496	0.30	8695
137	185	56	0.628	0.43	8700
92	185	56	0.279	0.14	8705
190	185	56	1.039	1.00	8710
200	185	56	1.116	1.00	8715
178	185	56	0.946	0.88	8720
200	185	56	1.116	1.00	8725
168	185	56	0.868	0.74	8730
150	185	56	0.729	0.54	8735
179	185	56	0.953	0.90	8740
177	185	56	0.938	0.87	8745
170	185	56	0.884	0.77	8750
198	185	56	1.101	1.00	8755
190	185	56	1.039	1.00	8760
170	185	56	0.884	0.77	8765
197	185	56	1.093	1.00	8770
137	185	56	0.628	0.43	8775
200	185	56	1.116	1.00	8780
140	185	56	0.651	0.45	8785

Vsh.calculation (Clavier Eq.)					Depth
GR.	Max	Min	GR.fraction	Vsh.	(feet)
185	185	56	1.000	1.00	8790
135	185	56	0.612	0.41	8795
100	185	56	0.341	0.18	8800
118	185	56	0.481	0.29	8805
180	185	56	0.961	0.91	8810
200	185	56	1.116	1.00	8815
185	185	56	1.000	1.00	8820
165	185	56	0.845	0.70	8825
101	185	56	0.349	0.19	8830
167	185	56	0.860	0.73	8835
170	185	56	0.884	0.77	8840
187	185	56	1.016	1.00	8845
180	185	56	0.961	0.91	8850
110	185	56	0.419	0.24	8855
160	185	56	0.806	0.65	8860
80	185	56	0.186	0.09	8865
180	185	56	0.961	0.91	8870
200	185	56	1.116	1.00	8875
118	185	56	0.481	0.29	8880
187	185	56	1.016	1.00	8885
133	185	56	0.597	0.40	8890
197	185	56	1.093	1.00	8895
187	185	56	1.016	1.00	8900
192	185	56	1.054	1.00	8905
145	185	56	0.690	0.50	8910
200	185	56	1.116	1.00	8915
100	185	56	0.341	0.18	8920
200	185	56	1.116	1.00	8925
67	185	56	0.085	0.04	8930
190	185	56	1.039	1.00	8935
145	185	56	0.690	0.50	8940
190	185	56	1.039	1.00	8945
180	185	56	0.961	0.91	8950
95	185	56	0.302	0.16	8955
127	185	56	0.550	0.35	8960

Table A.9 Shale volume (Vsh) calculation from **well: J**

Vsh.calculation (Clavier Eq.)					Depth
GR.	Max	Min	GR.fraction	Vsh.	(feet)
110	167	53	0.5000	0.31	4500
95	167	53	0.3684	0.20	4505
78	167	53	0.2193	0.11	4510
73	167	53	0.1754	0.08	4515
57	167	53	0.0351	0.01	4520
70	167	53	0.1491	0.07	4525
63	167	53	0.0877	0.04	4530
62	167	53	0.0789	0.03	4535
60	167	53	0.0614	0.03	4540
52	167	53	-0.0088	0.00	4545
175	167	53	1.0702	1.00	4550
160	167	53	0.9386	0.87	4555
168	167	53	1.0088	1.00	4560
142	167	53	0.7807	0.61	4565
158	167	53	0.9211	0.83	4570
154	167	53	0.8860	0.77	4575
150	167	53	0.8509	0.71	4580
130	167	53	0.6754	0.48	4585
158	167	53	0.9211	0.83	4590
168	167	53	1.0088	1.00	4595
140	167	53	0.7632	0.59	4600
140	167	53	0.7632	0.59	4605
113	167	53	0.5263	0.33	4610
52	167	53	-0.0088	0.00	4615
65	167	53	0.1053	0.05	4620
58	167	53	0.0439	0.02	4625
58	167	53	0.0439	0.02	4630
54	167	53	0.0088	0.00	4635
55	167	53	0.0175	0.01	4640
53	167	53	0.0000	0.00	4645
54	167	53	0.0088	0.00	4650
55	167	53	0.0175	0.01	4655
55	167	53	0.0175	0.01	4660
60	167	53	0.0614	0.03	4665
62	167	53	0.0789	0.03	4670
55	167	53	0.0175	0.01	4675
60	167	53	0.0614	0.03	4680
55	167	53	0.0175	0.01	4685
58	167	53	0.0439	0.02	4690
78	167	53	0.2193	0.11	4695
73	167	53	0.1754	0.08	4700
72	167	53	0.1667	0.08	4705
62	167	53	0.0789	0.03	4710
67	167	53	0.1228	0.06	4715
60	167	53	0.0614	0.03	4720
145	167	53	0.8070	0.65	4725
130	167	53	0.6754	0.48	4730

Vsh.calculation (Clavier Eq.)					Depth
GR.	Max	Min	GR.fraction	Vsh.	(feet)
87	167	53	0.2982	0.16	4735
63	167	53	0.0877	0.04	4740
132	167	53	0.6930	0.50	4745
158	167	53	0.9211	0.83	4750
128	167	53	0.6579	0.46	4755
77	167	53	0.2105	0.10	4760
60	167	53	0.0614	0.03	4765
70	167	53	0.1491	0.07	4770
70	167	53	0.1491	0.07	4775
65	167	53	0.1053	0.05	4780
68	167	53	0.1316	0.06	4785
73	167	53	0.1754	0.08	4790
65	167	53	0.1053	0.05	4795
138	167	53	0.7456	0.56	4800
137	167	53	0.7368	0.55	4805
88	167	53	0.3070	0.16	4810
80	167	53	0.2368	0.12	4815
75	167	53	0.1930	0.09	4820
78	167	53	0.2193	0.11	4825
67	167	53	0.1228	0.06	4830
120	167	53	0.5877	0.39	4835
75	167	53	0.1930	0.09	4840
112	167	53	0.5175	0.32	4845
147	167	53	0.8246	0.67	4850
142	167	53	0.7807	0.61	4855
125	167	53	0.6316	0.43	4860
150	167	53	0.8509	0.71	4865
158	167	53	0.9211	0.83	4870
190	167	53	1.2018	1.00	4875
200	167	53	1.2895	1.00	4880
162	167	53	0.9561	0.90	4885
153	167	53	0.8772	0.76	4890
127	167	53	0.6491	0.45	4895
160	167	53	0.9386	0.87	4900
132	167	53	0.6930	0.50	4905
152	167	53	0.8684	0.74	4910
170	167	53	1.0263	1.00	4915
163	167	53	0.9649	0.92	4920
165	167	53	0.9825	0.96	4925
153	167	53	0.8772	0.76	4930
155	167	53	0.8947	0.79	4935
145	167	53	0.8070	0.65	4940
140	167	53	0.7632	0.59	4945
163	167	53	0.9649	0.92	4950
175	167	53	1.0702	1.00	4955
135	167	53	0.7193	0.53	4960
185	167	53	1.1579	1.00	4965

Table A.9 Shale volume (Vsh) calculation from **well: J** (continued)

Vsh.calculation (Clavier Eq.)					Depth
GR.	Max	Min	GR.fraction	Vsh.	(feet)
132	167	53	0.6930	0.50	4970
140	167	53	0.7632	0.59	4975
150	167	53	0.8509	0.71	4980
128	167	53	0.6579	0.46	4985
130	167	53	0.6754	0.48	4990
90	167	53	0.3246	0.17	4995
147	167	53	0.8246	0.67	5000
60	167	53	0.0614	0.03	5005
65	167	53	0.1053	0.05	5010
60	167	53	0.0614	0.03	5015
60	167	53	0.0614	0.03	5020
200	167	53	1.2895	1.00	5025
195	167	53	1.2456	1.00	5030
170	167	53	1.0263	1.00	5035
123	167	53	0.6140	0.41	5040
158	167	53	0.9211	0.83	5045
151	167	53	0.8596	0.73	5050
120	167	53	0.5877	0.39	5055
140	167	53	0.7632	0.59	5060
97	167	53	0.3860	0.22	5065
79	167	53	0.2281	0.11	5070
93	167	53	0.3509	0.19	5075
60	167	53	0.0614	0.03	5080
61	167	53	0.0702	0.03	5085
97	167	53	0.3860	0.22	5090
105	167	53	0.4561	0.27	5095
165	167	53	0.9825	0.96	5100
173	167	53	1.0526	1.00	5105
162	167	53	0.9561	0.90	5110
185	167	53	1.1579	1.00	5115
138	167	53	0.7456	0.56	5120
150	167	53	0.8509	0.71	5125
160	167	53	0.9386	0.87	5130
135	167	53	0.7193	0.53	5135
150	167	53	0.8509	0.71	5140
160	167	53	0.9386	0.87	5145
152	167	53	0.8684	0.74	5150
150	167	53	0.8509	0.71	5155
140	167	53	0.7632	0.59	5160
132	167	53	0.6930	0.50	5165
78	167	53	0.2193	0.11	5170
70	167	53	0.1491	0.07	5175
67	167	53	0.1228	0.06	5180
162	167	53	0.9561	0.90	5185
145	167	53	0.8070	0.65	5190
150	167	53	0.8509	0.71	5195
137	167	53	0.7368	0.55	5200

Vsh.calculation (Clavier Eq.)					Depth
GR.	Max	Min	GR.fraction	Vsh.	(feet)
130	167	53	0.6754	0.48	5205
125	167	53	0.6316	0.43	5210
73	167	53	0.1754	0.08	5215
65	167	53	0.1053	0.05	5220
65	167	53	0.1053	0.05	5225
65	167	53	0.1053	0.05	5230
60	167	53	0.0614	0.03	5235
55	167	53	0.0175	0.01	5240
65	167	53	0.1053	0.05	5245
65	167	53	0.1053	0.05	5250
84	167	53	0.2719	0.14	5255
138	167	53	0.7456	0.56	5260
126	167	53	0.6404	0.44	5265
130	167	53	0.6754	0.48	5270
73	167	53	0.1754	0.08	5275
70	167	53	0.1491	0.07	5280
70	167	53	0.1491	0.07	5285
65	167	53	0.1053	0.05	5290
65	167	53	0.1053	0.05	5295
60	167	53	0.0614	0.03	5300
63	167	53	0.0877	0.04	5305
75	167	53	0.1930	0.09	5310
68	167	53	0.1316	0.06	5315
110	167	53	0.5000	0.31	5320
140	167	53	0.7632	0.59	5325
150	167	53	0.8509	0.71	5330
147	167	53	0.8246	0.67	5335
175	167	53	1.0702	1.00	5340
171	167	53	1.0351	1.00	5345
150	167	53	0.8509	0.71	5350
155	167	53	0.8947	0.79	5355
165	167	53	0.9825	0.96	5360
120	167	53	0.5877	0.39	5365
120	167	53	0.5877	0.39	5370
200	167	53	1.2895	1.00	5375
70	167	53	0.1491	0.07	5380
67	167	53	0.1228	0.06	5385
73	167	53	0.1754	0.08	5390
80	167	53	0.2368	0.12	5395
73	167	53	0.1754	0.08	5400
75	167	53	0.1930	0.09	5405
82	167	53	0.2544	0.13	5410
78	167	53	0.2193	0.11	5415
153	167	53	0.8772	0.76	5420
158	167	53	0.9211	0.83	5425
152	167	53	0.8684	0.74	5430
170	167	53	1.0263	1.00	5435

Table A.9 Shale volume (Vsh) calculation from **well: J** (continued)

Vsh.calculation (Clavier Eq.)					Depth
GR.	Max	Min	GR.fraction	Vsh.	(feet)
145	167	53	0.8070	0.65	5440
158	167	53	0.9211	0.83	5445
145	167	53	0.8070	0.65	5450
150	167	53	0.8509	0.71	5455
165	167	53	0.9825	0.96	5460
160	167	53	0.9386	0.87	5465
153	167	53	0.8772	0.76	5470
180	167	53	1.1140	1.00	5475
137	167	53	0.7368	0.55	5480
138	167	53	0.7456	0.56	5485
160	167	53	0.9386	0.87	5490
110	167	53	0.5000	0.31	5495
131	167	53	0.6842	0.49	5500
70	167	53	0.1491	0.07	5505
82	167	53	0.2544	0.13	5510
163	167	53	0.9649	0.92	5515
155	167	53	0.8947	0.79	5520
150	167	53	0.8509	0.71	5525
135	167	53	0.7193	0.53	5530
130	167	53	0.6754	0.48	5535
155	167	53	0.8947	0.79	5540
142	167	53	0.7807	0.61	5545
105	167	53	0.4561	0.27	5550
98	167	53	0.3947	0.22	5555
110	167	53	0.5000	0.31	5560
80	167	53	0.2368	0.12	5565
65	167	53	0.1053	0.05	5570
60	167	53	0.0614	0.03	5575
58	167	53	0.0439	0.02	5580
73	167	53	0.1754	0.08	5585
68	167	53	0.1316	0.06	5590
68	167	53	0.1316	0.06	5595
140	167	53	0.7632	0.59	5600
180	167	53	1.1140	1.00	5605
160	167	53	0.9386	0.87	5610
130	167	53	0.6754	0.48	5615
150	167	53	0.8509	0.71	5620
167	167	53	1.0000	1.00	5625
147	167	53	0.8246	0.67	5630
180	167	53	1.1140	1.00	5635
142	167	53	0.7807	0.61	5640
155	167	53	0.8947	0.79	5645
143	167	53	0.7895	0.62	5650
110	167	53	0.5000	0.31	5655
150	167	53	0.8509	0.71	5660
200	167	53	1.2895	1.00	5665
138	167	53	0.7456	0.56	5670

Vsh.calculation (Clavier Eq.)					Depth
GR.	Max	Min	GR.fraction	Vsh.	(feet)
110	167	53	0.5000	0.31	5675
100	167	53	0.4123	0.24	5680
150	167	53	0.8509	0.71	5685
140	167	53	0.7632	0.59	5690
125	167	53	0.6316	0.43	5695
122	167	53	0.6053	0.41	5700
140	167	53	0.7632	0.59	5705
155	167	53	0.8947	0.79	5710
137	167	53	0.7368	0.55	5715
125	167	53	0.6316	0.43	5720
122	167	53	0.6053	0.41	5725
120	167	53	0.5877	0.39	5730
160	167	53	0.9386	0.87	5735
165	167	53	0.9825	0.96	5740
177	167	53	1.0877	1.00	5745
145	167	53	0.8070	0.65	5750
132	167	53	0.6930	0.50	5755
140	167	53	0.7632	0.59	5760
158	167	53	0.9211	0.83	5765
143	167	53	0.7895	0.62	5770
141	167	53	0.7719	0.60	5775
102	167	53	0.4298	0.25	5780
185	167	53	1.1579	1.00	5785
182	167	53	1.1316	1.00	5790
160	167	53	0.9386	0.87	5795
145	167	53	0.8070	0.65	5800
168	167	53	1.0088	1.00	5805
127	167	53	0.6491	0.45	5810
108	167	53	0.4825	0.29	5815
80	167	53	0.2368	0.12	5820
65	167	53	0.1053	0.05	5825
58	167	53	0.0439	0.02	5830
73	167	53	0.1754	0.08	5835
75	167	53	0.1930	0.09	5840
140	167	53	0.7632	0.59	5845
130	167	53	0.6754	0.48	5850
138	167	53	0.7456	0.56	5855
135	167	53	0.7193	0.53	5860
175	167	53	1.0702	1.00	5865
105	167	53	0.4561	0.27	5870
167	167	53	1.0000	1.00	5875
142	167	53	0.7807	0.61	5880
200	167	53	1.2895	1.00	5885
118	167	53	0.5702	0.37	5890
138	167	53	0.7456	0.56	5895
147	167	53	0.8246	0.67	5900
135	167	53	0.7193	0.53	5905

Table A.9 Shale volume (Vsh) calculation from **well: J** (continued)

Vsh.calculation (Clavier Eq.)					Depth
GR.	Max	Min	GR.fraction	Vsh.	(feet)
155	167	53	0.8947	0.79	5910
90	167	53	0.3246	0.17	5915
120	167	53	0.5877	0.39	5920
200	167	53	1.2895	1.00	5925
160	167	53	0.9386	0.87	5930
150	167	53	0.8509	0.71	5935
153	167	53	0.8772	0.76	5940
140	167	53	0.7632	0.59	5945
100	167	53	0.4123	0.24	5950
147	167	53	0.8246	0.67	5955
162	167	53	0.9561	0.90	5960
163	167	53	0.9649	0.92	5965
200	167	53	1.2895	1.00	5970
200	167	53	1.2895	1.00	5975
115	167	53	0.5439	0.35	5980
153	167	53	0.8772	0.76	5985
153	167	53	0.8772	0.76	5990
150	167	53	0.8509	0.71	5995
170	167	53	1.0263	1.00	6000
148	167	53	0.8333	0.69	6005
157	167	53	0.9123	0.82	6010
135	167	53	0.7193	0.53	6015
157	167	53	0.9123	0.82	6020
150	167	53	0.8509	0.71	6025
167	167	53	1.0000	1.00	6030
150	167	53	0.8509	0.71	6035
148	167	53	0.8333	0.69	6040
140	167	53	0.7632	0.59	6045
130	167	53	0.6754	0.48	6050
92	167	53	0.3421	0.19	6055
80	167	53	0.2368	0.12	6060
87	167	53	0.2982	0.16	6065
65	167	53	0.1053	0.05	6070
60	167	53	0.0614	0.03	6075
140	167	53	0.7632	0.59	6080
103	167	53	0.4386	0.26	6085
160	167	53	0.9386	0.87	6090
160	167	53	0.9386	0.87	6095
115	167	53	0.5439	0.35	6100
78	167	53	0.2193	0.11	6105
62	167	53	0.0789	0.03	6110
53	167	53	0.0000	0.00	6115
63	167	53	0.0877	0.04	6120
55	167	53	0.0175	0.01	6125
160	167	53	0.9386	0.87	6130
150	167	53	0.8509	0.71	6135
132	167	53	0.6930	0.50	6140

Vsh.calculation (Clavier Eq.)					Depth
GR.	Max	Min	GR.fraction	Vsh.	(feet)
174	167	53	1.0614	1.00	6145
158	167	53	0.9211	0.83	6150
140	167	53	0.7632	0.59	6155
145	167	53	0.8070	0.65	6160
150	167	53	0.8509	0.71	6165
120	167	53	0.5877	0.39	6170
158	167	53	0.9211	0.83	6175
130	167	53	0.6754	0.48	6180
127	167	53	0.6491	0.45	6185
73	167	53	0.1754	0.08	6190
65	167	53	0.1053	0.05	6195
82	167	53	0.2544	0.13	6200
168	167	53	1.0088	1.00	6205
172	167	53	1.0439	1.00	6210
110	167	53	0.5000	0.31	6215
158	167	53	0.9211	0.83	6220
138	167	53	0.7456	0.56	6225
110	167	53	0.5000	0.31	6230
130	167	53	0.6754	0.48	6235
131	167	53	0.6842	0.49	6240
110	167	53	0.5000	0.31	6245
153	167	53	0.8772	0.76	6250
160	167	53	0.9386	0.87	6255
150	167	53	0.8509	0.71	6260
145	167	53	0.8070	0.65	6265
117	167	53	0.5614	0.36	6270
150	167	53	0.8509	0.71	6275
150	167	53	0.8509	0.71	6280
155	167	53	0.8947	0.79	6285
170	167	53	1.0263	1.00	6290
200	167	53	1.2895	1.00	6295
200	167	53	1.2895	1.00	6300
160	167	53	0.9386	0.87	6305
120	167	53	0.5877	0.39	6310
158	167	53	0.9211	0.83	6315
150	167	53	0.8509	0.71	6320
140	167	53	0.7632	0.59	6325
145	167	53	0.8070	0.65	6330
140	167	53	0.7632	0.59	6335
120	167	53	0.5877	0.39	6340
140	167	53	0.7632	0.59	6345
140	167	53	0.7632	0.59	6350
137	167	53	0.7368	0.55	6355
130	167	53	0.6754	0.48	6360
150	167	53	0.8509	0.71	6365
150	167	53	0.8509	0.71	6370
100	167	53	0.4123	0.24	6375

Table A.9 Shale volume (Vsh) calculation from **well: J** (continued)

Vsh.calculation (Clavier Eq.)					Depth
GR.	Max	Min	GR.fraction	Vsh.	(feet)
150	167	53	0.8509	0.71	6380
160	167	53	0.9386	0.87	6385
127	167	53	0.6491	0.45	6390
90	167	53	0.3246	0.17	6395
165	167	53	0.9825	0.96	6400
90	167	53	0.3246	0.17	6405
180	167	53	1.1140	1.00	6410
167	167	53	1.0000	1.00	6415
150	167	53	0.8509	0.71	6420
150	167	53	0.8509	0.71	6425
155	167	53	0.8947	0.79	6430
140	167	53	0.7632	0.59	6435
180	167	53	1.1140	1.00	6440
150	167	53	0.8509	0.71	6445
166	167	53	0.9912	0.98	6450
128	167	53	0.6579	0.46	6455
151	167	53	0.8596	0.73	6460
140	167	53	0.7632	0.59	6465
100	167	53	0.4123	0.24	6470
85	167	53	0.2807	0.14	6475
60	167	53	0.0614	0.03	6480
67	167	53	0.1228	0.06	6485
68	167	53	0.1316	0.06	6490
82	167	53	0.2544	0.13	6495
200	167	53	1.2895	1.00	6500
105	167	53	0.4561	0.27	6505
143	167	53	0.7895	0.62	6510
147	167	53	0.8246	0.67	6515
140	167	53	0.7632	0.59	6520
178	167	53	1.0965	1.00	6525
145	167	53	0.8070	0.65	6530
125	167	53	0.6316	0.43	6535
180	167	53	1.1140	1.00	6540
173	167	53	1.0526	1.00	6545
120	167	53	0.5877	0.39	6550
159	167	53	0.9298	0.85	6555
168	167	53	1.0088	1.00	6560
150	167	53	0.8509	0.71	6565
147	167	53	0.8246	0.67	6570
163	167	53	0.9649	0.92	6575
110	167	53	0.5000	0.31	6580
117	167	53	0.5614	0.36	6585
41	167	53	-0.1053	0.00	6590
50	167	53	-0.0263	0.00	6595
52	167	53	-0.0088	0.00	6600
50	167	53	-0.0263	0.00	6605
50	167	53	-0.0263	0.00	6610

Vsh.calculation (Clavier Eq.)					Depth
GR.	Max	Min	GR.fraction	Vsh.	(feet)
155	167	53	0.8947	0.79	6615
162	167	53	0.9561	0.90	6620
170	167	53	1.0263	1.00	6625
143	167	53	0.7895	0.62	6630
200	167	53	1.2895	1.00	6635
174	167	53	1.0614	1.00	6640
153	167	53	0.8772	0.76	6645
153	167	53	0.8772	0.76	6650
135	167	53	0.7193	0.53	6655
120	167	53	0.5877	0.39	6660
143	167	53	0.7895	0.62	6665
158	167	53	0.9211	0.83	6670
115	167	53	0.5439	0.35	6675
145	167	53	0.8070	0.65	6680
60	167	53	0.0614	0.03	6685
115	167	53	0.5439	0.35	6690
120	167	53	0.5877	0.39	6695
120	167	53	0.5877	0.39	6700
200	167	53	1.2895	1.00	6705
150	167	53	0.8509	0.71	6710
188	167	53	1.1842	1.00	6715
170	167	53	1.0263	1.00	6720
139	167	53	0.7544	0.58	6725
125	167	53	0.6316	0.43	6730
160	167	53	0.9386	0.87	6735
160	167	53	0.9386	0.87	6740
115	167	53	0.5439	0.35	6745
80	167	53	0.2368	0.12	6750
60	180	45	0.1111	0.05	6755
60	180	45	0.1111	0.05	6760
65	180	45	0.1481	0.07	6765
60	180	45	0.1111	0.05	6770
65	180	45	0.1481	0.07	6775
65	180	45	0.1481	0.07	6780
60	180	45	0.1111	0.05	6785
87	180	45	0.3111	0.16	6790
117	180	45	0.5333	0.34	6795
100	180	45	0.4074	0.23	6800
78	180	45	0.2444	0.12	6805
80	180	45	0.2593	0.13	6810
70	180	45	0.1852	0.09	6815
65	180	45	0.1481	0.07	6820
65	180	45	0.1481	0.07	6825
120	180	45	0.5556	0.36	6830
130	180	45	0.6296	0.43	6835
100	180	45	0.4074	0.23	6840
50	180	45	0.0370	0.02	6845

Table A.9 Shale volume (Vsh) calculation from **well: J** (continued)

Vsh.calculation (Clavier Eq.)					Depth
GR.	Max	Min	GR.fraction	Vsh.	(feet)
60	180	45	0.1111	0.05	6850
100	180	45	0.4074	0.23	6855
57	180	45	0.0889	0.04	6860
173	180	45	0.9481	0.89	6865
170	180	45	0.9259	0.84	6870
139	180	45	0.6963	0.50	6875
200	180	45	1.1481	1.00	6880
170	180	45	0.9259	0.84	6885
163	180	45	0.8741	0.75	6890
140	180	45	0.7037	0.51	6895
150	180	45	0.7778	0.61	6900
145	180	45	0.7407	0.56	6905
190	180	45	1.0741	1.00	6910
160	180	45	0.8519	0.71	6915
150	180	45	0.7778	0.61	6920
170	180	45	0.9259	0.84	6925
178	180	45	0.9852	0.97	6930
153	180	45	0.8000	0.64	6935
178	180	45	0.9852	0.97	6940
139	180	45	0.6963	0.50	6945
180	180	45	1.0000	1.00	6950
117	180	45	0.5333	0.34	6955
198	180	45	1.1333	1.00	6960
139	180	45	0.6963	0.50	6965
200	180	45	1.1481	1.00	6970
139	180	45	0.6963	0.50	6975
163	180	45	0.8741	0.75	6980
147	180	45	0.7556	0.58	6985
160	180	45	0.8519	0.71	6990
128	180	45	0.6148	0.41	6995
90	180	45	0.3333	0.18	7000
160	180	45	0.8519	0.71	7005
188	180	45	1.0593	1.00	7010
170	180	45	0.9259	0.84	7015
165	180	45	0.8889	0.78	7020
173	180	45	0.9481	0.89	7025
127	180	45	0.6074	0.41	7030
182	180	45	1.0148	1.00	7035
125	180	45	0.5926	0.39	7040
147	180	45	0.7556	0.58	7045
152	180	45	0.7926	0.63	7050
110	180	45	0.4815	0.29	7055
68	180	45	0.1704	0.08	7060
68	180	45	0.1704	0.08	7065
60	180	45	0.1111	0.05	7070
55	180	45	0.0741	0.03	7075
68	180	45	0.1704	0.08	7080

Vsh.calculation (Clavier Eq.)					Depth
GR.	Max	Min	GR.fraction	Vsh.	(feet)
58	180	45	0.0963	0.04	7085
70	180	45	0.1852	0.09	7090
78	180	45	0.2444	0.12	7095
200	180	45	1.1481	1.00	7100
150	180	45	0.7778	0.61	7105
167	180	45	0.9037	0.80	7110
172	180	45	0.9407	0.87	7115
160	180	45	0.8519	0.71	7120
110	180	45	0.4815	0.29	7125
168	180	45	0.9111	0.81	7130
178	180	45	0.9852	0.97	7135
152	180	45	0.7926	0.63	7140
133	180	45	0.6519	0.45	7145
113	180	45	0.5037	0.31	7150
130	180	45	0.6296	0.43	7155
70	180	45	0.1852	0.09	7160
80	180	45	0.2593	0.13	7165
60	180	45	0.1111	0.05	7170
60	180	45	0.1111	0.05	7175
60	180	45	0.1111	0.05	7180
50	180	45	0.0370	0.02	7185
53	180	45	0.0593	0.03	7190
50	180	45	0.0370	0.02	7195
142	180	45	0.7185	0.53	7200
140	180	45	0.7037	0.51	7205
64	180	45	0.1407	0.07	7210
130	180	45	0.6296	0.43	7215
165	180	45	0.8889	0.78	7220
168	180	45	0.9111	0.81	7225
150	180	45	0.7778	0.61	7230
167	180	45	0.9037	0.80	7235
160	180	45	0.8519	0.71	7240
183	180	45	1.0222	1.00	7245
145	180	45	0.7407	0.56	7250
147	180	45	0.7556	0.58	7255
100	180	45	0.4074	0.23	7260
55	180	45	0.0741	0.03	7265
55	180	45	0.0741	0.03	7270
55	180	45	0.0741	0.03	7275
58	180	45	0.0963	0.04	7280
108	180	45	0.4667	0.28	7285
160	180	45	0.8519	0.71	7290
145	180	45	0.7407	0.56	7295
160	180	45	0.8519	0.71	7300
110	180	45	0.4815	0.29	7305
141	180	45	0.7111	0.52	7310
118	180	45	0.5407	0.34	7315

Table A.9 Shale volume (Vsh) calculation from **well: J** (continued)

Vsh.calculation (Clavier Eq.)					Depth
GR.	Max	Min	GR.fraction	Vsh.	(feet)
150	180	45	0.7778	0.61	7320
177	180	45	0.9778	0.95	7325
140	180	45	0.7037	0.51	7330
177	180	45	0.9778	0.95	7335
100	180	45	0.4074	0.23	7340
90	180	45	0.3333	0.18	7345
90	180	45	0.3333	0.18	7350
92	180	45	0.3481	0.19	7355
50	180	45	0.0370	0.02	7360
115	180	45	0.5185	0.32	7365
100	180	45	0.4074	0.23	7370
128	180	45	0.6148	0.41	7375
134	180	45	0.6593	0.46	7380
90	180	45	0.3333	0.18	7385
60	180	45	0.1111	0.05	7390
57	180	45	0.0889	0.04	7395
112	180	45	0.4963	0.30	7400
122	180	45	0.5704	0.37	7405
120	180	45	0.5556	0.36	7410
63	180	45	0.1333	0.06	7415
110	180	45	0.4815	0.29	7420
170	180	45	0.9259	0.84	7425
160	180	45	0.8519	0.71	7430
180	180	45	1.0000	1.00	7435
139	180	45	0.6963	0.50	7440
170	180	45	0.9259	0.84	7445
137	180	45	0.6815	0.49	7450
113	180	45	0.5037	0.31	7455
170	180	45	0.9259	0.84	7460
168	180	45	0.9111	0.81	7465
125	180	45	0.5926	0.39	7470
165	180	45	0.8889	0.78	7475
200	180	45	1.1481	1.00	7480
190	180	45	1.0741	1.00	7485
178	180	45	0.9852	0.97	7490
139	180	45	0.6963	0.50	7495
165	180	45	0.8889	0.78	7500
157	180	45	0.8296	0.68	7505
120	180	45	0.5556	0.36	7510
180	180	45	1.0000	1.00	7515
150	180	45	0.7778	0.61	7520
145	180	45	0.7407	0.56	7525
155	180	45	0.8148	0.66	7530
173	180	45	0.9481	0.89	7535
113	180	45	0.5037	0.31	7540
50	180	45	0.0370	0.02	7545
50	180	45	0.0370	0.02	7550

Vsh.calculation (Clavier Eq.)					Depth
GR.	Max	Min	GR.fraction	Vsh.	(feet)
50	180	45	0.0370	0.02	7555
57	180	45	0.0889	0.04	7560
55	180	45	0.0741	0.03	7565
50	180	45	0.0370	0.02	7570
53	180	45	0.0593	0.03	7575
60	180	45	0.1111	0.05	7580
160	180	45	0.8519	0.71	7585
200	180	45	1.1481	1.00	7590
155	180	45	0.8148	0.66	7595
200	180	45	1.1481	1.00	7600
158	180	45	0.8370	0.69	7605
165	180	45	0.8889	0.78	7610
165	180	45	0.8889	0.78	7615
148	180	45	0.7630	0.59	7620
110	180	45	0.4815	0.29	7625
180	180	45	1.0000	1.00	7630
175	180	45	0.9630	0.92	7635
178	180	45	0.9852	0.97	7640
200	180	45	1.1481	1.00	7645
200	180	45	1.1481	1.00	7650
50	180	45	0.0370	0.02	7655
160	180	45	0.8519	0.71	7660
65	180	45	0.1481	0.07	7665
65	180	45	0.1481	0.07	7670
65	180	45	0.1481	0.07	7675
70	180	45	0.1852	0.09	7680
120	180	45	0.5556	0.36	7685
160	180	45	0.8519	0.71	7690
110	180	45	0.4815	0.29	7695
80	180	45	0.2593	0.13	7700
70	180	45	0.1852	0.09	7705
74	180	45	0.2148	0.11	7710
70	180	45	0.1852	0.09	7715
74	180	45	0.2148	0.11	7720
65	180	45	0.1481	0.07	7725
68	180	45	0.1704	0.08	7730
55	180	45	0.0741	0.03	7735
173	180	45	0.9481	0.89	7740
180	180	45	1.0000	1.00	7745
150	180	45	0.7778	0.61	7750
120	180	45	0.5556	0.36	7755
93	180	45	0.3556	0.19	7760
50	180	45	0.0370	0.02	7765
60	180	45	0.1111	0.05	7770
44	180	45	-0.0074	0.00	7775
48	180	45	0.0222	0.01	7780
55	180	45	0.0741	0.03	7785

Table A.9 Shale volume (Vsh) calculation from **well: J** (continued)

Vsh.calculation (Clavier Eq.)					Depth
GR.	Max	Min	GR.fraction	Vsh.	(feet)
50	180	45	0.0370	0.02	7790
165	180	45	0.8889	0.78	7795
159	180	45	0.8444	0.70	7800
145	180	45	0.7407	0.56	7805
192	180	45	1.0889	1.00	7810
170	180	45	0.9259	0.84	7815
160	180	45	0.8519	0.71	7820
175	180	45	0.9630	0.92	7825
176	180	45	0.9704	0.93	7830
200	180	45	1.1481	1.00	7835
123	180	45	0.5778	0.38	7840
195	180	45	1.1111	1.00	7845
180	180	45	1.0000	1.00	7850
157	180	45	0.8296	0.68	7855
137	180	45	0.6815	0.49	7860
80	180	45	0.2593	0.13	7865
40	180	45	-0.0370	0.00	7870
123	180	45	0.5778	0.38	7875
150	180	45	0.7778	0.61	7880
190	180	45	1.0741	1.00	7885
150	180	45	0.7778	0.61	7890
185	180	45	1.0370	1.00	7895
142	180	45	0.7185	0.53	7900
150	180	45	0.7778	0.61	7905
200	180	45	1.1481	1.00	7910
192	180	45	1.0889	1.00	7915
200	180	45	1.1481	1.00	7920
147	180	45	0.7556	0.58	7925
60	180	45	0.1111	0.05	7930
59	180	45	0.1037	0.05	7935
60	180	45	0.1111	0.05	7940
87	180	45	0.3111	0.16	7945
78	180	45	0.2444	0.12	7950
53	180	45	0.0593	0.03	7955
63	180	45	0.1333	0.06	7960
81	180	45	0.2667	0.14	7965
85	180	45	0.2963	0.15	7970
157	180	45	0.8296	0.68	7975
80	180	45	0.2593	0.13	7980
80	180	45	0.2593	0.13	7985
75	180	45	0.2222	0.11	7990
82	180	45	0.2741	0.14	7995
133	180	45	0.6519	0.45	8000
130	180	45	0.6296	0.43	8005
160	180	45	0.8519	0.71	8010
72	180	45	0.2000	0.10	8015
75	180	45	0.2222	0.11	8020

Vsh.calculation (Clavier Eq.)					Depth
GR.	Max	Min	GR.fraction	Vsh.	(feet)
75	180	45	0.2222	0.11	8025
65	180	45	0.1481	0.07	8030
58	180	45	0.0963	0.04	8035
63	180	45	0.1333	0.06	8040
55	180	45	0.0741	0.03	8045
60	180	45	0.1111	0.05	8050
155	180	45	0.8148	0.66	8055
180	180	45	1.0000	1.00	8060
177	180	45	0.9778	0.95	8065
180	180	45	1.0000	1.00	8070
139	180	45	0.6963	0.50	8075
172	180	45	0.9407	0.87	8080
132	180	45	0.6444	0.45	8085
170	180	45	0.9259	0.84	8090
178	180	45	0.9852	0.97	8095
120	180	45	0.5556	0.36	8100
195	180	45	1.1111	1.00	8105
183	180	45	1.0222	1.00	8110
195	180	45	1.1111	1.00	8115
133	180	45	0.6519	0.45	8120
127	180	45	0.6074	0.41	8125
142	180	45	0.7185	0.53	8130
125	180	45	0.5926	0.39	8135
73	180	45	0.2074	0.10	8140
74	180	45	0.2148	0.11	8145
57	180	45	0.0889	0.04	8150
57	180	45	0.0889	0.04	8155
50	180	45	0.0370	0.02	8160
160	180	45	0.8519	0.71	8165
170	180	45	0.9259	0.84	8170
175	180	45	0.9630	0.92	8175
145	180	45	0.7407	0.56	8180
177	180	45	0.9778	0.95	8185
145	180	45	0.7407	0.56	8190
95	180	45	0.3704	0.21	8195
180	180	45	1.0000	1.00	8200
170	180	45	0.9259	0.84	8205
190	180	45	1.0741	1.00	8210
147	180	45	0.7556	0.58	8215
170	180	45	0.9259	0.84	8220
170	180	45	0.9259	0.84	8225
160	180	45	0.8519	0.71	8230
162	180	45	0.8667	0.74	8235
107	180	45	0.4593	0.27	8240
160	180	45	0.8519	0.71	8245
150	180	45	0.7778	0.61	8250
180	180	45	1.0000	1.00	8255

Table A.9 Shale volume (Vsh) calculation from **well: J** (continued)

Vsh.calculation (Clavier Eq.)					Depth
GR.	Max	Min	GR.fraction	Vsh.	(feet)
160	180	45	0.8519	0.71	8260
115	180	45	0.5185	0.32	8265
185	180	45	1.0370	1.00	8270
110	180	45	0.4815	0.29	8275
110	180	45	0.4815	0.29	8280
120	180	45	0.5556	0.36	8285
180	180	45	1.0000	1.00	8290
170	180	45	0.9259	0.84	8295
120	180	45	0.5556	0.36	8300
138	180	45	0.6889	0.50	8305
138	180	45	0.6889	0.50	8310
92	180	45	0.3481	0.19	8315
115	180	45	0.5185	0.32	8320
100	180	45	0.4074	0.23	8325
70	180	45	0.1852	0.09	8330
50	180	45	0.0370	0.02	8335
160	180	45	0.8519	0.71	8340
173	180	45	0.9481	0.89	8345
180	180	45	1.0000	1.00	8350
187	180	45	1.0519	1.00	8355
177	180	45	0.9778	0.95	8360
190	180	45	1.0741	1.00	8365
130	180	45	0.6296	0.43	8370
187	180	45	1.0519	1.00	8375
140	180	45	0.7037	0.51	8380
195	180	45	1.1111	1.00	8385
165	180	45	0.8889	0.78	8390
80	180	45	0.2593	0.13	8395
110	180	45	0.4815	0.29	8400
125	180	45	0.5926	0.39	8405
80	180	45	0.2593	0.13	8410
60	180	45	0.1111	0.05	8415
63	180	45	0.1333	0.06	8420
50	180	45	0.0370	0.02	8425
52	180	45	0.0519	0.02	8430
142	180	45	0.7185	0.53	8435
180	180	45	1.0000	1.00	8440
180	180	45	1.0000	1.00	8445
178	180	45	0.9852	0.97	8450
185	180	45	1.0370	1.00	8455
120	180	45	0.5556	0.36	8460
200	180	45	1.1481	1.00	8465
190	180	45	1.0741	1.00	8470
130	180	45	0.6296	0.43	8475
200	180	45	1.1481	1.00	8480
107	180	45	0.4593	0.27	8485
125	180	45	0.5926	0.39	8490

Vsh.calculation (Clavier Eq.)					Depth
GR.	Max	Min	GR.fraction	Vsh.	(feet)
117	180	45	0.5333	0.34	8495
160	180	45	0.8519	0.71	8500
197	180	45	1.1259	1.00	8505
145	180	45	0.7407	0.56	8510
140	180	45	0.7037	0.51	8515
160	180	45	0.8519	0.71	8520
170	180	45	0.9259	0.84	8525
142	180	45	0.7185	0.53	8530
175	180	45	0.9630	0.92	8535
70	180	45	0.1852	0.09	8540
58	180	45	0.0963	0.04	8545
75	180	45	0.2222	0.11	8550
70	180	45	0.1852	0.09	8555
187	180	45	1.0519	1.00	8560
190	180	45	1.0741	1.00	8565
187	180	45	1.0519	1.00	8570
120	180	45	0.5556	0.36	8575
197	180	45	1.1259	1.00	8580
139	180	45	0.6963	0.50	8585
180	180	45	1.0000	1.00	8590
200	200	60	1.0000	1.00	8595
180	200	60	0.8571	0.72	8600
179	200	60	0.8500	0.71	8605
125	200	60	0.4643	0.28	8610
72	200	60	0.0857	0.04	8615
200	200	60	1.0000	1.00	8620
200	200	60	1.0000	1.00	8625
120	200	60	0.4286	0.25	8630
180	200	60	0.8571	0.72	8635
200	200	60	1.0000	1.00	8640
100	200	60	0.2857	0.15	8645
97	200	60	0.2643	0.13	8650
157	200	60	0.6929	0.50	8655
70	200	60	0.0714	0.03	8660
200	200	60	1.0000	1.00	8665
200	200	60	1.0000	1.00	8670
175	200	60	0.8214	0.67	8675
170	200	60	0.7857	0.62	8680
128	200	60	0.4857	0.29	8685
108	200	60	0.3429	0.19	8690
128	200	60	0.4857	0.29	8695
200	200	60	1.0000	1.00	8700
200	200	60	1.0000	1.00	8705
125	200	60	0.4643	0.28	8710
190	200	60	0.9286	0.85	8715
178	200	60	0.8429	0.70	8720

APPENDIX B

REPEAT FORMATION TEST

REPEAT FORMATION TESTER DATA:

Well: **F**

Horizon/ test#: **U-C6/ # 19,20,21,22,23,24,25,26,27,28,28.**

Record test			Fluid type
Pressure (psi.)	Depth (ft.)	Grad. To depth above	from log
2817.60	6574.3		oil
2819.40	6580.9	0.2727	oil
2822.08	6589.2	0.3229	oil
2824.60	6597.4	0.3073	oil
2829.80	6614.0	0.3133	oil
2832.00	6621.5	0.2933	oil
2834.13	6629.0	0.2840	oil

Linear equasion from pressure Vs. depth plot.

Oil Y1 = 3.2692X1 - 2636.7

Estimate water Y2 = 2.4386X2 - 266.73

Solve for fluid contact:

		Slope	Cons
Equation 1	y1	3.2692	-2636.7
Equation 2	y2	2.4386	-266.73
Co-ordinate	x =	2853.32	
Hydrocarbon contact depth	y =	6691	ft.

Formation data:

	depth (feet)	Pressure (psi)
Top sand:	6564	2800
	6564	2860
Base sand:	6634	2800
	6634	2860

Contact plot:

Xw1 =	2805	Yw1 =	6573.54	ft.
Xw2 =	2845	Yw2 =	6671.09	ft.

OWC:

x =	2800	y =	6691
	2860		6691

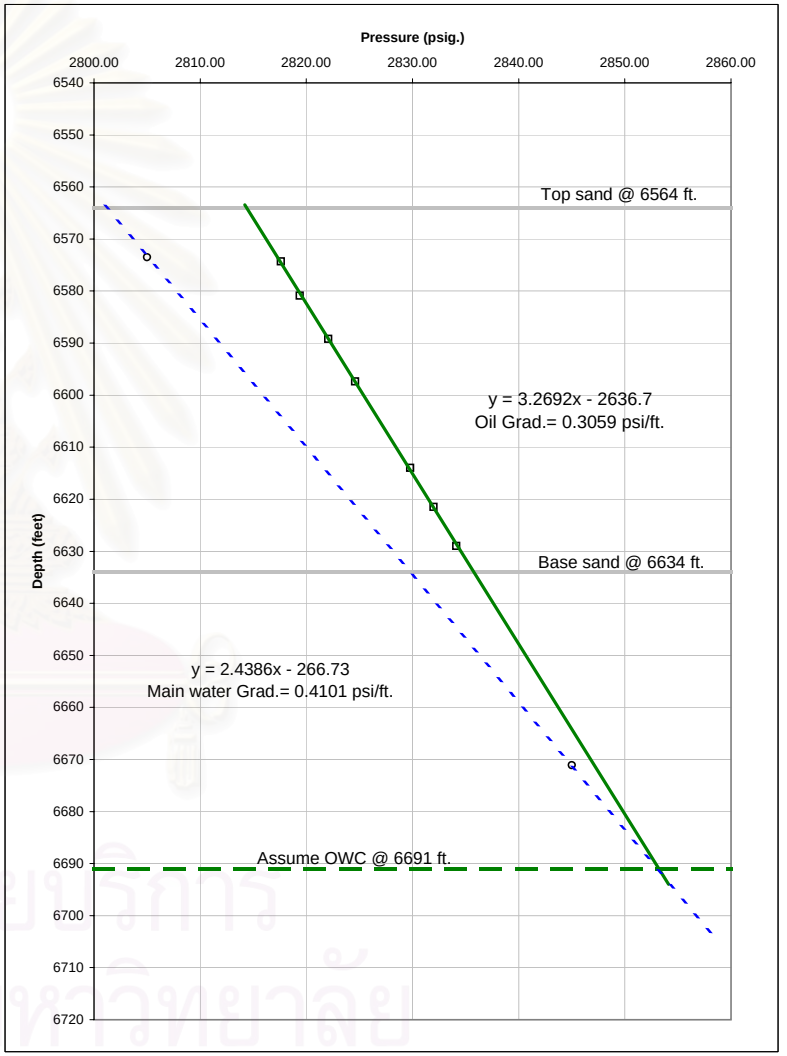

Figure B.1 Pressure-depth diagram represents pore-pressure profile in horizon U-C6 of well F

REPEAT FORMATION TESTER DATA:

Well: **I**
Horizon/ test#: **U-C6/ # 5,6,9,10,11.**

Record test			Fluid type
Pressure (psi.)	Depth (ft.)	Grad. To depth above	from log
2910.05	6812.7		oil
2915.11	6829.7	0.2976	oil
2923.54	6859.0	0.2877	oil
2921.88	6852.0	0.2371	oil
2926.50	6869.5	0.2640	oil

Linear equasion from pressure Vs. depth plot.

Oil Y1 = 3.4365X1 - 3188.1
Estimate water Y2 = 2.4115X2 - 177.63

Solve for fluid contact:

		Slope	Cons
Equation 1	y1	3.4365	-3188.1
Equation 2	y2	2.4115	-177.63
Co-ordinate	x =	2937.04	
Hydrocarbon contact depth	y =	6905	ft.

Formation data:

	depth (feet)	Pressure (psi)
Top sand:	6809	2890
	6809	2950
Base sand:	6878	2890
	6878	2950

Contact plot:

Xw1 =	2905	Yw1 =	6827.78	ft.
Xw2 =	2940	Yw2 =	6912.18	ft.

OWC:

x =	2890	y =	6905
	2950		6905

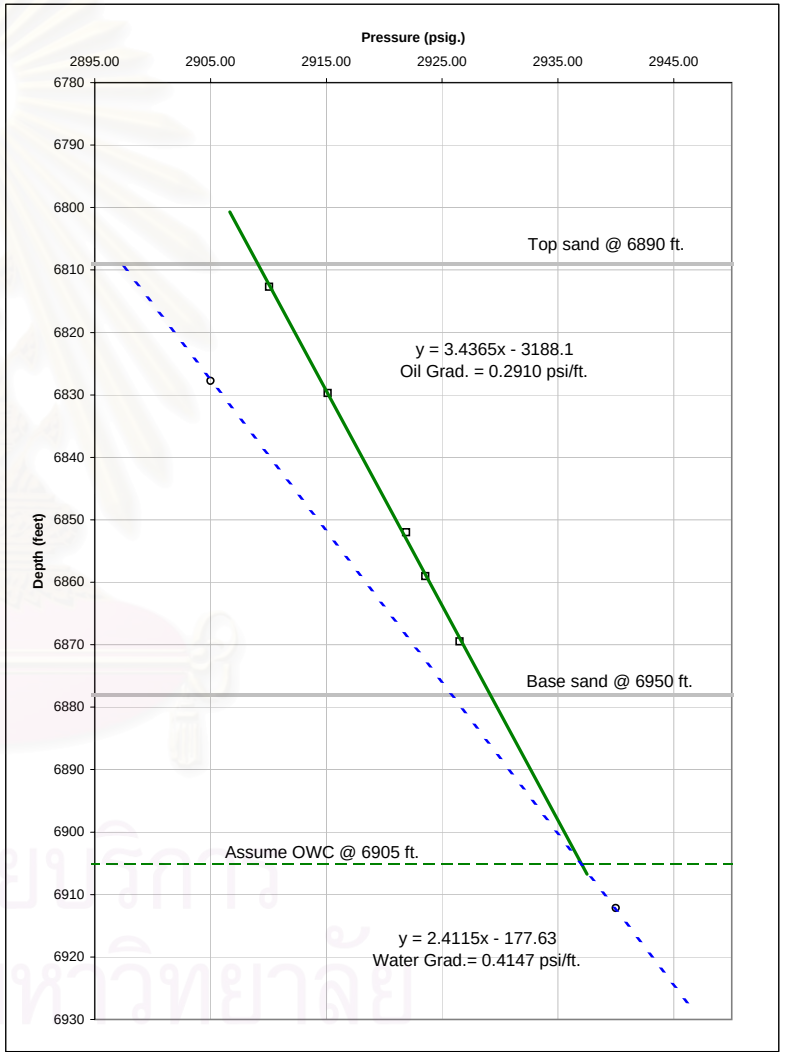

Figure B.2 Pressure-depth diagram represents pore-pressure profile in horizon U-C6 of well I

REPEAT FORMATION TESTER DATA:

Well: **F**
Horizon/ test#: **U-B2/ # 30,31,32,33.**

Record test			Fluid type
Pressure (psi.)	Depth (ft.)	Grad. To depth above	from log
2945.12	6916.0		water
2949.00	6924.5	0.4565	water
2952.73	6933.1	0.4337	water
2960.61	6952.7	0.4020	water

Linear equasion from pressure Vs. depth plot.

Sand wet Y1 = 2.3783X1 - 88.801
Estimate water Y2 = 2.4386X2 - 266.73

Solve for fluid contact:

		Slope	Cons
Equation 1	y1	2.3783	-88.801
Equation 2	y2	2.4386	-266.73
Co-ordinate	x =	2950.73	
Main water contact depth	y =	6929	ft.

Formation data:

	depth (feet)	Pressure (psi)
Top sand:	6905	2930
	6905	2980
Base sand:	6955	2930
	6955	2980

Contact plot:

Xw1 =	2940	Yw1 =	6902.75	ft.
Xw2 =	2970	Yw2 =	6975.91	ft.

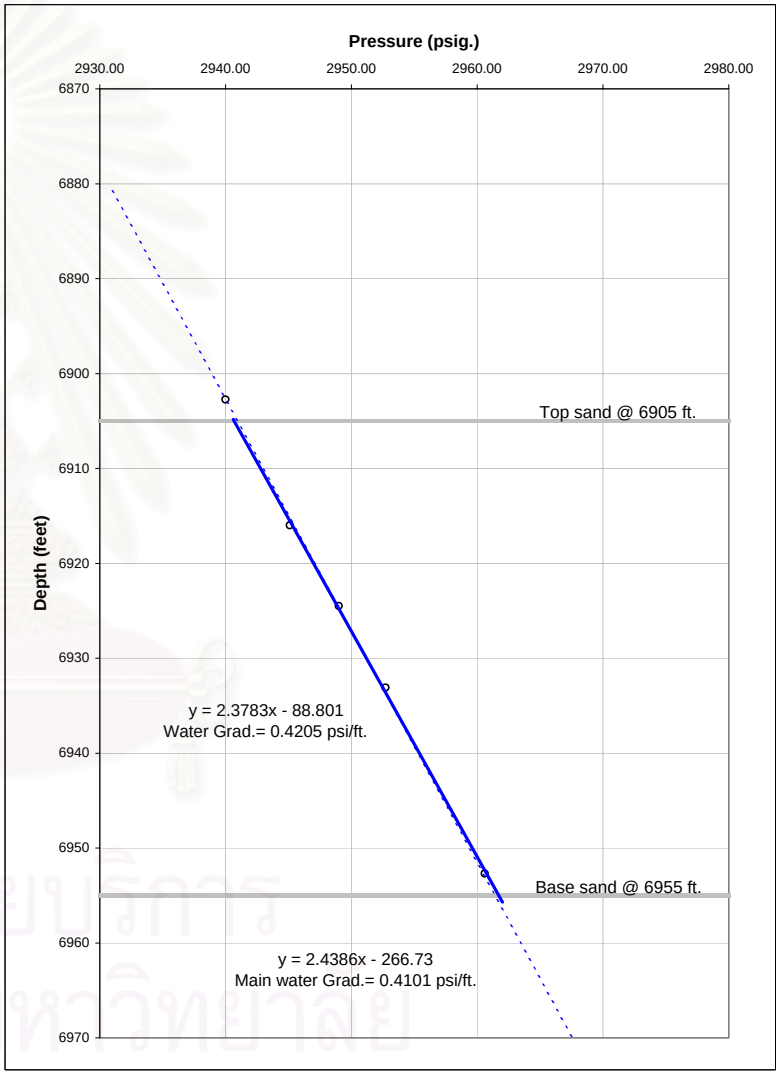

Figure B.3 Pressure-depth diagram represents pore-pressure profile in horizon U-B2 of well F

REPEAT FORMATION TESTER DATA:

Well: **I**
Horizon/ test#: **U-B2/ # 16,17,18,19,20.**

Record test			Fluid type
Pressure (psi.)	Depth (ft.)	Grad. To depth above	from log
3069.21	7181.0		gas
3069.92	7190.1	0.0780	gas
3070.78	7199.1	0.0956	gas
3071.43	7206.4	0.0890	gas

Linear equasion from pressure Vs. depth plot.

Gas Y1 = 11.32X1 - 27562
Estimate water Y2 = 2.4115X2 - 177.63

Solve for fluid contact:

		Slope	Cons	
Equation 1	y1	11.32	-27562	
Equation 2	y2	2.4115	-177.63	
Co-ordinate	x =	3073.96		
Hydrocarbon contact depth	y =	7235		ft.

Formation data:

	depth (feet)	Pressure (psi)
Top sand:	7173	3050
	7173	3090
Base sand:	7212	3050
	7212	3090

Contact plot:

Xw1 =	3055	Yw1 =	7189.50	ft.
Xw2 =	3080	Yw2 =	7249.79	ft.

GWC:

x =	3050	y =	7235
	3090		7235

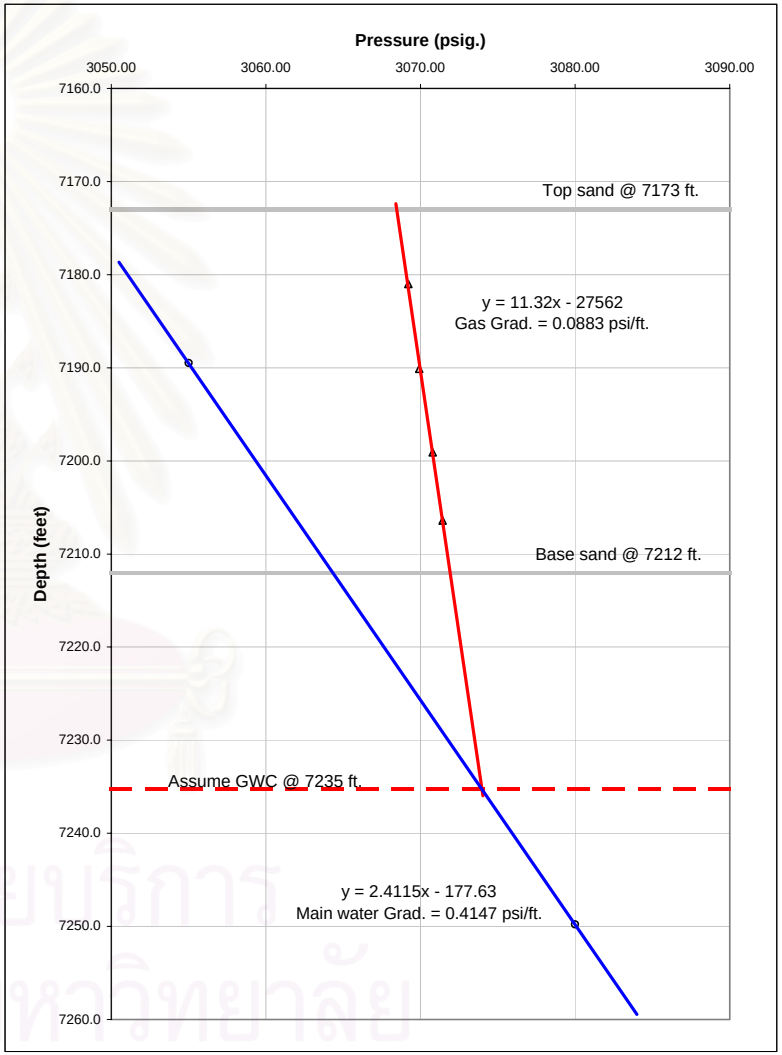

Figure B.4 Pressure-depth diagram represents pore-pressure profile in horizon U-B2 of well I

REPEAT FORMATION TESTER DATA:

Well: **F**
Horizon/ test#: **U-B3/ # 34,35,37,42.**

Record test			Fluid type
Pressure (psi.)	Depth (ft.)	Grad. To depth above	from log
3086.89	7037.5		gas
3087.43	7044.3	0.0794	gas
3087.90	7049.5	0.0904	gas

Linear equasion from pressure Vs. depth plot.

Gas Y1 = 11.899X1 - 29692
Estimate water Y2 = 2.4386X2 - 266.73

Solve for fluid contact:

			Slope	Cons
	Equation 1	y1	11.899	-29692
	Equation 2	y2	2.4386	-266.73
	Co-ordinate	x =	3110.36	
Hydrocarbon contact depth		y = (possible)	7318	ft.

Formation data:

	depth (feet)	Pressure (psi)
Top sand:	7034	3060
	7034	3120
Base sand:	7053	3060
	7053	3120

Contact plot:

Xw1 =	3070	Yw1 =	7219.77	ft.
Xw2 =	3110	Yw2 =	7317.32	ft.

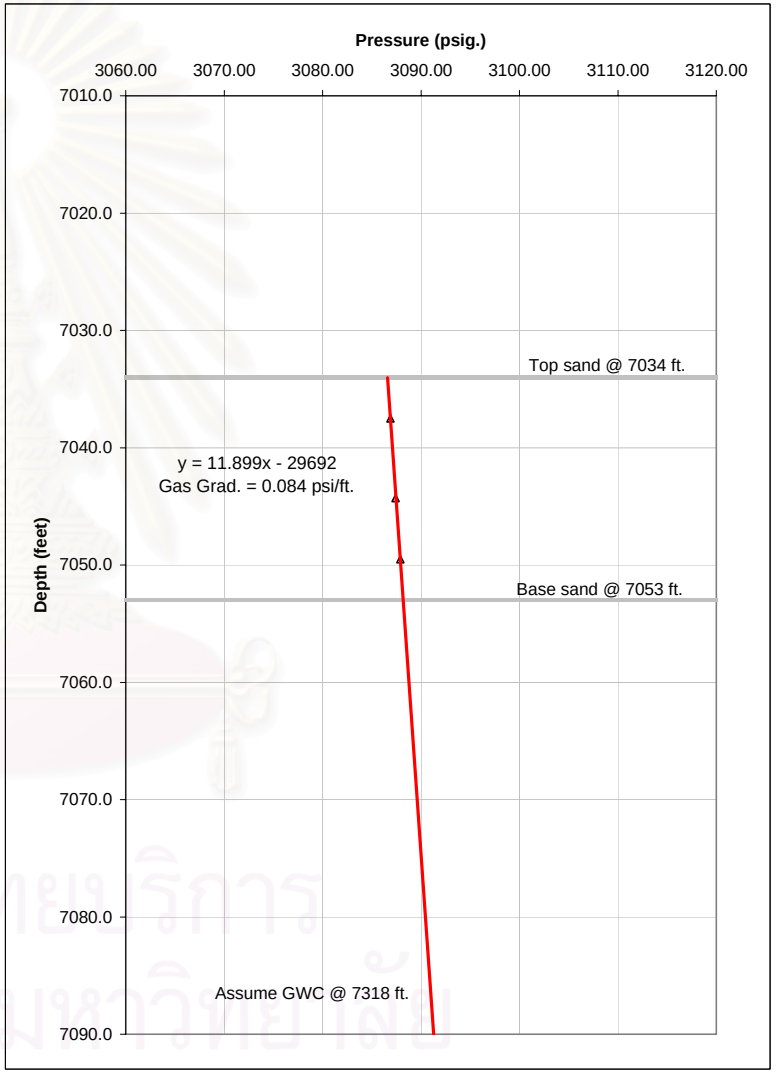

Figure B.5 Pressure-depth diagram represents pore-pressure profile in horizon U-B3 of well F

REPEAT FORMATION TESTER DATA:

Well: **E**
Horizon/ test#: **U-B3/ # 4,5,6.**

Record test			Fluid type
Pressure (psi.)	Depth (ft.)	Grad. To depth above	from log
3095.82	7144.5		gas
3096.20	7153.2	0.0437	gas
3096.75	7160.3	0.0775	gas

Linear equasion from pressure Vs. depth plot.

Gas Y1 = 16.698X1 - 44550
Estimate water Y2 = 2.4246X2 - 231.88

Solve for fluid contact:

			Slope	Cons
	Equation 1	y1	16.698	-44550
	Equation 2	y2	2.4246	-231.88
	Co-ordinate	x =	3104.94	
Hydrocarbon contact depth		y = (possible)	7296	ft.

Formation data:

	depth (feet)	Pressure (psi)
Top sand:	7140	3070
	7140	3130
Base sand:	7165	3070
	7165	3130

Contact plot:

Xw1 =	3070	Yw1 =	7211.64	ft.
Xw2 =	3110	Yw2 =	7308.63	ft.

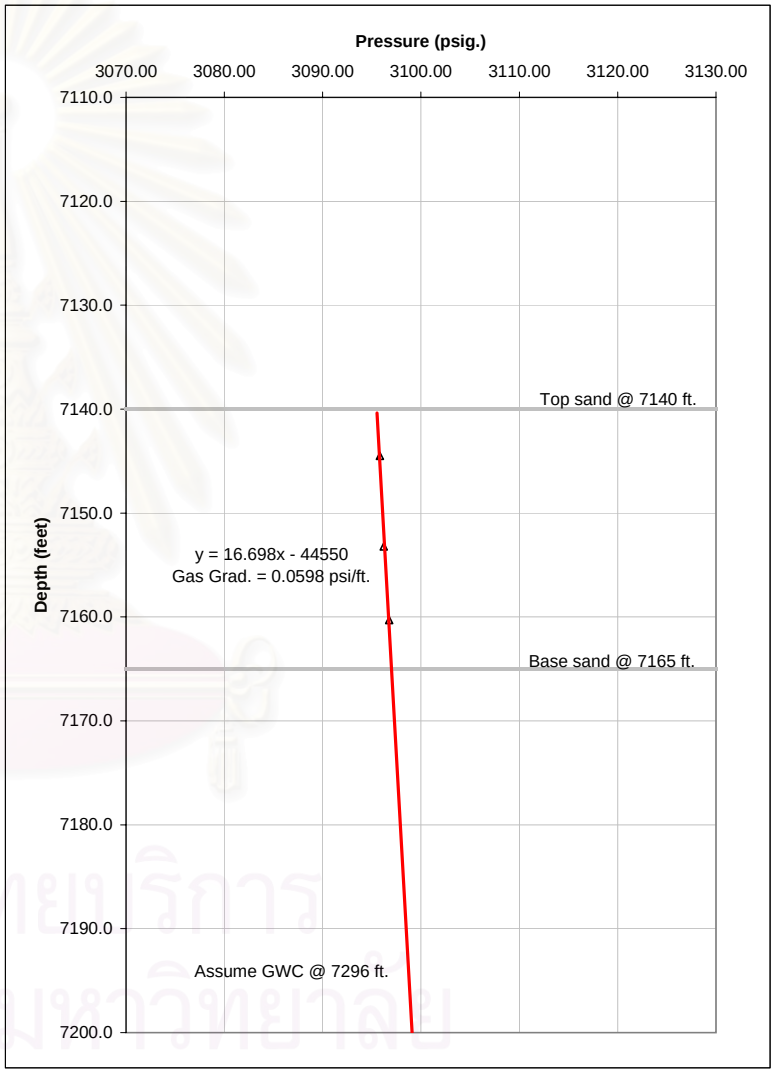

Figure B.6 Pressure-depth diagram represents pore-pressure profile in horizon U-B3 of well E

REPEAT FORMATION TESTER DATA:

Well: **D**
Horizon/ test#: **U-B3/ # 6,7,8.**

Record test			Fluid type
Pressure (psi.)	Depth (ft.)	Grad. To depth above	from log
3100.82	7172.2		gas
3101.53	7178.8	0.1076	gas
3101.73	7186.3	0.0267	gas

Linear equasion from pressure Vs. depth plot.

Gas Y1 = 13.859X1 - 35802
Estimate water Y2 = 2.3927X2 - 132.51

Solve for fluid contact:

		Slope	Cons
Equation 1	y1	13.859	-35802
Equation 2	y2	2.3927	-132.51
Co-ordinate	x =	3110.81	
Hydrocarbon contact depth	y = (possible)	7311	ft.

Formation data:

	depth (feet)	Pressure (psi)
Top sand:	7167	3070
	7167	3130
Base sand:	7192	3070
	7192	3130

Contact plot:

Xw1 =	3070	Yw1 =	7213.08	ft.
Xw2 =	3110	Yw2 =	7308.79	ft.

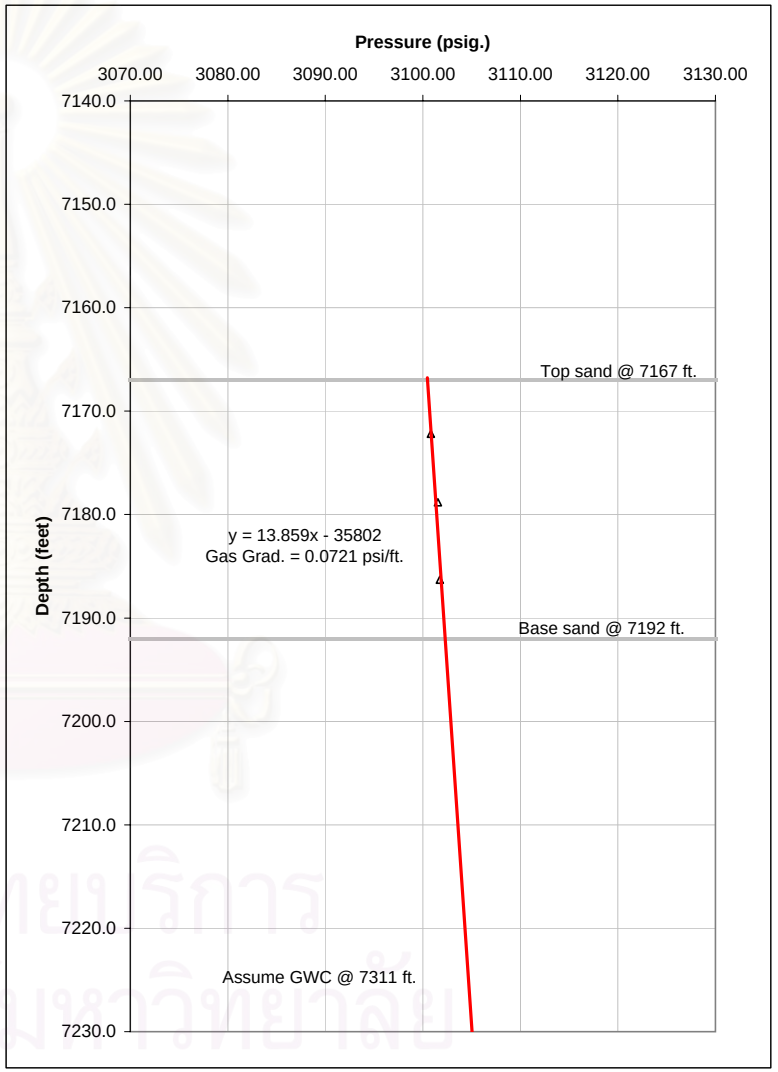

Figure B.7 Pressure-depth diagram represents pore-pressure profile in horizon U-B3 of well D

REPEAT FORMATION TESTER DATA:

Well: **J**
Horizon/ test#: **U-B3/ # 6,7,8.**

Record test			Fluid type
Pressure (psi.)	Depth (ft.)	Grad. To depth above	from log
3103.42	7269.0		gas
3103.63	7271.7	0.0778	gas
3103.92	7277.1	0.0537	gas
3104.61	7282.5	0.1278	gas

Linear equasion from pressure Vs. depth plot.

Gas Y1 = 11.315X1 - 27847
Estimate water Y2 = 2.3033X2 + 137.96

Solve for fluid contact:

		Slope	Cons
Equation 1	y1	11.315	-27847
Equation 2	y2	2.3033	137.96
Co-ordinate	x =	3105.40	
Hydrocarbon contact depth	y = (possible)	7291	ft.

Formation data:

	depth (feet)	Pressure (psi)
Top sand:	7260	3080
	7260	3130
Base sand:	7286	3080
	7286	3130

Contact plot:

Xw1 =	3070	Yw1 =	7209.09	ft.
Xw2 =	3110	Yw2 =	7301.22	ft.

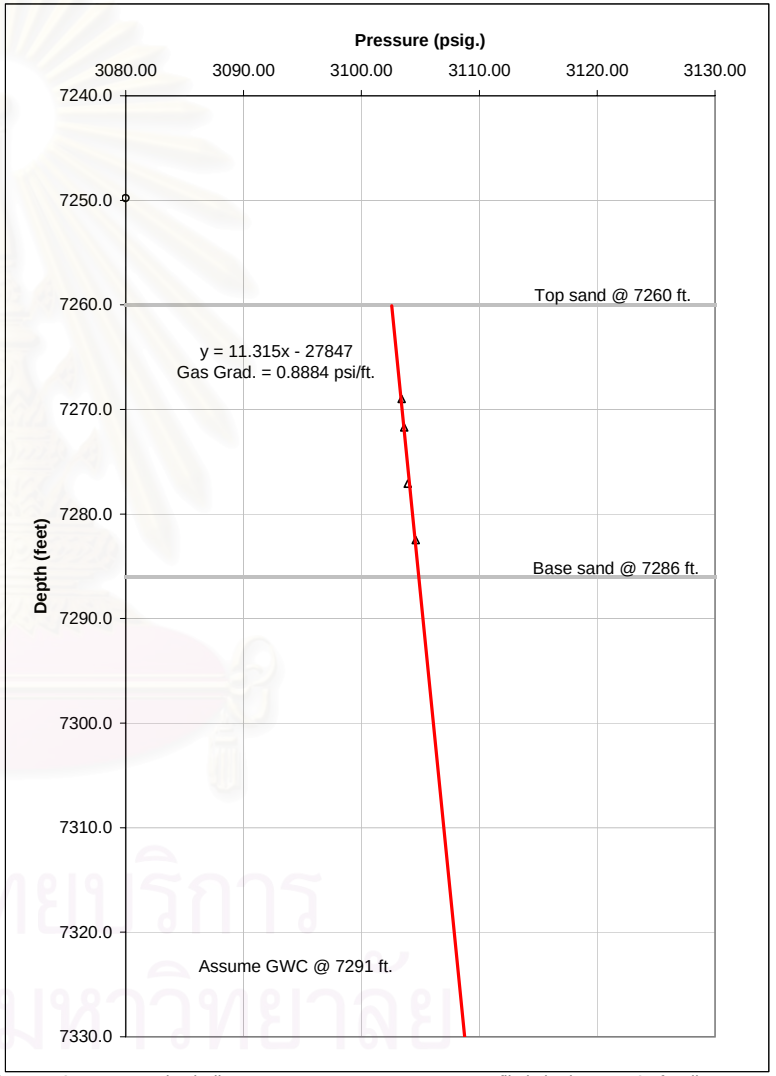

Figure B.8 Pressure-depth diagram represents pore-pressure profile in horizon U-B3 of well J

REPEAT FORMATION TESTER DATA:

Well: **I**
Horizon/ test#: **U-B3/ # 24,25,26.**

Record test			Fluid type
Pressure (psi.)	Depth (ft.)	Grad. To depth above	from log
3090.40	7286.9		water
3094.77	7297.9	0.3973	water
3100.10	7310.7	0.4164	water

Linear equasion from pressure Vs. depth plot.

Sand wet Y1 = 2.4517X1 - 289.81
Estimate water Y2 = 2.4168X2 - 189.35

Solve for fluid contact:

			Slope	Cons
	Equation 1	y1	2.4517	-289.81
	Equation 2	y2	2.4168	-189.35
	Co-ordinate	x =	2878.51	
Main water contact depth		y = (possible)	6767	ft.

Formation data:

	depth (feet)	Pressure (psi)
Top sand:	7282	3060
	7282	3130
Base sand:	7313	3060
	7313	3130

Contact plot:

Xw1 =	3080	Yw1 =	7254.39	ft.
Xw2 =	3110	Yw2 =	7326.90	ft.

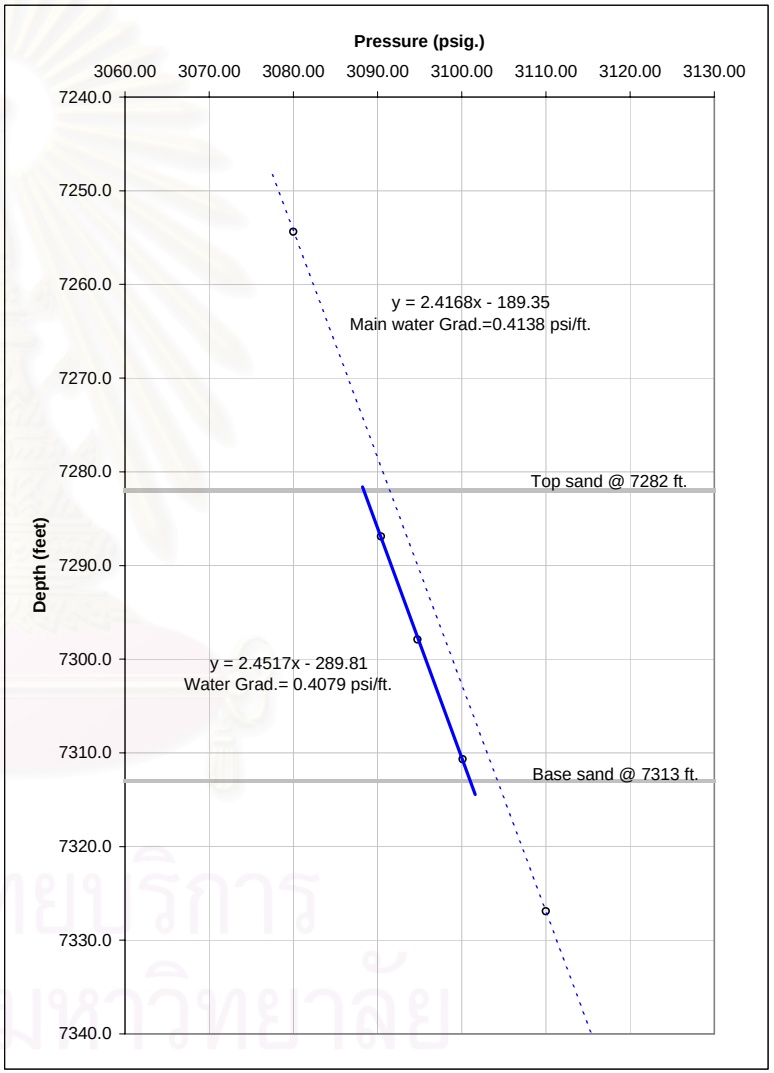

Figure B.9 Pressure-depth diagram represents pore-pressure profile in horizon U-B3 of well I

REPEAT FORMATION TESTER RESERVOIR ZONE DATA:

Well: **F,E,D,J (Upthrown side)**
Horizon: **U-B3**

Record test			Well
Pressure (psi.)	Depth (ft.)	Fluid type	Test
3086.89	7037.5	gas	F
3087.43	7044.3	gas	F
3087.90	7049.5	gas	F
3095.82	7144.5	gas	E
3096.20	7153.2	gas	E
3096.75	7160.3	gas	E
3100.82	7172.2	gas	D
3101.53	7178.8	gas	D
3101.73	7186.3	gas	D
3103.42	7269.0	gas	J
3103.63	7271.7	gas	J
3103.92	7277.1	gas	J
3104.61	7282.5	gas	J

Linear equasion from pressure Vs. depth plot.

GAS $Y_1 = 12.894X_1 - 32772$
MAIN WATER $Y_2 = 2.377X_2 - 93.778$

Solve for fluid contact:			Slope	Cons
	Equation 1	y1	12.894	-32772
	Equation 2	y2	2.377	-93.778
	Co-ordinate	x =	3107.18	
Hydrocarbon contact depth		y = (GWC)	7292	ft.

	Contact plot X	Y
GWC	2900	7292
	3250	7292

Main water			
X1 =	3000	Y1 =	7037.222
X2 =	3200	Y2 =	7512.622

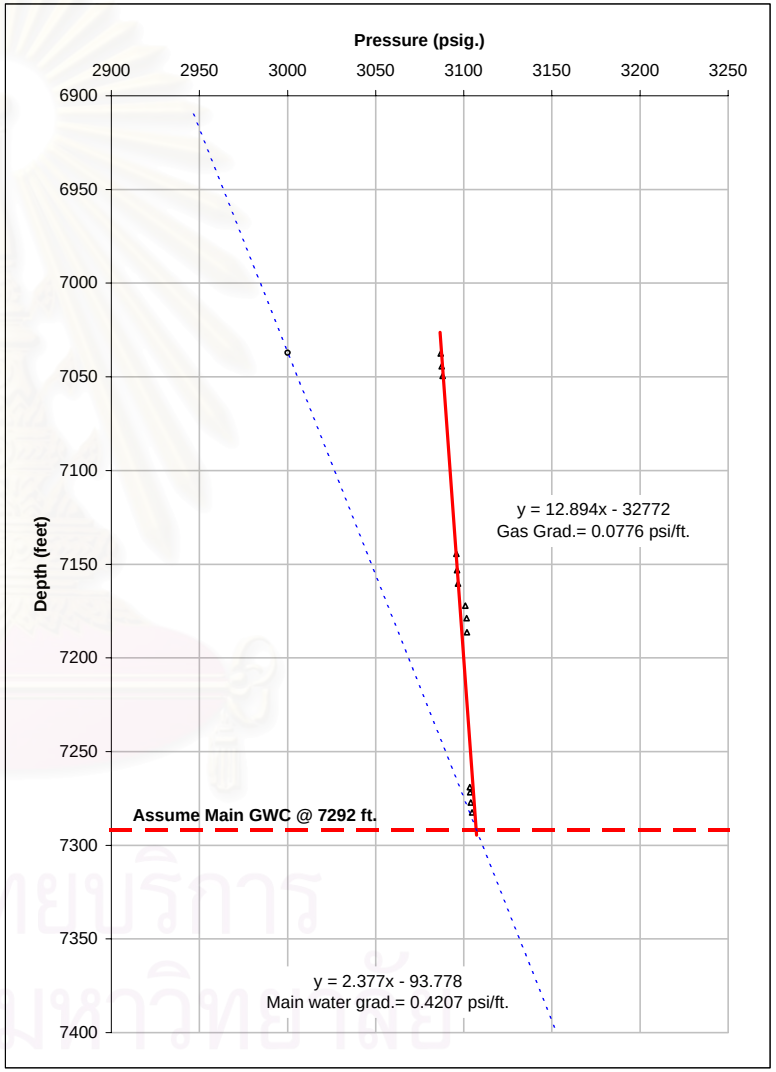

Figure B.10 Pressure-depth diagram represents pore-pressure profile in horizon U-B3 of well F, E, D.

REPEAT FORMATION TESTER RESERVOIR ZONE DATA:

Well: **I (Down thrown side)**
Horizon: **U-B3**

Record test			Well
Pressure (psi.)	Depth (ft.)	Fluid type	Test
3090.40	7286.9	water	I
3094.77	7297.9	water	I
3100.10	7310.7	water	I

Linear equasion from pressure Vs. depth plot.

Sand wet Y1 = 2.4517X1 - 289.81
Main water Y2 = 2.4168X2 - 189.35

Main water

X1 =	3050	Y1 =	7181.89
X2 =	3150	Y2 =	7423.57

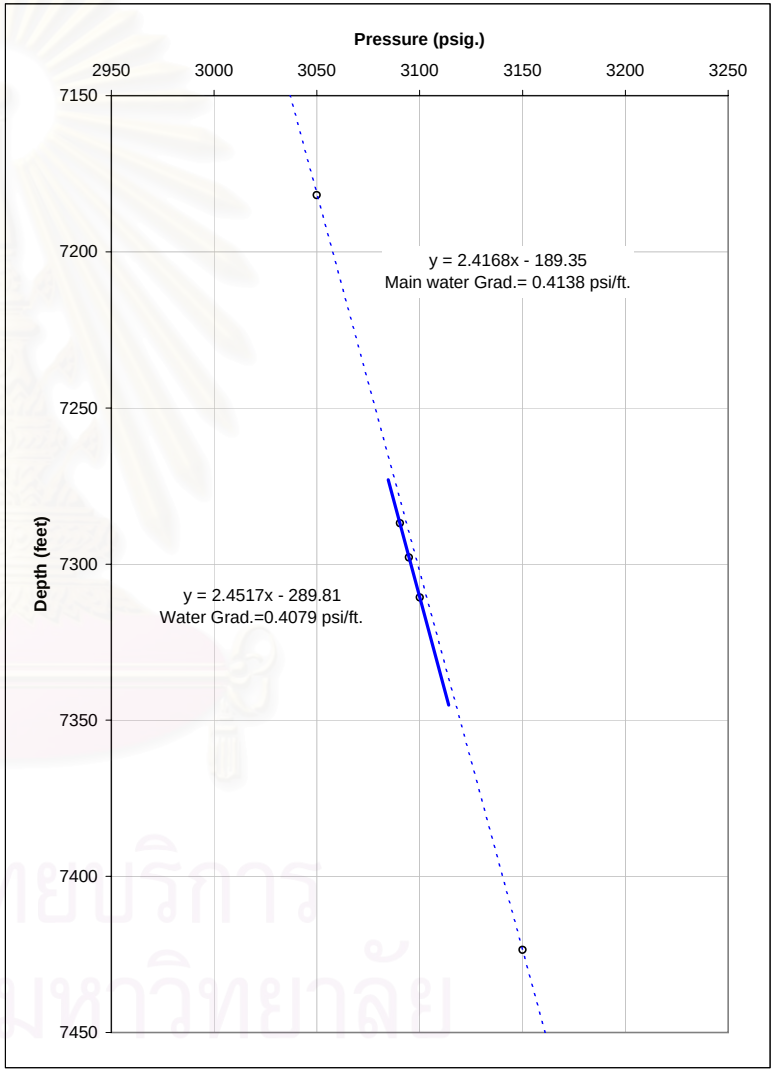

Figure B.11 Pressure-depth diagram represents pore-pressure profile in horizon U-B3 of well I.

REPEAT FORMATION TESTER DATA:

Well: **F**
Horizon/ test#: **U-B4/ # 43,44,45,46,47.**

Record test			Fluid type
Pressure (psi.)	Depth (ft.)	Grad. To depth above	from log
3042.9	7143.5		
3043.90	7144.4	1.1111	water
3046.71	7151.2	0.4132	water
3049.88	7158.0	0.4662	water
3054.61	7171.6	0.3478	water

0.4091

Linear equasion from pressure Vs. depth plot.

Sand wet Y1 = 2.523X1 - 535.61
Estimate water Y2 = 2.386X2 - 266.73

Solve for fluid contact:

			Slope	Cons
	Equation 1	y1	2.523	-535.61
	Equation 2	y2	2.4386	-266.73
	Co-ordinate	x =	3185.78	
Main water contact depth		y =	7502	ft.

Formation data:

	depth (feet)	Pressure (psi)
Top sand:	7135	3020
	7135	3080
Base sand:	7172	3020
	7172	3080

Contact plot:

Xw1 =	3030	Yw1 =	7122.23	ft.
Xw2 =	3060	Yw2 =	7195.39	ft.

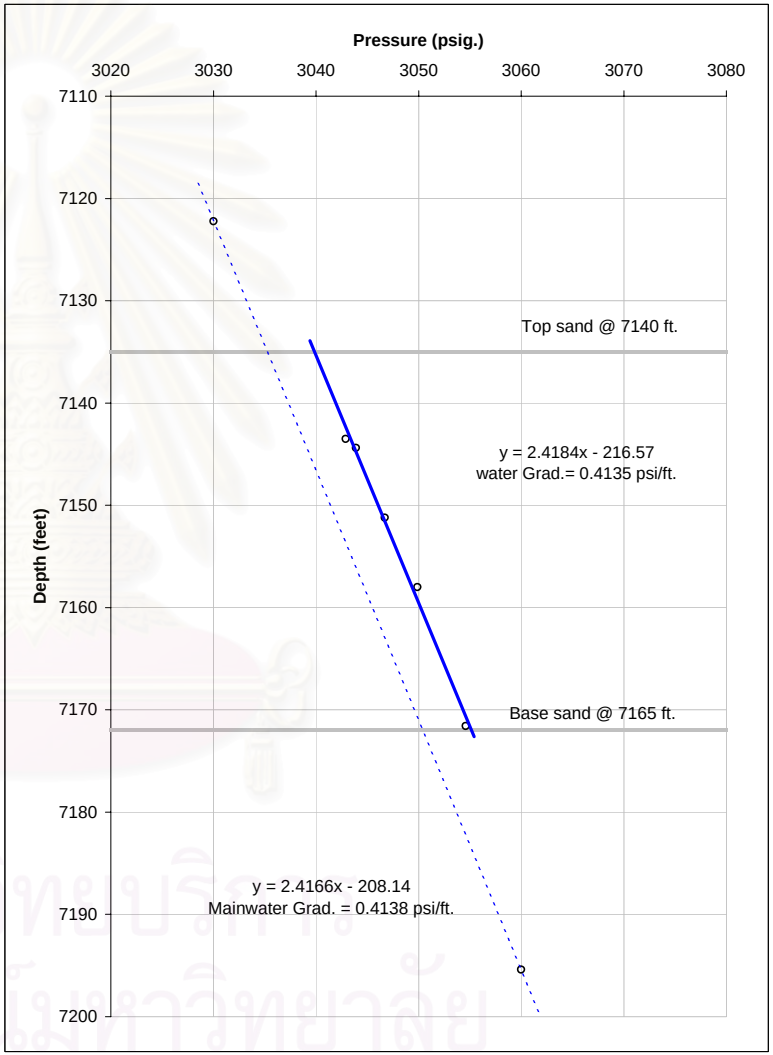

Figure B.12 Pressure-depth diagram represents pore-pressure profile in horizon U-B4 of well F.

REPEAT FORMATION TESTER DATA:

Well: I
Horizon/ test#: U-B4/ # 27,28,29.

Record test			Fluid type
Pressure (psi.)	Depth (ft.)	Grad. To depth above	from log
3154.57	7371.8		
3154.97	7379.9	0.0494	gas
3155.98	7390.8	0.0927	gas

Linear equasion from pressure Vs. depth plot.

Gas Y1 = 12.953X1 - 33489
Estimate water Y2 = 2.4115X2 - 177.63

Solve for fluid contact:

			Slope	Cons
	Equation 1	y1	12.953	-33489
	Equation 2	y2	2.4115	-177.63
	Co-ordinate	x =	3160.02	
Hydrocarbon contact depth		y =(possible)	7443	ft.

Formation data:

	depth (feet)	Pressure (psi)
Top sand:	7370	3130
	7370	3180
Base sand:	7400	3130
	7400	3180

Contact plot:

Xw1 =	3135	Yw1 =	7382.42	ft.
Xw2 =	3170	Yw2 =	7466.83	ft.

GWC:

x =	3130	y =	7443
	3180		7443

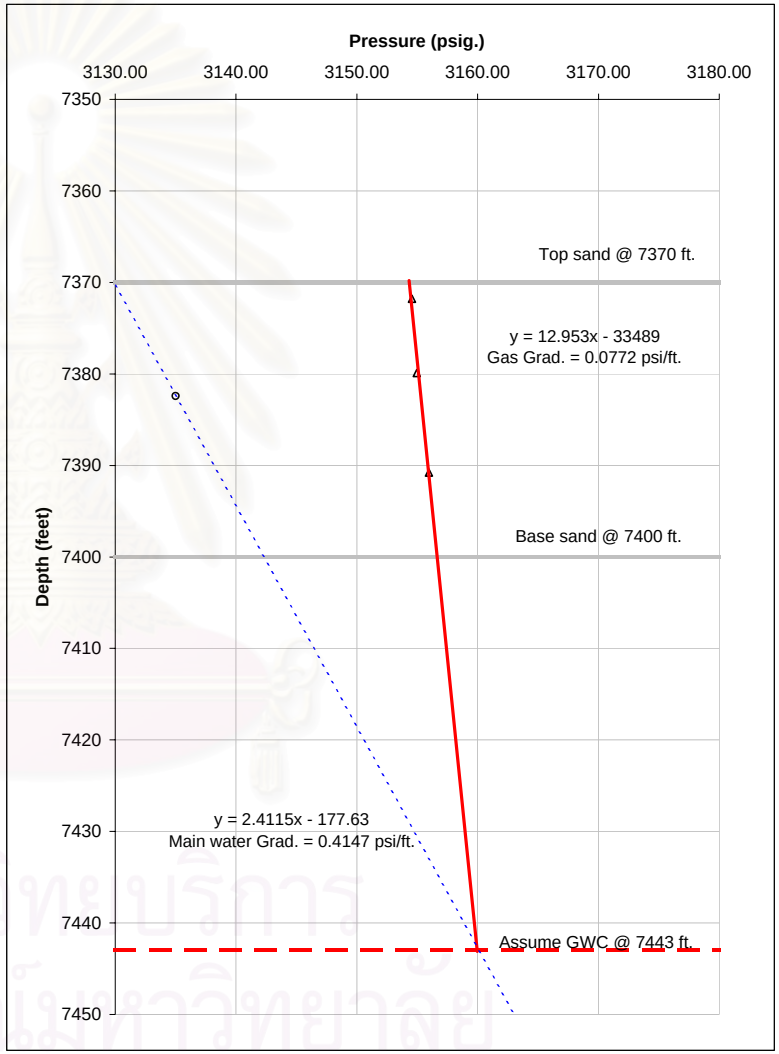

Figure B.13 Pressure-depth diagram represents pore-pressure profile in horizon U-B4 of well I.

REPEAT FORMATION TESTER DATA:

Well: **B**
Horizon/ test#: **U-B4/ # 11,12,13,14.**

Record test			Fluid type
Pressure (psi.)	Depth (ft.)	Grad. To depth above	from log
3014.48	7425.5		
3014.57	7433.1	0.0118	gas
3024.54	7450.3	0.5797	water
3039.23	7472.7	0.6558	water

Linear equasion from pressure Vs. depth plot.

Gas	Y1 = 84.444X1 - 247131
Water zone	Y2 = 1.5248X2 + 2838.3
Estimate water	Y3 = 2.219X3 + 440.02

Solve for fluid contact:

		Slope	Cons
Equation 1	y1	84.444	-247131
Equation 2	y2	1.5248	2838.3
Co-ordinate	x1 =	3014.61	
Hydrocarbon contact depth	y =(GWC)	7435	ft.

Formation data:

	depth (feet)	Pressure (psi)
Top sand:	7423	2990
	7423	3090
Base sand:	7474	2990
	7474	3090

Contact plot:

Xw1 =	3100	Yw1 =	7318.92	ft.
Xw2 =	3150	Yw2 =	7429.87	ft.

GWC:

x =	2990	y =	7435
	3090		7435

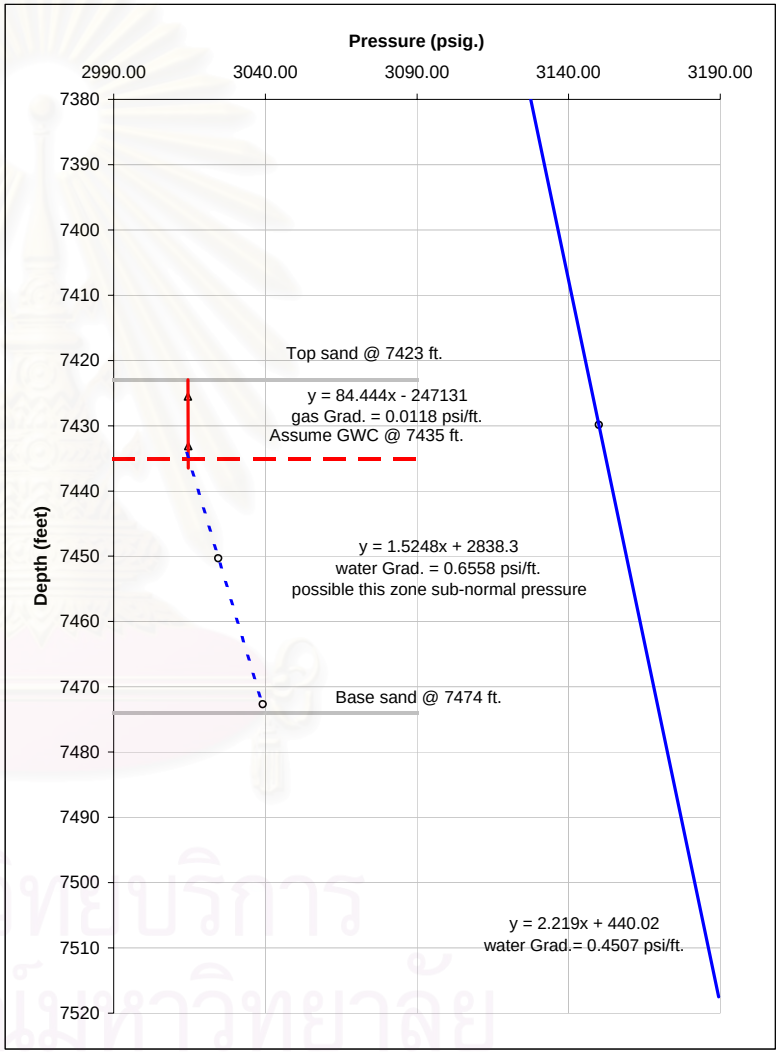

Figure B.14 Pressure-depth diagram represents pore-pressure profile in horizon U-B4 of well B.

REPEAT FORMATION TESTER RESERVOIR ZONE DATA:

Well: **F,E,D,J (Upthrown side)**
Horizon: **U-B4**

Record test			Well
Pressure (psi.)	Depth (ft.)	Fluid type	Test
3042.90	7143.5	water	F
3043.90	7144.4	water	F
3046.71	7151.2	water	F
3049.88	7158.0	water	F
3054.61	7171.6	water	F

Linear equasion from pressure Vs. depth plot.

Sand wet 2.6058X1 - 787.82
Estimate water : 2.377X2 - 93.778

Solve for fluid contact:

			Slope	Cons
	Equation 1	y1	2.6058	-787.82
	Equation 2	y2	2.377	-93.778
	Co-ordinate	x =	3033.40	
Main water contact depth		y =	7117	ft.

Main water
X1 = 3000 Y1 = 7037.222
X2 = 3150 Y2 = 7393.772

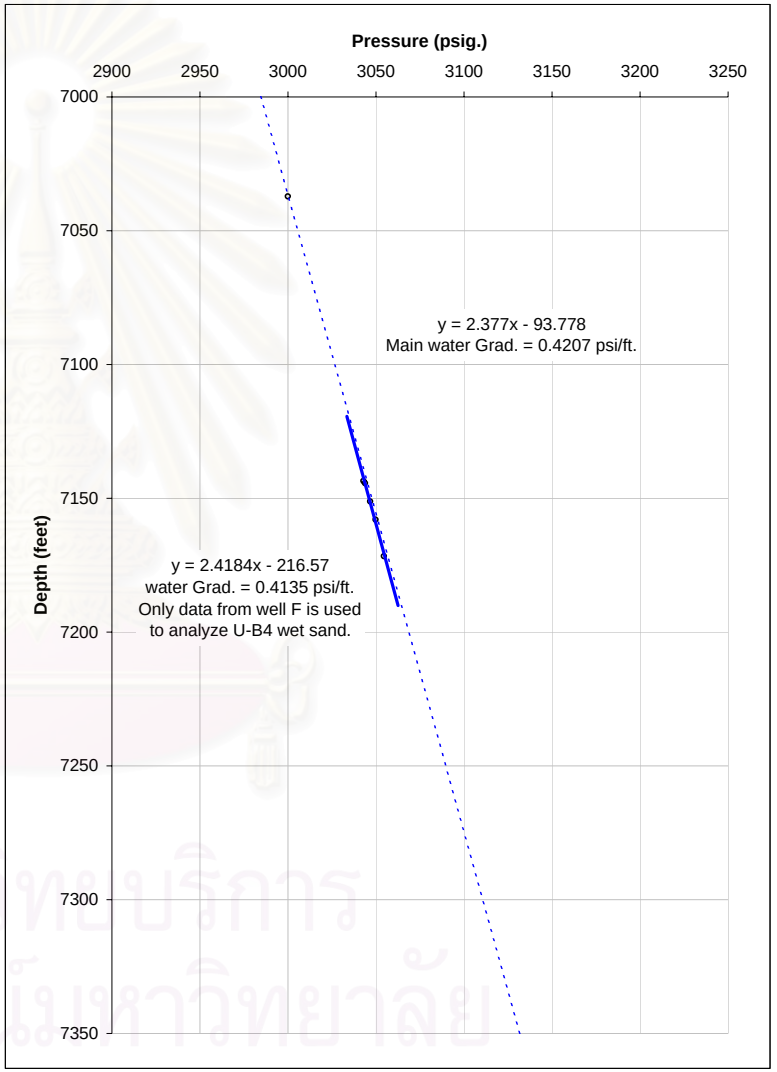

Figure B.15 Pressure-depth diagram represents pore-pressure profile in horizon U-B4 of well F, E, D, J.

REPEAT FORMATION TESTER RESERVOIR ZONE DATA:

Well: **I and B (Down thrown side)**
Horizon: **U-B4**

Record test			Well
Pressure (psi.)	Depth (ft.)	Fluid type	Test
3154.57	7371.8	gas	I
3154.97	7379.9	gas	I
3155.98	7390.8	gas	I
3014.48	7425.5	gas	B
3014.57	7433.1	gas	B
3024.54	7450.3	water	B
3039.23	7472.7	water	B

Linear equasion from pressure Vs. depth plot.

GAS (main)	Y1 = 12.953X1 - 33489
WATER	Y2 = 2.4115X2 - 177.63
GAS (well B)	Y3 = 84.444X3 - 247131
Water (well B)	Y4 = 1.5248X4 + 2838.3
Water(down th)	Y5 = 2.4168X5 - 189.35

Solve for fluid contact:			Slope	Cons	
	Equation 1	y1	12.953	-33489	
	Equation 2	y2	2.4115	-177.63	
	Equation 3	y3	84.444	-247131	
	Equation 4	y4	1.5248	2838.3	
	Equation 5	y5	2.4168	-189.35	
	Co-ordinate	x1 =	3160.02		
Hydrocarbon contact depth		y1 = (GWC) well I	7443	ft.	
	Co-ordinate	x3 =	3014.61		
Hydrocarbon contact depth		y3 = (GWC) sub.	7435	ft.	
	Co-ordinate	x1 =	3160.50		
Hydrocarbon contact depth		y1 = (GWC) main	7449	ft.	

Contact plot

	X	Y
GWC well B	2950	7443
	3350	7443
GWC sub.	2950	7435
	3100	7435
GWC main	2950	7449
	3350	7449

Main water down throw side.

X1 =	3100	Y1 =	7302.73
X2 =	3200	Y2 =	7544.41

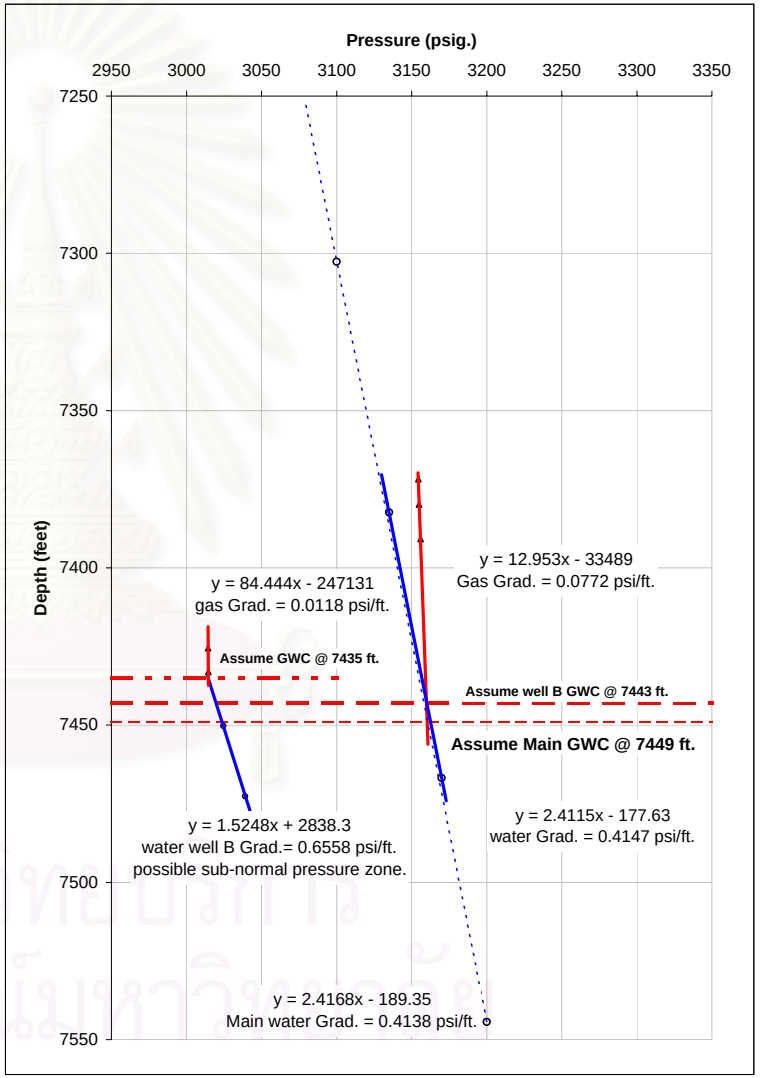

Figure B.16 Pressure-depth diagram represents pore-pressure profile in horizon U-B4 of well B, I.

REPEAT FORMATION TESTER DATA:

Well: **I**
Horizon/ test#: **U-B5/ # 40,41,42.**

Record test			Fluid type
Pressure (psi.)	Depth (ft.)	Grad. To depth above	from log
3371.39	7740.9		gas
3372.96	7755.7	0.1061	gas
3373.70	7769.5	0.0536	gas

Linear equasion from pressure Vs. depth plot.

Gas Y1 = 11.92X1 - 32446
Estimate water Y2 = 2.4115X2 - 177.63

Solve for fluid contact:

			Slope	Cons
	Equation 1	y1	11.92	-32446
	Equation 2	y2	2.4115	-177.63
	Co-ordinate	x =	3393.63	
Hydrocarbon contact depth		y =(possible)	8006	ft.

Formation data:

	depth (feet)	Pressure (psi)
Top sand:	7738	3350
	7738	3400
Base sand:	7771	3350
	7771	3400

Contact plot:

Xw1 =	3360	Yw1 =	7925.01	ft.
Xw2 =	3390	Yw2 =	7997.36	ft.

GWC:

x =	3350	y =	8006
	3400		8006

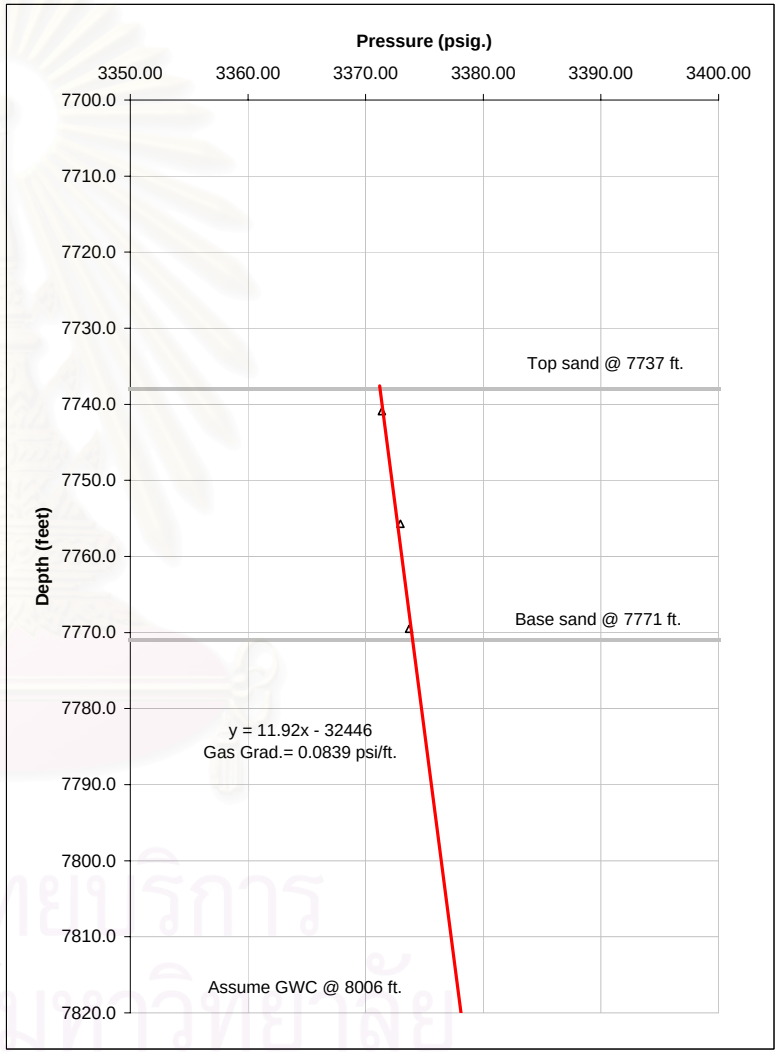

Figure B.17 Pressure-depth diagram represents pore-pressure profile in horizon U-B5 of well I.

REPEAT FORMATION TESTER DATA:

Well: **B**
Horizon/ test#: **U-B5/ # 27,28,29.**

Record test			Fluid type
Pressure (psi.)	Depth (ft.)	Grad. To depth above	from log
3385.87	7878.0		gas
3386.29	7885.3	0.0575	gas
3387.02	7894.1	0.0830	gas

Linear equasion from pressure Vs. depth plot.

Gas Y1 = 13.783X1 - 38790
Estimate water Y2 = 2.219X2 + 440.02

Solve for fluid contact:

		Slope	Cons
Equation 1	y1	13.783	-38790
Equation 2	y2	2.219	440.02
Co-ordinate	x =	3392.43	
Hydrocarbon contact depth	y =(possible)	7968	ft.

Formation data:

	depth (feet)	Pressure (psi)
Top sand:	7876	3360
	7876	3410
Base sand:	7897	3360
	7897	3410

Contact plot:

Xw1 =	3370	Yw1 =	7918.05	ft.
Xw2 =	3390	Yw2 =	7962.43	ft.

GWC:

x =	3360	y =	7968
	3410		7968

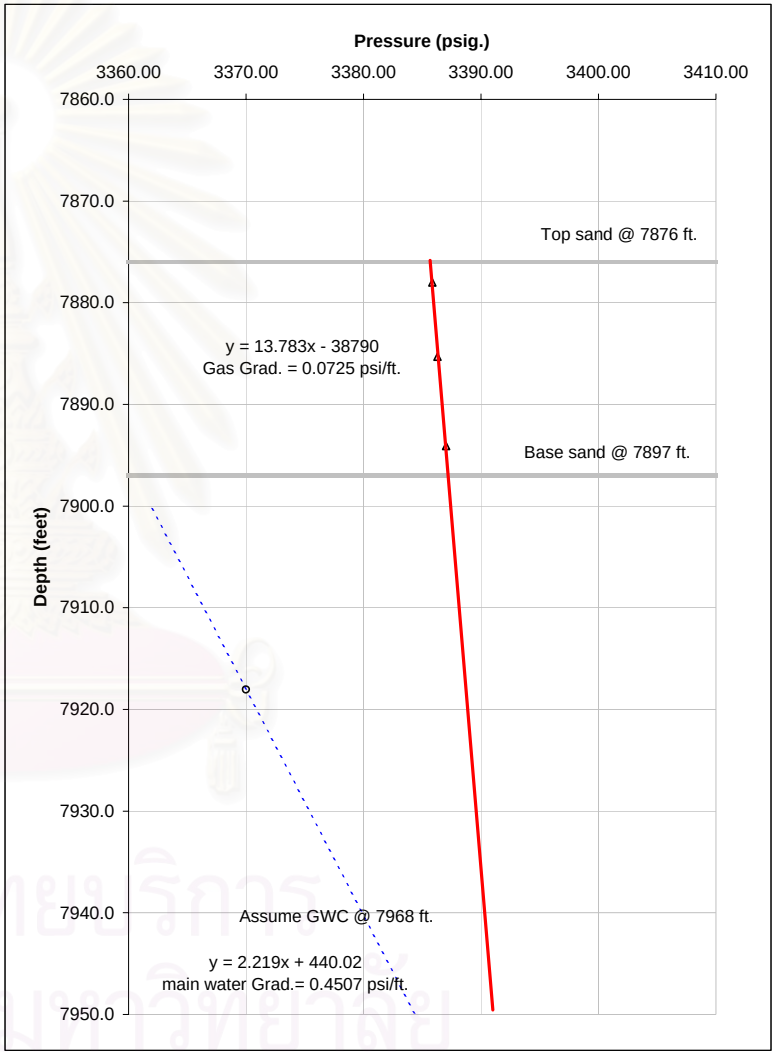

Figure B.18 Pressure-depth diagram represents pore-pressure profile in horizon U-B5 of well B.

REPEAT FORMATION TESTER DATA:

Well: **F**
Horizon/ test#: **U-B5/ # 58,59.**

Record test			Fluid type
Pressure (psi.)	Depth (ft.)	Grad. To depth above	from log
3246.08	7459.3		gas
3247.23	7472.3	0.0885	gas

Linear equasion from pressure Vs. depth plot.

Gas Y1 = 11.304X1 - 29236
Estimate water Y2 = 2.4386X2 - 266.73

Solve for fluid contact:

		Slope	Cons
Equation 1	y1	11.304	-29236
Equation 2	y2	2.4386	-266.73
Co-ordinate	x =	3267.68	
Hydrocarbon contact depth	y =(possible GWC)	7702	ft.

Formation data:

	depth (feet)	Pressure (psi)
Top sand:	7450	3220
	7450	3270
Base sand:	7479	3220
	7479	3270

Contact plot:

Xw1 =	3230	Yw1 =	7609.95	ft.
Xw2 =	3250	Yw2 =	7658.72	ft.

GWC:

x =	3220	y =	7702	
	3270		7702	

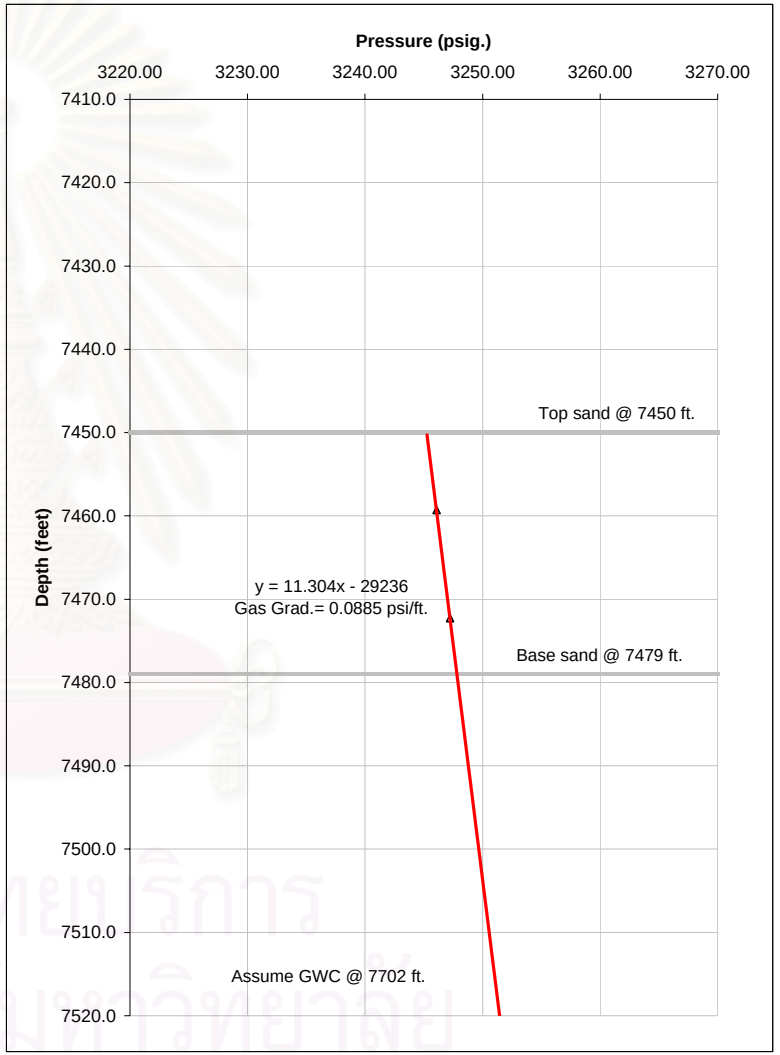

Figure B.19 Pressure-depth diagram represents pore-pressure profile in horizon U-B5 of well F.

REPEAT FORMATION TESTER DATA:

Well: **E**
Horizon/ test#: **U-B5/ # 11,12,13,14.**

Record test			Fluid type
Pressure (psi.)	Depth (ft.)	Grad. To depth above	from log
3251.09	7513.5		gas
3251.88	7523.8	0.0767	gas
3252.67	7533.2	0.0840	gas
3253.52	7543.5	0.0825	gas

Linear equasion from pressure Vs. depth plot.

Gas Y1 = 12.3X1 - 32473
Estimate water Y2 = 2.4246X2 - 231.88

Solve for fluid contact:

		Slope	Cons
Equation 1	y1	12.3	-32473
Equation 2	y2	2.4246	-231.88
Co-ordinate	x =	3264.79	
Hydrocarbon contact depth	y =(possible)	7684	ft.

Formation data:

	depth (feet)	Pressure (psi)
Top sand:	7508	3220
	7508	3280
Base sand:	7555	3220
	7555	3280

Contact plot:

Xw1 =	3230	Yw1 =	7599.58	ft.
Xw2 =	3250	Yw2 =	7648.07	ft.

GWC:

x =	3220	y =	7684
	3280		7684

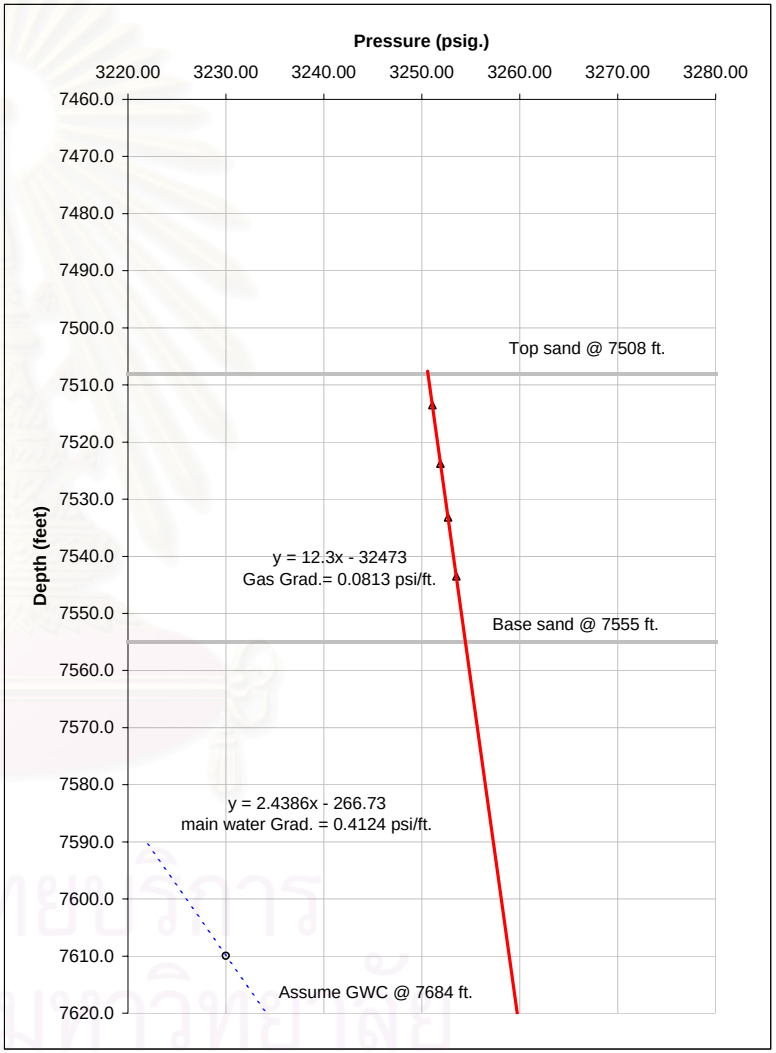

Figure B.20 Pressure-depth diagram represents pore-pressure profile in horizon U-B5 of well E.

REPEAT FORMATION TESTER DATA:

Well: **D**
Horizon/ test#: **U-B5/ # 13,12,11,10.**

Record test			Fluid type
Pressure (psi.)	Depth (ft.)	Grad. To depth above	from log
3255.90	7555.3		gas
3256.23	7565.2	0.0333	gas
3257.19	7573.5	0.1157	gas
3257.83	7582.6	0.0703	gas

Linear equasion from pressure Vs. depth plot.

Gas Y1 = 12.894X1 - 34425
Estimate water Y2 = 2.3927X2 - 132.51

Solve for fluid contact:

		Slope	Cons
Equation 1	y1	12.894	-34425
Equation 2	y2	2.3927	-132.51
Co-ordinate	x =	3265.55	
Hydrocarbon contact depth	y =(possible)	7681	ft.

Formation data:

	depth (feet)	Pressure (psi)
Top sand:	7548	3220
	7548	3290
Base sand:	7588	3220
	7588	3290

Contact plot:

Xw1 =	3230	Yw1 =	7595.91	ft.
Xw2 =	3250	Yw2 =	7643.77	ft.

GWC:

x =	3220	y =	7681	
	3290		7681	

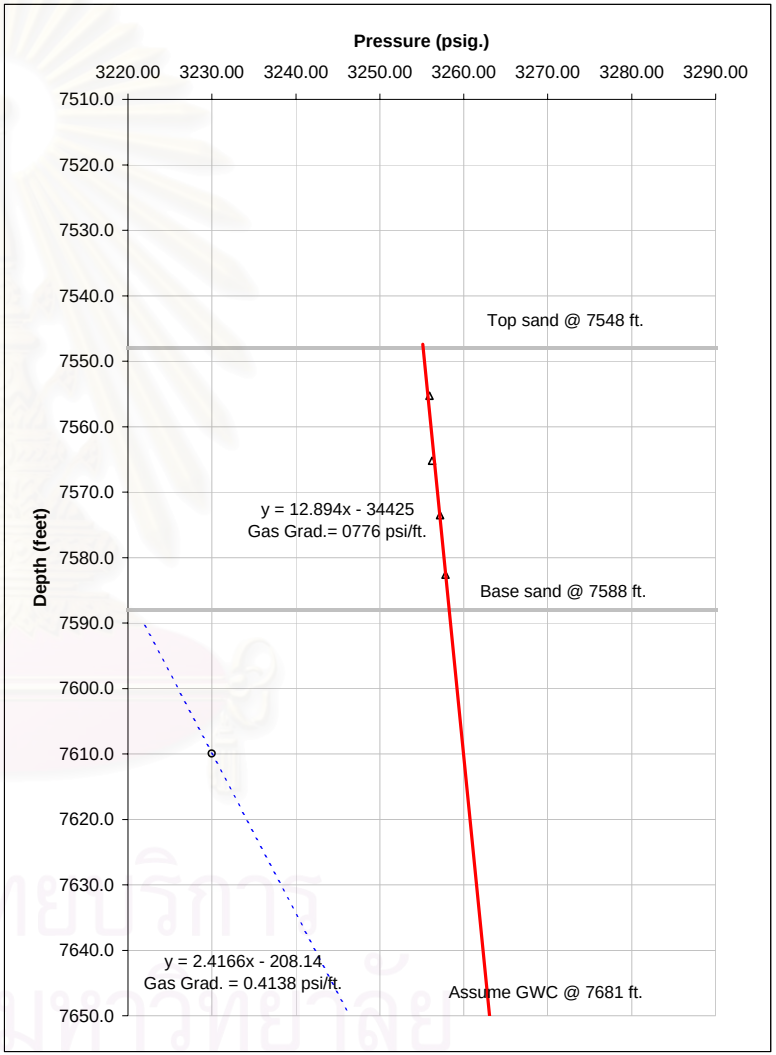

Figure B.21 Pressure-depth diagram represents pore-pressure profile in horizon U-B5 of well D.

REPEAT FORMATION TESTER RESERVOIR ZONE DATA:

Well: **F,E,D (Upthrown side)**
Horizon: **U-B5**

Record test			Well
Pressure (psi.)	Depth (ft.)	Fluid type	Test
3246.08	7459.3	gas	F
3247.23	7472.3	gas	F
3251.09	7513.5	gas	E
3251.88	7523.8	gas	E
3252.67	7533.2	gas	E
3253.52	7543.5	gas	E
3255.90	7555.3	gas	D
3256.23	7565.2	gas	D
3257.19	7573.5	gas	D
3257.83	7582.6	gas	D

Linear equasion from pressure Vs. depth plot.

GAS Y1 = 10.199X1 - 25645
WATER Y2 = 2.3949X2 - 142.97

Solve for fluid contact:			Slope	Cons
	Equation 1	y1	10.199	-25645
	Equation 2	y2	2.3949	-142.97
	Co-ordinate	x =	3267.77	
Hydrocarbon contact depth		y = (GWC)	7683	ft.

Contact plot

	X	Y
GWC	3150	7683
	3350	7683

Main water

X1 =	3200	Y1 =	7520.71
X2 =	3300	Y2 =	7760.2

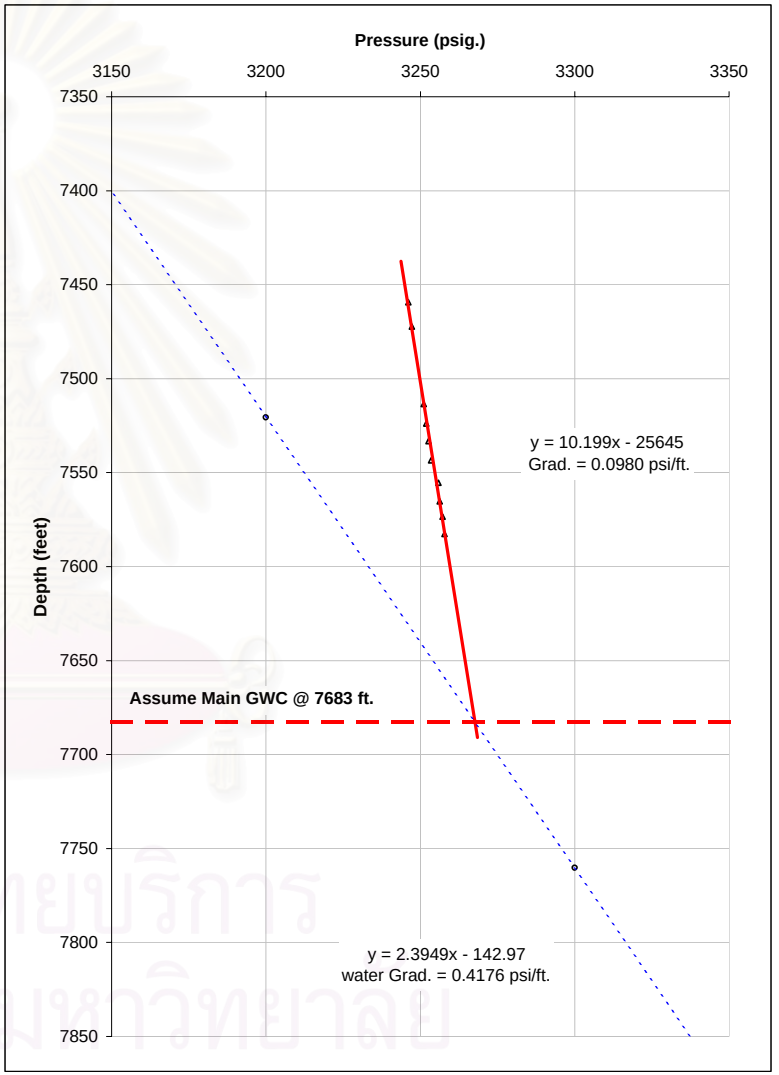

Figure B.22 Pressure-depth diagram represents pore-pressure profile in horizon U-B5 of well F, E, D.

REPEAT FORMATION TESTER RESERVOIR ZONE DATA:

Well: **I,B (Down thrown side)**
Horizon: **U-B5**

Record test			Well
Pressure (psi.)	Depth (ft.)	Fluid type	Test
3371.39	7740.9	gas	I
3372.96	7755.7	gas	I
3373.70	7769.5	gas	I
3385.87	7878.0	gas	B
3386.29	7885.3	gas	B
3387.02	7894.1	gas	B

Linear equasion from pressure Vs. depth plot.

GAS Y1 = 9.5473X1 - 24445
WATER Y2 = 2.4138X2 - 189.35

Solve for fluid contact:

			Slope	Cons
	Equation 1	y1	9.5473	-24445
	Equation 2	y2	2.4138	-189.35
	Co-ordinate	x =	3400.25	
Hydrocarbon contact depth		y = (GWC)	8018	ft.

Contact plot

	X	Y
GWC	3250	8018
	3450	8018

Main water

X1 =	3300	Y1 =	7776.19
X2 =	3400	Y2 =	8017.57

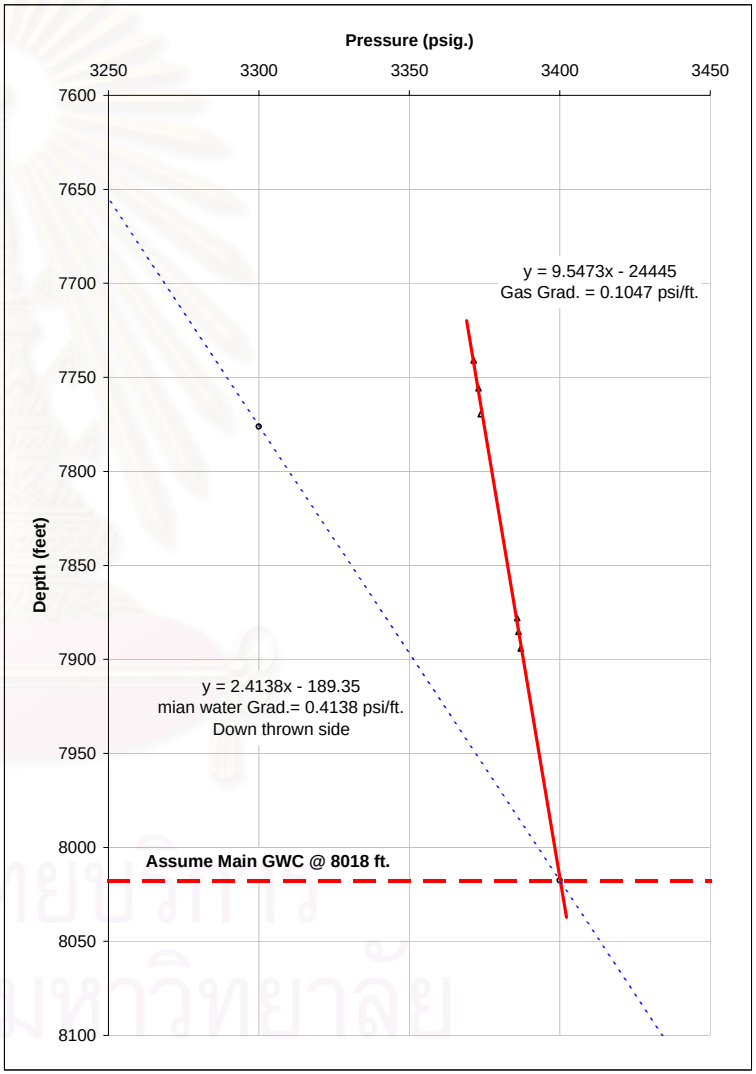

Figure B.23 Pressure-depth diagram represents pore-pressure profile in horizon U-B5 of well B, I.

REPEAT FORMATION TESTER DATA:

Well: **F**
Horizon/ test#: **U-B6/ # 60,61,62,63,64.**

Record test			Fluid type
Pressure (psi.)	Depth (ft.)	Grad. To depth above	from log
3364.02	7754.7		gas
3364.97	7764.6	0.0960	gas
3368.41	7799.8	0.0977	gas
3369.14	7808.8	0.0811	gas
3369.96	7817.8	0.0911	gas

Linear equasion from pressure Vs. depth plot.

Gas Y1 = 10.559X1 - 27765
Estimate water Y2 = 2.4386X2 - 266.73

Solve for fluid contact:

		Slope	Cons
Equation 1	y1	10.559	-27765
Equation 2	y2	2.4386	-266.73
Co-ordinate	x =	3386.32	
Hydrocarbon contact depth	y =(possible)	7991	ft.

Formation data:

	depth (feet)	Pressure (psi)
Top sand U-B6/1:	7748	3340
	7748	3390
Base sand:	7770	3340
	7770	3390
Top sand U-B6/2:	7789	3340
	7789	3390
	7821	3340
	7821	3390

Contact plot:

Xw1 =	3360	Yw1 =	7926.97	ft.
Xw2 =	3380	Yw2 =	7975.74	ft.

GWC:

x =	3220	y =	7991
	3270		7991

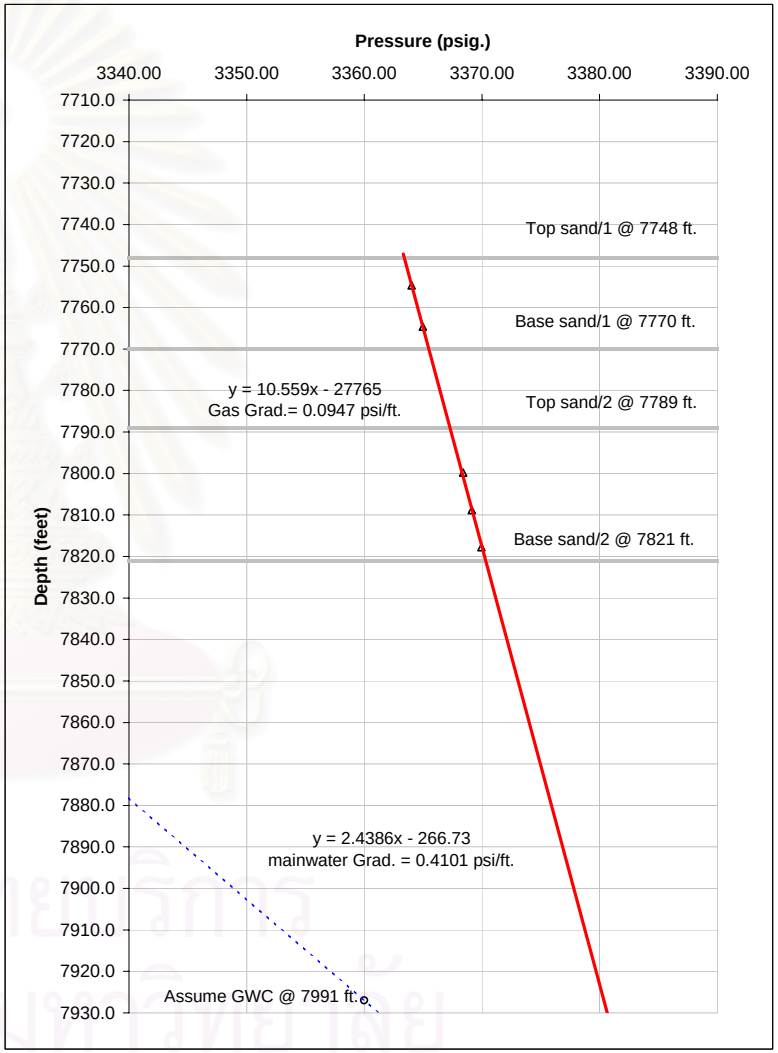

Figure B.24 Pressure-depth diagram represents pore-pressure profile in horizon U-B5 of well F.

REPEAT FORMATION TESTER DATA:

Well: **E**

Horizon/ test#: **U-B6/ # 68,69,70,71,72,73,74,75,76,77,78.**

Record test			Fluid type
Pressure (psi.)	Depth (ft.)	Grad. To depth above	from log
3366.59	7778.4		gas
3367.20	7785.7	0.0836	gas
3368.18	7794.7	0.1089	gas
3369.59	7811.0	0.0865	gas
3370.23	7819.2	0.0780	gas
3370.63	7824.9	0.0702	gas
3374.50	7858.3	0.1159	oil
3378.76	7873.0	0.2898	oil
3380.64	7880.3	0.2575	oil
3382.45	7886.8	0.2785	oil

Linear equasion from pressure Vs. depth plot.

Gas Y1 = 10.559X1 - 27765

Oil Y1 = 3.5898X1 - 4255.6

Estimate water Y3 = 2.4246X2 - 231.88

Solve for fluid contact:

			Slope	Cons	
	Equation 1	y1	11.322	-30338	
	Equation 2	y2	3.5898	-4255.6	
	Equation 3	y3	2.4246	-231.88	
	Co-ordinate	x1 =	3373.22		
Hydrocarbon contact depth		y = (GOC)	7854		ft.
	Co-ordinate	x2 =	3453.24		
Hydrocarbon contact depth		y = possible (OWC)	8141		ft.

Formation data:

	depth (feet)	Pressure (psi)
Top sand U-B6/1:	7770	3340
	7770	3410
Base sand:	7830	3340
	7830	3410
Top sand U-B6/2:	7849	3340
	7849	3410
	7890	3340
	7890	3410

Contact plot:

Xw1 =	3350	Yw1 =	7890.53	ft.
Xw2 =	3390	Yw2 =	7987.51	ft.

GOC:	x =	3340	y =	7854
		3410		7854
OWC:	x =	3340	y =	8141
		3410		8141

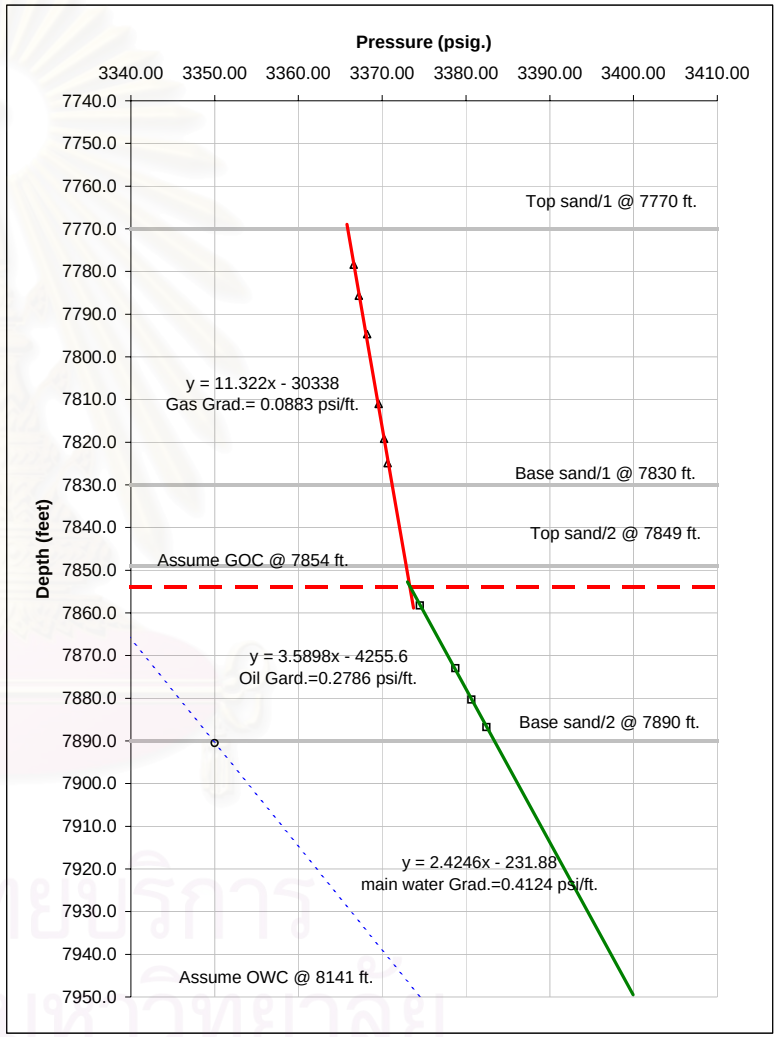

Figure B.25 Pressure-depth diagram represents pore-pressure profile in horizon U-B5 of well E.

REPEAT FORMATION TESTER DATA:

Well: **D**

Horizon/ test#: **U-B6/ # 16,15,14,19,18,17,20.**

Record test			Fluid type
Pressure (psi.)	Depth (ft.)	Grad. To depth above	from log
3369.86	7826.7		gas
3370.55	7835.1	0.0821	gas
3371.42	7843.5	0.1036	gas
3375.01	7870.4	0.1335	oil
3377.27	7878.8	0.2690	oil
3380.09	7889.0	0.2765	oil
3383.16	7899.0	0.3070	oil

Linear equasion from pressure Vs. depth plot.

Gas	Y1 = 10.722X1 - 28303
Oil	Y1 = 3.5139X1 - 3988.9
Estimate water	Y3 = 2.3927X2 - 132.51

Solve for fluid contact:

		Slope	Cons	
Equation 1	y1	10.722	-28303	
Equation 2	y2	3.5139	-3988.9	
Equation 3	y3	2.3927	-132.51	
Co-ordinate	x1 =	3373.16		
Hydrocarbon contact depth	y = (GOC)	7864	ft.	
Co-ordinate	x2 =	3439.52		
Hydrocarbon contact depth	y = possible (OWC)	8097	ft.	

Formation data:

	depth (feet)	Pressure (psi)
Top sand U-B6/1:	7823	3340
	7823	3410
Base sand:	7848	3340
	7848	3410
Top sand U-B6/2:	7859	3340
	7859	3410
	7908	3340
	7908	3410

Contact plot:

Xw1 =	3350	Yw1 =	7883.04	ft.
Xw2 =	3390	Yw2 =	7978.74	ft.

GOC:	x =	3340	y =	7864	
		3410		7864	
OWC:	x =	3340	y =	8097	
		3410		8097	

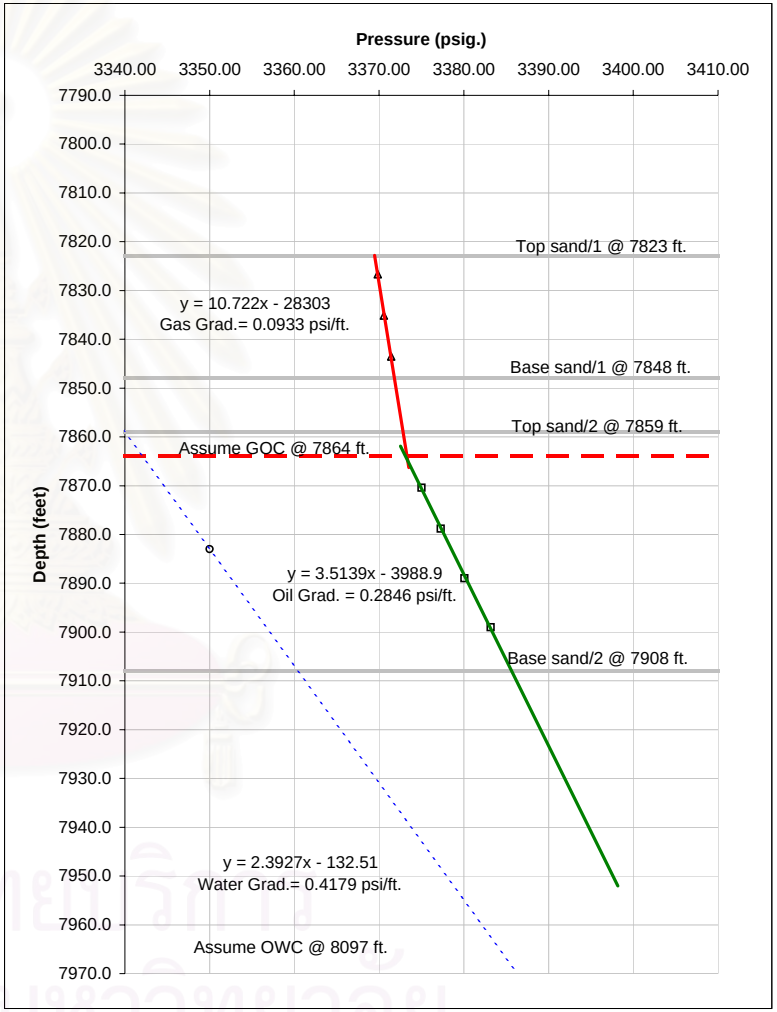

Figure B.26 Pressure-depth diagram represents pore-pressure profile in horizon U-B5 of well D.

REPEAT FORMATION TESTER DATA:

Well: **J**
Horizon/ test#: **U-B6/ # 21,22,23,24,25,26,27.**

Record test			Fluid type
Pressure (psi.)	Depth (ft.)	Grad. To depth above	from log
3392.95	7937.5		oil
3397.03	7955.2	0.2305	oil
3399.40	7964.0	0.2693	oil
3410.52	7989.7	0.4327	water
3432.62	8044.7	0.4018	water
3485.22	8154.7	0.4782	water

Linear equasion from pressure Vs. depth plot.

Oil	Y1 = 4.1336X1 - 6087.4
Water zone	Y1 = 2.1875X1 + 531.99
Estimate water	Y3 = 2.3033X2 + 137.96

Solve for fluid contact:

			Slope	Cons	
	Equation 1	y1	4.1336	-6087.4	
	Equation 2	y2	2.1875	531.99	
	Equation 3	y3	2.3033	137.96	
	Co-ordinate	x1 =	3401.36		
Hydrocarbon contact depth		y = (OWC)	7972	ft.	
	Co-ordinate	x2 =	3402.68		
Main water contact depth		y = possible	7975	ft.	

Formation data:

	depth (feet)	Pressure (psi)
Top sand U-B6/1:	7930	3370
	7930	3440
Base sand:	7968	3370
	7968	3440
Top sand U-B6/2:	7978	3370
	7978	3440
	7996	3370
	7996	3440

Contact plot:

Xw1 =	3390	Yw1 =	7946.15	ft.
Xw2 =	3420	Yw2 =	8015.25	ft.

OWC:	x =	3370	y =	7972
		3440		7972

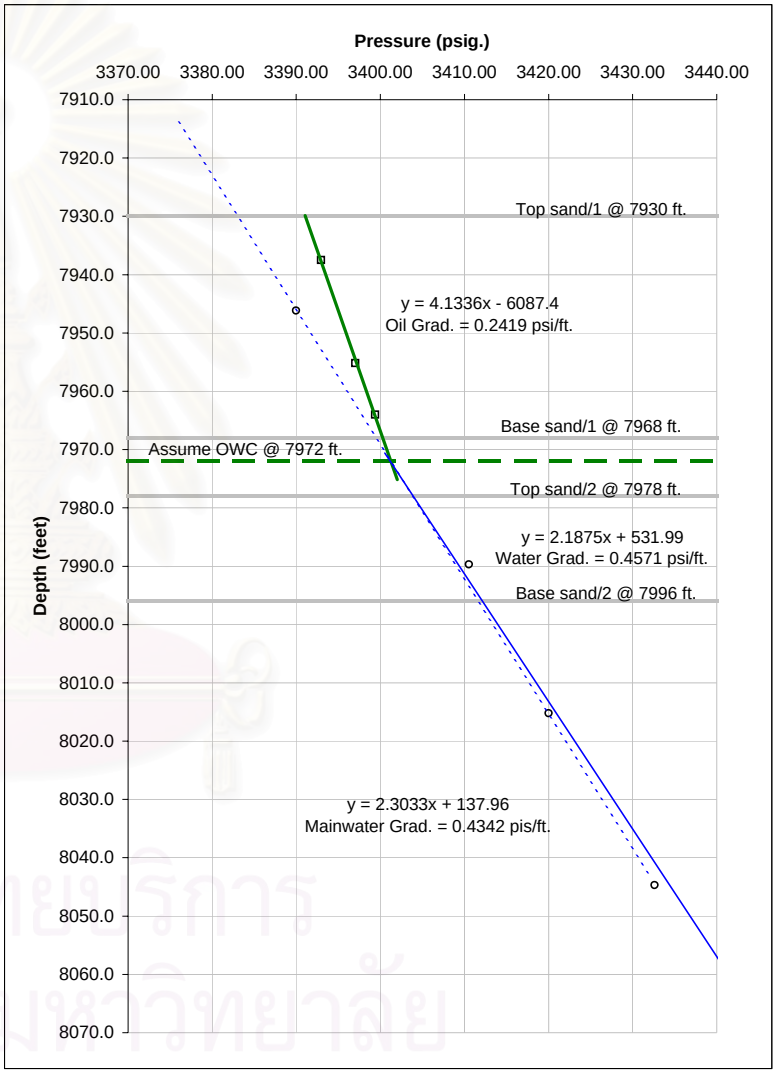

Figure B.27 Pressure-depth diagram represents pore-pressure profile in horizon U-B5 of well J.

REPEAT FORMATION TESTER DATA:

Well: **I**
Horizon/ test#: **U-B6/ # 45,47,48,49.**

Record test			Fluid type
Pressure (psi.)	Depth (ft.)	Grad. To depth above	from log
3500.36	8100.0		gas
3500.53	8110.5	0.0162	gas
3502.00	8124.8	0.1028	gas
3503.33	8134.3	0.1400	gas

Linear equasion from pressure Vs. depth plot.

Gas Y1 = 10.495X1 - 28631
Estimate water Y2 = 2.4115X2 - 177.63

Solve for fluid contact:

		Slope	Cons
Equation 1	y1	10.495	-28631
Equation 2	y2	2.4115	-177.63
Co-ordinate	x =	3519.93	
Hydrocarbon contact depth	y =(possible)	8311	ft.

Formation data:

	depth (feet)	Pressure (psi)
Top sand :	8090	3470
	8090	3530
Base sand:	8140	3470
	8140	3530

Contact plot:

Xw1 =	3490	Yw1 =	8238.51	ft.
Xw2 =	3510	Yw2 =	8286.74	ft.

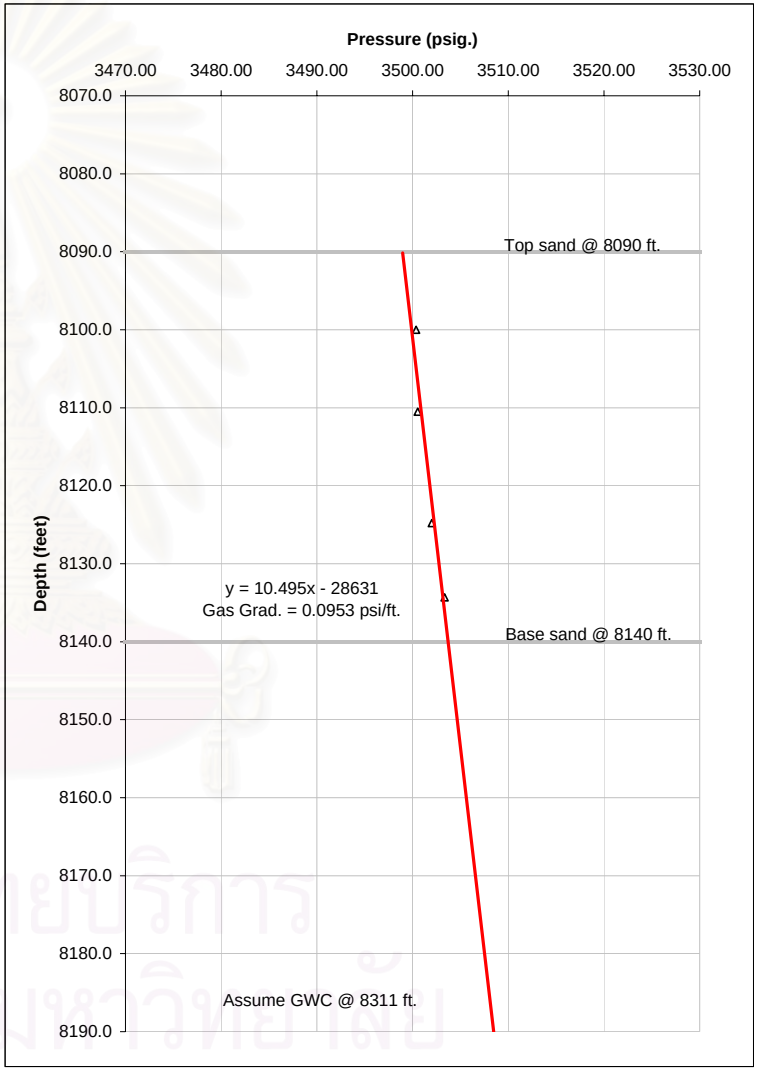

Figure B.28 Pressure-depth diagram represents pore-pressure profile in horizon U-B5 of well I.

REPEAT FORMATION TESTER DATA:

Well: **B**
Horizon/ test#: **U-B6/ # 36,37.**

Record test			Fluid type
Pressure (psi.)	Depth (ft.)	Grad. To depth above	from log
3209.24	8142.2		gas
3210.00	8162.1	0.0382	gas

Linear equasion from pressure Vs. depth plot.

Gas Y1 = 26.184X1 - 7588
Estimate water Y2 = 2.219X2 + 440.02

Solve for fluid contact:

		Slope	Cons	
Equation 1	y1	26.184	-75889	
Equation 2	y2	2.219	440.02	
Co-ordinate	x =	3185.02		
Hydrocarbon contact depth	y =	7508		ft. (possible subnormal Press.)

Formation data:

	depth (feet)	Pressure (psi)
Top sand :	8133	3190
	8133	3230
Base sand:	8198	3190
	8198	3230

Contact plot:

Xw1 =	3210	Yw1 =	7563.01	ft.
Xw2 =	3230	Yw2 =	7607.39	ft.

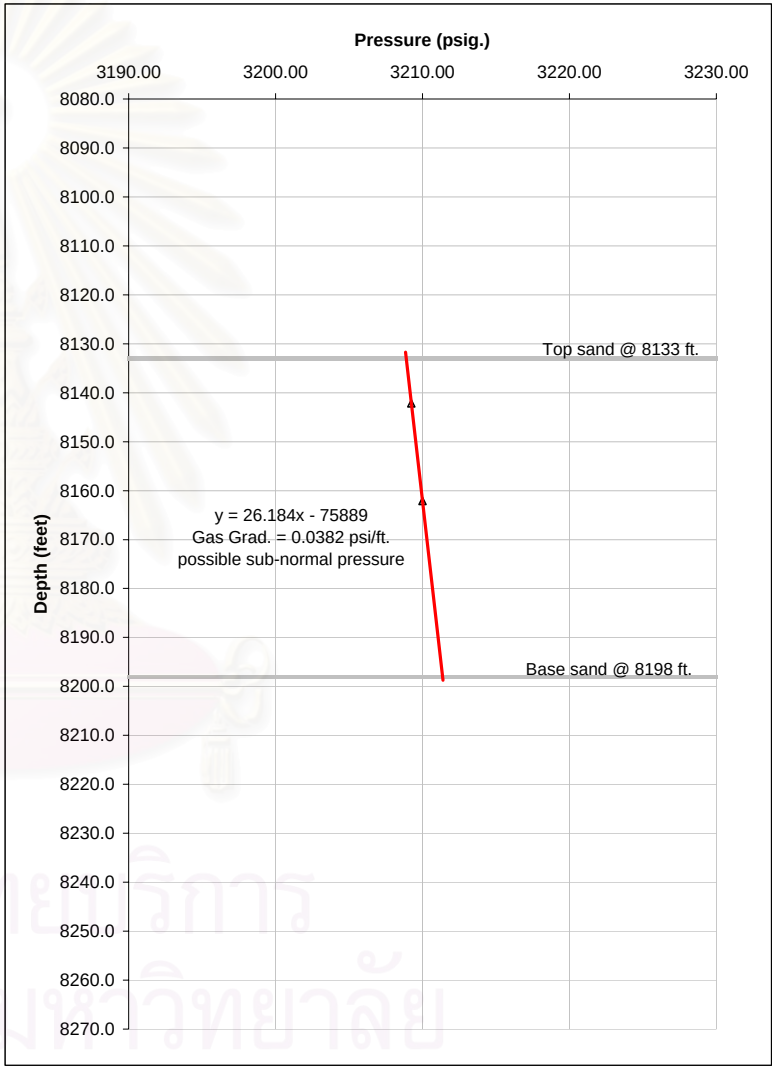

Figure B.29 Pressure-depth diagram represents pore-pressure profile in horizon U-B5 of well B.

REPEAT FORMATION TESTER RESERVOIR ZONE DATA:

Well: **F,E,D,J (Upthrown side)**
Horizon: **U-B6**

Record test			Well		Contact plot	
Pressure (psi.)	Depth (ft.)	Fluid type	Test		X	Y
3364.02	7754.7	gas	F			
3364.97	7764.6	gas	F			
3366.59	7778.4	gas	E			
3367.20	7785.7	gas	E	GOC	3300	7854
3368.18	7794.7	gas	E		3500	7854
3368.41	7799.8	gas	F			
3369.14	7808.8	gas	F	OWC	3300	7974
3369.59	7811.0	gas	E		3500	7974
3369.96	7817.8	gas	F			
3370.23	7819.2	gas	E	Main	3300	8017
3370.63	7824.9	gas	E	OWC	3500	8017
3369.86	7826.7	gas	D			
3370.55	7835.1	gas	D			
3371.42	7843.5	gas	D			
3374.50	7858.3	oil	E			
3375.01	7870.4	oil	D			
3378.76	7873.0	oil	E			
3377.27	7878.8	oil	D			
3380.64	7880.3	oil	E			
3382.45	7886.8	oil	E			
3380.09	7889.0	oil	D			
3383.16	7899.0	oil	D			
3392.95	7937.5	oil	J			
3397.03	7955.2	oil	J			
3399.40	7964.0	oil	J			
3410.52	7989.7	water	J			
3432.62	8044.7	water	J			
3485.22	8154.7	water	J			

Linear equasion from pressure Vs. depth plot.

GAS	Y1 = 11.738X1 - 31735	MAIN WATER	Y4 = 2.378X4 - 98.081
OIL	Y2 = 4.100X2 - 5974.2		
WATER	Y3 = 2.377X3 - 93.778		

Solve for fluid contact:

			Slope	Cons	
	Equation 1	y1	11.738	-31735	
	Equation 2	y2	4.1	-5974.2	
	Equation 3	y3	2.377	-93.778	
	Co-ordinate	x1 =	3372.72		
Hydrocarbon contact depth		y = (GOC)	7854	ft.	
	Co-ordinate	x2 =	3412.90		3412.38
Hydrocarbon contact depth		y = possible (OWC)	8019	ft.	8017

Main water	X	Y
	3360	7891.999
	3430	8058.459

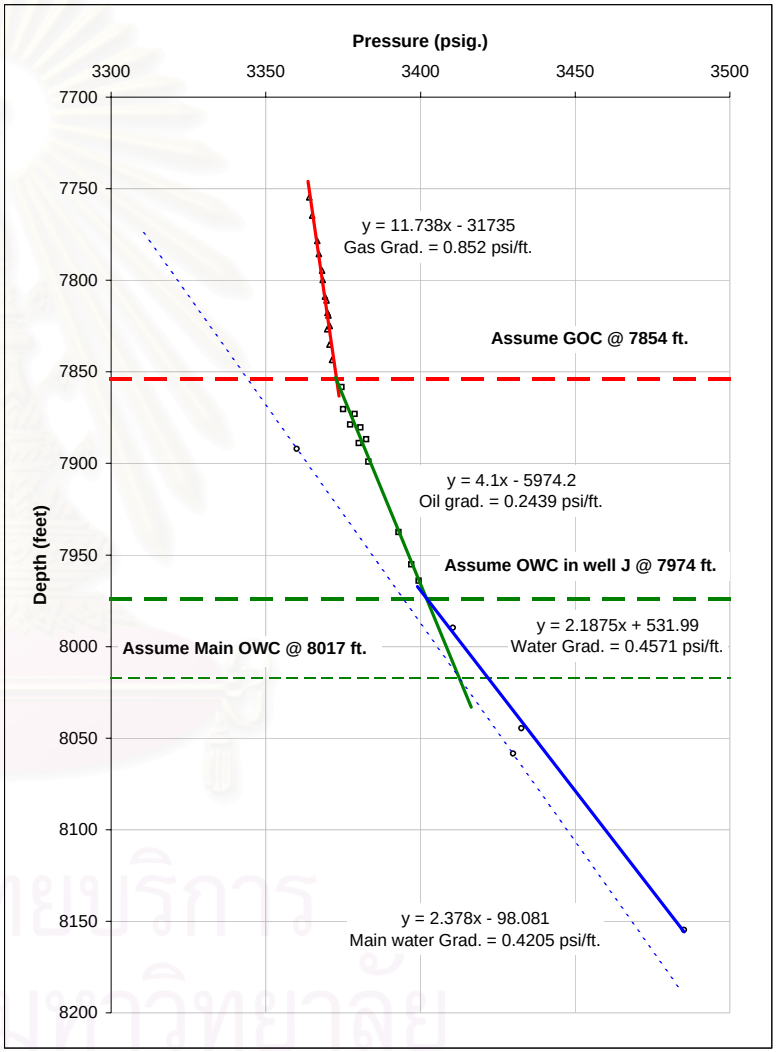

Figure B.30 Pressure-depth diagram represents pore-pressure profile in horizon U-B5 of well F, E, D, and J.

REPEAT FORMATION TESTER RESERVOIR ZONE DATA:

Well: **I,B (Down thrown side).**
Horizon: **U-B6**

Record test			Well
Pressure (psi.)	Depth (ft.)	Fluid type	Test
3500.36	8100.0	gas	I
3500.53	8110.5	gas	I
3502.00	8124.8	gas	I
3503.33	8134.3	gas	I
3209.24	8142.2	gas	B
3210.00	8162.1	gas	B

Linear equasion from pressure Vs. depth plot.

Gas	Y1 = 10.495X1 - 28631	(Well I)
Gas	Y2 = 26.184X2 - 7588	(Well B)
Estimate water	Y3 = 2.4115X3 - 177.63	(Well I)
Main water	Y4 = 2.4168X4 - 189.35	(well I,B)

Water plot line:

X3 =	3350	Y3 =	7900.895
X3 =	3550	Y3 =	8383.195
X4 =	3330	Y4 =	7858.594
X4 =	3530	Y4 =	8341.954

Solve for fluid contact:

			Slope	Cons	
	Equation 1	y1	10.495	-28631	
	Equation 3	y3	2.4115	-177.63	
	Equation 4	y4	2.4168	-189.35	
	Co-ordinate	x1 =	3519.93		
Hydrocarbon contact depth		y = (GOC)	8311		ft.
	Co-ordinate	x2 =	3520.79		
Hydrocarbon contact depth		y = possible (GWC)	8320		ft.

Contact plot		
	X	Y
GWC	3150	8311
well I	3600	8311
Main	3150	8320
GWC	3600	8320

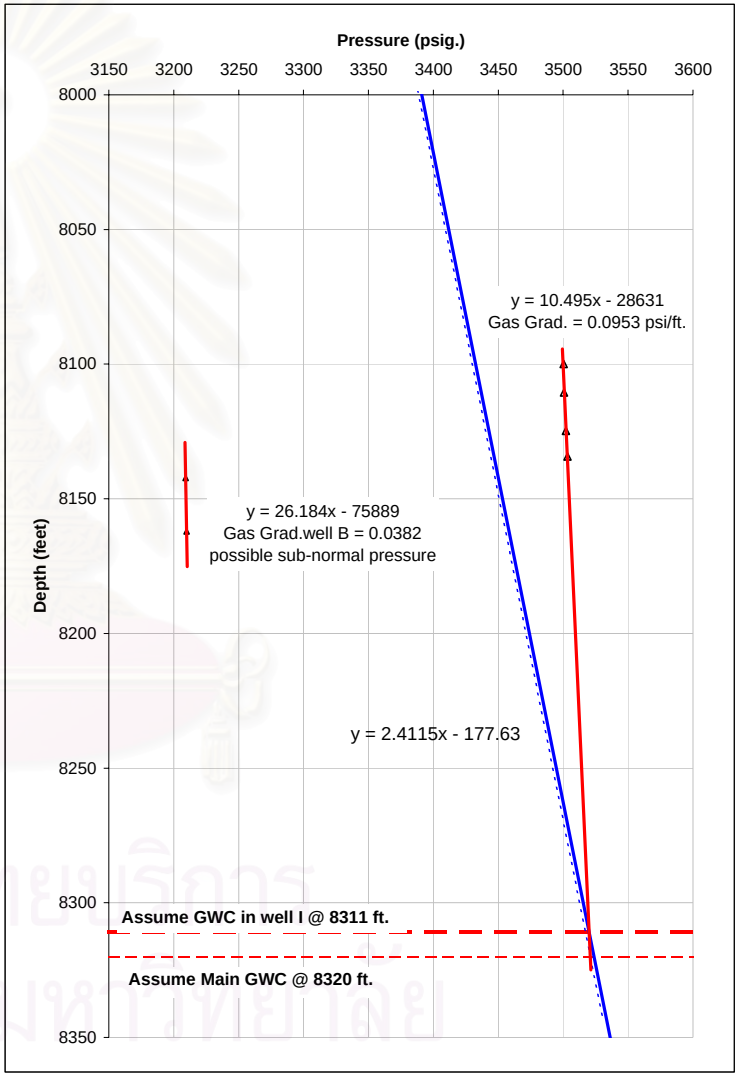

Figure B.31 Pressure-depth diagram represents pore-pressure profile in horizon U-B5 of well B and I.

APPENDIX C

SHALE GOUGE RATIO

Table C.1 Shale gouge ratio (SGR) calculated from dataset well F and I

Depth	Horizon	Vsh.	Throw (feet.)																							
feet	name	avg.	0-25	25-50	50-75	75-100	100-125	125-150	150-175	175-200	200-225	225-250	250-275	275-300	300-325	325-350	350-375	375-400	400-425	425-450	450-475	475-500	500-525	525-550	550-575	575-600	600-625	625-650
0-25		0.20	0.20	0.26	0.21	0.37	0.48	0.53	0.56	0.60	0.72	0.59	0.58	0.54	0.56	0.59	0.56	0.53	0.55	0.543	0.523	0.54	0.56	0.570	0.549	0.57	0.565	0.550
25-50	U-C6	0.32	0.32	0.21	0.43	0.55	0.60	0.62	0.66	0.70	0.71	0.61	0.57	0.59	0.62	0.58	0.55	0.57	0.564	0.541	0.56	0.57	0.587	0.565	0.58	0.580	0.564	0.57
50-75		0.10	0.10	0.49	0.62	0.67	0.68	0.71	0.75	0.67	0.73	0.59	0.62	0.64	0.60	0.57	0.59	0.579	0.554	0.57	0.59	0.601	0.577	0.59	0.591	0.575	0.58	0.60
75-100		0.87	0.87	0.89	0.86	0.82	0.83	0.86	0.75	0.71	0.73	0.67	0.69	0.65	0.60	0.62	0.61	0.58	0.60	0.61	0.63	0.60	0.62	0.61	0.60	0.60	0.61	0.62
100-125		0.90	0.90	0.86	0.81	0.83	0.85	0.73	0.69	0.62	0.73	0.68	0.63	0.58	0.60	0.59	0.56	0.58	0.60	0.61	0.59	0.60	0.60	0.58	0.59	0.60	0.61	0.59
125-150		0.81	0.81	0.76	0.80	0.84	0.70	0.66	0.58	0.62	0.73	0.60	0.55	0.58	0.57	0.54	0.56	0.58	0.60	0.57	0.59	0.59	0.57	0.57	0.59	0.60	0.58	0.59
150-175		0.71	0.71	0.80	0.85	0.67	0.63	0.54	0.59	0.63	0.65	0.53	0.56	0.55	0.52	0.54	0.56	0.58	0.55	0.58	0.57	0.56	0.56	0.58	0.59	0.57	0.58	0.60
175-200		0.88	0.88	0.93	0.65	0.61	0.51	0.57	0.62	0.56	0.57	0.54	0.53	0.50	0.53	0.55	0.57	0.55	0.57	0.57	0.55	0.56	0.58	0.58	0.56	0.58	0.59	0.58
200-225		0.97	0.97	0.54	0.51	0.42	0.51	0.58	0.51	0.46	0.57	0.50	0.47	0.50	0.53	0.55	0.52	0.55	0.55	0.53	0.54	0.56	0.57	0.55	0.57	0.58	0.57	0.56
225-250		0.11	0.11	0.29	0.23	0.39	0.498	0.435	0.389	0.45	0.503	0.418	0.46	0.49	0.521	0.491	0.52	0.523	0.503	0.52	0.54	0.549	0.529	0.55	0.564	0.550	0.547	0.56
250-275		0.46	0.46	0.30	0.49	0.595	0.500	0.435	0.50	0.489	0.509	0.49	0.53	0.555	0.520	0.55	0.550	0.528	0.54	0.56	0.572	0.550	0.57	0.585	0.569	0.565	0.577	0.562
275-300		0.13	0.13	0.50	0.640	0.510	0.430	0.502	0.493	0.451	0.56	0.53	0.56	0.53	0.56	0.556	0.532	0.54	0.57	0.578	0.555	0.57	0.590	0.574	0.570	0.582	0.566	0.58
300-325		0.87	0.87	0.90	0.64	0.51	0.58	0.55	0.50	0.54	0.65	0.61	0.56	0.59	0.59	0.56	0.57	0.60	0.60	0.58	0.60	0.61	0.60	0.59	0.60	0.58	0.60	0.61
325-350		0.92	0.92	0.52	0.38	0.50	0.49	0.44	0.50	0.54	0.65	0.53	0.57	0.57	0.54	0.55	0.58	0.59	0.56	0.58	0.60	0.58	0.58	0.59	0.57	0.59	0.60	0.60
350-375	U-B2	0.12	0.12	0.12	0.36	0.383	0.338	0.43	0.49	0.535	0.548	0.53	0.53	0.51	0.52	0.55	0.566	0.539	0.56	0.582	0.564	0.559	0.574	0.556	0.57	0.58	0.59	0.60
375-400		0.11	0.11	0.49	0.470	0.393	0.49	0.55	0.594	0.533	0.65	0.58	0.54	0.56	0.59	0.598	0.567	0.59	0.609	0.588	0.582	0.597	0.577	0.59	0.60	0.61	0.62	0.63
400-425		0.86	0.86	0.65	0.49	0.58	0.64	0.68	0.59	0.64	0.71	0.58	0.60	0.63	0.64	0.60	0.62	0.64	0.62	0.61	0.62	0.60	0.62	0.63	0.63	0.64	0.65	0.66
425-450		0.44	0.44	0.30	0.49	0.58	0.64	0.55	0.60	0.60	0.62	0.57	0.60	0.62	0.58	0.60	0.63	0.60	0.59	0.61	0.59	0.60	0.62	0.62	0.63	0.64	0.65	0.66
450-475	U-B3	0.16	0.16	0.51	0.63	0.69	0.57	0.63	0.62	0.57	0.66	0.62	0.63	0.59	0.62	0.64	0.61	0.60	0.62	0.60	0.61	0.62	0.63	0.64	0.65	0.66	0.67	0.67
475-500		0.86	0.86	0.86	0.86	0.67	0.73	0.70	0.62	0.64	0.76	0.68	0.63	0.65	0.68	0.64	0.63	0.65	0.62	0.64	0.65	0.65	0.67	0.67	0.68	0.69	0.69	0.70
500-525		0.86	0.86	0.87	0.61	0.69	0.66	0.59	0.60	0.65	0.74	0.61	0.64	0.66	0.63	0.62	0.63	0.61	0.62	0.64	0.64	0.66	0.66	0.67	0.68	0.69	0.69	0.70
525-550		0.87	0.87	0.49	0.64	0.62	0.53	0.56	0.62	0.64	0.65	0.61	0.64	0.61	0.60	0.62	0.59	0.61	0.62	0.63	0.65	0.65	0.66	0.67	0.68	0.69	0.69	0.70
550-575	U-B4	0.10	0.10	0.52	0.53	0.45	0.50	0.58	0.60	0.54	0.66	0.62	0.58	0.58	0.598	0.569	0.59	0.61	0.62	0.63	0.64	0.65	0.66	0.67	0.68	0.69	0.69	0.67
575-600		0.94	0.94	0.75	0.56	0.60	0.67	0.69	0.61	0.65	0.76	0.63	0.62	0.64	0.60	0.63	0.64	0.65	0.66	0.67	0.68	0.69	0.70	0.70	0.71	0.72	0.70	0.68
600-625		0.55	0.55	0.37	0.49	0.61	0.63	0.55	0.60	0.65	0.67	0.59	0.61	0.58	0.60	0.62	0.63	0.65	0.66	0.67	0.68	0.69	0.69	0.70	0.71	0.69	0.67	
625-650		0.19	0.19	0.46	0.62	0.66	0.55	0.612	0.659	0.61	0.66	0.62	0.58	0.61	0.63	0.63	0.65	0.66	0.68	0.68	0.69	0.70	0.71	0.715	0.692	0.671		
650-675		0.72	0.72	0.84	0.81	0.64	0.70	0.74	0.66	0.64	0.75	0.62	0.65	0.66	0.67	0.69	0.70	0.71	0.71	0.72	0.73	0.74	0.74	0.72	0.69			
675-700		0.96	0.96	0.86	0.61	0.69	0.74	0.66	0.63	0.66	0.68	0.64	0.66	0.66	0.68	0.69	0.71	0.71	0.72	0.73	0.74	0.74	0.71	0.69				
700-725		0.75	0.75	0.44	0.60	0.69	0.59	0.57	0.62	0.56	0.68	0.63	0.64	0.66	0.67	0.69	0.70	0.71	0.71	0.72	0.73	0.70	0.68					
725-750		0.13	0.13	0.53	0.66	0.56	0.54	0.593	0.536	0.58	0.69	0.63	0.65	0.67	0.68	0.69	0.70	0.71	0.72	0.728	0.700	0.675						
750-775		0.92	0.92	0.93	0.70	0.64	0.69	0.60	0.65	0.67	0.77	0.71	0.72	0.73	0.74	0.74	0.75	0.76	0.76	0.73	0.70							
775-800		0.94	0.94	0.59	0.55	0.63	0.54	0.60	0.64	0.65	0.77	0.70	0.71	0.72	0.73	0.74	0.75	0.75	0.72	0.69								
800-825		0.23	0.23	0.35	0.52	0.44	0.54	0.59	0.61	0.65	0.75	0.69	0.70	0.71	0.72	0.74	0.741	0.707	0.676									
825-850		0.47	0.47	0.67	0.51	0.61	0.66	0.67	0.71	0.72	0.83	0.75	0.76	0.76	0.77	0.778	0.739	0.704										
850-875		0.87	0.87	0.53	0.66	0.71	0.71	0.75	0.76	0.77	0.88	0.78	0.79	0.80	0.80	0.76	0.72											
875-900	U-B5	0.19	0.19	0.56	0.65	0.68	0.72	0.74	0.76	0.77	0.87	0.78	0.79	0.796	0.749	0.709												
900-925		0.92	0.92	0.89	0.84	0.86	0.85	0.85	0.85	0.85	0.96	0.85	0.85	0.80	0.75													
925-950		0.85	0.85	0.80	0.84	0.84	0.84	0.84	0.84	0.84	0.95	0.84	0.78	0.74														
950-975		0.74	0.74	0.83	0.83	0.84	0.84	0.84	0.84	0.85	0.95	0.78	0.72															
975-1000		0.92	0.92	0.88	0.87	0.86	0.85	0.86	0.86	0.86	0.88	0.72																
1000-1025		0.83	0.83	0.85	0.84	0.84	0.84	0.85	0.85	0.77	0.79																	
1025-1050		0.86	0.86	0.85	0.84	0.85	0.85	0.85	0.76	0.69																		
1050-1075		0.83	0.83	0.83	0.84	0.85	0.85	0.74	0.66																			
1075-1100		0.83	0.83	0.85	0.86	0.85	0.72	0.63																				
1100-1125		0.86	0.86	0.88	0.86	0.69	0.59																					
1125-1150		0.89	0.89	0.86	0.64	0.53																						
1150-1175		0.83	0.83	0.51	0.40																							
1175-1200	U-B6	0.190	0.190	0.190																								
1200-1225		0.190	0.190																									

Table C.1 (continued)

Depth feet	Horizon name	Vsh. avg.	Throw (feet.) 650-675	675-700	700-725	725-750	750-775	775-800	800-825	825-850	850-875	875-900	900-925	925-950	950-975	975-1000	1000-1025	1025-1050	1050-1075	1075-1100	1100-1125	1125-1150	1150-1175	1175-1200	1200-1225
0-25		0.20	0.56	0.57	0.577	0.562	0.57	0.585	0.575	0.571	0.580	0.569	0.58	0.59	0.59	0.60	0.60	0.61	0.61	0.62	0.63	0.63	0.64	0.63	0.617
25-50	**U-C6**	0.32	0.58	0.591	0.575	0.59	0.598	0.586	0.583	0.591	0.580	0.59	0.60	0.60	0.61	0.61	0.62	0.62	0.63	0.63	0.64	0.64	0.63	0.63	
50-75		0.10	0.601	0.584	0.60	0.607	0.595	0.591	0.599	0.587	0.60	0.60	0.61	0.62	0.62	0.63	0.63	0.64	0.64	0.65	0.65	0.64	0.63		
75-100		0.87	0.60	0.61	0.62	0.61	0.61	0.62	0.60	0.61	0.62	0.62	0.63	0.64	0.64	0.65	0.65	0.66	0.66	0.66	0.65	0.64			
100-125		0.90	0.60	0.62	0.60	0.60	0.61	0.59	0.60	0.61	0.61	0.62	0.63	0.63	0.64	0.64	0.65	0.66	0.66	0.65	0.64				
125-150		0.81	0.61	0.59	0.59	0.60	0.58	0.59	0.60	0.61	0.62	0.62	0.63	0.63	0.64	0.64	0.65	0.65	0.64	0.63					
150-175		0.71	0.58	0.58	0.59	0.58	0.59	0.60	0.60	0.61	0.62	0.62	0.63	0.63	0.64	0.65	0.65	0.64	0.63						
175-200		0.88	0.57	0.59	0.57	0.58	0.59	0.60	0.61	0.61	0.62	0.63	0.63	0.64	0.64	0.65	0.64	0.63							
200-225		0.97	0.57	0.56	0.57	0.58	0.59	0.60	0.60	0.61	0.62	0.62	0.63	0.64	0.64	0.63	0.62								
225-250		0.11	0.55	0.56	0.57	0.57	0.59	0.59	0.60	0.61	0.61	0.62	0.63	0.634	0.623	0.612									
250-275		0.46	0.58	0.59	0.59	0.60	0.61	0.62	0.62	0.63	0.64	0.64	0.648	0.636	0.625										
275-300		0.13	0.59	0.60	0.61	0.61	0.62	0.63	0.63	0.64	0.65	0.653	0.641	0.629											
300-325		0.87	0.61	0.62	0.63	0.64	0.64	0.65	0.66	0.66	0.67	0.66	0.64												
325-350		0.92	0.61	0.62	0.63	0.64	0.64	0.65	0.66	0.66	0.65	0.64													
350-375	**U-B2**	0.12	0.61	0.62	0.63	0.63	0.64	0.65	0.655	0.641	0.628														
375-400		0.11	0.64	0.65	0.65	0.66	0.67	0.671	0.657	0.643															
400-425		0.86	0.67	0.67	0.68	0.68	0.69	0.67	0.66																
425-450		0.44	0.66	0.67	0.68	0.68	0.67	0.65																	
450-475	**U-B3**	0.16	0.68	0.69	0.692	0.675	0.660																		
475-500		0.86	0.71	0.71	0.69	0.68																			
500-525		0.86	0.71	0.69	0.67																				
525-550		0.87	0.68	0.66																					
550-575	**U-B4**	0.10	0.66																						
575-600		0.94																							
600-625		0.55																							
625-650		0.19																							
650-675		0.72																							
675-700		0.96																							
700-725		0.75																							
725-750		0.13																							
750-775		0.92																							
775-800		0.94																							
800-825		0.23																							
825-850		0.47																							
850-875		0.87																							
875-900	**U-B5**	0.19																							
900-925		0.92																							
925-950		0.85																							
950-975		0.74																							
975-1000		0.92																							
1000-1025		0.83																							
1025-1050		0.86																							
1050-1075		0.83																							
1075-1100		0.83																							
1100-1125		0.86																							
1125-1150		0.89																							
1150-1175		0.83																							
1175-1200	**U-B6**	0.190																							
1200-1225		0.190																							

Table C.2 Shale gouge ratio (SGR) calculated from dataset well H and J

Depth feet	Formation name	Vsh. avg.	Throw (feet.) 0-25	25-50	50-75	75-100	100-125	125-150	150-175	175-200	200-225	225-250	250-275	275-300	300-325	325-350	350-375	375-400	400-425	425-450	450-475	475-500	500-525	525-550	550-575	575-600	600-625
0-25		0.21	0.210	0.160	0.117	0.27	0.37	0.445	0.443	0.46	0.528	0.439	0.46	0.46	0.495	0.472	0.442	0.47	0.489	0.478	0.49	0.508	0.488	0.472	0.49	0.504	0.497
25-50	U-C6	0.11	0.110	0.070	0.29	0.42	0.492	0.482	0.50	0.501	0.523	0.49	0.49	0.518	0.492	0.459	0.49	0.507	0.494	0.51	0.524	0.502	0.485	0.50	0.517	0.509	0.516
50-75		0.03	0.030	0.38	0.52	0.588	0.556	0.56	0.557	0.509	0.59	0.52	0.555	0.524	0.485	0.52	0.533	0.518	0.53	0.547	0.523	0.504	0.52	0.535	0.527	0.533	0.528
75-100		0.72	0.72	0.76	0.77	0.69	0.67	0.65	0.58	0.59	0.65	0.61	0.57	0.52	0.56	0.57	0.55	0.57	0.58	0.55	0.53	0.55	0.56	0.55	0.55	0.55	0.55
100-125		0.80	0.80	0.80	0.68	0.66	0.63	0.55	0.57	0.56	0.67	0.55	0.51	0.54	0.56	0.54	0.56	0.57	0.54	0.52	0.54	0.55	0.54	0.55	0.54	0.54	0.54
125-150		0.80	0.80	0.62	0.61	0.59	0.50	0.53	0.53	0.57	0.59	0.48	0.52	0.54	0.52	0.54	0.55	0.52	0.50	0.52	0.54	0.53	0.53	0.53	0.53	0.53	0.54
150-175		0.43	0.430	0.52	0.517	0.430	0.48	0.48	0.537	0.493	0.495	0.49	0.514	0.495	0.52	0.535	0.505	0.483	0.508	0.524	0.51	0.522	0.517	0.52	0.52	0.53	0.53
175-200		0.60	0.60	0.56	0.43	0.49	0.49	0.56	0.50	0.44	0.56	0.52	0.50	0.53	0.54	0.51	0.49	0.51	0.53	0.52	0.53	0.52	0.52	0.53	0.54	0.54	0.56
200-225		0.52	0.52	0.35	0.46	0.46	0.55	0.49	0.42	0.48	0.58	0.49	0.52	0.54	0.50	0.48	0.51	0.53	0.51	0.52	0.52	0.52	0.52	0.53	0.54	0.56	0.54
225-250		0.17	0.170	0.43	0.44	0.553	0.478	0.402	0.48	0.513	0.549	0.52	0.540	0.503	0.475	0.51	0.525	0.513	0.522	0.517	0.52	0.52	0.53	0.54	0.557	0.543	0.55
250-275		0.68	0.68	0.58	0.68	0.56	0.45	0.53	0.56	0.53	0.63	0.58	0.53	0.50	0.53	0.55	0.54	0.54	0.54	0.54	0.54	0.55	0.55	0.57	0.56	0.57	0.58
275-300		0.48	0.48	0.68	0.51	0.39	0.50	0.54	0.51	0.54	0.64	0.52	0.48	0.52	0.54	0.53	0.54	0.53	0.53	0.53	0.55	0.55	0.57	0.55	0.56	0.57	0.58
300-325		0.88	0.88	0.53	0.36	0.51	0.55	0.51	0.55	0.58	0.59	0.48	0.52	0.55	0.53	0.54	0.53	0.53	0.54	0.55	0.55	0.57	0.56	0.56	0.58	0.58	0.56
325-350	U-B2	0.18	0.180	0.100	0.38	0.473	0.436	0.50	0.533	0.478	0.495	0.49	0.515	0.500	0.513	0.506	0.51	0.51	0.53	0.53	0.557	0.541	0.55	0.56	0.568	0.548	0.56
350-375		0.02	0.020	0.48	0.570	0.500	0.56	0.592	0.520	0.473	0.59	0.549	0.529	0.541	0.532	0.53	0.54	0.55	0.55	0.578	0.560	0.57	0.58	0.586	0.564	0.57	0.588
375-400		0.94	0.94	0.85	0.66	0.69	0.71	0.60	0.54	0.59	0.68	0.58	0.59	0.57	0.57	0.57	0.59	0.59	0.61	0.59	0.60	0.61	0.61	0.59	0.60	0.61	0.60
400-425		0.75	0.75	0.52	0.61	0.65	0.54	0.47	0.53	0.57	0.61	0.55	0.54	0.54	0.54	0.56	0.56	0.59	0.57	0.58	0.59	0.60	0.57	0.58	0.60	0.59	0.60
425-450	U-B3	0.29	0.290	0.54	0.613	0.483	0.414	0.50	0.540	0.514	0.598	0.520	0.52	0.53	0.55	0.55	0.580	0.558	0.57	0.58	0.588	0.564	0.57	0.591	0.579	0.59	0.597
450-475		0.79	0.79	0.78	0.55	0.45	0.54	0.58	0.55	0.56	0.61	0.55	0.55	0.57	0.57	0.60	0.58	0.59	0.60	0.61	0.58	0.59	0.61	0.59	0.61	0.61	0.59
475-500		0.76	0.76	0.43	0.33	0.48	0.54	0.51	0.53	0.52	0.58	0.53	0.55	0.55	0.59	0.56	0.57	0.59	0.59	0.57	0.58	0.60	0.58	0.60	0.60	0.58	0.59
500-525	U-B4	0.09	0.090	0.115	0.38	0.485	0.454	0.490	0.480	0.49	0.56	0.53	0.53	0.572	0.545	0.56	0.58	0.584	0.555	0.57	0.587	0.574	0.59	0.595	0.575	0.59	0.598
525-550		0.14	0.140	0.53	0.617	0.545	0.570	0.545	0.55	0.55	0.65	0.58	0.615	0.583	0.59	0.61	0.617	0.584	0.60	0.615	0.599	0.62	0.619	0.597	0.61	0.620	0.602
550-575		0.92	0.92	0.86	0.68	0.68	0.63	0.61	0.61	0.63	0.70	0.66	0.62	0.63	0.65	0.65	0.61	0.63	0.64	0.62	0.64	0.64	0.62	0.63	0.64	0.62	0.61
575-600		0.79	0.79	0.56	0.60	0.55	0.55	0.56	0.59	0.59	0.71	0.59	0.61	0.63	0.63	0.59	0.61	0.63	0.61	0.63	0.63	0.60	0.62	0.63	0.61	0.60	0.59
600-625		0.33	0.330	0.50	0.473	0.49	0.51	0.56	0.56	0.615	0.572	0.59	0.61	0.617	0.576	0.59	0.615	0.596	0.62	0.619	0.594	0.61	0.620	0.600	0.593	0.578	
625-650		0.67	0.67	0.55	0.55	0.56	0.60	0.60	0.66	0.60	0.69	0.64	0.64	0.60	0.61	0.64	0.61	0.63	0.64	0.61	0.62	0.63	0.61	0.60	0.59		
650-675		0.42	0.420	0.49	0.52	0.58	0.58	0.653	0.593	0.61	0.72	0.640	0.590	0.61	0.632	0.609	0.63	0.634	0.605	0.62	0.633	0.611	0.601	0.585			
675-700		0.55	0.55	0.57	0.64	0.63	0.70	0.62	0.64	0.67	0.75	0.61	0.62	0.65	0.62	0.65	0.65	0.62	0.63	0.64	0.62	0.61	0.59				
700-725		0.58	0.58	0.68	0.65	0.74	0.64	0.65	0.68	0.68	0.69	0.63	0.66	0.63	0.65	0.66	0.62	0.64	0.65	0.62	0.61	0.59					
725-750		0.78	0.78	0.69	0.79	0.65	0.66	0.70	0.69	0.62	0.72	0.67	0.63	0.66	0.66	0.62	0.64	0.65	0.63	0.62	0.60						
750-775		0.59	0.59	0.80	0.61	0.64	0.68	0.68	0.59	0.62	0.74	0.62	0.65	0.65	0.61	0.63	0.65	0.62	0.61	0.59							
775-800		1.00	1.00	0.62	0.65	0.71	0.70	0.60	0.62	0.66	0.70	0.66	0.66	0.61	0.63	0.65	0.62	0.61	0.58								
800-825	U-B5	0.23	0.230	0.48	0.61	0.620	0.514	0.56	0.614	0.576	0.70	0.622	0.578	0.60	0.623	0.592	0.581	0.559									
825-850		0.72	0.72	0.80	0.75	0.59	0.63	0.68	0.63	0.67	0.75	0.61	0.64	0.66	0.62	0.61	0.58										
850-875		0.87	0.87	0.77	0.54	0.61	0.67	0.61	0.66	0.66	0.68	0.63	0.65	0.61	0.60	0.57											
875-900		0.66	0.66	0.38	0.52	0.62	0.56	0.62	0.63	0.57	0.68	0.63	0.59	0.57	0.55												
900-925		0.09	0.090	0.45	0.607	0.533	0.62	0.623	0.554	0.59	0.624	0.581	0.566	0.538													
925-950		0.80	0.80	0.87	0.68	0.75	0.73	0.63	0.66	0.69	0.72	0.61	0.58														
950-975		0.93	0.93	0.62	0.73	0.71	0.60	0.64	0.68	0.62	0.67	0.56															
975-1000		0.31	0.310	0.630	0.640	0.515	0.58	0.633	0.570	0.551	0.580																
1000-1025		0.95	0.95	0.81	0.58	0.65	0.70	0.61	0.59	0.54																	
1025-1050		0.66	0.66	0.40	0.55	0.64	0.55	0.53	0.48																		
1050-1075		0.14	0.140	0.50	0.627	0.518	0.498	0.453																			
1075-1100		0.86	0.86	0.87	0.64	0.59	0.52																				
1100-1125		0.88	0.88	0.54	0.50	0.43																					
1125-1150		0.19	0.190	0.305	0.280																						
1150-1175	U-B6	0.42	0.420	0.325																							
1175-1200		0.23	0.230																								

Table C.2 (continued)

Depth feet	Formation name	Vsh. avg.	Throw (feet) 625-650	650-675	675-700	700-725	725-750	750-775	775-800	800-825	825-850	850-875	875-900	900-925	925-950	950-975	975-1000	1000-1025	1025-1050	1050-1075	1075-1100	1100-1125	1125-1150	1150-1175	1175-1200
0-25		0.21	0.504	0.501	0.50	0.51	0.51	0.52	0.532	0.523	0.53	0.54	0.542	0.529	0.54	0.547	0.541	0.55	0.553	0.544	0.55	0.558	0.550	0.547	0.541
25-50	U-C6	0.11	0.512	0.51	0.52	0.52	0.53	0.542	0.533	0.54	0.55	0.551	0.538	0.55	0.556	0.549	0.56	0.562	0.552	0.56	0.566	0.558	0.555	0.548	
50-75		0.03	0.53	0.53	0.54	0.54	0.557	0.546	0.55	0.56	0.564	0.551	0.56	0.568	0.561	0.57	0.573	0.562	0.57	0.577	0.568	0.565	0.557		
75-100		0.72	0.55	0.56	0.56	0.57	0.56	0.57	0.58	0.58	0.57	0.57	0.58	0.58	0.59	0.59	0.58	0.58	0.59	0.58	0.58	0.57			
100-125		0.80	0.55	0.55	0.57	0.56	0.56	0.57	0.58	0.56	0.57	0.58	0.57	0.58	0.58	0.57	0.58	0.59	0.58	0.57	0.57				
125-150		0.80	0.54	0.56	0.55	0.56	0.57	0.57	0.55	0.56	0.57	0.56	0.58	0.58	0.57	0.57	0.58	0.57	0.57	0.56					
150-175		0.43	0.552	0.540	0.55	0.56	0.561	0.546	0.55	0.565	0.558	0.57	0.571	0.560	0.57	0.576	0.566	0.562	0.555						
175-200		0.60	0.54	0.55	0.56	0.57	0.55	0.56	0.57	0.56	0.57	0.58	0.56	0.57	0.58	0.57	0.57	0.56							
200-225		0.52	0.55	0.56	0.56	0.55	0.56	0.57	0.56	0.57	0.57	0.56	0.57	0.58	0.57	0.56	0.56								
225-250		0.17	0.56	0.566	0.549	0.56	0.570	0.562	0.57	0.576	0.564	0.57	0.581	0.570	0.566	0.557									
250-275		0.68	0.58	0.56	0.57	0.58	0.57	0.59	0.59	0.58	0.58	0.59	0.58	0.58	0.57										
275-300		0.48	0.56	0.57	0.58	0.57	0.58	0.59	0.57	0.58	0.59	0.58	0.57	0.56											
300-325		0.88	0.57	0.58	0.57	0.59	0.59	0.58	0.58	0.59	0.58	0.58	0.57												
325-350	U-B2	0.18	0.573	0.563	0.58	0.580	0.565	0.57	0.584	0.572	0.568	0.558													
350-375		0.02	0.578	0.59	0.594	0.578	0.59	0.597	0.584	0.579	0.569														
375-400		0.94	0.61	0.62	0.60	0.61	0.62	0.60	0.60	0.59															
400-425		0.75	0.60	0.59	0.60	0.61	0.59	0.59	0.57																
425-450	U-B3	0.29	0.579	0.59	0.600	0.586	0.580	0.569																	
450-475		0.79	0.60	0.61	0.60	0.59	0.58																		
475-500		0.76	0.60	0.59	0.58	0.57																			
500-525	U-B4	0.09	0.583	0.577	0.564																				
525-550		0.14	0.595	0.582																					
550-575		0.92	0.60																						
575-600		0.79																							
600-625		0.33																							
625-650		0.67																							
650-675		0.42																							
675-700		0.55																							
700-725		0.58																							
725-750		0.78																							
750-775		0.59																							
775-800		1.00																							
800-825	U-B5	0.23																							
825-850		0.72																							
850-875		0.87																							
875-900		0.66																							
900-925		0.09																							
925-950		0.80																							
950-975		0.93																							
975-1000		0.31																							
1000-1025		0.95																							
1025-1050		0.66																							
1050-1075		0.14																							
1075-1100		0.86																							
1100-1125		0.88																							
1125-1150	U-B6	0.19																							
1150-1175		0.42																							
1175-1200		0.23																							

Table C.3 Shale gouge ratio calculation was used to display in Figure 5.19

Using for cal. SGR on allan diagram (U-B2 vs. U-B4)			
	Throw	SGR	Shale volume
Dataset from well F and I	258	0.42	4.38
	258	0.42	
	257	0.43	
	257	0.43	
	260	0.42	
	260	0.42	
	260	0.42	
	259	0.42	
	259	0.42	
	257	0.43	
	256	0.43	
	256	0.43	
	258	0.42	
	265	0.41	
	266	0.41	
	266	0.41	
	268	0.41	
	270	0.41	
	272	0.40	
Using for cal. SGR on allan diagram (U-B5 vs. U-B6)			
	Throw	SGR	Shale volume
Dataset from well F and I	300	0.83	9.93
	287	0.86	
	288	0.86	
	292	0.85	
	295	0.84	
	296	0.84	
	298	0.83	
	299	0.83	
	300	0.83	
	302	0.82	
	303	0.82	
	304	0.82	
	305	0.81	
Dataset from well H and B	307	0.73	8.94
	309	0.72	
	311	0.72	
	313	0.71	
	316	0.71	
	322	0.69	
	335	0.67	
	339	0.66	
	343	0.65	
	347	0.64	
	350	0.64	
	352	0.63	
	355	0.63	
	356	0.63	
	357	0.63	
	360	0.62	
	361	0.62	

Table C.4 Shale gouge ratio calculation was used to display in Figure 5.40 **(a)**

Assuming Litho. Across The Benchamas-B Fault by using data from well F, H, E and C.											
					SGR calculation						
Horizon	Thickness	Depth interval	Vsh. Average	Vsh.*thickness	Throw (Juxtaposed unit)						
	(feet)	(feet)	(fraction)		U-C6	U-B2	U-B3	U-B4	U-B5	U-B6
U-C6	93	0-93	0.23	21.39	0.23	0.61	0.60	0.58	0.603	0.62
	142	93-235	0.77	109.34						
U-B1	21	235-256	0.14	2.94						
	78	256-334	0.53	41.34						
U-B2	59	334-393	0.12	7.08		0.12	0.64	0.57	0.61	0.63
	79	393-472	0.75	59.25						
U-B3	31	472-503	0.13	4.03			0.13	0.53	0.62	0.64
	64	503-567	0.71	45.44						
U-B4	35	567-602	0.08	2.8				0.08	0.65	0.66
	277	602-879	0.71	196.67						
U-B5	34	879-913	0.12	4.08					0.12	0.67
	248	913-1161	0.81	200.88						
U-B6	81	1161-1242	0.19	15.39						0.19

Table C.5 Shale gouge ratio calculation was used to display in Figure 5.40 **(b)**

Assuming Litho. Across Benchamas-B Fault by using data from well B and I.											
					SGR calculation						
Horizon	Thickness (feet)	Depth interval (feet)	Vsh. Average (fraction)	Vsh.*thickness	Throw (Juxtaposed unit)						
					U-C6	U-B2	U-B3	U-B4	U-B5	U-B6
U-C6	45	0-45	0.27	12.15	0.27	0.73	0.62	0.60	0.61	0.64
SH1	103	45-148	0.79	81.37						
S1	60	148-208	0.28	16.8						
U-B1	18	208-226	0.25	4.5						
SH2	58	226-284	0.91	52.78						
U-B2	35	284-319	0.18	6.3		0.18	0.64	0.58	0.61	0.64
SH3	60	319-379	0.7	42						
U-B3	23	379-401	0.17	3.91			0.17	0.57	0.62	0.44
SH4	40	401-441	0.9	36						
U-B4	40	441-481	0.15	6				0.15	0.65	0.67
SH5	65	481-546	0.8	52						
S2	28	546-574	0.14	3.92						
SH6	68	574-642	0.77	52.36						
S3	28	642-670	0.16	4.48						
SH7	30	670-700	0.92	27.6						
S4	18	700-718	0.24	4.32						
SH8	53	718-771	0.92	48.76						
U-B5	25	771-796	0.17	4.25					0.17	0.69
SH9,10,11,12+ S5,6,7	315	796-1111	0.76	239.4						
U-B6	53	1111-1164	0.21	11.13						0.21

BIOGRAPHY

Mr. Thammasak Koednok was born in Nakorn Ratchasima province on January 22, 1975. In 1998, he graduated with B.Eng. degree in Geotechnology from Suranaree University of Technology. After graduation, he studied the M.Sc. degree in Geology at Chulalongkok University.